frontiers | Research Topics

Advances and challenges in stroke therapy: a regenerative prospective, volume II

Edited by
Syed Shadab Raza, Viola B. Morris and Hassan Azari

Published in
Frontiers in Pharmacology
Frontiers in Cellular Neuroscience
Frontiers in Stroke

ISSN 1664-8714
ISBN 978-2-8325-5999-4
DOI 10.3389/978-2-8325-5999-4

About Frontiers

Frontiers is more than just an open access publisher of scholarly articles: it is a pioneering approach to the world of academia, radically improving the way scholarly research is managed. The grand vision of Frontiers is a world where all people have an equal opportunity to seek, share and generate knowledge. Frontiers provides immediate and permanent online open access to all its publications, but this alone is not enough to realize our grand goals.

Frontiers journal series

The Frontiers journal series is a multi-tier and interdisciplinary set of open-access, online journals, promising a paradigm shift from the current review, selection and dissemination processes in academic publishing. All Frontiers journals are driven by researchers for researchers; therefore, they constitute a service to the scholarly community. At the same time, the *Frontiers journal series* operates on a revolutionary invention, the tiered publishing system, initially addressing specific communities of scholars, and gradually climbing up to broader public understanding, thus serving the interests of the lay society, too.

Dedication to quality

Each Frontiers article is a landmark of the highest quality, thanks to genuinely collaborative interactions between authors and review editors, who include some of the world's best academicians. Research must be certified by peers before entering a stream of knowledge that may eventually reach the public - and shape society; therefore, Frontiers only applies the most rigorous and unbiased reviews. Frontiers revolutionizes research publishing by freely delivering the most outstanding research, evaluated with no bias from both the academic and social point of view. By applying the most advanced information technologies, Frontiers is catapulting scholarly publishing into a new generation.

What are Frontiers Research Topics?

Frontiers Research Topics are very popular trademarks of the *Frontiers journals series*: they are collections of at least ten articles, all centered on a particular subject. With their unique mix of varied contributions from Original Research to Review Articles, Frontiers Research Topics unify the most influential researchers, the latest key findings and historical advances in a hot research area.

Find out more on how to host your own Frontiers Research Topic or contribute to one as an author by contacting the Frontiers editorial office: frontiersin.org/about/contact

Advances and challenges in stroke therapy: a regenerative prospective, volume II

Topic editors

Syed Shadab Raza — ERA's Lucknow Medical College, India

Viola B. Morris — Emory University, United States

Hassan Azari — Barry University, United States

Citation

Raza, S. S., Morris, V. B., Azari, H., eds. (2025). *Advances and challenges in stroke therapy: a regenerative prospective, volume II*. Lausanne: Frontiers Media SA.

doi: 10.3389/978-2-8325-5999-4

Table of contents

frontiers | Frontiers in Cellular Neuroscience

TYPE Review
PUBLISHED 24 May 2023
DOI 10.3389/fncel.2023.1191629

OPEN ACCESS

EDITED BY
Viola B. Morris,
Emory University, United States

REVIEWED BY
Qiong Cheng,
Nantong University, China
Jane Joy Thomas,
Northwestern Medicine, United States
Narayanaiah Cheedarla,
Emory University, United States

*CORRESPONDENCE
Zhigang Mei
✉ meizhigang@hnucm.edu.cn
Jinwen Ge
✉ 001267@hnucm.edu.cn

RECEIVED 22 March 2023
ACCEPTED 05 May 2023
PUBLISHED 24 May 2023

CITATION
She R, Liu D, Liao J, Wang G, Ge J and Mei Z (2023) Mitochondrial dysfunctions induce PANoptosis and ferroptosis in cerebral ischemia/reperfusion injury: from pathology to therapeutic potential.
Front. Cell. Neurosci. 17:1191629.
doi: 10.3389/fncel.2023.1191629

Mitochondrial dysfunctions induce PANoptosis and ferroptosis in cerebral ischemia/reperfusion injury: from pathology to therapeutic potential

Ruining She[1], Danhong Liu[2], Jun Liao[2], Guozuo Wang[1], Jinwen Ge[1,3]* and Zhigang Mei[1,4]*

[1]Key Laboratory of Hunan Province for Integrated Traditional Chinese and Western Medicine on Prevention and Treatment of Cardio-Cerebral Diseases, College of Integrated Traditional Chinese and Western Medicine, Hunan University of Chinese Medicine, Changsha, Hunan, China, [2]Medical School, Hunan University of Chinese Medicine, Changsha, Hunan, China, [3]Hunan Academy of Traditional Chinese Medicine, Changsha, Hunan, China, [4]Third-Grade Pharmacological Laboratory on Chinese Medicine Approved by State Administration of Traditional Chinese Medicine, China Three Gorges University, Yichang, Hubei, China

Ischemic stroke (IS) accounts for more than 80% of the total stroke, which represents the leading cause of mortality and disability worldwide. Cerebral ischemia/reperfusion injury (CI/RI) is a cascade of pathophysiological events following the restoration of blood flow and reoxygenation, which not only directly damages brain tissue, but also enhances a series of pathological signaling cascades, contributing to inflammation, further aggravate the damage of brain tissue. Paradoxically, there are still no effective methods to prevent CI/RI, since the detailed underlying mechanisms remain vague. Mitochondrial dysfunctions, which are characterized by mitochondrial oxidative stress, Ca^{2+} overload, iron dyshomeostasis, mitochondrial DNA (mtDNA) defects and mitochondrial quality control (MQC) disruption, are closely relevant to the pathological process of CI/RI. There is increasing evidence that mitochondrial dysfunctions play vital roles in the regulation of programmed cell deaths (PCDs) such as ferroptosis and PANoptosis, a newly proposed conception of cell deaths characterized by a unique form of innate immune inflammatory cell death that regulated by multifaceted PANoptosome complexes. In the present review, we highlight the mechanisms underlying mitochondrial dysfunctions and how this key event contributes to inflammatory response as well as cell death modes during CI/RI. Neuroprotective agents targeting mitochondrial dysfunctions may serve as a promising treatment strategy to alleviate serious secondary brain injuries. A comprehensive insight into mitochondrial dysfunctions-mediated PCDs can help provide more effective strategies to guide therapies of CI/RI in IS.

KEYWORDS

ischemic stroke, cerebral ischemia/reperfusion injury (CI/RI), mitochondrial dysfunctions, PANoptosis, PANoptosome, ferroptosis

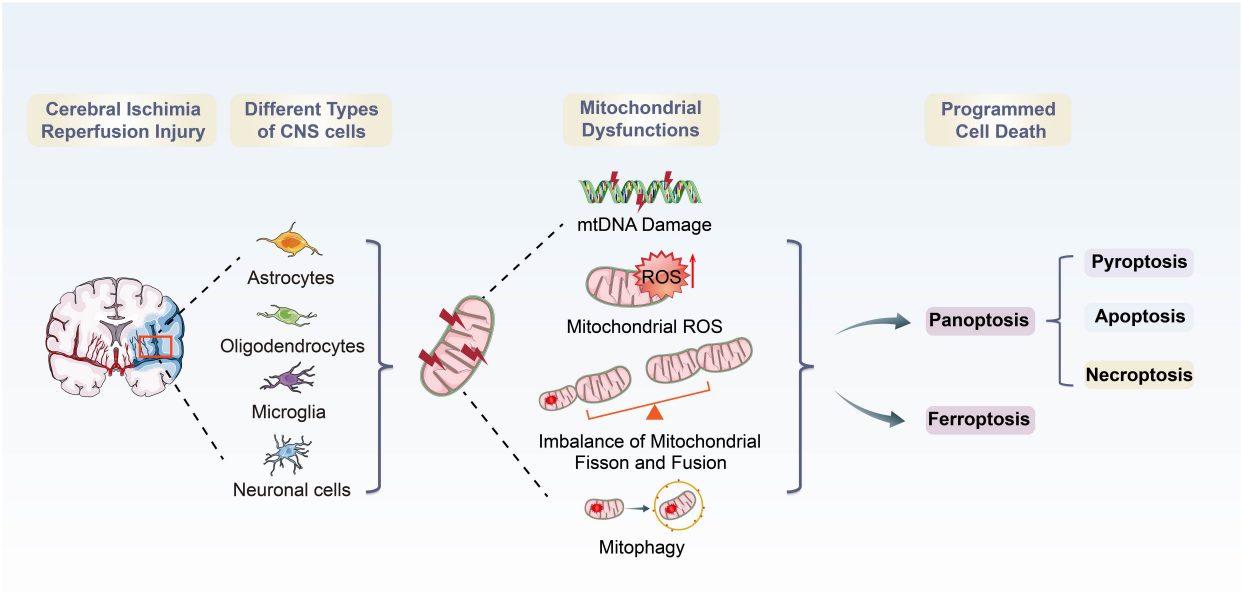

GRAPHICAL ABSTRACT
Overview of mitochondrial dysfunctions-induced PANoptosis and ferroptosis during CI/RI.

Introduction

Stroke is the second leading cause of death and the third major cause of disability globally (Pandian and Sebastian, 2021). In 2019, around 12.2 million people suffered from a new or recurrent stroke, which has increased substantially from 1990 to 2019 (Zhou et al., 2016; GBD 2019 Stroke Collaborators, 2021). Ischemic stroke (IS) accounts for more than 80% of all stroke types, and according to incomplete statistics, about 14 million people suffer from IS annually (Farina et al., 2021). During IS, blood flow is blocked, oxygen and nutrients are depleted, triggering a cascade of ischemic events in the brain (Magistretti and Allaman, 2015; Shen et al., 2021; Shi et al., 2021). Treatment for IS can be achieved through reperfusion, which restores blood flow/oxygenation to the brain in a timely fashion and efficiently salvaging the function of potentially reversible ischemic penumbra by thrombolysis such as intravenous recombinant tissue-type plasminogen activator (rtPA) or mechanical thrombectomy. Rapid reperfusion paradoxically has the constraint of a short recanalization time window and may result in irreparable neurological damage, a condition known as cerebral ischemia/reperfusion injury (CI/RI) (Gao et al., 2015).

Although recent clinical trials have shown that the administration of reperfusion therapy 24 h or more after stroke onset has a positive effect on the prognosis of patients with acute ischemic stroke (Ragoschke-Schumm and Walter, 2018), it often leads to additional cerebral damage, creating an important

Abbreviations: AMPK, AMP-activated protein kinase; ANT, adenine nucleotide translocator; APAF1, apoptotic protease activating factor-1; ASC, apoptosis-associated speck-like protein containing a caspase recruitment domain; ATP, adenosine triphosphate; BBB, blood-brain barrier; Bcl-2, B-cell leukemia/lymphoma 2; BER, base excision repair; CI/RI, cerebral ischemia/reperfusion injury; CNS, central nervous system; CoQ, coenzyme Q; CsA, cyclosporine-A; CypD, cyclophilin D; Cyt C, cytochrome C; DAMP, damage-associated molecular patterns; DHM, dihydromyricetin; DISC, death-induced signaling complex; DR, direct reversal; Drp1, dynamin-related protein 1; DSBs, double-strand breaks; EAA, excitatory amino acid; ETC, electron transportation chain; FADD, Fas-associated protein with a death domain; Fis1, mitochondrial fission protein 1; FtMt, mitochondrial ferritin; FUNDC1, FUN14 domain containing 1; Gln, glutamine; GLUD1, glutamate dehydrogenase 1; GPX4, glutathione peroxidase 4; GSDMD, Gasdermin D; GSH, glutathione; GTP, guanosine triphosphate; IMM, inner mitochondrial membrane; IMS, intermembrane space; IS, ischemic stroke; LC3, light chain 3; LIP, labile iron pool; L-OPA1, the long form of OPA-1; MDV, mitochondria derived vesicle; MFF, mitochondrial fission factor; MFN1/2, mitofusin 1/2; MiD49/MiD51, mitochondrial dynamics proteins of 49/51 kDa; MIMP, mitochondrial inner membrane permeabilization; miRNAs, microRNAs; MLKL, mixed lineage kinase domain-like protein; MMP, mitochondrial membrane potential; MMR, DNA mismatch repair; MO, mitochondrial outer membrane permeabilization; MPT, mitochondrial permeability transition; mPTP, mitochondrial permeability transition pore; MQC, mitochondrial quality control; mtDNA, mitochondrial DNA; mTORC1, mammalian target of rapamycin; mtROS, mitochondrial ROS; NADPH, nicotinamide adenine dinucleotide phosphate; NHE, Na/H exchanger; NLRC4, NOD-like receptors with caspase activation and recruitment domain 4; NLRP3, NOD-like receptor pyrin domain-containing 3; NMDA, N-methyl-D-aspartic acid; NO, nitric oxide; NOS, nitrogen species; NRF1/2, nuclear respiratory factor ½; OMM, outer mitochondrial membrane; OPA1, optic atrophy 1; OXPHOS, oxidative phosphorylation; PCD, programmed cell death; PDH, pyruvate dehydrogenase; PGAM5, phosphoglycerate mutase family member 5; PGC-1α, peroxisome proliferator-activated receptor-γ coactivator 1α; PINK1, PTEN-induced kinase 1; PUFAs, polyunsaturated fatty acids; PYGL, glycogen phosphorylase; RIPK, receptor-interacting protein kinase; RNS, reactive nitrogen species; ROS, reactive oxygen species; rtPA, recombinant tissue plasminogen activator; SIRT1, sirtuin 1; SLC3A2, solute carrier family 3 member 2; SLC7A11, solute carrier family 7 member 11; SMAC, second mitochondria-derived activator of caspase; SOD2, superoxide dismutase 2; S-OPA1, short form of OPA-1; system Xc-, cystine/glutamate antiporter system; TAK1, growth factor beta-activated kinase 1; tBIDa, truncated active BID; TCM, traditional Chinese medicine; TFAM, mitochondrial transcription factor A; TNF-α, tissue necrosis factor-alpha; TRADD, TNF receptor-associated death domain; TRAF, TNFR-associated factor; TRAIL, tumor necrosis factor-related apoptosis inducing ligand; UCP2, uncoupling protein 2; VDAC, voltage-dependent anion channel; XIAP, X-linked inhibitor of apoptosis protein; ZBP1, Z-DNA-binding protein; ΔpH, proton gradient; ΔΨm, mitochondrial membrane potential.

clinical dilemma. Reperfusion-induced reactive oxygen species (ROS) production overwhelms the cell's anti-oxidative defense mechanism, rendering it incapable of scavenging free radicals, disturbing neuronal homeostasis, which leads to inflammatory response, oxidative stress, apoptosis, necrosis, and other pathological processes, culminating in cell death (Deb et al., 2010).

Increasing evidence indicates that mitochondria play vital roles in improving neuronal survival and neurological function after IS (Deb et al., 2010; Anzell et al., 2018; Yang et al., 2021). Mitochondria are cellular organelles responsible for energy production and metabolism in cells, providing adenosine triphosphate (ATP) to active neurons (Sjostrand, 1953; Gustafsson et al., 2016; Xian and Liou, 2021). During CI/RI, energy balance is disturbed due to reduced blood supply and ATP synthesis is disturbed (Borutaite, 2010). One of the hallmarks of CI/RI are mitochondrial dysfunctions (Vosler et al., 2009), which are characterized by mitochondrial oxidative stress, mitochondrial Ca^{2+} overload, iron dyshomeostasis, mitochondrial DNA (mtDNA) defects and mitochondrial quality control (MQC) disruption. Following ischemia and reperfusion, mitochondrial dysfunctions initiate a cascade of events that result in acute and persistent inflammatory responses and activate the programmed cell deaths (PCDs), such as ferroptosis and PANoptosis, a recently proposed concept of programmed cell deaths characterized by a unique inflammatory cell death modality, including pyroptosis, apoptosis and necroptosis. These pathophysiological processes are intertwisted and deleterious to the neural cells, regulating the disease and immune response of CI/RI. However, how mitochondrial dysfunctions govern cell death has been unclear and somewhat controversial. A thorough understanding of mitochondrial dysfunctions in different physiological and pathological conditions is essential to provide therapeutic avenues for IS (Bock and Tait, 2020).

This review will offer an insight into the pathomechanism underlying the mitochondrial dysfunctions in various types of PCDs and mitochondria-targeted therapeutic potential against PCDs especially PANoptosis and ferroptosis in CI/RI. Clarifying the relationship of pathology between mitochondrial dysfunctions and PCDs and uncover the molecular pathways will not only contribute to a thorough understanding of the mitochondrial dysfunction-mediated PCDs machinery but also lighten potential novel pharmacological targets for IS.

2. CI/RI and mitochondrial dysfunctions

2.1. CI/RI pathology

The earliest symptom of IS is cerebral ischemia (Khoshnam et al., 2017). Protecting the ischemic penumbra and restoring brain function is critical. However, CI/RI is inevitable after restoration of blood flow and may be the most important determinant of poor prognosis (Kalogeris et al., 2016; Nentwich, 2016). Reperfusion produces paradoxical tissue responses, which lead to a severe imbalance of metabolic supply and demand, and eventually activates neuronal death and causes hippocampal and cortical damage, initiating cerebral hemorrhage and deteriorating the blood-brain barrier (BBB) (Kishimoto et al., 2019; Huang et al., 2021). CI/RI results from a complex series of pathophysiological events including burst of ROS, free radical damage, Ca^{2+} homeostasis disorder, EAA toxicity, neuroinflammation, and fat decomposition, etc., (Kalogeris et al., 2016; Wu M. et al., 2021). Ca^{2+} overload and ROS burst are the initial events of CI/RI (Pundik et al., 2012; Hayyan et al., 2016; Kalogeris et al., 2016; Wu M. Y. et al., 2018; Chen and Li, 2020).

During cerebral ischemia, ATP synthesis efficiency declines due to ischemia and hypoxia in the brain, along with acidic intracellular metabolites and purine bases surging. Thus, the Na^+/H^+ exchanger (NHE) exchanges for sodium ions (Sansbury and Spite, 2016) and the lack of oxygen supply forces cells to produce ATP, which is insufficient to maintain ATPases (e.g., Na^+/K^+ ATPase) function. This results in cellular Ca^{2+} overload and disruption of mitochondrial architecture. Once reperfusion, the oxygen and substrates required for aerobic ATP generation are restored, and hydrogen ions that accumulate in the extracellular space are removed, which promotes additional Ca^{2+} influx. At the same time, the oxygen influx could also fuel ROS production (Chen H. et al., 2011). Ca^{2+} accumulation also mediates the excitotoxicity and then promotes cerebral edema and activation of the intracellular self-destruction cascade. Mitochondria absorb excess Ca^{2+} when Ca^{2+} levels are elevated by excitotoxicity, leading to organelle enlargement and formation of the mitochondrial permeability transition pore (mPTP), which executes and activates cell death pathways (Andrabi et al., 2020). Reperfusion-promoted ROS damage and oxidative stress injure the proteins, lipids, as well as mtDNA, which causes straight damage to mitochondrial function after CI/RI (Borutaite, 2010). Moreover, CI/RI seriously affects glial cells, including oligodendrocytes, microglia, and astrocytes (Song et al., 2017). Oligodendrocytes are particularly sensitive to injuries, including hypoxia, ROS/nitrogen species (NOS) and excitotoxicity (Merrill and Scolding, 1999; Smith et al., 1999), which impair the functional activity of the mitochondrial respiratory chain (Ziabreva et al., 2010). Microglia are critical for regulating neuroinflammation. Mitochondrial dyshomeostasis injures microglial function and exacerbated the pathogenic process of IS (Zhou et al., 2019). Astrocytes communicate and protect neurons from hypoxia and excitotoxicity through the gap junction and BBB, whereas inhibition of astrocyte mitochondrial function leaves neurons vulnerable to cell death (Ouyang et al., 2013). Mitochondrial dysfunctions are the most critical link of CI/RI.

2.2. Mitochondrial abnormalities and dysfunctions in CI/RI

Mitochondria are the most vulnerable organelle to cerebral ischemic injury (Hill et al., 2018). Burst of ROS, Ca^{2+} overload, excitotoxicity and other consequences of CI/RI could trigger mitochondrial dysmorphology/dysfunctions (**Figure 1**). Notably, preserving or promoting mitochondrial function is a potential therapeutic target for treating CI/RI.

2.2.1. Mitochondrial structure abnormalities

In the brain, mitochondria generate ATP by electron transportation chain (ETC), which is composed of transmembrane

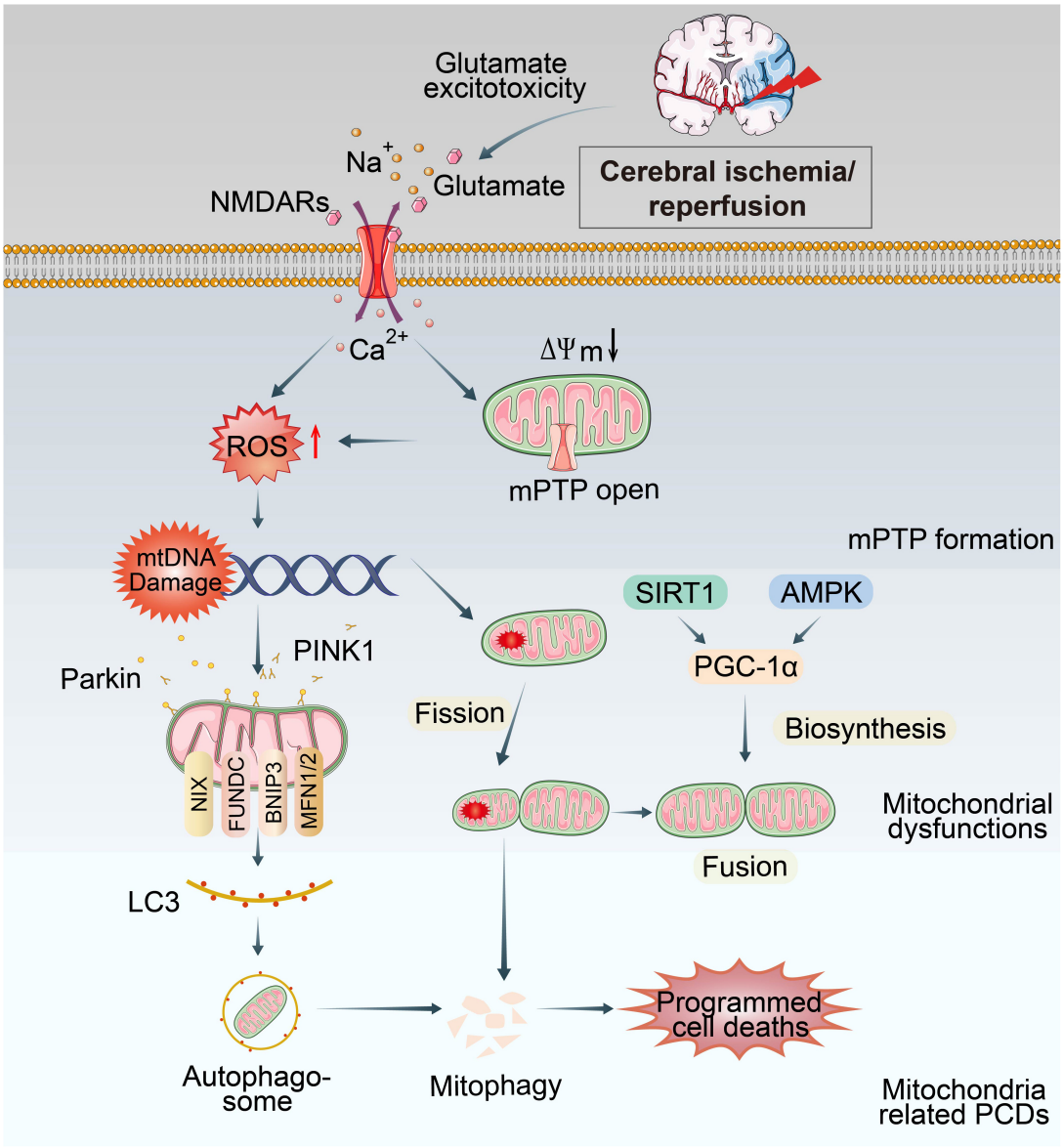

FIGURE 1
Overview of mitochondrial dysfunctions during CI/RI. Mitochondria are the most susceptible organelle to CI/RI. ATP consumption, glucose/O_2 deprivation, burst of ROS, Ca^{2+} overload, excitotoxicity, inflammatory response and other consequences of CI/RI could trigger mitochondrial dysfunctions including mitochondrial oxidative stress, Ca^{2+} overload, iron dyshomeostasis, mitochondrial DNA defects, mitochondrial quality control disruption as well as mitochondrial-induced PCDs. These cellular processes ultimately lead to the death of neuron.

protein complexes (I-IV) embedded in the inner mitochondrial membrane (IMM) (Tang et al., 2016; Zhao et al., 2019). During cerebral ischemia, the energy supply is drastically reduced. IMM and mitochondrial cristae structure deform due to oxygen radicals and Ca^{2+} overload, triggering mitochondrial response, including excessive ROS production, mitochondrial Ca^{2+} overloading, and disrupted MQC. During reperfusion, Ca^{2+} influx and ROS burst promote the mitochondria's swelling, increasing cytoplasmic density, depolarization of mitochondrial membrane potential ($\Delta\Psi m$) and opening of the mPTP (Solenski et al., 2002).

The mPTP is a high-conductance channel that composed of three proteins: the voltage-dependent anion channel (VDAC) in the outer mitochondrial membrane (OMM), the adenine nucleotide translocator (ANT) in the IMM and cyclophilin D (CypD) in the mitochondrial matrix (Rao et al., 2014; Pérez and Quintanilla, 2017; Rottenberg and Hoek, 2017), regulating molecular exchange between the mitochondrial matrix and cytoplasm. The mPTP regulation by CypD is the most critical for mitochondrial morphology. Under normal conditions, mPTP is closed, and the IMM selectively allows the passage of small metabolic substrates and ions. When the cell undergoes oxidative stress, Ca^{2+} and ROS concentrations burst and the permeability of mPTP increases, initiating further production and release of ROS that damage both mitochondrial and nuclear DNA, proteins, and phospholipids. Further, the opening of the mPTP forms the mitochondrial permeability transition (MPT). It releases cytochrome C (Cyt C) and serine protease into the cytosol (Tajeddine, 2016), which could trigger the

caspase cascade, leading to PCDs and a series of damage (Van Opdenbosch and Lamkanfi, 2019).

2.2.2. Mitochondrial oxidative stress

Oxidative phosphorylation (OXPHOS) is an oxygen-dependent process in mitochondria that consumes chemical energy from catabolism to produce ATP and power energy-dependent biological processes. The OXPHOS system works through a series of protein complexes, consisting of ETC complexes I, II, III, and IV, and ATP synthase (complex V), along with two electron carriers, Cyt C, and coenzyme Q (CoQ) (Zhao et al., 2022). Thus, mitochondria are famous as "the powerhouse of the cell".

Mitochondrial oxidative stress is a condition that arises from an imbalance between oxidation and antioxidation in the mitochondrial respiratory chain (Sinha et al., 2013). It plays an essential role in CI/RI development (Quesnelle et al., 2015). The reduction of oxygen in mitochondria following cerebral ischemia limits mitochondrial OXPHOS, which decreases ATP production, leading to the release of oxygen radicals from ETC and the eruption of incomplete metabolism such as superoxide anion (O_2^-), hydroxyl radicals (·OH), reactive nitrogen species (RNS) and nitric oxide (NO) (Vinogradov and Grivennikova, 2016; Trujillo-Rangel et al., 2022). While during reperfusion, after the oxygen supply is restored, the pro-oxidant enzyme system and mitochondria use oxygen as a substrate to produce oxygen radicals, generating transient but an exorbitant burst of ROS in cells and ultimately triggering a series of processes ranging from altered cell signaling pathways to cell death (Andrabi et al., 2020). Furthermore, the reperfusion process also significantly reduces the activity of succinic dehydrogenase and Cyt C oxidase and another key enzyme along the ETC, leading to a reduction in OXPHOS efficiency, which affects ATP production (Cadenas and Davies, 2000).

2.2.3. Mitochondrial Ca^{2+} overload

Normally, cytosolic Ca^{2+} is strictly regulated through the cell membrane, endoplasmic reticulum, and mitochondria. As Ca^{2+} buffer, mitochondria absorb substantial amounts of cytosolic Ca^{2+} at the expense of $\Delta\Psi m$. The pathways of Ca^{2+} entry into the mitochondrial matrix are known as the mitochondrial calcium uniporter (MCU), the "rapid mode" mechanism, and the mitochondrial ryanodine receptor (Feissner et al., 2009). When cerebral blood flow gets interrupted and oxygen supply is reduced, Na^+/K^+ ATPase and other ion channels are prevented from maintaining a regular electrochemical gradient, resulting in continued depolarization of glial and neuronal cells (Liao et al., 2019). Open voltage gated Ca^{2+} channels, insufficient Ca^{2+} pump activity, and ATP deficiency lead to increased intracellular Ca^{2+} concentration. Ca^{2+} overload causes the release of excitatory neurotransmitters, particularly glutamate extracellularly (Singh et al., 2019), which binds to NMDA (N-methyl-D-aspartic acid) and other ion receptors, causing massive Ca^{2+} influx and consequent excitotoxicity. Excessive matrix Ca^{2+} concentrations, especially when associated with oxidative stress, precipitate the opening of mPTP (Briston et al., 2017), which is associated with apoptosis via the mitochondrial pathway or other PCDs due to mitochondrial damage (Bernardi et al., 2022). There has also been evidence that mitochondrial Ca^{2+} uptake can be responsible for the production of free radicals (Feissner et al., 2009). The mechanism of mitochondrial Ca^{2+} overload is a topic of great debate in the field.

2.2.4. MtDNA defects

Mitochondria are the only organelle possessing their circular genome, which is 16.6 kb in mammals, encoding 13 subunits that are essential in the maintenance and regulation of mitochondrial functions, such as encoding essential proteins of ETC and OXPHOS system (Liu H. et al., 2022). As mtDNA exists within the mitochondrial matrix or attached to the IMM, it can be easily damaged by free radicals produced by the respiratory chain. However, it is barely protected by histones and cannot effectively synthesize glutathione to remove oxygen radicals (Fariss et al., 2005). Following CI/RI, mitochondria activate several mtDNA repair and clearance pathways such as direct reversal (DR), DNA mismatch repair (MMR), base excision repair (BER), double-strand breaks (DSBs) and other mtDNA repair pathways (Alexeyev et al., 2013). In mitochondria, BER is the most typical mechanism to repair various types of DNA damage affecting the nuclear genome (Fontana and Gahlon, 2020). If these repair mechanisms are not sufficient to restore mtDNA structure and function, irreversible defects occur, leading to mutations in mtDNA (Liu H. et al., 2022). Furthermore, mtDNA mutations alter tRNA structure, which defects the assembly of the respiratory chain complex and enzyme activity, further increasing ROS production and exacerbating mtDNA mutations, creating a vicious cycle in CI/RI. Chen H. et al. (2001) showed that CI/RI could cause mtDNA damage. Although mtDNA can repair itself after <30 min of transient cerebral ischemia, the damage is irreversible after prolonged ischemia, which reduces the activity of complexes I and IV in the ETC, thereby disrupting the integrity of the respiratory chain complex electron transport. The mtDNA mutation also affects mitochondrial autophagy. Compared to normal cells, mtDNA mutant cells show reduced expression of autophagy marker protein light chain 3 (LC3) and reduced accumulation of autophagic substrate p62, resulting in impaired mitochondrial autophagy and significantly increased ROS levels (Zhang et al., 2018). Mitochondrial DNA damage could induce ATP synthesis defect, aggravating the outcome of programmed cell deaths, with the poor clinical symptoms such as cognitive impairment, Alzheimer's disease (AD) and Parkinson's disease (PD) (Anzell et al., 2018). Consequently, mtDNA is an important driver of CI/RI and can be used as a marker from primary plasma samples or tissue (Chong et al., 2022; Salvador et al., 2023). Mitochondrial diseases stemming from mtDNA point mutations and deletions present a wide clinical spectrum of phenotypes (Nissanka and Moraes, 2018). ELISA, PCR amplifications, whole-genome sequencing could be used for detection (Bernal-Tirapo et al., 2023). Further investigation of mtDNA as a potentially sensitive marker of CI/RI and response to mitoprotective therapy is warranted.

2.2.5. Disrupted MQC

Mitochondrial quality control (MQC) is a significant process for maintaining mitochondrial health and function (Youle, 2019), which involves mitochondrial biogenesis, mitochondrial fission and fusion, and mitophagy (Pickles et al., 2018). These processes are essential for the production of energy, the maintenance of mitochondrial structure and function, and the removal of damaged or dysfunctional mitochondria.

2.2.5.1. Mitochondrial biosynthesis

Mitochondrial biogenesis refers to the generation of new mitochondrial mass and the replication of mitochondrial DNA by proliferation of pre-existing organelles, which is essential to meet increased cellular energy demands and to repopulate mitochondrial contents in newly generated cells during cell proliferation (Yang et al., 2019).

The key regulators of mitochondrial biosynthesis include peroxisome proliferator-activated receptor-γ coactivator 1α (PGC-1α), AMP-activated protein kinase (AMPK), nuclear respiratory factor 1/2 (NRF1/2), mitochondrial transcription factor A (TFAM) and sirtuin 1 (SIRT1) (Li et al., 2021). SIRT1-PGC-1α and AMPK-PGC-1α axes are key pathways that regulate mitochondrial biogenesis (Li et al., 2017). During CI/RI, PGC-1α is activated by upstream AMPK or SIRT1 and deacetylases through phosphorylation and deacetylation modifications. Meanwhile, upregulating the mammalian target of the rapamycin (mTORC1)/PGC-1 signaling pathway could activate mitochondrial biogenesis and cellular senescence (Summer et al., 2019). PGC-1α could improve ATP production and mitochondrial mass by activating NRF1/TFAM axis in oxidative stress environments (You et al., 2016). After IS, microglial PGC-1α expression upregulates for a short period of time, significantly reducing neurological deficits after ischemic injury, with reduced neuroinflammation and enhanced mitophagy (Han et al., 2021). Meanwhile, PGC1-α is a master regulator to activate superoxide dismutase 2 (SOD2) and the uncoupling protein 2 (UCP2); both are mitochondrial proteins and may contribute to neuronal survival and ROS scavenging (Chen S. D. et al., 2011). Furthermore, PGC-1α could regulate dynamin-related protein 1 (Drp1) protein expression and phosphorylation (Peng et al., 2017). In conclusion, activation of mitochondrial biosynthesis maintains mitochondrial homeostasis. It increases cellular antioxidant and anti-infective activity and has been proposed as a potential new target for mitigating mitochondrial damage during CI/RI disease.

2.2.5.2. Mitochondrial fission and fusion

Mitochondria are morphologically dynamic organelles that often undergo fission and fusion events that regulate mitochondrial integrity and bioenergetics and contribute to maintaining cellular homeostasis in healthy and diseased cells. Under normal conditions, mitochondria change shape, size and number by constantly fusing and dividing to meet the needs of cellular metabolism. However, under the induction of ischemia and hypoxia injury factors, ROS-induced mitochondrial oxidative stress can directly lead to a disruption of the relative mitochondrial fission/fusion balance, resulting in increased mitochondrial breakage and fragmentation and increased susceptibility of neurons to cell death.

In mitochondrial fission, Drp1 and fission protein 1 (Fis1) can divide mitochondria by binding to receptors on the OMM through multiple post-translational modifications, including S-nitrosylation, phosphorylation, SUMOylation, dephosphorylation, and ubiquitination (Qin et al., 2021). In CI/RI conditions, an increase in ROS levels disrupts mitochondrial membrane potential and mitochondrial depolarization, resulting in the translocation of Drp1 to the OMM via the recruitment of mitochondrial Fis1, fission factor (MFF) and mitochondrial dynamics proteins of 49/51 kDa (MiD49/MiD51), also known as MIEF1/MIEF2, where it promotes excessive mitochondrial fragmentation by coupling guanosine triphosphate (GTP) hydrolysis (Estaquier and Arnoult, 2007). Drp1-mediated mitochondrial fission is an initial event required for ischemic neuronal cell death (Fonseca et al., 2019). It has been suggested that the proapoptotic B-cell leukemia/lymphoma 2 (Bcl-2) family protein Bax function directly or indirectly as a Drp1 receptor to promote mitochondrial fission and cell death (Montessuit et al., 2010). Liu et al. (2012) found that Drp1 and P-Drp1 upregulation occurred after tMCAO, peaking at 2 and 14 days, respectively, suggesting an increase in mitochondrial fission in I/R condition. *In vitro* and *in vivo* studies shows that the mitochondrial fission inhibition by the Drp1 inhibitor or siRNA had beneficial effects on cerebral ischemia (Grohm et al., 2012; Flippo et al., 2020). Drp1 inhibition may have therapeutic value in treating stroke and neurodegeneration.

Mitochondrial fusion shares the mitochondrial matrix or metabolites such as proteins, mtDNA, or membrane components where the ETC occurs (Anzell et al., 2018). At the same time, damaged mitochondria can be repaired through fusion with healthy mitochondria to integrate contents and promote cell survival by complementation (Liu et al., 2018). Fusion proteins, including optic atrophy 1 (OPA1) and mitofusin 1/2 (MFN1/2), can protect tissues and neurons from death under CI/RI through their pro-fusion function (Dimmer and Scorrano, 2006). MFN1 and MFN2 proteins, which contain two transmembrane domains in the OMM with a GTPase domain, provide energy for OMM fusion by mixing the mitochondrial lipid bilayer. Similarly, OPA1 performs a similar function to enable IMM fusion (El-Hattab et al., 2018). The short form of OPA-1 (S-OPA1) mediates inner mitochondrial membrane fission, while the long form of OPA-1 (L-OPA1) has been reported to protect ischemic injuries by maintaining mitochondrial functions and attenuating neuronal apoptosis (Cipolat et al., 2004). Moreover, elevated levels of MIEFs promote in a manner that is mediated by MFN1/2 and OPA1 but independent of Drp1, and MIEF1/2 can alleviate hFis1-induced mitochondrial fragmentation and contribute to mitochondrial fusion (Yu et al., 2021). In hypoxic situations, CI/RI can impair mitochondrial fusion by decreasing OPA1 or depleting MFN2, thereby undermining intracellular homeostasis and inducing neuronal death (Peng et al., 2018; Wei et al., 2019; Chen Y. et al., 2020). Under I/R conditions, the upregulation of OPA1 expression greatly facilitates mitochondrial fusion, reversing the interconnected mitochondrial morphology and alleviates I/R-induced neuronal apoptosis, thereby reducing infarct volume (Wei et al., 2019). Furthermore, the downregulation of MFN2 aggravated the CI/RI by inhibiting autophagosome formation and the fusion of autophagosomes and lysosomes, demonstrating that MFN2 could ameliorate CI/RI by promoting autophagy (Peng et al., 2018).

Therefore, a delicate dynamic balance between fission and fusion is essential to maintain the structure and function of mitochondria (Li and Liu, 2018; Zhang et al., 2019). Excessive mitochondrial fission or insufficient fusion promotes the decreased ATP production and mtDNA stability, impaired mitochondrial permeability transition pore sensitivity, and cell death (Chen et al., 2010; Zhou et al., 2017; Wei et al., 2019).

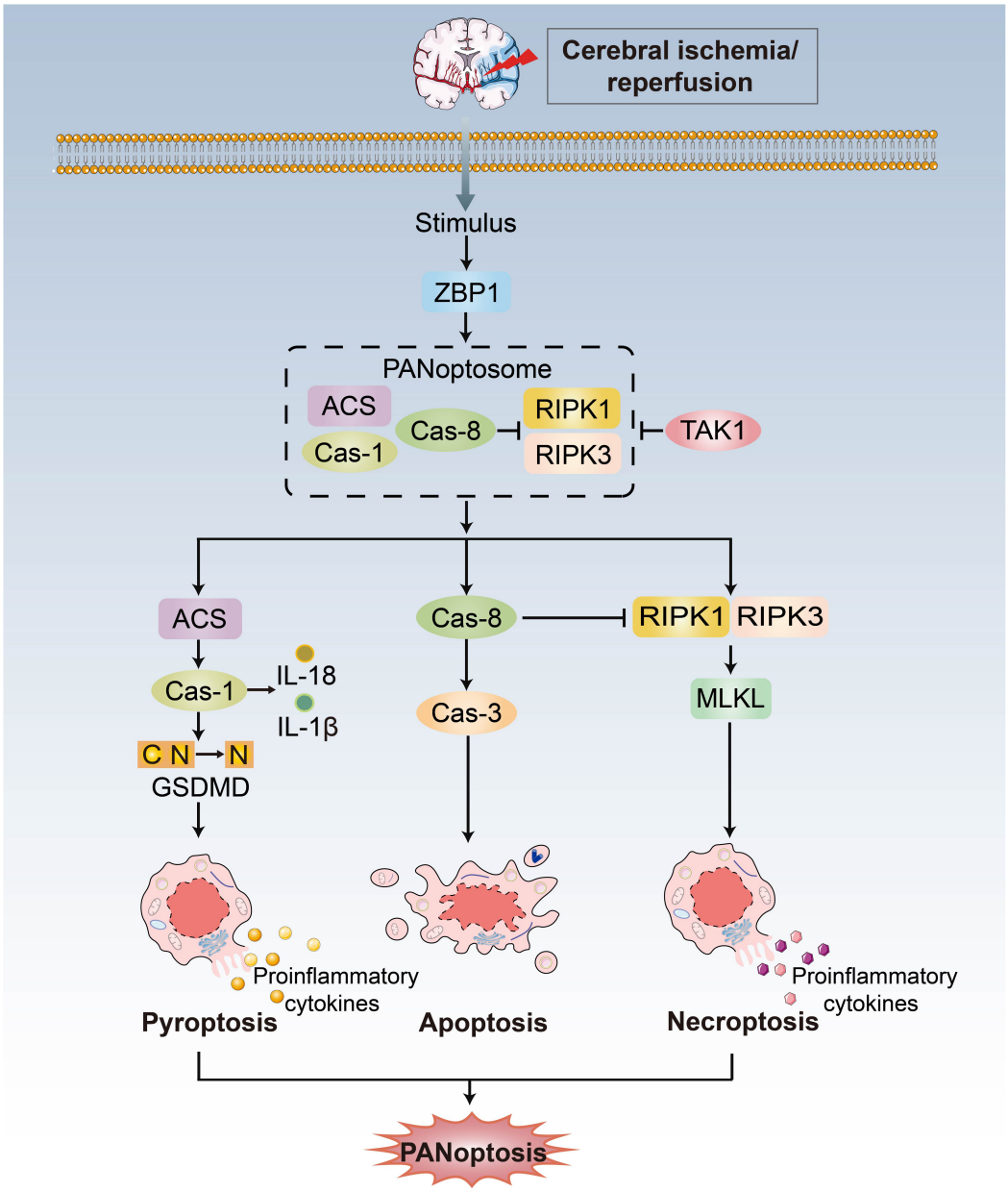

FIGURE 2
PANoptosis pathways. Exposure to stimulus during CI/RI can lead to the initiation of the apical sensors, such as ZBP1, which then induces the activation of proteins involved in pyroptosis, apoptosis, and necroptosis to form the ZBP1-PANoptosome and mediate PANoptosis. Three arms of cell death are executed by GSDMD family proteins (pyoptosis), caspase-3/7/8 (apoptosis) and MLKL (necroptosis). TAK1 could block formation of the PANoptosome and induction of PANoptosis.

2.2.5.3. Mitophagy

Mitochondrial autophagy, also known as mitophagy, is a cellular process that selectively removes the dysfunctional and damaged mitochondria by coordinated mitophagy pathways. Under ROS stress, cell aging, nutritional deprivation, and other conditions, mitochondrial depolarization damage will manifest. To preserve the integrity of the mitochondrial network and restore cellular homeostasis, an autophagy system is activated to encase and degrade dysfunctional mitochondria selectively. This mechanism consists primarily of four steps (Xu et al., 2020): 1) External stimuli dissipate mitochondria and disrupt mitochondrial membrane potential (MMP), which is the prerequisite for mitophagy to occur. 2) Mitochondrial autophagosomes take shape. 3) Mitochondrial autophagosomes are delivered to the lysosome for degradation. 4) Lysosomes degrade mitochondrial contents. In mammalian cells, PINK1/Parkin axis is one of the most studied mitophagy mechanisms. The serine/threonine kinase PINK1 and the E3 ubiquitin ligase Parkin cooperatively sense cellular stress and promote the binding of ubiquitinated proteins to microtubule-associated protein LC3 to form autophagosomes and then initiate the autophagy mechanism (Zhang et al., 2021). Additionally, there are other receptors which can directly bind to LC3 without ubiquitination, thus initiating mitophagy, which mainly includes the Nip3-like protein X (NIX)/BCL2-interacting protein 3-like

(BNIP3L) receptor, BCL2-interacting protein 3 (BNIP3) receptor, FUN14 domain containing 1 (FUNDC1) receptor (Villa et al., 2018; Ma et al., 2020; Poole et al., 2021).

Under physiological conditions, autophagy is capable of removing the abnormally aggregated proteins and degenerated subcellular organelles, while excessive autophagy may result in massive and unnecessary cell death (Wang Y. et al., 2020). After CI/RI, fluorescence results show that PINK1 accumulates on OMM and Parkin translocation occurs in the penumbra of rat cortex, and the levels of other related autophagy proteins such as LC3 and Beclin1 are elevated (Lan et al., 2018). Researchers have found that promoting mitophagy via PINK1/Parkin could decrease the accumulation of damaged mitochondria and ameliorate neuronal injury during CI/RI (Wu X. et al., 2018; Ma et al., 2020; Wang H. et al., 2020; Mao et al., 2022). Wu X. et al. (2021) found that NIX degradation leads to mitophagy deficiency in ischemic brains, indicating that NIX may be a potential therapeutic target for ischemic stroke. Overexpression of FUNDC1 inhibits apoptosis and improves mitochondrial function against CI/RI (Cai et al., 2021). In myocardial ischemia/reperfusion, hypoxic preconditioning could induce FUNDC1-dependent mitophagy to resist ischemia/reperfusion injury (Zhang W. et al., 2017). This indicates that similar mechanisms may exist in CI/RI. The dynamic balance between these three processes of MQC is essential for maintaining mitochondrial homeostasis and function.

3. PANoptosis/ferroptosis in CI/RI

3.1. PANoptosis

Initially, pyroptosis, apoptosis and necroptosis were considered different and independent (Chen X. et al., 2022). The crosstalk between these pathways has therefore led to the establishment of the concept of PANoptosis, defined as an inflammatory PCD pathway with key features of pyroptosis, apoptosis, and necroptosis that cannot be accounted for by any of these three PCDs pathways alone (**Figure 2**; Kuriakose et al., 2016; Kesavardhana et al., 2017; Malireddi et al., 2018, 2019, 2020a). Pathogen- or pharmacologically mediated obstruction of survival signaling acts as a key danger signal to trigger the assembly of PANoptotic cell death complexes (Wang and Kanneganti, 2021). Recent progress has shown that receptor-interacting protein kinase (RIPK)1/RIPK3, Fas-associated protein with a death domain (FADD), caspase-8 and apoptosis-associated speck-like protein containing a caspase recruitment domain (ASC) are the master regulators to form a PANoptosome and then activate PANoptosis (Malireddi et al., 2019), which is equivalent to providing a molecular scaffold that allows engagement of key pyroptotic, apoptotic, and necroptotic machinery (Briard et al., 2021; Chen X. et al., 2022).

Z-DNA-binding protein (ZBP1) acts as an innate immune sensor to activate all three pathways and inflammation that contemporaneously engages key molecules from pyroptosis, apoptosis and necroptosis. Upon sensing stimulus, ZBP1 activation leads to its interaction with RIPK1/RIPK3, FADD and caspase-8 to form cell death signaling scaffolds (Malireddi et al., 2019). Additionally, growth factor beta-activated kinase 1 (TAK1) acts as a master switch for PANoptosis quiescence (Malireddi et al., 2019). TAK1 inhibition/deletion leads to the activation of apoptosis, pyroptosis, and necroptosis (Malireddi et al., 2018, 2020b; Orning et al., 2018; Sarhan et al., 2018). In the absence of external stimuli, TAK1 deficiency causes loss of cellular homeostasis and unleashes inflammatory signaling and PANoptosis (Malireddi et al., 2020b). There are still unanswered questions concerning the mechanistic details of PANoptosis, even though ZBP1 and TAK1 are known as regulators.

3.2. Ferroptosis

Ferroptosis is a distinct PCD type characterized by lipid peroxidation relying on ROS generation and severe iron overload (Yang and Stockwell, 2008; Dixon et al., 2012). This pathway is essential in neuronal cell death (Lu et al., 2017; Wu J. R. et al., 2018). Morphologically, ferroptosis causes reduction or vanishing of mitochondria crista, condensed mitochondrial membrane densities, and OMM rupture (Xie et al., 2016; Wang H. et al., 2020), a unique feature that is distinguishable from other forms of cell death (Dixon et al., 2012). Emerging evidence suggests that stroke is associated with iron buildup, lipid peroxidation, and a reduction of glutathione (GSH) and glutathione peroxidase 4. (GPX4). In neurons, GPX4 can inhibit excessive lipid peroxidation. Hence GPX4 activity inhibition triggers ferroptosis (Gaschler et al., 2018; Ingold et al., 2018; Kang et al., 2018). The lethal metabolic imbalance resulting from GSH depletion or inactivation of GPX4 is the executor of ferroptosis within the neural cell (Stockwell et al., 2017). The injury of the cystine/glutamate antiporter system (system Xc-), which consists of solute carrier family 3 member 2 (SLC3A2) and solute carrier family 7 member 11 (SLC7A11), lessens GSH production and GPX4 activation, resulting in lipid peroxidation of polyunsaturated fatty acids (PUFAs) and the accumulation of PUFAs-O-OH that can form lipid ROS. In contrast, Fe^{2+} ions are present in large quantities, which bind to PUFAs-O-OH and then initiate lipid ROS by the Fenton reaction, leading to iron death and neuronal damage (Cao and Dixon, 2016; Yang et al., 2016; Yang and Stockwell, 2016). PANoptosis and ferroptosis differ in morphological characteristics, signaling pathways, inhibitors/key regulators, and mitochondrial association (**Table 1**).

3.3. PANoptosis in CI/RI

The recent progress in understanding of the extensive crosstalk between different PCDs and signaling cascades unequivocally establishes the existence of multifaceted signaling platforms. It is well established that pyroptosis, apoptosis, and necroptosis occur simultaneously during CI/RI in diverse passage cell lines or primary neurons. Moreover, PANoptosis can contribute to neuroinflammation, which has widespread repercussions on the body. Since the components of the PANoptosome are widely implicated in neurological disorders, an improved understanding of the molecular underpinnings of the PANoptosis will be able to inform the development of new and improved therapeutic strategies (Malireddi et al., 2020b).

There are many central nervous systems (CNS) diseases characterized PANoptosis (Yuan and Yankner, 2000;

McKenzie et al., 2020; Yan et al., 2021), which is generally associated with inflammatory reactions (Pender and Rist, 2001; Degterev et al., 2019; Lünemann et al., 2021). The inflammasome (Friedlander et al., 1997), caspase-8 (Krajewska et al., 2011), RIPK1 (Xu et al., 2018; Degterev et al., 2019) and other core components of the PANoptosome, are implicated in neuronal death (Fricker et al., 2018). Inflammation and immune system activation are often involved in the CI/RI pathophysiology, which can cause serious brain damage (Chamorro et al., 2016; Lambertsen et al., 2019; Shi et al., 2019; Zhang F. et al., 2022). In the existing studies of PANoptosis, the expression of cell death and the pathophysiological mechanism related to inflammation in IS are similar to the phenotype and mechanism, which provides basic evidence for the possible existence of PANoptosis and PANoptosomes (Yan et al., 2022). Otherwise, glial cells have been reported to interfere with these three forms of cell death after being stimulated by injury (Zhao et al., 2017; Xu et al., 2019; Naito et al., 2020; Liu X. et al., 2022), which overlaps with the inflammation-related and immune-related reports of existing studies of PANoptosis (Yan et al., 2022). Moreover, studies have shown that some molecules can simultaneously interfere with two PANoptosis components under CI/RI. RIPK3, as the key molecule of necroptosis, can interact with the Jun N-terminal kinase-mediated inflammatory signaling pathway, which is closely related to neuronal apoptosis (Hu et al., 2020). Blocking of thromboxane A synthase/thromboxane A2/thromboxane prostanoid signal can inhibit apoptosis and pyroptosis concurrently (Chueh et al., 2020). Moreover, the nucleotide oligomerization domain-like receptors with caspase activation and recruitment domain 4 (NLRC4) inflammasome complex can simultaneously regulate apoptosis and pyroptosis (Poh et al., 2019). Hence, PANoptosis induced by CI/RI could be regulated and intervened simultaneously.

Although there is no study on the PANoptosome in CI/RI, the existing data of the components that make up a PANoptosome are highly expressed in the brain. Studies have shown that inhibiting TAK1 can reduce neuronal death induced by CI/RI (Neubert et al., 2011; Wang L. et al., 2019; Wu et al., 2020). Additionally, TAK1 affects the microglia's function and interacts with an inflammatory pathway to activate neuronal apoptosis and pyroptosis (Gong et al., 2015; Zeyen et al., 2020). Furthermore, it is vital in the interaction between necroptosis and apoptosis of neurons during CI/RI (Naito et al., 2020). All these findings show that molecules like TAK1 may regulate PANoptosomes in CI/RI.

3.4. Ferroptosis in CI/RI

There is considerable evidence that ferroptosis plays a significant role in CI/RI pathogenesis. Research indicates that ferroptosis occurs mainly in neurons and exacerbates CI/RI (Guan et al., 2019; Yuan et al., 2021; Liu W. et al., 2022). The CI/RI pathogenesis results in increased vulnerability to oxidative stress and ATP production, which is impeded to maintaining metabolic activity and the activity of system Xc-. Meanwhile, neuronal membranes are rich in PUFAs, which are easy to lipid hydroperoxides and induce ferroptosis (Conrad and Pratt, 2019).

Moreover, under CI/RI conditions, iron accumulation in affected brain areas is the key mediator of neuronal damage and death (Castellanos et al., 2002). Iron chelation therapy, such as deferoxamine, has been shown to attenuate the cellular damage observed in the brains of experimental I/RI animal models (Prass et al., 2002; Hanson et al., 2009). Another study demonstrates that ferroptosis inhibition by GPX4 provides protective mechanisms against neurodegeneration (Zou and Schreiber, 2020; Li et al., 2022). Alim et al. (2019) reported that pharmacological selenium could augment GPX4 expression, which inhibits ferroptosis and protect neurons from CI/RI in C57BL/6 mice. Furthermore, dihydromyricetin (DHM) represses ferroptosis by SPHK1/mTOR signaling pathway inhibition, thereby alleviating CI/RI, suggesting that DHM may be a candidate drug for CI/RI treatment (Xie J. et al., 2022). Additionally, CI/RI-related neuronal damage can be rescued by ferroptosis inhibitors such as liprostatin-1 and ferrostatin-1, strongly suggesting a direct involvement of ferroptosis in CI/RI (Tuo et al., 2017). Primarily, additional research into the involvement of ferroptosis in CI/RI is required. Ferroptosis is the primary cause and a potential treatment for IS and other cerebrovascular disorders.

4. Mitochondrial dysfunctions in cell death

4.1. Mitochondrial dysfunctions and pyroptosis

Mitochondrial ROS (mtROS) has long been considered a key signaling molecule for pyroptosis since it promotes the efficiency of the GSDMD (Gasdermin D) cleavage by caspase-1 (Wang C. et al., 2019). Active GSDMD forms pore permeabilizes, leading to pyroptosis. In turn, active GSDMD and inflammasome can cause MOMP (mitochondrial outer membrane permeabilization), which induces mitochondrial dysfunctions and forms extensive crosstalk between pyroptosis and mitochondrial apoptosis (Rogers et al., 2019; Tsuchiya et al., 2019). Additionally, Yeon et al. (2017) showed that phospholipid oxidation and accumulation of oxidized phosphatidylcholine during cell injury could induce the production of mtROS, which then activates the NLRP3 inflammasome. The mtROS, mitochondrial Ca^{2+} and mitochondrial destabilization can induce NLRP3 inflammasome activation and activate pyroptosis (Yeon et al., 2017; Yu et al., 2019). Suppression of mitochondrial mitophagy also slows the pyroptosis progression (Yu et al., 2019).

4.2. Mitochondrial dysfunctions and apoptosis

Mitochondria are key factors in triggering apoptosis. The intrinsic pathway is related to mitochondria (Wei et al., 2001). Upon induction of mitochondrial apoptosis effectors, MOMP is driven by pro–apoptotic members of the BCL–2 family of proteins (prominently BAX and BAK). Activation of the pro–apoptotic effectors BAX and BAK are usually essential for MOMP and cell death (Wei et al., 2001). Under normal conditions, inactive BAX localizes to the cytoplasm and inactive BAK to the mitochondria. Once activated, they can directly bond to a subclass of BH3–only

TABLE 1 Hallmarks of four types of programmed cell death (PCD).

	Pyroptosis	Apoptosis	Necroptosis	Ferroptosis
Morphological changes	Cellular swelling, membrane rupture, and cellular contents flowing out	Wrinkled cells, nuclear condensation, cell membrane ectropion, and apoptotic body formation	Cell enlargement, cellular swelling, and membrane rupture	Shrunken mitochondria, mitochondrial membrane condensation, mitochondria crista reduction, and outer mitochondrial membrane rupture, and mitochondria fragment
Signaling pathway	Pyroptosis pathway: caspase1-dependent pyroptosis and caspase1-independent pyroptosis	Apoptosis pathway: extrinsic pathway (receptor-mediated) and intrinsic pathway (mitochondria-mediated); p53-mediated apoptosis pathway	Necroptosis pathway and TNF pathway	Ferroptosis pathway and p53 pathway
Inhibitors	VX765 (Chen Y. et al., 2022)	Z-VAD FMK (Yu et al., 2022)	Necrostatin-1 (Dong et al., 2022)	Ferrostatin-1 (Liu et al., 2020c), liproxstatin-1 (Fan et al., 2021), DFO (Shen et al., 2022)
Key regulators	GSDMD, caspase-1/4/5/11, IL-1β, and IL-18	Fas/TNFR/TRAILR, caspase-3/8/9, Bax/Bcl-2, Cyt C, and APAF-1	RIP1, RIP3, MLKL, and Fas/TNFR	GPX4, JAK, SLC7A11, ACSL4, FPN, p53, and NADPH oxidase
Mitochondrial dysfunction	ROS and Ca^{2+} overload	Cyt C releases, BAX/BAK, and Bcl family protein interact	ROS burst, Drp1 activation, and mitochondrial fisson	Mitochondrial lipid peroxidation and Ca^{2+} overload

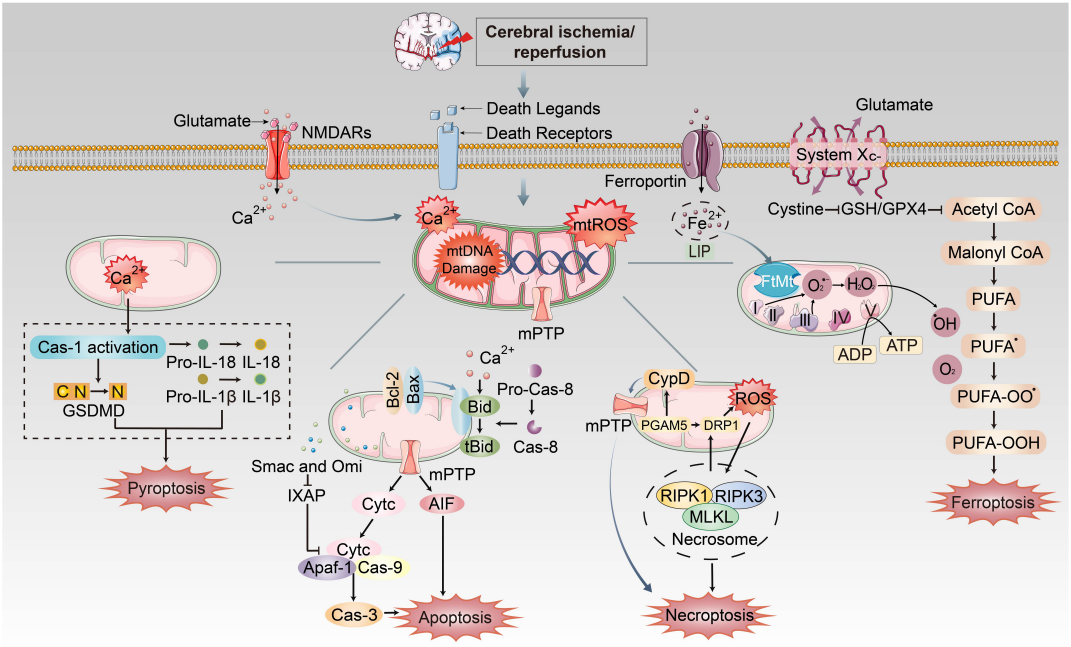

FIGURE 3
The mechanism of mitochondrial dysfunctions induced PANoptosis and ferroptosis during CI/RI. Mitochondria play essential roles in pathological conditions after ischemic stroke and reperfusion. During ischemia, oxygen–glucose deprivation will cause ATP consumption and the bind of death ligands to death receptors on the membrane. Na^+/K^+ ATPase pump failure that induces depolarization of neuronal membranes and extreme release of glutamate, burst of ROS, free radical damage, Ca^{2+} homeostasis disorder and EAA toxicity, etc. Iron was released into the brain parenchyma, which accelerates lipid ROS accumulation and ferroptosis via Fenton reaction. The extracellular death ligands bind to death receptors, which triggers the recruitment of FADD or TRADD to induce apoptosis and necroptosis, respectively. These mechanisms cause mitochondrial dysfunctions such as formation of mPTP, burst of mtROS, mitochondrial Ca^{2+} overload and mtDNA damage, which could execute different cell death pathways.

proteins like tBID (truncated active BID) (Letai et al., 2002), and BAX will accumulate in the mitochondria (Edlich et al., 2011; Schellenberg et al., 2013; Todt et al., 2015). BAX/BAK commits the release of soluble proteins-Cyt C, which activates the downstream caspase cascade (Wei et al., 2001).

Most Cyt C resides within mitochondrial cristae and is regulated by cristae junctions (van der Laan et al., 2016). Mitochondria, the dynamic organelles, can constantly undergo fission cycles and fusion by mitochondrial fission protein Drp1 (Frank et al., 2001; Bhola et al., 2009) to remodel mitochondrial cristae, which has been proposed to facilitate Cyt C release. Mdivi-1 is a Drp1 inhibitor that prevents mitochondria division and Bax-mediated MOMP during apoptosis (Tanaka and Youle, 2008; Nhu et al., 2021). Cyt C also induces tumor gene p53. Recent investigations show that the p53 protein can defect MOMP by forming an inhibitory complex with the Bcl-2 family protein, leading to Cyt C release (Bakthavachalam and Shanmugam, 2017). Meanwhile, MOMP causes the release of proteins, including the second mitochondria-derived activator of caspase (SMAC) and OMI/HTRA2 that block the caspase-7/9 inhibitor X-linked inhibitor of apoptosis protein (XIAP), facilitating apoptosis

TABLE 2 Therapeutic strategy by targeting mitochondrial dysfunctions to inhibit cerebral ischemia/reperfusion injury (CI/RI).

Cell deaths	Interventions	Model	Subjects	Mitochondrial associated targets	Functions	References
Pyroptosis	Idebenone	OGD/R and tMCAO	PC12 cells, BV2 cells, and rat	mtDNA and mtROS	Idebenone suppresses activation of NLRP3 and ameliorates NLRP3-mediating damage in I/R.	Peng et al., 2020
	Medioresinol	OGD, tMCAO	bEnd.3 cells, BMVECs, and mice	mtROS	MDN decreases mtROS through PPARα/GOT1 axis and ameliorate the pyroptosis and ischemic brain injury.	Wang Y. et al., 2021
	Umbelliferone	MCAO/R	Rat	ROS/TXNIP	UMB protects focal cerebral ischemic through the inhibition of TXNIP/NLRP3 inflammasome and activation of PPAR-γ.	Wang et al., 2015
Apoptosis	miR-668 inhibitor	tMCAO/R	Rat	Drp1, mtROS, Bax/Bcl-2	The miR-668 inhibitor prevents neuronal apoptosis in CI/RI by modulating mitochondrial function and regulating NLRP3 signaling.	He and Zhang, 2020
	Candesartan	OGD/R	PC12 cells	Bax	Candesartan inhibits apoptosis by downregulation of Bax and cleaved caspase-3 in OGD/R-PC12 cells.	Ding et al., 2022
	Edaravone dexborneol	Four-vessel occlusion (4-VO)	Rat	Bax/Bcl-2	Edaravone-Dexborneol alleviates cerebral ischemic injury via reduction of apoptosis and neuron damage.	Zhang W. et al., 2022
	Tong-Qiao-Huo-Xue-Decoction formula	MCAO	Rat	Bax/Bcl-2	TQHXD protects neurons from I/R damage and prevents apoptosis.	Yuan et al., 2022
	CsA	BBCAO/R	Rat	Bax/Bcl-2	CsA decreases Bax/Bcl-2 ratio as well as caspase-3 activation.	Fakharnia et al., 2017
Necroptosis	CsA	BBCAO/R	Rat	mPTP	CsA inhibits mPTP opening and reduces RIP1 and RIP3 levels.	Fakharnia et al., 2017
	Infliximab	tMCAO	Rat	Mitochondrial membrane potential	Infliximab ameliorates endothelial necroptosis and reduces mitochondrial damage, cytoplasm transparency, and BBB permeability.	Chen et al., 2019
	rhTrx-1	MCAO	C57BL/6 mice	Mitochondrial membrane potential	rhTrx-1 provides neuroprotection in IS-induced microglial neuroinflammation by inhibiting RIPK1 expression	Jiao et al., 2020
Ferroptosis	UBIAD1	MCAO/R, OGD/R	Rat, primary neurons	Mitochondrial protein complexes	UBIAD1 modulates I/R-mediated ferroptosis by restoring mitochondrial dysfunctions and enhances antioxidative capacities.	Huang et al., 2022
	FtMt	MCAO/R	Mice	FtMt	FtMt protects against CI/RI-induced ferroptosis.	Wang P. et al., 2021
	Ferrostatin-1	t-BHP treatment	PC12 cells	Mitochondrial membrane potential, ATP production, and mtROS	Ferrostatin-1 reverses ferroptosis-induced mitochondrial dysfunctions	Wu C. et al., 2018

(Bock and Tait, 2020). Even in the absence of caspase activity, cells usually die following BAX/BAK-dependent MOMP, which releases mtDNA by mitochondrial inner membrane permeabilization (MIMP) and then activates cGAS-STING signaling during apoptosis (Riley et al., 2018). Elevated levels of mtROS also induces cell oxidative stress and destroy the cellular structure and MOMP. ROS are involved in both caspase-dependent and caspase-independent pathways, which is an important bridge between these two apoptosis types (Chen C. et al., 2020). The extrinsic pathway is activated at the plasma membrane by death receptor ligands binding to their related receptors, interacting with the pro-caspase-8 and forming a death-induced signaling complex (DISC), leading to activation of caspase-8 and activate pro-caspase-3/7. Caspase-8 is the crosstalk to the mitochondrial pathway (Datta et al., 2020).

4.3. Mitochondrial dysfunctions and necroptosis

Necroptosis is morphologically characterized by electron-lucent cytoplasm, cell swelling, shrinking of organelles, cell membrane rupture, dilation of the perinuclear space and spilling of intracellular damage-associated molecular patterns (DAMPs) out of the cell (Kaczmarek et al., 2013), which can trigger an inflammatory response (Chen et al., 2019; Miyake et al., 2020). RIPK1-RIPK3-MLKL necrosome is essential in necroptosis through mitochondria (Zhe-Wei et al., 2018; Zhou et al., 2018).

TNF-α (tissue necrosis factor-alpha) binds to TNFR on cell surface and transmits death signals via RIPK1 and RIPK3, forming RIPK1-RIPK3-MLKL necrosome. RIPK3 and MLKL

phosphorylation upregulate phosphoglycerate mutase family member 5 (PGAM5) expression on the mitochondrial membrane. PGAM5 can increase CypD phosphorylation, which obligated endothelial cells to undergo necroptosis by augmenting mPTP opening. Blocking the RIPK3-PGAM5-CypD signal pathways can suppress mPTP opening and interrupt necroptosis (Zhou et al., 2018). PGAM5 enters the cytoplasm to collaborate with Drp1 (Feng et al., 2020), which inhibits glutathione production and disrupts mitochondrial metabolism, leading to reduced free radical removal capacity and increased mtROS (Wang et al., 2012; Zhou et al., 2018; Xiao et al., 2020). Moreover, the necrosome can also affect metabolic enzymes glutamate dehydrogenase 1 (GLUD1), glycogen phosphorylase (PYGL), and pyruvate dehydrogenase (PDH) to promote the production of mtROS (Zhang et al., 2009; Han et al., 2018; Yang et al., 2018; Zhao et al., 2021). In turn, the released mtROS can facilitate the RIPK1 autophosphorylation and RIPK3 recruitment, which are critical for necroptosis (Schenk and Fulda, 2015; Zhang Y. et al., 2017).

4.4. Mitochondrial dysfunctions and ferroptosis

Ferroptosis is characterized morphologically by abnormal mitochondrial architecture, including mitochondrial fragmentation, shrunken mitochondria, rupture of OMM and vanished mitochondrial cristae (Xie et al., 2016; Miyake et al., 2020; Wang H. et al., 2020). Abnormal mitochondrial architecture, including mitochondrial fragmentation, shrunken mitochondria and rupture of the mitochondrial outer membrane, and vanished mitochondrial cristae, is regarded as the typical morphological characteristic of ferroptosis.

Currently, whether mitochondria have an impact on ferroptosis remains a controversial research topic. Furthermore, recent nervous system studies have revealed that the burst of lethal mtROS and the accumulation of lipid peroxidation products affect proteins related to iron metabolism in the mitochondrial membrane, which is the main reason to mediate ferroptosis in neurons (Gao and Chang, 2014; Xie et al., 2016; Liu et al., 2020a,b). Meanwhile, iron overload, one of the mechanisms of ferroptosis, has been shown to trigger mPTP opening and necroptosis by ROS accumulation (Tian et al., 2020).

Mitochondria are vital in ferroptosis induced by the lack of cysteine. Cysteine deprivation induces the decomposition of glutamine (Gln), a non-essential amino acid that serves as the major respiratory fuel for energy production and lipid biosynthesis. Gln drives the hyperpolarization of MMP and feeds the tricarboxylic acid (TCA) cycle (Gao et al., 2019), thereby increasing mitochondrial respiration by ETC in consequence, augmenting levels of mitochondrial ROS to initiate the Fenton reaction (Gao et al., 2019; Bock and Tait, 2020). Additionally, increased mtROS induced by Gln facilitates the overload of mitochondrial Ca^{2+} (Maher et al., 2018) and the mPTP opening, causing dissipation of the mitochondrial transmembrane potential and subsequent ATP depletion (Bernardi and Di Lisa, 2015; Ying and Padanilam, 2016; Novgorodov et al., 2018). Furthermore, the mitochondrial VDACs were proved to be a potential target of erastin by decreasing $\Delta\Psi m$ (Yagoda et al., 2007). Opening VDACs leads to an increase in MMP, and then mtROS generates (Yagoda et al., 2007; DeHart et al., 2018). Mitochondrial ferritin (FtMt), an iron-storage protein, has been reported to protect mitochondria from iron-induced oxidative damage, presumably through the chelation of potentially harmful excess free iron (Nie et al., 2005; Gao and Chang, 2014). It also participates in the regulation of iron distribution between cytosol and mitochondrial contents. FtMt has been shown to significantly inhibit the cellular labile iron pool (LIP) level, ROS and subsequent ferroptosis by the Fenton reaction (Yarmohammadi et al., 2021; Boag et al., 2022).

During CI/RI, mitochondrial dysfunctions play essential roles in pathological conditions in PANoptosis and ferroptosis, as previously stated (**Figure 3**). The mtROS burst, mtDNA defects, mPTP formation, mitochondrial Ca^{2+} overload and iron dyshomeostasis are central parts of cell death. It has been demonstrated that mitochondrial dysfunctions are closely associated with various PCDs in the pathophysiological process of CI/RI, and therefore the rational use of these mechanisms in the biomedical field to address mitochondria as the target for drug development and therapeutic strategies to ameliorate PCD in IS could be a promising option.

5. Therapeutical potential of targeting the mitochondrial dysfunctions against CI/RI in ischemic encephalopathy

Mitochondrial dysfunctions are the main feature seen during the initiation of stroke pathophysiology. Consequently, targeting mitochondria dysfunctions represents a promising strategy to attenuate CI/RI-induced diseases (Carinci et al., 2021). Interventions that directly target mitochondrial dysfunctions by alleviating different cell death during CI/RI are summarized in the present review (**Table 2**).

Idebenone is a well-appreciated mitochondrial protectant in cerebral ischemia and reperfusion. Peng et al. (2020) found that mitochondrial dysfunctions in OGD/R leads to accumulation of oxidized mtDNA and mtROS generation, dramatically augments inflammation in BV2 and PC12 cells. Idebenone inhibits the process and attenuates cerebral inflammatory injury in ischemia and reperfusion by dampening NLRP3 inflammasome activity. MicroRNAs (miRNAs) are a group of small non-coding RNA molecules that regulate gene expression at the post-transcriptional level. The miR-668 expression level has been reported to be altered under ischemic conditions in cell culture and animal models (Chun et al., 2018). The miR-668 inhibition prevents neuronal apoptosis in CI/RI by modulating mitochondrial functions such as reduction of Drp1 and melioration of the expression of Bax/Bcl-2 protein (He and Zhang, 2020). CypD is a prominent mediator of mPTP, which leads to mitochondrial swelling and dissipation of MMP on necroptosis, autophagy, and apoptosis beyond CI/RI. Cyclosporine-A (CsA) is a potent inhibitor of CypD. Fakharnia et al. (2017) found that CsA reduces necroptosis markers, RIP1 and RIP3. Furthermore, the Bax/Bcl-2 ratio and caspase-3 activation, as the executioner of apoptosis, noticeably decreases by CsA pretreatment (Fakharnia et al., 2017). It suggests that CsA-mediated CypD inhibition may provide a promising therapeutic potential

for protecting against CI/RI-mediated mitochondrial dysfunctions. UBIAD1 is a newly identified antioxidant enzyme that acts on the Golgi apparatus membrane and mitochondria (Nakagawa et al., 2010; Mugoni et al., 2013). Upregulated UBIAD1 protects against brain tissue damage and neuronal death by rescuing the morphology and bio functions of the mitochondria and Golgi apparatus in CI/RI, thus alleviating I/R-mediated lipid peroxidation and ferroptosis (Huang et al., 2022). Moreover, the rescue of impaired mitochondrial as a possible mechanism of regulating ferroptosis neuronal death is a potential treatment strategy for IS. FtMt is a key mitochondrial iron storage protein that protects cells from iron-dependent oxidative damage rather than being directly related to cellular iron levels (Nie et al., 2005). Mice lacking FtMt experience more severe brain damage and neurological deficits, accompanied by typical molecular features of ferroptosis after CI/RI. Conversely, FtMt overexpression reverses these changes, which limits CI/RI-induced iron overload and iron-dependent lipid peroxidation and suppresses ferroptosis in the penumbra (Wang P. et al., 2021). FtMt may be a potential therapeutic target in ischemic stroke.

In conclusion, we have discussed the therapeutic potential of targeting mitochondrial dysfunctions on PCDs in IS or CI/RI and the associated mechanisms. New therapeutic strategies that target mitochondrial dysfunctions may be used to mitigate the devastating effects of CI/RI.

6. Conclusion and perspective

As stated above, mitochondrial dysfunctions highlight the essential role of cell death during CI/RI, providing us with a more comprehensive and profound understanding of pathogenesis of which is associated with mitochondrial oxidative stress, Ca^{2+} overload, iron dyshomeostasis, mtDNA defects and MQC disruption, eventually triggering programmed cell deaths (Giorgi et al., 2018). Emerging researches have indicated that mitochondrial molecules such as mPTP, FtMt, proteins of MQC, Bax/Bcl-2 might be the crosstalk between mitochondrial dysfunctions and PCD pathways. These markers have diagnostic or prognostic values for patients with IS.

Furthermore, the study of mitochondrial dysfunctions is conducive to developing potential molecular therapeutic strategies that target CI/RI. The natural inhibitors or small molecules modifying mitochondrial dysfunctions are of high efficacy for the treatment and prevention of the cell death pathways (Egawa et al., 2017). For example, CsA, a potent inhibitor of CypD and mPTP, could decrease Bax/Bcl-2 ratio as well as caspase-3 activation for apoptosis intervention, while it also reduces RIP1 and RIP3 levels to suppress necroptosis (Fakharnia et al., 2017). Currently, stem cells have shown the ability to transfer mitochondria to the injured cells, which helps to protect mitochondria and revive cell energetics (Sarmah et al., 2018). Additionally, traditional Chinese medicine (TCM) acts as a promising candidate in breaking the vicious cycle between mitochondrial dysfunctions and PCD pathways, improving the quality of life of the stroke patients. It provides a multiple-target approach rather than a single-target approach and thus can target multiple pathways involved in CI/RI at once. Taken together, further studies targeting mitochondrial dysfunctions will provide novel opportunities for the treatment of IS.

However, some limitations exist in the current studies. Firstly, the molecular mechanisms underlying mitochondria-targeted cell death pathways has not been fully elucidated. Secondly, under different pathological injury states of IS, the role of mitochondria is dissimilar. Additionally, the activation of molecular executioner signatures of pyroptosis, apoptosis, necroptosis, and ferroptosis are not required simultaneously in an individual cell for a cell death process to fit (Gullett et al., 2022), which remains optimal time window of intervention unclear. Thirdly, current studies might be limited by the lack of clinical tests to assess the status of mitochondrial dysfunctions. Besides, other clinical biomarkers have poor sensitivity and specificity to predict the outcome of CI/RI.

Consequently, further studies are recommended to develop novel and targeted mechanisms centered on the mitochondrial dysfunctions to improve prognosis in patients with CI/RI. Genome, transcriptome, proteome, epigenome sequencing techniques and radiomics can identify the molecular heterogeneity that reveals the crosstalk between mitochondrial dysfunctions and PCDs in a patient-specific manner. Meanwhile, investigating the expression of PCDs markers as well as mitochondrial morphological changes and dysfunctions at different phases of functional recovery after CI/RI can provide valuable insights into best time-window of treatment for CI/RI. Furthermore, we anticipate that in clinical trials, combining ultrasound, CT, serum markers and other technologies can effectively improve the diagnostic accuracy of mitochondrial dysfunctions in the early stage, and guide the clinical treatment. We hold the view that the in-depth study of mitochondrial dysfunctions-induced PANoptosis and ferroptosis would provide new perspectives, potential therapeutic targets for ischemic stroke and other ischemia-induced diseases of CNS.

Author contributions

ZM and JG conceived and supervised the work and revised the manuscript. RS drafted the initial manuscript. DL, JL, and GW provided some positive suggestions and amended the manuscript. All authors contributed to manuscript revision, read, and approved the submitted version.

Funding

This work was supported from the National Natural Science Foundation of China (82174167), the Key Project of Hunan Province Education Department (20A366), the Project of Natural Science Foundation of Hunan Province (2021JJ30499), and the Fund for Youth Top Talent Project of Hubei Provincial Health and Family Planning Commission (EWT-2019-48).

Conflict of interest

The authors declare that the research was conducted in the absence of any commercial or financial relationships that could be construed as a potential conflict of interest.

Publisher's note

References

Alexeyev, M., Shokolenko, I., Wilson, G., and LeDoux, S. (2013). The maintenance of mitochondrial DNA integrity–critical analysis and update. *Cold Spring Harb. Perspect. Biol.* 5:a012641. doi: 10.1101/cshperspect.a012641

Alim, I., Caulfield, J. T., Chen, Y., Swarup, V., Geschwind, D. H., Ivanova, E., et al. (2019). Selenium drives a transcriptional adaptive program to block ferroptosis and treat stroke. *Cell* 177, 1262–1279.e25. doi: 10.1016/j.cell.2019.03.032

Andrabi, S. S., Parvez, S., and Tabassum, H. (2020). Ischemic stroke and mitochondria: mechanisms and targets. *Protoplasma* 257, 335–343. doi: 10.1007/s00709-019-01439-2

Anzell, A. R., Maizy, R., Przyklenk, K., and Sanderson, T. H. (2018). Mitochondrial quality control and disease: insights into ischemia-reperfusion injury. *Mol. Neurobiol.* 55, 2547–2564. doi: 10.1007/s12035-017-0503-9

Bakthavachalam, P., and Shanmugam, P. (2017). Mitochondrial dysfunction - Silent killer in cerebral ischemia. *J. Neurol. Sci.* 375, 417–423. doi: 10.1016/j.jns.2017.02.043

Bernal-Tirapo, J., Bayo Jiménez, M. T., Yuste-García, P., Cordova, I., Peñas, A., García-Borda, F. J., et al. (2023). Evaluation of mitochondrial function in blood samples shows distinct patterns in subjects with thyroid carcinoma from those with Hyperplasia. *Int. J. Mol. Sci.* 24:6543. doi: 10.3390/ijms24076453

Bernardi, P., Carraro, M., and Lippe, G. (2022). The mitochondrial permeability transition: recent progress and open questions. *FEBS J.* 289, 7051–7074. doi: 10.1111/febs.16254

Bernardi, P., and Di Lisa, F. (2015). The mitochondrial permeability transition pore: molecular nature and role as a target in cardioprotection. *J. Mol. Cell. Cardiol.* 78, 100–106. doi: 10.1016/j.yjmcc.2014.09.023

Bhola, P. D., Mattheyses, A. L., and Simon, S. M. (2009). Spatial and temporal dynamics of mitochondrial membrane permeability waves during apoptosis. *Biophys. J.* 97, 2222–2231. doi: 10.1016/j.bpj.2009.07.056

Boag, M. K., Roberts, A., Uversky, V. N., Ma, L., Richardson, D. R., and Pountney, D. L. (2022). Ferritinophagy and α-Synuclein: pharmacological targeting of autophagy to restore iron regulation in Parkinson's disease. *Int. J. Mol. Sci.* 23:2378. doi: 10.3390/ijms23042378

Bock, F. J., and Tait, S. (2020). Mitochondria as multifaceted regulators of cell death. *Nat. Rev. Mol. Cell Biol.* 21, 85–100. doi: 10.1038/s41580-019-0173-8

Borutaite, V. (2010). Mitochondria as decision-makers in cell death. *Environ. Mol. Mutagen.* 51, 406–416. doi: 10.1002/em.20564

Briard, B., Malireddi, R., and Kanneganti, T. D. (2021). Role of inflammasomes/pyroptosis and PANoptosis during fungal infection. *PLoS Pathog.* 17:e1009358. doi: 10.1371/journal.ppat.1009358

Briston, T., Roberts, M., Lewis, S., Powney, B., Staddon, M. J., Szabadkai, G., et al. (2017). Mitochondrial permeability transition pore: sensitivity to opening and mechanistic dependence on substrate availability. *Sci. Rep.* 7:10492. doi: 10.1038/s41598-017-10673-8

Cadenas, E., and Davies, K. J. (2000). Mitochondrial free radical generation, oxidative stress, and aging. *Free Radic. Biol. Med.* 29, 222–230. doi: 10.1016/s0891-5849(00)00317-8

Cai, Y., Yang, E., Yao, X., Zhang, X., Wang, Q., Wang, Y., et al. (2021). FUNDC1-dependent mitophagy induced by tPA protects neurons against cerebral ischemia-reperfusion injury. *Redox Biol.* 38:101792. doi: 10.1016/j.redox.2020.101792

Cao, J. Y., and Dixon, S. J. (2016). Mechanisms of ferroptosis. *Cell. Mol. Life Sci.* 73, 2195–2209. doi: 10.1007/s00018-016-2194-1

Carinci, M., Vezzani, B., Patergnani, S., Ludewig, P., Lessmann, K., Magnus, T., et al. (2021). Different roles of mitochondria in cell death and inflammation: focusing on mitochondrial quality control in ischemic stroke and reperfusion. *Biomedicines* 9:169. doi: 10.3390/biomedicines9020169

Castellanos, M., Puig, N., Carbonell, T., Castillo, J., Martinez, J., Rama, R., et al. (2002). Iron intake increases infarct volume after permanent middle cerebral artery occlusion in rats. *Brain Res.* 952, 1–6. doi: 10.1016/s0006-8993(02)03179-7

Chamorro, Á, Dirnagl, U., Urra, X., and Planas, A. M. (2016). Neuroprotection in acute stroke: targeting excitotoxicity, oxidative and nitrosative stress, and inflammation. *Lancet Neurol.* 15, 869–881. doi: 10.1016/S1474-4422(16)00114-9

Chen, A. Q., Fang, Z., Chen, X. L., Yang, S., Zhou, Y. F., Mao, L., et al. (2019). Microglia-derived TNF-α mediates endothelial necroptosis aggravating blood brain-barrier disruption after ischemic stroke. *Cell Death Dis.* 10:487. doi: 10.1038/s41419-019-1716-9

Chen, C., Zhang, J., Guo, Z., Shi, X., Zhang, Y., Zhang, L., et al. (2020). Effect of oxidative stress on AIF-mediated apoptosis and bovine muscle tenderness during postmortem aging. *J. Food Sci.* 85, 77–85. doi: 10.1111/1750-3841.14969

Chen, H., Hu, C. J., He, Y. Y., Yang, D. I., Xu, J., and Hsu, C. Y. (2001). Reduction and restoration of mitochondrial dna content after focal cerebral ischemia/reperfusion. *Stroke* 32, 2382–2387. doi: 10.1161/hs1001.097099

Chen, H., Vermulst, M., Wang, Y. E., Chomyn, A., Prolla, T. A., McCaffery, J. M., et al. (2010). Mitochondrial fusion is required for mtDNA stability in skeletal muscle and tolerance of mtDNA mutations. *Cell* 141, 280–289. doi: 10.1016/j.cell.2010.02.026

Chen, H., Yoshioka, H., Kim, G. S., Jung, J. E., Okami, N., Sakata, H., et al. (2011). Oxidative stress in ischemic brain damage: mechanisms of cell death and potential molecular targets for neuroprotection. *Antioxid. Redox Signal.* 14, 1505–1517. doi: 10.1089/ars.2010.3576

Chen, S. D., Yang, D. I., Lin, T. K., Shaw, F. Z., Liou, C. W., and Chuang, Y. C. (2011). Roles of oxidative stress, apoptosis, PGC-1α and mitochondrial biogenesis in cerebral ischemia. *Int. J. Mol. Sci.* 12, 7199–7215. doi: 10.3390/ijms12107199

Chen, W., and Li, D. (2020). Reactive Oxygen Species (ROS)-Responsive nanomedicine for solving ischemia-reperfusion injury. *Front. Chem.* 8:732. doi: 10.3389/fchem.2020.00732

Chen, X., Zhang, W., Yi, W., Yang, L., Bi, X., Lin, Y., et al. (2022). Pathway of cell death and its role in virus infection. *Viral Immunol.* Online ahead of print. doi: 10.1089/vim.2022.0010

Chen, Y., Guo, S., Tang, Y., Mou, C., Hu, X., Shao, F., et al. (2020). Mitochondrial fusion and fission in neuronal death induced by cerebral ischemia-reperfusion and its clinical application: a mini-review. *Med. Sci. Monit.* 26:e928651. doi: 10.12659/MSM.928651

Chen, Y., Ma, S., Pi, D., Wu, Y., Zuo, Q., Li, C., et al. (2022). Luteolin induces pyroptosis in HT-29 cells by activating the Caspase1/Gasdermin D signalling pathway. *Front. Pharmacol.* 13:952587. doi: 10.3389/fphar.2022.952587

Chong, M., Mohammadi-Shemirani, P., Perrot, N., Nelson, W., Morton, R., Narula, S., et al. (2022). GWAS and ExWAS of blood mitochondrial DNA copy number identifies 71 loci and highlights a potential causal role in dementia. *eLife* 11:e70382. doi: 10.7554/eLife.70382

Chueh, T. H., Cheng, Y. H., Chen, K. H., and Chien, C. T. (2020). Thromboxane A2 synthase and thromboxane receptor deletion reduces ischaemia/reperfusion-evoked inflammation, apoptosis, autophagy and pyroptosis. *Thromb. Haemost.* 120, 329–343. doi: 10.1055/s-0039-3400304

Chun, N., Coca, S. G., and He, J. C. (2018). A protective role for microRNA-688 in acute kidney injury. *J. Clin. Invest.* 128, 5216–5218. doi: 10.1172/JCI124923

Cipolat, S., Martins, de Brito, O., Dal Zilio, B., and Scorrano, L. (2004). OPA1 requires mitofusin 1 to promote mitochondrial fusion. *Proc. Natl. Acad. Sci. U S A.* 101, 15927–15932. doi: 10.1073/pnas.0407043101

Conrad, M., and Pratt, D. A. (2019). The chemical basis of ferroptosis. *Nat. Chem. Biol.* 15, 1137–1147. doi: 10.1038/s41589-019-0408-1

Datta, A., Sarmah, D., Mounica, L., Kaur, H., Kesharwani, R., Verma, G., et al. (2020). Cell death pathways in ischemic stroke and targeted pharmacotherapy. *Trans. Stroke Res.* 11, 1185–1202. doi: 10.1007/s12975-020-00806-z

Deb, P., Sharma, S., and Hassan, K. M. (2010). Pathophysiologic mechanisms of acute ischemic stroke: an overview with emphasis on therapeutic significance beyond thrombolysis. *Pathophysiology.* 17, 197–218. doi: 10.1016/j.pathophys.2009.12.001

Degterev, A., Ofengeim, D., and Yuan, J. (2019). Targeting RIPK1 for the treatment of human diseases. *Proc. Natl. Acad. Sci. U S A.* 116, 9714–9722. doi: 10.1073/pnas.1901179116

DeHart, D. N., Fang, D., Heslop, K., Li, L., Lemasters, J. J., and Maldonado, E. N. (2018). Opening of voltage dependent anion channels promotes reactive oxygen species generation, mitochondrial dysfunction and cell death in cancer cells. *Biochem. Pharmacol.* 148, 155–162. doi: 10.1016/j.bcp.2017.12.022

Dimmer, K. S., and Scorrano, L. (2006). (De)constructing mitochondria: what for. *Physiology (Bethesda)* 21, 233–241. doi: 10.1152/physiol.00010.2006

Ding, Y., Lang, Y., Zhang, H., Li, Y., Liu, X., and Li, M. (2022). Candesartan reduces neuronal apoptosis caused by ischemic stroke via regulating the FFAR1/ITGA4 pathway. *Med. Inflamm.* 2022:2356507. doi: 10.1155/2022/2356507

Dixon, S. J., Lemberg, K. M., Lamprecht, M. R., Skouta, R., Zaitsev, E. M., Gleason, C. E., et al. (2012). Ferroptosis: an iron-dependent form of nonapoptotic cell death. *Cell* 149, 1060–1072. doi: 10.1016/j.cell.2012.03.042

Dong, L., Liang, F., Lou, Z., Li, Y., Li, J., Chen, Y., et al. (2022). Necrostatin-1 alleviates lung ischemia-reperfusion injury via inhibiting necroptosis and apoptosis of lung epithelial cells. *Cells* 11:3139. doi: 10.3390/cells11193139

Edlich, F., Banerjee, S., Suzuki, M., Cleland, M. M., Arnoult, D., Wang, C., et al. (2011). Bcl-x(L) retrotranslocates Bax from the mitochondria into the cytosol. *Cell* 145, 104–116. doi: 10.1016/j.cell.2011.02.034

Egawa, N., Lok, J., Washida, K., and Arai, K. (2017). Mechanisms of axonal damage and repair after central nervous system injury. *Trans. Stroke Res.* 8, 14–21. doi: 10.1007/s12975-016-0495-1

El-Hattab, A. W., Suleiman, J., Almannai, M., and Scaglia, F. (2018). Mitochondrial dynamics: biological roles, molecular machinery, and related diseases. *Mol. Genet. Metab.* 125, 315–321. doi: 10.1016/j.ymgme.2018.10.003

Estaquier, J., and Arnoult, D. (2007). Inhibiting Drp1-mediated mitochondrial fission selectively prevents the release of cytochrome c during apoptosis. *Cell Death Differ.* 14, 1086–1094. doi: 10.1038/sj.cdd.4402107

Fakharnia, F., Khodagholi, F., Dargahi, L., and Ahmadiani, A. (2017). Prevention of cyclophilin D-mediated mPTP opening using cyclosporine-a alleviates the elevation of necroptosis, autophagy and apoptosis-related markers following global cerebral ischemia-reperfusion. *J. Mol. Neurosci.* 61, 52–60. doi: 10.1007/s12031-016-0843-3

Fan, B. Y., Pang, Y. L., Li, W. X., Zhao, C. X., Zhang, Y., Wang, X., et al. (2021). Liproxstatin-1 is an effective inhibitor of oligodendrocyte ferroptosis induced by inhibition of glutathione peroxidase 4. *Neural Regen. Res.* 16, 561–566. doi: 10.4103/1673-5374.293157

Farina, M., Vieira, L. E., Buttari, B., Profumo, E., and Saso, L. (2021). The Nrf2 pathway in ischemic stroke: a review. *Molecules* 26:5001. doi: 10.3390/molecules26165001

Fariss, M. W., Chan, C. B., Patel, M., Van Houten, B., and Orrenius, S. (2005). Role of mitochondria in toxic oxidative stress. *Mol. Interv.* 5, 94–111. doi: 10.1124/mi.5.2.7

Feissner, R. F., Skalska, J., Gaum, W. E., and Sheu, S. S. (2009). Crosstalk signaling between mitochondrial Ca2+ and ROS. *Front. Biosci. (Landmark Ed).* 14:1197–1218. doi: 10.2741/3303

Feng, S. T., Wang, Z. Z., Yuan, Y. H., Wang, X. L., Sun, H. M., Chen, N. H., et al. (2020). Dynamin-related protein 1: a protein critical for mitochondrial fission, mitophagy, and neuronal death in Parkinson's disease. *Pharmacol. Res.* 151:104553. doi: 10.1016/j.phrs.2019.104553

Flippo, K. H., Lin, Z., Dickey, A. S., Zhou, X., Dhanesha, N. A., Walters, G. C., et al. (2020). Deletion of a neuronal Drp1 activator protects against cerebral ischemia. *J. Neurosci.* 40, 3119–3129. doi: 10.1523/JNEUROSCI.1926-19.2020

Fonseca, T. B., Sánchez-Guerrero, Á, Milosevic, I., and Raimundo, N. (2019). Mitochondrial fission requires DRP1 but not dynamins. *Nature* 570, E34–E42. doi: 10.1038/s41586-019-1296-y

Fontana, G. A., and Gahlon, H. L. (2020). Mechanisms of replication and repair in mitochondrial DNA deletion formation. *Nucleic Acids Res.* 48, 11244–11258. doi: 10.1093/nar/gkaa804

Frank, S., Gaume, B., Bergmann-Leitner, E. S., Leitner, W. W., Robert, E. G., Catez, F., et al. (2001). The role of dynamin-related protein 1, a mediator of mitochondrial fission, in apoptosis. *Dev. Cell.* 1, 515–525. doi: 10.1016/s1534-5807(01)00055-7

Fricker, M., Tolkovsky, A. M., Borutaite, V., Coleman, M., and Brown, G. C. (2018). Neuronal cell death. *Physiol. Rev.* 98, 813–880. doi: 10.1152/physrev.00011.2017

Friedlander, R. M., Gagliardini, V., Hara, H., Fink, K. B., Li, W., MacDonald, G., et al. (1997). Expression of a dominant negative mutant of interleukin-1 beta converting enzyme in transgenic mice prevents neuronal cell death induced by trophic factor withdrawal and ischemic brain injury. *J. Exp. Med.* 185, 933–940.

Gao, G., and Chang, Y. Z. (2014). Mitochondrial ferritin in the regulation of brain iron homeostasis and neurodegenerative diseases. *Front. Pharmacol.* 5:19. doi: 10.3389/fphar.2014.00019

Gao, H. J., Liu, P. F., Li, P. W., Huang, Z. Y., Yu, F. B., Lei, T., et al. (2015). Ligustrazine monomer against cerebral ischemia/reperfusion injury. *Neural Regen. Res.* 10, 832–840. doi: 10.4103/1673-5374.156991

Gao, M., Yi, J., Zhu, J., Minikes, A. M., Monian, P., Thompson, C. B., et al. (2019). Role of mitochondria in ferroptosis. *Mol. Cell* 73, 354–363.e3.

Gaschler, M. M., Andia, A. A., Liu, H., Csuka, J. M., Hurlocker, B., Vaiana, C. A., et al. (2018). FINO(2) initiates ferroptosis through GPX4 inactivation and iron oxidation. *Nat. Chem. Biol.* 14, 507–515. doi: 10.1038/s41589-018-0031-6

GBD 2019 Stroke Collaborators (2021). Global, regional, and national burden of stroke and its risk factors, 1990-2019: a systematic analysis for the Global Burden of Disease Study 2019. *Lancet Neurol.* 20, 795–820. doi: 10.1016/S1474-4422(21)00252-0

Giorgi, C., Marchi, S., Simoes, I., Ren, Z., Morciano, G., Perrone, M., et al. (2018). Mitochondria and reactive oxygen species in aging and age-related diseases. *Int. Rev. Cell Mol. Biol.* 340, 209–344. doi: 10.1016/bs.ircmb.2018.05.006

Gong, J., Li, Z. Z., Guo, S., Zhang, X. J., Zhang, P., Zhao, G. N., et al. (2015). Neuron-Specific tumor necrosis factor receptor-associated factor 3 is a central regulator of neuronal death in acute ischemic stroke. *Hypertension* 66, 604–616. doi: 10.1161/HYPERTENSIONAHA.115.05430

Grohm, J., Kim, S. W., Mamrak, U., Tobaben, S., Cassidy-Stone, A., Nunnari, J., et al. (2012). Inhibition of Drp1 provides neuroprotection in vitro and in vivo. *Cell Death Differ.* 19, 1446–1458. doi: 10.1038/cdd.2012.18

Guan, X., Li, X., Yang, X., Yan, J., Shi, P., Ba, L., et al. (2019). The neuroprotective effects of carvacrol on ischemia/reperfusion-induced hippocampal neuronal impairment by ferroptosis mitigation. *Life Sci.* 235:116795. doi: 10.1016/j.lfs.2019.116795

Gullett, J. M., Tweedell, R. E., and Kanneganti, T. D. (2022). It's all in the PAN: crosstalk, plasticity, redundancies, switches, and interconnectedness encompassed by PANoptosis underlying the totality of cell death-associated biological effects. *Cells* 11:1495. doi: 10.3390/cells11091495

Gustafsson, C. M., Falkenberg, M., and Larsson, N. G. (2016). Maintenance and expression of mammalian mitochondrial DNA. *Annu. Rev. Biochem.* 85, 133–160. doi: 10.1146/annurev-biochem-060815-014402

Han, B., Jiang, W., Cui, P., Zheng, K., Dang, C., Wang, J., et al. (2021). Microglial PGC-1α protects against ischemic brain injury by suppressing neuroinflammation. *Genome Med.* 13:47. doi: 10.1186/s13073-021-00863-5

Han, Q., Ma, Y., Wang, H., Dai, Y., Chen, C., Liu, Y., et al. (2018). Resibufogenin suppresses colorectal cancer growth and metastasis through RIP3-mediated necroptosis. *J. Transl. Med.* 16:201. doi: 10.1186/s12967-018-1580-x

Hanson, L. R., Roeytenberg, A., Martinez, P. M., Coppes, V. G., Sweet, D. C., Rao, R. J., et al. (2009). Intranasal deferoxamine provides increased brain exposure and significant protection in rat ischemic stroke. *J. Pharmacol. Exp. Ther.* 330, 679–686. doi: 10.1124/jpet.108.149807

Hayyan, M., Hashim, M. A., and AlNashef, I. M. (2016). Superoxide ion: generation and chemical implications. *Chem. Rev.* 116, 3029–3085. doi: 10.1021/acs.chemrev.5b00407

He, J., and Zhang, X. (2020). miR-668 inhibitor attenuates mitochondrial membrane potential and protects against neuronal apoptosis in cerebral ischemic stroke. *Folia Neuropathol.* 58, 22–29. doi: 10.5114/fn.2020.94003

Hill, R. L., Kulbe, J. R., Singh, I. N., Wang, J. A., and Hall, E. D. (2018). Synaptic mitochondria are more susceptible to traumatic brain injury-induced oxidative damage and respiratory dysfunction than non-synaptic mitochondria. *Neuroscience* 386, 265–283. doi: 10.1016/j.neuroscience.2018.06.028

Hu, W., Wu, X., Yu, D., Zhao, L., Zhu, X., Li, X., et al. (2020). Regulation of JNK signaling pathway and RIPK3/AIF in necroptosis-mediated global cerebral ischemia/reperfusion injury in rats. *Exp. Neurol.* 331:113374. doi: 10.1016/j.expneurol.2020.113374

Huang, Y., Liu, J., He, J., Hu, Z., Tan, F., Zhu, X., et al. (2022). UBIAD1 alleviates ferroptotic neuronal death by enhancing antioxidative capacity by cooperatively restoring impaired mitochondria and Golgi apparatus upon cerebral ischemic/reperfusion insult. *Cell Biosci.* 12:42. doi: 10.1186/s13578-022-00776-9

Huang, Y., Wang, Y., Duan, Z., Liang, J., Xu, Y., Zhang, S., et al. (2021). Restored microRNA-326-5p inhibits neuronal apoptosis and attenuates mitochondrial damage via suppressing STAT3 in cerebral ischemia/reperfusion injury. *Nanoscale Res. Lett.* 16:63. doi: 10.1186/s11671-021-03520-3

Ingold, I., Berndt, C., Schmitt, S., Doll, S., Poschmann, G., Buday, K., et al. (2018). Selenium utilization by GPX4 is required to prevent hydroperoxide-induced ferroptosis. *Cell* 172, 409–422.e21. doi: 10.1016/j.cell.2017.11.048.

Jiao, Y., Wang, J., Zhang, H., Cao, Y., Qu, Y., Huang, S., et al. (2020). Inhibition of microglial receptor-interacting protein kinase 1 ameliorates neuroinflammation following cerebral ischaemic stroke. *J. Cell. Mol. Med.* 24, 12585–12598. doi: 10.1111/jcmm.15820

Kaczmarek, A., Vandenabeele, P., and Krysko, D. V. (2013). Necroptosis: the release of damage-associated molecular patterns and its physiological relevance. *Immunity* 38, 209–223. doi: 10.1016/j.immuni.2013.02.003

Kalogeris, T., Baines, C. P., Krenz, M., and Korthuis, R. J. (2016). Ischemia/Reperfusion. *Comprehens. Physiol.* 7, 113–170. doi: 10.1002/cphy.c160006

Kang, R., Zeng, L., Zhu, S., Xie, Y., Liu, J., Wen, Q., et al. (2018). Lipid peroxidation drives gasdermin d-mediated pyroptosis in lethal polymicrobial sepsis. *Cell Host Microbe* 24, 97–108.e4. doi: 10.1016/j.chom.2018.05.009.

Kesavardhana, S., Kuriakose, T., Guy, C. S., Samir, P., Malireddi, R., Mishra, A., et al. (2017). ZBP1/DAI ubiquitination and sensing of influenza vRNPs activate programmed cell death. *J. Exp. Med.* 214, 2217–2229. doi: 10.1084/jem.20170550

Khoshnam, S. E., Winlow, W., Farzaneh, M., Farbood, Y., and Moghaddam, H. F. (2017). Pathogenic mechanisms following ischemic stroke. *Neurol. Sci.* 38, 1167–1186. doi: 10.1007/s10072-017-2938-1

Kishimoto, M., Suenaga, J., Takase, H., Araki, K., Yao, T., Fujimura, T., et al. (2019). Oxidative stress-responsive apoptosis inducing protein (ORAIP) plays a critical role in cerebral ischemia/reperfusion injury. *Sci. Rep.* 9:13512. doi: 10.1038/s41598-019-50073-8

Krajewska, M., You, Z., Rong, J., Kress, C., Huang, X., Yang, J., et al. (2011). Neuronal deletion of caspase 8 protects against brain injury in mouse models of controlled cortical impact and kainic acid-induced excitotoxicity. *PLoS One* 6:e24341. doi: 10.1371/journal.pone.0024341

Kuriakose, T., Man, S. M., Malireddi, R. K., Karki, R., Kesavardhana, S., Place, D. E., et al. (2016). ZBP1/DAI is an innate sensor of influenza virus triggering the NLRP3 inflammasome and programmed cell death pathways. *Sci. Immunol.* 1:aag2045. doi: 10.1126/sciimmunol.aag2045

Lambertsen, K. L., Finsen, B., and Clausen, B. H. (2019). Post-stroke inflammation-target or tool for therapy. *Acta Neuropathol.* 137, 693–714. doi: 10.1007/s00401-018-1930-z

Lan, R., Wu, J. T., Wu, T., Ma, Y. Z., Wang, B. Q., Zheng, H. Z., et al. (2018). Mitophagy is activated in brain damage induced by cerebral ischemia and reperfusion via the PINK1/Parkin/p62 signalling pathway. *Brain Res. Bull.* 142, 63–77. doi: 10.1016/j.brainresbull.2018.06.018

Letai, A., Bassik, M. C., Walensky, L. D., Sorcinelli, M. D., Weiler, S., and Korsmeyer, S. J. (2002). Distinct BH3 domains either sensitize or activate mitochondrial apoptosis, serving as prototype cancer therapeutics. *Cancer Cell* 2, 183–192. doi: 10.1016/s1535-6108(02)00127-7

Li, L., Zhi, D., Cheng, R., Li, J., Luo, C., and Li, H. (2021). The neuroprotective role of SIRT1/PGC-1α signaling in limb postconditioning in cerebral ischemia/reperfusion injury. *Neurosci. Lett.* 749:135736. doi: 10.1016/j.neulet.2021.135736

Li, M., Meng, Z., Yu, S., Li, J., Wang, Y., Yang, W., et al. (2022). Baicalein ameliorates cerebral ischemia-reperfusion injury by inhibiting ferroptosis via regulating GPX4/ACSL4/ACSL3 axis. *Chem. Biol. Interact.* 366:110137. doi: 10.1016/j.cbi.2022.110137

Li, P. A., Hou, X., and Hao, S. (2017). Mitochondrial biogenesis in neurodegeneration. *J. Neurosci. Res.* 95, 2025–2029. doi: 10.1002/jnr.24042

Li, Y., and Liu, X. (2018). Novel insights into the role of mitochondrial fusion and fission in cardiomyocyte apoptosis induced by ischemia/reperfusion. *J. Cell. Physiol.* 233, 5589–5597. doi: 10.1002/jcp.26522

Liao, Q. S., Du, Q., Lou, J., Xu, J. Y., and Xie, R. (2019). Roles of Na(+)/Ca(2+) exchanger 1 in digestive system physiology and pathophysiology. *World J. Gastroenterol.* 25, 287–299. doi: 10.3748/wjg.v25.i3.287

Liu, F., Lu, J., Manaenko, A., Tang, J., and Hu, Q. (2018). Mitochondria in ischemic stroke: new insight and implications. *Aging Dis.* 9, 924–937. doi: 10.14336/AD.2017.1126

Liu, H., Liu, X., Zhou, J., and Li, T. (2022). Mitochondrial DNA is a vital driving force in ischemia-reperfusion injury in cardiovascular diseases. *Oxid. Med. Cell Longev.* 2022:6235747. doi: 10.1155/2022/6235747

Liu, J., Guo, Z. N., Yan, X. L., Huang, S., Ren, J. X., Luo, Y., et al. (2020a). Crosstalk between autophagy and ferroptosis and its putative role in ischemic stroke. *Front. Cell Neurosci.* 14:577403. doi: 10.3389/fncel.2020.577403

Liu, J., Kuang, F., Kroemer, G., Klionsky, D. J., Kang, R., and Tang, D. (2020b). Autophagy-Dependent ferroptosis: machinery and regulation. *Cell Chem. Biol.* 27, 420–435. doi: 10.1016/j.chembiol.2020.02.005

Liu, P., Feng, Y., Li, H., Chen, X., Wang, G., Xu, S., et al. (2020c). Ferrostatin-1 alleviates lipopolysaccharide-induced acute lung injury via inhibiting ferroptosis. *Cell. Mol. Biol. Lett.* 25:10. doi: 10.1186/s11658-020-00205-0

Liu, W., Tian, F., Kurata, T., Morimoto, N., and Abe, K. (2012). Dynamic changes of mitochondrial fusion and fission proteins after transient cerebral ischemia in mice. *J. Neurosci. Res.* 90, 1183–1189. doi: 10.1002/jnr.23016

Liu, W., Wang, L., Liu, C., Dai, Z., Li, T., and Tang, B. (2022). Edaravone ameliorates cerebral ischemia-reperfusion injury by downregulating ferroptosis via the Nrf2/FPN pathway in rats. *Biol. Pharm. Bull.* 45, 1269–1275. doi: 10.1248/bpb.b22-00186

Liu, X., Lv, X., Liu, Z., Zhang, M., and Leng, Y. (2022). MircoRNA-29a in astrocyte-derived extracellular vesicles suppresses brain ischemia reperfusion injury via TP53INP1 and the NF-κB/NLRP3 axis. *Cell. Mol. Neurobiol.* 42, 1487–1500. doi: 10.1007/s10571-021-01040-3

Lu, B., Chen, X. B., Ying, M. D., He, Q. J., Cao, J., and Yang, B. (2017). The role of ferroptosis in cancer development and treatment response. *Front. Pharmacol.* 8:992. doi: 10.3389/fphar.2017.00992

Lünemann, J. D., Malhotra, S., Shinohara, M. L., Montalban, X., and Comabella, M. (2021). Targeting inflammasomes to treat neurological diseases. *Ann. Neurol.* 90, 177–188. doi: 10.1002/ana.26158

Ma, K., Chen, G., Li, W., Kepp, O., Zhu, Y., and Chen, Q. (2020). Mitophagy, mitochondrial homeostasis, and cell fate. *Front. Cell Dev. Biol.* 8:467. doi: 10.3389/fcell.2020.00467

Magistretti, P. J., and Allaman, I. (2015). A cellular perspective on brain energy metabolism and functional imaging. *Neuron* 86, 883–901. doi: 10.1016/j.neuron.2015.03.035

Maher, P., van Leyen, K., Dey, P. N., Honrath, B., Dolga, A., and Methner, A. (2018). The role of Ca(2+) in cell death caused by oxidative glutamate toxicity and ferroptosis. *Cell Calcium* 70, 47–55. doi: 10.1016/j.ceca.2017.05.007

Malireddi, R., Gurung, P., Kesavardhana, S., Samir, P., Burton, A., Mummareddy, H., et al. (2020a). Innate immune priming in the absence of TAK1 drives RIPK1 kinase activity-independent pyroptosis, apoptosis, necroptosis, and inflammatory disease. *J. Exp. Med.* 217:jem.20191644. doi: 10.1084/jem.20191644

Malireddi, R., Tweedell, R. E., and Kanneganti, T. D. (2020b). PANoptosis components, regulation, and implications. *Aging (Albany)* 12, 11163–11164. doi: 10.18632/aging.103528

Malireddi, R., Gurung, P., Mavuluri, J., Dasari, T. K., Klco, J. M., Chi, H., et al. (2018). TAK1 restricts spontaneous NLRP3 activation and cell death to control myeloid proliferation. *J. Exp. Med.* 215, 1023–1034. doi: 10.1084/jem.20171922

Malireddi, R., Kesavardhana, S., and Kanneganti, T. D. (2019). ZBP1 and TAK1: master regulators of NLRP3 inflammasome/pyroptosis, apoptosis, and necroptosis (PAN-optosis). *Front. Cell Infect. Microbiol.* 9:406. doi: 10.3389/fcimb.2019.00406

Mao, Z., Tian, L., Liu, J., Wu, Q., Wang, N., Wang, G., et al. (2022). Ligustilide ameliorates hippocampal neuronal injury after cerebral ischemia reperfusion through activating PINK1/Parkin-dependent mitophagy. *Phytomedicine* 101:154111. doi: 10.1016/j.phymed.2022.154111

McKenzie, B. A., Dixit, V. M., and Power, C. (2020). Fiery cell death: pyroptosis in the central nervous system. *Trends Neurosci.* 43, 55–73. doi: 10.1016/j.tins.2019.11.005

Merrill, J. E., and Scolding, N. J. (1999). Mechanisms of damage to myelin and oligodendrocytes and their relevance to disease. *Neuropathol. Appl. Neurobiol.* 25, 435–458. doi: 10.1046/j.1365-2990.1999.00200.x

Miyake, S., Murai, S., Kakuta, S., Uchiyama, Y., and Nakano, H. (2020). Identification of the hallmarks of necroptosis and ferroptosis by transmission electron microscopy. *Biochem. Biophys. Res. Commun.* 527, 839–844. doi: 10.1016/j.bbrc.2020.04.127

Montessuit, S., Somasekharan, S. P., Terrones, O., Lucken-Ardjomande, S., Herzig, S., Schwarzenbacher, R., et al. (2010). Membrane remodeling induced by the dynamin-related protein Drp1 stimulates Bax oligomerization. *Cell* 142, 889–901. doi: 10.1016/j.cell.2010.08.017

Mugoni, V., Postel, R., Catanzaro, V., De Luca, E., Turco, E., Digilio, G., et al. (2013). Ubiad1 is an antioxidant enzyme that regulates eNOS activity by CoQ10 synthesis. *Cell* 152, 504–518. doi: 10.1016/j.cell.2013.01.013

Naito, M. G., Xu, D., Amin, P., Lee, J., Wang, H., Li, W., et al. (2020). Sequential activation of necroptosis and apoptosis cooperates to mediate vascular and neural pathology in stroke. *Proc. Natl. Acad. Sci. U S A.* 117, 4959–4970. doi: 10.1073/pnas.1916427117

Nakagawa, K., Hirota, Y., Sawada, N., Yuge, N., Watanabe, M., Uchino, Y., et al. (2010). Identification of UBIAD1 as a novel human menaquinone-4 biosynthetic enzyme. *Nature* 468, 117–121. doi: 10.1038/nature09464

Nentwich, L. M. (2016). Diagnosis of acute ischemic stoke. *Emerg. Med. Clin. North Am.* 34, 837–859. doi: 10.1016/j.emc.2016.06.008

Neubert, M., Ridder, D. A., Bargiotas, P., Akira, S., and Schwaninger, M. (2011). Acute inhibition of TAK1 protects against neuronal death in cerebral ischemia. *Cell Death Differ.* 18, 1521–1530. doi: 10.1038/cdd.2011.29

Nhu, N. T., Li, Q., Liu, Y., Xu, J., Xiao, S. Y., and Lee, S. D. (2021). Effects of Mdivi-1 on neural mitochondrial dysfunction and mitochondria-mediated apoptosis in ischemia-reperfusion injury after stroke: a systematic review of preclinical studies. *Front. Mol. Neurosci.* 14:778569. doi: 10.3389/fnmol.2021.778569

Nie, G., Sheftel, A. D., Kim, S. F., and Ponka, P. (2005). Overexpression of mitochondrial ferritin causes cytosolic iron depletion and changes cellular iron homeostasis. *Blood* 105, 2161–2167. doi: 10.1182/blood-2004-07-2722

Nissanka, N., and Moraes, C. T. (2018). Mitochondrial DNA damage and reactive oxygen species in neurodegenerative disease. *FEBS Lett.* 592, 728–742. doi: 10.1002/1873-3468.12956

Novgorodov, S. A., Voltin, J. R., Gooz, M. A., Li, L., Lemasters, J. J., and Gudz, T. I. (2018). Acid sphingomyelinase promotes mitochondrial dysfunction due to glutamate-induced regulated necrosis. *J. Lipid Res.* 59, 312–329. doi: 10.1194/jlr.M080374

Orning, P., Weng, D., Starheim, K., Ratner, D., Best, Z., Lee, B., et al. (2018). Pathogen blockade of TAK1 triggers caspase-8-dependent cleavage of gasdermin D and cell death. *Science* 362, 1064–1069. doi: 10.1126/science.aau2818

Ouyang, Y. B., Xu, L., Lu, Y., Sun, X., Yue, S., Xiong, X. X., et al. (2013). Astrocyte-enriched miR-29a targets PUMA and reduces neuronal vulnerability to forebrain ischemia. *Glia* 61, 1784–1794. doi: 10.1002/glia.22556

Pandian, J. D., and Sebastian, I. A. (2021). Integrated approach to stroke burden: are we doing enough. *Lancet Neurol.* 20, 774–775. doi: 10.1016/S1474-4422(21)00287-8

Pender, M. P., and Rist, M. J. (2001). Apoptosis of inflammatory cells in immune control of the nervous system: role of glia. *Glia* 36, 137–144. doi: 10.1002/glia.1103

Peng, C., Rao, W., Zhang, L., Gao, F., Hui, H., Wang, K., et al. (2018). Mitofusin 2 exerts a protective role in ischemia reperfusion injury through increasing autophagy. *Cell. Physiol. Biochem.* 46, 2311–2324. doi: 10.1159/000489621

Peng, J., Wang, H., Gong, Z., Li, X., He, L., Shen, Q., et al. (2020). Idebenone attenuates cerebral inflammatory injury in ischemia and reperfusion via dampening NLRP3 inflammasome activity. *Mol. Immunol.* 123, 74–87. doi: 10.1016/j.molimm.2020.04.013

Peng, K., Yang, L., Wang, J., Ye, F., Dan, G., Zhao, Y., et al. (2017). The interaction of mitochondrial biogenesis and fission/fusion mediated by PGC-1α regulates rotenone-induced dopaminergic neurotoxicity. *Mol. Neurobiol.* 54, 3783–3797. doi: 10.1007/s12035-016-9944-9

Pérez, M. J., and Quintanilla, R. A. (2017). Development or disease: duality of the mitochondrial permeability transition pore. *Dev. Biol.* 426, 1–7. doi: 10.1016/j.ydbio.2017.04.018

Pickles, S., Vigié, P., and Youle, R. J. (2018). Mitophagy and quality control mechanisms in mitochondrial maintenance. *Curr. Biol.* 28, R170–R185. doi: 10.1016/j.cub.2018.01.004

Poh, L., Kang, S. W., Baik, S. H., Ng, G., She, D. T., Balaganapathy, P., et al. (2019). Evidence that NLRC4 inflammasome mediates apoptotic and pyroptotic microglial death following ischemic stroke. *Brain Behav. Immun.* 75, 34–47. doi: 10.1016/j.bbi.2018.09.001

Poole, L. P., Bock-Hughes, A., Berardi, D. E., and Macleod, K. F. (2021). ULK1 promotes mitophagy via phosphorylation and stabilization of BNIP3. *Sci. Rep.* 11:20526. doi: 10.1038/s41598-021-00170-4

Prass, K., Ruscher, K., Karsch, M., Isaev, N., Megow, D., Priller, J., et al. (2002). Desferrioxamine induces delayed tolerance against cerebral ischemia in vivo and in vitro. *J. Cereb. Blood Flow Metab.* 22, 520–525. doi: 10.1097/00004647-200205000-00003

Pundik, S., Xu, K., and Sundararajan, S. (2012). Reperfusion brain injury: focus on cellular bioenergetics. *Neurology* 79, S44–S51. doi: 10.1212/WNL.0b013e3182695a14

Qin, Y., Li, Q., Liang, W., Yan, R., Tong, L., Jia, M., et al. (2021). TRIM28 SUMOylates and stabilizes NLRP3 to facilitate inflammasome activation. *Nat. Commun.* 12:4794. doi: 10.1038/s41467-021-25033-4

Quesnelle, K. M., Bystrom, P. V., and Toledo-Pereyra, L. H. (2015). Molecular responses to ischemia and reperfusion in the liver. *Arch. Toxicol.* 89, 651–657. doi: 10.1007/s00204-014-1437-x

Ragoschke-Schumm, A., and Walter, S. (2018). DAWN and DEFUSE-3 trials: is time still important. *Radiologe* 58, 20–23. doi: 10.1007/s00117-018-0406-4

Rao, V. K., Carlson, E. A., and Yan, S. S. (2014). Mitochondrial permeability transition pore is a potential drug target for neurodegeneration. *Biochim. Biophys. Acta* 1842, 1267–1272. doi: 10.1016/j.bbadis.2013.09.003

Riley, J. S., Quarato, G., Cloix, C., Lopez, J., O'Prey, J., Pearson, M., et al. (2018). Mitochondrial inner membrane permeabilisation enables mtDNA release during apoptosis. *EMBO J.* 37:e99238. doi: 10.15252/embj.201899238

Rogers, C., Erkes, D. A., Nardone, A., Aplin, A. E., Fernandes-Alnemri, T., and Alnemri, E. S. (2019). Gasdermin pores permeabilize mitochondria to augment caspase-3 activation during apoptosis and inflammasome activation. *Nat. Commun.* 10:1689. doi: 10.1038/s41467-019-09397-2

Rottenberg, H., and Hoek, J. B. (2017). The path from mitochondrial ROS to aging runs through the mitochondrial permeability transition pore. *Aging Cell.* 16, 943–955. doi: 10.1111/acel.12650

Salvador, C. L., Oppebøen, M., Vassli, A. Ø, Pfeiffer, H., Varhaug, K. N., Elgstøen, K., et al. (2023). Increased sphingomyelin and free sialic acid in cerebrospinal fluid of kearns-sayre syndrome: new findings using untargeted metabolomics. *Pediatr. Neurol.* 143, 68–76. doi: 10.1016/j.pediatrneurol.2023.02.016

Sansbury, B. E., and Spite, M. (2016). Resolution of acute inflammation and the role of resolvins in immunity, thrombosis, and vascular biology. *Circ. Res.* 119, 113–130. doi: 10.1161/CIRCRESAHA.116.307308

Sarhan, J., Liu, B. C., Muendlein, H. I., Li, P., Nilson, R., Tang, A. Y., et al. (2018). Caspase-8 induces cleavage of gasdermin D to elicit pyroptosis during Yersinia infection. *Proc. Natl. Acad. Sci. U S A.* 115, E10888–E10897. doi: 10.1073/pnas.1809548115

Sarmah, D., Kaur, H., Saraf, J., Vats, K., Pravalika, K., Wanve, M., et al. (2018). Mitochondrial dysfunction in stroke: implications of stem cell therapy. *Trans. Stroke Res.* Online ahead of print. doi: 10.1007/s12975-018-0642-y

Schellenberg, B., Wang, P., Keeble, J. A., Rodriguez-Enriquez, R., Walker, S., Owens, T. W., et al. (2013). Bax exists in a dynamic equilibrium between the cytosol and mitochondria to control apoptotic priming. *Mol. Cell* 49, 959–971. doi: 10.1016/j.molcel.2012.12.022

Schenk, B., and Fulda, S. (2015). Reactive oxygen species regulate Smac mimetic/TNFα-induced necroptotic signaling and cell death. *Oncogene* 34, 5796–5806. doi: 10.1038/onc.2015.35

Shen, L., Gan, Q., Yang, Y., Reis, C., Zhang, Z., Xu, S., et al. (2021). Mitophagy in cerebral ischemia and ischemia/reperfusion injury. *Front. Aging Neurosci.* 13:687246. doi: 10.3389/fnagi.2021.687246

Shen, Y., Shen, X., Wang, S., Zhang, Y., Wang, Y., Ding, Y., et al. (2022). Protective effects of Salvianolic acid B on rat ferroptosis in myocardial infarction through upregulating the Nrf2 signaling pathway. *Int. Immunopharmacol.* 112:109257. doi: 10.1016/j.intimp.2022.109257

Shi, K., Tian, D. C., Li, Z. G., Ducruet, A. F., Lawton, M. T., and Shi, F. D. (2019). Global brain inflammation in stroke. *Lancet Neurol.* 18, 1058–1066. doi: 10.1016/S1474-4422(19)30078-X

Shi, Q., Cheng, Q., and Chen, C. (2021). The role of autophagy in the pathogenesis of ischemic stroke. *Curr. Neuropharmacol.* 19, 629–640. doi: 10.2174/1570159X18666200729101913

Singh, V., Mishra, V. N., Chaurasia, R. N., Joshi, D., and Pandey, V. (2019). Modes of calcium regulation in ischemic neuron. *Indian J. Clin. Biochem.* 34, 246–253. doi: 10.1007/s12291-019-00838-9

Sinha, K., Das, J., Pal, P. B., and Sil, P. C. (2013). Oxidative stress: the mitochondria-dependent and mitochondria-independent pathways of apoptosis. *Arch. Toxicol.* 87, 1157–1180. doi: 10.1007/s00204-013-1034-4

Sjostrand, F. S. (1953). Electron microscopy of mitochondria and cytoplasmic double membranes. *Nature* 171, 30–32. doi: 10.1038/171030a0

Smith, K. J., Kapoor, R., and Felts, P. A. (1999). Demyelination: the role of reactive oxygen and nitrogen species. *Brain Pathol. (Zurich)* 9, 69–92. doi: 10.1111/j.1750-3639.1999.tb00212.x

Solenski, N. J., diPierro, C. G., Trimmer, P. A., Kwan, A. L., and Helm, G. A. (2002). Ultrastructural changes of neuronal mitochondria after transient and permanent cerebral ischemia. *Stroke* 33, 816–824. doi: 10.1161/hs0302.104541

Song, F. E., Huang, J. L., Lin, S. H., Wang, S., Ma, G. F., and Tong, X. P. (2017). Roles of NG2-glia in ischemic stroke. *CNS Neurosci. Ther.* 23, 547–553. doi: 10.1111/cns.12690

Stockwell, B. R., Friedmann Angeli, J. P., Bayir, H., Bush, A. I., Conrad, M., Dixon, S. J., et al. (2017). Ferroptosis: a regulated cell death nexus linking metabolism, redox biology, and disease. *Cell* 171, 273–285. doi: 10.1016/j.cell.2017.09.021

Summer, R., Shaghaghi, H., Schriner, D., Roque, W., Sales, D., Cuevas-Mora, K., et al. (2019). Activation of the mTORC1/PGC-1 axis promotes mitochondrial biogenesis and induces cellular senescence in the lung epithelium. *Am. J. Physiol. Lung Cell Mol. Physiol.* 316, L1049–L1060. doi: 10.1152/ajplung.00244.2018

Tajeddine, N. (2016). How do reactive oxygen species and calcium trigger mitochondrial membrane permeabilisation. *Biochim. Biophys. Acta* 1860, 1079–1088. doi: 10.1016/j.bbagen.2016.02.013

Tanaka, A., and Youle, R. J. (2008). A chemical inhibitor of DRP1 uncouples mitochondrial fission and apoptosis. *Mol. Cell* 29, 409–410. doi: 10.1016/j.molcel.2008.02.005

Tang, Y. C., Tian, H. X., Yi, T., and Chen, H. B. (2016). The critical roles of mitophagy in cerebral ischemia. *Protein Cell* 7, 699–713. doi: 10.1007/s13238-016-0307-0

Tian, Q., Qin, B., Gu, Y., Zhou, L., Chen, S., Zhang, S., et al. (2020). ROS-Mediated necroptosis is involved in iron overload-induced osteoblastic cell death. *Oxid. Med. Cell Longev.* 2020:1295382. doi: 10.1155/2020/1295382

Todt, F., Cakir, Z., Reichenbach, F., Emschermann, F., Lauterwasser, J., Kaiser, A., et al. (2015). Differential retrotranslocation of mitochondrial Bax and Bak. *EMBO J.* 34, 67–80. doi: 10.15252/embj.201488806

Trujillo-Rangel, W. Á, García-Valdés, L., Méndez-Del Villar, M., Castañeda-Arellano, R., Totsuka-Sutto, S. E., and García-Benavides, L. (2022). Therapeutic targets for regulating oxidative damage induced by ischemia-reperfusion injury: a study from a pharmacological perspective. *Oxid. Med. Cell Longev.* 2022:8624318. doi: 10.1155/2022/8624318

Tsuchiya, K., Nakajima, S., Hosojima, S., Thi Nguyen, D., Hattori, T., Manh, et al. (2019). Caspase-1 initiates apoptosis in the absence of gasdermin D. *Nat Commun.* 10:2091. doi: 10.1038/s41467-019-09753-2

Tuo, Q. Z., Lei, P., Jackman, K. A., Li, X. L., Xiong, H., Li, X. L., et al. (2017). Tau-mediated iron export prevents ferroptotic damage after ischemic stroke. *Mol. Psychiatry* 22, 1520–1530. doi: 10.1038/mp.2017.171

van der Laan, M., Horvath, S. E., and Pfanner, N. (2016). Mitochondrial contact site and cristae organizing system. *Curr. Opin. Cell Biol.* 41, 33–42. doi: 10.1016/j.ceb.2016.03.013

Van Opdenbosch, N., and Lamkanfi, M. (2019). Caspases in cell death, inflammation, and disease. *Immunity* 50, 1352–1364. doi: 10.1016/j.immuni.2019.05.020

Villa, E., Marchetti, S., and Ricci, J. E. (2018). No parkin zone: mitophagy without parkin. *Trends Cell Biol.* 28, 882–895. doi: 10.1016/j.tcb.2018.07.004

Vinogradov, A. D., and Grivennikova, V. G. (2016). Oxidation of NADH and ROS production by respiratory complex I. *Biochim. Biophys. Acta* 1857, 863–871. doi: 10.1016/j.bbabio.2015.11.004

Vosler, P. S., Graham, S. H., Wechsler, L. R., and Chen, J. (2009). Mitochondrial targets for stroke: focusing basic science research toward development of clinically translatable therapeutics. *Stroke* 40, 3149–3155. doi: 10.1161/STROKEAHA.108.543769

Wang, C., Cai, X., Hu, W., Li, Z., Kong, F., Chen, X., et al. (2019). Investigation of the neuroprotective effects of crocin via antioxidant activities in HT22 cells and in mice with Alzheimer's disease. *Int. J. Mol. Med.* 43, 956–966. doi: 10.3892/ijmm.2018.4032

Wang, H., Chen, S., Zhang, Y., Xu, H., and Sun, H. (2019). Electroacupuncture ameliorates neuronal injury by Pink1/Parkin-mediated mitophagy clearance in cerebral ischemia-reperfusion. *Nitric. Oxide.* 91, 23–34. doi: 10.1016/j.niox.2019.07.004

Wang, H., Liu, C., Zhao, Y., and Gao, G. (2020). Mitochondria regulation in ferroptosis. *Eur. J. Cell Biol.* 99:151058. doi: 10.1016/j.ejcb.2019.151058

Wang, L., Wu, D., and Xu, Z. (2019). USP10 protects against cerebral ischemia injury by suppressing inflammation and apoptosis through the inhibition of TAK1 signaling. *Biochem. Biophys. Res. Commun.* 516, 1272–1278. doi: 10.1016/j.bbrc.2019.06.042

Wang, P., Cui, Y., Ren, Q., Yan, B., Zhao, Y., Yu, P., et al. (2021). Mitochondrial ferritin attenuates cerebral ischaemia/reperfusion injury by inhibiting ferroptosis. *Cell Death Dis.* 12:447. doi: 10.1038/s41419-021-03725-5

Wang, X., Li, R., Wang, X., Fu, Q., and Ma, S. (2015). Umbelliferone ameliorates cerebral ischemia-reperfusion injury via upregulating the PPAR gamma expression and suppressing TXNIP/NLRP3 inflammasome. *Neurosci. Lett.* 600, 182–187. doi: 10.1016/j.neulet.2015.06.016

Wang, Y., Cai, J., Tang, C., and Dong, Z. (2020). Mitophagy in acute kidney injury and kidney repair. *Cells* 9:338. doi: 10.3390/cells9020338

Wang, Y., Guan, X., Gao, C. L., Ruan, W., Zhao, S., Kai, G., et al. (2021). Medioresinol as a novel PGC-1α activator prevents pyroptosis of endothelial cells in ischemic stroke through PPARα-GOT1 axis. *Pharmacol. Res.* 169:105640. doi: 10.1016/j.phrs.2021.105640

Wang, Y., and Kanneganti, T. D. (2021). From pyroptosis, apoptosis and necroptosis to PANoptosis: a mechanistic compendium of programmed cell death pathways. *Comput. Struct. Biotechnol. J.* 19, 4641–4657. doi: 10.1016/j.csbj.2021.07.038

Wang, Z., Jiang, H., Chen, S., Du, F., and Wang, X. (2012). The mitochondrial phosphatase PGAM5 functions at the convergence point of multiple necrotic death pathways. *Cell* 148, 228–243. doi: 10.1016/j.cell.2011.11.030

Wei, M. C., Zong, W. X., Cheng, E. H., Lindsten, T., Panoutsakopoulou, V., Ross, A. J., et al. (2001). Proapoptotic BAX and BAK: a requisite gateway to mitochondrial dysfunction and death. *Science* 292, 727–730. doi: 10.1126/science.1059108

Wei, N., Pu, Y., Yang, Z., Pan, Y., and Liu, L. (2019). Therapeutic effects of melatonin on cerebral ischemia reperfusion injury: role of Yap-OPA1 signaling pathway and mitochondrial fusion. *Biomed. Pharmacother* 110, 203–212. doi: 10.1016/j.biopha.2018.11.060

Wu, C., Zhao, W., Yu, J., Li, S., Lin, L., and Chen, X. (2018). Induction of ferroptosis and mitochondrial dysfunction by oxidative stress in PC12 cells. *Sci. Rep.* 8:574. doi: 10.1038/s41598-017-18935-1

Wu, J. R., Tuo, Q. Z., and Lei, P. (2018). Ferroptosis, a recent defined form of critical cell death in neurological disorders. *J. Mol. Neurosci.* 66, 197–206. doi: 10.1007/s12031-018-1155-6

Wu, M., Gu, X., and Ma, Z. (2021). Mitochondrial quality control in cerebral ischemia-reperfusion injury. *Mol. Neurobiol.* 58, 5253–5271. doi: 10.1007/s12035-021-02494-8

Wu, M. Y., Yiang, G. T., Liao, W. T., Tsai, A. P., Cheng, Y. L., Cheng, P. W., et al. (2018). Current mechanistic concepts in ischemia and reperfusion injury. *Cell. Physiol. Biochem.* 46, 1650–1667. doi: 10.1159/000489241

Wu, X., Li, X., Liu, Y., Yuan, N., Li, C., Kang, Z., et al. (2018). Hydrogen exerts neuroprotective effects on OGD/R damaged neurons in rat hippocampal by protecting mitochondrial function via regulating mitophagy mediated by PINK1/Parkin signaling pathway. *Brain Res.* 1698, 89–98. doi: 10.1016/j.brainres.2018.06.028

Wu, X., Lin, L., Qin, J. J., Wang, L., Wang, H., Zou, Y., et al. (2020). CARD3 promotes cerebral ischemia-reperfusion injury via activation of TAK1. *J. Am. Heart Assoc.* 9:e014920. doi: 10.1161/JAHA.119.014920

Wu, X., Zheng, Y., Liu, M., Li, Y., Ma, S., Tang, W., et al. (2021). BNIP3L/NIX degradation leads to mitophagy deficiency in ischemic brains. *Autophagy* 17, 1934–1946. doi: 10.1080/15548627.2020.1802089

Xian, H., and Liou, Y. C. (2021). Functions of outer mitochondrial membrane proteins: mediating the crosstalk between mitochondrial dynamics and mitophagy. *Cell Death Differ.* 28, 827–842. doi: 10.1038/s41418-020-00657-z

Xiao, K., Liu, C., Qin, Q., Zhang, Y., Wang, X., Zhang, J., et al. (2020). EPA and DHA attenuate deoxynivalenol-induced intestinal porcine epithelial cell injury and protect barrier function integrity by inhibiting necroptosis signaling pathway. *FASEB J.* 34, 2483–2496. doi: 10.1096/fj.201902298R

Xie, J., Zhang, T., Li, P., Wang, D., Liu, T., and Xu, S. (2022). Dihydromyricetin attenuates cerebral ischemia reperfusion injury by inhibiting SPHK1/mTOR signaling and targeting ferroptosis. *Drug Des. Devel. Ther.* 16, 3071–3085. doi: 10.2147/DDDT.S378786

Xie, Y., Hou, W., Song, X., Yu, Y., Huang, J., Sun, X., et al. (2016). Ferroptosis: process and function. *Cell Death Differ.* 23, 369–379. doi: 10.1038/cdd.2015.158

Xu, D., Jin, T., Zhu, H., Chen, H., Ofengeim, D., Zou, C., et al. (2018). TBK1 Suppresses RIPK1-Driven apoptosis and inflammation during development and in aging. *Cell* 174, 1477–1491.e19. doi: 10.1016/j.cell.2018.07.041.

Xu, P., Zhang, X., Liu, Q., Xie, Y., Shi, X., Chen, J., et al. (2019). Microglial TREM-1 receptor mediates neuroinflammatory injury via interaction with SYK in experimental ischemic stroke. *Cell Death Dis.* 10:555. doi: 10.1038/s41419-019-1777-9

Xu, Y., Shen, J., and Ran, Z. (2020). Emerging views of mitophagy in immunity and autoimmune diseases. *Autophagy* 16, 3–17. doi: 10.1080/15548627.2019.1603547

Yagoda, N., von Rechenberg, M., Zaganjor, E., Bauer, A. J., Yang, W. S., Fridman, D. J., et al. (2007). RAS-RAF-MEK-dependent oxidative cell death involving voltage-dependent anion channels. *Nature* 447, 864–868. doi: 10.1038/nature05859

Yan, W. T., Lu, S., Yang, Y. D., Ning, W. Y., Cai, Y., Hu, X. M., et al. (2021). Research trends, hot spots and prospects for necroptosis in the field of neuroscience. *Neural Regen. Res.* 16, 1628–1637. doi: 10.4103/1673-5374.303032

Yan, W. T., Yang, Y. D., Hu, X. M., Ning, W. Y., Liao, L. S., Lu, S., et al. (2022). Do pyroptosis, apoptosis, and necroptosis (PANoptosis) exist in cerebral ischemia? Evidence from cell and rodent studies. *Neural Regen. Res.* 17, 1761–1768. doi: 10.4103/1673-5374.331539

Yang, M., He, Y., Deng, S., Xiao, L., Tian, M., Xin, Y., et al. (2021). Mitochondrial quality control: a pathophysiological mechanism and therapeutic target for stroke. *Front. Mol. Neurosci.* 14:786099. doi: 10.3389/fnmol.2021.786099

Yang, M., Linn, B. S., Zhang, Y., and Ren, J. (2019). Mitophagy and mitochondrial integrity in cardiac ischemia-reperfusion injury. *Biochim Biophys. Acta Mol. Basis Dis.* 1865, 2293–2302. doi: 10.1016/j.bbadis.2019.05.007

Yang, W. S., Kim, K. J., Gaschler, M. M., Patel, M., Shchepinov, M. S., and Stockwell, B. R. (2016). Peroxidation of polyunsaturated fatty acids by lipoxygenases drives ferroptosis. *Proc. Natl. Acad. Sci. U S A.* 113, E4966–E4975. doi: 10.1073/pnas.1603244113

Yang, W. S., and Stockwell, B. R. (2008). Synthetic lethal screening identifies compounds activating iron-dependent, nonapoptotic cell death in oncogenic-RAS-harboring cancer cells. *Chem. Biol.* 15, 234–245.

Yang, W. S., and Stockwell, B. R. (2016). Ferroptosis: death by lipid peroxidation. *Trends Cell Biol.* 26, 165–176. doi: 10.1016/j.tcb.2015.10.014

Yang, Z., Wang, Y., Zhang, Y., He, X., Zhong, C. Q., Ni, H., et al. (2018). RIP3 targets pyruvate dehydrogenase complex to increase aerobic respiration in TNF-induced necroptosis. *Nat. Cell Biol.* 20, 186–197. doi: 10.1038/s41556-017-0022-y

Yarmohammadi, F., Hayes, A. W., and Karimi, G. (2021). The role of ferroptosis in organ toxicity. *Hum. Exp. Toxicol.* 40, S851–S860. doi: 10.1177/09603271211052987

Yeon, S. H., Yang, G., Lee, H. E., and Lee, J. Y. (2017). Oxidized phosphatidylcholine induces the activation of NLRP3 inflammasome in macrophages. *J. Leukoc. Biol.* 101, 205–215. doi: 10.1189/jlb.3VMA1215-579RR

Ying, Y., and Padanilam, B. J. (2016). Regulation of necrotic cell death: p53, PARP1 and cyclophilin D-overlapping pathways of regulated necrosis. *Cell. Mol. Life Sci.* 73, 2309–2324. doi: 10.1007/s00018-016-2202-5

You, Y., Hou, Y., Zhai, X., Li, Z., Li, L., Zhao, Y., et al. (2016). Protective effects of PGC-1α via the mitochondrial pathway in rat brains after intracerebral hemorrhage. *Brain Res.* 1646, 34–43. doi: 10.1016/j.brainres.2016.04.076

Youle, R. J. (2019). Mitochondria-Striking a balance between host and endosymbiont. *Science* 365:eaaw9855. doi: 10.1126/science.aaw9855

Yu, R., Liu, T., Jin, S. B., Ankarcrona, M., Lendahl, U., Nistér, M., et al. (2021). MIEF1/2 orchestrate mitochondrial dynamics through direct engagement with both the fission and fusion machineries. *BMC Biol.* 19:229.

Yu, T. J., Shiau, J. P., Tang, J. Y., Yen, C. H., Hou, M. F., Cheng, Y. B., et al. (2022). Physapruin a induces reactive oxygen species to trigger cytoprotective autophagy of breast cancer cells. *Antioxidants (Basel)* 11:1352. doi: 10.3390/antiox11071352

Yu, X., Hao, M., Liu, Y., Ma, X., Lin, W., Xu, Q., et al. (2019). Liraglutide ameliorates non-alcoholic steatohepatitis by inhibiting NLRP3 inflammasome and pyroptosis activation via mitophagy. *Eur. J. Pharmacol.* 864:172715. doi: 10.1016/j.ejphar.2019.172715

Yuan, J., and Yankner, B. A. (2000). Apoptosis in the nervous system. *Nature* 407, 802–809. doi: 10.1038/35037739

Yuan, M., Zhang, Y., Wang, L., Hua, Y., Wang, Y., Cheng, H., et al. (2022). Study on the mechanism of Tong-Qiao-Huo-Xue decoction regulating apoptosis via ASK1/MKK4/JNK pathway in MCAO/R rats. *Phytomedicine* 106:154437. doi: 10.1016/j.phymed.2022.154437

Yuan, Y., Zhai, Y., Chen, J., Xu, X., and Wang, H. (2021). Kaempferol ameliorates oxygen-glucose deprivation/reoxygenation-induced neuronal ferroptosis by activating Nrf2/SLC7A11/GPX4 Axis. *Biomolecules* 11:923. doi: 10.3390/biom11070923

Zeyen, T., Noristani, R., Habib, S., Heinisch, O., Slowik, A., Huber, M., et al. (2020). Microglial-specific depletion of TAK1 is neuroprotective in the acute phase after ischemic stroke. *J. Mol. Med. (Berlin)* 98, 833–847. doi: 10.1007/s00109-020-01916-9

Zhang, C. X., Cheng, Y., Liu, D. Z., Liu, M., Cui, H., Zhang, B. L., et al. (2019). Mitochondria-targeted cyclosporin A delivery system to treat myocardial ischemia reperfusion injury of rats. *J. Nanobiotechnol.* 17:18. doi: 10.1186/s12951-019-0451-9

Zhang, D. W., Shao, J., Lin, J., Zhang, N., Lu, B. J., Lin, S. C., et al. (2009). RIP3, an energy metabolism regulator that switches TNF-induced cell death from apoptosis to necrosis. *Science* 325, 332–336. doi: 10.1126/science.1172308

Zhang, F., Ran, Y., Tahir, M., Li, Z., Wang, J., and Chen, X. (2022). Regulation of N6-methyladenosine (m6A) RNA methylation in microglia-mediated inflammation and ischemic stroke. *Front. Cell Neurosci.* 16:955222. doi: 10.3389/fncel.2022.955222

Zhang, J., Chen, S., Li, Y., Xiao, W., and An, W. (2021). Alleviation of CCCP-induced mitochondrial injury by augmenter of liver regeneration via the PINK1/Parkin pathway-dependent mitophagy. *Exp. Cell Res.* 409:112866. doi: 10.1016/j.yexcr.2021.112866

Zhang, J., Ji, Y., Lu, Y., Fu, R., Xu, M., Liu, X., et al. (2018). Leber's hereditary optic neuropathy (LHON)-associated ND5 12338T > C mutation altered the assembly and function of complex I, apoptosis and mitophagy. *Hum. Mol. Genet.* 27, 1999–2011. doi: 10.1093/hmg/ddy107

Zhang, W., Siraj, S., Zhang, R., and Chen, Q. (2017). Mitophagy receptor FUNDC1 regulates mitochondrial homeostasis and protects the heart from I/R injury. *Autophagy* 13, 1080–1081. doi: 10.1080/15548627.2017.1300224

Zhang, W., Yang, H., Gao, M., Zhang, H., Shi, L., Yu, X., et al. (2022). Edaravone dexborneol alleviates cerebral ischemic injury via MKP-1-Mediated inhibition of MAPKs and activation of Nrf2. *Biomed. Res. Int.* 2022:4013707. doi: 10.1155/2022/4013707

Zhang, Y., Su, S. S., Zhao, S., Yang, Z., Zhong, C. Q., Chen, X., et al. (2017). RIP1 autophosphorylation is promoted by mitochondrial ROS and is essential for RIP3 recruitment into necrosome. *Nat. Commun.* 8:14329. doi: 10.1038/ncomms14329

Zhao, R. Z., Jiang, S., Zhang, L., and Yu, Z. B. (2019). Mitochondrial electron transport chain, ROS generation and uncoupling (Review). *Int. J. Mol. Med.* 44, 3–15. doi: 10.3892/ijmm.2019.4188

Zhao, S. C., Ma, L. S., Chu, Z. H., Xu, H., Wu, W. Q., and Liu, F. (2017). Regulation of microglial activation in stroke. *Acta Pharmacol. Sin.* 38, 445–458. doi: 10.1038/aps.2016.162

Zhao, X., Quan, J., Tan, Y., Liu, Y., Liao, C., Li, Z., et al. (2021). RIP3 mediates TCN-induced necroptosis through activating mitochondrial metabolism and ROS production in chemotherapy-resistant cancers. *Am. J. Cancer Res.* 11, 729–745.

Zhao, Z., Mei, Y., Wang, Z., and He, W. (2022). The effect of oxidative phosphorylation on cancer drug resistance. *Cancers (Basel)* 15:62. doi: 10.3390/cancers15010062

Zhe-Wei, S., Li-Sha, G., and Yue-Chun, L. (2018). The role of necroptosis in cardiovascular disease. *Front. Pharmacol.* 9:721. doi: 10.3389/fphar.2018.00721

Zhou, H., Li, D., Zhu, P., Ma, Q., Toan, S., Wang, J., et al. (2018). Inhibitory effect of melatonin on necroptosis via repressing the Ripk3-PGAM5-CypD-mPTP pathway attenuates cardiac microvascular ischemia-reperfusion injury. *J. Pineal Res.* 65:e12503. doi: 10.1111/jpi.12503

Zhou, K., Chen, J., Wu, J., Wu, Q., Jia, C., Xu, Y., et al. (2019). Atractylenolide III ameliorates cerebral ischemic injury and neuroinflammation associated with inhibiting JAK2/STAT3/Drp1-dependent mitochondrial fission in microglia. *Phytomedicine* 59:152922. doi: 10.1016/j.phymed.2019.152922

Zhou, M., Wang, H., Zhu, J., Chen, W., Wang, L., Liu, S., et al. (2016). Cause-specific mortality for 240 causes in China during 1990-2013: a systematic subnational analysis for the Global Burden of Disease Study 2013. *Lancet* 387, 251–272. doi: 10.1016/S0140-6736(15)00551-6

Zhou, X., Wang, H. Y., Wu, B., Cheng, C. Y., Xiao, W., Wang, Z. Z., et al. (2017). Ginkgolide K attenuates neuronal injury after ischemic stroke by inhibiting mitochondrial fission and GSK-3β-dependent increases in mitochondrial membrane permeability. *Oncotarget* 8, 44682–44693. doi: 10.18632/oncotarget.17967

Ziabreva, I., Campbell, G., Rist, J., Zambonin, J., Rorbach, J., Wydro, M. M., et al. (2010). Injury and differentiation following inhibition of mitochondrial respiratory chain complex IV in rat oligodendrocytes. *Glia* 58, 1827–1837. doi: 10.1002/glia.21052

Zou, Y., and Schreiber, S. L. (2020). Progress in understanding ferroptosis and challenges in its targeting for therapeutic benefit. *Cell Chem. Biol.* 27, 463–471. doi: 10.1016/j.chembiol.2020.03.015

frontiers | Frontiers in Cellular Neuroscience

TYPE Review
PUBLISHED 09 August 2023
DOI 10.3389/fncel.2023.1228761

OPEN ACCESS

EDITED BY
Syed Shadab Raza,
ERA's Lucknow Medical College, India

REVIEWED BY
Ahmet Burak Caglayan,
Istanbul Medipol University, Türkiye
Taha Kelestemur,
Columbia University, United States

*CORRESPONDENCE
Qin Yang
✉ xyqh200@126.com

†These authors have contributed equally to this work

RECEIVED 25 May 2023
ACCEPTED 25 July 2023
PUBLISHED 09 August 2023

CITATION
Tang H, Wen J, Qin T, Chen Y, Huang J, Yang Q, Jiang P, Wang L, Zhao Y and Yang Q (2023) New insights into Sirt1: potential therapeutic targets for the treatment of cerebral ischemic stroke.
Front. Cell. Neurosci. 17:1228761.
doi: 10.3389/fncel.2023.1228761

New insights into Sirt1: potential therapeutic targets for the treatment of cerebral ischemic stroke

Hao Tang[1†], Jun Wen[1†], Ting Qin[2†], Yue Chen[1], Jiagui Huang[1], Qinghuan Yang[1], Peiran Jiang[1], Ling Wang[1], Yong Zhao[1] and Qin Yang[1*]

[1]Department of Neurology, The First Affiliated Hospital of Chongqing Medical University, Chongqing, China, [2]Department of Respiratory Disease, Daping Hospital, Army Medical University, Chongqing, China

Ischemic stroke is one of the main causes of mortality and disability worldwide. However, the majority of patients are currently unable to benefit from intravenous thrombolysis or intravascular mechanical thrombectomy due to the limited treatment windows and serious complications. Silent mating type information regulation 2 homolog 1 (Sirt1), a nicotine adenine dinucleotide-dependent enzyme, has emerged as a potential therapeutic target for ischemic stroke due to its ability to maintain brain homeostasis and possess neuroprotective properties in a variety of pathological conditions for the central nervous system. Animal and clinical studies have shown that activation of Sirt1 can lessen neurological deficits and reduce the infarcted volume, offering promise for the treatment of ischemic stroke. In this review, we summarized the direct evidence and related mechanisms of Sirt1 providing neuroprotection against cerebral ischemic stroke. Firstly, we introduced the protein structure, catalytic mechanism and specific location of Sirt1 in the central nervous system. Secondly, we list the activators and inhibitors of Sirt1, which are primarily divided into three categories: natural, synthetic and physiological. Finally, we reviewed the neuroprotective effects of Sirt1 in ischemic stroke and discussed the specific mechanisms, including reducing neurological deficits by inhibiting various programmed cell death such as pyroptosis, necroptosis, ferroptosis, and cuproptosis in the acute phase, as well as enhancing neurological repair by promoting angiogenesis and neurogenesis in the later stage. Our review aims to contribute to a deeper understanding of the critical role of Sirt1 in cerebral ischemic stroke and to offer novel therapeutic strategies for this condition.

KEYWORDS

Sirt1, cerebral ischemic stroke, neuroprotection, deacetylation, programmed cell death

Introduction

Currently, ischemic stroke is one of the well-known leading causes of mortality and long-term disability globally (Ahmadi et al., 2020). Although substantial efforts have been made to search for better treatment modalities for ischemic stroke, remarkably few strategies are considered sufficiently effective due to their complex pathophysiological mechanism,

including excitotoxicity, oxidative stress, inflammation and blood-brain barrier (BBB) damage.

At present, thrombolysis and mechanical thrombectomy are the only authorized treatments for acute ischemic stroke clinically. However, its therapeutic application is severely constrained by the narrow time windows and secondary injury caused by vascular recanalization (Nogueira et al., 2018; Turc et al., 2019). Therefore, it is essential to seek for new alternatives that can prolong the time windows and improve the prognosis of ischemic stroke patients. Among the potential therapeutic targets, Silent mating type information regulation 2 homolog 1 (Sirt1) merits special attention. Because it can not only lessen the neurological injury in the acute phase, but also enhance neurorestoration in the later stage.

Sirt1, a nicotine adenine dinucleotide (NAD^+)-dependent enzyme, is the member of the sirtuins family, which can catalyze the deacetylation of histone and non-histone substrates (such as P53, FOXO3), and plays a crucial role in chromatin remodeling, gene regulation and metabolism (Meng et al., 2020). Sirt1 is abundant in early embryo and widely expressed in mature tissues (Chang and Guarente, 2014). In the central nervous system (CNS), Sirt1 is extensively expressed in neurons, neural stem cells, neural precursor cells, astrocytes and microglia of embryonic and adult brains. Further studies shows that Sirt1 is involved in the modulation of neurodevelopment, learning, memory and metabolic function (Chang and Guarente, 2014; Herskovits and Guarente, 2014; Zhou et al., 2018). It has been discovered that activated Sirt1 exhibits obviously potent neuroprotective effects on ischemic stroke and other neurodegenerative diseases.

In the review, we summarized the protective effects of Sirt1 on ischemic stroke and its related mechanisms, including reducing inflammatory response, inhibiting oxidative stress and ultimately modulating programmed cell death in the acute phase, and promoting neurological functional recovery through enhancing angiogenesis and neurogenesis in the later stage. The review may provide a fundamental basis for the design of new drugs for ischemic stroke.

Sirt1 protein structure

Sirtuins are a group of highly conserved NAD^+-dependent deacetylases. Mammalian sirtuins can be split into seven members (Sirt1∼7) according to their structure and function. Sirt1 is firstly discovered and the most studied. The human Sirt1 protein (747 amino acids) is composed of highly conserved catalytic domain, N-terminal domain and C-terminal domain. For human Sirt1, the catalytic core consists of two domains. The larger NAD^+-binding domain consists of a Rossmann fold, and the smaller domain composes of a helical structure and a zinc-binding module. The Sirt1-mediated catalytic reaction is initiated by the binding of acetylated residues of the target molecule with NAD^+ through the cleft between these two domains (Sauve et al., 2006), which eventually produces the deacetylated substrates, nicotinamide and 2′-O-acetyl-ADP-ribose (AADPR) (Tanner et al., 2000; **Figure 1**).

Sirt1 protein localization

Growing studies have verified that Sirt1 is widely distributed in human and rodent organs, including brain, heart and liver (Sakamoto et al., 2004; Tanno et al., 2010; Ogawa et al., 2011; Al-Bahrani et al., 2015; Cao et al., 2018). An anatomical study of rodent and human nervous system showed that Sirt1 was localized in the regions of the hippocampus, prefrontal cortex and basal ganglia (Zakhary et al., 2010). Subsequently, Sirt1 was also found to express in hypothalamus and cerebellum (Ramadori et al., 2008). In addition to neurons, Sirt1 has also been demonstrated to be expressed in various glial cells (Kannan et al., 2013; Prozorovski et al., 2019), such as microglia, astrocytes and oligodendrocytes (**Figure 2**). In summary, Sirt1 is widely distributed in the CNS.

Next, let us turn to the subcellular localization of Sirt1. The nuclear localization signal is found on residues 41–46 of the Sirt1 protein (Frye, 1999). Therefore, it makes sense that Sirt1 is classified as a nuclear protein. However, a variety of findings suggested that Sirt1 was also present in cytoplasm under certain conditions (Jin et al., 2007; Hisahara et al., 2008; Yu et al., 2020). Subsequent study confirmed that Sirt1 could shuttle between the nucleus and cytoplasm, which was mediated by the nuclear import and export sequences in the N-terminal region of Sirt1 (Tanno et al., 2007).

Activators and inhibitors of Sirt1

Sirt1 plays an important role in various physiological and pathological processes in organisms, and up or down regulation of Sirt1 often means completely different outcomes. Therefore, searching for the activator and inhibitors of Sirt1 remains significantly important for the prevention and treatment of various diseases, including cerebral ischemic stroke. Next, we will simply divide them into three categories: natural, synthetic and physiological (**Table 1**).

Physiological

Active regulator of Sirt1 (AROS) is seen as a direct interactant of Sirt1, which functions by directly binding at a site (amino acids 114–217) distal to the Sirt1 catalytic domain, thereby promoting Sirt1 deacetylation activity (Autiero et al., 2008). Kim et al. (2007) found that AROS can upregulate Sirt1 activity so as to inhibit P53-dependent transcriptional activation by directly binding to Sirt1. Nevertheless, AROS is considered as a weak activator of Sirt1, which requires strict conditions for this activation. The regulation of P53 acetylation by AROS depends to some extent on the cell context. Specifically, AROS suppressed the acetylation of P53 only during the process of cell damaging stress (Knight et al., 2013). Different from AROS, member of La ribonucleoprotein domain family 7 (LARP7) is an RNA binding protein and a strong activator of Sirt1, which has been reported to play a positive role in aging and heart failure by regulating Sirt1 (Yan et al., 2021; Yu H. et al., 2021). LARP7 strongly bound to Sirt1 residues 158–225 and allosterically enhances Sirt1 deacetylase activity, thereby inhibiting the acetylation of P53 and P65, respectively.

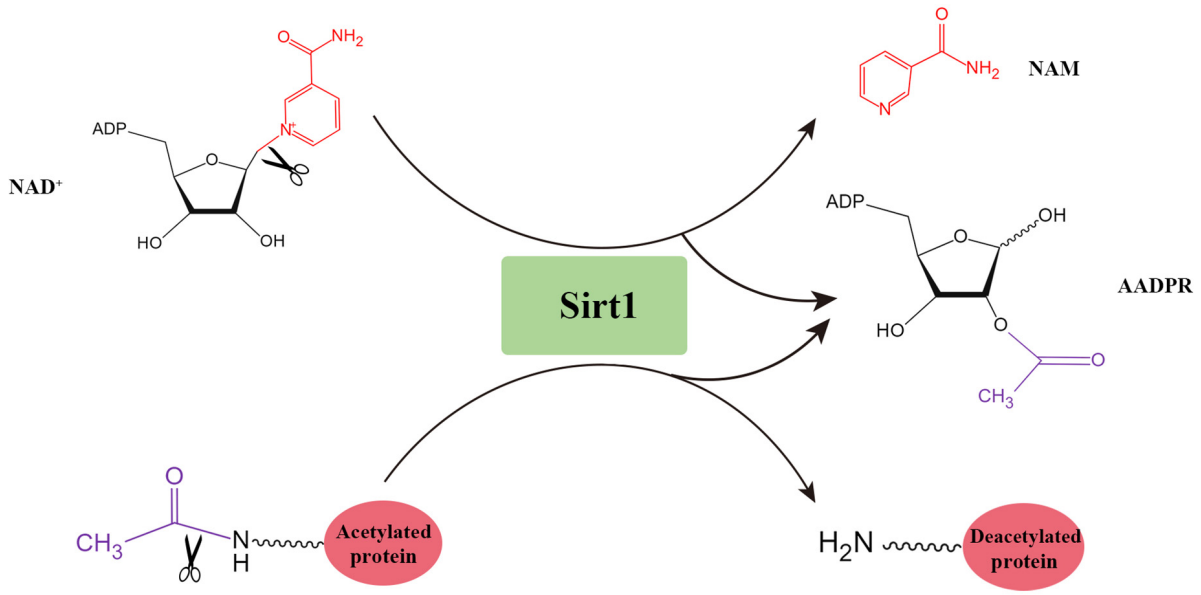

FIGURE 1
The deacetylation reaction catalyzed by Sirt1.

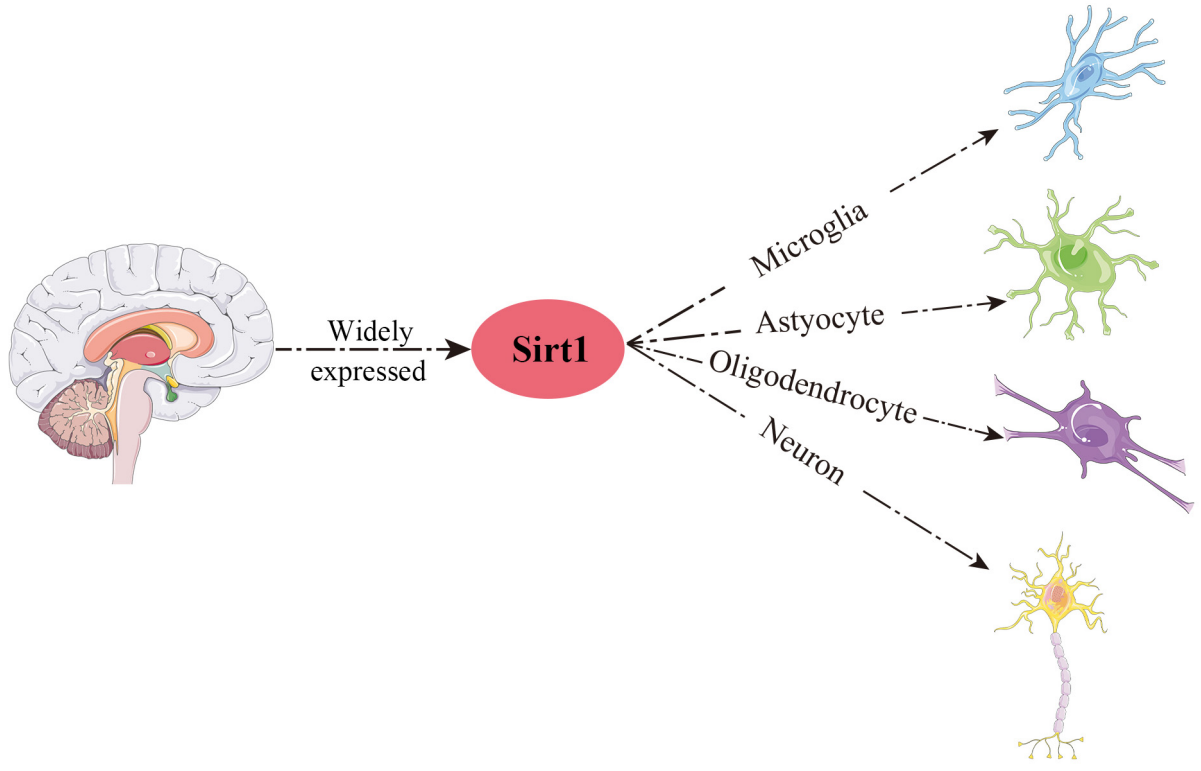

FIGURE 2
Schematic overview of the main distribution of Sirt1 in the CNS.

Conversely, Deleted in Breast Cancer-1 (DBC1) was reported to be a physiological inhibitor of Sirt1, which could directly interact with Sirt1 and suppress its activity (Kim et al., 2008). Deletion analysis revealed that the inhibition of Sirt1 deacetylation activity was attributed to DBC1's direct binding to the catalytic domain of Sirt1, which hindered the binding of Sirt1 with downstream molecules P53 and FOXO. And hyperacetylation of P53 and FOXO could augment cellular apoptosis under damaging stress, which may be the ability of DBC1 as a tumor suppressor (Kim et al., 2008).

TABLE 1 The major activators and inhibitors of Sirt1.

Sirt1 activators/inhibitors	Categories	Catalytic mechanism	References
Activators			
AROS	Physiological	Binding to the Sirt1 catalytic domain	Autiero et al., 2008
LARP7	Physiological	Strongly binding to the N-terminal domain of Sirt1	Yan et al., 2021; Yu H. et al., 2021
Resveratrol	Natural	(1) Binding with the N-terminal domain of Sirt1 and the related substrate at the same time (2) Interacting with LAMIN A	Liu et al., 2012; Cao et al., 2015
Quercetin	Natural	Binding to the helix2-turn-helix3 motif in the N-terminal domain of Sirt1	Zhang et al., 2021
Curcumin/Salvianolic acid B	Natural	Uncertain. Further studies are need to clarify the specific catalytic mechanism	Lv et al., 2015; Zhang et al., 2017; Ling et al., 2018
SRT1720	Synthetic	Binding to the Sirt1-substrate complex at the allosteric site of the amino terminal catalytic region	Milne et al., 2007
Inhibitors			
DBC1	Physiological	Binding to the catalytic domain of Sirt1	Kim et al., 2008
Suramin	Natural	Tightly binding to Sirt1 catalytic domain, and simultaneously occupy the binding region of NAD + and the substrate	Trapp et al., 2007
EX527	Synthetic	Specifically binding to Sirt1 to inhibit the formation of the Sirt1-substrate complex	Gertz et al., 2013

Natural

Resveratrol, a natural polyphenolic compound, presents in many plants and is identified as the natural activator of Sirt1, which plays an important role in several CNS disorders. Our previous studies found that resveratrol alleviated cerebral ischemic stroke injury by inhibiting neuronal apoptosis (Yu et al., 2017), attenuating oxidative stress (Shen et al., 2016), promoting synaptogenesis (Yu P. et al., 2021), and suppressing ferroptosis (Zhu et al., 2022). Some researchers also figured out that resveratrol could modulate autophagy (He et al., 2017) and inhibit activation of inflammasomes (Chiang et al., 2022) to improve the ischemic injury. As the activator of Sirt1, resveratrol functions by binding with the N-terminal domain of Sirt1 and the related substrate at the same time, thereby promoting the tighter combination of Sirt1 and substrate and Sirt1 deacetylation activity (Cao et al., 2015). In addition to directly activating Sirt1, resveratrol can also increase the activity of Sirt1 by interacting with LAMIN A, which is a key protein for maintaining nuclear structure (Liu et al., 2012).

Quercetin is a natural flavonoid, which exists in many fruits and vegetables (Cui et al., 2022). A recent study indicated that quercetin maintained the BBB integrity and inhibiting reactive oxygen species (ROS) generation through activating Sirt1, thereby improving neurological function after ischemic stroke (Yang R. et al., 2022). Recently, Zhang et al. (2021) found that quercetin activates Sirt1 activity by binding to the helix2-turn-helix3 motif in the N-terminal domain of Sirt1. Compared with resveratrol, quercetin can more effectively activate Sirt1 deacetylase activity and enhance the binding of Sirt1 to the substrate acetylated P53 (Zhang et al., 2021). Curcumin and salvianolic acid B, also as natural polyphenols, performs the similar characteristics of activating Sirt1 as resveratrol does. The neuroprotective effects mediated by them were mainly attributed by reducing the release of inflammatory factors and cellular apoptosis through activating Sirt1 (Lv et al., 2015; Zhang et al., 2017; Ling et al., 2018). However, although enough studies had confirmed that both of them could activate Sirt1 to exert their neuroprotection, the molecular mechanism of their activation of Sirt1 remains to be clarified.

Conversely, Suramin, extracted from pine needles, was first used to manage trypanosomiasis and nematode disease, and was later reported to have certain anti-tumor activity and anti-apoptosis effects. The co-crystal structure analysis showed that suramin can tightly bind to Sirt1 catalytic domain, and simultaneously occupy the binding region of NAD + and the substrate, thereby inhibiting Sirt1 deacetylase activity (Trapp et al., 2007).

Synthetic

High-throughput screening found that SRT1720 was a potential Sirt1 activator, and it performed a much stronger property to activate Sirt1 than resveratrol. Similar to resveratrol, SRT1720 binds to the Sirt1-substrate complex at the allosteric site of the amino terminal catalytic region, thereby promoting Sirt1 deacetylation activity (Milne et al., 2007). It was reported that application of SRT1720 could provide the neuroprotective effects by regulating autophagy (Bai et al., 2021), inhibiting neuroinflammation (Wang F. et al., 2019) and promoting microglia polarization (Xia et al., 2021) through activating Sirt1. Similar to SRT1720, SRT2104 was also found to efficiently activate Sirt1 to alleviate brain damage after ischemic stroke by regulating microglia polarization (Fu et al., 2021).

Conversely, several chemical compounds have performed their ability to suppress Sirt1 activity. Since its discovery in 2005, EX527 has become one of the most effective selective inhibitors of Sirt1. EX527 can specifically bind to Sirt1 to inhibit the formation of the Sirt1-substrate complex, which leads to the acceleration of substrate acetylation (Gertz et al., 2013). In addition to EX527, sirtinol is also the effective inhibitors of Sirt1 and involved in the development of cerebral ischemic injury and neurological damage (Tang et al., 2017).

Crucial role of Sirt1 in neurodegenerative diseases

Neurodegenerative diseases, such as Alzheimer's disease (AD), Parkinson's disease (PD), and Huntington's disease, are chronic conditions characterized by neuronal dysfunction and loss. Recent studies have highlighted the role of Sirt1 in regulating synaptic plasticity and mitigating neurodegenerative damage within the CNS. The levels of Sirt1 protein were found to be significantly reduced in patients with neurodegenerative diseases compared to those undergoing normal aging, suggesting that diminished Sirt1 expression and activity contribute to the pathological progression of these conditions (Cao et al., 2018). Moreover, overexpression of Sirt1 can modulate the impact of Aβ in AD and impede the formation of synuclein aggregates in PD. Conversely, the inactivation of Sirt1 has shown potential to ameliorate the mitochondrial apoptosis pathway, which is implicated in the pathogenesis of aging, metabolic disorders, and neurodegenerative diseases (Rana et al., 2019). In summary, Sirt1 may play a crucial role in neurodegenerative diseases.

Neuroprotective role of Sirt1 for ischemic stroke

As a survival factor against the aging process, Sirt1 has been shown to exert neuroprotective effects in the neurodegenerative diseases, such as AD, PD, and Huntington's disease. Recent studies have found that Sirt1 can alleviate ischemic stroke injury, including reducing cerebral infarcted volume and neurological deficits. Next, we will discuss the progresses of Sirt1 in animal models and clinical trials of ischemic stroke in recent years.

Clinical trials

In 2021, a case-control study showed that the activity of Sirt1 in the serum of patients with acute ischemic stroke (AIS) was significantly lower than that of the control group, and its levels were significantly negatively correlated with the stroke score, which suggested that Sirt1 could be used as a potential biomarker for predicting the risk of AIS (Esmayel et al., 2021). However, another clinical trial reached the opposite conclusion. The researchers found that Sirt1 activity increased sharply after ischemic stroke, and there was no significant correlation between its activity and stroke score, which blocked its opportunity as a biomarker for prognosticating the functional outcome of AIS patients (Liu et al., 2018). These studies suggest that Sirt1 expression may be a dynamic process after stroke, so further study with larger sample and more accurate grouping was needed to clarify its role in ischemic stroke.

Subsequently, a cohort study focused on evaluating the effects of Sirt1 activator resveratrol on blood pressure, weight status, glucose, and lipid profile which are the main risk factors for ischemic stroke. It was found that resveratrol can significantly reduce these parameters at 6 and 12 months after the initial evaluation, which suggested that resveratrol could serve as the promising drug to prevent ischemic stroke (Fodor et al., 2018). Another clinical trial also reported the neuroprotective effects of resveratrol on AIS patients. As the most effective method to treat ischemic stroke, recombinant tissue plasminogen activator (r-tPA) is severely limited by its narrow therapeutic window. Chen et al. (2016) found that resveratrol can prolong the clinical therapeutic window of r-tPA and reduce the MMP-induced neurological deficits, thus improving the prognosis of AIS patients receiving r-tPA treatment at a later stage.

These clinical evidences suggest that Sirt1 has potential as a target for prevention and treatment for AIS patients, and can be used as a prognostic indicator of ischemic stroke.

Animal studies

Similar to the results of clinical trials, Sirt1 expression in rodent models was modulated by ischemic injury as well. For instance, Sirt1 was upregulated significantly in ischemic penumbra from 18 h to 7 days after ischemic stroke (Hernández-Jiménez et al., 2013). However, another study reached the opposite conclusion. They found that compared with control group, the level of Sirt1 in middle cerebral artery occlusion (MCAO) group decreased sharply (Kalaivani et al., 2014). The huge difference in results may be attributed to different species and different model construction used in such two studies.

In order to further clarify the role of Sirt1 in cerebral ischemic/reperfusion (I/R) injury, researchers constructed its overexpression and knockout model through genetic manipulation technology. Compared with wild-type model, Sirt1$^{-/-}$ mice subjected to permanent MCAO performed the larger infarct size (Hernández-Jiménez et al., 2013). Conversely, overexpressing Sirt1 could reduce hippocampal injury after bilateral common carotid artery occlusion (Hattori et al., 2015). In summary, activation of Sirt1 has neuroprotective effects and regulates the outcome of cerebral ischemic injury.

Potential mechanisms of Sirt1 for ischemic stroke

Studies in animal models and clinical trials have shown that Sirt1 is an efficient treatment for ischemic stroke. How does Sirt1 play a therapeutic role? What are the therapeutic targets for Sirt1? The specific mechanisms of Sirt1 for regulating cerebral ischemic stroke will be discussed in the following section (**Figure 3**).

Anti-oxidative stress

Oxidative stress is one of the earliest outcomes in the period of ischemic stroke, causing cascades of cellular and molecular processes that leads to neurodegeneration and death of neurons. Increased levels of ROS in cells, such as hydroxyl radicals, can result in oxidative stress and mitochondrial dysfunction, which can lead to cerebral ischemia and further aggravate the cerebral injury. Sirt1 has been identified as playing an essential role in oxidative stress. Sirt1 is activated after the onset of stroke and can regulate multiple signaling pathways to affect oxidative stress, further modulating the pathological process of stroke.

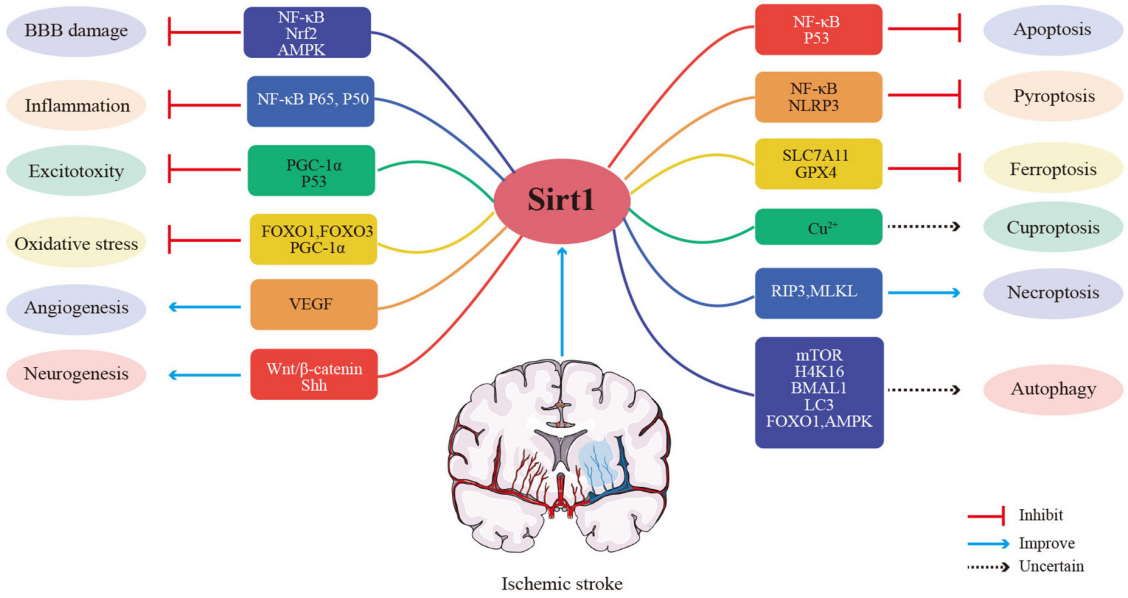

FIGURE 3
Potential mechanisms of Sirt1 for ischemic stroke.

The anti-oxidant properties of Sirt1 rely basically on targeting the FOXO transcription factors. Specifically, FOXO3 has been demonstrated to play an essential role in the regulation of oxidative stress, which can upregulate the expression of several antioxidant proteins, including superoxide dismutase, manganese superoxide dismutase, and catalase. FOXO3 can be phosphorylated and deacetylated to regulate its transcriptional activity.

In addition, deacetylation of FOXO3 by Sirt1 can prevent cell death induced by FOXO3. Zhang et al. (2022) found that Bergenin hampered the production of inflammatory factors and oxidative stress mediators by boosting the Sirt1/FOXO3 pathway. Similarly, the lncRNA SNHG12 also performed the anti-oxidant effects in ischemic model by activating Sirt1/FOXO3 pathway.

In addition, FOXO1 and FOXO3 can regulate the level of peroxisome proliferator-activated receptor gamma co-activator 1-α(PGC-1α). PGC-1α is involved to the oxidative phosphorylation and ROS detoxification, contributing to maintaining metabolic homeostasis. PGC-1α upregulation could reduce the oxidative stress-mediated neuronal death (St-Pierre et al., 2006). Reversely, PGC-1α depletion further increased the cellular injury induced by oxidative stress (Pérez et al., 2019). Moreover, Calycosin-7-glucoside reduced neuronal death mediated by oxidative stress through activating Sirt1/FOXO1/PGC-1α signaling pathway (Yan et al., 2019). Similarly, Xie et al. (2020) found that notoginseng leaf triterpenes, a natural ingredient, suppressed the excessive oxidative stress and mitochondrial damage at least partly via Sirt1/FOXO3/PGC-1α axis. These studies suggest that Sirt1 has anti-oxidant stress effect.

Anti-inflammation

Inflammatory response plays a crucial role in the pathophysiology of stroke because it runs through the whole process. The nuclear factor kappa B (NF-κB) is a major transcription factor of inflammation, which can be specifically activated after cerebral ischemic stroke. Sirt1 can alleviate cerebral ischemia/reperfusion injury by regulating NF-κB pathway. For example, Sirt1 regulated the transcriptional activity of NF-κB by directly deacetylating NF-κB P65, thereby modulating the expression of inflammatory cytokine TNF-α (Yeung et al., 2004). Sirt1 activator resveratrol could reduce OGD/R-mediated neuronal death and neuroinflammation by regulating NF-κB p50 deacetylation (Lanzillotta et al., 2010). Besides acetylation modification, Sirt1 can also mitigated NF-κB phosphorylation to alleviate microglia inflammation (Hu et al., 2022). In addition, Sirt1 can indirectly modulate NF-κB pathway through other targets, including TLR4, FOXO3, Nrf2 and so on. Specifically, Bergenin inhibited the expression of inflammatory factors in MCAO model via Sirt1/FOXO3/NF-κB pathway (Zhang et al., 2022). TLR4 was also involved in the regulation of Sirt1 on NF-κB-mediated inflammatory response (Le et al., 2019). And Sirt1 can modulate Nrf2-NF-κB signaling pathway thereby reducing inflammatory respose and protect neurons from OGD damage (Zheng et al., 2022). Taken together, Sirt1 can downregulate the inflammatory response after cerebral ischemia by directly or indirectly regulating NF-κB signaling pathway.

Affecting excitotoxicity

Glutamate is a primary excitatory amino acid neurotransmitter and activation of glutamate receptors including *N*-methyl-D-aspartate (NMDA) receptor plays crucial roles in the central nervous system. However, excessive NMDA receptor can result in intracellular calcium overload, leading to an enzymatic cascade of events resulting ultimately in cell death known as

excitotoxicity. NMDA-mediated excitotoxicity has been associated with a variety of nervous system diseases, including stroke and epilepsy. Therefore, better management of excitotoxicity is of great significance for maintaining brain homeostasis and alleviating neurological damage after cerebral ischemic stroke.

The recent study suggested that Ca-PKC-HuR-Sirt1 axis was involved in the glutamate-mediated excitotoxicity, and Sirt1 is the key node (Yang et al., 2020). Subsequently, it was reported that Sirt1 protected cerebral cortical and hippocampal neurons from glutamate-induced injury, which was mainly due to its ability to deacetylate PGC-1α (Jia et al., 2016; Yue et al., 2016). Interestingly, Yang et al. (2017) found that Sirt1 activator resveratrol could also shield cortical neurons from glutamate-induced excitotoxicity through suppressing P53 acetylation. Moreover, the inhibition of Sirt1 on excitotoxicity has also been verified in rodent model. Recent reportedly, α-amino-3-hydroxy-5-methyl-4-isoxazolepropionic acid-mediated excitotoxicity led to a progressive motor neuron degeneration and motor deficits. Quercetin could improve these neurological deficits, and its protective effects was reversed by Sirt1 inhibitor EX527, which implicated the crucial role of Sirt1 on exerting the neuroprotection by suppressing excitotoxicity (Lazo-Gomez and Tapia, 2017).

In summary, these evidences have proved that Sirt1 is a potential target for blocking glutamate-induced excitotoxicity. However, further study is needed to confirm whether and how Sirt1 diminishes excitotoxicity after ischemic stroke.

Regulating BBB damage

It is well known that BBB is served as the first line of defense to prevent harmful substances from entering the brain and is vital for maintaining brain homeostasis. BBB consists primarily of tightly connected brain microvascular endothelial cells (BMECs), basement membrane, astrocyte end-foot, and pericytes. Disruption of BBB integrity leads to further damage to the brain after ischemic stroke. Increasing evidence suggests that Sirt1 can regulate ischemia-induced BBB damage, thus providing neuroprotection.

BMECs play an essential role in maintaining BBB integrity. CaMKK (α and β), a major kinase activated by elevated intracellular calcium, has been shown to activate Sirt1, a key endothelial protector. Recently, Sun et al. found that CaMKK activation may attenuate ischemic brain injury by protecting the brain microvascular system through Sirt1. Another research implied that lncRNA Snhg8 could relieve ischemic injury of BMECs both *in vitro* and *in vivo* by targeting Sirt1-mediated NF-κB pathway through sponging miR-425-5p. It was suggested that Snhg8/miR-425-5p/Sirt1/NF-κB axis plays a critical role in the regulation of cerebral ischemia-induced BBB damage. Similarly, circHIPK3 acted as an endogenous sponge of miR-148b-3p to decrease its activity, resulting in downregulation of Sirt1 expression and subsequent BMEC apoptosis and mitochondrial dysfunction, further exacerbating BBB damage (Chen G. et al., 2022). In addition, Sirt1 agonist quercetin ameliorates neurological deficits and BBB integrity through Sirt1/Nrf2/HO-1 signaling, and its protective effect is partially reversed by the Sirt1 inhibitor EX527.

Although most investigators have confirmed the positive role of Sirt1 in improving BBB damage in ischemic stroke, there are still some studies that contradict these findings. It was reported that Sirt1 was involved to regulate expression of Sirt3, induction of apoptosis, and production of ROS by inhibiting AMPK-PGC1 pathway, thereby increasing BBB permeability.

Further studies are required to elucidate the specific mechanism of Sirt1 for regulating BBB and thus explain the contradiction in these studies.

Controlling programmed cell death

Cell death includes uncontrolled accidental cell death and programmed cell death (PCD), which can be activated during trauma, ischemia, hemorrhage, inflammation, oxidative stress, and so on. PCD is induced by one or more signals and can be managed through pharmacological or genetical intervention, including apoptosis, necroptosis, autophagy, pyroptosis and ferroptosis. Recently, cuproptosis has been recognized as a novel PCD. Growing studies have revealed that Sirt1 can alleviate cerebral ischemic injury by regulating the occurrence of PCD. Thus, we provided supporting data that Sirt1 regulated PCD in ischemic stroke.

Apoptosis

Apoptosis is a programmed cell death process that relies on caspase activity and is characterized by cell shrinkage, membrane blebbing, and chromatin condensation. It can be activated by either the intrinsic or extrinsic pathway (Carneiro and El-Deiry, 2020). Specifically, the pro-apoptotic proteins of the B-cell lymphoma 2 (Bcl-2) family increase the permeability of the outer mitochondrial membrane, which leads to the activation of caspase proteases and eventually, cell disintegration. Sirt1 plays an important role in endogenous neuroprotection against ischemic stroke due to its anti-apoptotic effects (Gao et al., 2022). Inhibition of Sirt1 exacerbates ischemic injury accompanied by increased acetylation of P53 and NF-κB P65, which are important factors in apoptotic pathways that cause brain damage (Hernández-Jiménez et al., 2013).

Maresin 1 (MaR1), a mediator released by M2 macrophages, has been shown to possess anti-inflammatory and anti-apoptotic properties in several diseases (Li et al., 2021; Li H. et al., 2022; Yang W. et al., 2022). In ischemic stroke, MaR1 inhibited apoptosis and reduced injury by up-regulating expression of Sirt1 and Bcl-2 and down-regulating expression of acetylated NF-κB and Bax, Sirt1 inhibitor EX527 could partially reverse the effects, which suggested that the Sirt1/P65 signaling was specifically involved in MaR1-mediated protection against ischemic stroke (Xian et al., 2019). In OGD model of PC12 cells, kaempferol, a natural flavonol, reduces P66shc expression, promotes the deacetylation of P66shc by up-regulating Sirt1, and inhibits cellular apoptosis and mitochondrial dysfunction. This suggested that kaempferol inhibited OGD-mediated apoptosis via Sirt1/p66shc axis (Zhou and Li, 2020).

QIK 6 is a member of the STAR family and has recently been found to be predominantly expressed in primary neurons.

Its neuroprotective effects against ischemic stroke have been demonstrated, and Sirt1 is considered the most critical node in this process. On the one hand, Sirt1 induced the deacetylation of QIK 6; on the other hand, Sirt1 activated PPARγ/PGC-1α Signal pathway, both of which could promote synthesis of triglyceride and inhibit neuronal apoptosis, thus slowing the progression of stroke. In a word, Sirt1 mediated the synthesis of triglyceride and inhibition of neuronal apoptosis after stroke, which was associated with the QKI 6 and the PPARγ/PGC-1α signaling pathway (Liu R. et al., 2021).

MicroRNAs (miRs) regulate gene expression by inhibiting protein translation and targeting mRNA destabilization/degradation (Szabo and Bala, 2013). Increasing evidence has indicated that miRs play a key role in various pathological processes, including inflammation, neurodegeneration and cellular apoptosis (Di Leva et al., 2014). It was reported that the miR-149-5p levels were markedly decreased at 24 h after cerebral I/R injury, and Sirt1 natural activator resveratrol could increase its activity accompanied by the downregulation of P53 and caspase-3. This implied that miR-149-5p was involved in the regulation of caspase-3- mediated apoptotic neuronal cell death via Sirt1/P53 axis (Teertam et al., 2020). Another study demonstrated that miR-489-3p was also involved in the regulation of Sirt1 on apoptosis in ischemic stroke (Song et al., 2022). After ischemic stroke, miR-489-3p was upregulated, while Sirt1 was downregulated. Silencing miR-489-3p inhibited neuronal apoptosis and improved neurological function by targeting Sirt1. Moreover, a recent report identified Sirt1 as a target gene of miR-142-3p. The study revealed that miR-142-3p can modulate neuronal apoptosis after ischemic stroke by targeting Sirt1 (Meng et al., 2023). These studies showed that the anti-apoptotic effects of various substances in ischemic stroke are achieved by targeting Sirt1. Therefore, Sirt1 may be one of the key targets for regulating apoptosis.

Pyroptosis

Pyroptosis is a form of regulated necrosis, triggered by inflammatory Caspase-1 after its activation by various inflammasomes, which can mediate the effect of Gasdermin-D protein, leading to cell lysis and extracellular release of the cytosolic contents and secretion of pro-inflammatory mediators, such as interleukin (IL)-1β and IL-18, resulting in the excessive inflammatory response (Sharma and Kanneganti, 2021). Specifically, The NLRP3 inflammasome is among the most prominent inflammasomes, with high expression levels in the brain, as it plays a crucial role in detecting cell damage and initiating an inflammatory cascade. Several studies have indicated that the NLRP3 inflammasome plays an essential part in the occurrence and development of cerebral I/R injury (Heinisch et al., 2022; Kerr et al., 2022), and the activation of Sirt1 can exert the neuroprotection via inhibition of this pathway (Zhou et al., 2023).

Growing evidence indicates that mesenchymal stem cells (MSCs) affect the pathological processes of ischemic stroke via multiple targets and multitemporal, including reducing inflammation, modulating immune function, inhibiting apoptosis, promoting neurovascular regeneration, enhancing autophagy, and more (Zhou et al., 2022; Szydlak, 2023; Xie et al., 2023; Xu et al., 2023). A recent study indicated neuroprotective effects of bone MSCs transplantation, including reducing infarct size, improving motor function and behavioral outcomes, and downregulating NLRP3 inflammasome expression. However, all these positive effects were reversed by the Sirt1 specific inhibitor EX-527 through the regulation of NF-κB pathway (Sarmah et al., 2022). During the hyperacute phase of ischemic stroke, researchers observed the suppression of Sirt1 and upregulation of TRFA6 protein and ROS levels were observed. Activation of Sirt1 exerted its neuroprotection by inhibiting cellular pyroptosis after stroke via the ROS-TRFA6 signaling pathway (Yan et al., 2020).

Resveratrol, a specific Sirt1 agonist, performed the positive effect on the inhibition of NLRP3 inflammasome and neuroprotection after embolic stroke. Furthermore, it attenuated I/R-induced NLRP3 inflammasome-derived inflammation and upregulated autophagy. Sirt1 knockdown significantly blocked resveratrol-induced enhancement of autophagy activity and suppression of NLRP3 inflammasome activation, which implied that resveratrol protects against cerebral I/R injury by inhibiting NLRP3 inflammasome activation through Sirt1-dependent autophagy activity (He et al., 2017).

Recently, several studies indicated that acetylation of NLRP3 is required for the assembly and activation of the NLRP3 inflammasome (Zhao et al., 2019). So, suppressing acetylation of NLRP3 can inhibit the incidence and development of pyroptosis. Zhang et al. demonstrated that Sirt2 improved aging-associated chronic inflammation and insulin resistance by promoting NLRP3 deacetylation (He et al., 2020). Moreover, the inhibitory effect of Sirt1 on NLRP3 acetylation was also found in adipose tissue inflammation (Chen C. et al., 2022). Although various inhibitory mechanisms of Sirt1 on NLRP3 inflammasome have been discussed, whether Sirt1 exerts a protective effect on ischemic stroke by directly regulating NLRP3 deacetylation to inhibit pyroptosis remains unknown.

Autophagy

Autophagy-dependent death, known as type 2 programmed cell death, is essential for maintaining cellular homeostasis in both physiological and pathological processes (Debnath et al., 2023). However, it is still unclear whether it has a positive or negative impact. Generally, in the nervous system, moderate autophagy has neuroprotective effects, while inadequate or excess autophagy may lead to neuronal death. Recently, autophagy has been recognized as a critical process in ischemic stroke in addition to neurodegenerative diseases (Yang Z. et al., 2022). And growing evidence suggests that Sirt1 may promote neuronal cell survival and alleviate cerebral I/R injury by modulating autophagy process (Tang et al., 2022; Teertam and Phanithi, 2022).

Nicotinamide phosphoribosyltransferase (Nampt), the rate-limiting enzyme in mammalian NAD^+ biosynthesis, has been found to have a positive effect on ischemic stroke treatment. Besides inhibiting neuronal apoptosis and necrosis, Nampt promotes neuronal survival through inducing autophagy via

regulating TSC2-mTOR-S6K1 signaling pathway in a Sirt1-dependent manner during cerebral ischemia (Wang et al., 2012). Nicotinamide mononucleotide adenylyltransferase also showed the similar therapeutic potential as Nampt for cerebral ischemia. It was reported that Nicotinamide mononucleotide adenylyltransferase protects against acute ischemic stroke in aged rats by inducing autophagy via regulating the Sirt1/mTOR pathway (Wang P. et al., 2019).

Electroacupuncture (EA) treatment is a promising therapy for ischemic stroke, however, the specific mechanism is still elusive. It is recently reported that EA treatment may inhibit apoptosis by regulating autophagy in the acute phase of ischemic stroke, thereby alleviating brain injury, and Sirt1 may play a crucial role in the regulation of autophagy in EA treatment for ischemic stroke (Xing et al., 2021). Xu et al. (2020) further tested the role of Sirt1 on regulating autophagy after ischemic stroke. They found that EA treatment inhibited the histone H4K16 acetylation process through Sirt1, facilitated autophagy, and alleviated I/R injury.

Diabetic brains are more vulnerable to I/R injury, but melatonin treatment has been found to protect against cerebral I/R-induced brain damage in both normal and diabetic mice by enhancing autophagy through the Sirt1-BMAL1 pathway (Liu L. et al., 2021).

Cerebral I/R injury induced by hemorrhagic shock and reperfusion is the main cause of death following trauma. Sirt1 was involved in the neuroprotective effects of sevoflurane post-conditioning on regulation of defective autophagy, mitochondrial oxidative injury, and neuronal death caused by hemorrhagic shock and reperfusion (Shu et al., 2022).

In addition to indirect regulation, Sirt1 can also directly modulate the deacetylation of the autophagy-related protein to induce autophagy. LC3, a key initiator of autophagy, became selectively activated in the nucleus during starvation through deacetylation by Sirt1. Deacetylation of LC3 at K49 and K51 by Sirt1 allows LC3 to interact with the nuclear protein DOR and return to the cytoplasm where it functioned as autophagy initiation (Huang et al., 2015). Recently reported, deacetylation of beclin1 was also mediated by Sirt1, which improved the acute kidney injury via activation of autophagy (Deng et al., 2021). However, the direct regulatory effect of Sirt1 on autophagy in stroke remains unclear and needs to be confirmed by further studies.

Interestingly, Sirt1 not only can induce autophagy after ischemic stroke, but also has a negative regulatory effect on autophagy.

The activation of Sirt1/FOXO1 pathway by Betulinic acid, a pentacyclic triterpene acid mainly extracted from birch bark, suppressed the autophagy, which improved the brain damage after ischemic stroke (Zhao et al., 2021). Magnoflorine, a natural compound with anti-oxidant and immunomodulatory effects, has also been found to protect against ischemic stroke by inhibiting autophagy through the activation of the Sirt1/AMPK pathway (Liang et al., 2022).

As mentioned above, there is bidirectional regulation of autophagy by Sirt1 in stroke. Further studies are needed to thoroughly understand the regulatory effect of Sirt1 on autophagy, which is of great significance for the prevention and treatment of stroke.

Necroptosis

Necroptosis is a programmed type of cell death mediated by receptor-interacting serine/threonine-protein kinase (RIPK) 1, RIPK3, and mixed lineage kinase like protein (MLKL), which is characterized by cellular organelle swelling and cell membrane rupture (Albani et al., 2010). This process plays a critical role in both physiological and pathological conditions, and Sirt1 has been shown to protect against necroptosis in various disease models, including cancer (Carafa et al., 2018), acute lung injury (Liu et al., 2022) and liver fibrosis (Sun et al., 2022). However, a study of ischemic stroke has yielded contradictory results. Specifically, RIP3 and MLKL levels were found to increase in the prefrontal cortex and hippocampus of rat brains during the 24 h after I/R injury.

Surprisingly, the Sirt1 inhibitor EX-527 was shown to be as effective as necrostatin-1 in suppressing the elevation of RIP3 and MLKL, leading to reduced infarct volumes, which indicated that suppression of Sirt1 provided the neuroprotection against ischemic stroke by inhibiting necroptosis. Further studies are needed to elucidate the interaction between Sirt1 and necroptosis following ischemic stroke.

Ferroptosis

Ferroptosis is a form of programmed cell death that depends on iron overload and lipid peroxidation, and has gained significant attention since its discovery in Lei et al. (2022). Excessive intracellular iron accumulation results in the production of reactive oxygen species (ROS) through the Fenton reaction, causing lipid peroxidation and subsequent ferroptosis. Studies have shown that iron deposition, lipid peroxidation, and neuronal death in the brain were significantly increased in an adult rat model of ischemic stroke (Ye et al., 2022).

Glutathione peroxidase 4 (GPX4) plays an important role in suppressing ferroptosis, which functions to reduce lipid peroxides in cellular membranes.

Silent mating type information regulation 2 homolog 1 activator resveratrol exhibited the positive effects on inhibiting ferroptosis via upregulation of GPX4, which exerted neuroprotection against ischemic stroke. Our previous research found that resveratrol pretreatment had a similar effect as ferroptosis inhibitors, ferrostatin-1 on inhibiting neuronal ferroptosis-related changes, such as iron overload, damages of oxidation-reduction system, and destruction of mitochondrial structure, with the upregulation of GPX4 (Zhu et al., 2022). Similarly, Li C. et al. (2022) found that resveratrol inhibited hippocampal neuronal ferroptosis by activating Sirt1/Nrf2/GPx4 signaling pathway, thereby improving the cognitive impairment.

Furthermore, it was recently demonstrated that Sirt1 participated in the neuroprotection against ischemic stroke both *in vivo* and *in vitro* by inhibiting ferroptosis via SLC7A11, another key executor of ferroptosis. Further researches are needed to determine whether Sirt1 can inhibit ferroptosis by directly regulating the deacetylation of ferroptosis-associated molecules and thus exert neuroprotective effects.

Cuproptosis

Copper is an indispensable cofactor for all organisms, but excessive intracellular copper induces cell death, thus causing toxic effects on the body. Recently, Todd R. Golub and Peter Tsvetkov et al. (2022) found a new sort of copper-dependent programmed cell death, and named it cuproptosis. Cuproptosis occurs through direct interaction of copper with the fatty acylated components of the tricarboxylic acid cycle, leading to excessive aggregation of fatty acylated proteins and loss of iron–sulfur cluster proteins, which stimulates proteotoxic stress and cell death. In ischemic stroke patients, the level of copper in serum and urine was significantly increased (Lai et al., 2016). However, it requires further to be clarification whether excessive copper induces cuproptosis of neurons and whether Sirt1 played a key role in regulating cuproptosis.

Promoting angiogenesis

Angiogenesis can promote the survival and recovery of patients with ischemic stroke by restoring blood supply to the affected regions. Emerging evidence has indicated the involvement of Sirt1 in post-stroke angiogenesis, which is a complicated process regulated by angiogenic factors, such as vascular endothelial growth factor (VEGF) (Simão et al., 2012; Hermann et al., 2015; Zheng et al., 2018).

Hypoxia inducible factor 1α (HIF-1α) is the core regulatory factor of post-stroke angiogenesis, which can upregulate the expression of key angiogenic factors, such as VEGF and its receptor, thereby promoting post-stroke angiogenesis. The interaction between Sirt1 and HIF-1α was first reported in Lim et al. (2010). It revealed that Sirt1 could interact with HIF-1α and deacetylate its 647 lysine to inhibit its activity and thereby suppressing angiogenesis. Conversely, a recent study has indicated that Sirt1 can promote the proliferation and migration of hypoxia/high glucose induced-BMECs by activating HIF-1α/VEGF pathway, which is the important process of angiogenesis (Mi et al., 2019). Further studies are needed to clarify the relationship between Sirt1 and HIF-1α-mediated angiogenesis.

Vascular endothelial growth factor acts directly on endothelial cells and is a critical node in the angiogenic process. Choi et al. (2017) found that Sirt1 could upregulate the expression of VEGF through inducing PGC-1α deacetylation and ubiquitination to promote angiogenesis. Furthermore, Donepezil was reported to increase the viability and migration of OGD/R-induced human BMECs and expression of VEGF via Sirt1/FOXO3a/NF-κB pathway (Sun and Liu, 2022). The Notch signaling pathway and VEGF exhibit a synergistic effect in angiogenesis, especially in the process of tube formation (Gerhardt et al., 2003). Notoginsenoside R1, a natural constituent, could promote angiogenesis via Notch/VEGF signaling pathway, which was partially reversed by Sirt1 inhibitor EX527 (Zhu et al., 2021). However, it remains unclear how Sirt1 regulates the interaction between Notch signaling and VEGF to promote angiogenesis in ischemic stroke.

Enhancing neurogenesis

Neurogenesis, which involves the proliferation and differentiation of neural stem cells (NSCs), is crucial for functional recovery after ischemic stroke. Sirt1 has shown the potential property of inducing neurogenesis primarily through sonic hedgehog (Shh) signaling and Wnt/β-catenin signaling.

It was found that up-regulation of Sirt1 activity by momordica charantia polysaccharides induced the cytoplasmic deacetylation of β-catenin, which mediated the translocation of β-catenin into the nucleus, thus promoting NSCs proliferation in the subventricular and subgranular zones of cerebral I/R rats on the one hand (Ma et al., 2021), and transferring the differentiation potential of NSCs from the gliogenic to neurogenic lineage under pathological conditions on the other hand (Hu et al., 2020). Taken together, Sirt1 can induce neurogenesis, including NSCs proliferation and differentiation, thereby promoting recovery from cerebral I/R injury.

Sonic hedgehog signaling plays a critical role in regulating stem cell behavior and promoting neurite outgrowth and synaptogenesis in both developing and adult brains. Our previous studies suggested that Sirt1 activator resveratrol pretreatment enhanced NSCs proliferation *in vitro* (Cheng et al., 2015) and *in vivo* (Yu H. et al., 2021) after cerebral I/R injury, and induced the differentiation of bone MSCs into neuronal-like cells via activation of the Shh signaling (Huang et al., 2014).

In conclusion, Sirt1 has shown its protective effects on endogenous NSCs proliferation and differentiation. However, further studies are necessary to clarify whether Sirt1 contributes to the survival of exogenous stem cell transplantation.

Conclusion and perspectives

Ischemic stroke has long caused concern among medical professionals as one of the leading causes of death worldwide. Therefore, the need for novel treatment modalities is urgent at the moment. The data we gathered has identified activated Sirt1 as a potential therapy. It is clear that Sirt1 is able to protect against pathological situations like cerebral ischemia injury and sustain brain homeostasis when acting physiologically. Numerous pharmacological agents that stimulate Sirt1 have been thoroughly described above and have demonstrated the potential for clinical transformation. However, despite these encouraging findings, there is still a lack of clinical proof to support the claim that Sirt1 protects against ischemia stroke. Additional research is needed to substantiate this claim.

The specific mechanism by which Sirt1 promotes neuroprotection in ischemic stroke is not yet completely clear. Therefore, further investigation is required to identify the precise target of Sirt1, which will aid in the development of novel treatment strategies for ischemic stroke. In summary, Sirt1 is undoubtedly a promising candidate therapeutic target for ischemic stroke.

Author contributions

HT, JW, and TQ: data curation. HT, JW, TQ, and YC: framework design. HT: writing and original draft preparation. JH, QhY, and PJ: language and format revision. QiY: review and editing. HT, LW, and YZ: revision and supervision. All authors contributed to the article and approved the submitted version.

Funding

This work was supported by grants from the National Natural Science Foundation of China (Grant nos. 82171456 and 81971229), the Natural Science Foundation of Chongqing (Grant no. cstc2021jcyj-msxmX0263).

Conflict of interest

The authors declare that the research was conducted in the absence of any commercial or financial relationships that could be construed as a potential conflict of interest.

Publisher's note

References

Ahmadi, M., Laumeier, I., Ihl, T., Steinicke, M., Ferse, C., Endres, M., et al. (2020). A support programme for secondary prevention in patients with transient ischaemic attack and minor stroke (INSPiRE-TMS): An open-label, randomised controlled trial. *Lancet Neurol.* 19, 49–60. doi: 10.1016/S1474-4422(19)30369-2

Al-Bahrani, R., Tuertcher, D., Zailaie, S., Abuetabh, Y., Nagamori, S., Zetouni, N., et al. (2015). Differential SIRT1 expression in hepatocellular carcinomas and cholangiocarcinoma of the liver. *Ann Clin. Lab. Sci.* 45, 3–9.

Albani, D., Polito, L., Signorini, A., and Forloni, G. (2010). Neuroprotective properties of resveratrol in different neurodegenerative disorders. *BioFactors* 36, 370–376. doi: 10.1002/biof.118

Autiero, I., Costantini, S., and Colonna, G. (2008). Human sirt-1: Molecular modeling and structure-function relationships of an unordered protein. *PLoS One* 4:e7350. doi: 10.1371/journal.pone.0007350

Bai, L., Liu, R., Wang, R., Xin, Y., Wu, Z., Ba, Y., et al. (2021). Attenuation of Pb-induced Aβ generation and autophagic dysfunction via activation of SIRT1: Neuroprotective properties of resveratrol. *Ecotoxicol. Environ. Safety* 222:112511. doi: 10.1016/j.ecoenv.2021.112511

Cao, D., Wang, M., Qiu, X., Liu, D., Jiang, H., Yang, N., et al. (2015). Structural basis for allosteric, substrate-dependent stimulation of SIRT1 activity by resveratrol. *Genes Dev.* 29, 1316–1325. doi: 10.1101/gad.265462.115

Cao, K., Dong, Y., Xiang, J., Xu, Y., Hong, W., Song, H., et al. (2018). Reduced expression of SIRT1 and SOD-1 and the correlation between these levels in various regions of the brains of patients with Alzheimer's disease. *J. Clin. Pathol.* 71, 1090–1099. doi: 10.1136/jclinpath-2018-205320

Carafa, V., Nebbioso, A., Cuomo, F., Rotili, D., Cobellis, G., Bontempo, P., et al. (2018). RIP1-HAT1-SIRT complex identification and targeting in treatment and prevention of cancer. *Clin. Cancer Res.* 24, 2886–2900. doi: 10.1158/1078-0432.CCR-17-3081

Carneiro, B., and El-Deiry, W. (2020). Targeting apoptosis in cancer therapy. *Nat. Rev. Clin. Oncol.* 17, 395–417. doi: 10.1038/s41571-020-0341-y

Chang, H., and Guarente, L. (2014). SIRT1 and other sirtuins in metabolism. *Trends Endocrinol. Metab.* 25, 138–145. doi: 10.1016/j.tem.2013.12.001

Chen, C., Ren, Y., Zhu, J., Chen, J., Feng, Z., Zhang, T., et al. (2022). Ainsliadimer C, a disesquiterpenoid isolated from Ainsliaea macrocephala, ameliorates inflammatory responses in adipose tissue via sirtuin 1-NLRP3 inflammasome axis. *Acta Pharmacol. Sin.* 43, 1780–1792. doi: 10.1038/s41401-021-00797-z

Chen, G., Shan, X., Li, L., Dong, L., Huang, G., and Tao, H. (2022). circHIPK3 regulates apoptosis and mitochondrial dysfunction induced by ischemic stroke in mice by sponging miR-148b-3p via CDK5R1/SIRT1. *Exp. Neurol.* 355:114115. doi: 10.1016/j.expneurol.2022.114115

Chen, J., Bai, Q., Zhao, Z., Sui, H., and Xie, X. (2016). Resveratrol improves delayed r-tPA treatment outcome by reducing MMPs. *Acta Neurol. Scand.* 134, 54–60. doi: 10.1111/ane.12511

Cheng, W., Yu, P., Wang, L., Shen, C., Song, X., Chen, J., et al. (2015). Sonic hedgehog signaling mediates resveratrol to increase proliferation of neural stem cells after oxygen-glucose deprivation/reoxygenation injury in vitro. *Cell. Physiol. Biochem.* 35, 2019–2032. doi: 10.1159/000374009

Chiang, M., Nicol, C., Lo, S., Hung, S., Wang, C., and Lin, C. (2022). Resveratrol mitigates oxygen and glucose deprivation-induced inflammation, NLRP3 inflammasome, and oxidative stress in 3D neuronal culture. *Int. J. Mol. Sci.* 23:11678. doi: 10.3390/ijms231911678

Choi, Y., Kim, J., Lee, D., Lee, K., Won, M., Jeoung, D., et al. (2017). Carbon monoxide potentiation of L-Type Ca channel activity increases HIF-1α-independent VEGF expression via an AMPKα/SIRT1-Mediated PGC-1α/ERRα Axis. *Antioxid. Redox Signal.* 27, 21–36. doi: 10.1089/ars.2016.6684

Cui, Z., Zhao, X., Amevor, F., Du, X., Wang, Y., Li, D., et al. (2022). Therapeutic application of quercetin in aging-related diseases: SIRT1 as a potential mechanism. *Front. Immunol.* 13:943321. doi: 10.3389/fimmu.2022.943321

Debnath, J., Gammoh, N., and Ryan, K. (2023). Autophagy and autophagy-related pathways in cancer. *Nat. Rev. Mol. Cell biol.* 24, 560–575. doi: 10.1038/s41580-023-00585-z

Deng, Z., Sun, M., Wu, J., Fang, H., Cai, S., An, S., et al. (2021). SIRT1 attenuates sepsis-induced acute kidney injury via beclin1 deacetylation-mediated autophagy activation. *Cell Death Dis.* 12:217. doi: 10.1038/s41419-021-03508-y

Di Leva, G., Garofalo, M., and Croce, C. (2014). MicroRNAs in cancer. *Annu. Rev. Pathol.* 9, 287–314. doi: 10.1093/neuonc/noz215

Esmayel, I., Hussein, S., Gohar, E., Ebian, H., and Mousa, M. (2021). Plasma levels of sirtuin-1 in patients with cerebrovascular stroke. *Neurol. Sci.* 42, 3843–3850. doi: 10.1007/s10072-021-05074-9

Fodor, K., Tit, D., Pasca, B., Bustea, C., Uivarosan, D., Endres, L., et al. (2018). Long-term resveratrol supplementation as a secondary prophylaxis for stroke. *Oxid. Med. Cell. Longev.* 2018:4147320. doi: 10.1155/2018/4147320

Frye, R. (1999). Characterization of five human cDNAs with homology to the yeast SIR2 gene: Sir2-like proteins (sirtuins) metabolize NAD and may have protein ADP-ribosyltransferase activity. *Biochem. Biophys. Res. Commun.* 260, 273–279. doi: 10.1006/bbrc.1999.0897

Fu, C., Zhong, C., Yang, Y., Zhang, M., Li, W., Zhou, Q., et al. (2021). Sirt1 activator SRT2104 protects against oxygen-glucose deprivation/reoxygenation-induced injury via regulating microglia polarization by modulating Sirt1/NF-κB pathway. *Brain Res.* 1753:147236. doi: 10.1016/j.brainres.2020.147236

Gao, H., Yang, L., and Shao, Y. (2022). SIRT1/NF-κB pathway on neuronal apoptosis in rats with ischemic stroke. *Cell. Mol. Biol.* 68, 77–82. doi: 10.26355/eurrev_201906_18214

Gerhardt, H., Golding, M., Fruttiger, M., Ruhrberg, C., Lundkvist, A., Abramsson, A., et al. (2003). VEGF guides angiogenic sprouting utilizing endothelial tip cell filopodia. *J Cell Biol.* 161, 1163–1177. doi: 10.1083/jcb.200302047

Gertz, M., Fischer, F., Nguyen, G., Lakshminarasimhan, M., Schutkowski, M., Weyand, M., et al. (2013). Ex-527 inhibits sirtuins by exploiting their unique NAD+-dependent deacetylation mechanism. *Proc. Natl. Acad. Sci. U. S. A.* 110, E2772–E2781. doi: 10.1073/pnas.1303628110

Hattori, Y., Okamoto, Y., Nagatsuka, K., Takahashi, R., Kalaria, R., Kinoshita, M., et al. (2015). SIRT1 attenuates severe ischemic damage by preserving cerebral blood flow. *Neuroreport* 26, 113–117. doi: 10.1097/WNR.0000000000000308

He, M., Chiang, H., Luo, H., Zheng, Z., Qiao, Q., Wang, L., et al. (2020). An acetylation switch of the NLRP3 inflammasome regulates aging-associated chronic inflammation and insulin resistance. *Cell Metab.* 31, 580–591.e5. doi: 10.1016/j.cmet.2020.01.009

He, Q., Li, Z., Wang, Y., Hou, Y., Li, L., and Zhao, J. (2017). Resveratrol alleviates cerebral ischemia/reperfusion injury in rats by inhibiting NLRP3 inflammasome activation through Sirt1-dependent autophagy induction. *Int. Immunopharmacol.* 50, 208–215. doi: 10.1016/j.intimp.2017.06.029

Heinisch, O., Zeyen, T., Goldmann, T., Prinz, M., Huber, M., Jung, J., et al. (2022). Erythropoietin abrogates post-ischemic activation of the NLRP3, NLRC4, and aim2 inflammasomes in microglia/macrophages in a TAK1-dependent manner. *Transl. Stroke Res.* 13, 462–482. doi: 10.1007/s12975-021-00948-8

Hermann, D., Zechariah, A., Kaltwasser, B., Bosche, B., Caglayan, A., Kilic, E., et al. (2015). Sustained neurological recovery induced by resveratrol is associated with angioneurogenesis rather than neuroprotection after focal cerebral ischemia. *Neurobiol. Dis.* 83, 16–25. doi: 10.1016/j.nbd.2015.08.018

Hernández-Jiménez, M., Hurtado, O., Cuartero, M., Ballesteros, I., Moraga, A., Pradillo, J., et al. (2013). Silent information regulator 1 protects the brain against cerebral ischemic damage. *Stroke* 44, 2333–2337. doi: 10.1161/STROKEAHA.113.001715

Herskovits, A., and Guarente, L. (2014). SIRT1 in neurodevelopment and brain senescence. *Neuron* 81, 471–483. doi: 10.1016/j.neuron.2014.01.028

Hisahara, S., Chiba, S., Matsumoto, H., Tanno, M., Yagi, H., Shimohama, S., et al. (2008). Histone deacetylase SIRT1 modulates neuronal differentiation by its nuclear translocation. *Proc. Natl. Acad. Sci. U. S. A.* 105, 15599–15604. doi: 10.1073/pnas.0800612105

Hu, C., Zhang, S., Chen, Q., and Wang, R. (2022). Ovatodiolide protects ischemia-reperfusion-induced neuronal injury via microglial neuroinflammation via mediating SIRT1/NF-κB pathway. *Brain Res. Bull.* 180, 97–107. doi: 10.1016/j.brainresbull.2021.12.010

Hu, Z., Li, F., Zhou, X., Zhang, F., Huang, L., Gu, B., et al. (2020). *Momordica charantia* polysaccharides modulate the differentiation of neural stem cells via SIRT1/B-catenin axis in cerebral ischemia/reperfusion. *Stem Cell Res. Therapy* 11:485. doi: 10.1186/s13287-020-02000-2

Huang, J., Shen, C., Wu, W., Ren, J., Xu, L., Liu, S., et al. (2014). Primary cilia mediate sonic hedgehog signaling to regulate neuronal-like differentiation of bone mesenchymal stem cells for resveratrol induction in vitro. *J. Neurosci. Res.* 92, 587–596. doi: 10.1002/jnr.23343

Huang, R., Xu, Y., Wan, W., Shou, X., Qian, J., You, Z., et al. (2015). Deacetylation of nuclear LC3 drives autophagy initiation under starvation. *Mol. Cell* 57, 456–466. doi: 10.1016/j.molcel.2014.12.013

Jia, N., Sun, Q., Su, Q., and Chen, G. (2016). SIRT1-mediated deacetylation of PGC1α attributes to the protection of curcumin against glutamate excitotoxicity in cortical neurons. *Biochem. Biophys. Res. Commun.* 478, 1376–1381.

Jin, Q., Yan, T., Ge, X., Sun, C., Shi, X., and Zhai, Q. (2007). Cytoplasm-localized SIRT1 enhances apoptosis. *J. Cell. Physiol.* 213, 88–97. doi: 10.1002/jcp.21091

Kalaivani, P., Ganesh, M., Sathiya, S., Ranju, V., Gayathiri, V., and Saravana Babu, C. (2014). Alteration in bioenergetic regulators, SirT1 and Parp1 expression precedes oxidative stress in rats subjected to transient cerebral focal ischemia: Molecular and histopathologic evidences. *J. Stroke Cerebrovasc. Dis.* 23, 2753–2766. doi: 10.1016/j.jstrokecerebrovasdis.2014.06.026

Kannan, V., Brouwer, N., Hanisch, U., Regen, T., Eggen, B., and Boddeke, H. (2013). Histone deacetylase inhibitors suppress immune activation in primary mouse microglia. *J. Neurosci. Res.* 91, 1133–1142. doi: 10.1002/jnr.23221

Kerr, N., Sanchez, J., O'Connor, G., Watson, B., Daunert, S., Bramlett, H., et al. (2022). Inflammasome-regulated pyroptotic cell death in disruption of the gut-brain axis after stroke. *Transl. Stroke Res.* 13, 898–912.

Kim, E. J., Kho, J. H., Kang, M. R., and Um, S. J. (2007). Active regulator of SIRT1 cooperates with SIRT1 and facilitates suppression of p53 activity. *Mol. Cell* 28, 277–290. doi: 10.1016/j.molcel.2007.08.030

Kim, J., Chen, J., and Lou, Z. (2008). DBC1 is a negative regulator of SIRT1. *Nature* 451, 583–586.

Knight, J., Allison, S., and Milner, J. (2013). Active regulator of SIRT1 is required for cancer cell survival but not for SIRT1 activity. *Open Biol.* 3:130130. doi: 10.1098/rsob.130130

Lai, M., Wang, D., Lin, Z., and Zhang, Y. (2016). Small molecule copper and its relative metabolites in serum of cerebral ischemic stroke patients. *J. Stroke cerebrovasc. Dis.* 25, 214–219. doi: 10.1016/j.jstrokecerebrovasdis.2015.09.020

Lanzillotta, A., Sarnico, I., Ingrassia, R., Boroni, F., Branca, C., Benarese, M., et al. (2010). The acetylation of RelA in Lys310 dictates the NF-κB-dependent response in post-ischemic injury. *Cell Death Dis.* 1:e96.

Lazo-Gomez, R., and Tapia, R. (2017). Quercetin prevents spinal motor neuron degeneration induced by chronic excitotoxic stimulus by a sirtuin 1-dependent mechanism. *Transl. Neurodegen.* 6:31. doi: 10.1186/s40035-017-0102-8

Le, K., Chibaatar Daliv, E., Wu, S., Qian, F., Ali, A., Yu, D., et al. (2019). SIRT1-regulated HMGB1 release is partially involved in TLR4 signal transduction: A possible anti-neuroinflammatory mechanism of resveratrol in neonatal hypoxic-ischemic brain injury. *Int. Immunopharmacol.* 75:105779. doi: 10.1016/j.intimp.2019.105779

Lei, G., Zhuang, L., and Gan, B. (2022). Targeting ferroptosis as a vulnerability in cancer. *Nature Rev. Cancer* 22, 381–396.

Li, C., Wu, Z., Xue, H., Gao, Q., Zhang, Y., Wang, C., et al. (2022). Ferroptosis contributes to hypoxic-ischemic brain injury in neonatal rats: Role of the SIRT1/Nrf2/GPx4 signaling pathway. *CNS Neurosci. Therap.* 28, 2268–2280. doi: 10.1111/cns.13973

Li, H., Li, X., Hao, Y., Wu, C., Fu, Y., Su, N., et al. (2022). Maresin 1 intervention reverses experimental pulmonary arterial hypertension in mice. *Br. J. Pharmacol.* 179, 5132–5147. doi: 10.1111/bph.15906

Li, J., Zhang, Z., Wang, L., Jiang, L., Qin, Z., Zhao, Y., et al. (2021). Maresin 1 Attenuates Lipopolysaccharide-Induced Acute Kidney Injury via Inhibiting NOX4/ROS/NF-κB Pathway. *Front. Pharmacol.* 12:782660. doi: 10.3389/fphar.2021.782660

Liang, H., Chang, X., Xia, R., Wu, W., Guo, H., and Yang, M. (2022). Magnoflorine attenuates cerebral ischemia-induced neuronal injury via autophagy/Sirt1/AMPK signaling pathway. *Evid. Based Complem. Altern. Med.* 2022:2131561. doi: 10.1155/2022/2131561

Lim, J., Lee, Y., Chun, Y., Chen, J., Kim, J., and Park, J. (2010). Sirtuin 1 modulates cellular responses to hypoxia by deacetylating hypoxia-inducible factor 1alpha. *Mol. Cell* 38, 864–878. doi: 10.1016/j.molcel.2010.05.023

Ling, C., Liang, J., Zhang, C., Li, R., Mou, Q., Qin, J., et al. (2018). Synergistic effects of salvianolic acid B and puerarin on cerebral ischemia reperfusion injury. *Molecules* 23:564. doi: 10.3390/molecules23030564

Liu, B., Ghosh, S., Yang, X., Zheng, H., Liu, X., Wang, Z., et al. (2012). Resveratrol rescues SIRT1-dependent adult stem cell decline and alleviates progeroid features in laminopathy-based progeria. *Cell Met.* 16, 738–750. doi: 10.1016/j.cmet.2012.11.007

Liu, L., Cao, Q., Gao, W., Li, B., Zeng, C., Xia, Z., et al. (2021). Melatonin ameliorates cerebral ischemia-reperfusion injury in diabetic mice by enhancing autophagy via the SIRT1-BMAL1 pathway. *FASEB J.* 35:e22040. doi: 10.1096/fj.202002718RR

Liu, R., Li, H., Deng, J., Wu, Q., Liao, C., Xiao, Q., et al. (2021). QKI 6 ameliorates CIRI through promoting synthesis of triglyceride in neuron and inhibiting neuronal apoptosis associated with SIRT1-PPARγ-PGC-1α axis. *Brain Behav.* 11:e2271.

Liu, Y., Jia, S., Liang, X., Dong, M., Xu, X., Lu, C., et al. (2018). Prognostic value of Sirtuin1 in acute ischemic stroke and its correlation with functional outcomes. *Medicine* 97:e12959. doi: 10.1097/MD.0000000000012959

Liu, Z., Li, C., Li, Y., Yu, L., and Qu, M. (2022). Propofol reduces renal ischemia reperfusion-mediated necroptosis by up-regulation of SIRT1 in rats. *Inflammation* 45, 2038–2051. doi: 10.1007/s10753-022-01673-6

Lv, H., Wang, L., Shen, J., Hao, S., Ming, A., Wang, X., et al. (2015). Salvianolic acid B attenuates apoptosis and inflammation via SIRT1 activation in experimental stroke rats. *Brain Res. Bull.* 115, 30–36. doi: 10.1016/j.brainresbull.2015.05.002

Ma, J., Fan, H., Cai, H., Hu, Z., Zhou, X., Li, F., et al. (2021). Promotion of *Momordica Charantia* polysaccharides on neural stem cell proliferation by increasing SIRT1 activity after cerebral ischemia/reperfusion in rats. *Brain Res. Bull.* 170, 254–263. doi: 10.1016/j.brainresbull.2021.02.016

Meng, F., Qian, M., Peng, B., Peng, L., Wang, X., Zheng, K., et al. (2020). Synergy between SIRT1 and SIRT6 helps recognize DNA breaks and potentiates the DNA damage response and repair in humans and mice. *eLife* 9:e55828. doi: 10.7554/eLife.55828

Meng, S., Wang, B., and Li, W. (2023). LncRNA MALAT1 improves cerebral ischemia-reperfusion injury and cognitive dysfunction by regulating miR-142-3p/SIRT1 axis. *Int J Neurosci.* 133, 740–753. doi: 10.1080/00207454.2021.1972999

Mi, D., Fang, H., Zheng, G., Liang, X., Ding, Y., Liu, X., et al. (2019). DPP-4 inhibitors promote proliferation and migration of rat brain microvascular endothelial cells under hypoxic/high-glucose conditions, potentially through the SIRT1/HIF-1/VEGF pathway. *CNS Neurosci. Therap.* 25, 323–332. doi: 10.1111/cns.13042

Milne, J., Lambert, P., Schenk, S., Carney, D., Smith, J., Gagne, D., et al. (2007). Small molecule activators of SIRT1 as therapeutics for the treatment of type 2 diabetes. *Nature* 450, 712–716.

Nogueira, R., Jadhav, A., Haussen, D., Bonafe, A., Budzik, R., Bhuva, P., et al. (2018). Thrombectomy 6 to 24 hours after stroke with a mismatch between deficit and infarct. *N. Engl. J. Med.* 378, 11–21.

Ogawa, T., Wakai, C., Saito, T., Murayama, A., Mimura, Y., Youfu, S., et al. (2011). Distribution of the longevity gene product. SIRT1, in developing mouse organs. *Congenital Anom.* 51, 70–79. doi: 10.1111/j.1741-4520.2010.00304.x

Pérez, S., Rius-Pérez, S., Finamor, I., Martí-Andrés, P., Prieto, I., García, R., et al. (2019). Obesity causes PGC-1α deficiency in the pancreas leading to marked IL-6 upregulation via NF-κB in acute pancreatitis. *J. Pathol.* 247, 48–59.

Prozorovski, T., Ingwersen, J., Lukas, D., Göttle, P., Koop, B., Graf, J., et al. (2019). Regulation of sirtuin expression in autoimmune neuroinflammation: Induction of SIRT1 in oligodendrocyte progenitor cells. *Neurosci. Lett.* 704, 116–125. doi: 10.1016/j.neulet.2019.04.007

Ramadori, G., Lee, C., Bookout, A., Lee, S., Williams, K., Anderson, J., et al. (2008). Brain SIRT1: Anatomical distribution and regulation by energy availability. *J. Neurosci.* 28, 9989–9996. doi: 10.1523/JNEUROSCI.3257-08.2008

Rana, P., Franco, E., Rao, Y., Syed, K., Barh, D., Azevedo, V., et al. (2019). Evaluation of the common molecular basis in Alzheimer's and Parkinson's diseases. *Int. J. Mol. Sci.* 20:3730.

Sakamoto, J., Miura, T., Shimamoto, K., and Horio, Y. (2004). Predominant expression of Sir2alpha, an NAD-dependent histone deacetylase, in the embryonic mouse heart and brain. *FEBS Lett.* 556, 281–286. doi: 10.1016/s0014-5793(03)01444-3

Sarmah, D., Datta, A., Kaur, H., Kalia, K., Borah, A., Rodriguez, A., et al. (2022). Sirtuin-1 – mediated NF-κB pathway modulation to mitigate inflammasome signaling and cellular apoptosis is one of the neuroprotective effects of intra-arterial mesenchymal stem cell therapy following ischemic stroke. *Stem Cell Rev. Rep.* 18, 821–838.

Sauve, A., Wolberger, C., Schramm, V., and Boeke, J. (2006). The biochemistry of sirtuins. *Annu. Rev. Biochem.* 75, 435–465.

Sharma, B., and Kanneganti, T. (2021). NLRP3 inflammasome in cancer and metabolic diseases. *Nat. Immunol.* 22, 550–559.

Shen, C., Cheng, W., Yu, P., Wang, L., Zhou, L., Zeng, L., et al. (2016). Resveratrol pretreatment attenuates injury and promotes proliferation of neural stem cells following oxygen-glucose deprivation/reoxygenation by upregulating the expression of Nrf2, HO-1 and NQO1 in vitro. *Mol. Med. Rep.* 14, 3646–3654. doi: 10.3892/mmr.2016.5670

Shu, J., Huang, X., Liao, Q., Wang, J., Zhou, Y., Chen, Y., et al. (2022). Sevoflurane improves hemorrhagic shock and resuscitation-induced cognitive impairments and mitochondrial dysfunctions through SIRT1-mediated autophagy. *Oxid. Med. Cell. Longev.* 2022:9771743. doi: 10.1155/2022/9771743

Simão, F., Pagnussat, A., Seo, J., Navaratna, D., Leung, W., Lok, J., et al. (2012). Pro-angiogenic effects of resveratrol in brain endothelial cells: Nitric oxide-mediated regulation of vascular endothelial growth factor and metalloproteinases. *J. Cereb. Blood Flow Metab.* 32, 884–895. doi: 10.1038/jcbfm.2012.2

Song, L., Mu, L., and Wang, H. (2022). MicroRNA-489-3p aggravates neuronal apoptosis and oxidative stress after cerebral ischemia-reperfusion injury. *Bioengineered* 13, 14047–14056. doi: 10.1080/21655979.2022.2062534

St-Pierre, J., Drori, S., Uldry, M., Silvaggi, J., Rhee, J., Jäger, S., et al. (2006). Suppression of reactive oxygen species and neurodegeneration by the PGC-1 transcriptional coactivators. *Cell* 127, 397–408. doi: 10.1016/j.cell.2006.09.024

Sun, S., Li, Z., Huan, S., Kai, J., Xia, S., Su, Y., et al. (2022). Modification of lysine deacetylation regulates curcumol-induced necroptosis through autophagy in hepatic stellate cells. *Phytother. Res.* 36, 2660–2676. doi: 10.1002/ptr.7483

Sun, X., and Liu, B. (2022). Donepezil ameliorates oxygen-glucose deprivation/reoxygenation-induced brain microvascular endothelial cell dysfunction via the SIRT1/FOXO3a/NF-κB pathways. *Bioengineered* 13, 7760–7770.

Szabo, G., and Bala, S. (2013). MicroRNAs in liver disease. *Nat. Rev. Gastroenterol. hepatol.* 10, 542–552.

Szydlak, R. (2023). Mesenchymal stem cells in ischemic tissue regeneration. *World J. Stem Cells* 15, 16–30.

Tang, F., Guo, S., Liao, H., Yu, P., Wang, L., Song, X., et al. (2017). Resveratrol enhances neurite outgrowth and synaptogenesis via sonic hedgehog signaling following oxygen-glucose deprivation/reoxygenation injury. *Cell. Physiol. Biochem.* 43, 852–869. doi: 10.1159/000481611

Tang, Y., Xie, J., Chen, X., Sun, L., Xu, L., and Chen, X. (2022). A novel link between silent information regulator 1 and autophagy in cerebral ischemia-reperfusion. *Front. Neurosci.* 16:1040182. doi: 10.3389/fnins.2022.1040182

Tanner, K., Landry, J., Sternglanz, R., and Denu, J. (2000). Silent information regulator 2 family of NAD- dependent histone/protein deacetylases generates a unique product, 1-O-acetyl-ADP-ribose. *Proc. Natl. Acad. Sci. U. S. A.* 97, 14178–14182.

Tanno, M., Kuno, A., Yano, T., Miura, T., Hisahara, S., Ishikawa, S., et al. (2010). Induction of manganese superoxide dismutase by nuclear translocation and activation of SIRT1 promotes cell survival in chronic heart failure. *J. Biol. Chem.* 285, 8375–8382. doi: 10.1074/jbc.M109.090266

Tanno, M., Sakamoto, J., Miura, T., Shimamoto, K., and Horio, Y. (2007). Nucleocytoplasmic shuttling of the NAD+-dependent histone deacetylase SIRT1. *J. Biol. Chem.* 282, 6823–6832.

Teertam, S., Jha, S., and Prakash Babu, P. (2020). Up-regulation of Sirt1/miR-149-5p signaling may play a role in resveratrol induced protection against ischemia via p53 in rat brain. *J. Clin. Neurosci.* 72, 402–411. doi: 10.1016/j.jocn.2019.11.043

Teertam, S., and Phanithi, P. (2022). Up-regulation of Sirtuin-1/autophagy signaling in human cerebral ischemia: Possible role in caspase-3 mediated apoptosis. *Heliyon* 8:e12278. doi: 10.1016/j.heliyon.2022.e12278

Trapp, J., Meier, R., Hongwiset, D., Kassack, M., Sippl, W., and Jung, M. (2007). Structure-activity studies on suramin analogues as inhibitors of NAD+-dependent histone deacetylases (sirtuins). *ChemMedChem* 2, 1419–1431. doi: 10.1002/cmdc.200700003

Tsvetkov, P., Coy, S., Petrova, B., Dreishpoon, M., Verma, A., Abdusamad, M., et al. (2022). Copper induces cell death by targeting lipoylated TCA cycle proteins. *Science* 375, 1254–1261.

Turc, G., Bhogal, P., Fischer, U., Khatri, P., Lobotesis, K., Mazighi, M., et al. (2019). European Stroke Organisation (ESO) – European Society for Minimally Invasive Neurological Therapy (ESMINT) guidelines on mechanical thrombectomy in acute ischaemic strokeendorsed by stroke alliance for Europe (SAFE). *Eur. Stroke J.* 4, 6–12. doi: 10.1177/2396987319832140

Wang, F., Shang, Y., Zhang, R., Gao, X., and Zeng, Q. A. (2019). SIRT1 agonist reduces cognitive decline in type 2 diabetic rats through antioxidative and anti-inflammatory mechanisms. *Mol. Med. Rep.* 19, 1040–1048. doi: 10.3892/mmr.2018.9699

Wang, P., Guan, Y., Du, H., Zhai, Q., Su, D., and Miao, C. (2012). Induction of autophagy contributes to the neuroprotection of nicotinamide phosphoribosyltransferase in cerebral ischemia. *Autophagy* 8, 77–87. doi: 10.4161/auto.8.1.18274

Wang, P., Lu, Y., Han, D., Wang, P., Ren, L., Bi, J., et al. (2019). Neuroprotection by nicotinamide mononucleotide adenylyltransferase 1 with involvement of autophagy in an aged rat model of transient cerebral ischemia and reperfusion. *Brain Res.* 1723:146391. doi: 10.1016/j.brainres.2019.146391

Xia, D., Yuan, J., Jiang, X., Qi, M., Lai, N., Wu, L., et al. (2021). viaSIRT1 promotes M2 microglia polarization reducing ROS-mediated NLRP3 inflammasome signaling after subarachnoid hemorrhage. *Front. Immunol.* 12:770744. doi: 10.3389/fimmu.2021.770744

Xian, W., Li, T., Li, L., Hu, L., and Cao, J. (2019). Maresin 1 attenuates the inflammatory response and mitochondrial damage in mice with cerebral ischemia/reperfusion in a SIRT1-dependent manner. *Brain Res.* 1711, 83–90. doi: 10.1016/j.brainres.2019.01.013

Xie, W., Zhu, T., Zhou, P., Xu, H., Meng, X., Ding, T., et al. (2020). Notoginseng leaf triterpenes ameliorates OGD/R-induced neuronal injury via SIRT1/2/3-Foxo3a-MnSOD/PGC-1α signaling pathways mediated by the NAMPT-NAD pathway. *Oxid. Med. Cell. Longev.* 2020:7308386.

Xie, X., Cao, Y., Dai, L., and Zhou, D. (2023). Bone marrow mesenchymal stem cell-derived exosomal lncRNA KLF3-AS1 stabilizes Sirt1 protein to improve cerebral ischemia/reperfusion injury via miR-206/USP22 axis. *Mol. Med.* 29:3. doi: 10.1186/s10020-022-00595-1

Xing, Y., Zhang, M., Wang, M., Feng, Y., Dong, F., and Zhang, F. (2021). The anti-apoptosis effect of single electroacupuncture treatment via suppressing neuronal autophagy in the acute stage of ischemic stroke without infarct alleviation. *Front. Cell. Neurosci.* 15:633280. doi: 10.3389/fncel.2021.633280

Xu, Q., Zhou, D., and Yu, D. (2023). Bone marrow mesenchymal stem cells-derived exosomal long non-coding RNA KLF3 antisense RNA 1 enhances autophagy to protect against cerebral ischemia/reperfusion injury via ETS variant transcription factor 4/silent information regulator 1 axis. *Neuroscience* 521, 44–57. doi: 10.1016/j.neuroscience.2023.02.021

Xu, S., Lv, H., Li, W., Hong, H., Peng, Y., and Zhu, B. (2020). Electroacupuncture alleviates cerebral ischemia/reperfusion injury in rats by histone H4 lysine 16 acetylation-mediated autophagy. *Front. Psychiatry* 11:576539. doi: 10.3389/fpsyt.2020.576539

Yan, P., Li, Z., Xiong, J., Geng, Z., Wei, W., Zhang, Y., et al. (2021). LARP7 ameliorates cellular senescence and aging by allosterically enhancing SIRT1 deacetylase activity. *Cell Rep.* 37:110038. doi: 10.1016/j.celrep.2021.110038

Yan, W., Sun, W., Fan, J., Wang, H., Han, S., Li, J., et al. (2020). Sirt1-ROS-TRAF6 signaling-induced pyroptosis contributes to early injury in ischemic mice. *Neurosci. Bull.* 36, 845–859. doi: 10.1007/s12264-020-00489-4

Yan, X., Yu, A., Zheng, H., Wang, S., He, Y., and Wang, L. (2019). OCalycosin-7—-glucoside attenuates OGD/R-induced damage by preventing oxidative stress and neuronal apoptosis via the SIRT1/FOXO1/PGC-1 pathway in HT22 cells. *Neural Plast.* 2019:8798069. doi: 10.1155/2019/8798069

Yang, R., Shen, Y., Chen, M., Zhao, J., Chen, S., Zhang, W., et al. (2022). Quercetin attenuates ischemia reperfusion injury by protecting the blood-brain barrier through Sirt1 in MCAO rats. *J. Asian Natl. Products Res.* 24, 278–289. doi: 10.1080/10286020.2021.1949302

Yang, W., Tao, K., Zhang, P., Chen, X., Sun, X., and Li, R. (2022). Maresin 1 protects against lipopolysaccharide/d-galactosamine-induced acute liver injury by inhibiting macrophage pyroptosis and inflammatory response. *Biochem. Pharmacol.* 195:114863. doi: 10.1016/j.bcp.2021.114863

Yang, X., Si, P., Qin, H., Yin, L., Yan, L., and Zhang, C. (2017). The neuroprotective effects of SIRT1 on NMDA-induced excitotoxicity. *Oxid. Med. Cell. Longev.* 2017:2823454.

Yang, X., Sun, X., Wu, J., Ma, J., Si, P., Yin, L., et al. (2020). Regulation of the SIRT1 signaling pathway in NMDA-induced Excitotoxicity. *Toxicol. Lett.* 322, 66–76.

Yang, Z., Huang, C., Wen, X., Liu, W., Huang, X., Li, Y., et al. (2022). Circular RNA circ-FoxO3 attenuates blood-brain barrier damage by inducing autophagy during ischemia/reperfusion. *Mol. Therapy* 30, 1275–1287. doi: 10.1016/j.ymthe.2021.11.004

Ye, J., Zhang, F., Li, B., Liu, Q., and Zeng, G. (2022). Knockdown of ATF3 suppresses the progression of ischemic stroke through inhibiting ferroptosis. *Front. Mol. Neurosci.* 15:1079338. doi: 10.3389/fnmol.2022.1079338

Yeung, F., Hoberg, J., Ramsey, C., Keller, M., Jones, D., Frye, R., et al. (2004). Modulation of NF-kappaB-dependent transcription and cell survival by the SIRT1 deacetylase. *EMBO J.* 23, 2369–2380. doi: 10.1038/sj.emboj.7600244

Yu, H., Kim, Y., and Cho, M. (2020). Cytoplasm-localized SIRT1 downregulation attenuates apoptosis and cell cycle arrest in cisplatin-resistant lung cancer A549 cells. *J. Cancer* 11, 4495–4509. doi: 10.7150/jca.44383

Yu, H., Zhang, F., Yan, P., Zhang, S., Lou, Y., Geng, Z., et al. (2021). LARP7 protects against heart failure by enhancing mitochondrial biogenesis. *Circulation* 143, 2007–2022. doi: 10.1161/CIRCULATIONAHA.120.050812

Yu, P., Wang, L., Tang, F., Guo, S., Liao, H., Fan, C., et al. (2021). Resveratrol-mediated neurorestoration after cerebral ischemic injury – Sonic Hedgehog signaling pathway. *Life Sci.* 280:119715. doi: 10.1016/j.lfs.2021.119715

Yu, P., Wang, L., Tang, F., Zeng, L., Zhou, L., Song, X., et al. (2017). Resveratrol pretreatment decreases ischemic injury and improves neurological function via sonic hedgehog signaling after stroke in rats. *Mol. Neurobiol.* 54, 212–226. doi: 10.1007/s12035-015-9639-7

Yue, L., Zhao, L., Liu, H., Li, X., Wang, B., Guo, H., et al. (2016). Adiponectin protects against glutamate-induced excitotoxicity via activating SIRT1-dependent PGC-1α expression in HT22 hippocampal neurons. *Oxid. Med. Cell. Longev.* 2016:2957354.

Zakhary, S., Ayubcha, D., Dileo, J., Jose, R., Leheste, J., Horowitz, J., et al. (2010). Distribution analysis of deacetylase SIRT1 in rodent and human nervous systems. *Anatomical Rec.* 293, 1024–1032. doi: 10.1002/ar.21116

Zhang, M., Lu, P., Terada, T., Sui, M., Furuta, H., Iida, K., et al. (2021). Quercetin 3,5,7,3',4'-pentamethyl ether from Kaempferia parviflora directly and effectively activates human SIRT1. *Commun. Biol.* 4:209. doi: 10.1038/s42003-021-01705-1

Zhang, X., Zhang, F., Yao, F., Wang, P., Xiong, Q., and Neng, P. (2022). Bergenin has neuroprotective effects in mice with ischemic stroke through antioxidative stress and anti-inflammation via regulating Sirt1/FOXO3a/NF-κB signaling. *Neuroreport* 33, 549–560.

Zhang, Y., Yan, Y., Cao, Y., Yang, Y., Zhao, Q., Jing, R., et al. (2017). Potential therapeutic and protective effect of curcumin against stroke in the male albino stroke-induced model rats. *Life Sci.* 183, 45–49. doi: 10.1016/j.lfs.2017.06.023

Zhao, K., Zhang, Y., Xu, X., Liu, L., Huang, L., Luo, R., et al. (2019). Acetylation is required for NLRP3 self-aggregation and full activation of the inflammasome. *bioRxiv* [preprint]. doi: 10.1101/2019.12.31.891556

Zhao, Y., Shi, X., Wang, J., Mang, J., and Xu, Z. (2021). Betulinic acid ameliorates cerebral injury in middle cerebral artery occlusion rats through regulating autophagy. *ACS Chem. Neurosci.* 12, 2829–2837. doi: 10.1021/acschemneuro.1c00198

Zheng, X., Shan, C., Xu, Q., Wang, Y., Shi, Y., Wang, Y., et al. (2018). Buyang huanwu decoction targets SIRT1/VEGF pathway to promote angiogenesis after cerebral ischemia/reperfusion injury. *Front. Neurosci.* 12:911. doi: 10.3892/mmr.2021.12431

Zheng, Y., Li, L., Chen, B., Fang, Y., Lin, W., Zhang, T., et al. (2022). Chlorogenic acid exerts neuroprotective effect against hypoxia-ischemia brain injury in neonatal rats by activating Sirt1 to regulate the Nrf2-NF-κB signaling pathway. *Cell Commun. Signal.* 20:84.

Zhou, D., Chen, L., Wang, Y., Gan, L., Yuan, M., Zhang, L., et al. (2023). RNA binding protein RPS3 mediates microglial polarization by activating NLRP3 inflammasome via SIRT1 in ischemic stroke. *J. Stroke Cerebrovasc. Dis.* 32:107132. doi: 10.1016/j.jstrokecerebrovasdis.2023.107132

Zhou, L., Zhu, H., Bai, X., Huang, J., Chen, Y., Wen, J., et al. (2022). Potential mechanisms and therapeutic targets of mesenchymal stem cell transplantation for ischemic stroke. *Stem Cell Res. Therapy* 13:195.

Zhou, S., Qiao, B., Chu, X., and Kong, Q. (2018). Oxymatrine attenuates cognitive deficits through SIRT1-mediated autophagy in ischemic stroke. *J. Neuroimmunol.* 323, 136–142. doi: 10.1016/j.jneuroim.2018.06.018

Zhou, Y., and Li, G. (2020). Kaempferol protects cell damage in in vitro ischemia reperfusion model in rat neuronal PC12 cells. *BioMed Res. Int.* 2020:2461079. doi: 10.1155/2020/2461079

Zhu, H., Huang, J., Chen, Y., Li, X., Wen, J., Tian, M., et al. (2022). Resveratrol pretreatment protects neurons from oxygen-glucose deprivation/reoxygenation and ischemic injury through inhibiting ferroptosis. *Biosci. Biotechnol. Biochem.* 86, 704–716. doi: 10.1093/bbb/zbac048

Zhu, T., Xie, W., Wang, L., Jin, X., Meng, X., Sun, G., et al. (2021). Notoginsenoside R1 activates the NAMPT-NAD-SIRT1 cascade to promote postischemic angiogenesis by modulating Notch signaling. *Biomed. Pharmacother.* 140:111693.

frontiers | Frontiers in Pharmacology

TYPE Review
PUBLISHED 07 September 2023
DOI 10.3389/fphar.2023.1261326

OPEN ACCESS

EDITED BY
Viola B. Morris,
Emory University, United States

REVIEWED BY
Manju Saraswathy,
Sree Chitra Tirunal Institute for Medical Sciences and Technology (SCTIMST), India
Yule Wang,
Zhejiang University, China

*CORRESPONDENCE
Yanxia Wang,
394019707@qq.com

†These authors have contributed equally to this work

RECEIVED 19 July 2023
ACCEPTED 28 August 2023
PUBLISHED 07 September 2023

CITATION
Wang Q, Yang Z, Guo L, Li Z, Liu Y, Feng S and Wang Y (2023), Chemical composition, pharmacology and pharmacokinetic studies of GuHong injection in the treatment of ischemic stroke.
Front. Pharmacol. 14:1261326.
doi: 10.3389/fphar.2023.1261326

Chemical composition, pharmacology and pharmacokinetic studies of GuHong injection in the treatment of ischemic stroke

Qiuyue Wang[1†], Zhihua Yang[1,2†], Liuli Guo[1], Zhenzhen Li[2], Yangxi Liu[3], Shaoling Feng[3] and Yanxia Wang[4*]

[1]Graduate School, Tianjin University of Traditional Chinese Medicine, Tianjin, China, [2]Institute of Traditional Chinese Medicine, Tianjin University of Traditional Chinese Medicine, Tianjin, China, [3]National Clinical Research Center for Chinese Medicine Acupuncture and Moxibustion, First Teaching Hospital of Tianjin University of Traditional Chinese Medicine, Tianjin, China, [4]Tianjin Beichen Traditional Chinese Medicine Hospital, Tianjin, China

GuHong injection is composed of safflower and *N*-acetyl-L-glutamine. It is widely used in clinical for cerebrovascular diseases, such as ischemic stroke and related diseases. The objective of this review is to comprehensively summarize the most recent information related to GuHong in the treatment of stroke, including chemical composition, clinical studies, potential pharmacological mechanisms and pharmacokinetics. Additionally, it examines possible scientific gaps in current study and aims to provide a reliable reference for future GuHong studies. The systematic review reveals that the chemical composition of safflower in GuHong is more than 300 chemical components in five categories. GuHong injection is primarily used in clinical applications for acute ischemic stroke and related diseases. Pharmacological investigations have indicated that GuHong acts in the early and recovery stages of ischemic stroke by anti-inflammatory, anti-oxidative stress, anti-coagulation, neuroprotective and anti-apoptotic mechanisms simultaneously. Pharmacokinetic studies found that the main exposed substances in rat plasma after GuHong administration are hydroxysafflor yellow A and *N*-acetyl-L-glutamine, and *N*-acetyl-L-glutamine could exert its pharmacological effect across the blood-brain barrier. As a combination of Chinese herb and chemical drug, GuHong injection has great value in drug research and clinical treatment, especially for ischemic stroke disease. This article represents a comprehensive and systematic review of existing studies on GuHong injection, including chemical composition, pharmacological mechanism, and pharmacokinetics, which provides reference significance for the clinical treatment of ischemic stroke with GuHong, as well as provides guidance for further study.

KEYWORDS

GuHong injection, ischemic stroke, phytochemistry, pharmacology, pharmacokinetics

1 Introduction

Stroke is the second highest cause of death globally and a leading cause of disability, with an increasing incidence in China. Stroke can be broadly classified into two categories: ischemic stroke and hemorrhagic stroke. Ischemic stroke is characterized by the occurrence of infarction in the brain, spinal cord, or retina, and it accounts for approximately 71% of all

strokes worldwide (Campbell et al., 2019; Wu et al., 2019), which causes neuronal cell death and neurological deficits, such as learning/memory and locomotor deficiencies (Lee et al., 2018). According to TOAST (Trial of Org 10172 in Acute Stroke Treatment) criteria, ischaemic stroke was categorized into large-artery atherosclerosis, cardioembolism, small-vessel occlusion, stroke of other determined and undetermined etiology, of which arterial occlusion is responsible for the majority of strokes (Adams et al., 1993; Donnan et al., 2008). The classification of time post-stroke was based on the review of participants' time post-stroke, and four categories regarding time post-stroke emerged: acute, subacute, post-acute, and chronic stroke (Esposito et al., 2021). The development mechanisms are complex and diverse among all possible pathological processes occurring after ischemic stroke, which includes energy failure, excitotoxicity, neuroinflammation, apoptosis and oxidative stress as shown in Figure 1 (Moskowitz et al., 2010; Campbell et al., 2019). Clinically, ischemic stroke has high mortality and disability rate. Rapid restoration of blood flow to blocked cerebral vessels is the main goal of ischemic stroke treatment and a prerequisite for neuroprotective therapy.

GuHong, a sterile, non-pyrogenic injection for intravenous administration, is prepared from *Carthamus tinctorius* flowers (Honghua in Chinese) and *N*-acetyl-L-glutamine (NAG), and approved by the Chinese National Medical Products Administration (NMPA) as an add-on therapy in the treatment of acute ischaemic stroke. Several clinical meta-analyses and clinical efficacy analyses have demonstrated the effectiveness of adding GuHong to the conventional management of acute ischemic stroke in the first week post-stroke (He et al., 2014; Liu et al., 2020). *Carthamus tinctorius* L. (C. tinctorius) or safflower, commonly called Honghua in Chinese, is an annual or biennial herbal plant in the family of Compositae. With the increasing extensiveness of studies on chemical constituents of Chinese Material Medica, investigations concerning phytochemistry have also been conducted on safflower. The dried florets of *Carthamus tinctorius* have mainly been used as injections in clinical practice. Modern pharmacological experiments have shown that *Carthamus tinctorius*, with its active compounds, possesses wide-reaching biological activities, including dilating coronary artery, improving ischemia, anti-coagulation, anti-thrombosis, anti-oxidation, and anti-inflammation, etc (Zhou et al., 2014).

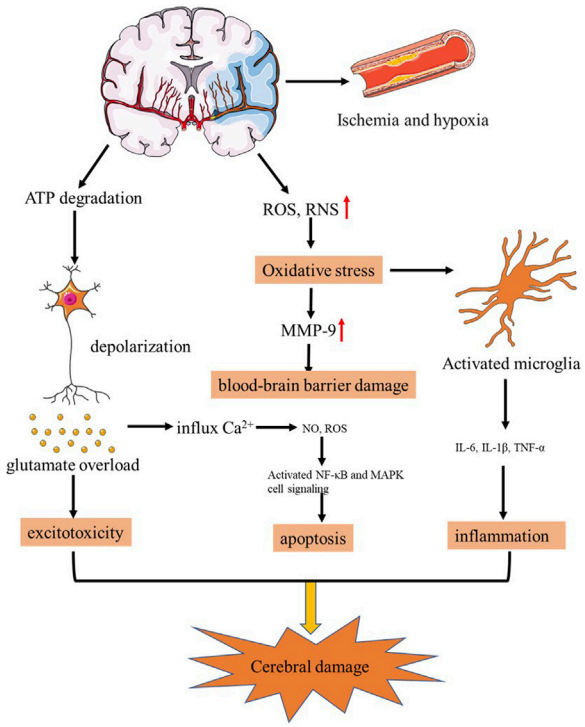

FIGURE 1
Pathogenesis of strok.

Glutamine, which has traditionally been considered as a non-essential amino acid in healthy individuals, is now known to be 'conditionally essential' in states of serious illness or injury (Bollhalder et al., 2013; Tao et al., 2014). States of critical illness lead to significant decreases in plasma levels of glutamine and when this decrease is severe, it is correlated with increasing mortality (Oudemans van Straaten et al., 2001; Kelly and Wischmeyer, 2003; Wischmeyer, 2008). Glutamine has multiple physiological roles and functions: a precursor of nucleic acids, amino sugars, and proteins; an important nitrogen transporter; and a carrier of ammonia (Snowden et al., 2002). Glutamine acts not only as a precursor for protein synthesis and glutathione but also as a preferred fuel for the immune system and other cells involved in wound repair (Wang et al., 2010). Therefore, glutamine supplementation can protect the brain from oxidative stress during ischemic stroke (Luo et al., 2019). However, glutamine is not adequately stable in aqueous solution and is also unstable in heat treatment of liquid nutritional products (Snowden et al., 2002). NAG is a glutamine acetyl derivative which is a liquid-stable source of glutamine. As a neuropeptide, it exhibits the ability to enhance nerve cell metabolism, preserve nerve stress function, and reduce blood ammonia levels. These actions contribute to the improvement of brain function and nerve activity. (López Pedrosa et al., 2007; Zhang et al., 2015; Deng et al., 2018).

GuHong injection is composed of safflower extract and NAG. Each milliliter of the injection contains 0.5 g Carthamus tinctorius flowers (Honghua) and 30 mg NAG. GuHong injection has multi-substance and multi-target characteristics in the treatment of ischemic stroke. Pharmacological studies have shown that GuHong injection has multiple pharmacological activities, such as anti-inflammatory, antioxidant, neuroprotective, and anti-apoptotic. However, to date, there are no published comprehensive and systematic reviews on GuHong injection. In this review, studies on phytochemistry, pharmacology, pharmacokinetics and clinical application of GuHong are presented to provide comprehensive and updated information on research on GuHong in the past few decades and to investigate the therapeutic potential and safety of its components in clinical application.

2 Phytochemistry

GuHong injection is formulated with a combination of safflower extract and NAG. NAG is a monomer compound, whereas safflower contains a complex chemical composition.

TABLE 1 Chemical composition in GuHong injection.

No.	Compound	Molecular formula	Molecular weight (Da)	References
1	*N*-acetyl-L-glutamine	$C_7H_{12}N_2O_4$	188.181	Wang et al. (2022a)
2	Hydroxysafflor yellow A	$C_{27}H_{32}O_{16}$	612.533	Wang et al. (2022b)
3	Quercetin-3-O-sophoroside-7-O-glucoside	$C_{33}H_{40}O_{22}$	788.660	Wang et al. (2022a)
4	Notoginsenic acid beta-sophoroside	$C_{22}H_{32}O_{13}$	504.184	Wang et al. (2022a)
5	Quercetin 3-glucosyl-(1->6)-glucosyl-(1->4)-rhamnoside	$C_{33}H_{40}O_{21}$	772.658	Wang et al. (2022a)
6	Quercetin 3-laminaribioside	$C_{27}H_{30}O_{17}$	626.148	Wang et al. (2022a)
7	Okanin 3′,4′-diglucoside	$C_{27}H_{32}O_{16}$	612.533	Wang et al. (2022a)
8	Rutin	$C_{27}H_{30}O_{16}$	610.518	Wang et al. (2022b)
9	Scutellarin	$C_{21}H_{18}O_{12}$	462.360	Wang et al. (2022a)
10	Kaempferol-3-O-β-rutinoside	$C_{27}H_{30}O_{15}$	594.518	Wang et al. (2022a)
11	Isorhamnetin 3-neohesperidoside	$C_{28}H_{32}O_{16}$	624.544	Wang et al. (2022a)
12	Quercitrin	$C_{21}H_{20}O_{11}$	448.377	Wang et al. (2022b)
13	Kaempferol	$C_{15}H_{10}O_6$	286.236	Wang et al. (2022a)
14	Baicalin	$C_{21}H_{18}O_{11}$	446.361	Wang et al. (2022b)
15	Safflomin C	$C_{30}H_{30}O_{14}$	614.551	Wang et al. (2022a)
16	Safflower Yellow	$C_{43}H_{42}O_{22}$	910.780	Wang et al. (2022a)
17	Syringin	$C_{17}H_{24}O_9$	372.367	Wang et al. (2022a)
18	Meglumin	$C_7H_{17}NO_5$	195.214	Wang et al. (2022a)
19	Guanosine	$C_{10}H_{13}N_5O_5$	283.241	Wang et al. (2022a)
20	L-phenylalanine	$C_9H_{11}NO_2$	165.189	Wang et al. (2022a)
21	p-Hydroxy benzaldehyde	$C_7H_6O_2$	122.032	Wang et al. (2022b)
22	Neochlorogenic acid	$C_{16}H_{18}O_9$	354.309	Wang et al. (2022a)
23	4-O-beta-D-glucosyl-4-coumaric acid	$C_{15}H_{18}O_8$	326.299	Wang et al. (2022a)
24	Chlorogenic acid	$C_{16}H_{18}O_9$	354.309	Wang et al. (2022b)
25	Cryptochlorogenic acid	$C_{16}H_{18}O_9$	354.309	Wang et al. (2022a)
26	Gallic acid	$C_7H_6O_5$	170.120	Wang et al. (2022b)

More than 300 compounds such as flavonoids, organic acids, alkaloids, and polyacetylenes have been isolated from safflower, among which flavonoid is the main active component. Given the widespread clinical usage of GuHong injection, acquiring a comprehensive understanding of its chemical composition would greatly facilitate more effective treatment of ischemic stroke and related symptoms. There are three literature references which provide the most comprehensive information on the chemical constituents present in Honghua (Zhou et al., 2014; Zhang et al., 2016; Lu et al., 2019; Xian et al., 2022). Currently, there are few studies on the composition of GuHong injection. It was found that researchers used UPLC-Q-TOF-MS/M to identify a total of 26 components in GuHong as listed in Table 1. Among these components, the majority originate from safflower, with only a small quantity of pharmaceutical excipients derived from the preparation process. It is crucial to emphasize that these excipients are generally not exhibit biological activity. Hence, apart from NAG, the main active ingredients in GuHong are predominantly from safflower.

2.1 Flavonoids

The flavonoids found in safflower are an important class of pharmacologically active ingredients and the most reported class of major compounds, which can be classified as quinonechalcones, flavonols, flavonoids and dihydroflavonoids according to their chemical structure. Its structure is distinguished by the oxidation of the A ring of the parent nucleus of the flavonoid (Figure 2), in the form of quinone or quinone analogues, and all of them are C-glycosides (Yue et al., 2013). The specific ingredients are as follow: hydroxysafflor yellow A, hydroxysafflor yellow B, hydroxysafflor yellow C (Feng et al., 2013; Yue et al., 2014), safflor yellow A, safflor yellow B (Zhou et al., 2014), saffloquinoside A, saffloquinoside B,

Carthamus tinctorius L.

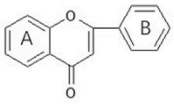

Flavonoid parent nucleus

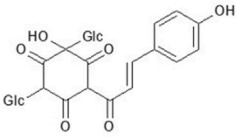

Hydroxysafflor yellow A

FIGURE 2
Chemical structure of flavonoids from Safflower.

saffloquinoside C, saffloquinoside D, saffloquinoside E (Jiang et al., 2013; Yue et al., 2014), cartormin, isocartormin (Li F. et al., 2017), safflomin A, safflomin C (Zhao et al., 2022), etc. The most representative of flavonoids is hydroxysafflor yellow A, which is considered as a quality marker in the Pharmacopoeia of the People's Republic of China (2020). In addition, another major class of flavonoid components in safflower is flavonols with quercetin and kaempferol as the parent structure (Jin et al., 2008; Xie et al., 2016), mostly in the form of O-glucosides. They are usually substituted by monosaccharide (mainly including glucose, rhamnose, glucuronide) or disaccharide (mainly including rutinose, sophorose) at the 3, 6, and 7 positions of their original nucleus (Jin et al., 2008), such as quercetin-3-*O*-β-D-glucoside, quercetin-7-*O*-β-D-glucoside, kaempferol-3-*O*-β-D-glucoside, kaempferol-3-*O*-β-rutinoside, kaempferol-3-*O*-β-sophoroside, 6-hydroxykaempferol, 6-hydroxykaempferol-3-*O*-β-D-glucoside, 6-hydroxykaempferol-7-*O*-β-D-glucoside (Hattori et al., 1992; Kazuma et al., 2000; Hu et al., 2013; Lu et al., 2019). Apart from the above compounds, there are flavonoids and dihydroflavonoids in safflower.

2.2 Organic acids

As a class of acidic organic compounds containing carboxyl groups, organic acids are also one of the pharmacologically active components in safflower. Currently, the organic acids isolated from safflower mainly include *p*-coumaric acid, coumaric acid glycosides (Zhou et al., 2008), chlorogenic acid, butyric acid, *p*-hydroxybenzoic acid, ferulic acid, gallic acid and caffeic acid (Jiang et al., 2008b; Lu et al., 2019).

2.3 Alkaloids

The alkaloids extracted and isolated from safflower contain indole rings and *p*-hydroxycinnamamide groups in their molecules, which are 5-hydroxytryptamine derivatives of indole alkaloids and have anti-oxidant pharmacological activities. Such alkaloids include *N*-feruloyl-5-hydroxytryptamine, *N*-(p-coumaroyl)-5-hydroxytryptamine, *N*-feruloyltryptamine, 4,4″-bis(*N*-p-coumaroyl)5-hydroxytryptamine, 4,4″-bis(*N*-p-coumaroyl)-5-hydroxytryptamine (Jiang et al., 2008b; Zhou et al., 2014).

2.4 Polyacetylenes

The polyacetylene compounds in safflower are mainly ten-, thirteen- and fourteen-carbon compounds with unsaturated double bonds mainly in trans configuration (Li et al., 2021). These components are unstable, prone to decomposition and conformational transformation when exposed to light, and have relatively weak anti-inflammatory effects (Xian et al., 2022), such as (2E, 8Z)-decadiene-4,6-diyne-1-ol-1-*O*-β-D-glucopyranoside, (2E,8E, 10E)-tridecatriene-4,6-diyne-1,12,13-triol-1-*O*-β-D-glucopyranoside, (2E)-tetradecaene-4,6-diyne-1,10,14-triol-1-*O*-β-D-glucopyranoside, (2E, 8E)-tetradecadiene-4,6-diyne-1,12,14-triol-1-*O*-β-D-Glucopyranoside, (2Z, 8Z)-tetradecadiene-4,6-diyne-1,12,14-triol-1-*O*-β-D-glucopyranoside, (2Z, 8E)-tetradecadiene-4,6-diyne-1,12,14-triol-1-O-β-D-Glucopyranoside, (2E, 8Z)-tetradecadiene-4,6-diyne-1,12,14-triol-1-*O*-β-D-glucopyranoside (Liu et al., 2017), etc.

2.5 Spermidines

Spermidines are low molecular weight aliphatic carbons containing three amine groups (Li et al., 2013), and the main spermidine compounds isolated from safflower are safflospermidine A, safflospermidine B, N^1,N^5,N^{10}-(Z)-tri-p-coumaroyl spermidine, N^1,N^5,N^{10}-(E)-tri-p-coumaroyl spermidine, N^1,N^5-(Z)-N^{10}-(E)-tri-p-coumaroyl spermidine (Jiang et al., 2008a; Zhao et al., 2009; Li et al., 2016).

3 Pharmacological mechanisms of GuHong injection for ischemic stroke treatment

Pharmacological investigations have observed that GuHong exhibits brain protective effects on ischemic by reducing thrombosis, anti-oxidation, inhibiting inflammation and apoptosis, maintaining mitochondrial integrity, and improving microvasculature and microcirculation. GuHong is comprised of safflower and NAG, which is a glutamine acetyl derivative and a stable form of glutamine. When GuHong is introduced into the body, NAG is mainly metabolized into glutamine to play its drug effect. This section focuses on a review of pharmacological mechanisms of GuHong, safflower and its chemical composition, NAG and its metabolites, which are shown in Table 2.

TABLE 2 Pharmacological effects of GuHong injection.

Pharmacological activity	Effective dose	Animal/ Cell	Route	Positive control	Effects	Mechanisms	Application	References
Anti-inflammatory	2.5, 5, 10 mL/kg	Male SD rats MCAO model	i.p	Nimodipine 10 mL/kg	Inhibition inflammatory response to ameliorative effect on cerebral I/R injury in rats	NO ↓ iNOS ↓ TNF-α ↓ IL-1β ↓ MPO ↓ CPR ↓ ICAM-1 ↓ NF-κB p65 ↓	*In vivo*	Ai et al. (2017)
	2.5, 5, 10 mL/kg	Male C57BL/ 6 J mice MCAO model	i.p	Minocycline 45 mg/kg	Decreased the abnormally elevated concentrations of proinflammatory cytokines in damaged cortex tissues	TNF-α ↓ IL-1β ↓ IL-6 ↓	*In vivo*	Wang et al. (2022a)
	1.25, 5 mL/kg	Male SD rats MCAO model	i.p	Ginaton 8 mL/kg	Decreased these inflammatory cytokines enhance the expression of molecules that maintain the blood-brain barrier	C5AR1 ↓ C5A ↓ CASP3 ↓ 8-OHdG ↓ TNF ↓ IL-1β ↓ IL-6 ↓ ICAM-1 ↓ MMP-9 ↓ MCP-1 ↓ TIMP1 ↑ JAM-A ↑ laminin ↑	*In vivo*	Zhang et al. (2022a)
Anti-oxidative stress	2.5 mL/kg	Male SD rats MCAO model	i.p	Ginaton 8 mL/kg	enhanced anti-oxidant systems prevented ASK1 activation and suppressed subsequent p38 and JNK cascade-mediated apoptosis	GSH ↑ Trx ↑ Nrf2 ↑	*In vivo*	Zhang et al. (2020)
	5 mL/kg	Male SD rats cerebral ischemia/ reperfusion	i.v./i.g. (postive)	Nimodipine (i.g) 9.375 mg/kg	Increase the anti-oxidant stress and decrease the apoptotic rate	SOD ↑ MDA ↓	*In vivo* and *in vitro*	Wang et al. (2021)
	2.5, 5, 10 mL/kg	Male SD rats MCAO model	i.p	N.d	Enhance anti-oxidant factors and related enzymes to prevent cell damage	SOD ↑ MDA ↓ LDH ↓ MMP-9 ↓	*In vivo*	Zhou et al. (2021)
Anti-coagulant and anti-thrombotic	2.5, 5, 10 mL/kg	Male SD rats MCAO model	i.p	Nimodipine 10 mL/kg	Prevent thrombosis and regulate local blood flow	t-PA ↑ 6-keto-$PGF_{1\alpha}$ ↑ PAI ↓ TXB_2 ↓	*In vivo*	Shu et al. (2014)

(Continued on following page)

TABLE 2 (*Continued*) Pharmacological effects of GuHong injection.

Pharmacological activity	Effective dose	Animal/ Cell	Route	Positive control	Effects	Mechanisms	Application	References
Neuroprotection	2.5, 5, 10 mL/kg	Male SD rats MCAO model	i.p	N.d	Repair brain microvascular and mitochondria, maintain the normal function of nerve cells	BFGF ↑	*In vivo*	Zhou et al. (2021)
						VEGF ↑		
						TGF-β1 ↑		
Anti-apoptosis	2.5, 5, 10 mL/kg	Male C57BL/ 6 J mice or Male SD rats MCAO model	i.p	Minocycline 45 mg/kg	Regulate P13K/AKT pathways to maintain anti-apoptotic, cerebral microvascular and mitochondrial integrity	Cyt-c ↓	*In vivo*	Zhou et al. (2021); Wang et al. (2022a)
						Bax ↓ caspase-3 ↓		
						Bc-2 ↑		
	10 mL/kg	Male SD rats MCAO model	i.p	Nimodipine 10 mL/kg	Through PKC/HIF-1α pathway to ameliorate cerebral I/R injury	HIF-1α↓	*In vivo*	Yu et al. (2021)
						PKC ↓		
						Erythropoietin ↓		

Note: MCAO, middle cerebral artery occlusion.

Safflower is one of the commonly used drugs in the treatment of ischemic cardiovascular and cerebrovascular diseases, which has the effect on activating blood and removing stasis (Yu et al., 2019). It is mainly used in traditional medicine for amenorrhea, dysmenorrhea and lochia. Recent studies have showed that flavonoids are the main bioactive components in safflower, which have anti-inflammatory, anti-oxidant, anti-apoptosis, anti-cerebral ischemic reperfusion injury and protection of cardiovascular and cerebrovascular effects (Asgarpanah and Kazemivash, 2013). However, there are relatively few reports on the pharmacodynamics of NAG. Since NAG is a derivative of glutamine, it acts primarily as glutamine after introducing into the body. Clinically, glutamine plays a versatile role in cellular metabolism. It acts as a crucial nitrogen source for cells, serving as an essential precursor for the synthesis of proteins and nucleic acids. Additionally, it enhances immunity by promoting replication of immune cells and maintaining their functionality. Glutamine also aids in reducing muscle catabolism and improving nitrogen balance. (Andrews and Griffiths, 2002; Cruzat et al., 2018). Furthermore, it exhibits antioxidant effects by promoting the synthesis of glutathione, reducing oxygen free radicals, and alleviating inflammatory responses. (Amores Sanchez and Medina, 1999); Lastly, glutamine serves as a cellular energy source by acting as a substrate for the tricarboxylic acid (TCA) cycle, (Xiao et al., 2016), generating adenosine triphosphate (ATP) to support cellular functions and safeguard intercellular material metabolism. (Yoo et al., 2020). Its pharmacological mechanisms are shown in Figure 3.

3.1 Anti-inflammatory

After ischemic stroke occurs, the accumulation of reactive oxygen species (ROS), inflammatory factors, and necrotic cells will trigger an inflammatory response (Khoshnam et al., 2017). The main pathological mechanism of ischaemic stroke is the excessive release of inflammatory factors. Many studies have shown that post-stroke neuroinflammation is an important factor affecting long-term ischemic prognosis. Thus, neuroinflammation has been regarded as a vital pathological process following cerebral ischemia-reperfusion injury (Yu et al., 2022).

Research finding indicate that the administration of GuHong can significantly decrease the levels of nitric oxide (NO), inducible NO synthase (iNOS), myeloperoxidase (MPO), interleukin-1β (IL-1β), TNF-α (tumor necrosis factor-α) and C reactive protein (CRP) in serum induced by ischemia reperfusion injury in rats. Further, histological examination by H&E staining revealed that after the intervention of GuHong in rats, the cell outlines appeared distinct and a substantial number of neurons were survived. The immunohistochemical staining revealed that GuHong administration significantly attenuated expressions of intercellular cell adhesion molecule-1 (ICAM-1) and nuclear factor-κB p65 (NF-κB p65) in rat brain tissues to exert anti-inflammatory effects (Ai et al., 2017). Besides, the interaction between the active components of GuHong and NF-κB p65 was determined by molecular docking. GuHong and its active substances partially prevent thrombosis and ischemic stroke by regulating NF-κB mediated inflammatory responses (Wang et al., 2022b). According to the results of immunofluorescence and ELISA, the administration of GuHong (10 mL/kg) to mice with ischemic stroke decreased NF-κB p65 nuclear translocation and regulated the content of pro-inflammatory factors including TNF-α, IL-6, and IL-1β in the damaged cortical tissue of mice with subacute stroke (Wang et al., 2022a). Moreover, C5ar1 (CD88) is considered to be an important potential therapeutic target for the regulation of inflammation in ischemic stroke. Experiments demonstrated that the administration of GuHong could lead to a decrease of C5AR1, C5A, CASP3, 8-OHdG, as well as inflammatory factors covering IL-1β, TNF, IL6, ICAM-1, MMP9, MCP-1 in MCAO rat model. Additionally, GuHong also enhanced the expression of tissue inhibitor of metalloproteinases 1 (TIMP1), junctional adhesion molecule 1 (JAM-A) and laminin to regulated cell growth and differentiation (Zhang J. J. et al., 2022).

The content of safflower in GuHong injection is equivalent to 0.5 g raw drug, in which hydroxylsafflower yellow A (HSYA) is used as the quality control component (0.410–0.437 mg/mL).

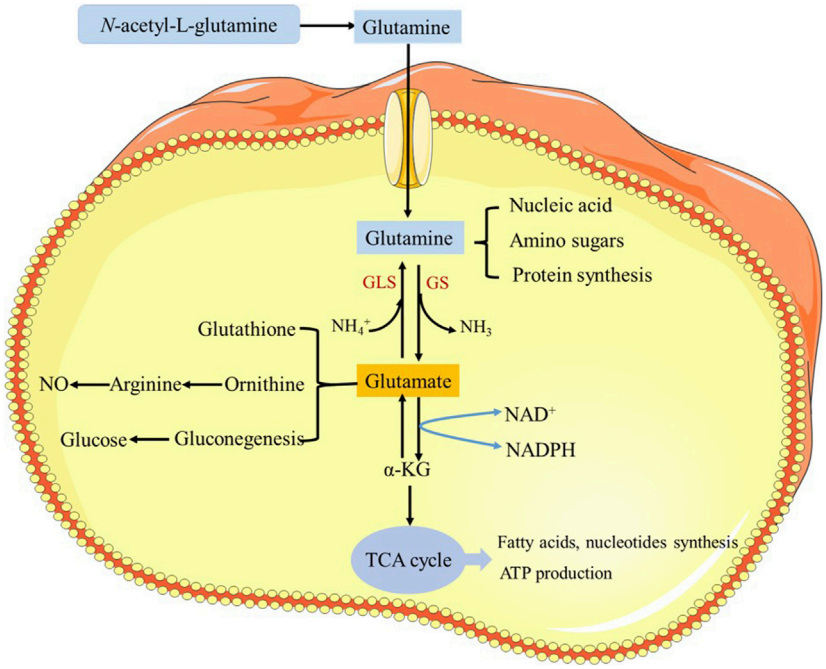

FIGURE 3
Pharmacological mechanism of *N*-acetyl-L-glutamine.

Experimental data have demonstrated that safflower extract also has anti-inflammatory effects on brain infarct areas by reducing free radical levels in the blood and inhibiting the expression of TNF-α and IL-1β (Fu et al., 2016). Different extraction methods of safflower can affect the type and content of chemical components, resulting in different drug effects. Safflower aqueous and methanol extracts were shown to inhibit inducible iNOS and cyclooxygenase-2 (COX-2) protein expression and to diminish LPS-induced release of NO, prostaglandin E2 (PGE2) and IL-1β as well as to translocated nuclear factor (red-like derivative 2)-like 2 (Nrf2) from the cytoplasm to the nucleus and significantly reduced NF-κB binding and NF-κB luciferase activity. In addition, safflower methanol extract also significantly attenuated tumor necrosis factor (TNF-α)-mediated vascular cell adhesion protein 1 (VCAM-1) expression in endothelial cells, thus, regardless of the extraction method, safflower exhibited significant anti-inflammatory effects (Jun et al., 2011; Wang et al., 2011). HSYA is the main representative component of safflower in GuHong injection. In the literature, HSYA has been reported to decrease brain infarct volume in ischemia-reperfused rats, increase GSK-3β phosphorylation levels, downregulate the expression of several key pro-inflammatory cytokines, and inhibit the activation of iNOS, NF-κB and caspase-3, These actions collectively contribute to its anti-inflammatory and anti-apoptotic effects (Ye and Gao, 2008; Yang et al., 2020). In addition, HSYA inhibits LPS-induced reduction in pro-inflammatory factor levels and suppress VSMC proliferation and migration by inhibiting the TLR-/Rac1/Akt pathway (Yang et al., 2015). Under the condition of pathological injury, oral supplementation with glutamine can significantly reduce TNF-α and IL-1β (Cruzat et al., 2014).

3.2 Anti-oxidative stress

Due to high oxygen demand and limited anti-oxidant capacity, the brain is quite sensitive to hypoxia and susceptible to oxidative damage. Ischemia-reperfusion leads to the production of highly harmful ROS, and then trigger oxidative stress (OS), which is responsible for most of the ischemia-reperfusion-induced brain damage. In addition, OS can lead to apoptosis, autophagy, and necrosis of brain cells (Rodrigo et al., 2013; Orellana Urzúa et al., 2020).

The triple anti-oxidant system of Nrf2, glutathione (GSH) and thioredoxin (Trx) could be enhanced by GuHong, which were more effective than its two combinations in ameliorating oxidative damage after brain I/R. Moreover, GuHong enhanced the triple anti-oxidant system while blocked the activation of ASK1 and subsequently inhibited the activation of p38 and JNK signaling cascades, preventing oxidative damage and apoptosis (Zhang et al., 2020). Glutathione-s-transferase (GST) is a detoxification enzyme that exerts cellular detoxification by catalyzing the reaction of reduced glutathione (GSH) with electrophilic reagents substance (Ji et al., 2019). GuHong can increase the expression levels of GST P mRNA and protein, and regulate oxidative stress (Chen et al., 2023). GuHong injection increases SOD (superoxide dismutase) levels and reduces MDA (malondialdehyde) levels in patients with ischemia-reperfusion to prevent oxidative damage (Wang et al., 2021; Zhou et al., 2021).

Under pathological conditions, brain tissue experiences ischemia and hypoxia, leading to the excessive production of reactive oxygen species and an accumulation of free radicals. This process results in brain lipid peroxidation and exacerbates injury to the brain tissue. Flavonoids are the main components of

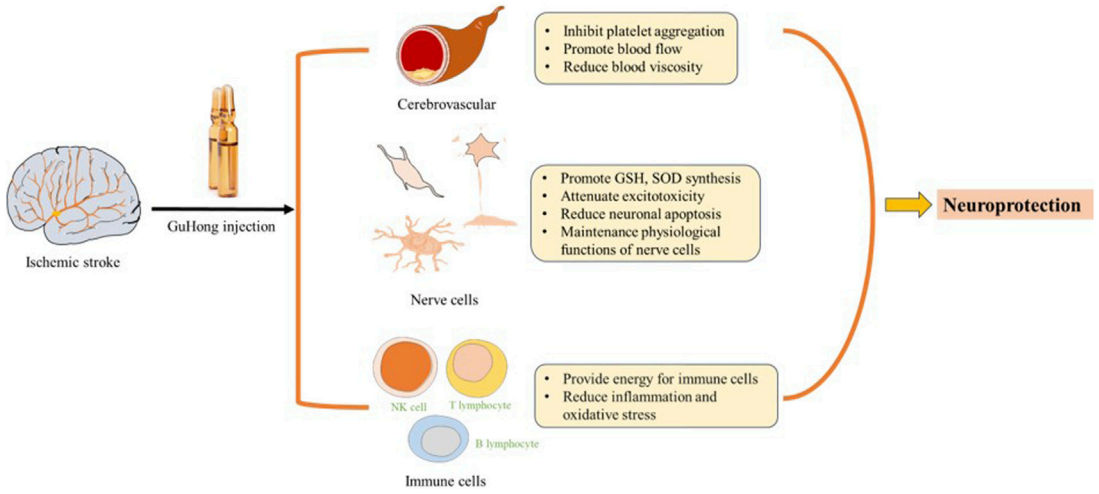

FIGURE 4
Neuroprotective mechanism of GuHong injection3.5 Anti-apoptosis.

safflower extracts in GuHong and are active in scavenging radicals including O^{2-}, –OH, and DPPH in a dose-dependent manner (Han et al., 2010). HSYA, as one of the main quinonechalcones in GuHong, can inhibit Ca^{2+} and H_2O_2 induced swelling of rat brain mitochondria and decreased the production of ROS. HSYA treatment can significantly reduce the MDA content in the ipsilateral hemisphere and serum, and increase the activity of SOD and total anti-oxidant capacity (Wei et al., 2005; Tian et al., 2008). The tripeptide GSH is the most important intracellular anti-oxidant. Glutamine is an important precursor compound for glutamate, and the synthesis of GSH depends on the supply of glutamine to glutamate. Glutamine, as a precursor for glutathione synthesis, is clinically added to patients against oxidative stress (Amores Sanchez and Medina, 1999). NAG can also enhance the anti-oxidant system and effectively improve the oxidative damage of ischemia reperfusion, although less effective than combined safflower extract (Zhang et al., 2020).

3.3 Anti-coagulant and anti-thrombotic effect

Platelet activating factor (PAF), the most potent platelet activator known, has a wide range of biological activities and can be synthesized by a variety of cells including platelets, leukocytes and endothelial cells. It was found that GuHong could significantly increase the contents of tissue-type plasminogen activator (t-PA) and 6-keto prostaglandin $F_{1\alpha}$ (6-keto-$PGF_{1\alpha}$), and decrease the contents of plasminogen activator inhibitor (PAI) and thromboxane B_2 (TXB_2) in serum of rats with ischemia reperfusion. The dynamic balance between TXB_2/6-keto-$PGF_{1\alpha}$ are important factor in regulating vascular wall tension, platelet function, preventing thrombosis and regulating local blood flow. These results showed that GuHong had good anti-thrombotic effects in the treatment of stroke (Shu et al., 2014). Safflower yellow, the main active ingredient in safflower, is extracted from the aqueous extract of safflower and has anti-coagulant pharmacological activity. Safflower yellow could inhibit PAF induced platelet activation and suppress platelet aggregation, release reaction, and increase intracellular free calcium (Zang et al., 2002; Jin et al., 2004; Huang et al., 2012). Experimental data in the literature showed that safflower yellow could significantly prolong plasma prothrombin time (PT), thromboplastin time (TT) and activated partial thromboplastin time (APTT), reduce plasma fibrinogen content and inhibit ADP-induced platelet aggregation in rats. Moreover, it significantly reduced whole blood viscosity, plasma viscosity and erythrocyte aggregation index in rats with blood stasis models (Li et al., 2009). Coagulation factors F7 and F2 were recognized as crucial factors in the extrinsic coagulation pathway. Studies have revealed that GuHong can significantly decrease the mRNA expression of coagulation factors F7 and F2. This suggests that the coagulation cascade regulated by these factors may serve as targets for GuHong's anti-thrombotic effect (Wang et al., 2022b).

3.4 Neuroprotection effect

Neuroprotective therapy is aimed at the main pathological mechanism of ischemic stroke and the biochemical and metabolic disorders of ischemic brain injury through drugs or other means to block cell necrosis, increase cell survival ability, and promote the recovery of neurological function. Neuroprotective agents play a vital role in reducing cell damage following ischemia. Their primary objective are to extend the time window for cerebral perfusion therapy, delay nerve cell death, and alleviate brain dysfunction. (Tuo et al., 2022). Neuroprotection and neurorestoration therapy are the two main drug intervention strategies for ischemic stroke. Neuroprotective therapy can significantly prolong the time window of thrombolytic therapy and reduce cerebral ischemic injury (Zhu et al., 2022). Immunohistochemical staining of rat cerebral tissues revealed a significant increase in the expression of BFGF, VEGF, and TGF-β1 following the administration of GuHong (Zhou et al., 2021). GuHong injection promotes the expression of vascular

TABLE 3 Pharmacokinetic parameters of GuHong injection and its components.

Species	Drug/dose	Analyses	Analyte methods	Measure sample	C_{max} (ng/mL)	$T_{1/2}$ (h)	AUC_{0-t} (mg·h/L)	$AUC_{0-\infty}$ (mg·h/L)	MRT (h)	Reference
Normal SD rats (n = 6)	GuHong injection, 2.10 mL/kg	HSYA	HPLC	plasma	15.15 ± 0.39	2.29 ± 0.55	47.25 ± 0.45	57.16 ± 3.42	2.10 ± 0.47	Yu et al. (2018)
Normal SD rats (n = 6)	GuHong injection, 2.10 mL/kg	NAG	HPLC	plasma	338.83 ± 7.01	0.78 ± 0.26	1282.41 ± 32.91	1292.41 ± 29.48	1.19 ± 0.04	
MCAO SD rats (n = 6)	GuHong injection, 2.10 mL/kg	HSYA	HPLC	plasma	8.84 ± 0.05	2.83 ± 1.29	31.69 ± 0.36	54.53 ± 13.27	3.64 ± 1.60	
MCAO SD rats (n = 6)	GuHong injection, 2.10 mL/kg	NAG	HPLC	plasma	175.13 ± 86.11	0.57 ± 0.28	435.04 ± 213.19	442.44 ± 216.82	0.92 ± 0.45	
Normal SD rats (n = 6)	Acetyl-L-glutamine 75 mg/kg	NAG	LC-MS/MS	Blood microdialysis	74350 ± 4400	0.74 ± 0.05	358.49 ± 18.49	359.75 ± 18.45	0.93 ± 0.03	Xu et al. (2020)
Normal SD rats (n = 6)	Acetyl-L-glutamine 150 mg/kg	NAG	LC-MS/MS	Blood microdialysis	118610 ± 6670	0.64 ± 0.11	594.74 ± 16.74	595.82 ± 16.61	0.94 ± 0.04	
Normal SD rats (n = 6)	Acetyl-L-glutamine 300 mg/kg	NAG	LC-MS/MS	Blood microdialysis	128250 ± 6240	0.50 ± 0.20	793.88 ± 52.77	797.78 ± 54.73	1.24 ± 0.07	
Normal SD rats (n = 6)	GuHong injection, 10 mL/kg	NAG	LC-MS/MS	Blood microdialysis	118370 ± 6500	0.76 ± 0.22	750.82 ± 64.56	755.12 ± 65.32	1.29 ± 0.06	
Normal SD rats (n = 6)	Acetyl-L-glutamine 75 mg/kg	NAG	LC-MS/MS	Brain microdialysis	7760 ± 500	2.01 ± 0.30	50.14 ± 1.37	58.69 ± 3.48	2.84 ± 0.42	
Normal SD rats (n = 6)	Acetyl-L-glutamine 150 mg/kg	NAG	LC-MS/MS	Brain microdialysis	30570 ± 3330	0.96 ± 0.06	163.15 ± 7.62	165.27 ± 7.32	1.44 ± 0.03	
Normal SD rats (n = 6)	Acetyl-L-glutamine 300 mg/kg	NAG	LC-MS/MS	Brain microdialysis	53440 ± 4710	0.96 ± 0.10	275.07 ± 13.99	278.67 ± 14.04	N.d	
Normal SD rats (n = 6)	GuHong injection, 10 mL/kg	NAG	LC-MS/MS	Brain microdialysis	41480 ± 3340	1.25 ± 0.25	226.34 ± 14.10	241.01 ± 25.23	N.d	
MCAO SD rats (n = 10)	HSYA 4 mg/kg	HSYA	HPLC	plasma	N.d	0.84 ± 0.21	51296.40 ± 7095.60	51645.60 ± 7481.40	1.00 ± 0.10	Chen et al. (2016)
MCAO SD rats (n = 10)	GuHong injection, 10 mL/kg (equal to HSYA 4 mg/kg)	HSYA	HPLC	plasma	N.d	1.06 ± 0.26	95102.40 ± 17421.00	97941.00 ± 20107.80	1.64 ± 0.28	
Normal SD rats (n = 4)	Safflower injection 1 mL/kg	HSYA	LC-MS/MS	plasma	2624.50 ± 660.17	0.47 ± 0.07	2.48 ± 1.31	2.49 ± 1.32	0.78 ± 0.19	Shi et al. (2022)
Normal SD rats (n = 3)	Safflower injection 2 mL/kg	HSYA	LC-MS/MS	plasma	5628.33 ± 405.14	0.64 ± 0.08	5.07 ± 3.29	5.46 ± 2.02	0.97 ± 0.06	
Normal SD rats (n = 3)	Safflower injection 4 mL/kg	HSYA	LC-MS/MS	plasma	14077.33 ± 17.21	0.46 ± 0.12	11.02 ± 1.03	11.45 ± 6.68	0.78 ± 0.11	
Healthy volunteers (n = 12)	HSYA 25 mg/kg	HSYA	LC-MS/MS	plasma	1736 ± 381	4.10 ± 0.42	6.80 ± 1.25	6.89 ± 1.28	N.d	Li et al. (2015)

(Continued on following page)

TABLE 3 (*Continued*) Pharmacokinetic parameters of GuHong injection and its components.

Species	Drug/dose	Analyses	Analyte methods	Measure sample	C_{max} (ng/mL)	$T_{1/2}$ (h)	AUC_{0-t} (mg·h/L)	$AUC_{0-\infty}$ (mg·h/L)	MRT (h)	Reference
Healthy volunteers (n = 12)	HSYA 50 mg/kg	HSYA	LC-MS/MS	plasma	3207 ± 582	3.91 ± 0.39	12.66 ± 2.23	6.89 ± 1.28	N.d	
Healthy volunteers (n = 12)	HSYA 75 mg/kg	HSYA	LC-MS/MS	plasma	3603 ± 554	4.18 ± 0.29	16.33 ± 2.13	16.56 ± 2.16	N.d	

Note: HSYA, hydroxysafflor yellow A; NAG, *N*-acetyl-L-glutamine; HPLC, high performance liquid chromatography; LC-MS/MS, liquid chromatography tandem mass spectrometry; C_{max}, maximum plasma concentration; $T_{1/2}$, elimination half-life; AUC_{0-t}, area under the plasma concentration-time curve from 0 to last measurable time point after dosing; $AUC_{0-\infty}$, area under the plasma concentration-time curve from zero to infinity; MRT, mean residence time. N.d., not detected.

endothelial growth factor (VEGF-B), nerve growth factor (NGF) and glial cell line-derived neurotrophic factor (GDNF) to reduce nerve damage caused by diabetic peripheral neuropathy (Martel et al., 2017). Studies have revealed that stroke disrupts glycolysis, the TCA cycle, the malate-aspartate cycle, the glutamate-glutamine cycle, nucleic acid metabolism, and phospholipid metabolism in the affected regions of the ischemic hemisphere in rats. However, administration of GuHong injection has been found to regulate the levels of these metabolites, leading to significant improvements in cerebral infarction rate, neurological deficits, cerebral blood flow, and neuronal damage. (Wang et al., 2023).

Excitotoxicity is one of the molecular mechanisms of post-ischaemic stroke injury. During cerebral ischemia and hypoxia, the brain experiences an elevation in the release of excitatory neurotransmitters and a disruption in their reuptake due to metabolic abnormalities. This results in the levels of excitatory neurotransmitters escalate rapidly within the ischemic regions of the brain. When the brain is in a state of ischemia and hypoxia, increased excitatory neurotransmitter release and impaired reuptake due to metabolic disorders result in rapidly increasing levels of excitatory neurotransmitters in ischaemic areas of the brain. Ischemic neuronal injury causes a massive release of glutamate, leading to excessive activation of NMDA receptors and a massive influx of Ca^{2+} into cells, resulting in excitotoxic cell death (Orrenius et al., 2003; Maida et al., 2020). According to the literature, Except for NAG, HSYA is the most abundant chemical ingredient in GuHong and is also the quality control ingredient in safflower (Li X. et al., 2017). HSYA protects the hippocampal neurons from excitatory toxic damage by inhibiting NMDARs and regulating the Bcl-2 family as the main component of GuHong (Yang et al., 2010; Wang et al., 2016). HSYA treatment can also significantly attenuate the neurological defects caused by ischemic stroke and reduce the volume of cerebral infarction. To protect the nerves from damage, it has been observed that decreased hippocampal expression levels of LC3, HIF-1, BNIP3, and Notch1 are effective. (Zhang Y. L. et al., 2022). As a neuroprotective agent, NAG has been proved to improve behavioral functions, reduce infarct volume and elevate the number of TH-positive neurons in the substantia nigra (SN) (Zhang et al., 2015). Safflower and NAG in GuHong injection can synergistically play a neuroprotective role, and the specific mechanism is shown in Figure 4.

Apoptosis is a normal physiological phenomenon of genetically controlled cell death to maintain the homeostasis of the internal environment. When cerebral ischemia and reperfusion occur, excessive apoptosis of neurons in brain tissue can largely exacerbate brain injury and cause a series of normal physiological dysfunctions in the body (Radak et al., 2017).

It has been found that a decrease in Bcl-2 or overexpression of Bax causes neuronal apoptosis after cerebral ischemia. (Love, 2003). GuHong injection was effective to upregulate Bax, Caspase-3 and Cleaved-Caspase-3 while increasing Bcl-2 protein expression after continuous administration to acute ischemic stroke rats significantly (Zhou et al., 2021; Wang et al., 2022a). GuHong alleviated brain I/R injury in MCAO rats by decreasing plasma EPO (erythropoietin), HIF-1α (hypoxia-inducible factor-1α), PKC (protein kinase C), upregulating prolyl hydroxylase structural domain 2 (PHD2) protein, downregulating HIF-1α and iNOS protein, and decreasing nicotinamide adenine dinucleotide phosphate oxidase 4 (NOX4) and HIF-1α mRNA, which can regulate apoptosis (Yu et al., 2021).

GuHong injection effectively inhibits the expression of ASK1, JNK, and p38 mRNA. It also decreases the expression of Bax while elevating the expression of Bcl-2, resulting in a reduction in caspase-3 expression and exerting anti-apoptotic effect (Chen et al., 2023). HSYA could inhibit apoptosis in I/R-injured rat penumbra cortical cells by increasing Bcl-2/Bax ratio and this neuroprotective effect may be related to the activation of PI3K/Akt/GSK3β signaling pathway (Yang et al., 2010; Chen et al., 2013). NAG also reduces apoptosis in nigrostriatal neurons by inhibiting the apoptosis-related factor tumor necrosis factor receptor-associated factor 1 (TRAF1) and by upregulating the P-Akt and Bcl-2 signaling pathways, which can increase the number of Th-positive nigrostriatal neurons and reduce neuronal apoptosis (Zhang et al., 2015). Apart from HSYA and NAG, GuHong contains other active substances that contribute to stroke management. These include baicalin, scutellarin, gallic acid, chlorogenic acid, kaempferol, kaempferol-3-O-β-rutinoside, and rutin. These substances work synergistically to target central pathways involved in inflammation and apoptosis, such as NF-κB p65, TNF-α, IL-6, IL-1β, Bax, Bcl-2, and Caspase-3 (Wang et al., 2022a).

4 Pharmacokinetics

Pharmacokinetics is the quantitative study of drug absorption, distribution, metabolism and excretion in the body, which is regulated by many factors (such as dose, administration mode, species and drug interactions). Pharmacokinetic studies are also effective way to discover active ingredients and determine quality

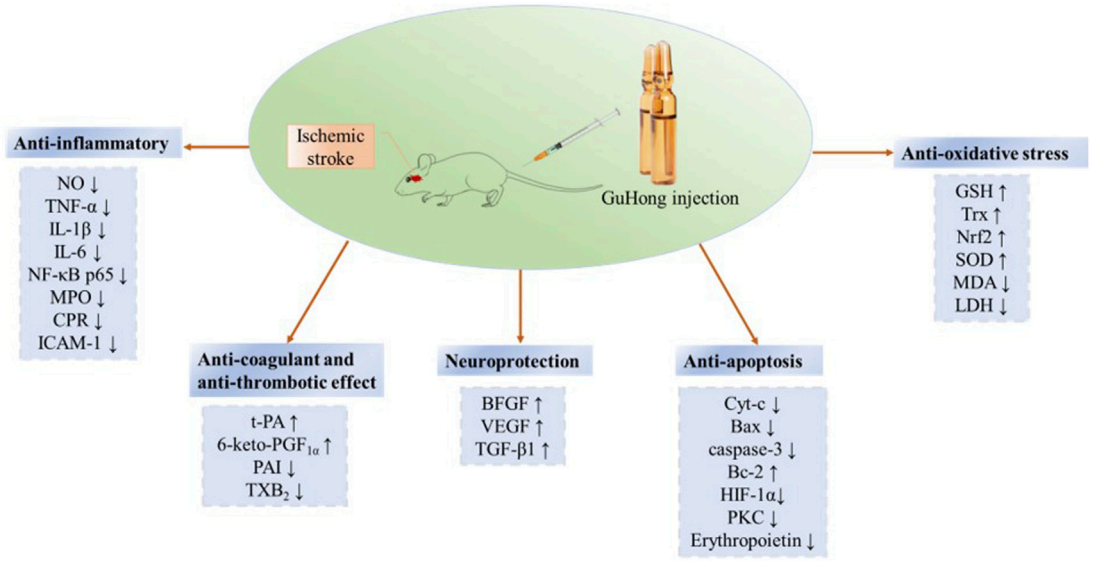

FIGURE 5
Pharmacological mechanism of GuHong Injection.

markers in Chinese medicine. The specific pharmacokinetic parameters of GuHong injection and its components are summarized in Table 3.

According to current literature reports, after the administration of GuHong, most scholars mainly studied the pharmacokinetic characteristics of target compounds, NAG and HSYA in safflower. Yu et al. studied the pharmacokinetics of intravenous glutamine injection (2.1 mg/kg) in healthy and MCAO pathological rats using HPLC analysis method (Yu et al., 2018). The results showed that the main exposed substances in plasma were NAG and HSYA after intravenous glutamine injection. The C_{max}, $t_{1/2}$, $AUC_{0-\infty}$ and MRT of HSYA in healthy rats and MCAO model rats were 15.15 ± 0.39 vs. 8.84 ± 0.05 μg/L, 137.47 ± 32.91 vs. 169.76 ± 77.50 min, 952.89 ± 57.00 vs. 909.84 ± 221.11 μg/L*min, 125.81 ± 28.01 vs. 218.51 ± 95.87min, respectively. The C_{max}, $t_{1/2}$, $AUC_{0-\infty}$ and MRT of NAG in healthy rats and MCAO model rats were 338.83 ± 7.01 vs. 175.13 ± 86.11 μg/L, 46.91 ± 15.87 vs. 34.48 ± 16.96 min, 21373.54 ± 548.58 vs. 7250.72 ± 3553.22 μg/L*min, 71.61 ± 2.59 vs. 55.39 ± 27.15 min, respectively. In the rats of MCAO group, the C_{max} and $AUC_{0-\infty}$ of HSYA and NAG were significantly higher than those of the healthy group. This results indicate that under the pathological condition of MCAO, compounds of GuHong may enter the brain and be utilized due to the disruption of the blood-brain barrier, thereby reducing their exposure in the plasma. Healthy rats were treated with low (75 mg/kg), medium (150 mg/kg) and high (300 mg/kg) doses of NAG and GuHong injection (10 mL/kg, equivalent to 150 mg/kg containing NAG), and the dialysate of blood and brain was collected by LC-MS/MS combined with microdialysis sampling technique. According to the $AUC_{0-\infty,\ brain}/AUC_{0-\infty,\ blood}$ results (Liu and Li, 2010), NAG can cross the blood-brain barrier and act on the central nervous system. Comparing its half-life in blood and brain, NAG is eliminated faster in blood than in brain (Xu et al., 2020). Besides, according to the administration of NAG at low, medium and high doses, the dose-exposure relationship of C_{max} and $AUC_{0-\infty}$ in blood and brain was not proportional (Smith et al., 2000). Healthy volunteers were given 25, 50 and 75 mg/kg HSYA respectively, and the dose-exposure relationship of $AUC_{0-\infty}$ was linear (Li et al., 2015). According to the results of the literature, rats were given 4 mg/kg HSYA and 10 mL/kg GuHong injection (equal to HSYA 4 mg/kg), and the $t_{1/2}$ and $AUC_{0-\infty}$ were 50.11 ± 12.62 vs. 63.53 ± 15.84 min, 860.76 ± 124.69 vs. 1632.35 ± 335.13 respectively. GuHong injection contains both safflower and NAG, which may have pharmacokinetic matrix effect in the body and affect the pharmacokinetic characteristics of HSYA (Chen et al., 2016).

5 Clinical application of GuHong injection

GuHong injection was approved for marketing in 2003 and has been in clinical use for about 20 years. The main ingredients are NAG and safflower extract, which complement each other. NAG can improve nerve cell metabolism and brain function; *Carthamus tinctorius L.* is included in the Chinese Pharmacopoeia from the 1963 to 2020 editions and it is a commonly utilized Chinese herb with the effect of promoting blood circulation to remove blood stasis. GuHong has been extensively employed in clinical for the treatment of diverse cardiovascular and cerebrovascular diseases. It exhibits several beneficial pharmacological effects such as enhancing coagulation function, suppressing inflammation, exerting antioxidant properties, preventing neuronal damage, and mitigating ischemia-reperfusion injury. These effects are illustrated in Figure 5. GuHong injection is recommended by the

TABLE 4 The clinical application of GuHong injection.

Disease	Sample size		Gender (M/F)		Age (years)		Medication		Treatment time	Clinical therapeutic effect evaluation	References
	T	C	T	C	T	C	T	C			
Acute ischemic stroke	30	30	16/14	16/14	43–73	43–74	GuHong injection, i.v	MaiLuoNing injection, i.v	14 days	NIH Stroke Scale Glasgow Coma Scale	Cai et al. (2006)
Acute ischemic stroke	42	42	22/20	24/18	47–85	47–83	GuHong injection, i.v	compound danshen injections, i.v	14 days	Clinical neurological deficit score in Chinese stroke patients (1995)	He (2006)
Acute ischemic stroke	50	45	32/18	30/15	60–72	61–75	GuHong injection, i.v	compound danshen injections, i.v	14 days	Scandinavian stroke scale	Wang and Dong (2006)
Acute ischemic stroke	60	60	37/23	35/25	40–72	38–73	GuHong injection, i.v	compound danshen injections, i.v	15 days	Clinical neurological deficit score in Chinese stroke patients (1995)	Li et al. (2007)
Acute ischemic stroke	50	50	24/26	21/29	57–88	61–93	GuHong injection, i.v	Saiviae Miltiorrhizae and Ligustrazine Hydrochloride Injection, i.v	14 days	NIH Stroke Scale	Zhang and Ning (2015)
Acute ischemic stroke	138	143	80/58	93/50	50–73	52–72	Initial therapy + GuHong injection, i.v	Initial therapy	14 days	NIH Stroke Scale, Glasgow Coma Scale Modified Rankin Scale	Zhang (2010)
Acute ischemic stroke	40	40	19/21	20/20	40–75	41–75	Initial therapy + GuHong injection, i.v	Initial therapy	14 days	NIH Stroke Scale, Glasgow Coma Scale Modified Rankin Scale	Jiang et al. (2016)
Acute ischemic stroke	68	68	39/29	41/27	48–85	46–83	Butylphthalide and Sodium Chloride injection + GuHong injection, i.v	Butylphthalide and Sodium Chloride injections, i.v	14 days	NIH Stroke Scale	Li and Zhang (2018)
Acute ischemic stroke	38	38	21/17	23/15	46–82	45–82	Ozagrel Sodium injection + GuHong injection, i.v	Ozagrel Sodium injection, i.v	14 days	NIH Stroke Scale	Sheng (2019)
vascular cognitive impairment	186	143	106/80	83/60	56–60	56–70	GuHong injection, i.v	Dengzhanxixin injection, i.v	14 days	Basic cognitive ability test	Zhao (2006)
vascular cognitive impairment	35	35	18/17	16/19	56–79	60–78	GuHong injection, i.v	Danshen injections, i.v	14 days	Neurological impairment score	Liu (2017)
vascular cognitive impairment	30	30	15/15	18/12	67–85	68–85	Initial therapy + GuHong injection, i.v	Initial therapy	14 days	Montreal Cognitive Assessment	Jia (2019)
vascular cognitive impairment	38	38	24/14	22/16	55–82	54–81	GuHong injection, i.v	Acetamide Pyrrolidone injection, i.v	21 days	Montreal Cognitive Assessment	Wang (2020)

(Continued on following page)

10.3389/fphar.2023.1261326

TABLE 4 (*Continued*) The clinical application of GuHong injection.

Disease	Sample size		Gender (M/F)		Age (years)		Medication		Treatment time	Clinical therapeutic effect evaluation	References
	T	C	T	C	T	C	T	C			
Coronary heart disease	33	33	20/13	21/12	55–81	52–82	Initial therapy + GuHong injection, i.v	Initial therapy	10 days	Resting electrocardiogram	He et al. (2019)
Coronary heart disease	38	38	25/13	27/11	61–76	60–72	Initial therapy + GuHong injection, i.v	Initial therapy	ND	hematological examination	Chen and Xu (2020)
Coronary heart disease	130	130	N.d	N.d	N.d	N.d	GuHong injection, i.v	physiological saline, i.v	10 days	anginal attack frequency Electrocardiogram changes TCM symptoms and signs scores	Zhuang et al. (2020)
Coronary heart disease	58	58	33/25	32/26	51–76	52–75	GuHong injection, i.v	Metoprolol Tartrate Tablets, p.o	15 days	hemorheology	Xu (2020)

Note: T, treatment group; C, control group; M, male; F, female; i. v., intravenous; p. o., peros.

"Expert Consensus on Integrated Chinese and Western Medicine Treatment of Chronic Cerebral Ischemia" (Gao, 2018) and used as intravenous preparation in clinical practice (Liu et al., 2020). According to the results of the meta-analysis of clinical application of GuHong injection, it is mainly used in acute ischemic stroke and vascular cognitive impairment caused by cerebrovascular disease. The summary results of meta-analysis literature on the clinical application of GuHong are shown in Table 4.

6 Discussion and conclusion

In the present review, we systematically summarized the informations about GuHong injection, including the phytochemistry, pharmacokinetics, pharmacological effects and clinical studies. Ischemic stroke is mainly caused by thrombosis, embolism and focal hypoperfusion, which can result in cerebral ischemia and hypoxia. The pathophysiology is complex and can cause a range of responses including energy depletion, excitotoxicity, oxidative stress, blood-brain barrier disruption (BBB), inflammation, necrosis or apoptosis (Campbell et al., 2019). Previous studies have shown that GuHong is a multi-component, multi-target and multi-pathway agent with anti-inflammatory, anti-oxidant, anti-apoptotic and neuroprotective effects. It is mainly used clinically for the treatment of cardiovascular and cerebrovascular diseases. The pharmacokinetics-based identification of these exposure compounds, together with metabolites after dosing GuHong injection, will facilitate uncovering active constituents responsible for the injection's therapeutic action. GuHong injection has significant advantages in the treatment of ischemic stroke through multi-substance, multi-pathway mechanism of action.

Moreover, although GuHong has shown some efficacy in the treatment of ischemic stroke, there are still many problems and challenges. First of all, there are few literatures available that report the composition spectrum of GuHong, and it is unclear about how many chemical compositions are contained in GuHong injection from safflower. Secondly, there is a lack of overall pharmacodynamic studies on NAG, and it is not possible to state whether it is the original form or the metabolite that exerts the pharmacological effect. Thirdly, Pharmacokinetics of the bioactive components of GuHong are absent in experimental animals, healthy volunteers and patients with ischemic stroke. The available pharmacokinetic studies are insufficient of distribution, metabolism and excretion. Fourthly, multicentre, large-scale, methodologically reliable trials are still needed to verify the efficacy of GuHong in the treatment of ischemic stroke. Finally, more high-quality designed experiments and literature are needed to provide more credible evidence for the effectiveness and safety of GuHong.

In short, it is the first time to systematically summarize the basic information about GuHong, which might provide relatively comprehensive basic data for the related research of GuHong. Although GuHong has shown some efficacy in the treatment of ischemic stroke, there are some scientific gaps that need to be filled currently. More research concerning pharmacokinetics, interactions with other drugs, clinical efficacy and safety, pharmacological mechanisms of bioactive components, and large-scale clinical trials should be conducted in the future.

Author contributions

QW: Writing–original draft, Writing–review and editing. ZY: Writing–original draft. LG: Investigation, Visualization, Writing–review and editing. ZL: Software, Writing–review and editing. YL: Data curation, Visualization, Writing–review and editing. SF: Supervision, Writing–original draft. YW: Funding acquisition, Investigation, Writing–review and editing.

Funding

The author(s) declare that no financial support was received for the research, authorship, and of this article.

Conflict of interest

The authors declare that the research was conducted in the absence of any commercial or financial relationships that could be construed as a potential conflict of interest.

Publisher's note

All claims expressed in this article are solely those of the authors and do not necessarily represent those of their affiliated organizations, or those of the publisher, the editors and the reviewers. Any product that may be evaluated in this article, or claim that may be made by its manufacturer, is not guaranteed or endorsed by the publisher.

References

Adams, H. P., Jr., Bendixen, B. H., Kappelle, L. J., Biller, J., Love, B. B., Gordon, D. L., et al. (1993). Classification of subtype of acute ischemic stroke. Definitions for us e in a multicenter clinical trial. TOAST. Trial of Org 10172 in Acute Stroke Treatment. *Stroke* 24, 35–41. doi:10.1161/01.str.24.1.35

Ai, J. C., Wan, H. T., Shu, M. C., Zhou, H. F., Zhao, T., Fu, W., et al. (2017). Guhong injection protects against focal cerebral ischemia-reperfusion injury via anti-inflammatory effects in rats. *Archives Pharmacal Res.* 40, 610–622. doi:10.1007/s12272-016-0835-4

Amores Sanchez, M. I., and Medina, M. A. (1999). Glutamine, as a precursor of glutathione, and oxidative stress. *Mol. Genet. Metabolism* 67, 100–105. doi:10.1006/mgme.1999.2857

Andrews, F. J., and Griffiths, R. D. (2002). Glutamine: Essential for immune nutrition in the critically ill. *Br. J. Nutr.* 87, S3–S8. doi:10.1079/bjn2001451

Asgarpanah, J., and Kazemivash, N. (2013). Phytochemistry, pharmacology and medicinal properties of Carthamus tin ctorius L. *Chin. J. Integr. Med.* 19, 153–159. doi:10.1007/s11655-013-1354-5

Bollhalder, L., Pfeil, A. M., Tomonaga, Y., and Schwenkglenks, M. (2013). A systematic literature review and meta-analysis of randomized clinica l trials of parenteral glutamine supplementation. *Clin. Nutr. Edinb. Scotl.* 32, 213–223. doi:10.1016/j.clnu.2012.11.003

Cai, Y., Lu, G. L., Che, J. M., and Wu, H. R. (2006). Clinical study of Guhong injection in the treatment of acute cerebral infarction in 30 cases. *Pract. J. Cardiac Cereb. Pneumal Vasc. Dis.* 2006, 724–725. doi:10.3969/j.issn.1673-5110.2007.02.011

Campbell, B. C. V., De Silva, D. A., Macleod, M. R., Coutts, S. B., Schwamm, L. H., Davis, S. M., et al. (2019). Ischaemic stroke. *Nat. Rev. Dis. Prim.* 5, 70. doi:10.1038/s41572-019-0118-8

Chen, H. Y., Zhou, H. F., Yang, J. H., Wan, H. T., and He, Y. (2023). Guhong injection mitigates myocardial ischemia/reperfusion injury by activating GST P to inhibit ASK1-JNK/p38 pathway. *Phytomedicine* 109, 154603. doi:10.1016/j.phymed.2022.154603

Chen, J., and Xu, H. (2020). Clinical observation of guhong injection in treatment of stable coronary heart disease. *Clin. Observation Guhong Inject. Treat. Stable Coron. Heart Dis.* 47, 137–139. doi:10.13192/j.issn.1000-1719.2020.03.042

Chen, L., Xiang, Y., Kong, L., Zhang, X., Sun, B., Wei, X., et al. (2013). Hydroxysafflor yellow A protects against cerebral ischemia-reperfusion injury by anti-apoptotic effect through PI3K/Akt/GSK3β pathway in rat. *Neurochem. Res.* 38, 2268–2275. doi:10.1007/s11064-013-1135-8

Chen, J. K., Wan, H. J., Zhou, H. F., Peng, X. Q., Zhao, T., Fu, W., et al. (2016). Correlation study on *in vivo* pharmacokinetics and anti-oxidation of Guhong Injection in cerebral ischemia reperfusion injury model of rats. *Chin. Traditional Herb. Drugs* 47, 447–453. doi:10.7501/j.issn.0253-2670.2016.03.016

Cruzat, V. F., Pantaleão, L. C., Donato, J., Jr., De Bittencourt, P. I. H., Jr., and Tirapegui, J. (2014). Oral supplementations with free and dipeptide forms of L-glutamine in endotoxemic mice: Effects on muscle glutamine-glutathione axis and hea t shock proteins. *J. Nutr. Biochem.* 25, 345–352. doi:10.1016/j.jnutbio.2013.11.009

Cruzat, V., Rogero, M. M., Keane, K. N., Curi, R., and Newsholme, P. (2018). Glutamine: Metabolism and immune function, supplementation and clinical translation. *Nutrients* 10, 31. doi:10.3390/nu10111564

Deng, L., Wan, H. T., Yu, L., Zhou, H. F., Chen, J. Z., and He, Y. (2018). Analysis on blood and brain microdialysis probes recovery of N-acetyl-L-glutamine,Glutamic acid and γ aminobutyric acid *in vitro* using LC-MS/MS. *Chin. Pharm. J.* 53, 719–724. doi:10.11669/cpj.2018.09.012

Donnan, G. A., Fisher, M., Macleod, M., and Davis, S. M. (2008). Stroke. *Lancet (London, Engl.* 371, 1612–1623. doi:10.1016/S0140-6736(08)60694-7

Esposito, E., Shekhtman, G., and Chen, P. (2021). Prevalence of spatial neglect post-stroke: A systematic review. *Ann. Phys. rehabilitation Med.* 64, 101459. doi:10.1016/j.rehab.2020.10.010

Feng, Z. M., He, J., Jiang, J. S., Chen, Z., Yang, Y. N., and Zhang, P. C. (2013). NMR solution structure study of the representative component hydroxysa fflor yellow A and other quinochalcone C-glycosides from Carthamus tin ctorius. *J. Nat. Prod.* 76, 270–274. doi:10.1021/np300814k

Fu, P. K., Pan, T. L., Yang, C. Y., Jeng, K. C., Tang, N. Y., and Hsieh, C. L. (2016). Carthamus tinctorius L. ameliorates brain injury followed by cerebral ischemia-reperfusion in rats by antioxidative and anti-inflammatory mechanisms. *Iran. J. Basic Med. Sci.* 19, 1368–1375. doi:10.22038/ijbms.2016.7925

Gao, L. (2018). Expert consensus on the diagnosis and treatment of chronic cerebral ischemia by integrated Chinese and Western medicine. *Chin. J. Integr. Traditional West. Med.* 38, 1161–1167. doi:10.7661/j.cjim.20180908.258

Han, S., Li, H., Bai, C., Wang, L., and Tu, P. (2010). Component analysis and free radical-scavenging potential of Panax noto ginseng and Carthamus tinctorius extracts. *Chem. Biodivers.* 7, 383–391. doi:10.1002/cbdv.200800313

Hattori, M., Huang, X. L., Che, Q. M., Kawata, Y., Tezuka, Y., Kikuchi, T., et al. (1992). 6-hydroxykaempferol and its glycosides from Carthamus tinctorius petals. *Phytochemistry* 31, 4001–4004. doi:10.1016/s0031-9422(00)97572-1

He, Q. D., Huang, M. S., Zhang, L. B., Shen, J. C., Lian, L. Y., Zhang, Y., et al. (2019). Effect of moxibustion on intestinal microbiome in acute gastric ulcer rats. *Evidence-Based Complementary Altern. Med.* 2019, 6184205. doi:10.1155/2019/6184205

He, T. W. (2006). Clinical investigation of guhong injection in the treatment of acute cerebral infarction. *Mod. J. Integr. Tradit. Chin. west. med.* 15, 2654.

He, X. W., Fan, X. P., Zhong, T., Yao, B., and He, Y. (2014). Meta-analysis of guhong injection on acute cerebral infarction. *Chin. Archives Traditional Chin. Med.* 32, 2602–2605. doi:10.13193/j.issn.1673-7717.2014.11.012

Hu, X. J., Yin, S., Yuan, T. T., Wang, Y. J., Huang, Z. R., and Lu, Y. (2013). Chemical constituents and pharmacological activities of Carthamus tinctorius L. *J. Pharm. Pract.* 31, 161–168+197. doi:10.3969/j.issn.1006-0111.2013.03.001

Huang, D. M., Lu, Y. M., Luo, X. H., Shi, L. X., Zhang, J. C., Shen, J. X., et al. (2012). Effect of safflower yellow on platelet activating factor mediated platelet activation in patients with coronary heart disease. *Bangladesh J. Pharmacol.* 7, 140–144. doi:10.3329/bjp.v7i2.11094

Ji, Y., Dai, F., Yan, S., Shi, J. Y., and Zhou, B. (2019). Identification of catechol-type diphenylbutadiene as a tyrosinase-activated pro-oxidative chemosensitizer against melanoma A375 cells via glutathione S-transferase inhibition. *J. Agric. Food Chem.* 67, 9060–9069. doi:10.1021/acs.jafc.9b02875

Jia, J. (2019). Effect of Guhong Injection on senile patients with vascular mild cognitive impairment. *World Latest Med. Inf.* 19, 97+106. doi:10.19613/j.cnki.1671-3141.2019.49.060

Jiang, J. S., Chen, Z., Yang, Y. N., Feng, Z. M., and Zhang, P. C. (2013). Two new glycosides from the florets of Carthamus tinctorius. *J. Asian Nat. Prod. Res.* 15, 427–432. doi:10.1080/10286020.2013.780046

Jiang, J. S., Lu, L., Yang, Y. J., Zhang, J. L., and Zhang, P. C. (2008a). New spermidines from the florets of Carthamus tinctorius. *J. Asian Nat. Prod. Res.* 10, 447–451. doi:10.1080/10286020801948540

Jiang, J. S., Xia, P. F., Feng, Z. M., and Zhang, P. C. (2008b). Chemical constituents from flowers of Carthamus tinctorius. *China J. Chin. Materia Medica* 33, 2911–2913.

Jiang, S. D., Zou, Y. B., Xiao, J., Tang, M. S., and Pan, C. D. (2016). Guhong injection for treating acute cerebral infarction in 40 cases. *China Pharm.* 25, 40–42.

Jin, Y., Xiao, Y. S., Zhang, F. F., Xue, X. Y., Xu, Q., and Liang, X. M. (2008). Systematic screening and characterization of flavonoid glycosides in C arthamus tinctorius L. by liquid chromatography/UV diode-array detecti on/electrospray ionization tandem mass spectrometry. *J. Pharm. Biomed. analysis* 46, 418–430. doi:10.1016/j.jpba.2007.10.036

Jin, M., Gao, Z. C., and Wang, J. F. (2004). Research on the inhibitory effects of hydroxysafflor yellow A on the rabbit platelet activation induced by platelet activating factor. *J. Beijing Univ. Traditional Chin. Med.* 2004, 32–35.

Jun, M. S., Ha, Y. M., Kim, H. S., Jang, H. J., Kim, Y. M., Lee, Y. S., et al. (2011). Anti-inflammatory action of methanol extract of Carthamus tinctorius involves in heme oxygenase-1 induction. *J. Ethnopharmacol.* 133, 524–530. doi:10.1016/j.jep.2010.10.029

Kazuma, K., Takahashi, T., Sato, K., Takeuchi, H., Matsumoto, T., and Okuno, T. (2000). Quinochalcones and flavonoids from fresh florets in different cultivar s of Carthamus tinctorius L. *Biosci. Biotechnol. Biochem.* 64, 1588–1599. doi:10.1271/bbb.64.1588

Kelly, D., and Wischmeyer, P. E. (2003). Role of L-glutamine in critical illness: New insights. *Curr. Opin. Clin. Nutr. metabolic care* 6, 217–222. doi:10.1097/00075197-200303000-00011

Khoshnam, S. E., Winlow, W., Farzaneh, M., Farbood, Y., and Moghaddam, H. F. (2017). Pathogenic mechanisms following ischemic stroke. *Neurol. Sci.* 38, 1167–1186. doi:10.1007/s10072-017-2938-1

Lee, R. H. C., Lee, M. H. H., Wu, C. Y. C., Couto E Silva, A., Possoit, H. E., Hsieh, T.-H., et al. (2018). Cerebral ischemia and neuroregeneration. *Neural Regen. Res.* 13, 373–385. doi:10.4103/1673-5374.228711

Li, C. Y., Yin, J. G., Zhang, J., Wang, X. X., Xu, M. J., Liu, F., et al. (2015). Pharmacokinetic profiles of hydroxysafflor yellow A following intraven ous administration of its pure preparations in healthy Chinese volunte ers. *J. Ethnopharmacol.* 162, 225–230. doi:10.1016/j.jep.2014.12.068

Li, F., He, Z., and Ye, Y. (2017a). Isocartormin, a novel quinochalcone C-glycoside from Carthamus tinctorius. *Acta Pharm. Sin. B* 7, 527–531. doi:10.1016/j.apsb.2017.04.005

Li, H. X., Han, S. Y., Wang, X. W., Ma, X., Zhang, K., Wang, L., et al. (2009). Effect of the carthamins yellow from Carthamus tinctorius L. on hemorh eological disorders of blood stasis in rats. *Food Chem. Toxicol. Int. J. Publ. Br. Industrial Biol. Res. Assoc.* 47, 1797–1802. doi:10.1016/j.fct.2009.04.026

Li, S. F., Yuan, M. Y., and Zhang, L. W. (2016). Simultaneous determination of four coumaroylspermidine constituents in Carthamus tinctorius by HPLC-DAD. *China J. Chin. Materia Medica* 41, 1480–1484. doi:10.4268/cjcmm20160819

Li, W. C., Wang, X. Y., Lin, P. C., Hu, N., Zhang, Q. L., Suo, Y. R., et al. (2013). Preparative separation and purification of four cis-trans isomers of coumaroylspermidine analogs from safflower by high-speed counter-current chromatography. *J. Chromatogr. B-Analytical Technol. Biomed. Life Sci.* 938, 75–79. doi:10.1016/j.jchromb.2013.08.012

Li, X. R., Liu, J., Peng, C., Zhou, Q. M., Liu, F., Guo, L., et al. (2021). Polyacetylene glucosides from the florets of Carthamus tinctorius and their anti-inflammatory activity. *Phytochemistry* 187, 112770. doi:10.1016/j.phytochem.2021.112770

Li, X., Wang, J. P., Liu, C. L., Li, N., and Bai, H. Y. (2007). Clinical study of Guhong injection in the treatment of acute cerebral infarction. *Chin. J. Pract. Nerv. Dis.* 2007, 19–21.

Li, X., Wu, Y., Zhi, X. R., Li, Q., Li, Y., Wang, Q. M., et al. (2017b). Simultaneous determination of seven active components in guhong injection. *Chin. J. Exp. Traditional Med. Formulae* 23, 64–69. doi:10.13422/j.cnki.syfjx.2017210064

Li, Y. P., and Zhang, Q. S. (2018). Clinical study on Guhong Injection combined with butylphthalide in treatment of acute cerebral infarction. *Drugs & Clin.* 33, 41–45. doi:10.7501/j.issn.1674-5515.2018.01.010

Liu, L. T., Fu, C. G., and Wang, S. Z. (2020). Chinese expert consensus on the clinical application of guhong injection. *Chin. J. Integr. Med. Cardio-Cerebrovascular Dis.* 18, 1665–1670. doi:10.12102/ji.ssn.1672-1349.2020.11.001

Liu, S. J., Tang, Z. S., Cui, C. L., Liu, H. B., Liang, Y. N., Zhang, Y., et al. (2017). Research progress of the chemical components of Chinese herb Honghua (flos carthami). *Henan Tradit. Chin. Med.* 37, 168–171. doi:10.16367/j.issn.1003-5028.2017.01.0059

Liu, X. Y. (2017). Effect of Guhong Injection on improving nerve function in cerebral infarction. *J. Pract. Traditional Chin. Med.* 33, 51–52.

Liu, Y. P., and Li, H. D. (2010). Pharmacokinetic parameters and its significances in central nervous system. *Chin. J. Clin. Pharmacol.* 26, 154–156. doi:10.13699/j.cnki.1001-6821.2010.02.022

López Pedrosa, J. M., Manzano, M., Baxter, J. H., and Rueda, R. (2007). N-acetyl-L-glutamine, a liquid-stable source of glutamine, partially p revents changes in body weight and on intestinal immunity induced by p rotein energy malnutrition in pigs. *Dig. Dis. Sci.* 52, 650–658. doi:10.1007/s10620-006-9500-y

Love, S. (2003). Apoptosis and brain ischaemia. *Prog. Neuro-Psychopharmacology Biol. Psychiatry* 27, 267–282. doi:10.1016/S0278-5846(03)00022-8

Lu, J. X., Zhang, C. X., Hu, Y., Zhang, M. H., Wang, Y. N., Qian, Y. X., et al. (2019). Application of multiple chemical and biological approaches for quality assessment of Carthamus tinctorius L. (safflower) by determining both the primary and secondary metabolites. *Phytomedicine Int. J. phytotherapy Phytopharm. ology* 58, 152826. doi:10.1016/j.phymed.2019.152826

Luo, L. L., Li, Y. F., Shan, H. M., Wang, L. P., Yuan, F., Ma, Y. Y., et al. (2019). L-glutamine protects mouse brain from ischemic injury via up-regulatin g heat shock protein 70. *CNS Neurosci. Ther.* 25, 1030–1041. doi:10.1111/cns.13184

Maida, C. D., Norrito, R. L., Daidone, M., Tuttolomondo, A., and Pinto, A. (2020). Neuroinflammatory mechanisms in ischemic stroke: Focus on cardioemboli c stroke, background, and therapeutic approaches. *Int. J. Mol. Sci.* 21, 6454. doi:10.3390/ijms21186454

Martel, J., Ko, Y. F., Ojcius, D. M., Lu, C. C., Chang, C. J., Lin, C. S., et al. (2017). Immunomodulatory properties of plants and mushrooms. *Trends Pharmacol. Sci.* 38, 967–981. doi:10.1016/j.tips.2017.07.006

Moskowitz, M. A., Lo, E. H., and Iadecola, C. (2010). The science of stroke: Mechanisms in search of treatments. *Neuron* 67, 181–198. doi:10.1016/j.neuron.2010.07.002

Orellana Urzúa, S., Rojas, I., Líbano, L., and Rodrigo, R. (2020). Pathophysiology of ischemic stroke: Role of oxidative stress. *Curr. Pharm. Des.* 26, 4246–4260. doi:10.2174/1381612826666200708133912

Orrenius, S., Zhivotovsky, B., and Nicotera, P. (2003). Regulation of cell death: The calcium-apoptosis link. *Nat. Rev. Mol. Cell Biol.* 4, 552–565. doi:10.1038/nrm1150

Oudemans Van Straaten, H. M., Bosman, R. J., Treskes, M., Van Der Spoel, H. J., and Zandstra, D. F. (2001). Plasma glutamine depletion and patient outcome in acute ICU admissions. *Intensive care Med.* 27, 84–90. doi:10.1007/s001340000703

Radak, D., Katsiki, N., Resanovic, I., Jovanovic, A., Sudar-Milovanovic, E., Zafirovic, S., et al. (2017). Apoptosis and acute brain ischemia in ischemic stroke. *Curr. Vasc. Pharmacol.* 15, 115–122. doi:10.2174/1570161115666161104095522

Rodrigo, R., Fernández Gajardo, R., Gutiérrez, R., Matamala, J. M., Carrasco, R., Miranda-Merchak, A., et al. (2013). Oxidative stress and pathophysiology of ischemic stroke: Novel therape utic opportunities. *CNS neurological Disord. drug targets* 12, 698–714. doi:10.2174/18715273113120500 15

Sheng, F. (2019). Effect of guhong injection combined with ozagrel sodium on NIHSS score and hemorheology of acute cerebral infarction. *Chin. Foreign Med. Res.* 17, 11–13. doi:10.14033/j.cnki.cfmr.2019.10.005

Shi, P., Ruan, Y., Zhong, C., Teng, L., Ke, L., and Yao, H. (2022). Identification of pharmacokinetic markers for safflower injection usin g a combination of system pharmacology, multicomponent pharmacokinetic s, and quantitative proteomics study. *Front. Pharmacol.* 13, 1062026. doi:10.3389/fphar.2022.1062026

Shu, M. C., Wan, H. T., Zhou, H. F., Yang, J. H., Zhao, T., Fu, W., et al. (2014). Effect and mechanism of Guhong injection against cerebral ischemia reperfusion injury. *China J. Chin. Materia Medica* 39, 4829–4833. doi:10.4268/cjcmm20142425

Smith, B. P., Vandenhende, F. R., Desante, K. A., Farid, N. A., Welch, P. A., Callaghan, J. T., et al. (2000). Confidence interval criteria for assessment of dose proportionality. *Pharm. Res.* 17, 1278–1283. doi:10.1023/a:1026451721686

Snowden, M. K., Baxter, J. H., Bergana, M. M., Reyzer, I., and Pound, V. (2002). Stability of N-acetylglutamine and glutamine inAqueous solution and in a liquid NutritionalProduct by an improved HPLC method. *J. food sicence* 67, 384–389. doi:10.1111/j.1365-2621.2002.tb11415.x

Tao, K. M., Li, X. Q., Yang, L. Q., Yu, W. F., Lu, Z. J., Sun, Y. M., et al. (2014). Glutamine supplementation for critically ill adults. *Cochrane database Syst. Rev.* 2014, CD010050. doi:10.1002/14651858.CD010050.pub2

Tian, J., Li, G., Liu, Z., and Fu, F. (2008). Hydroxysafflor yellow A inhibits rat brain mitochondrial permeability transition pores by a free radical scavenging action. *Pharmacology* 82, 121–126. doi:10.1159/000141653

Tuo, Q. Z., Zhang, S. T., and Lei, P. (2022). Mechanisms of neuronal cell death in ischemic stroke and their therape utic implications. *Med. Res. Rev.* 42, 259–305. doi:10.1002/med.21817

Wang, C. C., Choy, C. S., Liu, Y. H., Cheah, K. P., Li, J. S., Wang, J. T. J., et al. (2011). Protective effect of dried safflower petal aqueous extract and its main constituent, carthamus yellow, against lipopolysaccharide-induced inflammation in RAW264.7 macrophages. *J. Sci. Food Agric.* 91, 218–225. doi:10.1002/jsfa.4172

Wang, H. H., Li, Z. K., Cao, G. Z., Tang, L. Y., Zhou, R., Li, C. F., et al. (2023). Targeted energy metabolomics combined with spatial metabolomics study on the efficacy of guhong injection against cerebral ischemia reperfusion. *Mol. Neurobiol.* 2023. doi:10.1007/s12035-023-03403-x

Wang, H. T., and Dong, Y. (2006). Observation of therapeutic effects of Guhong injection on acute cerebral infraction. *Pract. J. Cardiac Cereb. Pneumal Vasc. Dis.* 2006, 641–642.

Wang, H. Y., Zhou, H. F., He, Y., Yu, L., Li, C., Yang, J. H., et al. (2021). Protective effect of naoxintong capsule combined with guhong inject ion on rat brain

microvascular endothelial cells during cerebral is chemia-reperfusion injury. *Chin. J. Integr. Med.* 27, 744–751. doi:10.1007/s11655-020-3215-3

Wang, S. L. (2020). Effect analysis of Guhong Injection on vascular dementia patients. *J. Med. Theory Pract.* 33, 1269–1271. doi:10.19381/j.issn.1001-7585.2020.08.028

Wang, X., Ma, Z., Fu, Z., Gao, S., Yang, L., Jin, Y., et al. (2016). Hydroxysafflor yellow A protects neurons from excitotoxic death throug h inhibition of NMDARs. *ASN neuro* 8, 1759091416642345. doi:10.1177/1759091416642345

Wang, Y., Jiang, Z., Nolan, M. T., Jiang, H., Han, H., Yu, K., et al. (2010). The impact of glutamine dipeptide-supplemented parenteral nutrition on outcomes of surgical patients: A meta-analysis of randomized clinical trials. *JPEN. J. Parenter. Enter. Nutr.* 34, 521–529. doi:10.1177/0148607110362587

Wang, Y. L., Wu, H. M., Han, Z., Sheng, H. D., Wu, Y. H., Wang, Y. C., et al. (2022a). Guhong injection promotes post-stroke functional recovery via attenuating cortical inflammation and apoptosis in subacute stage of ischemic stroke. *Phytomedicine* 99, 154034. doi:10.1016/j.phymed.2022.154034

Wang, Y. L., Wu, H. M., Sheng, H. D., Wang, Y. C., Li, X. C., Wang, Y., et al. (2022b). Discovery of anti-stroke active substances in Guhong injection based on multi-phenotypic screening of zebrafish. *Biomed. Pharmacother.* 155, 113744. doi:10.1016/j.biopha.2022.113744

Wei, X., Liu, H., Sun, X., Fu, F., Zhang, X., Wang, J., et al. (2005). Hydroxysafflor yellow A protects rat brains against ischemia-reperfusi on injury by antioxidant action. *Neurosci. Lett.* 386, 58–62. doi:10.1016/j.neulet.2005.05.069

Wischmeyer, P. E. (2008). Glutamine: Role in critical illness and ongoing clinical trials. *Curr. Opin. gastroenterology* 24, 190–197. doi:10.1097/MOG.0b013e3282f4db94

Wu, S., Wu, B., Liu, M., Chen, Z., Wang, W., Anderson, C. S., et al. (2019). Stroke in China: Advances and challenges in epidemiology, prevention, and management. *Lancet. Neurology* 18, 394–401. doi:10.5582/bst.2019.01186

Xian, B., Wang, R., Jiang, H., Zhou, Y., Yan, J., Huang, X., et al. (2022). Comprehensive review of two groups of flavonoids in Carthamus tinctori us L. *Biomed. Pharmacother. = Biomedecine Pharmacother.* 153, 113462. doi:10.1016/j.biopha.2022.113462

Xiao, D. F., Zeng, L. M., Yao, K., Kong, X. F., Wu, G. Y., and Yin, Y. L. (2016). The glutamine-alpha-ketoglutarate (AKG) metabolism and its nutritional implications. *Amino Acids* 48, 2067–2080. doi:10.1007/s00726-016-2254-8

Xie, X., Zhou, J., Sun, L., Zhang, H., Zhao, Y., Song, Y., et al. (2016). A new flavonol glycoside from the florets of Carthamus tinctorius L. *Nat. Prod. Res.* 30, 150–156. doi:10.1080/14786419.2015.1045905

Xu, J. Z. (2020). Effect of Guhong Injection on angina pectoris of coronary heart disease and blood flow. *China Rural. Health* 12, 17.

Xu, S., Li, C., Zhou, H., Yu, L., Deng, L., Zhu, J., et al. (2020). A study on acetylglutamine pharmacokinetics in rat blood and brain bas ed on liquid chromatography-tandem mass spectrometry and microdialysis technique. *Front. Pharmacol.* 11, 508. doi:10.3389/fphar.2020.00508

Yang, G., Zhou, X., Chen, T., Deng, Y., Yu, D., Pan, S., et al. (2015). Hydroxysafflor yellow A inhibits lipopolysaccharide-induced proliferat ion and migration of vascular smooth muscle cells via Toll-like recept or-4 pathway. *Int. J. Clin. Exp. Med.* 8, 5295–5302.

Yang, Q., Yang, Z. F., Liu, S. B., Zhang, X. N., Hou, Y., Li, X. Q., et al. (2010). Neuroprotective effects of hydroxysafflor yellow A against excitotoxic neuronal death partially through down-regulation of NR2B-containing N MDA receptors. *Neurochem. Res.* 35, 1353–1360. doi:10.1007/s11064-010-0191-6

Yang, X., Chen, L., Li, Y., Gao, F., Yan, Z., Zhang, P., et al. (2020). Protective effect of Hydroxysafflor Yellow A on cerebral ischemia reperfusion-injury by regulating GSK3?-mediated pathways. *Neurosci. Lett.* 736, 135258. doi:10.1016/j.neulet.2020.135258

Ye, S. Y., and Gao, W. Y. (2008). Hydroxysafflor yellow A protects neuron against hypoxia injury and sup presses inflammatory responses following focal ischemia reperfusion in rats. *Archives pharmacal Res.* 31, 1010–1015. doi:10.1007/s12272-001-1261-y

Yoo, H. C., Yu, Y. C., Sung, Y., and Han, J. M. (2020). Glutamine reliance in cell metabolism. *Exp. Mol. Med.* 52, 1496–1516. doi:10.1038/s12276-020-00504-8

Yu, G. H., Luo, Z. Q., Zhou, Y. T., Zhang, L., Wu, Y., Ding, L., et al. (2019). Uncovering the pharmacological mechanism of Carthamus tinctorius L. on cardiovascular disease by a systems pharmacology approach. *Biomed. Pharmacother. = Biomedecine Pharmacother.* 117, 109094. doi:10.1016/j.biopha.2019.109094

Yu, L., Jin, Z., Li, M. C., Liu, H. F., Tao, J., Xu, C., et al. (2022). Protective potential of hydroxysafflor yellow A in cerebral ischemia and reperfusion injury: An overview of evidence from experimental studies. *Front. Pharmacol.* 13, 1063035. doi:10.3389/fphar.2022.1063035

Yu, L., Wan, H. F., Li, C., Yang, J. H., Zhou, H. F., Wan, H. T., et al. (2018). Pharmacokinetics of active components from guhong injection in normal and pathological rat models of cerebral ischemia: A comparative study. *Front. Pharmacol.* 9, 493. doi:10.3389/fphar.2018.00493

Yu, L., Zhang, Y. Y., Zhao, X., Wan, H. T., He, Y., and Jin, W. F. (2021). Guhong injection alleviates cerebral ischemia-reperfusion injury via t he PKC/HIF-1α pathway in rats. *Front. Pharmacol.* 12, 716121. doi:10.3389/fphar.2021.716121

Yue, S. J., Tang, Y. P., Li, S. J., and Duan, J. A. (2013). Chemical and biological properties of quinochalcone C-glycosides from the florets of Carthamus tinctorius. *Mol. (Basel, Switz.* 18, 15220–15254. doi:10.3390/molecules181215220

Yue, S. J., Tang, Y. P., Xu, C. M., Li, S. J., Zhu, Y., and Duan, J. A. (2014). Two new quinochalcone C-glycosides from the florets of Carthamus tinct orius. *Int. J. Mol. Sci.* 15, 16760–16771. doi:10.3390/ijms150916760

Zang, B. X., Jin, M., Si, N., Zhang, Y., Wu, W., and Piao, Y. Z. (2002). Antagonistic effect of hydroxysafflor yellow A on the platelet activat ing factor receptor. *Acta Pharm. Sin.* 37, 696–699.

Zhang, B., and Ning, Y. (2015). Clinical efficacy and safety of guhong injection in the treatment of acute cerebral in farction. *Pract. Pharm. Clin. Remedies* 18, 1129–1132. doi:10.14053/j.cnki.ppcr.201509033

Zhang, J. J., Zhou, R., Cao, G. Z., Zhang, Y., Xu, H., and Yang, H. J. (2022a). Guhong injection prevents ischemic stroke-induced neuro-inflammation and neuron loss through regulation of C5ar1. *Front. Pharmacol.* 13, 818245. doi:10.3389/fphar.2022.818245

Zhang, J. J., Zhou, R., Xiang, C. P., Fan, F. F., Gao, J. H., Zhang, Y., et al. (2020). Enhanced thioredoxin, glutathione and Nrf2 antioxidant systems by saff lower extract and aceglutamide attenuate cerebral ischaemia/reperfusio n injury. *J. Cell. Mol. Med.* 24, 4967–4980. doi:10.1111/jcmm.15099

Zhang, L. L., Tian, K., Tang, Z. H., Chen, X. J., Bian, Z. X., Wang, Y. T., et al. (2016). Phytochemistry and pharmacology of Carthamus tinctorius L. *Am. J. Chin. Med.* 44, 197–226. doi:10.1142/S0192415X16500130

Zhang, R., Yang, N., Ji, C., Zheng, J., Liang, Z., Hou, C. Y., et al. (2015). Neuroprotective effects of Aceglutamide on motor function in a rat mod el of cerebral ischemia and reperfusion. *Restor. neurology Neurosci.* 33, 741–759. doi:10.3233/RNN-150509

Zhang, Y. L., Liu, Y., Cui, Q., Fu, Z. T., Yu, H. Y., Liu, A., et al. (2022b). Hydroxysafflor yellow A alleviates ischemic stroke in rats via HIF-1[F ormula: See text], BNIP3, and notch1-mediated inhibition of autophagy. *Am. J. Chin. Med.* 50, 799–815. doi:10.1142/S0192415X22500331

Zhang, Z. (2010). multi-center, randomized and open clinical study on the efficacy and safety of GuHong injection in patients with acute cerebral infraction. *Mod. Prev. Med.* 37, 4382–4383+4385.

Zhao, G., Gai, Y., Chu, W. J., Qin, G. W., and Guo, L. H. (2009). A novel compound N(1),N(5)-(Z)-N(10)-(E)-tri-p-coumaroylspermidine iso lated from Carthamus tinctorius L. and acting by serotonin transporter inhibition. *Eur. Neuropsychopharmacol. J. Eur. Coll. Neuropsychopharmacol.* 19, 749–758. doi:10.1016/j.euroneuro.2009.06.009

Zhao, L. W., Ren, C. J., Xue, X. F., Lu, H. X., Wang, K., and Wu, L. M. (2022). Safflomin A: A novel chemical marker for Carthamus tinctorius L. (saff lower) monofloral honey. *Food Chem.* 366, 130584. doi:10.1016/j.foodchem.2021.130584

Zhao, S. J. (2006). Analysis of curative effect of Guhong Injection on 186 cases of cognitive impairment after cerebral infarction. *Pract. J. Cardiac Cereb. Pneumal Vasc. Dis.* 893.

Zhou, H. F., He, Y., Zhu, J. Q., Lin, X. J., Chen, J., Shao, C. Y., et al. (2021). Guhong injection protects against apoptosis in cerebral ischemia by ma intaining cerebral microvasculature and mitochondrial integrity throug h the PI3K/AKT pathway. *Front. Pharmacol.* 12, 650983. doi:10.3389/fphar.2021.650983

Zhou, X. D., Tang, L. Y., Xu, Y. L., Zhou, G. H., and Wang, Z. J. (2014). Towards a better understanding of medicinal uses of carthamus tinctori us L. In traditional Chinese medicine: A phytochemical and pharmacolog ical review. *J. Ethnopharmacol.* 151, 27–43. doi:10.1016/j.jep.2013.10.050

Zhou, Y. Z., Chen, H., Qiao, L., Xu, N., Cao, J. Q., and Pei, Y. H. (2008). Two new compounds from Carthamus tinctorius. *J. Asian Nat. Prod. Res.* 10, 429–433. doi:10.1080/10286020801892425

Zhu, T., Wang, L., Wang, L. P., and Wan, Q. (2022). Therapeutic targets of neuroprotection and neurorestoration in ischemic stroke: Applications for natural compounds from medicinal herbs. *Biomed. Pharmacother.* 148, 112719. doi:10.1016/j.biopha.2022.112719

Zhuang, J. Q., Liu, S. L., Cai, H. R., Dai, X. Z., Chen, Y. H., Jin, Z. L., et al. (2020). Efficacy and safety of guhong injection for treating coronary microvas cular disease: Study protocol for a randomized controlled trial. *Trials* 21, 75. doi:10.1186/s13063-019-3990-3

Glossary

ATP	Adenosine triphosphate
BFGF	Basic fibroblast growth factor
Bax	BCL2-associated X protein
Bcl-2	B cell leukemia/lymphoma 2
Cyt-c	Cytochrome c
C5AR1	C5a anaphylatoxin chemotactic receptor 1
CRP	C reactive protein
GSH	Glutathione
HIF-1α	Hypoxia-inducible factor-1α
H&E	Hematoxylin and eosin staining
HSYA	Hydroxysafflor yellow A
iNOS	Inducible NO synthase
IL-1β	Interleukin-1β
ICAM-1	Intercellular cell adhesion molecule-1
IL-6	Interleukin-6
LDH	Lactate dehydrogenase
MPO	Myeloperoxidase
MDA	Malondialdehyde
MMP-9	Matrix metalloproteinase-9
NF-κB p65	Nuclear factor-κB p65
Nrf2	Nuclear factor (erythroid-derived 2)-like 2
NO	Nitric oxide
NAG	N-acetyl-L-glutamine
PAI	Plasminogen activator inhibitor
PKC	Protein kinase C
SOD	Superoxide dismutase
TNF-α	Tumor necrosis factor-α
Trx	Thioredoxin
TXB2	Thromboxane B2
TGF-β1	Transforming growth factor-β1
t-PA	Tissue-type plasminogen activator
VEGF	Vascular endothelial growth factor
TCA	Tricarboxylic Acid Cycle
VCAM-1	Vascular cell adhesion protein 1
6-Keto-PGF1α	6-keto prostaglandin F1α
8-OHdG	8-hydroxy-2′-deoxyguanosine

frontiers | Frontiers in Stroke

TYPE Systematic Review
PUBLISHED 17 January 2024
DOI 10.3389/fstro.2023.1339331

OPEN ACCESS

EDITED BY
Viola B. Morris,
Emory University, United States

REVIEWED BY
Sivakumar Vijayaraghavalu,
Manipur University, India
Mario Antony,
Krishna Institute of Medical Sciences, India

*CORRESPONDENCE
Mahmoud Tarek Hefnawy
✉ Mahmoudhefnawy77@gmail.com

RECEIVED 15 November 2023
ACCEPTED 22 December 2023
PUBLISHED 17 January 2024

CITATION
Hassanein ME, Fayad J, Shabana JA, AlEdani EM, Hefnawy MT, Ghaith HS and Negida A (2024) Efficacy and safety of intravenous mesenchymal stem cells for ischemic stroke patients, a systematic review and meta-analysis. *Front. Stroke* 2:1339331. doi: 10.3389/fstro.2023.1339331

Efficacy and safety of intravenous mesenchymal stem cells for ischemic stroke patients, a systematic review and meta-analysis

Maged Elsayed Hassanein[1], Jaber Fayad[2], Jilan Ali Shabana[1], Esraa M. AlEdani[3], Mahmoud Tarek Hefnawy[1]*, Hazem S. Ghaith[4] and Ahmed Negida[1]

[1]Faculty of Medicine, Zagazig University, Zagazig, Egypt, [2]Klinik für Neurologie und Neurophysiologie, Katholisches Klinikum Essen, Philippusstift, Essen, Germany, [3]Faculty of Medicine, Basra University, Basra, Iraq, [4]Faculty of Medicine, Al-Azhar University, Cairo, Egypt

Background: Clinical trials have evaluated the efficacy of intravenous mesenchymal stem cells (MSCs) for acute and subacute ischemic stroke. Therefore, we conducted this meta-analysis to investigate the efficacy and safety of intravenous MSC treatments compared to placebo for acute and subacute ischemic stroke patients.

Methods: We searched PubMed, SCOPUS, Web of Science, and Cochrane CENTRAL for randomized controlled trials evaluating any clinical trials of intravenous MSCs for acute and subacute ischemic stroke patients. The efficacy outcomes of this study were the rates of improvement in National Institutes of Health Stroke Scale (NIHSS) scores, good scores on the modified Rankin Scale (mRS), and Barthel Index (BI) scores, while the safety outcomes were the rates of mortality and stroke recurrence. We compared intravenous MSC and placebo treatments on a fixed-effect meta-analysis model in R software.

Results: Four randomized controlled studies involving 97 patients were included in the analysis. In the meta-analysis, MSC treatments were superior to placebo treatments in good mRS (MD −0.95, 95% CI [−1.39, −0.52]) or BI (MD 21.36, 95% CI [9.96, 32.75]) scores, and MSC treatments were not superior to placebo treatments in the rate of improvement of the NIHSS scores (MD −1.81, 95% CI [−4.123, 0.494]). MSCs were associated with neither decreased mortality nor stroke recurrence (risk ratio 0.58 and 0.59, respectively; p-value = 0.51 and p-value = 0.533, respectively).

Conclusion: For patients with acute and subacute ischemic stroke who are eligible for further damage to neural tissue, MSCs achieve high efficacy and acceptable safety.

Systematic review registration: Prospero, unique ID: CRD42023457655.

KEYWORDS

humans, ischemic stroke, cerebral infarction, mesenchymal stem cells, stroke

1 Introduction

Stroke is the second-most common cause of death worldwide, accounting for 11.6% of fatalities in 2019. The most common type of stroke is ischemic stroke, accounting for 62.4% of all stroke incidents globally in 2019. Worldwide, 77.19 million people had an ischemic stroke in 2019, which resulted in 63.48 million disability-adjusted life years and

3.29 million fatalities (El-Hajj et al., 2016). The Middle East experiences a varying incidence of ischemic stroke, with reported rates ranging from 43.17 to 164 per 100,000 population per year (El-Hajj et al., 2016).

The standard therapy for acute ischemic stroke is tissue plasminogen activator therapy, which is a clot-busting medication that must be administered within 4.5 h of symptom onset (Broderick et al., 2013). Additionally, endovascular thrombectomy, a procedure that involves physically removing the clot from the blocked blood vessel, is also considered standard therapy for select patients with acute ischemic stroke (Badhiwala et al., 2015).

Recent research has suggested that stem cell therapy may hold promise as a potential treatment option for acute and subacute ischemic stroke. Stem cells can differentiate into various cell types and can potentially regenerate damaged tissue, making them a promising therapeutic approach for neurological disorders such as stroke (Ebrahimi et al., 2021).

Several types of stem cells can be used in the treatment of ischemic stroke, including embryonic stem cells, induced pluripotent stem cells, mesenchymal stem cells (MSCs), and neural stem cells (Marei et al., 2018). Embryonic stem cells are derived from embryos and can differentiate into any cell type in the body. These cells have the potential to replace damaged neurons and restore lost function in the brain after a stroke (Cui et al., 2010). MSCs are derived from the bone marrow or adipose tissue and can differentiate into several cell types, including neural cells. MSCs have been shown to have neuroprotective effects and can improve functional recovery after stroke (Li et al., 2016).

In this review, we sought to examine the effectiveness and safety of stem cell therapy for acute and subacute ischemic stroke. To evaluate the effect of stem cell therapy on functional outcomes, rates of mortality, and stroke recurrence in patients with acute and subacute ischemic stroke, we conducted a systematic literature search and analysis. Despite mixed findings, the potential advantages of stem cell treatments for acute and subacute ischemic stroke remain unknown. Therefore, it is crucial to properly evaluate the available research in order to present an up-to-date summary of the information on MSC therapy for acute and subacute ischemic stroke.

2 Methods

Throughout this systematic review and meta-analysis, we adhered to the Preferred Reporting Items for Systematic Reviews and Meta-Analysis (PRISMA statement) criteria (Page et al., 2021). The *Cochrane Handbook of Systematic Reviews and Meta-Analyses of Interventions*, version 5.1.0, was strictly followed in the execution of the techniques (Cumpston et al., 2019; Shaheen et al., 2023).

2.1 Eligibility criteria

We included all studies satisfying the following criteria:

Population: patients with acute and subacute ischemic stroke.
Intervention: MSCs (any dose).
Comparator: placebo.
Outcomes: We included studies reporting at least one of the following outcomes: (1) clinical improvement in National Institutes of Health Stroke Scale (NIHSS) scores, (2) good modified Rankin Scale (mRS) scores (0–1), (3) Barthel Index (BI) scores, (4) mortality, and (5) stroke recurrence.
Study design: Only randomized controlled trials (RCTs).

We excluded studies that were not in the English language and studies that used an observational design.

2.2 Literature search

We performed a comprehensive literature search of four electronic databases (PubMed, Scopus, Web of Science, and Cochrane CENTRAL) from inception until July 2023 using this search query ((Stem cells OR Stem Cell OR Progenitor Cell* OR Mother Cell* OR Colony-Forming Unit*) AND (Ischemic Stroke* OR Cryptogenic Stroke* OR Cryptogenic Embolism Stroke* OR Wake-up Stroke* OR wake up stroke*)). All duplicates were removed, and all references in the included articles were screened manually for any eligible studies.

2.3 Screening of the literature search results

The literature search results passed a two-step screening process. All paper titles and abstracts were initially reviewed for eligibility. The full-text articles of accepted abstracts were then obtained and checked for acceptance.

2.4 Data extraction

A standard data extraction sheet was used for data extraction. The retrieved data contained the following: (1) study characteristics, (2) study characteristics, (3) risk-of-bias domains, and (4) outcome measures.

2.5 Outcome measures

2.5.1 mRS

The mRS is a scale with values ranging from 0 to 6 that is frequently used to measure the level of dependency or disability in people who have experienced a stroke or other neurological diseases (Runde, 2019). For statistical purposes, studies provide data as means and standard deviations.

2.5.2 BI

The BI is a tool that is frequently utilized in rehabilitation settings. When someone enters a rehabilitation program, their functional state is evaluated, their progress is tracked over time, and the efficacy of rehabilitation therapies is assessed. A higher score on the BI, which has a total value that can vary from 0 to 100, indicates a higher level of independence (Prodinger et al.,

2017). For statistical purposes, studies provide data as means and standard deviations.

2.5.3 Clinical improvement in the NIHSS

The NIHSS is an established method for assessing the severity of neurological impairments caused by a stroke. These deficiencies, which include those in motor function, sensory perception, language skills, and vision, give unbiased information that aids medical personnel in assessing the success of interventions and the patient's condition during therapy. A higher score indicates more neurological impairments; the total score goes from 0 to 42 (National Cancer Institute, 2018). For statistical purposes, studies provide data as means and standard deviations.

2.5.4 Mortality

Mortality is defined as the proportion of patients who died; it is represented as the risk ratio (RR) between the two groups.

2.5.5 Stroke recurrence

The incidence of stroke recurrence is expressed as the RR between the two groups.

2.6 Synthesis of results

Using the metafor package in the R programming language, we created the generic inverse variance analysis and compared MSCs to placebos. Results for efficacy were presented as Mean Differences (MDs) with matching 95% confidence intervals.

2.7 Heterogeneity assessment

The chi-square test (Cochran's Q test) was used to assess the statistical heterogeneity between studies. The I^2 was then calculated using the chi-square statistic, Cochran's Q, using the formula $I^2 = (Q - df) * 100\%/Q$. Significant heterogeneity was defined as a chi-squared p-value of 0.1. I^2 values of 0% indicated that there was no heterogeneity (Bergh, 2015).

2.8 Risk of bias across studies

Following the guidelines of the *Cochrane Handbook of Systematic Reviews of Interventions*, two authors independently evaluated the effectiveness of the included clinical trials. Using the quality assessment table from the same book (Cumpston et al., 2019), we looked at the likelihood of bias in a number of domains, including random sequence generation, allocation concealment, the blinding of participants and study staff, the blinding of outcome assessors, complete data, and selective outcome reporting.

2.9 Assessment of publication bias

Due to the low number of included RCTs (fewer than 10) and the advice given by Egger et al. (1997) we were unable to accurately quantify the publication bias using a funnel plot and Egger's test.

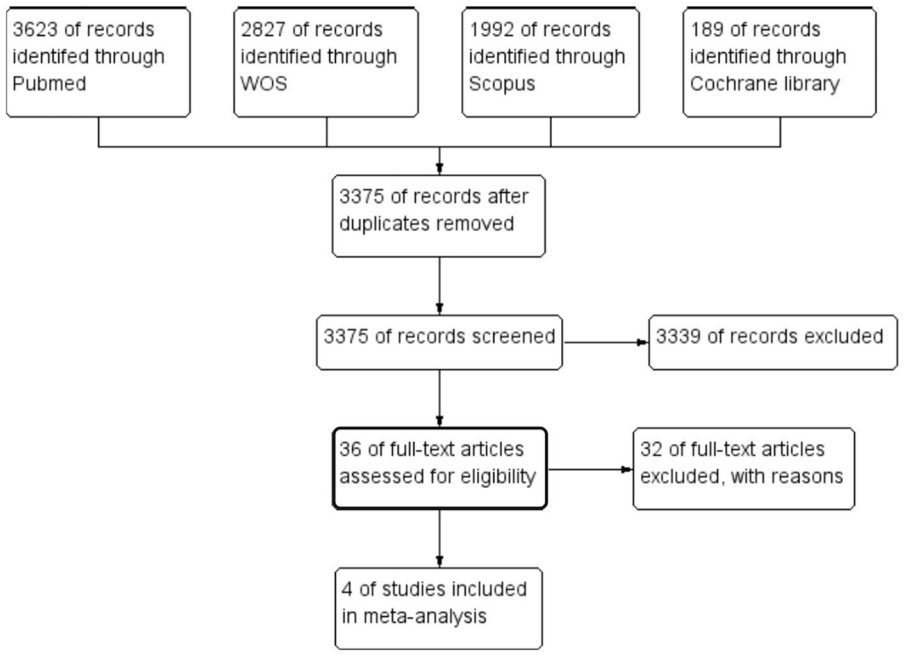

FIGURE 1
The preferred reporting items for systematic reviews and meta-analysis flow diagram of the study selection process.

3 Results

3.1 Literature search results and study selection

Our search for relevant literature turned up 8,646 results. Of those, 36 articles qualified for full-text screening after being subjected to title and abstract screening. Four RCTs from these 36 trials were included in the meta-analysis. Additionally, no additional publications were included despite carefully searching the references of the listed research. The PRISMA flow diagram in Figure 1 provides the flowchart for the study selection approach.

3.2 Study characteristics

The four RCTs (Bang et al., 2005; Jaillard et al., 2020; Law et al., 2021; de Celis-Ruiz et al., 2022) involved 97 ischemic stroke patients. Table 1 provides more information on the characteristics of each study group, including age, sex distribution, baseline NIHSS scores, mRS scores, infarct volume, site of stroke, and follow-up durations. Table 2 summarizes the major information from various studies regarding the use of stem cells for treating stroke, the measured outcomes, and the key findings.

3.3 Risk of bias within studies

According to the Cochrane risk-of-bias assessment method, the included studies' quality ranged from moderate concerns to high risk. Due to the patients' and research staff's lack of blinding, two studies had a high risk of performance bias, and one study had a high risk of proper analysis. Except for the 2005 Bang trial, which did not disclose the methods used for sequence generation or allocation concealment, all studies had acceptable random sequence generation and minimal risk of selection bias in the allocation procedure. In 2019, Jaillard conducted an open-label RCT. Figure 2 provides the specific risk-of-bias domains by study ID (Sterne et al., 2019).

3.4 Clinical improvement in the NIHSS

MSC treatments showed no significant improvement compared to the placebo treatment (common effect model; MD −1.81, 95% CI [−4.123; 0.494], p-value = 0.1234; Figure 3). The calculated effect size using the inverted variance method was not statistically significant (p = 0.1234), indicating that the treatment strategies did not have a significant impact on the NIHSS scores in the analyzed studies. Pooled studies were homogenous (I^2 = 0.0%; chi-square p = 1.00). Subgroup analyses were conducted based on different time points (3 months, 6 months, 12 months, and 24 months). A test for subgroup differences was performed to evaluate whether there were significant differences between the subgroups. The "between-groups" p-value was 1.00, indicating no significant subgroup differences. The

TABLE 1 Summary and characteristics of the population of included studies.

Refernces	Study group	Age	Sex, male: n (%)	Baseline NIHSS	Baseline mRS	Infarct volume	Site of stroke	Follow up duration(s)
Bang et al. (2005)	MSC group	63.0 ± 7.5	4 (80%)	10.6 ± 2.6	4.8 ± 5	127.4 ± 70.3	Middle cerebral artery (MCA)	3 m, 6 m, 12 m
	Control group	59.3 ± 11.5	14 (56%)	11.6 ± 4.9	4.6 ± 0.7	89.1 ± 77.4	Middle cerebral artery (MCA)	3 m, 6 m, 12 m
de Celis-Ruiz et al. (2022)	AD-MSC group	78 (70.5–82)	1 (11.1%)	10 ± 7.64	mRS 0 = 7 (77.8%) mRS 1 = 2 (22.2%)	43.22 (37.57–94.01)	Middle cerebral artery (MCA)	2 h, 24 h, 7 d, 3 m, 6 m, 12 m, 18 m, 24 m
	Control group	76 (69–80.25)	3 (30.0%)	8.83 ± 4.81	mRS 0 = 9 (90%) mRS 1 = 1 (10%)	88.165 (55.06–130.75)	Middle cerebral artery (MCA)	2 h, 24 h, 7 d, 3 m, 6 m, 12 m, 18 m, 24 m
Jaillard et al. (2020)	MSC group	55 (46–58)	11 (68.8%)	14 ± 6.5	3.83 ± 0.4	84 ± 66.65	Middle cerebral artery (MCA)	6 m, 12 m, 24 m
	Control group	53 (45–63)	11 (73.3%)	13 ± 4.09	3.74 ± 0.178	113 ± 48.15	Middle cerebral artery (MCA)	6 m, 12 m, 24 m
Law et al. (2021)	BM-MSC group	54.6 (13.2)	8 (88.89%)	17.166 ± 5.68	4.33 ± 0.874	68.2 ± 41	Middle cerebral artery (MCA)	1.5 m, 3 m, 6 m, 9 m, 12 m
	Control group	64 (13.9)	2 (25%)	15.5 ± 10.27	4.5 ± 0.89	38 ± 30.1	Middle cerebral artery (MCA)	1.5 m, 3 m, 6 m, 9 m, 12 m

TABLE 2 Summary and characteristics of the included studies.

References	Population	Intervention	Types of stem cells	Dose of injection	Frequency of injection	Control group	Measured outcomes	Key findings
Bang et al. (2005)	Acute Ischemic Stroke patients	IV infusion of MSC	Autologous Mesenchymal Stem Cell (MSC)	5 * 107	Twice	Standard medical care	NIHSS–BI–MRS–change in infarct sizze–ventricular dilation	Intravenous injection of *ex vivo*–cultured autologous MSCs is a safe and feasible method of treatment for ischemic stroke.
de Celis-Ruiz et al. (2022)	Acute Ischemic Stroke patients	Intravenous infusion of allogeneic AD-MSCs coupled with conventional treatment	Adipose tissue–derived mesenchymal stem cells (AD-MSCs)	1 million cells per kilogram	-	Conventional treatment for ischemic stroke according to the valid guidelines	NIHSS, infarct size, mRS, blood biomarkers.	The intravenous administration of AD-MSCs within the first 2 weeks of ischemic stroke onset is safe at 24 months of follow-up. Although no efficacy end points were statistically significant between treatment groups
(Jaillard et al., 2020)	Subacute Ischemic Stroke patients	Received IV injection of MSCs coupled with rehabilitation MSCs	Mesenchymal stem cells (MSCs)	The first ten patients assigned to treatment received low-dose MSCs (100 million) and the next ten patients received high-dose MSCs (300 million)	Once	Rehabilitation alone	mRS- BI- NIHSS-n-NIHSS–Motor FMS-MI-BA 4a -MI-BA 4p	Autologous MSC treatment is safe and feasible for treating moderate to severe stroke.
Law et al. (2021)	Subacute Ischemic Stroke patients	Standard medical care and culture expanded autologous BMMSCs	Autologous bone marrow derived MSCs (BMMSCs)	2.05 ± 0.20 * 106 BMMSCs per kg	Once	Standard medical care, which included treatment to prevent recurrence, optimal control of risk factors and post-stroke follow-up rehabilitative therapies.	NIHSS, mRS, BI, Infarct volume change	BMMSCs administered intravenously in the subacute period following MCA infarct were safe but did not improve functional outcome at 12 months. Improvements in radiological outcome were observed in the treatment group.

10.3389/fstro.2023.1339331

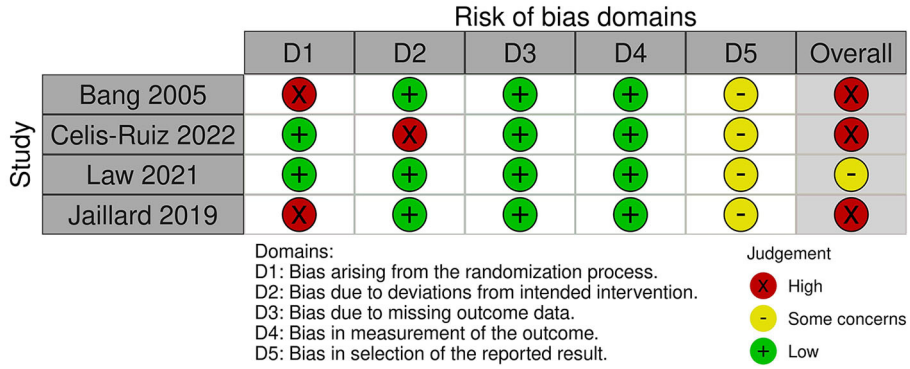

FIGURE 2
Risk of bias 2.

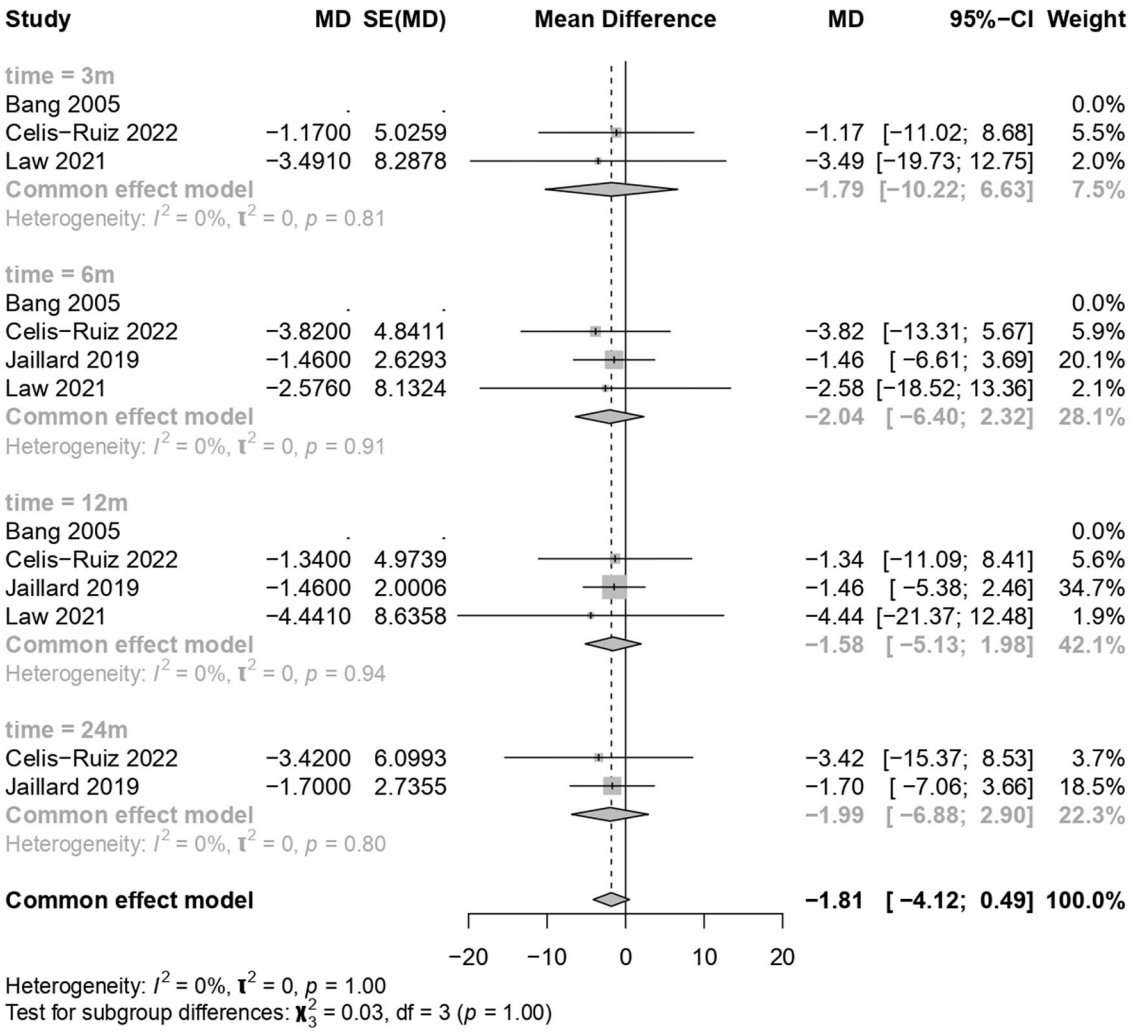

FIGURE 3
Forest plot for clinical improvement in the national institutes of health stroke scale.

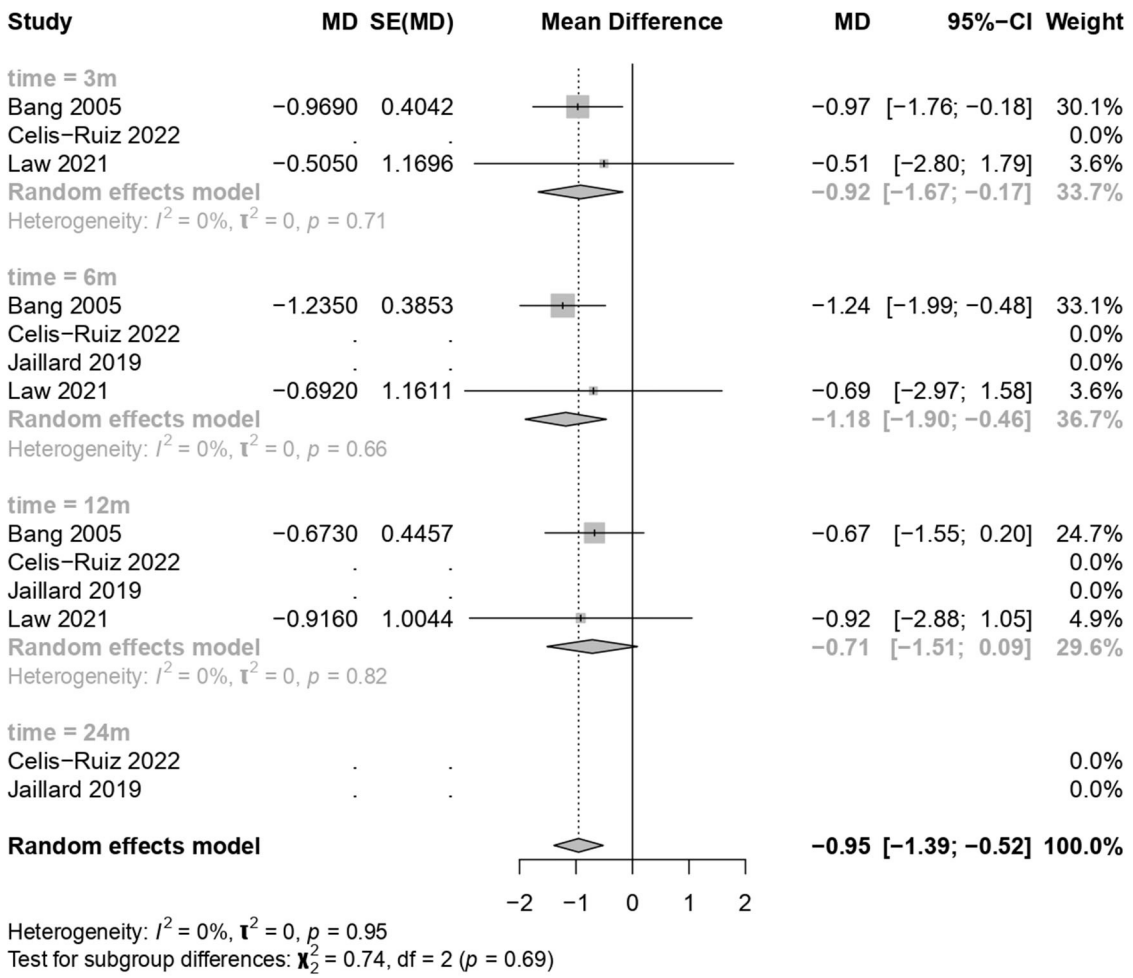

FIGURE 4
Forest plot for good neurological outcome on modified Rankin scale.

"within-groups" p-value was 1.00, suggesting consistency within the subgroups.

3.5 Good neurological outcome on the mRS

MSC treatments showed a significant improvement over the placebo treatment (common effect model; MD −0.95, 95% CI [−1.39; −0.52], p-value < 0.0001; Figure 4). The calculated effect size using the inverted variance method was statistically significant (p < 0.0001), indicating that the treatment strategies had a significant impact on the mRS scores in the analyzed studies. Pooled studies were homogeneous (I^2 = 0.0%; chi-square p = 0.95). Subgroup analyses were conducted based on different time points (3 months, 6 months, and 12 months). A test for subgroup differences was performed to evaluate whether there were significant differences between the subgroups. The between-groups p-value was 0.6894, indicating no significant subgroup differences. The within-groups p-value was 0.9430, suggesting consistency within the subgroups.

3.6 Clinical improvement in the BI

MSC treatments showed a significant improvement over the placebo treatment (common effect model; MD 21.36, 95% CI [9.96, 32.75], p-value = 0.0002; Figure 5). The calculated effect size using the inverted variance method was statistically significant (p = 0.0002), indicating that the treatment strategies had a significant impact on the BI scores in the analyzed studies. Pooled studies were homogeneous (I^2 = 0.0%; chi-square p = 0.53). Subgroup analyses were conducted based on different time points (3 months, 6 months, 12 months, and 24 months). A test for subgroup differences was performed to evaluate whether there were significant differences between the subgroups. The between-groups p-value was 0.35, indicating no significant subgroup differences. The within-groups p-value was 0.57, suggesting consistency within subgroups.

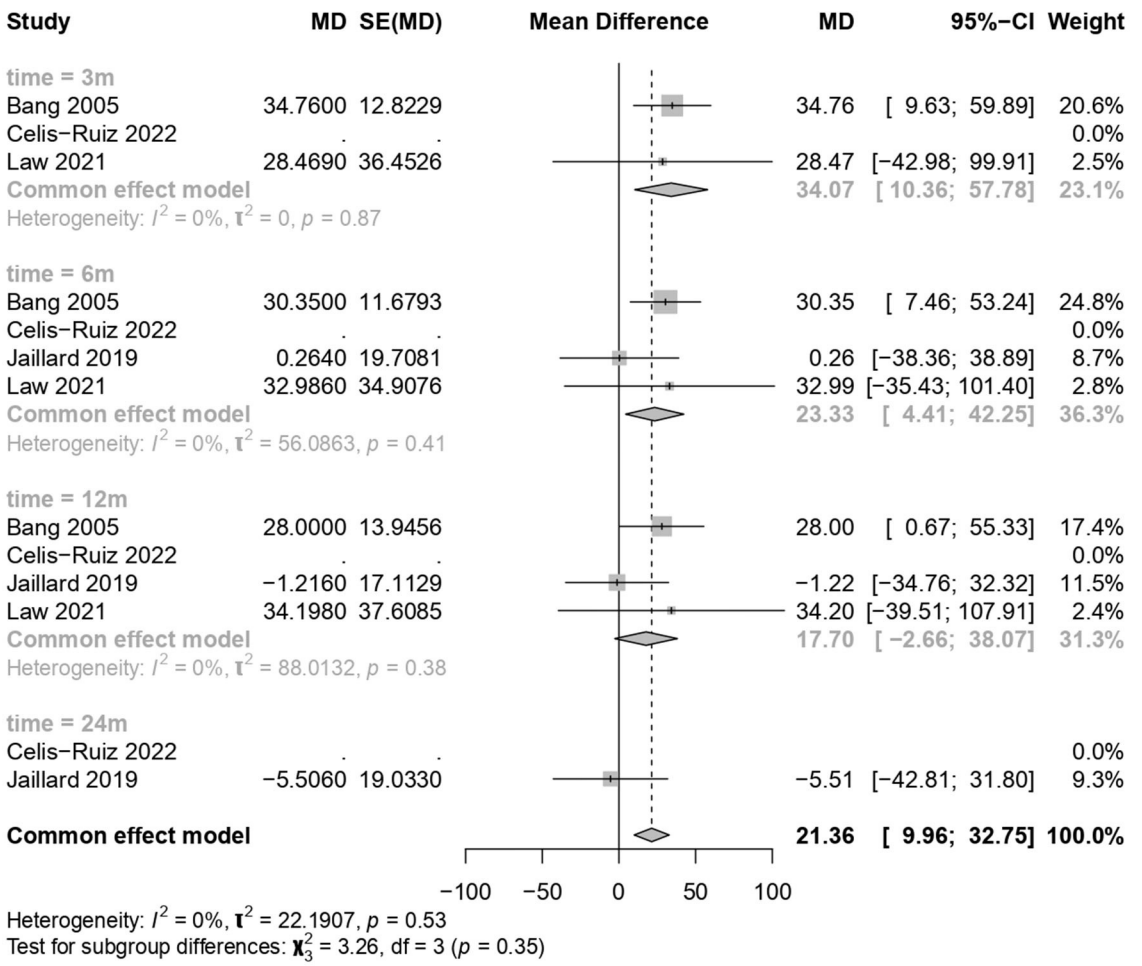

FIGURE 5
Forest plot for clinical improvement in the Barthel Index.

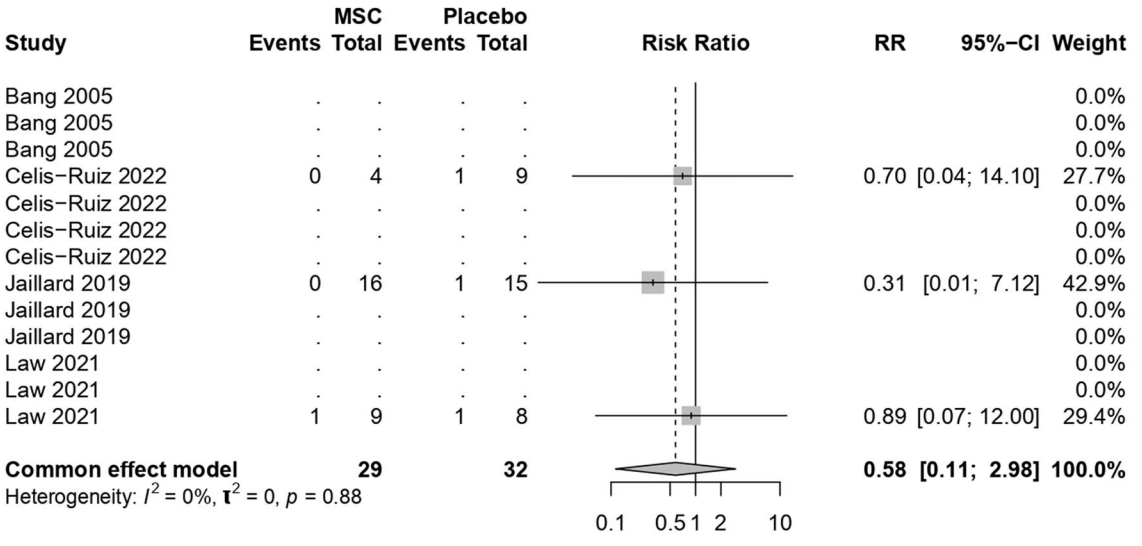

FIGURE 6
Forest plot for mortality rates.

3.7 Mortality rates

MSC treatments were not associated with increased mortality (common effect model; RR 0.58, 95% CI [0.11, 2.97], p-value = 0.51; Figure 6). The calculated effect size using the Mantel–Haenszel method was not statistically significant ($p = 0.51$), indicating that the treatment strategies did not have a significant impact on the mortality rate in the analyzed studies. Pooled studies were homogeneous ($I^2 = 0.0\%$; chi-square $p = 0.53$).

3.8 Stroke recurrence rates

MSC treatments were not associated with increased mortality (common effect model; RR 0.59, 95% CI [0.1122; 3.0588], p-value = 0.53; Figure 7). The calculated effect size using the Mantel–Haenszel method was not statistically significant ($p = 0.53$), indicating that the treatment strategies did not have a significant impact on the mortality rate in the analyzed studies. Pooled results were ($I^2 = 36.5\%$; chi-square $p = 0.21$). The moderate I^2 value, along with the non-significant chi-square test, suggests that the observed heterogeneity might not be strong enough to undermine the overall findings of the stroke recurrence. However, potential sources of heterogeneity, such as sample size, among the included studies need further exploration and interpretation.

4 Discussion

4.1 Summary of the main findings

The meta-analysis findings from different outcome measures are as follows: (1) Clinical improvement in the NIHSS scores did not show significant differences between the MSCs and placebo groups (MD −1.81, 95% CI [−4.123, 0.494], $p = 0.1234$), indicating a negligible impact on the scores. (2) On the mRS outcomes, MSC treatments demonstrated a significant positive effect (MD −0.95, 95% CI [−1.39, −0.52], $p < 0.0001$), indicating a substantial improvement over placebo treatments. (3) The BI scores showed significant improvement with the use of MSCs (MD 21.36, 95% CI [9.96, 32.75], $p = 0.0002$). (4) The mortality and stroke recurrence rates did not exhibit significant differences between MSC and placebo treatments. (5) Heterogeneity was low for most analyses ($I^2 = 0.0\%$) except for stroke recurrence rates ($I^2 = 36.5\%$), where moderate heterogeneity was observed (chi-square $p = 0.21$). Despite this, the moderate I^2 value, along with non-significant chi-square tests, suggests that heterogeneity might not significantly impact the overall findings. Furthermore, subgroup analyses and tests for subgroup differences showed consistent results within subgroups, reinforcing the consistency of the treatment effects across different time points.

4.2 Explanation of the study findings

Adult stem cells, known as MSCs, have the capacity to differentiate into a variety of mesoderm-derived cells, including osteoblasts, chondrocytes, myoblasts, and adipocytes, among others. They can be present in the bone marrow, fat tissue, and other connective tissues, among other bodily tissues (Orbay et al., 2012). MSCs are advantageous in the therapeutic setting due to their multipotency, immunomodulation, secretome, and low immunogenicity (Miceli et al., 2021). MSCs are being researched for a variety of therapeutic uses due to these attributes, including the treatment of neurological conditions including acute and subacute ischemic stroke (Li et al., 2016), as well as others like Parkinson's disease (Kitada and Dezawa, 2012) and Alzheimer's disease (Lee et al., 2012). MSCs are thought to provide neuroprotection, enhanced neurological recovery, and immune response regulation, according to a preclinical study (Uccelli et al., 2011). All of these elements benefit ischemic stroke patients by reducing the severity of tissue damage, preventing more cell death, and reducing oxidative stress, all of which are caused by the heightened immune response that occurs during the acute phase of a stroke. Since MSCs encourage the growth of new blood vessels (angiogenesis) (Velazquez, 2007), which increases blood flow and oxygen supply to brain areas, functional outcomes—whether motor or cognitive—are improved. Based on the previously stated principles, the results of MSCs on the mRS and the BI are predictable.

4.3 Significance of the work

Despite the promising results of MSCs in animal models of stroke, RCTs on MSCs have utilized small sample numbers, making the results less credible due to their effect size. By assessing the overall effect size of intravenous MSCs in patients with acute and subacute ischemic stroke, the current meta-analysis offers robust evidence. The study was the most rigorous meta-analysis to date addressing this research question, analyzing data from four studies involving a total of 97 participants. The study provided the most recent information on the safety and effectiveness of MSCs in acute and subacute ischemic stroke patients in an attempt to aid decision-making.

4.4 Agreement and disagreement with previous studies

Other delivery routes and cell types besides MSCs were taken into consideration in earlier individual patient data meta-analyses of RCTs and non-randomized trials. Furthermore, these meta-analyses did not separate patients with acute stroke and chronic ischemic stroke into separate groups. Additionally, in 2022, Yang et al. (2022) used a prior Bayesian model–based network meta-analysis that heavily relied on animal studies. Other meta-analyses performed by Ouyang et al. (2019) and Sarmah et al. (2018) had similar issues. The current study, in contrast, is founded on trustworthy human data and attempts to inform decision-making by presenting the most recent information on the safety and effectiveness of MSCs in patients with acute and subacute ischemic stroke. We found that the stem cell group was not superior to the placebo group in terms of NIHSS scores in contrast to the findings of Li et al. (2020) which found that participants in the stem cell

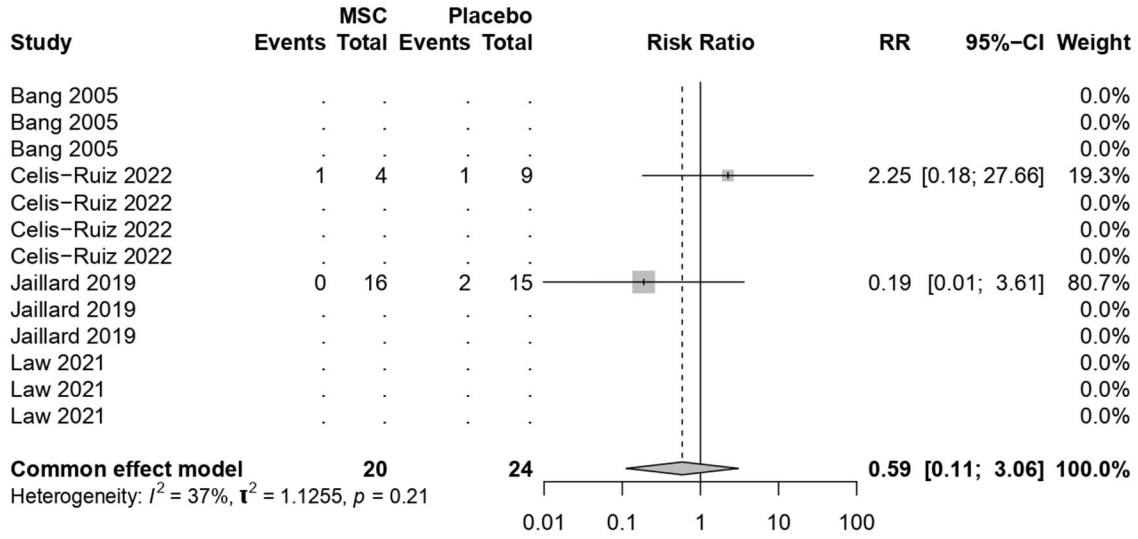

FIGURE 7
Forest plot for stroke recurrence rates.

group had significant outcomes in NIHSS score than the placebo group as reported in RCTs; however, in non-randomized studies, stem cell groups were not superior to placebo groups. We believe that our findings were achieved by including three randomized studies in the analysis (Jaillard et al., 2020; Law et al., 2021; de Celis-Ruiz et al., 2022) that were missing in the analysis by Li et al. (2020).

We conducted a systematic review and meta-analysis of clinical trials in acute and subacute ischemic stroke that compared safety outcomes (such as death and adverse effects) and efficacy outcomes (measured by scales such as the NIHSS, the mRS, or the BI) between the groups receiving stem cell–based therapies and control groups. The study adhered to the procedures outlined in the *Cochrane Handbook of Systematic Reviews for Interventions*, and it was presented using the PRISMA declaration, which is the standard format for systematic reviews and meta-analyses. The study maintains the accuracy and comprehensiveness of the findings by applying these strict processes and including only studies that provide detailed descriptions of their methodologies and analyses.

4.5 Strength points and limitations

This study has several strengths, which are as follows: (1) The study was conducted according to the methods explained in the *Cochrane Handbook of Systematic Reviews for Interventions* and reported according to the PRISMA statement (Cumpston et al., 2019; Page et al., 2021). This ensured that the study followed rigorous guidelines for conducting and reporting systematic reviews. (2) For the literature search and identification, the researchers searched multiple electronic databases to ensure a comprehensive literature search. They also examined all existing records on clinicaltrials.gov, including stopped, incomplete, and ongoing studies. This thorough approach increases the likelihood of capturing relevant studies and data. (3) Only studies whose data were published as full-text journal articles with a complete description of the methods and analysis were included in this study. This inclusion criterion helps ensure that the selected studies provide sufficient information for a comprehensive analysis. However, this study also has a few limitations: (1) The current evidence on the safety and efficacy of MSCs in acute and subacute ischemic stroke patients is limited by the small number of available RCTs. This suggests that more research is needed to draw definitive conclusions. (2) The findings of this study may not be generalizable to the entire population of acute and subacute ischemic stroke patients. It is important to consider individual patient characteristics and other factors when interpreting the results.

4.6 Ongoing studies and implications for clinical practice

We are aware of several ongoing clinical trials on MSCs (clinicaltrials.gov identifier: NCT05522569, NCT04097652, NCT04434768, NCT04093336, NCT03384433, and NCT03186456) for which the data are not yet available. In the future, as further data from these ongoing RCTs become available, this current meta-analysis will provide the most up-to-date information on the safety and efficacy of MSCs in acute and subacute ischemic stroke patients.

5 Conclusion

The use of intravenous MSCs in acute and subacute stroke patients showed positive results in terms of the mRS and the BI, indicating improved functional recovery and quality of life. However, while there were no substantial changes in NIHSS scores, mortality rates, or stroke recurrence, these outcomes emphasize

MSCs' potential to enhance rehabilitation and highlight the need for further research to uncover the complex impacts of MSC therapy on stroke outcomes.

Data availability statement

The original contributions presented in the study are included in the article/supplementary material, further inquiries can be directed to the corresponding author.

Author contributions

MH: Data curation, Methodology, Supervision, Validation, Writing – original draft, Writing – review & editing. JF: Conceptualization, Data curation, Methodology, Writing – original draft. JS: Data curation, Methodology, Writing – original draft. EA: Data curation, Writing – original draft. MH: Conceptualization, Methodology, Validation, Visualization, Writing – original draft, Writing – review & editing. HG: Writing – review & editing. AN: Writing – original draft, Writing – review & editing.

Funding

The author(s) declare that no financial support was received for the research, authorship, and/or publication of this article.

Acknowledgments

We would like to thank Negida Academy Internship Program the information we gained through has helped us in conducting this work. Also we would like to extend their gratitude to Dr. Ibrahim Abdelmonaem for his assistance during statical analysis.

Conflict of interest

The authors declare that the research was conducted in the absence of any commercial or financial relationships that could be construed as a potential conflict of interest.

The author(s) declared that they were an editorial board member of Frontiers, at the time of submission. This had no impact on the peer review process and the final decision.

Publisher's note

References

Badhiwala, J. H., Nassiri, F., Alhazzani, W., Selim, M. H., Farrokhyar, F., Spears, J., et al. (2015). Endovascular thrombectomy for acute ischemic stroke: a meta-analysis. *JAMA* 314, 1832–1843. doi: 10.1001/jama.2015.13767

Bang, O. Y., Lee, J. S., Lee, P. H., and Lee, G. (2005). Autologous mesenchymal stem cell transplantation in stroke patients. *Ann. Neurol.* 57, 874–882. doi: 10.1002/ana.20501

Bergh, D. (2015). Chi-squared test of fit and sample size-a comparison between a random sample approach and a chi-square value adjustment method. *J. Appl. Meas.* 16, 204–217. doi: 10.1007/978-3-662-47490-7_15

Broderick, J. P., Palesch, Y. Y., Demchuk, A. M., Yeatts, S. D., Khatri, P., Hill, M. D., et al. (2013). Endovascular therapy after intravenous t-PA versus t-PA alone for stroke. *N. Engl. J. Med.* 368, 893–903. doi: 10.1056/NEJMoa1214300

Cui, Y.-F., Hargus, G., Xu, J.-C., Schmid, J. S., Shen, Y.-Q., Glatzel, M., et al. (2010). Embryonic stem cell-derived L1 overexpressing neural aggregates enhance recovery in Parkinsonian mice. *Brain* 133, 189–204. doi: 10.1093/brain/awp290

Cumpston, M., Li, T., Page, M. J., Chandler, J., Welch, V. A., Higgins, J. P., et al. (2019). Updated guidance for trusted systematic reviews: a new edition of the Cochrane Handbook for Systematic Reviews of Interventions. *Cochr. Datab. Syst. Rev.* 10, ED000142. doi: 10.1002/14651858.ED000142

de Celis-Ruiz, E., Fuentes, B., Alonso de Leciñana, M., Gutiérrez-Fernández, M., Borobia, A. M., Gutiérrez-Zúñiga, R., et al. (2022). Final results of allogeneic adipose tissue-derived mesenchymal stem cells in acute ischemic stroke (AMASCIS): a phase II, randomized, double-blind, placebo-controlled, single-center, pilot clinical trial. *Cell Transplant.* 31, 9636897221083864. doi: 10.1177/09636897221083863

Ebrahimi, T., Abasi, M., Seifar, F., Eyvazi, S., Hejazi, M. S., Tarhriz, V., et al. (2021). Transplantation of stem cells as a potential therapeutic strategy in neurodegenerative disorders. *Curr. Stem Cell Res. Ther.* 16, 133–144. doi: 10.2174/22123946MTA33NzUey

Egger, M., Smith, G., Schneider, M., and Minder, C. (1997). Bias in meta-analysis detected by a simple, graphical test. *BMJ* 315, 629–634. doi: 10.1136/bmj.315.7109.629

El-Hajj, M., Salameh, P., Rachidi, S., and Hosseini, H. (2016). The epidemiology of stroke in the Middle East. *Eur. Stroke J.* 1, 180–198. doi: 10.1177/2396987316654338

Jaillard, A., Hommel, M., Moisan, A., Zeffiro, T. A., Favre-Wiki, I. M., Barbieux-Guillot, M., et al. (2020). Autologous mesenchymal stem cells improve motor recovery in subacute ischemic stroke: a randomized clinical trial. *Transl. Stroke Res.* 11, 910–923. doi: 10.1007/s12975-020-00787-z

Kitada, M., and Dezawa, M. (2012). Parkinson's disease and mesenchymal stem cells: potential for cell-based therapy. *Parkinsons Dis.* 2012, 873706. doi: 10.1155/2012/873706

Law, Z. K., Tan, H. J., Chin, S. P., Wong, C. Y., Wan Yahya, W. N. N., Muda, A. S., et al. (2021). The effects of intravenous infusion of autologous mesenchymal stromal cells in patients with subacute middle cerebral artery infarct: a phase 2 randomized controlled trial on safety, tolerability and efficacy. *Cytotherapy* 23, 833–840. doi: 10.1016/j.jcyt.2021.03.005

Lee, H. J., Lee, J. K., Lee, H., Carter, J. E., Chang, J. W., Oh, W., et al. (2012). Human umbilical cord blood-derived mesenchymal stem cells improve neuropathology and cognitive impairment in an Alzheimer's disease mouse model through modulation of neuroinflammation. *Neurobiol. Aging* 33, 588–602. doi: 10.1016/j.neurobiolaging.2010.03.024

Li, G., Yu, F., Lei, T., Gao, H., Li, P., Sun, Y., et al. (2016). Bone marrow mesenchymal stem cell therapy in ischemic stroke: mechanisms of action and treatment optimization strategies. *Neural Regen. Res.* 11, 1015–1024. doi: 10.4103/1673-5374.184506

Li, Z., Dong, X., Tian, M., Liu, C., Wang, K., Li, L., et al. (2020). Stem cell-based therapies for ischemic stroke: a systematic review and meta-analysis of clinical trials. *Stem. Cell Res. Ther.* 11, 252. doi: 10.1186/s13287-020-01762-z

Marei, H. E., Hasan, A., Rizzi, R., Althani, A., Afifi, N., Cenciarelli, C., et al. (2018). Potential of stem cell-based therapy for ischemic stroke. *Front. Neurol.* 9, 34. doi: 10.3389/fneur.2018.00034

Miceli, V., Bulati, M., Iannolo, G., Zito, G., Gallo, A., and Conaldi, P. G. (2021). Therapeutic properties of mesenchymal stromal/stem cells: the need of cell priming for cell-free therapies in regenerative medicine. *Int. J. Mol. Sci.* 22, 763. doi: 10.3390/ijms22020763

National Cancer Institute (2018). "National institute of neurological disorders and stroke." in *Definitions* (Qeios).

Orbay, H., Tobita, M., and Mizuno, H. (2012). Mesenchymal stem cells isolated from adipose and other tissues: basic biological properties and clinical applications. *Stem. Cells Int*. 2012, 461718. doi: 10.1155/2012/461718

Ouyang, Q., Li, F., Xie, Y., Han, J., Zhang, Z., Feng, Z., et al. (2019). Meta-analysis of the safety and efficacy of stem cell therapies for ischemic stroke in preclinical and clinical studies. *Stem Cells Dev*. 28, 497–514. doi: 10.1089/scd.2018.0218

Page, M. B., Boutron, H., Mulrow, C. D., Shamseer, L., Tetzlaff, J. M., Akl, E. A., et al. (2021). The PRISMA 2020 statement: an updated guideline for reporting systematic reviews. *BMJ* 372, n71. doi: 10.1136/bmj.n71

Prodinger, B., O'Connor, R. J., Stucki, G., and Tennant, A. (2017). Establishing score equivalence of the functional independence measure motor scale and the barthel index, utilising the international classification of functioning, disability and health and rasch measurement theory. *J. Rehabil. Med*. 49, 416–422. doi: 10.2340/16501977-2225

Runde, D. (2019). Calculated decisions: modified rankin scale (mrs) for neurologic disability. *Emerg. Med. Pract*. 21, CD4–CD5.

Sarmah, D., Agrawal, V., Rane, P., Bhute, S., Watanabe, M., Kalia, K., et al. (2018). Mesenchymal stem cell therapy in ischemic stroke: a meta-analysis of preclinical studies. *Clin. Pharmacol. Ther*. 103, 990–998. doi: 10.1002/cpt.927

Shaheen, N., Shaheen, A., Ramadan, A., Hefnawy, M. T., Ramadan, A., Ibrahim, I. A., et al. (2023). Appraising systematic reviews: a comprehensive guide to ensuring validity and reliability. *Front. Res. Metr. Anal*. 8:1268045. doi: 10.3389/frma.2023.1268045

Sterne, J. A. C., Savović, J., Page, M. J., Elbers, R. G., Blencowe, N. S., Boutron, I., et al. (2019). RoB 2: a revised tool for assessing risk of bias in randomised trials. *BMJ* 366, l4898. doi: 10.1136/bmj.l4898

Uccelli, A., Laroni, A., and Freedman, M. S. (2011). Mesenchymal stem cells for the treatment of multiple sclerosis and other neurological diseases. *Lancet Neurol*. 10, 649–656. doi: 10.1016/S1474-4422(11)70121-1

Velazquez, O. C. (2007). Angiogenesis and vasculogenesis: inducing the growth of new blood vessels and wound healing by stimulation of bone marrow-derived progenitor cell mobilization and homing. *J. Vasc. Surg*. 45, A39–47. doi: 10.1016/j.jvs.2007.02.068

Yang, Y., Hu, X., Qin, Q., Kong, F., Peng, X., Zhao, J., et al. (2022). Optimal therapeutic conditions for the neural stem cell-based management of ischemic stroke: a systematic review and network meta-analysis based on animal studies. *BMC Neurol*. 22, 345. doi: 10.1186/s12883-022-02875-z

frontiers | Frontiers in Pharmacology

TYPE Review
PUBLISHED 27 March 2024
DOI 10.3389/fphar.2024.1250918

OPEN ACCESS

EDITED BY
Viola B. Morris,
Emory University, United States

REVIEWED BY
Junping Zhang,
First Teaching Hospital of Tianjin University of Traditional Chinese Medicine, China
Roger Gutiérrez-Juárez,
National Autonomous University of Mexico, Mexico
Yi Li,
China Pharmaceutical University, China

*CORRESPONDENCE
Jinwen Ge,
001267@hnucm.edu.cn

†These authors share first authorship

RECEIVED 30 June 2023
ACCEPTED 11 January 2024
PUBLISHED 27 March 2024

CITATION
Yang K, Zeng L, He Q, Wang S, Xu H and Ge J (2024), Advancements in research on the immune-inflammatory mechanisms mediated by NLRP3 inflammasome in ischemic stroke and the regulatory role of natural plant products. *Front. Pharmacol.* 15:1250918. doi: 10.3389/fphar.2024.1250918

Advancements in research on the immune-inflammatory mechanisms mediated by NLRP3 inflammasome in ischemic stroke and the regulatory role of natural plant products

Kailin Yang[1,2†], Liuting Zeng[3†], Qi He[4†], Shanshan Wang[1], Hao Xu[1] and Jinwen Ge[1,2*]

[1]Key Laboratory of Hunan Province for Integrated Traditional Chinese and Western Medicine on Prevention and Treatment of Cardio-Cerebral Diseases, School of Integrated Chinese and Western Medicine, Hunan University of Chinese Medicine, Changsha, China, [2]Hunan Academy of Chinese Medicine, Changsha, Hunan, China, [3]Graduate School, Chinese Academy of Medical Sciences and Peking Union Medical College, Beijing, China, [4]Department of Critical Care Medicine, People's Hospital of Ningxiang City, Ningxiang, China

Ischemic stroke (IS) is a major cause of mortality and disability among adults. Recanalization of blood vessels to facilitate timely reperfusion is the primary clinical approach; however, reperfusion itself may trigger cerebral ischemia-reperfusion injury. Emerging evidence strongly implicates the NLRP3 inflammasome as a potential therapeutic target, playing a key role in cerebral ischemia and reperfusion injury. The aberrant expression and function of NLRP3 inflammasome-mediated inflammation in cerebral ischemia have garnered considerable attention as a recent research focus. Accordingly, this review provides a comprehensive summary of the signaling pathways, pathological mechanisms, and intricate interactions involving NLRP3 inflammasomes in cerebral ischemia-reperfusion injury. Moreover, notable progress has been made in investigating the impact of natural plant products (e.g., Proanthocyanidins, methylliensinine, salidroside, α-asarone, acacia, curcumin, morin, ginsenoside Rd, paeoniflorin, breviscapine, sulforaphane, etc.) on regulating cerebral ischemia and reperfusion by modulating the NLRP3 inflammasome and mitigating the release of inflammatory cytokines. These findings aim to present novel insights that could contribute to the prevention and treatment of cerebral ischemia and reperfusion injury.

KEYWORDS

ischemic stroke, NLRP3 inflammasome, immune mechanism, inflammatory mechanism, natural plant products

1 Introduction

Stroke, the second most lethal disease globally, is a highly disabling condition causing approximately 6 million deaths annually (Feske, 2021). In China, the number of stroke patients exceeds 13 million, a figure projected to surpass 30 million by 2030, imposing a substantial burden on patients and their families (Hussain et al., 2021; Saini et al., 2021). Stroke manifests as either ischemic stroke (IS), resulting from embolic blockage of cerebral

artery blood flow, or hemorrhagic stroke caused by blood vessel rupture within the brain. Pathophysiological processes underlying stroke encompass disorders in bioenergy metabolism, cellular ion homeostasis imbalances, acidosis, elevation of intracellular calcium concentration, excitotoxicity, superoxide dismutase-mediated neurotoxicity, increased arachidonic acid expression, cytokine-mediated cytotoxicity, complement system activation, glial cell activation, leukocyte infiltration, and disruption of the blood-brain barrier. Inflammation constitutes a critical pathogenic mechanism in IS, as the inflammatory response can trigger both ischemic brain injury and facilitate tissue repair following damage (Qiu et al., 2021). Activated neurons, astrocytes, microglia, and endothelial cells in IS release pro-inflammatory factors such as tumor necrosis factor-α (TNF-α), interleukin-1β (IL-1β), IL-6, and IL-18, ultimately leading to neuronal and glial cell death (Ajoolabady et al., 2021; Zhu et al., 2022a). Recent studies have highlighted the potential importance of NOD-like receptors Pyrin Containing 1 (NLRP1) and NLRP3 inflammasome in neurons and glial cells for detecting IS-induced cell damage and immune response regulation (Xu et al., 2021; Wang et al., 2022; Zhang et al., 2022). The human NLRP1 inflammasome is composed of four cytoplasmic components, including NLRP1, an apoptosis-associated speck-like protein (ASC) harboring N-terminal pyrin domain (PYD) and caspase recruitment domain (CARD), a caspase-1 precursor, and either a caspase-4 precursor or a caspase-5 precursor (Piancone et al., 2021). The composition of the NLRP1 inflammasome in mice slightly differs and consists of NLRP1, ASC, caspase-1 precursor, caspase-11 precursor (homologous to caspase-4 precursor and caspase-5 precursor), and X-linked inhibitor of apoptosis (XIAP) (Huang et al., 2021a). On the other hand, the NLRP3 inflammasome comprises three cytoplasmic components, namely, NLRP3, ASC, and caspase-1 precursor (Sharma and Kanneganti, 2021). Although the mechanisms underlying NLRP1 and NLRP3 inflammasome activation in IS remain incompletely understood, several pathways potentially implicated in their stimulation have been identified, including ATP-mediated activation, acidosis-mediated activation, cathepsin-mediated activation, potassium-mediated activation, ROS-mediated activation, calcium ion-mediated activation, and cell edema-mediated activation (Pandey et al., 2021; Zhang et al., 2021a; Liu et al., 2021).

Following ischemic stroke (IS), the NLRP3 or NLRP1 protein forms a multi-protein complex known as the NLRP3 or NLRP1 inflammasome by binding with Caspase-1 precursor and ASC (Lin et al., 2021). Once formed, the inflammasome activates the caspase-1 precursor through inter-neighbor autocatalysis. Activated caspase-1 then cleaves the precursors of IL-1β and IL-18, generating active mature forms that are subsequently released into the extracellular environment to bind to corresponding cell membrane receptors. This triggers downstream MAPK and nuclear factor kappa B (NF-κB) pathways, leading to the re-transcription of IL-1β and IL-18 precursors, NLRP1, and NLRP3 (Li et al., 2022a). In IS, excessive production of IL-18 by neurons and glial cells induces an increase in IFN-γ levels and the release and maturation of IL-1β, promoting a state of brain tissue inflammation and causing severe damage (Mi et al., 2022). Additionally, activated caspase-1 can cleave and activate caspase-3 and caspase-7, leading to apoptosis through the internal and external pathways of cells, respectively (Wang et al., 2022). Recent studies have highlighted the regulatory role of natural plant products in modulating the cerebral ischemic inflammasome (Tao et al., 2022). This discovery opens up new avenues for exploring lead compounds as inflammasome inhibitors. This review aims to summarize the mechanisms of the inflammasome in IS and the regulatory effects of natural plant products. These findings serve as a theoretical reference for future drug development and clinical treatment.

2 Inflammation as the core pathological process of IS

Inflammation serves as the innate immune response of the body, playing a crucial role in eliminating harmful stimuli and promoting tissue repair initiation (Lee et al., 2018). The inflammatory response elicited by ischemic stroke (IS) extends throughout the entire IS process, starting from the activation of endothelial cells shortly after IS onset to the post-injury repair phase occurring several days to months later. It represents one of the key factors influencing neuronal death. However, an exaggerated inflammatory response can lead to significant harm. In the presence of cerebral ischemia, activated cells (including neurons, astrocytes, and endothelial cells) release pro-inflammatory cytokines such as IL-1β, IL-6, and IL-18, which induce the death of neurons and glial cells. Microglia in the central nervous system (CNS) are the first to be activated, secreting numerous inflammatory mediators and exacerbating the inflammatory response in the ischemic region, damaging the blood-brain barrier, and releasing various danger-associated molecular patterns (DAMPs) (Tang et al., 2023). These factors collectively induce the recruitment of peripheral immune cells to the lesion and its surroundings, extensively contributing to the inflammation and immune response in IS. Recent work by Dai et al. (2020) demonstrated that D-carvone attenuated the cerebral ischemia-reperfusion-induced inflammatory response in rats, reducing damage to the hippocampus and cortex. Additionally, released pro-inflammatory cytokines can induce the expression of adhesion molecules such as intercellular adhesion molecule-1 (ICAM-1), vascular cell adhesion molecule (VCAM), selectins (e.g., P-selectin, E-selectin), and integrins. These adhesion molecules are crucial for the infiltration of immune cells, especially neutrophils and monocytes/macrophages, into the ischemic area during reperfusion. Unfortunately, this often leads to secondary injuries in ischemia-reperfusion injury. Moreover, activated neurons and glial cells release monocyte chemotactic protein-1 (MCP-1/CCL2), promoting leukocyte migration to damaged tissues. However, a recent study revealed that the accumulation of leukocytes in nerves and blood vessels did not spatially correlate with increased vascular permeability or enhanced expression of endothelial cell adhesion molecules (Enzmann et al., 2013). Although the mechanism underlying ischemia-reperfusion injury remains unclear, it has been observed that leukocyte infiltration can lead to the release of various cytotoxic agents, including additional pro-inflammatory cytokines (e.g., IL-1β, IL-6), reactive oxygen species (ROS)

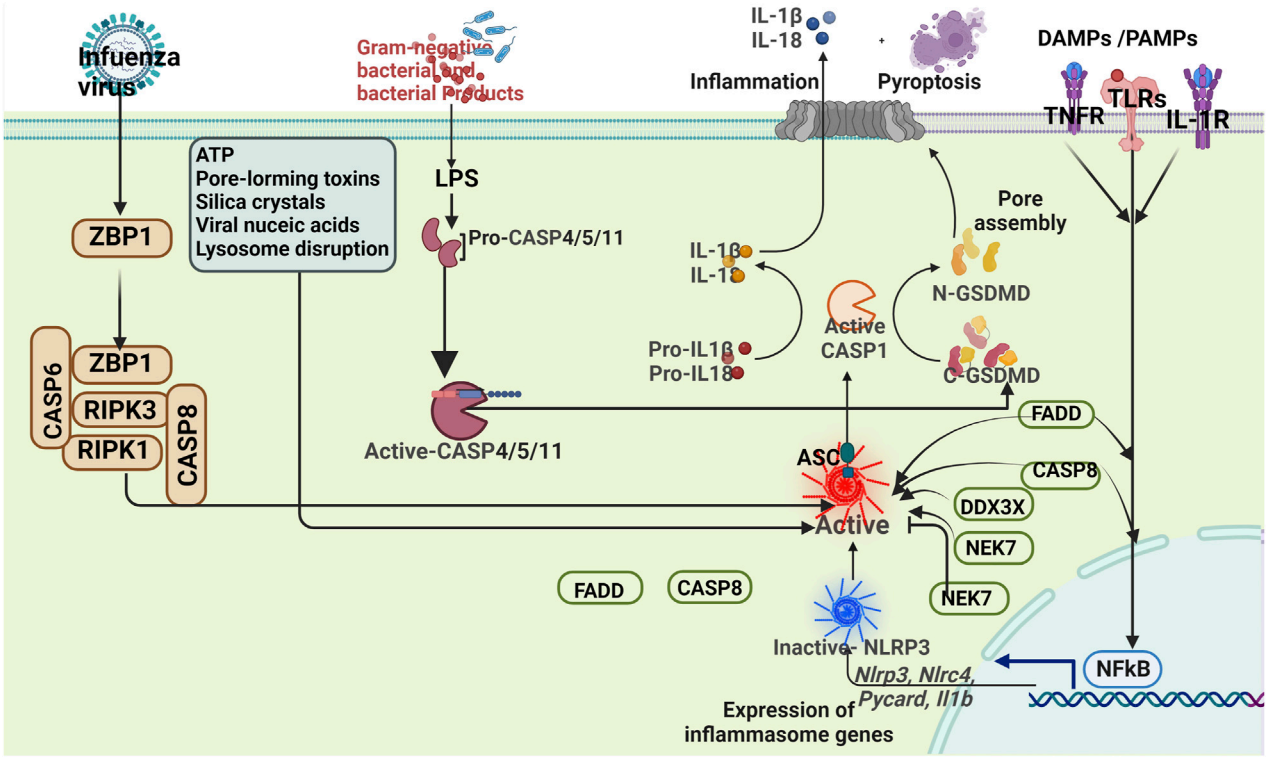

FIGURE 1
Mechanisms of the inflammasome.

produced by reduced nicotinamide adenine dinucleotide phosphate oxidase, as well as nitric oxide, induced by inducible nitric oxide synthase (iNOS) and matrix metalloproteinases (MMP). These MMPs can contribute to extracellular matrix damage and blood-brain barrier disruption, ultimately exacerbating cerebral edema and hemorrhage, leading to neuronal and glial cell death (Shen et al., 2023).

3 Inflammasome participates in the pathological process of IS

The inflammasome is characterized by three components: a receptor protein, ASC, and Pro-caspase-1. Among the pattern recognition receptors investigated, the most extensively studied ones are nucleotide-binding and oligomerization domain-like receptors (NLRs) and absent in melanoma 2-like receptors (ALRs) (Huang et al., 2021a; Pandey et al., 2021). The NLR family comprises five subtypes: NLRA with an acidic transactivation domain, NLRB with baculovirus inhibitor repeat, NLRC with CARD (NOD1, NOD2, NLRC3-5), NLRPs containing protein domains (NLRP1-14), and NLRXs with unknown domains (Li et al., 2021a; Zhang et al., 2021b). The ALR family consists of AIM2 protein and IFN-γ inducible protein 16 (IFI16) protein (Zheng et al., 2021). Extensively studied inflammasomes include NLRP1, NLRP3, NLRC4, and AIM2 (Zheng et al., 2021). Several studies have reported the significant involvement of NLR containing pyrin domain (NLRP) in the inflammatory response among ischemic stroke patients (Seoane et al., 2020). The mechanism of the inflammasome was summarized in Figure 1.

3.1 NLRP1

The NLRP1 inflammasome consists of the NLRP1 receptor, ASC and Pro-caspase-1, is a member of the NLRs family, and is highly expressed in brain tissue. The NLRP1 receptor is characterized by 5 domains: PYD, nucleotide-binding oligomerization (NACHT), C-terminus is leucine repeat domains (LRRs), function-to-find domain (FIIND) and CARD. When the NLRP1 receptor is activated, the FIND domain is automatically cleaved (Ciążyńska et al., 2021; de Brito Toscano et al., 2021). Cao et al. showed that NLRP1 is a target gene of miR-9a-5p and is involved in the NLRP1 inflammasome-mediated inflammatory response induced by ischemic injury (Cao et al., 2020). Overexpression of miR-9a-5p downregulates NLRP1. Overexpression of miR-9a5p not only reduced the levels of NLRP1, Asc and Pro-caspase-1, but also decreased the levels of IL-1β and IL-18, suggesting that overexpression of miR-9a5p can improve brain injury after IS (Cao et al., 2020).

3.2 NLRP3

The NLRP3 inflammasome consists of the NLRP3 receptor, ASC, and Pro-caspase-1. The NLRP3 receptor, a member of the NLR

family, exhibits three structural features: N-terminal PYD, central NACHT, and C-terminal LRR domains (Zhang et al., 2021a; Zhao et al., 2021). The N-terminal PYD domain enables interaction with the downstream adaptor protein ASC via dual ligand binding. The NACHT domain regulates the activation of NLRP1 and NLRP3 receptors, initiating oligomerization and formation of the central core of the inflammasome, an ATP-dependent process (Levinsohn et al., 2012). The LRR domain is believed to participate in ligand sensing and autoregulation (Levinsohn et al., 2012). Recent studies have explored potential interventions targeting the NLRP3 inflammasome for neuroprotection in ischemic stroke. For instance, Ma et al. discovered that salvianolic acid for injection can inhibit the activation of microglial NLRP3 inflammasome, facilitate the transition of microglial phenotype from M1 to M2, and reduce neuronal apoptosis, thereby exerting neuroprotective effects (Ma et al., 2021). Yin et al. also revealed the involvement of TET2 in the inflammatory response induced by cerebral ischemia-reperfusion through the demethylation of TUG1 and regulation of the TUG1/miR-200A-3p/NLRP3 pathway (Yin et al., 2021). Sun et al. identified the role of the low-density lipoprotein receptor (LDLR) in mediating NLRP3-dependent neuronal pyroptosis and neuroinflammation after ischemic stroke, suggesting LDLR as a potential therapeutic target for neuroinflammatory responses in acute cerebral ischemic injury (Sun et al., 2020). Assembly and activation of the NLRP3 inflammasome rely on two complementary signals associated with cellular damage. One initiation signal involves the NF-κB and mitogen-activated protein kinase (MAPK) signaling pathways. These pathways upregulate the expression of NLRP3 inflammasome complex proteins, precursor IL-1β, and precursor IL-18 (Paerewijck and Lamkanfi, 2022). The other complementary signal mediates NLRP3 activation and ASC phosphorylation, initiating NLRP3 inflammasome assembly, caspase-1 activation, and processing of Pro-IL-1β and Pro-IL-18, ultimately resulting in the secretion of IL-1β and IL-18 (Takahashi, 2022).

3.2.1 Initiation regulation of NLRP3 inflammasome activation

In the resting state, the expression levels of NLRP3, Pro-IL-1β and Pro-IL-18 in cells are low, and they cannot directly assemble or activate the NLRP3 inflammasome. Therefore, upregulation of priming signals, especially NLRP3-related proteins, is required for activation of the NLRP3 inflammasome (Coll et al., 2022). Fann et al. found that intravenous injection of immunoglobulin preparations could reduce the activation of NF-κB and MAPK signaling pathways, resulting in decreased expression and activation of NLRP3 inflammasomes (Fann et al., 2018). This suggests that NF-κB and MAPK signaling pathways play critical roles in regulating the expression and activation of the NLRP3 inflammasome in primary cortical neurons and brain tissue under ischemic conditions (Huang et al., 2021a).

3.2.2 Activation regulation of NLRP3 inflammasome activation

After activation of the priming signal, the adaptor protein ASC recruits the NLRP3 protein to form the NLRP3 inflammasome complex (Chen et al., 2021a). Currently, the NLRP3 inflammasome has multiple activation mechanisms, including K+ efflux, ROS overproduction, mitochondrial dysfunction, Ca overload, and lysosomal rupture (Milner et al., 2021). Among the extracellular and intracellular factors, K+ efflux plays an important role in activating the NLRP3 inflammasome (Muñoz-Planillo et al., 2013). This non-selective K+ cation channel located on the cell surface can change intracellular ion content depending on the binding of adenosine triphosphate, activate downstream signals, and induce the maturation and secretion of IL-1β. Studies have shown that downregulation of intracellular K+ levels is essential for activation of the NLRP3 inflammasome pathway compared to other known stimuli, highlighting the important role of K+ efflux in this process. Purinergic ion channel receptor 7 (P2X7R) is one of the receptors associated with K+ efflux, and its activation may induce the release of proinflammatory cytokines and amplify ischemic injury via ATP (Kelley et al., 2019). Ye et al. found that the expressions of P2X7R, NLRP3 inflammatory components and cleaved caspase-3 were significantly enhanced in ischemic brain tissue after stroke (Ye et al., 2017). However, the expression of cleaved caspase-3 was significantly attenuated after stroke treatment with a P2X7R antagonist (BBG) or an NLRP3 inhibitor (MCC950), which significantly reduced brain infarct volume, neuronal apoptosis, and nerve damage. Mitochondrial damage is another important activation mechanism of the NLRP3 inflammasome. Mitochondria are double-membrane-bound organelles that are the main site for energy and ROS production in cells (Peng and Jou, 2010). Previous studies have shown that under various cellular stresses, especially high levels of ROS produced by mitochondria activate the NLRP3 inflammasome signaling pathway (Heid et al., 2013). A large amount of ROS-induced ROS scavenger thioredoxin is cleaved from thioredoxin-interacting protein (TXNIP), which then directly binds to NLRP3 protein and regulates its assembly through oligomerization (Yin et al., 2017). Ishrat et al.showed that the expression of TXNIP in brain tissue increased after IS, and ROS can lead to the dissociation of TXNIP and thioredoxin 1 (TRX1), which can quickly bind to NLRP3, induce the activation of NLRP3 inflammasome, inhibit the activation of NLRP3 inflammasome by inhibiting TXNIP, and reduce ischemic brain injury (Ishrat et al., 2015). Dysfunctional mitochondria also release mitochondrial DNA into the cytoplasm, which directly induces the assembly of the NLRP3 inflammasome complex through molecular self-association (Ip and Medzhitov, 2015).

3.3 AIM2

The AIM2 inflammasome is a cytoplasmic sensor that recognizes double-stranded DNA (dsDNA) from viruses, bacteria, or the host itself. AIM2 consists of PYD and HIN-200 domains, and AIM2 protein is the activating component of the AIM2 inflammasome. Li et al. found that cytosolic DNA participates in a variety of independent but complementary DNA sensing signals through cyclic adenosine monophosphate synthase and AIM2, and synergistically exerts the greatest inflammatory response during ischemia (Li Q. et al., 2020a). The inhibitor of cytoplasmic double-stranded DNA, A151, significantly reduced cerebral infarct volume, alleviated neurological deficits, and reduced cell death, inhibited the overall neuroinflammatory

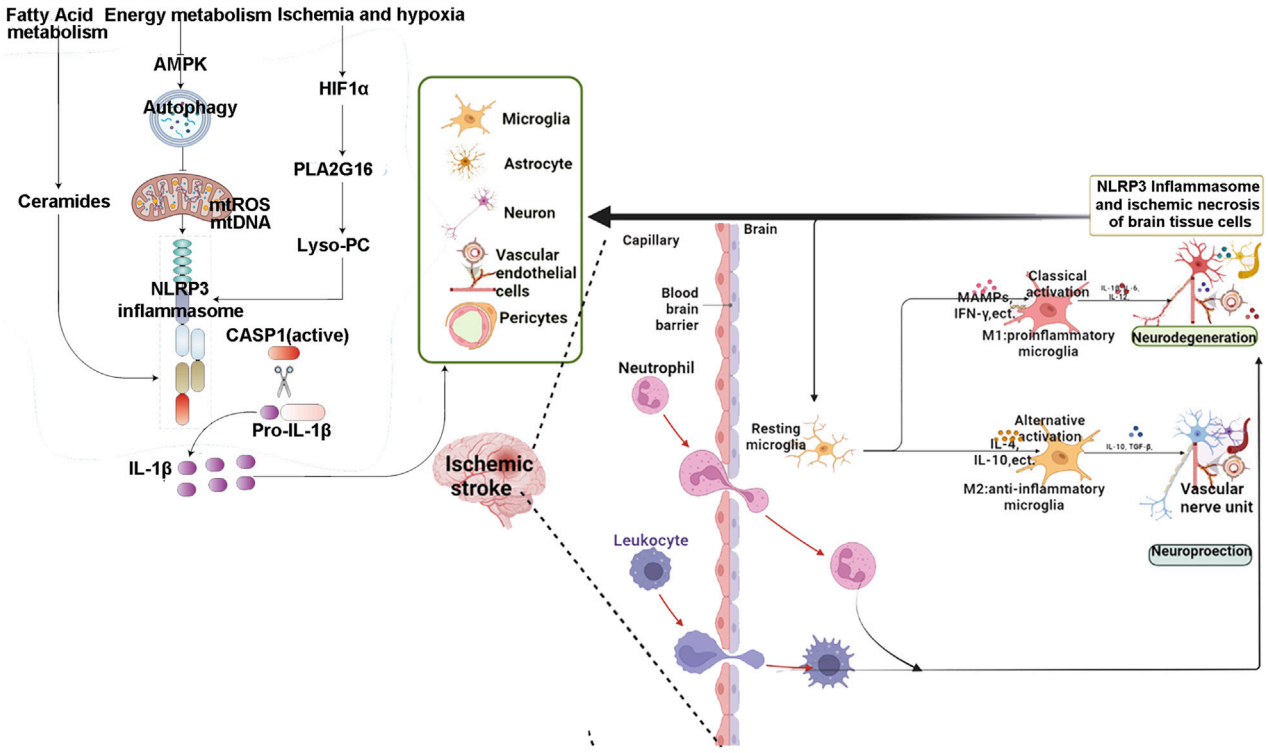

FIGURE 2
The mechanisms of inflammasome involvement in IS.

response, and may provide a new therapeutic concept for IS. Liang et al. found that MEG3 knockout could inhibit oxygen-glucose deprivation/reoxygenation-induced pyroptosis and inflammatory responses (Liang et al., 2020). Lack of MEG3 inhibits caspase-1 signaling and reduces the expression of AIM2, ASC, cleaved caspase-1 and GSDMD-N. This suggests that the MEG3/miR-485/AIM2 axis is involved in pyroptosis by activating the caspase-1 signaling pathway during cerebral ischemia-reperfusion, and may be an effective therapeutic target for IS (Liang et al., 2020).

3.4 NLRC4

NLRC4, also known as IL-1β converting enzyme protease activating factor (IPAF), is a member of the NLR family (Sundaram and Kanneganti, 2021). The NLRC4 receptor is characterized by three domains: its N-terminus is the caspase recruitment domain (CARD), which is an effector domain that recruits and activates Pro-caspase-1 and is responsible for downstream signal transduction. In the middle is the NACHT domain, which is a characteristic domain shared by members of the NLR family, NBD-HD1-WHD-HD2 from the N-terminal to the C-terminal, which can mediate the oligomerization of NLR molecules and change its configuration. The LRRs, which are responsible for the recognition and binding of ligands such as PAMP (Andrade and Zamboni, 2020; Bauer and Rauch, 2020). Recent studies have shown that inflammasome activation can lead to the death of neurons and glial cells, which in turn leads to brain damage and nervous system damage after ischemic stroke (Wen et al., 2021a). Wang et al. found that in microglia induced by high glucose hypoxia/reoxygenation (H/R), knockout of the long non-coding RNA-Fendrr (LncRNA-Fendrr) gene reduced NLRC4 and inflammatory cytokines (Wang et al., 2021a). LncRNA-Fendrr can protect the ubiquitination and degradation of NLRC4 protein through the E3 ubiquitin ligase HERC2, thereby accelerating the pyroptosis of microglia.

The mechanisms of inflammasome involvement in IS were summarized in Figure 2.

4 Inflammasomes involves in cerebral ischemia-induced cell damage

4.1 Inflammasome and apoptosis

Apoptosis is an active process involving activation, expression and regulation of a series of genes. Activation of classical apoptosis occurs mainly through two pathways (Christgen et al., 2022). One is the extrinsic pathway, which is activated by activating apoptosis receptors on the cell surface, ultimately activating caspase-8 or caspase-10 (Gudipaty et al., 2018). The other is the endogenous pathway, also known as the mitochondrial apoptosis pathway, which starts with mitochondrial cytochrome C and activates caspase-9 (Tang et al., 2019a). Both pathways lead to a signal transduction cascade that ultimately leads to apoptosis through activation of caspase-3 (Wu et al., 2020a). Previous studies have shown that free radicals generated by cerebral ischemia-reperfusion are mainly released by mitochondria, leading to oxidative stress in neurons.

Excessive production of reactive oxygen species in mitochondria can damage mitochondria and lipids, thereby impairing mitochondrial function and leading to increased permeability. Increased permeability of mitochondria releases cytochrome C, which activates caspases and leads to cell death after cerebral ischemia-reperfusion (DArcy, 2019). Kang et al. found that TRIM22 gene silencing inhibited the activation of NF-κB/NLRP3, thereby inhibiting neuroinflammation and apoptosis, indicating that TRIM22 may be a potential target for the treatment of brain I/R injury (Kang et al., 2021).

4.2 Inflammasome and autophagy

In the process of autophagy, autophagic vesicles are formed in cells, which wrap their own proteins or organelles, and then fuse with lysosomes and degrade them. There is a close relationship between the NLRP3 inflammasome and autophagy (Nakatogawa, 2020). On the one hand, the activation of NLRP3 inflammasome can regulate the induction of autophagy (Zhao and Zhang, 2019); on the other hand, autophagy can control the activation of inflammasome and its activity (Deretic et al., 2013). Together, they regulate the balance between host defense, inflammatory responses, and prevention of excessive inflammation, and form the necessary positive and negative feedback loops. Activation of caspase-1 inhibits autophagy induction and activates the inflammatory response, which is required for pathogen clearance (Kimmey and Stallings, 2016). However, excessive inflammatory responses can lead to organ and tissue damage and induce inflammatory diseases. Autophagy suppresses inflammatory responses by removing NLRP3 inflammasome activators and inflammatory components (Chang et al., 2021). Wang et al. found that inhibition of GSK-3β could downregulate NLRP3 expression by enhancing autophagy activity in cerebral ischemia-reperfusion injury, suggesting that GSK-3β may be its specific target (Wang et al., 2019). He et al. found that cerebral ischemia-reperfusion injury activates the NLRP3 inflammasome, increases the levels of caspase-1, IL-1β and IL-18, and enhances autophagy activity. Resveratrol is a specific NAD-dependent deacetylase sirtuin-1 (Sirt1) agonist. Cerebral infarct volume and cerebral water content decreased and neurological scores improved after resveratrol treatment. Intraventricular injection of 3-MA to inhibit autophagy blocked the inhibitory effect of resveratrol on NLRP3 inflammasome activation. Knockdown of Sirt1 significantly blocked resveratrol-induced autophagy activity and inhibition of NLRP3 inflammasome activation, and upregulated autophagy. This suggests that resveratrol has a protective effect on cerebral ischemia-reperfusion injury by inhibiting the activation of NLRP3 inflammasome by inhibiting Sirt1-dependent autophagy activity (He et al., 2017).

4.3 Inflammasome and pyroptosis

Pyroptosis is a programmed cell death that occurs in two main ways. The classical pyroptotic pathway of caspase-1 is that the pyrin domain of the NLR family binds to ASC by recognizing cognate ligands, and then binds and activates the precursor of caspase-1 to form active caspase-1 (Rao et al., 2022). Activated caspase-1 cleaves GSDMD into a 22 kDa C-terminal fragment and a 31 kDa N-terminal fragment. The production of GSDMD-N directly induces cell membrane perforation and rupture, and the release of cellular contents triggers an inflammatory response (Feng et al., 2022). Meanwhile, activated IL-1β and IL-18 proteins are released to the outside of the cell through stomata on the cell membrane (Xu et al., 2017). Under the stimulation of various infectious factors represented by Gram-negative surface endotoxin (LPS), the non-classical pathway of pyroptosis will be activated. Caspase-11 has been shown to bind to LPS as a natural receptor, and LPS can enter the cell in the form of endocytosis and bind to and activate the caspase-11 precursor. Active IL-1β and IL-18 are released along with the rupture and perforation of the cell membrane, triggering an inflammatory response. Meanwhile, the N-terminal fragment of GSDMD activates NLRP3 through the canonical pathway, thereby inducing pyroptosis (Chen et al., 2018). Li et al. found that indobufen or aspirin pretreatment combined with clopidogrel or ticagrelor can reduce rat cerebral ischemia-reperfusion and PC12 cell oxygen glucose deprivation/reoxygenation inflammatory corpuscle mediated pyroptosis by inhibiting the NF-κB/NLRP3 signaling pathway (Li F. et al., 2021b). Fann et al. (2018) showed that when cerebral ischemia-reperfusion injury occurs, peripheral inflammatory cells can release pro-inflammatory cytokines such as IL-18 and IL-1β through the blood-brain barrier and activated microglia in the central system. This resulted in high expression of pyroptosis-related proteins, resulting in extensive glial and neuronal cell death, suggesting that pyroptosis plays an important role in the process of cerebral ischemia-reperfusion injury. Inhibition of NLRP3 inflammasome expression can simultaneously inhibit the expression of downstream pyroptosis pathway-related proteins, limit the inflammatory response and alleviate cerebral ischemia-reperfusion injury. Therefore, therapeutic interventions targeting neuronal inflammasome activation may provide new opportunities for the treatment of IS.

5 Modulation of inflammasome in IS by natural plant products

5.1 Natural compounds

5.1.1 Toona polyphenols

The fruit of Toona sinensis is a member of the Meliaceae and is commonly used to prepare tea to prevent various diseases. Its main active ingredients are polyphenolic compounds. In recent years, numerous studies have confirmed the beneficial effects of Toona sinensis in treating various diseases, including central nervous system diseases, cardiovascular diseases, and diabetes (Zhao et al., 2023a; Wu et al., 2023). Zhao et al. found that Toona polyphenols can reduce the infarct volume and improve neural function in mice with chronic intermittent hypoxia (CIR). The optimal protection dosage is 100 mg/kg. The mechanism of protection may involve regulation of the prefrontal cortex and hippocampal MAPK pathways, NLRP3 inflammasome pathways, and inhibition of neural inflammation and cell apoptosis (Zhao, 2022).

5.1.2 Proantho cyanidins (PC)

PC are a class of large flavonoid polyphenols widely found in the plant kingdom (Gupta et al., 2022). Their molecular structure contains multiple hydroxyl structures that can effectively combine with oxygen radical anions to exhibit antioxidant and reduce inflammation properties. Since the 1980s, multiple studies have shown that PC extracts from various plants have pharmaceutical and biological activities, including reducing inflammatory responses, treating antioxidant therapy, antineoplastic therapy, and protecting the cardiovascular system (Pinent et al., 2006; Holt et al., 2012; Lee, 2017; Osakabe et al., 2022). Yang et al. found that PC can inhibit the activation of the TLR4-NLRP3 signaling pathway and the upregulation of caspase-1 and IL-1β in BV2 cells induced by OGD/R. The results of the *in vitro* experiment were consistent with those obtained using Cli-095 pretreatment. The study concluded that PC can protect neurons *in vitro* by downregulating the TLR4-NLRP3 inflammatory signaling pathway induced by OGD/R, and the protection is related to time and concentration (Yang, 2022).

5.1.3 Panax notoginseng saponins (PNS)

PNS is the main active ingredient in Sanqi, with the functions of dilating arteries, inhibiting platelet aggregation, reducing blood lipid levels, relieving inflammation, and antioxidant activity (Xie et al., 2018; Liu et al., 2020). Pharmacological studies have shown that PNS can reduce the release of chemotactic cytokines such as tumor necrosis factor-α (TNF-α) and interleukin-1 (IL-1), inhibit the activation of nuclear factor-κB (NF-κB), and the formation of NLRP3 inflammasomes, thereby suppressing inflammation responses (Song et al., 2017; Xu et al., 2018; Qu et al., 2020). PNS also protects myocardial mitochondria and reduces the leakage of lactate dehydrogenase (LDH) to improve myocardial energy metabolism. PNS can also inhibit the abnormal activation of platelets and the abnormal activation of the coagulation system to improve microcirculatory flow. PNS increases the activity of endogenous antioxidant enzymes and reduces the production of active oxygen to alleviate oxidative stress responses. PNS also regulates the concentration of intracellular calcium ions and reduces the abnormal expression of cancer genes to inhibit cell apoptosis. Zhou et al. found that the mechanism by which PNS improves I/RI may be related to the downregulation of NF-κB protein activation, the reduction in NLRP3 inflammasome formation, and the downregulation of chemotactic cytokines such as IL-1β secretion (Zhou et al., 2021).

5.1.4 Neferine

Neferine is a dimeric quinolinone alkaloid extracted from the embryo of the mature seeds of the water chestnut plant *Nelumbo nucifera* (MarthandamAsokan et al., 2018), a member of the Nelumbonaceae family. Neferine has various effects such as anti-atherosclerosis, anti-hypertension, anti-thrombosis, anti-diabetic vascular complications, and vascular protection, as well as anti-arrhythmia (Tang et al., 2019b; Bharathi Priya et al., 2021; Qi et al., 2021). Studies have shown that Neferine has good therapeutic effects and low side effects in the treatment and prevention of cardiovascular and cerebrovascular diseases. Huang et al. found that methylnelumbellate can alleviate brain ischemic reperfusion injury and immune dysregulation in mice by inhibiting the activation of NLRP3 inflammasome (Huang et al., 2021).

5.1.5 Salvianolic acid

Salvianolic acid has the function of blood purification and is used for cerebral infarction (Xiao et al., 2020). The main chemical components of salvianolic acid include D-(−)-pinoresinol-β-D-glucoside, rosmarinic acid, p-coumaric acid, ferulic acid, pinoresinol, and salvianolic acid B water-soluble phenolic acids (Guo and Wang, 2022). Modern pharmacological studies have shown that salvianolic acid has analgesic, anti-inflammatory, antioxidant, neurotrophic, and neuroprotective effects (Wu et al., 2020b; Xin et al., 2020), which can significantly improve the nerve function damage in patients with ischemic stroke, restore their daily life behavior, and improve the prognosis and quality of life (Lyu et al., 2019). Ma et al. found that salvianolic acid may inhibit the activation and cell apoptosis of small glial cells through the P2X7/NLRP3/GSDMD pathway, thus reducing the downstream inflammatory cascade reaction and exerting a nerve protection effect on experimental brain ischemic reperfusion injury (Ma, 2021).

5.1.6 Salidroside

Salidroside, the main active ingredient in Rhodiola rosea, has been shown to possess broad biological activities, including anti-inflammatory, antioxidant, antitumor, immune regulatory, and protective effects on the lungs, kidneys, liver, cardiovascular system, and nervous system (Xu et al., 2019; Qu et al., 2022). In terms of cerebral ischemia, Salidroside can improve energy metabolism disorders, metabolic acidosis, Ca2+ overload, and inhibit oxidative stress, inflammatory response, cell apoptosis, and autophagy (Fan et al., 2020; Magani et al., 2020; Zhang et al., 2021d). Liu et al. found that Salidroside may inhibit the activation of NLRP3 inflammasome and cell apoptosis in microglia by suppressing the TLR4/NF-κB signaling pathway, thereby reducing neuronal damage. Salidroside may also inhibit the activation of NLRP3 inflammasome and TLR4/NF-κB signaling pathway in rat cerebral ischemia-reperfusion injury by increasing the expression of miR-370-3p (Liu, 2022).

5.1.7 α-Asarone

α-Asarone is the main active component of Acorus tatarinowii, a perennial herb of the Araceae family. Studies have found that besides having antitumor, insecticidal, antibacterial, antitussive, bronchodilatory, neuroprotective, antiepileptic, and antidepressant effects, α-Asarone and beta-asarone also exhibit good pharmacological activities in cardiovascular and cerebrovascular diseases, such as protecting myocardial and vascular cells (including endothelial cells and vascular smooth muscle cells), preventing thrombosis, lowering blood lipids, and improving vascular function (Chellian et al., 2017; Uebel et al., 2021; Uebel et al., 2021). In the context of cerebral ischemia, α-Asarone exerts its effects by alleviating energy metabolism and ion metabolism disorders, reducing excitotoxicity, oxidative stress, inflammatory factor expression, protecting the blood-brain barrier, and other mechanisms (Liu et al., 2019; Balakrishnan et al., 2022). Xu et al.

found that α-Asarone has a significant protective effect against cerebral ischemia/reperfusion injury, mainly by regulating ROS activity, inhibiting NF-κB phosphorylation, reducing the excessive activation of NLRP3 inflammasomes, and exerting anti-inflammatory effects to protect against cerebral ischemia/reperfusion injury (Fei-Fei et al., 2022).

5.1.8 Acacia

Acacetin is a natural flavonoid drug that can be extracted from various plants and has attracted the attention of many researchers due to its wide range of pharmacological effects (Wu et al., 2022). Increasing evidence indicates that acacetin has potential in the treatment of various diseases such as anti-tumor, cardioprotective, anti-inflammatory, and neuroprotective effects (Singh et al., 2020; Cui et al., 2022). In the case of cerebral ischemia, acacetin may reduce the permeability of the blood-brain barrier by increasing the expression of Occludin, Claudin-5, and ZO-1 proteins, thereby exerting a neuroprotective effect in cerebral ischemia-reperfusion injury (Niu and Yang, 2020). Bu et al. found that acacetin can increase the survival rate of astrocytes after OGD/R injury, reduce the release of LDH, decrease ROS generation, increase the expression of LC3-II and beclin-1 proteins, and further downregulate the expression of NLRP3, caspase-1, and IL-1β. In summary, Acacetin can alleviate OGD/R-induced damage to astrocytes, thereby exerting a protective effect on cerebral ischemia-reperfusion injury. Its mechanism of action may be related to the inhibition of ROS production, activation of autophagy, and inhibition of NLRP3 inflammasome (Juan et al., 2023).

5.1.9 Curcumin

Curcumin is a polyphenolic substance extracted from the rhizomes of turmeric, which is commonly used as a food coloring agent. Curcumin has been found to possess a wide range of pharmacological activities, such as antibacterial, antioxidant, anti-apoptotic, anti-tumor, anti-oxidative stress, anti-inflammatory, anti-viral, lipid-lowering, liver-protective, bile-stimulating, and neuroprotective effects (Termini et al., 2020; Jabczyk et al., 2021). Curcumin has also been shown to improve age-related diseases such as atherosclerosis, diabetes, cardiovascular disease, and chronic kidney disease (Peng et al., 2021). Curcumin can exert neuroprotective effects in cerebral ischemia, intracerebral hemorrhage (ICH), and subarachnoid hemorrhage (SAH) through various pathways such as anti-inflammatory reactions, anti-oxidative stress, anti-apoptosis, and autophagy (Li et al., 2020b; Fan and Lei, 2022; Marques et al., 2022). Zhang et al. (2023) found that curcumin can reduce the volume of cerebral infarction and improve neurological function in rats, possibly by reducing the inflammatory response in the brain after cerebral infarction; the anti-inflammatory mechanism of curcumin may be related to its blockade of the NLRP3/Caspase-1 signaling axis, inhibition of NLRP3 inflammasome function, and reduction of the synthesis and release of inflammatory cytokines. Zhao et al., 2023b found that curcumin can alleviate cortical neuronal inflammation and synaptic injury caused by cerebral ischemia-reperfusion in rats by inhibiting inflammatory cytokine levels and reducing brain damage.

5.1.10 Morin

Morin, a natural active substance extracted from various plants, belongs to the flavonoid class of compounds and is a secondary metabolite of phenols in plants, widely distributed in nature (Caselli et al., 2016). Morin displays its pharmacological activity by modulating various cell signaling pathways, such as nuclear factor-kappa B (NF-κB), mitogen-activated protein kinase (MAPK), Janus kinase/signal transducer and activator of transcription (JAKs/STATs), Kelch-like ECH-associated protein1/Nuclear erythroid-2-related factor (Keap1/Nrf2), endoplasmic reticulum (ER), mitochondria-mediated apoptosis, Wnt/β-catenin, and Rapamycin (mTOR) signaling pathways (Sinha et al., 2016; Rajput et al., 2021). Extensive evidence has shown that morin plays a beneficial role in various chronic and life-threatening degenerative diseases (Kataria et al., 2018; Solairaja et al., 2021). Xue et al. found that morin can alleviate cerebral ischemia-reperfusion injury in rats, inhibit neuronal apoptosis, and its mechanism may be related to the inhibition of TXNIP/NLRP3/Caspase-1 signaling pathway activation (Xue et al., 2023).

5.1.11 Ginsenoside Rd

Ginsenoside Rd is one of the major active monomers of ginsenosides and belongs to the dammarane-type ginsenosides with a diol structure (Chen et al., 2022a). Although ginsenoside Rd is present in low concentrations in Panax species, it has attracted wide attention from scholars due to its strong biological activity. Studies have shown that ginsenoside Rd exhibits various pharmacological effects, such as protecting cardiovascular and renal functions, exerting anti-tumor and immunomodulatory activities, and showing good neuroprotective effects on the central nervous system (Li et al., 2022b; Tang et al., 2022). In terms of cerebral ischemia, ginsenoside Rd can improve ischemic stroke-induced damage by inhibiting oxidative stress and inflammation. Its mechanism mainly involves upregulating the endogenous antioxidant system, the phosphatidylinositol 3-kinase/protein kinase B and extracellular signal-regulated kinase 1/2 pathways, protecting mitochondrial membrane potential to prolong the survival of neuronal cells, inhibiting the activation of nuclear factor kappa B, transient receptor potential melastatin, acid-sensing ion channel 1a, poly(ADP-ribose) polymerase-1, and protein tyrosine kinase, as well as reducing the release of cytochrome c and apoptosis-inducing factor (Ye et al., 2013; Nabavi et al., 2015; Song et al., 2022). Yao et al. found that ginsenoside Rd can inhibit the expression levels of cell death-associated proteins, IL-18 and IL-1β secretion, intracellular ROS content, cell death ratio, and the interaction between TXNIP and NLRP3. Furthermore, ginsenoside Rd exerts a protective effect on neurons after cerebral ischemia/reperfusion injury, which is associated with upregulating the expression level of miR-139-5p, decreasing the expression levels of FoxO1 and Keap1, and activating the Nrf2 antioxidant signaling pathway, thereby inhibiting cell death induced by the ROS-TXNIP-NLRP3 inflammasome axis (Yao, 2022).

5.1.12 Paeoniflorin

Paeoniflorin is the main active monomer component of Paeonia. Previous studies have shown that paeoniflorin exhibits various activities, such as anti-free radical damage, inhibition of

intracellular calcium overload, and neuroprotection. *In vivo* experiments have demonstrated that paeoniflorin has effects on reducing blood viscosity, anti-platelet aggregation, vasodilation, improving microcirculation, and exerting antioxidative and anticonvulsant effects (Zhang and Wei, 2020; Zhou et al., 2020; Wang et al., 2021b). In cerebral ischemia research, paeoniflorin has been found to protect PC12 cells against calcium overload-induced injury. Additionally, paeoniflorin has been shown to protect against neurotoxicity induced by calcium overload in PC12 cells (Hu et al., 2019; Long et al., 2020; Tang et al., 2021). In terms of inhibiting the inflammasome, He et al. found that paeoniflorin has a protective effect on nerve damage in OGD-induced rat hippocampal slices, which may be related to the downregulation of the expression of NLRP3 and NLRP1 inflammasome components, thereby affecting the release of downstream inflammatory factors and cell apoptosis (He, 2016). A recent study also detected paeoniflorin in the colon and found that it improved UC symptoms in mice, inhibited the infiltration of macrophages in the mesentery and colon tissue, suppressed NLRP3 protein in colon macrophages, and inhibited the release of cytokine IL-1β (Liu et al., 2018). Moreover, a recent study showed that paeoniflorin can improve neuronal functional impairment mediated by ACI by inhibiting the activation of NLRP3 and Caspase-1, reducing microglial cell activation, and inhibiting neuronal necrosis (Aikmu et al., 2021).

5.1.13 Astragaloside IV

Astragalus membranaceus (AM) is a commonly used Chinese herbal medicine for the treatment of cardiovascular and cerebrovascular diseases. It has the effects of promoting diuresis, reducing edema, tonifying qi, and enhancing the immune system (Zhang et al., 2020). Modern medicine has also shown that AM has the ability to reduce oxidative stress, inhibit apoptosis, and decrease edema (Zang et al., 2020; Chen et al., 2021b). Astragaloside IV (AST-IV) is the main active component of AM responsible for its cardiovascular effects and is used as an important indicator for the evaluation of AM content. Experimental studies have demonstrated that AST-IV can improve neurological function, reduce cerebral infarct volume, and decrease blood-brain barrier permeability, thus exerting a protective effect in cerebral ischemia. The mechanism is mainly related to its anti-oxidant, anti-inflammatory, and anti-apoptotic properties, which are achieved by inhibiting the expression of MPO, TNF- α, IL-1?, iNOS, intracellular adhesion molecules, and NF-κB (Tang et al., 2019c; Tang, 2019). These findings suggest that PNS and AST-IV can play a protective role in ischemic brain injury through multiple targets and pathways. Tang et al. used an improved thread embolization method to prepare a rat model of middle cerebral artery occlusion/reperfusion to evaluate the effect of AST-IV on cerebral ischemia-reperfusion injury. Compared with the model group, AST-IV significantly reduced the neurological function deficit score, cerebral infarct volume, and the protein levels of NLRP3, Caspase-1, pro-IL-1β, IL-1β, pro-IL-18, and IL-18 in brain tissue, and inhibited the expression of phosphorylated NF-κB protein. These results suggest that AST-IV has a protective effect against cerebral ischemia-reperfusion injury, and its mechanism may be related to the inhibition of NF-κB protein phosphorylation and the inhibition of NLRP3 inflammasome activation (Tang et al., 2019c; Tang, 2019).

5.1.14 Breviscapine

The first record of Erigeron breviscapus (Vant) Hand-Mazz, commonly known as "Dengzhanhua," can be traced back to the book "Dian Nan Ben Cao." Breviscapine, extracted from Dengzhanhua, is one of its major active monomers (Gao et al., 2017; Wen et al., 2021b; Zhu et al., 2022b). Currently, evidence-based studies have shown that Breviscapine has significant clinical efficacy and good safety for treating stroke (Zhi et al., 2018; Lyu et al., 2020). Breviscapine has various functions, such as reducing autophagy of neurons and astrocytes in the ischemic penumbra, promoting nitric oxide synthesis in endothelial cells, reducing the synthesis of vascular wall and thromboxane A2, inhibiting platelet activation and aggregation, and reducing the risk of thrombosis (Li et al., 2020c; Chen et al., 2022b). In both *in vivo* and *in vitro* models of cerebral ischemia, the neuroprotective mechanism of Dengzhanhua may be related to reducing inflammatory responses, decreasing cell apoptosis, alleviating brain edema, promoting angiogenesis, and increasing brain-derived neurotrophic factor (Pengyue et al., 2017; Long et al., 2020; Chen et al., 2022b). A recent study indicated that Breviscapine could significantly improve the cognitive function of rats with CCI and alleviate the pathological damage of ischemic neurons. The mechanism of this effect may be related to the inhibition of NLRP3 inflammasome activation and cell pyroptosis pathways in brain tissue (Wang et al., 2020).

5.1.15 Sulforaphane

Sulforaphane (SFN), mainly derived from cruciferous vegetables such as broccoli and mustard greens (Vanduchova et al., 2019), is an isothiocyanate with strong bioactivities such as anticancer, antioxidative, immunomodulatory, antibacterial, and anti-inflammatory effects (Huang et al., 2019; Yagishita et al., 2019; Wu et al., 2020c; Nandini et al., 2020; Schepici et al., 2020; Kaiser et al., 2021; Xie et al., 2021). In improving brain ischemia, SFN was found to reduce cortical neuron damage caused by oxygen-glucose deprivation (OGD)/reoxygenation after primary culture of cortical neurons from Sprague Dawley (SD) rats aged 0–1 day (Li et al., 2022c). SFN also significantly inhibited oxidative stress damage and peripheral neuronal degeneration in traumatic brain injury (TBI) models (Calabrese and Kozumbo, 2021). SFN increased the expression of Bcl-2 and decreased the expression of cleaved caspase-3 to inhibit apoptosis of neurons after OGD (Alfieri et al., 2013). Additionally, SFN produced neuroprotective effects through the activation of phosphatidylinositol 3-kinase (PI3K)/Akt signaling pathway. As an effective antioxidant, SFN can activate the Nrf2-ARE signaling pathway to improve oxidative stress and exert neuroprotective effects in epilepsy-induced brain damage (Sun et al., 2017). David Vauzour et al. found that SFN protected neurons from Parkinson's disease by activating the Nrf2 pathway to upregulate the expression of antioxidant genes (Wei et al., 2022). Soane et al. found that SFN protected hippocampal neurons of mice from death caused by OGD or hemoglobin (Soane et al., 2010). Zhang et al. confirmed that SFN exerted neuroprotective effects by increasing the expression of Nrf2 and HO-1 (Ping et al., 2010). Deng et al. (2012) showed that SFN induced the nuclear translocation of Nrf2 and increased the expression of HO-1 to protect neurons from dopamine neurotoxicity damage via the PI3K/Akt pathway. In animal models of Parkinson's disease, SFN was found to counteract

TABLE 1 Summary of the mechanisms of natural plant products.

Natural plant products	Functions	Reference
Toona polyphenols	Regulate the prefrontal cortex and hippocampal MAPK pathways and NLRP3 inflammasome pathways	Zhao (2022)
Proantho Cyanidins	Downregulate the TLR4-NLRP3 inflammatory signaling pathway	Yang (2022)
Panax notoginseng saponins	Downregulate the NF-κB protein activation and NLRP3 inflammasome formation	Zhou et al. (2021)
Neferine	Inhibite the activation of NLRP3 inflammasome	Huang et al. (2021b)
Salvianolic acid	Inhibit the activation and cell apoptosis of small glial cells through the P2X7/NLRP3/GSDMD pathway	Ma (2021)
Salidroside	Inhibit the activation of NLRP3 inflammasome and TLR4/NF-κB signaling pathway	Liu (2022)
α-Asarone	Reduce the excessive activation of NLRP3 inflammasomes	Fei-Fei et al. (2022)
Acacia	Inhibite of NLRP3 inflammasome	Juan et al. (2023)
Curcumin	Inhibite the NLRP3/Caspase-1 signaling axis and NLRP3 inflammasome function	Zhang et al. (2023)
Morin	Inhibite the TXNIP/NLRP3/Caspase-1 signaling pathway	Xue et al. (2023)
Ginsenoside Rd	Decrease the expression levels of FoxO1 and Keap1, and activating the Nrf2 antioxidant signaling pathway	Yao (2022)
Paeoniflorin	Inhibite the activation of NLRP3 and Caspase-1, reduce microglial cell activation, and inhibite neuronal necrosis	Aikmu et al. (2021)
Astragaloside IV	Inhibite NF-κB protein phosphorylation and NLRP3 inflammasome activation	Tang et al., 2019c; Tang (2019)
Breviscapine	Inhibite NLRP3 inflammasome activation and cell pyroptosis pathways	Wang et al. (2020)
Sulforaphane	Activate the JAK2-STAT3 signaling pathway and inhibite the activation of NLRP3 inflammasomes	Chang (2017)
Metformin	Reduce cell necrosis caused by NLRP3 inflammasome activation	Yuan et al. (2021)

the toxic effects of 6-hydroxydopamine-1-methyl-4-phenyl-1,2,3,6-tetrahydropyridine-mediated damage and reduce degeneration and death of striatal dopaminergic neurons (Siebert et al., 2009; Jazwa et al., 2011). Vauzour et al. (2010) found that SFN could resist the toxic effects of 5-S-cysteinyl-dopamine on cortical neurons by activating extracellular signal-regulated kinase 1/2, Nrf2, and detoxifying enzymes. In terms of inhibiting inflammasomes, the latest study found that SFN can improve neurological function deficits, reduce cerebral infarct volume, and alleviate the inflammatory response after cerebral ischemia-reperfusion, thus achieving a neuroprotective effect on rat cerebral ischemia-reperfusion injury. This may be achieved by activating the JAK2-STAT3 signaling pathway, inhibiting the activation of NLRP3 inflammasomes, and reducing the inflammatory response during ischemia-reperfusion (Chang, 2017).

5.1.16 Metformin

Recently, it has been found that metformin, a traditional antidiabetic drug, originally derived from a guanidine compound found in plants and modified, has the potential to reduce brain damage caused by ischemia/reperfusion injury and protect neurological function without affecting blood glucose levels (Lee et al., 2021; Sharma et al., 2021). This may be due to its ability to activate AMPK-induced autophagy, reduce brain tissue damage, promote vascular and neural regeneration, inhibit inflammatory responses, and promote central nervous system recovery (Jia et al., 2015; Arbeláez-Quintero and Palacios, 2017). Recent studies have shown that metformin can protect against ischemia/reperfusion injury by inhibiting TLR4 and NF-κB protein expression, reducing inflammatory reactions, and providing neuroprotective effects (Liu et al., 2022). Deng et al. found that metformin preconditioning is necessary for its neuroprotective effects during the acute phase of cerebral ischemic injury. Pre-treatment with 10 mg/kg/d of metformin for 7 days significantly reduced ischemic brain damage, and the protective effect of metformin may be related to the downregulation of AMPK (Deng, 2016). In terms of inhibiting inflammasomes, Yuan et al. (2021) found that metformin has a protective effect on brain damage caused by ischemia/reperfusion, and its mechanism of action includes activating the AMPK pathway, promoting autophagy, removing damaged mitochondria through autophagy, reducing cell necrosis caused by NLRP3 inflammasome activation by damaged mitochondria, and thereby protecting against ischemia/reperfusion brain damag.

It is noteworthy that metformin, as a member of the guanidine family, was originally derived from a molecular modification of guanidine, which in turn is derived from an extract of Galega officinalis, a plant commonly known as goat's rue. This is a classic case of using natural compounds as lead compounds for drug development. In the future, we hope to discover more natural compounds as lead compounds and develop specific inflammasome-targeting drugs, providing safe and effective new drug formulations for future clinical applications.

The mechanisms of natural plant products were summarized in Table 1.

6 Prospects

This review provides a summary of the neuroinflammatory mechanism mediated by the NLRP3 inflammasome in the context of cerebral ischemia-reperfusion injury. Accumulating evidence from both *in vitro* and *in vivo* studies supports the involvement of the inflammasome signaling pathway in the pathogenesis of cerebral ischemia-reperfusion injury, demonstrated by direct activation of inflammasomes in animal models and patients. Importantly, the inflammasome-mediated inflammatory mechanism persists from the early to late stages of cerebral ischemia-reperfusion injury, indicating its potential as a therapeutic target. Modulating the activity of the inflammasome may help mitigate its impact on pathogenic cells, such as microglia and neurons, and the associated structural damage observed in the progression of cerebral ischemic disease. Currently, clinically approved therapeutic drugs like Anakinra, Canakinumab, and Ilorinase effectively target IL-1β. Recent clinical studies have shown that Canakinumab can improve cardiovascular conditions, including atherosclerosis, an independent risk factor for stroke. Additionally, clinical trials are underway for drugs that neutralize IL-18, such as Tadekinig alfa and GSK1070806. Nevertheless, it is crucial to consider potential side effects when targeting the NLRP3 inflammasome and to ensure patient protection against pathogenic microbial infections while reducing inflammatory activity. Finding therapeutic interventions that selectively target specific types of inflammasome complexes may offer enhanced safety and long-term efficacy, particularly for neurodegenerative diseases like cerebral ischemia-reperfusion injury.

Currently, there is growing interest in exploring natural plant products for the treatment of NLRP3 inflammasome-mediated neuroinflammation in cerebral ischemia/reperfusion injury. These natural products mainly consist of flavonoids, alkaloids, polysaccharides, quinones, terpenes, lignans, coumarins, phenolic acids, and saponins. Most studies conducted thus far have relied on *in vitro* and *in vivo* experiments. While certain natural compounds, such as total glucosides of paeony, have been utilized in cerebral ischemia treatment, there is a lack of large-scale, long-term clinical studies to validate their efficacy. This calls for further investigation. The aim of reviewing natural compounds is to identify potential lead compounds capable of inhibiting the NLRP3 inflammasome in cerebral ischemia. These findings can subsequently contribute to the development of specific inflammasome inhibitors. A comprehensive management strategy for patients with cerebral ischemia represents a promising direction for future research. The key focus for both basic researchers and clinical physicians is to devise rational treatment plans that can alleviate complications by targeting inflammatory processes. Ultimately, understanding the mechanisms underlying inflammatory processes in cerebral ischemia/reperfusion injury will open up new avenues for the comprehensive treatment of cerebral ischemia and its associated complications.

This review reveals a structural commonality among several compounds - the presence of a phenol unit. Examples of such compounds include chimonanthus polyphenols, anthocyanins, ellagic acid, curcumin, and luteolin. Based on this finding, it is speculated that the inhibition of NLRP3 inflammasome activity by polyphenolic compounds and their metabolites mainly depends on the type, number, and arrangement of functional groups on the core structure. This, in turn, affects their anti-inflammatory activity. It suggests that future design of NLRP3 inflammasome inhibitors can be based on this class of phenolic structures, necessitating further research and structural modifications by future investigators.

Furthermore, another class of compounds based on sapogenin glycosides, such as total saponins of Panax notoginseng, salidroside, ginsenoside Rd, paeoniflorin, and astragaloside IV, is identified. These compounds exhibit structural characteristics that involve spirosolane, related steroidal compounds, or triterpenes. From a structure-activity standpoint, the complex nature of these structures requires further clarification of their structure-activity relationship in inhibiting NLRP3 inflammasome activity. This could provide new perspectives for structural modifications from different angles in future studies.

Author contributions

KY and LZ are responsible for the study concept and design. KY, LZ, QH, SW, HX, and JG are responsible for the data collection, data analysis, and interpretation; KY and LZ drafted the paper; JG supervised the study. All authors contributed to the article and approved the submitted version.

Funding

The research is supported by National Key Research and Development Project of China (No. 2018YFC1704904), the National Natural Science Foundation of China (81774174), the Provincial Discipline Construction Project of Hunan University of Chinese Medicine (Integrated Traditional Chinese and Western Medicine) and the Postgraduate Scientific Research Innovation Project of Hunan Province (CX20230800).

Acknowledgments

Thanks to Xing Li for assisting with the English translation and writing.

Conflict of interest

The authors declare that the research was conducted in the absence of any commercial or financial relationships that could be construed as a potential conflict of interest.

Publisher's note

References

Aikmu, Z., Uppur, M., Xing, H., Fan, M., and Zhang, J. (2021). Effects of paeoniflorin on neuronal scorch death regulated by microglia activation in rats with acute cerebral infarction. *J. Brain Neurological Disord.* 29 (08), 469–474.

Ajoolabady, A., Wang, S., Kroemer, G., Penninger, J. M., Uversky, V. N., Pratico, D., et al. (2021). Targeting autophagy in ischemic stroke: from molecular mechanisms to clinical therapeutics. *Pharmacol. Ther.* 225, 107848. doi:10.1016/j.pharmthera.2021.107848

Alfieri, A., Srivastava, S., Siow, R. C. M., Cash, D., Modo, M., Duchen, M. R., et al. (2013). Sulforaphane preconditioning of the Nrf2/HO-1 defense pathway protects the cerebral vasculature against blood-brain barrier disruption and neurological deficits in stroke. *Free Radic. Biol. Med.* 65, 1012–1022. doi:10.1016/j.freeradbiomed.2013.08.190

Andrade, W. A., and Zamboni, D. S. (2020). NLRC4 biology in immunity and inflammation. *J. Leukoc. Biol.* 108 (4), 1117–1127. doi:10.1002/JLB.3MR0420-573R

Arbeláez-Quintero, I., and Palacios, M. (2017). To use or not to use metformin in cerebral ischemia: a review of the application of metformin in stroke rodents. *Stroke Res. Treat.* 2017, 9756429. doi:10.1155/2017/9756429

Balakrishnan, R., Cho, D. Y., Kim, I. S., Seol, S. H., and Choi, D. K. (2022). Molecular mechanisms and therapeutic potential of α- and β-asarone in the treatment of neurological disorders. *Antioxidants (Basel)* 11 (2), 281. doi:10.3390/antiox11020281

Bauer, R., and Rauch, I. (2020). The NAIP/NLRC4 inflammasome in infection and pathology. *Mol. Asp. Med.* 76, 100863. doi:10.1016/j.mam.2020.100863

Bharathi Priya, L., Huang, C. Y., Hu, R. M., Balasubramanian, B., and Baskaran, R. (2021). An updated review on pharmacological properties of neferine-A bisbenzylisoquinoline alkaloid from *Nelumbo nucifera*. *J. Food Biochem.* 45 (12), e13986. doi:10.1111/jfbc.13986

Calabrese, E. J., and Kozumbo, W. J. (2021). The phytoprotective agent sulforaphane prevents inflammatory degenerative diseases and age-related pathologies via Nrf2-mediated hormesis. *Pharmacol. Res.* 163, 105283. doi:10.1016/j.phrs.2020.105283

Cao, Y., Zhang, H., Lu, X., Wang, J., Zhang, X., Sun, S., et al. (2020). Overexpression of MicroRNA-9a-5p ameliorates NLRP1 inflammasome-mediated ischemic injury in rats following ischemic stroke. *Neuroscience* 444, 106–117. doi:10.1016/j.neuroscience.2020.01.008

Caselli, A., Cirri, P., Santi, A., and PaoliMorin, P. (2016). Morin: a promising natural drug. *Curr. Med. Chem.* 23 (8), 774–791. doi:10.2174/0929867323666160106150821

Chang, P., Li, H., Hu, H., Li, Y., and Wang, T. (2021). The role of HDAC6 in autophagy and NLRP3 inflammasome. *Front. Immunol.* 12, 763831. doi:10.3389/fimmu.2021.763831

Chang, Yu (2017). *Preliminary study on the protective effect of lycopene on focal cerebral ischemia-reperfusion injury in rats and its anti-inflammatory mechanism[D]*. China: Chongqing Medical University.

Chellian, R., Pandy, V., and Mohamed, Z. (2017). Pharmacology and toxicology of α- and β-Asarone: a review of preclinical evidence. *Phytomedicine* 32, 41–58. doi:10.1016/j.phymed.2017.04.003

Chen, H. D., Jiang, M. Z., Zhao, Y. Y., Li, X., Lan, H., Yang, W. Q., et al. (2022b). Effects of breviscapine on cerebral ischemia-reperfusion injury and intestinal flora imbalance by regulating the TLR4/MyD88/NF-κB signaling pathway in rats. *J. Ethnopharmacol.* 300, 115691. doi:10.1016/j.jep.2022.115691

Chen, R., Yin, C., Fang, J., and Liu, B. (2021a). The NLRP3 inflammasome: an emerging therapeutic target for chronic pain. *J. Neuroinflammation* 18 (1), 84. doi:10.1186/s12974-021-02131-0

Chen, T., Yang, P., and Jia, Y. (2021b). Molecular mechanisms of astragaloside-IV in cancer therapy (Review). *Int. J. Mol. Med.* 47 (3), 13. doi:10.3892/ijmm.2021.4846

Chen, Y., Qin, X., An, Q., Yi, J., Feng, F., Yin, D., et al. (2018). Mesenchymal stromal cells directly promote inflammation by canonical NLRP3 and non-canonical caspase-11 inflammasomes. *EBioMedicine* 32, 31–42. doi:10.1016/j.ebiom.2018.05.023

Chen, Y. Y., Liu, Q. P., An, P., Jia, M., Luan, X., Tang, J. Y., et al. (2022a). Ginsenoside Rd: a promising natural neuroprotective agent. *Phytomedicine* 95, 153883. doi:10.1016/j.phymed.2021.153883

Christgen, S., Tweedell, R. E., and Kanneganti, T. D. (2022). Programming inflammatory cell death for therapy. *Pharmacol. Ther.* 232, 108010. doi:10.1016/j.pharmthera.2021.108010

Ciążyńska, M., Olejniczak-Staruch, I., Sobolewska-Sztychny, D., Narbutt, J., Skibińska, M., and Lesiak, A. (2021). The role of NLRP1, NLRP3, and AIM2 inflammasomes in psoriasis: review. *Int. J. Mol. Sci.* 22 (11), 5898. doi:10.3390/ijms22115898

Coll, R. C., Schroder, K., and Pelegrín, P. (2022). NLRP3 and pyroptosis blockers for treating inflammatory diseases. *Trends Pharmacol. Sci.* 43 (8), 653–668. doi:10.1016/j.tips.2022.04.003

Cui, Y. K., Hong, Y. X., Wu, W. Y., Han, W. M., Wu, Y., Wu, C., et al. (2022). Acacetin ameliorates cardiac hypertrophy by activating Sirt1/AMPK/PGC-1α pathway. *Eur. J. Pharmacol.* 920, 174858. doi:10.1016/j.ejphar.2022.174858

Dai, M., Wu, L., Yu, K., Xu, R., Wei, Y., Chinnathambi, A., et al. (2020). D-Carvone inhibit cerebral ischemia/reperfusion induced inflammatory response TLR4/NLRP3 signaling pathway. *Biomed. Pharmacother.* 132, 110870. doi:10.1016/j.biopha.2020.110870

DArcy, M. S. (2019). Cell death: a review of the major forms of apoptosis, necrosis and autophagy. *Cell Biol. Int.* 43 (6), 582–592. doi:10.1002/cbin.11137

de Brito Toscano, E. C., Rocha, N. P., Lopes, B. N. A., Suemoto, C. K., and Teixeira, A. L. (2021). Neuroinflammation in alzheimer's disease: focus on NLRP1 and NLRP3 inflammasomes. *Curr. Protein Pept. Sci.* 22 (8), 584–598. doi:10.2174/1389203722666210916141436

Deng, C., Tao, R., Yu, S. Z., and Jin, H. (2012). Sulforaphane protects against 6-hydroxydopamine-induced cytotoxicity by increasing expression of heme oxygenase-1 in a PI3K/Akt-dependent manner. *Mol. Med. Rep.* 5 (3), 847–851. doi:10.3892/mmr.2011.731

Deng, T. (2016). *Study on the effect of metformin pretreatment against acute ischemic brain injury in mice[D]*. China: Zhejiang University.

Deretic, V., Saitoh, T., and Akira, S. (2013). Autophagy in infection, inflammation and immunity. *Nat. Rev. Immunol.* 13, 722–737. doi:10.1038/nri3532

Enzmann, G., Mysiorek, C., Gorina, R., Cheng, Y. J., Ghavampour, S., Hannocks, M. J., et al. (2013). The neurovascular unit as a selective barrier to polymorphonuclear granulocyte (PMN) infiltration into the brain after ischemic injury. *Acta Neuropathol.* 125 (3), 395–412. doi:10.1007/s00401-012-1076-3

Fan, F., and Lei, M. (2022). Mechanisms underlying curcumin-induced neuroprotection in cerebral ischemia. *Front. Pharmacol.* 13, 893118. doi:10.3389/fphar.2022.893118

Fan, F., Yang, L., Li, R., Zou, X., Li, N., Meng, X., et al. (2020). Salidroside as a potential neuroprotective agent for ischemic stroke: a review of sources, pharmacokinetics, mechanism and safety. *Biomed. Pharmacother.* 129, 110458. doi:10.1016/j.biopha.2020.110458

Fann, D. Y., Lim, Y. A., Cheng, Y. L., Lok, K. Z., Chunduri, P., Baik, S. H., et al. (2018). Evidence that NF-κB and MAPK signaling promotes NLRP inflammasome activation in neurons following ischemic stroke. *Mol. Neurobiol.* 55 (2), 1082–1096. doi:10.1007/s12035-017-0394-9

Fei-Fei, Xu, Cui, K., and Wang, L.-Y. (2022). α-Fine octyl ether protects oxygen glucose deprivation/reperfusion injured BV2 cells by regulating NLRP3 pathway. *Chin. J. Pharmacol.* 38 (08), 1209–1218.

Feng, Y., Li, M., Yangzhong, X., Zhang, X., Zu, A., Hou, Y., et al. (2022). Pyroptosis in inflammation-related respiratory disease. *J. PhysiolBiochem* 78, 721–737. doi:10.1007/s13105-022-00909-1

Feske, S. K. (2021). Ischemic stroke. *Am. J. Med.* 134 (12), 1457–1464. doi:10.1016/j.amjmed.2021.07.027

Gao, J., Chen, G., He, H., Liu, C., Xiong, X., Li, J., et al. (2017). Therapeutic effects of breviscapine in cardiovascular diseases: a review. *Front. Pharmacol.* 8, 289. doi:10.3389/fphar.2017.00289

Gudipaty, S. A., Conner, C. M., Rosenblatt, J., and Montell, D. J. (2018). Unconventional ways to live and die: cell death and survival in development, homeostasis, and disease. *Annu. Rev. Cell Dev. Biol.* 34, 311–332. doi:10.1146/annurev-cellbio-100616-060748

Guo, S. S., and Wang, Z. G. (2022). Salvianolic acid B from Salvia miltiorrhizabunge: a potential antitumor agent. *Front. Pharmacol.* 13, 1042745. doi:10.3389/fphar.2022.1042745

Gupta, A. K., Talukder, M., and Bamimore, M. A. (2022). Natural products for male androgenetic alopecia. *Dermatol Ther.* 35 (4), e15323. doi:10.1111/dth.15323

He, Q., Li, Z., Wang, Y., Hou, Y., Li, L., and Zhao, J. (2017). Resveratrol alleviates cerebral ischemia/reperfusion injury in rats by inhibiting NLRP3 inflammasome activation through Sirt1-dependent autophagy induction. *Int. Immunopharmacol.* 50, 208–215. doi:10.1016/j.intimp.2017.06.029

He, Y.-B. (2016). *Exploring the effects of paeoniflorin on NLRP3 and NLRP1 inflammatory vesicles based on rat OGD hippocampal brain slices[D]*. China: Fujian University of Traditional Chinese Medicine.

Heid, M. E., Keyel, P. A., Kamga, C., Shiva, S., Watkins, S. C., and Salter, R. D. (2013). Mitochondrial reactive oxygen species induces NLRP3-dependent lysosomal damage and inflammasome activation. *J. Immunol.* 191 (10), 5230–5238. doi:10.4049/jimmunol.1301490

Holt, R. R., Heiss, C., Kelm, M., and Keen, C. L. (2012). The potential of flavanol and procyanidin intake to influence age-related vascular disease. *J. NutrGerontolGeriatr* 31 (3), 290–323. doi:10.1080/21551197.2012.702541

Hu, M. Z., Wang, A. R., Zhao, Z. Y., Chen, X. Y., Li, Y. B., and Liu, B. (2019). Antidepressant-like effects of paeoniflorin on post-stroke depression in a rat model. *Neurol. Res.* 41 (5), 446–455. doi:10.1080/01616412.2019.1576361

Huang, C., Wu, J., Chen, D., Jin, J., Wu, Y., and Chen, Z. (2019). Effects of sulforaphane in the central nervous system. *Eur. J. Pharmacol.* 853, 153–168. doi:10.1016/j.ejphar.2019.03.010

Huang, H., Qi, S., and Zhang, K. (2021b). Inhibition of NLRP3 inflammatory vesicle activation by methyllysine alleviates brain tissue injury and immune disorders in rats with cerebral ischemia-reperfusion. *J. Immunol.* 37 (08), 704–709. doi:10.13431/j.cnki.immunol.j.20210098

Huang, Y., Xu, W., and Zhou, R. (2021a). NLRP3 inflammasome activation and cell death. *Cell Mol. Immunol.* 18 (9), 2114–2127. doi:10.1038/s41423-021-00740-6

Hussain, A., Lee, M., Rana, J., and Virani, S. S. (2021). Epidemiology and risk factors for stroke in young individuals: implications for prevention. *CurrOpinCardiol* 36 (5), 565–571. doi:10.1097/HCO.0000000000000894

Ip, W. K., and Medzhitov, R. (2015). Macrophages monitor tissue osmolarity and induce inflammatory response through NLRP3 and NLRC4 inflammasome activation. *Nat. Commun.* 6, 6931. doi:10.1038/ncomms7931

Ishrat, T., Mohamed, I. N., Pillai, B., Soliman, S., Fouda, A. Y., Ergul, A., et al. (2015). Thioredoxin-interacting protein: a novel target for neuroprotection in experimental thromboembolic stroke in mice. *Mol. Neurobiol.* 51 (2), 766–778. doi:10.1007/s12035-014-8766-x

Jabczyk, M., Nowak, J., Hudzik, B., and Zubelewicz-Szkodzińska, B. (2021). Curcumin in metabolic health and disease. *Nutrients* 13 (12), 4440. doi:10.3390/nu13124440

Jazwa, A., Rojo, A. I., Innamorato, N. G., Hesse, M., Fernández-Ruiz, J., and Cuadrado, A. (2011). Pharmacological targeting of the transcription factor Nrf2 at the basal ganglia provides disease modifying therapy for experimental parkinsonism. *Antioxid. Redox Signal* 14 (12), 2347–2360. doi:10.1089/ars.2010.3731

Jia, J., Cheng, J., Ni, J., and Zhen, X. (2015). Neuropharmacological actions of metformin in stroke. *CurrNeuropharmacol* 13 (3), 389–394. doi:10.2174/1570159x13666150205143555

Juan, T., Guoqing, Ji, and Mahan, Y. (2023). Acanthocyanin plays a protective role against cerebral ischemia-reperfusion injury through autophagy-regulated ROS/NLRP3 signaling pathway. *J. Stroke Neurological Disord.* 40 (02), 99–102. doi:10.19845/j.cnki.zfysjjbzz.2023.0025

Kaiser, A. E., Baniasadi, M., Giansiracusa, D., Giansiracusa, M., Garcia, M., Fryda, Z., et al. (2021). Sulforaphane: a broccoli bioactive phytocompound with cancer preventive potential. *Cancers (Basel)* 13 (19), 4796. doi:10.3390/cancers13194796

Kang, C., Lu, Z., Zhu, G., Chen, Y., and Wu, Y. (2021). Knockdown of TRIM22 relieves oxygen-glucose deprivation/reoxygenation-induced apoptosis and inflammation through inhibition of NF-κB/NLRP3 Axis. *Cell Mol. Neurobiol.* 41 (2), 341–351. doi:10.1007/s10571-020-00855-w

Kataria, R., Sobarzo-Sanchez, E., and Khatkar, A. (2018). Role of morin in neurodegenerative diseases: a review. *Curr. Top. Med. Chem.* 18 (11), 901–907. doi:10.2174/1568026618666180711153416

Kelley, N., Jeltema, D., Duan, Y., and He, Y. (2019). The NLRP3 inflammasome: an overview of mechanisms of activation and regulation. *Int. J. Mol. Sci.* 20 (13), 3328. doi:10.3390/ijms20133328

Kimmey, J. M., and Stallings, C. L. (2016). Bacterial pathogens versus autophagy: implications for therapeutic interventions. *Trends Mol. Med.* 22 (12), 1060–1076. doi:10.1016/j.molmed.2016.10.008

Lee, J., Noh, S., Lim, S., and Kim, B. (2021). Plant extracts for type 2 diabetes: from traditional medicine to modern drug discovery. *Antioxidants (Basel)* 10 (1), 81. doi:10.3390/antiox10010081

Lee, R. H. C., Lee, M. H. H., Wu, C. Y. C., Couto E Silva, A., Possoit, H. E., Hsieh, T. H., et al. (2018). Cerebral ischemia and neuroregeneration. *Neural Regen. Res.* 13 (3), 373–385. doi:10.4103/1673-5374.228711

Lee, Y. (2017). Cancer chemopreventive potential of procyanidin. *Toxicol. Res.* 33 (4), 273–282. doi:10.5487/TR.2017.33.4.273

Levinsohn, J. L., Newman, Z. L., Hellmich, K. A., Fattah, R., Getz, M. A., Liu, S., et al. (2012). Anthrax lethal factor cleavage of Nlrp1 is required for activation of the inflammasome. *PLoS Pathog.* 8 (3), e1002638. doi:10.1371/journal.ppat.1002638

Li, Q., Cao, Y., Dang, C., Han, B., Han, R., Ma, H., et al. (2020a). Inhibition of double-strand DNA-sensing cGAS ameliorates brain injury after ischemic stroke. *EMBO Mol. Med.* 12 (4), e11002. doi:10.15252/emmm.201911002

Li, H., Sureda, A., Devkota, H. P., Pittalà, V., Barreca, D., Silva, A. S., et al. (2020b). Curcumin, the golden spice in treating cardiovascular diseases. *Biotechnol. Adv.* 38, 107343. doi:10.1016/j.biotechadv.2019.01.010

Li, Y., Li, S., and Li, D. (2020c). Breviscapine alleviates cognitive impairments induced by transient cerebral ischemia/reperfusion through its anti-inflammatory and anti-oxidant properties in a rat model. *ACS Chem. Neurosci.* 11 (24), 4489–4498. doi:10.1021/acschemneuro.0c00697

Li, Y., Ling, J., and Jiang, Q. (2021a). Inflammasomes in alveolar bone loss. *Front. Immunol.* 12, 691013. doi:10.3389/fimmu.2021.691013

Li, F., Xu, D., Hou, K., Gou, X., Lv, N., Fang, W., et al. (2021b). Pretreatment of indobufen and aspirin and their combinations with clopidogrel or ticagrelor alleviates inflammasome mediated pyroptosis via inhibiting NF-κB/NLRP3 pathway in ischemic stroke. *J. Neuroimmune Pharmacol.* 16 (4), 835–853. doi:10.1007/s11481-020-09978-9

Li, Z., Ji, S., Jiang, M. L., Xu, Y., and Zhang, C. J. (2022a). The regulation and modification of GSDMD signaling in diseases. *Front. Immunol.* 13, 893912. doi:10.3389/fimmu.2022.893912

Li, J., Huang, Q., Yao, Y., Ji, P., Mingyao, E., Chen, J., et al. (2022b). Biotransformation, pharmacokinetics, and pharmacological activities of ginsenoside Rd against multiple diseases. *Front. Pharmacol.* 13, 909363. doi:10.3389/fphar.2022.909363

Li, Q., Fadoul, G., Ikonomovic, M., Yang, T., and Zhang, F. (2022c). Sulforaphane promotes white matter plasticity and improves long-term neurological outcomes after ischemic stroke via the Nrf2 pathway. *Free Radic. Biol. Med.* 193 (Pt 1), 292–303. doi:10.1016/j.freeradbiomed.2022.10.001

Liang, J., Wang, Q., Li, J. Q., Guo, T., and Yu, D. (2020). Long non-coding RNA MEG3 promotes cerebral ischemia-reperfusion injury through increasing pyroptosis by targeting miR-485/AIM2 axis. *Exp. Neurol.* 325, 113139. doi:10.1016/j.expneurol.2019.113139

Lin, H. B., Li, F. X., Zhang, J. Y., You, Z. J., Xu, S. Y., Liang, W. B., et al. (2021). Cerebral-Cardiac syndrome and diabetes: cardiac damage after ischemic stroke in diabetic state. *Front. Immunol.* 12, 737170. doi:10.3389/fimmu.2021.737170

Liu, H., Lu, X., Hu, Y., and Fan, X. (2020). Chemical constituents of Panax ginseng and Panax notoginseng explain why they differ in therapeutic efficacy. *Pharmacol. Res.* 161, 105263. doi:10.1016/j.phrs.2020.105263

Liu, H., Zhang, M., Liu, T., Shi, L., and Wang, C. (2022). Effects of intermittent fasting and metformin on Toll-like receptor 4/nuclear transcription factor-κB pathway after cerebral ischemia-reperfusion injury. *Chin. J. Geriatric Cardiovasc. Dis.* 24 (07), 760–764.

Liu, J. (2022). *Study on the anti-inflammatory effect and mechanism of rhodiogenin in cerebral ischemia-reperfusion injury in rats[D]*. China: Kunming Medical University. doi:10.27202/d.cnki.gkmyc.2022.000819

Liu, J. X., Wang, D., and Liu, S. (2019). Advances in the role and mechanism of α- and β-fosetyl ether in cardiovascular and cerebrovascular diseases. *Adv. Mod. Biomed.* 19 (09), 1797–1800. doi:10.13241/j.cnki.pmb.2019.09.044

Liu, P., Zhang, Z., and Li, Y. (2021). Relevance of the pyroptosis-related inflammasome pathway in the pathogenesis of diabetic kidney disease. *Front. Immunol.* 12, 603416. doi:10.3389/fimmu.2021.603416

Liu, Q., Luo, X., Luo, X., Luo, X., He, J. R., Deng, X. L., et al. (2018). Study on the treatment of ulcerative colitis mice by peonidin through inhibition of NLRP3 inflammatory vesicles. *New Drugs Chin. Med. Clin. Pharmacol.* 29 (04), 409–414. doi:10.19378/j.issn.1003-9783.2018.04.006

Long, Y., Yang, Q., Xiang, Y., Zhang, Y., Wan, J., Liu, S., et al. (2020). Nose to brain drug delivery - a promising strategy for active components from herbal medicine for treating cerebral ischemia reperfusion. *Pharmacol. Res.* 159, 104795. doi:10.1016/j.phrs.2020.104795

Lyu, J., Xie, Y., Sun, M., and Zhang, L. (2020). Clinical evidence and GRADE assessment for breviscapine injection (DengZhanHuaSu) in patients with acute cerebral infarction. *J. Ethnopharmacol.* 262, 113137. doi:10.1016/j.jep.2020.113137

Lyu, J., Xie, Y., Wang, Z., and Wang, L. (2019). Salvianolic acids for injection combined with conventional treatment for patients with acute cerebral infarction: a systematic review and meta-analysis of randomized controlled trials. *Med. Sci. Monit.* 25, 7914–7927. doi:10.12659/MSM.917421

Ma, D. C. (2021). *Effects of salvianolic acid on cerebral ischemia reperfusion injury via microglia P2X7/NLRP3/GSDMD pathway [D]*. China: Liaoning university of traditional Chinese medicine. doi:10.27213/d.cnki.glnzc.2021.000034

Ma, D. C., Zhang, N. N., Zhang, Y. N., and Chen, H. S. (2021). Salvianolic Acids for Injection alleviates cerebral ischemia/reperfusion injury by switching M1/M2 phenotypes and inhibiting NLRP3 inflammasome/pyroptosis axis in microglia *in vivo* and *in vitro*. *J. Ethnopharmacol.* 270, 113776. doi:10.1016/j.jep.2021.113776

Magani, S. K. J., Mupparthi, S. D., Gollapalli, B. P., Shukla, D., Tiwari, A. K., Gorantala, J., et al. (2020). Salidroside - can it be a multifunctional drug? *Curr. Drug Metab.* 21 (7), 512–524. doi:10.2174/1389200221666200610172105

Marques, M. S., Marinho, M. A. G., Vian, C. O., and Horn, A. P. (2022). The action of curcumin against damage resulting from cerebral stroke: a systematic review. *Pharmacol. Res.* 183, 106369. doi:10.1016/j.phrs.2022.106369

MarthandamAsokan, S., Mariappan, R., Muthusamy, S., and Velmurugan, B. K. (2018). Pharmacological benefits of neferine - a comprehensive review. *Life Sci.* 199, 60–70. doi:10.1016/j.lfs.2018.02.032

Mi, L., Min, X., Chai, Y., Zhang, J., and Chen, X. (2022). NLRP1 inflammasomes: a potential target for the treatment of several types of brain injury. *Front. Immunol.* 13, 863774. doi:10.3389/fimmu.2022.863774

Milner, M. T., Maddugoda, M., Götz, J., Burgener, S. S., and Schroder, K. (2021). The NLRP3 inflammasome triggers sterile neuroinflammation and Alzheimer's disease. *Curr. Opin. Immunol.* 68, 116–124. doi:10.1016/j.coi.2020.10.011

Muñoz-Planillo, R., Kuffa, P., Martínez-Colón, G., Smith, B. L., Rajendiran, T. M., and Núñez, G. (2013). K^+ efflux is the common trigger of NLRP3 inflammasome activation by bacterial toxins and particulate matter. *Immunity* 38 (6), 1142–1153. doi:10.1016/j.immuni.2013.05.016

Nabavi, S. F., Sureda, A., Habtemariam, S., and Nabavi, S. M. (2015). Ginsenoside Rd and ischemic stroke; a short review of literatures. *J. Ginseng Res.* 39 (4), 299–303. doi:10.1016/j.jgr.2015.02.002

Nakatogawa, H. (2020). Mechanisms governing autophagosome biogenesis. *Nat. Rev. Mol. Cell. Biol.* 21, 439–458. doi:10.1038/s41580-020-0241-0

Nandini, D. B., Rao, R. S., Deepak, B. S., and Reddy, P. B. (2020). Sulforaphane in broccoli: the green chemoprevention!! Role in cancer prevention and therapy. *J. Oral MaxillofacPathol* 24 (2), 405. doi:10.4103/jomfp.JOMFP_126_19

Niu, X. S., and Yang, L. J. (2020). Effect of acanthin on blood-brain barrier after ischemia-reperfusion injury in mouse brain. *Stroke Neurological Dis.* 27 (05), 572–575+603.

Osakabe, N., Fushimi, T., and Fujii, Y. (2022). Hormetic response to B-type procyanidin ingestion involves stress-related neuromodulation via the gut-brain axis: preclinical and clinical observations. *Front. Nutr.* 9, 969823. doi:10.3389/fnut.2022.969823

Paerewijck, O., and Lamkanfi, M. (2022). The human inflammasomes. *Mol. Asp. Med.* 88, 101100. doi:10.1016/j.mam.2022.101100

Pandey, A., Shen, C., Feng, S., and Man, S. M. (2021). Cell biology of inflammasome activation. *Trends Cell Biol.* 31 (11), 924–939. doi:10.1016/j.tcb.2021.06.010

Peng, T. I., and Jou, M. J. (2010). Oxidative stress caused by mitochondrial calcium overload. *Ann. N. Y. Acad. Sci.* 1201, 183–188. doi:10.1111/j.1749-6632.2010.05634.x

Peng, Y., Ao, M., Dong, B., Jiang, Y., Yu, L., Chen, Z., et al. (2021). Anti-inflammatory effects of curcumin in the inflammatory diseases: status, limitations and countermeasures. *Drug Des. DevelTher* 15, 4503–4525. doi:10.2147/DDDT.S327378

Pengyue, Z., Tao, G., Hongyun, H., Liqiang, Y., and Yihao, D. (2017). Breviscapine confers a neuroprotective efficacy against transient focal cerebral ischemia by attenuating neuronal and astrocytic autophagy in the penumbra. *Biomed. Pharmacother.* 90, 69–76. doi:10.1016/j.biopha.2017.03.039

Piancone, F., La Rosa, F., Marventano, I., Saresella, M., and Clerici, M. (2021). The role of the inflammasome in neurodegenerative diseases. *Molecules* 26 (4), 953. doi:10.3390/molecules26040953

Pinent, M., Bladé, C., Salvadó, M. J., Blay, M., Pujadas, G., Fernández-Larrea, J., et al. (2006). Procyanidin effects on adipocyte-related pathologies. *Crit. Rev. Food Sci. Nutr.* 46 (7), 543–550. doi:10.1080/10408390500354537

Ping, Z., Liu, W., Kang, Z., Cai, J., Wang, Q., Cheng, N., et al. (2010). Sulforaphane protects brains against hypoxic-ischemic injury through induction of Nrf2-dependent phase 2 enzyme. *Brain Res.* 1343, 178–185. doi:10.1016/j.brainres.2010.04.036

Qi, Z., Wang, R., Liao, R., Xue, S., and Wang, Y. (2021). Neferine ameliorates sepsis-induced myocardial dysfunction through anti-apoptotic and antioxidative effects by regulating the PI3K/AKT/mTOR signaling pathway. *Front. Pharmacol.* 12, 706251. doi:10.3389/fphar.2021.706251

Qiu, Y. M., Zhang, C. L., Chen, A. Q., Wang, H. L., Zhou, Y. F., Li, Y. N., et al. (2021). Immune cells in the BBB disruption after acute ischemic stroke: targets for immune therapy? *Front. Immunol.* 12, 678744. doi:10.3389/fimmu.2021.678744

Qu, B., Liu, X., Liang, Y., Zheng, K., Zhang, C., and Lu, L. (2022). Salidroside in the treatment of NAFLD/NASH. *Chem. Biodivers.* 19 (12), e202200401. doi:10.1002/cbdv.202200401

Qu, J., Xu, N., Zhang, J., Geng, X., and Zhang, R. (2020). Panax notoginseng saponins and their applications in nervous system disorders: a narrative review. *Ann. Transl. Med.* 8 (22), 1525. doi:10.21037/atm-20-6909

Rajput, S. A., Wang, X. Q., and Yan, H. C. (2021). Morin hydrate: a comprehensive review on novel natural dietary bioactive compound with versatile biological and pharmacological potential. *Biomed. Pharmacother.* 138, 111511. doi:10.1016/j.biopha.2021.111511

Rao, Z., Zhu, Y., Yang, P., Chen, Z., Xia, Y., Qiao, C., et al. (2022). Pyroptosis in inflammatory diseases and cancer. *Theranostics* 12 (9), 4310–4329. doi:10.7150/thno.71086

Saini, V., Guada, L., and Yavagal, D. R. (2021). Global epidemiology of stroke and access to acute ischemic stroke interventions. *Neurology* 97 (20), S6–S16. doi:10.1212/WNL.0000000000012781

Schepici, G., Bramanti, P., and Mazzon, E. (2020). Efficacy of sulforaphane in neurodegenerative diseases. *Int. J. Mol. Sci.* 21 (22), 8637. doi:10.3390/ijms21228637

Seoane, P. I., Lee, B., Hoyle, C., Yu, S., Lopez-Castejon, G., Lowe, M., et al. (2020). The NLRP3-inflammasome as a sensor of organelle dysfunction. *J. Cell Biol.* 219 (12), e202006194. doi:10.1083/jcb.202006194

Sharma, B. R., and Kanneganti, T. D. (2021). NLRP3 inflammasome in cancer and metabolic diseases. *Nat. Immunol.* 22 (5), 550–559. doi:10.1038/s41590-021-00886-5

Sharma, S., Nozohouri, S., Vaidya, B., and Abbruscato, T. (2021). Repurposing metformin to treat age-related neurodegenerative disorders and ischemic stroke. *Life Sci.* 274, 119343. doi:10.1016/j.lfs.2021.119343

Shen, X., Li, M., Shao, K., Li, Y., and Ge, Z. (2023). Post-ischemic inflammatory response in the brain: targeting immune cell in ischemic stroke therapy. *Front. Mol. Neurosci.* 16, 1076016. doi:10.3389/fnmol.2023.1076016

Siebert, A., Desai, V., Chandrasekaran, K., Fiskum, G., and Jafri, M. S. (2009). Nrf2 activators provide neuroprotection against 6-hydroxydopamine toxicity in rat organotypic nigrostriatal cocultures. *J. Neurosci. Res.* 87 (7), 1659–1669. doi:10.1002/jnr.21975

Singh, S., Gupta, P., Meena, A., and Luqman, S. (2020). Acacetin, a flavone with diverse therapeutic potential in cancer, inflammation, infections and other metabolic disorders. *Food Chem. Toxicol.* 145, 111708. doi:10.1016/j.fct.2020.111708

Sinha, K., Ghosh, J., and Sil, P. C. (2016). Morin and its role in chronic diseases. *Adv. Exp. Med. Biol.* 928, 453–471. doi:10.1007/978-3-319-41334-1_19

Soane, L., Li Dai, W., Fiskum, G., and Bambrick, L. L. (2010). Sulforaphane protects immature hippocampal neurons against death caused by exposure to hemin or to oxygen and glucose deprivation. *J. Neurosci. Res.* 88 (6), 1355–1363. doi:10.1002/jnr.22307

Solairaja, S., Andrabi, M. Q., Dunna, N. R., and Venkatabalasubramanian, S. (2021). Overview of morin and its complementary role as an adjuvant for anticancer agents. *Nutr. Cancer* 73 (6), 927–942. doi:10.1080/01635581.2020.1778747

Song, H., Wang, P., Liu, J., and Wang, C. (2017). Panax notoginseng preparations for unstable angina pectoris: a systematic review and meta-analysis. *Phytother. Res.* 31 (8), 1162–1172. doi:10.1002/ptr.5848

Song, X., Wang, L., and Fan, D. (2022). Insights into recent studies on biotransformation and pharmacological activities of ginsenoside Rd. *Biomolecules* 12 (4), 512. doi:10.3390/biom12040512

Sun, R., Peng, M., Xu, P., Huang, F., Xie, Y., Li, J., et al. (2020). Low-density lipoprotein receptor (LDLR) regulates NLRP3-mediated neuronal pyroptosis following cerebral ischemia/reperfusion injury. *J. Neuroinflammation* 17 (1), 330. doi:10.1186/s12974-020-01988-x

Sun, Y., Yang, T., Mao, L., and Zhang, F. (2017). Sulforaphane protects against brain diseases: roles of cytoprotective enzymes. *Austin J. Cerebrovasc. Dis. Stroke* 4 (1), 1054. doi:10.26420/austinjcerebrovascdisstroke.2017.1054

Sundaram, B., and Kanneganti, T. D. (2021). Advances in understanding activation and function of the NLRC4 inflammasome. *Int. J. Mol. Sci.* 22 (3), 1048. doi:10.3390/ijms22031048

Takahashi, M. (2022). NLRP3 inflammasome as a key driver of vascular disease. *Cardiovasc Res.* 118 (2), 372–385. doi:10.1093/cvr/cvab010

Tang, B. (2019). *The role of mitochondrial autophagy -NLRP3 inflammatory body pathway in cerebral ischemia-reperfusion injury and the intervention of total saponins of Pantoginseng and Astragaloside IV [D]*. China: Hunan university of Chinese medicine.

Tang, B., Tang, W., Tang, Y., and Deng, C. (2019c). Astragaloside IV attenuates cerebral ischemia and reperfusion injury and reduces activation of NLRP3 inflammasome and NF-κB phosphorylation in rats following a transient middle cerebral artery occlusion. *J. physiology* 71 (03), 424–430. doi:10.13294/j.aps.2019.0007

Tang, D., Kang, R., Berghe, T. V., Vandenabeele, P., and Kroemer, G. (2019a). The molecular machinery of regulated cell death. *Cell Res.* 29 (5), 347–364. doi:10.1038/s41422-019-0164-5

Tang, H., Wu, L., Chen, X., Li, H., Huang, B., Huang, Z., et al. (2021). Paeoniflorin improves functional recovery through repressing neuroinflammation and facilitating neurogenesis in rat stroke model. *PeerJ* 9, e10921. doi:10.7717/peerj.10921

Tang, K., Qin, W., Wei, R., Jiang, Y., Fan, L., Wang, Z., et al. (2022). Ginsenoside Rd ameliorates high glucose-induced retinal endothelial injury through AMPK-STRT1 interdependence. *Pharmacol. Res.* 179, 106123. doi:10.1016/j.phrs.2022.106123

Tang, Y. L., Tao, Y., Zhu, L., Shen, J. L., and Cheng, H. (2023). Role of NLRP3 inflammasome in hepatocellular carcinoma: a double-edged sword. *Int. Immunopharmacol.* 118, 110107. doi:10.1016/j.intimp.2023.110107

Tang, Y. S., Zhao, Y. H., Zhong, Y., Li, X. Z., Pu, J. X., Luo, Y. C., et al. (2019b). Neferine inhibits LPS-ATP-induced endothelial cell pyroptosis via regulation of ROS/NLRP3/Caspase-1 signaling pathway. *Inflamm. Res.* 68 (9), 727–738. doi:10.1007/s00011-019-01256-6

Tao, Y. W., Yang, L., Chen, S. Y., Zhang, Y., Zeng, Y., Wu, J. S., et al. (2022). Pivotal regulatory roles of traditional Chinese medicine in ischemic stroke via inhibition of NLRP3 inflammasome. *J. Ethnopharmacol.* 294, 115316. doi:10.1016/j.jep.2022.115316

Termini, D., Den Hartogh, D. J., Jaglanian, A., and Tsiani, E. (2020). Curcumin against prostate cancer: current evidence. *Biomolecules* 10 (11), 1536. doi:10.3390/biom10111536

Uebel, T., Hermes, L., Haupenthal, S., Müller, L., and Esselen, M. (2021). α-Asarone, β-asarone, and γ-asarone: current status of toxicological evaluation. *J. Appl. Toxicol.* 41 (8), 1166–1179. doi:10.1002/jat.4112

Vanduchova, A., Anzenbacher, P., and Anzenbacherova, E. (2019). Isothiocyanate from broccoli, sulforaphane, and its properties. *J. Med. Food* 22 (2), 121–126. doi:10.1089/jmf.2018.0024

Vauzour, D., Buonfiglio, M., Corona, G., Chirafisi, J., Vafeiadou, K., Angeloni, C., et al. (2010). Sulforaphane protects cortical neurons against 5-S-cysteinyl-dopamine-induced toxicity through the activation of ERK1/2, Nrf-2 and the upregulation of detoxification enzymes. *Mol. Nutr. Food Res.* 54 (4), 532–542. doi:10.1002/mnfr.200900197

Wang, L. Q., Zheng, Y. Y., Zhou, H. J., Zhang, X. X., Wu, P., and Zhu, S. M. (2021a). LncRNA-Fendrr protects against the ubiquitination and degradation of NLRC4 protein through HERC2 to regulate the pyroptosis of microglia. *Mol. Med.* 27 (1), 39. doi:10.1186/s10020-021-00299-y

Wang, M., Pan, W., Xu, Y., Zhang, J., Wan, J., and Jiang, H. (2022). Microglia-mediated neuroinflammation: a potential target for the treatment of cardiovascular diseases. *J. Inflamm. Res.* 15, 3083–3094. doi:10.2147/JIR.S350109

Wang, S., Sun, F., Xue, W., Jiang, Q., and Dong, L. (2020). Breviscapine regulates the activation of NLRP3 inflammatory bodies and inhibits pyrodeath and apoptosis of neuronal cells in rats with chronic cerebral ischemia. *J. anhui Med. Univ.* (9), 1321–1326.

Wang, X. L., Feng, S. T., Wang, Y. T., Chen, N. H., Wang, Z. Z., and Zhang, Y. (2021b). Paeoniflorin: a neuroprotective monoterpenoid glycoside with promising anti-depressive properties. *Phytomedicine* 90, 153669. doi:10.1016/j.phymed.2021.153669

Wang, Y., Meng, C., Zhang, J., Wu, J., and Zhao, J. (2019). Inhibition of GSK-3β alleviates cerebral ischemia/reperfusion injury in rats by suppressing NLRP3 inflammasome activation through autophagy. *Int. Immunopharmacol.* 68, 234–241. doi:10.1016/j.intimp.2018.12.042

Wei, L. Y., Zhang, J. K., Zheng, L., and Chen, Y. (2022). The functional role of sulforaphane in intestinal inflammation: a review. *Food Funct.* 13 (2), 514–529. doi:10.1039/d1fo03398k

Wen, J., Xuan, B., Liu, Y., Wang, L., He, L., Meng, X., et al. (2021a). Updating the NLRC4 inflammasome: from bacterial infections to autoimmunity and cancer. *Front. Immunol.* 12, 702527. doi:10.3389/fimmu.2021.702527

Wen, L., He, T., Yu, A., Sun, S., Li, X., Wei, J., et al. (2021b). Breviscapine: a review on its phytochemistry, pharmacokinetics and therapeutic effects. *Am. J. Chin. Med.* 49 (6), 1369–1397. doi:10.1142/S0192415X21500646

Wu, C., Yan, J., and Li, W. (2022). Acacetin as a potential protective compound against cardiovascular diseases. *Evid. Based Complement. Altern. Med.* 2022, 6265198. doi:10.1155/2022/6265198

Wu, G., Yan, Y., Zhou, Y., Duan, Y., Zeng, S., Wang, X., et al. (2020c). Sulforaphane: expected to become a novel antitumor compound. *Oncol. Res.* 28 (4), 439–446. doi:10.3727/096504020X15828892654385

Wu, G. X., Li, S. X., and Li, R. Y. (2023). Effects of total polyphenols of Toona sinensis seeds on apoptosis in rats with myocardial ischemia/reperfusion injury. *Chin. J. Hosp. Pharm.* 43 (02), 145–149. doi:10.13286/j.1001-5213.2023.02.04

Wu, Y., Dong, G., and Sheng, C. (2020a). Targeting necroptosis in anticancer therapy: mechanisms and modulators. *Acta Pharm. Sin. B* 10 (9), 1601–1618. doi:10.1016/j.apsb.2020.01.007

Wu, Y., Xu, S., and Tian, X. Y. (2020b). The effect of salvianolic acid on vascular protection and possible mechanisms. *Oxid. Med. Cell Longev.* 2020, 5472096. doi:10.1155/2020/5472096

Xiao, Z., Liu, W., Mu, Y. P., Zhang, H., Wang, X. N., Zhao, C. Q., et al. (2020). Pharmacological effects of salvianolic acid B against oxidative damage. *Front. Pharmacol.* 11, 572373. doi:10.3389/fphar.2020.572373

Xie, H., Chun, F. K., Rutz, J., and Blaheta, R. A. (2021). Sulforaphane impact on reactive oxygen species (ROS) in bladder carcinoma. *Int. J. Mol. Sci.* 22 (11), 5938. doi:10.3390/ijms22115938

Xie, W., Meng, X., Zhai, Y., Zhou, P., Ye, T., Wang, Z., et al. (2018). Panax notoginseng saponins: a review of its mechanisms of antidepressant or anxiolytic effects and network analysis on phytochemistry and Pharmacology. *Molecules* 23 (4), 940. doi:10.3390/molecules23040940

Xin, M., Hao, Y., Huang, G., Wang, X., Liang, Z., Miao, J., et al. (2020). The efficacy and safety of salvianolic acids on acute cerebral infarction treatment: a protocol for systematic review and meta analysis. *Med. Baltim.* 99 (23), e20059. doi:10.1097/MD.0000000000020059

Xu, F., Xu, J., Xiong, X., and Deng, Y. (2019). Salidroside inhibits MAPK, NF-κB, and STAT3 pathways in psoriasis-associated oxidative stress via SIRT1 activation. *Redox Rep.* 24 (1), 70–74. doi:10.1080/13510002.2019.1658377

Xu, Q., Zhao, B., Ye, Y., Li, Y., Zhang, Y., Xiong, X., et al. (2021). Relevant mediators involved in and therapies targeting the inflammatory response induced by activation of the NLRP3 inflammasome in ischemic stroke. *J. Neuroinflammation* 18 (1), 123. doi:10.1186/s12974-021-02137-8

Xu, Y., Tan, H. Y., Li, S., Wang, N., and Feng, Y. (2018). Panax notoginseng for inflammation-related chronic diseases: a review on the modulations of multiple pathways. *Am. J. Chin. Med.* 46 (5), 971–996. doi:10.1142/S0192415X18500519

Xu, Y., Yao, J., Zou, C., Zhang, H., Zhang, S., Liu, J., et al. (2017). Asiatic acid protects against hepatic ischemia/reperfusion injury by inactivation of Kupffer cells via PPARγ/NLRP3 inflammasome signaling pathway. *Oncotarget* 8 (49), 86339–86355. doi:10.18632/oncotarget.21151

Xue, Li, Han, H., and Zhang, Li (2023). Effect of sanlutein on neuronal apoptosis in cerebral ischemia reperfusion rats by inhibiting TXNIP/NLRP3/Caspase-1 signaling pathway. *Tianjin Pharm.* 51 (05), 487–491.

Yagishita, Y., Fahey, J. W., Dinkova-Kostova, A. T., and Kensler, T. W. (2019). Broccoli or sulforaphane: is it the source or dose that matters? *Molecules* 24 (19), 3593. doi:10.3390/molecules24193593

Yang, Bo (2022). *Study on the protective effect of proanthocyanidins on cerebral ischemia-reperfusion injury through inhibition of TLR4-NLRP3 pathway[D]*. China: Southern Medical University. doi:10.27003/d.cnki.gojyu.2022.000267

Yao, Y. Q. (2022). *Effect of ginsenoside Rd on pyrodeath after cerebral ischemia reperfusion injury and its mechanism based on miR-139-5p/FoxO1/Keap1/Nrf2 pathway [D]*. China: Xinjiang medical university.

Ye, R., Zhao, G., and Liu, X. (2013). Ginsenoside Rd for acute ischemic stroke: translating from bench to bedside. *Expert Rev. Neurother.* 13 (6), 603–613. doi:10.1586/ern.13.51

Ye, X., Shen, T., Hu, J., Zhang, L., Zhang, Y., Bao, L., et al. (2017). Purinergic 2X7 receptor/NLRP3 pathway triggers neuronal apoptosis after ischemic stroke in the mouse. *Exp. Neurol.* 292, 46–55. doi:10.1016/j.expneurol.2017.03.002

Yin, M., Chen, W. P., Yin, X. P., Tu, J. L., Hu, N., and Li, Z. Y. (2021). LncRNA TUG1 demethylated by TET2 promotes NLRP3 expression, contributes to cerebral ischemia/reperfusion inflammatory injury. *ASN Neuro* 13, 17590914211003247. doi:10.1177/17590914211003247

Yin, Y., Zhou, Z., Liu, W., Chang, Q., Sun, G., and Dai, Y. (2017). Vascular endothelial cells senescence is associated with NOD-like receptor family pyrin domain-containing 3 (NLRP3) inflammasome activation via reactive oxygen species (ROS)/thioredoxin-interacting protein (TXNIP) pathway. *Int. J. Biochem. Cell Biol.* 84, 22–34. doi:10.1016/j.biocel.2017.01.001

Yuan, Y., Jiang, X., Lu, L., Chen, S., Chen, X., and Deng, Z. (2021). Mechanisms of protective effect of metformin on cerebral ischemia-reperfusion injury by regulating cellular autophagy and scorch death. *Chin. J. Pharmacol.* 56 (05), 359–367.

Zang, Y., Wan, J., Zhang, Z., Huang, S., Liu, X., and Zhang, W. (2020). An updated role of astragaloside IV in heart failure. *Biomed. Pharmacother.* 126, 110012. doi:10.1016/j.biopha.2020.110012

Zhang, J., Wu, C., Gao, L., Du, G., and Qin, X. (2020). Astragaloside IV derived from Astragalus membranaceus: a research review on the pharmacological effects. *Adv. Pharmacol.* 87, 89–112. doi:10.1016/bs.apha.2019.08.002

Zhang, L., and Wei, W. (2020). Anti-inflammatory and immunoregulatory effects of paeoniflorin and total glucosides of paeony. *PharmacolTher* 207, 107452. doi:10.1016/j.pharmthera.2019.107452

Zhang, W. J., Chen, S. J., Zhou, S. C., Wu, S. Z., and Wang, H. (2021b). Inflammasomes and fibrosis. *Front. Immunol.* 12, 643149. doi:10.3389/fimmu.2021.643149

Zhang, X., Xie, L., Long, J., Xie, Q., Zheng, Y., Liu, K., et al. (2021d). Salidroside: a review of its recent advances in synthetic pathways and pharmacological properties. *Chem. Biol. Interact.* 339, 109268. doi:10.1016/j.cbi.2020.109268

Zhang, X., Zeng, W., Zhang, Y., Yu, Q., Zeng, M., Gan, J., et al. (2022). Focus on the role of mitochondria in NLRP3 inflammasome activation: a prospective target for the treatment of ischemic stroke (Review). *Int. J. Mol. Med.* 49 (6), 74. doi:10.3892/ijmm.2022.5130

Zhang, Y., Yang, W., Li, W., and Zhao, Y. (2021a). NLRP3 inflammasome: checkpoint connecting innate and adaptive immunity in autoimmune diseases. *Front. Immunol.* 12, 732933. doi:10.3389/fimmu.2021.732933

Zhang, Z., Huang, X., and Deng, X. (2023). Curcumin ameliorates neurological dysfunction in cerebral ischemic rats by modulating NLRP3/Caspase-1 signaling pathway. *Clin. J. Traditional Chin. Med.* 35 (01), 104–109. doi:10.16448/j.cjtcm.2023.0124

Zhao, H. (2022). *Exploring the neuroprotective effects of Toon seed polyphenols on focal cerebral ischemia from MAPK and NLRP3 inflammatory vesicle pathways[D]*. China: Three Gorges University. doi:10.27270/d.cnki.gsxau.2022.000257

Zhao, H., Wang, Q., and Shu, Y. X. (2023a). Research progress on the chemical composition and pharmacological activity of Aconite seeds. *Chin. Wild Plant Resour.* 42 (01), 63–69.

Zhao, M. H., Shang, H. H., and Li, F. Q. (2023b). The role of curcumin in inhibiting inflammation in alleviating brain ischemia-reperfusion synaptic injury[J/OL]. *Public Health Prev. Med.* 1-5.

Zhao, N., Di, B., and Xu, L. L. (2021). The NLRP3 inflammasome and COVID-19: activation, pathogenesis and therapeutic strategies. *Cytokine Growth Factor Rev.* 61, 2–15. doi:10.1016/j.cytogfr.2021.06.002

Zhao, Y. G., and Zhang, H. (2019). Autophagosome maturation: an epic journey from the ER to lysosomes. *J. Cell Biol.* 218, 757–770. doi:10.1083/jcb.201810099

Zheng, D., Kern, L., and Elinav, E. (2021). The NLRP6 inflammasome. *Immunology* 162 (3), 281–289. doi:10.1111/imm.13293

Zhi, Y., Zhao, J., Zhao, H., and Yu, D. (2018). Efficacy and safety of breviscapine injection in treatment of unstable angina pectoris: systematic review and Meta-analysis. *Chin. J. traditional Chin. Med.* 43 (19), 3940–3955. doi:10.19540/j.cnki.cjcmm.20180611.009

Zhou, Y., Zhang, Z.-C., and Zhou, J. (2021). Effects of early intervention of Panax ginseng total saponin on the expression of NLRP3/IL-1β signaling pathway-related factors in rats with cerebral ischemia-reperfusion injury. *Chin. J. Traditional Chin. Med.* 36 (12), 7275–7278.

Zhou, Y. X., Gong, X. H., Zhang, H., and Peng, C. (2020). A review on the pharmacokinetics of paeoniflorin and its anti-inflammatory and immunomodulatory effects. *Biomed. Pharmacother.* 130, 110505. doi:10.1016/j.biopha.2020.110505

Zhu, H., Hu, S., Li, Y., Sun, Y., Xiong, X., Hu, X., et al. (2022a). Interleukins and ischemic stroke. *Front. Immunol.* 13, 828447. doi:10.3389/fimmu.2022.828447

Zhu, T., Wang, L., Wang, L. P., and Wan, Q. (2022b). Therapeutic targets of neuroprotection and neurorestoration in ischemic stroke: applications for natural compounds from medicinal herbs. *Biomed. Pharmacother.* 148, 112719. doi:10.1016/j.biopha.2022.112719

frontiers | Frontiers in Pharmacology

TYPE Systematic Review
PUBLISHED 25 April 2024
DOI 10.3389/fphar.2023.1236684

OPEN ACCESS

EDITED BY
Syed Shadab Raza,
ERA's Lucknow Medical College, India

REVIEWED BY
Yuyan Zhang,
Zhejiang Chinese Medical University, China
Genxiang Mao,
Zhejiang Hospital, China

*CORRESPONDENCE
Jinmin Liu,
jmvip@vip.163.com

RECEIVED 09 June 2023
ACCEPTED 04 August 2023
PUBLISHED 25 April 2024

CITATION
Yan M, Wu J, Wang L, Wang K, Li L, Sun T, Zhang H, Zhang M, Zou L, Yang S and Liu J (2024), Ginkgolide injections in meglumine, combined with edaravone, significantly increases the efficacy in acute ischemic stroke: A meta-analysis.
Front. Pharmacol. 14:1236684.
doi: 10.3389/fphar.2023.1236684

Ginkgolide injections in meglumine, combined with edaravone, significantly increases the efficacy in acute ischemic stroke: A meta-analysis

Mingyuan Yan[1], Jing Wu[2], Le Wang[3], Kaiyue Wang[1], Lili Li[1], Tianye Sun[1], Han Zhang[1], Mi Zhang[1], Lin Zou[1], Songyi Yang[1] and Jinmin Liu[3]*

[1]Beijing University of Chinese Medicine, Beijing, China, [2]Dongzhimen Hospital, University of Chinese Medicine, Beijing, China, [3]Encephalopathy Department I, Dongfang Hospital, Beijing University of Chinese Medicine, Beijing, China

Objective: This study aimed to evaluate the efficacy of combining diterpene ginkgolide meglumine injection (DGMI) with edaravone for the treatment of acute ischemic stroke. This is particularly relevant because Western drugs, excluding intravenous thrombolysis, have shown limited success.

Methods: A comprehensive search was conducted using multiple databases, including PubMed, Cochrane Library, Web of Science, China National Knowledge Infrastructure WanFang, VIP, and Chinese Biomedical Database (CBM) until June 2023. The data were analyzed using fixed-effects and random-effects models in Review Manager. The mean difference with 95% confidence interval was calculated for each outcome.

Results: Eighteen studies involving 1,636 participants were included in the analysis. The DGMI group showed significant reductions in the National Institutes of Health Stroke Scale (NIHSS) score, modified Rankin Scale (mRS) score, and C-reactive protein (CRP) level, compared to the control group. Furthermore, the DGMI group showed a significant improvement in superoxide dismutase (SOD) levels and a reduction in malondialdehyde (MDA) levels. The combination of DGMI and edaravone was more effective in reducing neuron-specific enolase (NSE) levels following brain tissue injury than edaravone alone. Additionally, DGMI complemented edaravone in reducing rheological parameters associated with ischemic stroke, including hematocrit, plasma viscosity, platelet adhesion rate, and erythrocyte deformation index.

Conclusion: The combination of DGMI and edaravone significantly improved the therapeutic efficacy in patients with acute ischemic stroke. However, more extensive and high-quality clinical trials are required to validate these underlying mechanisms.

Systematic Review Registration: https://www.crd.york.ac.uk/PROSPERO/display_record.php?RecordID=260215, identifier: PROSPERO (CRD42021260215)

KEYWORDS

diterpene ginkgolides meglumine injection, traditional Chinese medicine, acute ischemic stroke, NIHSS, meta-analysis

Introduction

Acute ischemic stroke occurs when the blood supply to the brain is suddenly blocked or severely reduced, leading to ischemia, hypoxic necrosis, and softening of local brain tissue, resulting in rapid loss of brain function in the affected area. Ischemia-induced stroke is responsible for 68% of all strokes worldwide, ranking as the second leading cause of death and the third leading cause of disability. Despite primary prevention efforts, the annual incidence of stroke has continued to increase (GBD, 2019 Stroke Collaborators, 2021). China has the highest global incidence and death rate of stroke (Feigin et al., 2014; Wang et al., 2017; Song et al., 2019), posing a significant and urgent public health concern. Prompt revascularization of the occluded blood vessels is crucial for stroke management. Revascularization therapies, including intravenous thrombolysis, intravascular mechanical thrombus retrieval, and antiplatelet therapy, are effective interventions for improving cerebral infarction and are recommended by the Chinese Medical Association guidelines for ischemic stroke (Peng and Wu, 2018). However, the use of intravenous thrombolysis is limited owing to time constraints, stringent criteria, and limited hospital accessibility, among other factors. Traditional Chinese Medicine (TCM) plays an important role in the treatment of various diseases. The modernization of Chinese medicine has established an effective stroke treatment system that includes the use of herbal extracts. Given the limited success of Western medicine alone in acute ischemic stroke patients who cannot undergo thrombolysis, Chinese doctors have traditionally used a combination of Western and Chinese medicine (Gao et al., 2017). This combination of Western medicine and Chinese herbal extracts has proven beneficial for many stroke patients, particularly in improving brain microcirculation, reducing inflammation and edema, and providing antioxidant effects.

The diterpene ginkgolide meglumine injection (DGMI) is a Chinese medicinal product derived from *Ginkgo biloba* extract. The primary constituents of this drug are ginkgolides A, B, and K. To ensure a rigorous scientific conclusion, we referred to the ConPhyMP statement, which provides a comprehensive classification of drugs derived from plant extracts (Heinrich et al., 2022). The name of *G. biloba* has been verified in two databases (Plant of the World Online and The World Flora Online). They belong to a category of drugs that enhance blood circulation and resolve blood stasis. According to this statement, drugs composed of plant extracts can be categorized into three types, and DGMI meets the criteria for Type A extraction. DGMI is derived from the leaf extract of *G. biloba*, a plant belonging to the Ginkgoaceae family. Traditional medicine has been extensively researched and developed, revealing its potent antioxidant and anti-free-radical properties. The active components of DGMI are GA, GB, and GK, which are present at a ratio of 15:30:1 in this injection. Meglumine serves as a co-solvent in this injection, without contributing to its therapeutic effect. The intellectual property of the DGMI is exclusively owned and produced by Kanion Pharmaceutical, a Chinese company. Currently, the drugs used in all hospitals in China are uniform and adhere to certain specifications. Each bottle contains 5 mL of an injection with *G. biloba* diterpenoid lactone (25 mg and is administered as an injection. This TCM was approved by the SFDA on 30 October 2012, with approval number Z20120024. To minimize heterogeneity, all studies included in the analysis used the DGMI produced by the same manufacturer. More information about this drug has been listed in Table 1.

Modern medicine acknowledges the potential of these drugs to improve cerebral blood circulation, increase blood flow, and prevent platelet aggregation (Zhang Q. et al., 2021; Sun et al., 2021). DGMI is typically used in the treatment of cerebral infarction, often in combination with Western drugs, resulting in superior outcomes compared with Western drugs alone. These benefits are evident in NIHSS scores, blood rheological indicators, and other serum indicators (Zhang et al., 2017; Li, 2019; Liu et al., 2019; Wang, 2019). Moreover, animal studies have suggested that ginkgolides A, B, and K have potential as PAFR antagonists, offering unique advantages in protecting the blood-brain barrier, reducing brain edema, and exhibiting antioxidant effects. These mechanisms involve regulation of inflammatory molecule release, vascular endothelial growth factor expression, and neurogenesis (Wang et al., 2007; Liu et al., 2010; Ma et al., 2012; Nabavi et al., 2015; Liu et al., 2017; Zhong, 2020; Yang et al., 2021). Although several clinical studies have reported the efficacy of DGMI in combination with Western drugs for the treatment of cerebral infarction, these studies used different Western drugs, and there has been no systematic evaluation or analysis. Therefore, to minimize bias and provide evidence-based treatment for ischemic stroke using DGMI, we selected edaravone as the preferred Western drug in our study.

Methods

Systematic review protocol and registration

This study followed the guidelines outlined in the Preferred Reporting Items for Systematic Reviews and Meta-Analyses (PRISMA) statement (Moher et al., 2009) and the methodology recommended by the Cochrane Handbook for Systematic Reviews of Interventions. The protocol for this study was registered in PROSPERO (CRD42021260215).

Search strategy

A comprehensive search was conducted in three English databases (PubMed, Cochrane Library, and Web of Science) and four Chinese databases (CNKI, WanFang, VIP, and CBM) until June 2023. The databases were searched using terms such as stroke, ischemic stroke, cerebral infarction, diterpene ginkgolide meglumine injection, *Ginkgo* diterpene lactone meglumine, *G. biloba* diterpene lactone glucosamine, and randomized controlled trials. The search encompassed both electronic and manual sources of information. The identified studies were compiled, and duplicates, animal experiments, reviews, studies with unextractable data, and studies that could not be systematically evaluated were excluded, resulting in the selection of studies for

TABLE 1 Detailed information of DMGI accroding to the ConPhyMP statement.

Injection name	Injection sourse	Botanical plant name	Species	Plant part used	Origin and harvest time	Extraction and production methods
Diterpene ginkgolide meglumine injection	Jiangsu Kanion Pharmaceutical Co., Ltd	Ginkgo biloba L	Ginkgoaceae	Dry leaves of Ginkgo biloba L	China. Autumn	Under patent protection, we are unable to obtain specific information about the extraction and production process

Drug efficacy in TCM	Functional Indications	Quality control reported?	Chemical analysis report?	Injection composition	Proportion of main components and excipients	Drug properties
Promoting blood circulation to remove meridian obstruction	Used for cerebral infarction, symptoms such as hemiplegia, crooked tongue, awkward speech, numbness of limbsetc.	Yes. Z20120024, approved by China Foods Limited and Drug Administration	No.	Main components: Ginkgolides A, Ginkgolides B, Ginkgolides K(15:30:1). Excipients: Meglumine, Citric Acid, Sodium chloride	98:2	Colorless to yellowish clear liquid

Adverse reactions
1. Allergic reactions: chills, fever, panic, discomfort in the back pillow, slight cyanosis of the lips and claws, shaking of the lower limbs, skin rash, flushing, Telangiectasia, sweating, skin itching and chest tightness, cough, nasal congestion and runny nose, etc. 2. Systemic damage: fever, back pain, neck distension, discomfort in the occipital region. 3. Respiratory system: coughing, stuffy and runny nose, chest tightness, chest discomfort. 4. Cardiovascular system: blood pressure fluctuations mainly include blood pressure reduction, palpitation, palpitation, supraventricular premature contraction, complete or incomplete Right bundle branch block, first degree atrioventricular block, atrial fibrillation and other ECG abnormalities. 5. Neuropsychiatric system: dizziness, headache, drowsiness, insomnia, lower limb shaking, abnormal coordination function. 6. Digestive system: nausea, vomiting, loss of appetite, abdominal discomfort, diarrhea, positive fecal occult blood, alanine aminotransferase, Asparagus cochinchinensis aminotransferase, Alkaline phosphatase and γ- Glutamic transferase, single or multiple elevated. 7. Blood system: thrombocytopenia, red blood cell decline, hemoglobin decline, Prothrombin time extension, activated partial thromboplastin time extension, fibrinogen reduction. 8. Skin and its accessories: Phlebitis and ecchymosis at the infusion site. 9. Kidney and Urinary system: excessive urination, increased nocturnal urine, abnormal blood creatinine, abnormal Blood urea nitrogen, positive urine red blood cells, positive urine protein, positive urine sugar

further analysis. The screening process for these studies is depicted in Figure 1.

Eligibility criteria

The inclusion criteria were as follows: 1) Participants who met the diagnostic criteria for acute ischemic stroke and exhibited significant symptoms. 2) Patients aged between 18 and 90 years in whom the time from onset to consultation did not exceed 72 h. 3) The included literature reported at least the NIHSS score as an outcome indicator. 4) The study was approved by the ethics committees of the participating hospitals. 5) The study design was a randomized controlled trial. 6) The control group intervention involved edaravone, whereas the experimental group intervention involved a combination of edaravone and diterpene ginkgolide meglumine injection. 7) Studies limited to English and Chinese languages.

The exclusion criteria were as follows: 1) Duplicate publications, animal studies, and reviews. 2) Studies that did not align with the diagnosis of acute ischemic stroke, including transient ischemic attack. 3) Studies with incomplete data on relevant outcome indicators.

Study selection and data extraction

Two researchers (MY Yan and J Wu) independently screened the titles and abstracts of the studies based on the inclusion and exclusion criteria. The investigators compared their screening results and consulted a third person (L Wang) for a final decision in case of disagreement. Data extraction involved collecting information, such as the first author's name, year of publication, study design, participant characteristics, interventions, control measures, duration of intervention, outcome indicators, adverse effects, and continuous data are presented as mean ± standard deviation.

Assessment of risk of bias in individual studies

The studies were assessed for quality using the Cochrane "Bias Risk Assessment Tool," (Higgins et al., 2011) which evaluated randomization methods, allocation concealment, blinding, completeness of outcome data, selective reporting, and other biases. Other biases were identified by thoroughly analyzing the articles and assessing the adequacy of baseline characteristics and outcome indicators. The evaluations were categorized as "low risk of bias", "high risk of bias," or "unclear." All included studies acknowledged random allocation, with ten reporting the use of a random number table, one reporting a random lottery, and one using a random coin flip, with a minimal risk of bias. The method of randomization in the six remaining studies was unclear, resulting in an uncertain risk of bias. Allocation concealment was not addressed in these studies, resulting in a risk of bias. All studies had a high risk of performance bias owing to a lack of blinding reporting. Insufficient data hindered the evaluation of additional biases, resulting in uncertain risks. All the included studies were assessed as having a low risk of incomplete outcome data. The risk of selective reporting in these studies could not be determined

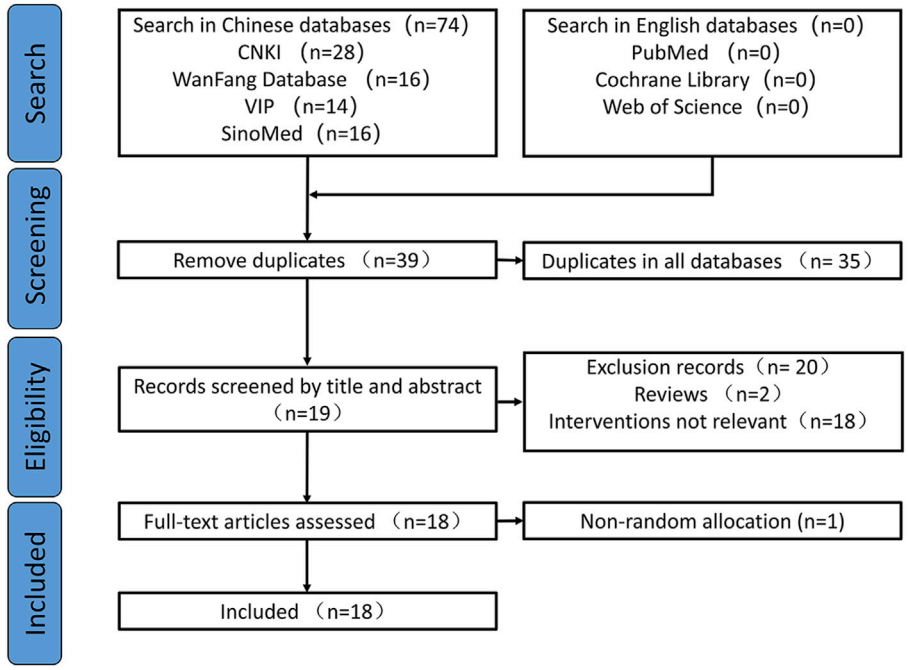

FIGURE 1
Flowchart for study screening.

due to insufficient evidence. These trials did not provide information on data management, statistical strategies, or implementation processes, resulting in ambiguous risk assessments. Based on these factors, it is reasonable to assume that all the included studies were of low quality. The quality assessment of the studies is presented in Figures 2, 3.

Statistical analysis

Statistical analyses were conducted using Review Manager 5.3 (Cochrane Collaboration, Copenhagen, Denmark). We estimated the combined effects of the interventions on continuous outcomes using the mean differences(MDs) with 95% confidence intervals (CIs). Meta-analyses were performed using Mantel-Haenszel fixed-effects models in the absence of significant statistical heterogeneity among the included studies. A significance level of 5% was used throughout the study. Heterogeneity between studies was assessed using the Q and I^2 methods. A p-value >0.1 and an I^2 value <50% indicated homogeneity in the literature and were analyzed using a fixed-effects model. Conversely, if heterogeneity was detected (p-value ≤0.1 or, $I^2 \geq 50\%$), a random-effects model was used. Sensitivity tests and subgroup analyses were performed to investigate the possible causes of heterogeneity.

Outcomes

The primary outcome indicator was the National Institute of Health Stroke Scale (NIHSS), while the additional outcome indicators included the Barthel index (BI), neuron-specific enolase (NSE), C-reactive protein (CRP), malondialdehyde (MDA), superoxide dismutase (SOD), modified Rankin scale (mRS), and hemorheological indices such as hematocrit, plasma viscosity (PV), erythrocyte deformation index, and platelet adhesion rate.

Results

Compilation of studies and characteristics

A total of 76 Chinese studies were initially retrieved. Through a rigorous process involving the careful evaluation of titles and abstracts and thorough screening by two reviewers, 18 randomized controlled trials (Li et al., 2017a; Luo et al., 2017; Zhao et al., 2017; Bao and Peng, 2019; Luo and Chen, 2019; Yang, 2019; Chen et al., 2020; Liu, 2020; Lv et al., 2020; Shi and Fan, 2020; Sun, 2020; Xiao, 2020; Zhu, 2020; Zhang et al., 2021b; Wang et al. 2024; Hu et al., 2021; Lu, 2021; Wang and Fan, 2021) conducted in China were selected for this meta-analysis. The analyzed studies were published between 2017 and 2021 and included 1,636 participants, with 820 assigned to the control group and 816 assigned to the experimental group. All studies reported NIHSS scores, and four studies (Luo et al., 2017; Luo and Chen, 2019; Hu et al., 2021; Wang et al. 2024) included data on BI post-treatment. Four studies reported NSE levels (Li et al., 2017a; Luo and Chen, 2019; Yang, 2019; Zhang et al., 2021b), while three studies reported CRP levels (Sun, 2020; Zhang et al., 2021b; Wang and Fan, 2021). Two studies reported MDA and SOD levels (Sun, 2020; Wang and Fan, 2021), and three studies reported hemorheological indices, including hematocrit, plasma viscosity, erythrocyte deformation index, and platelet adhesion rate (Chen et al., 2020; Zhang et al.,

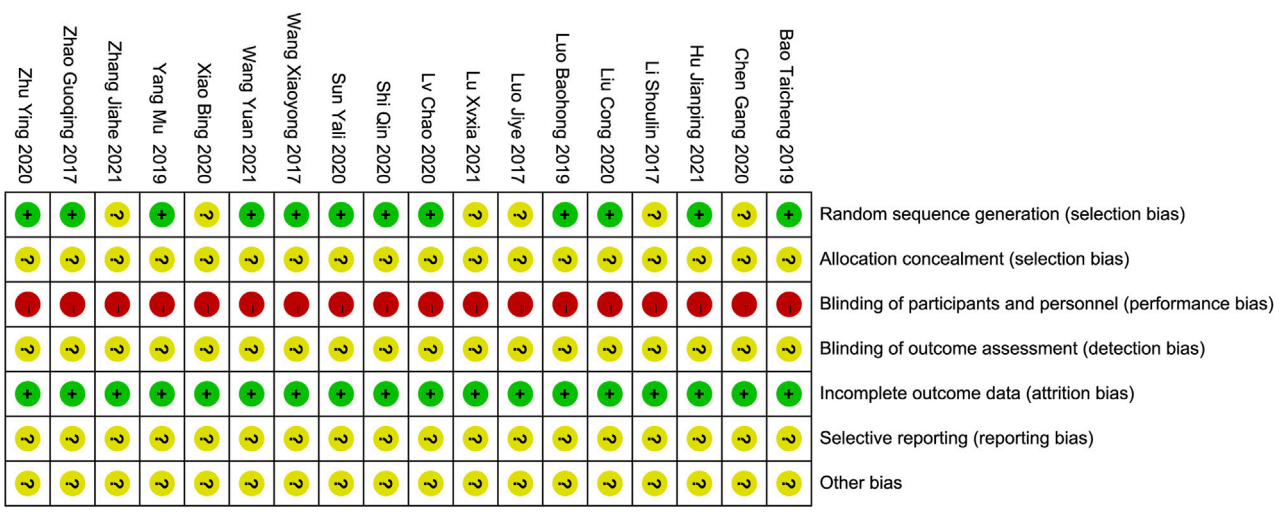

FIGURE 2
Risk of bias summary.

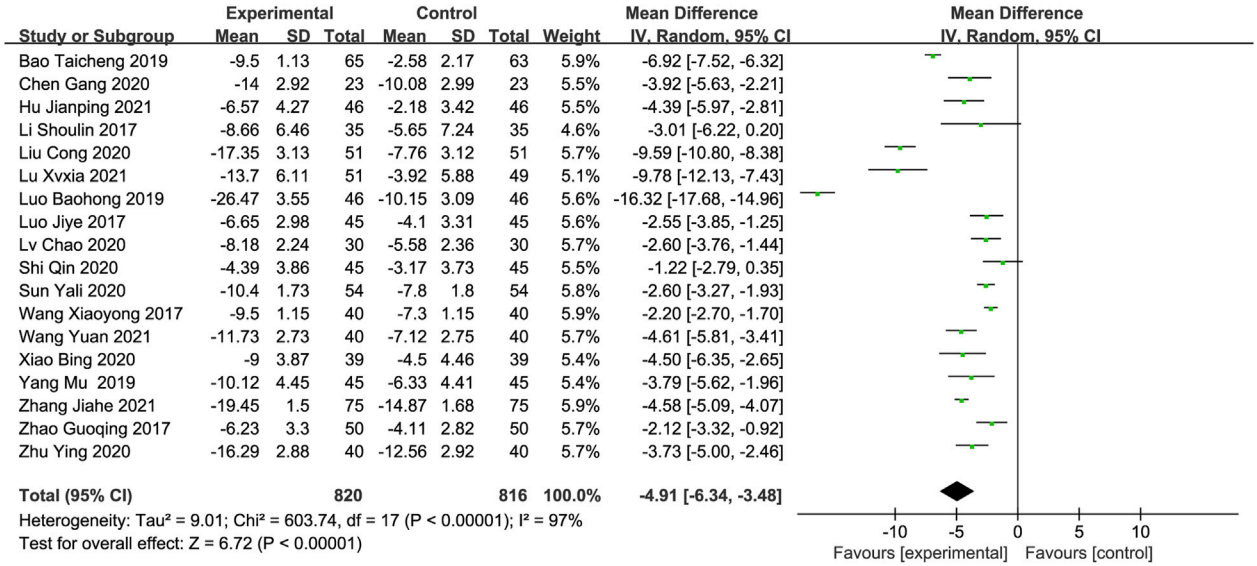

FIGURE 3
Risk of bias graph.

2021b; Lu, 2021). Two studies reported the mRS scores (Bao and Peng, 2019; Wang et al. 2024). Basic information and details of the included studies are presented in Tables 2 and 3, respectively.

Outcomes measurements

The National Institutes of Health Stroke Scalev (NIHSS)

All included studies (1,636 participants) reported the NIHSS score as an outcome measure. The meta-analysis found that the combination of DGMI and edaravone was more effective in reducing NIHSS scores than edaravone alone, based on the random-effects model (MD: −4.91; 95% CI: −6.34, −3.48; $p < 0.00001$, Figure 4). The studies showed significant heterogeneity ($Chi^2 = 603.74$; $I^2 = 97\%$; $p < 0.00001$), and the cause of this heterogeneity could not be determined using the sensitivity analysis.

Barthel Index (BI)

Only four studies (Luo and Chen, 2019; Zhang et al., 2021b; Hu et al., 2021; Wang and Fan, 2021), with 206 participants in each group, reported the BI score as an outcome measure. The meta-analysis demonstrated that the experimental group showed significantly greater improvement in BI than the control group, using a random-effects model. Sensitivity analysis revealed that the study conducted by Wang et al. (Wang and Fan, 2021) significantly

TABLE 2 Basic characteristics of the included studies.

Study	Sample size E C	Age (years) E/C	Male/ female E C	Population	Interventions E/C	Duration
Luo et al. Luo and Chen, (2019)	46 46	58.62 ± 5.14/58.58 ± 5.11	20/26 21/25	AIS within 6 h	DGMI + edaravone/ edaravone	14 d
Li et al. Li et al. (2017a)	35 35	66.40 ± 7.65/65.31 ± 7.81	20/15 23/12	AIS within 48 h	DGMI + edaravone + RT/edaravone + RT	14 d
Xiao et al. Xiao, (2020)	39 39	65.2 ± 6.5/66.0 ± 6.0	24/15 22/17	AIS within 48 h	DGMI + edaravone + RT/edaravone + RT	14 d
Shi et al. Shi and Fan, (2020)	45 45	69.5 ± 4.8/68.4 ± 5.1	28/17 26/19	AIS	DGMI + edaravone + RT/edaravone + RT	14 d
Lv et al. Lv et al. (2020)	30 30	62.20 ± 5.41/62.15 ± 5.36	17/13 18/12	AIS within 24 h	DGMI + edaravone + RT/edaravone + RT	14 d
Hu et al. Hu et al. (2021)	46 46	62.27 ± 3.68/62.35 ± 3.59	35/11 37/9	AIS within 6 h	DGMI + edaravone + RT/edaravone + RT	28 d
Liu et al. Liu, (2020)	51 51	60.62 ± 6.54/60.59 ± 6.51	31/20 30/21	AIS within 7 h	DGMI + edaravone/edaravone	14 d
Sun et al. Sun, (2020)	54 54	60 ± 6/60 ± 6	32/22 30/24	AIS within 24 h	DGMI + edaravone/edaravone	14 d
Yang et al. Yang, (2019)	45 45	53.04 ± 4.02/51.79 ± 4.33	25/20 29/16	AIS within 48 h	DGMI + edaravone + RT/edaravone + RT	14 d
Zhao et al. Zhao et al. (2017)	50 50	52.19 ± 2.28/53.18 ± 2.16	28/22 24/26	AIS within 7d	DGMI + edaravone/edaravone	14 d
Chen et al. Chen et al. (2020)	23 23	51.49 ± 2.71/51.57 ± 2.19	14/9 13/10	AIS within 6 h	DGMI + edaravone + RT/edaravone + RT	14 d
Zhu et al. Zhu, (2020)	40 40	64.29 ± 9.7/63.65 ± 9.3	21/19 22/18	AIS	DGMI + edaravone/edaravone	14 d
Bao et al. Bao and Peng, (2019)	65 63	64.50 ± 5.50/66.50 ± 5.00	30/35 30/33	AIS within 12 h	DGMI + edaravone + RT/edaravone + RT	14 d
Lu et al. Lu, (2021)	51 49	59.85 ± 10.24/60.02 ± 10.31	26/25 27/22	AIS	DGMI + edaravone + RT/edaravone + RT	NR
Zhang et al. Zhang et al. (2021b)	75 75	63.29 ± 3.62/62.38 ± 3.47	42/33 41/34	AIS within 6 h	DGMI + edaravone + RT/edaravone + RT	14 d
Wang et al. Wang et al. (2024)	40 40	75.5 ± 5.25/76.6 ± 5.25	22/18 19/21	AIS within 72 h	DGMI + edaravone + RT/edaravone + RT	14 d
Wang et al. Wang and Fan, (2021)	40 40	56.12 ± 1.42/55.86 ± 1.37	25/15 23/17	AIS within 48 h	DGMI + edaravone + RT/edaravone + RT	14 d
Luo et al. Luo et al. (2017)	45 45	75.46 ± 5.83/73.54 ± 6.32	27/18 28/17	AIS within 48 h	DGMI + edaravone + RT/edaravone + RT	14 d

RT: routine treatment; **AIS**: acute ischemic stroke; **E**: experimental group; **C**: control group; **DGMI**: diterpene ginkgolides meglumine injection; **NR**: not report.

10.3389/fphar.2023.1236684

TABLE 3 Additional information on the included studies.

Study	Drug dosage		Outcomes	Adverse effects
	DGMI	Edaravone		E/C
Luo et al. Luo and Chen, (2019)	25 mg + 250mL0.9%NS ivgtt qd	30 mg + 100mL0.9% NS ivgtt qd	effectiveness, NIHSS	1 case of diarrhea, 1 case of rash/1 case of diarrhea, 1 case of rash, 1 case of nausea
Li et al. Li et al. (2017a)	25 mg + 250mL0.9%NS ivgtt qd	30 mg + 100mL0.9% NS ivgtt bid	effectiveness, NIHSS	no adverse effects occurred
Xiao et al. Xiao, (2020)	25 mg + 250mL0.9%NS ivgtt qd	30 mg + 100mL0.9% NS ivgtt bid	effectiveness, NIHSS	not report
Shi et al. Shi and Fan, (2020)	25 mg ivgtt qd	30 mg ivgtt bid	NIHSS,Lp-PLA2,NSE,GFAP	not report
Lv et al. Lv et al. (2020)	25 mg + 250mL0.9%NS ivgtt qd	30 mg + 250mL0.9% NS ivgtt bid	NIHSS,ADL	not report
Hu et al. Hu et al. (2021)	25 mg ivgtt qd	30 mg ivgtt qd	NIHSS,FAM,BI,GABA,Gly,Hcy,NE,MPO,TNF	3 cases of cerebral vasospasm, 1 case of hydrocephalus, and 1 case of subcutaneous hemorrhage/cerebral vasospasm 10 cases, hydrocephalus 4 cases, subcutaneous hemorrhage 4 cases hydrocephalus 4 cases, subcutaneous hemorrhage 4 cases
Liu et al. Liu, (2020)	25 mg + 250mL0.9%NS ivgtt qd	30 mg + 150mL0.9% NS ivgtt qd	NIHSS, effectiveness,PV	not report
Sun et al. Sun, (2020)	25 mg + 250mL0.9%NS ivgtt qd	15 mg ivgtt qd	NIHSS,SOD,MDA,IL-6,CRP	not report
Yang et al. Yang, (2019)	25 mg + 250mL0.9%NS ivgtt qd	30 mg + 100mL0.9% NS ivgtt bid	NIHSS,Hcy,NSE	not report
Zhao et al. Zhao et al. (2017)	25 mg + 250mL0.9%NS ivgtt qd	30 mg + 100mL0.9% NS ivgtt qd	NIHSS, effectiveness	not report
Chen et al. Chen et al. (2020)	25 mg + 250mL0.9%NS ivgtt qd	30 mg + 100mL0.9% NS ivgtt bid	NIHSS,ADL,hematocrit,PV, erythrocyte deformation index, platelet adhesion rate	not report
Zhu et al. Zhu, (2020)	25 mg + 250mL0.9%NS ivgtt qd	30 mg + 100mL0.9% NS ivgtt bid	NIHSS	not report
Bao et al. Bao and Peng, (2019)	20 mg + 250mL0.9%NS ivgtt qd	30 mg + 100mL0.9% NS ivgtt bid	NIHSS,mRS	not report
Lu et al. Lu, (2021)	25 mg + 250mL0.9%NS ivgtt qd	30 mg ivgtt bid	NIHSS,FAM,MMSE, effectiveness,hematocrit, platelet adhesion rate,PV	1 case of headache, 1 case of nausea, 1 case of diarrhea, 1 case of chills/1 case of fever, 1 case of chest tightness, 1 case of rash, 1 case of dyspnea, 1 case of palpitations
Zhang et al. Zhang et al. (2021b)	25 mg + 250mL0.9%NS ivgtt qd	30 mg + 100mL0.9% NS ivgtt bid	NIHSS,BI,QOLISP,NSE,CRP,hematocrit,PV, erythrocyte deformation index, platelet adhesion rate	not report
Wang et al. Wang et al. (2024)	25 mg + 250mL0.9%NS ivgtt qd	30 mg + 100mL0.9% NS ivgtt bid	NIHSS,mRS,effectiveness	no adverse effects occurred
Wang et al. Wang and Fan, (2021)	25 mg + 250mL0.9%NS ivgtt qd	30 mg + 100mL0.9% NS ivgtt bid	NIHSS,BI,SOD,MDA,CRP,effectiveness	not report

(Continued on following page)

TABLE 3 (*Continued*) Additional information on the included studies.

Study	Drug dosage		Outcomes	Adverse effects
	DGMI	Edaravone		E/C
Luo et al. Luo et al. (2017)	25 mg + 100mL0.9%NS ivgtt qd	30 mg + 100mL0.9% NS ivgtt bid	NIHSS,BI,hs-CRP,NSE,effectiveness	not report

NS: normal saline; **Lp-PLA2**: lipoprotein-associated phospholipaseA2; **CRP**: C-reactive protein; **GABA**: gamma-aminobutyric acid; **Gly**: glycine; **Hcy**: homocysteine; **NE**: noradrenaline; **MPO**: myeloperoxidase; **TNF**: tumor necrosis factor-α; **PV**: plasma viscosity; **BI**: barthel index; **NSE**: neuron-specific enolase; **GFAP**: glial fibrillary acidic protein; **SOD**: superoxide dismutase; **IL-6**: Interleukin-6; **mRS**: modified Rankin scale; **hs-CRP**: high sensitivity C-reactive protein; **QOLISP**: quality of life inventory for stroke patients; **MMSE**: Mini-mental State Examination; **DGMI**: diterpene ginkgolides meglumine injection; **MDA**: Malondialdehyde.

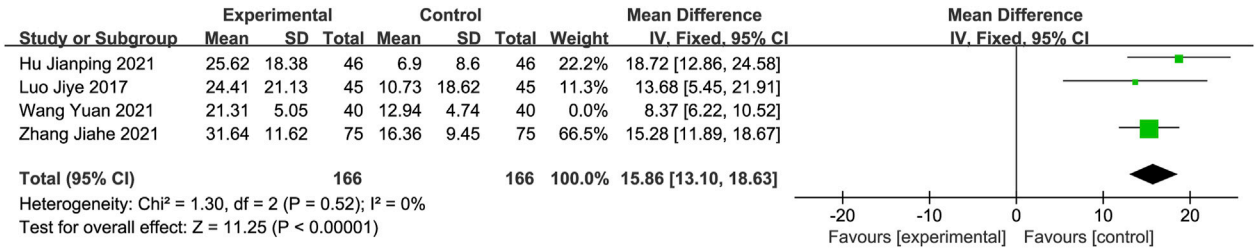

FIGURE 4
Forest plot of NIHSS scores.

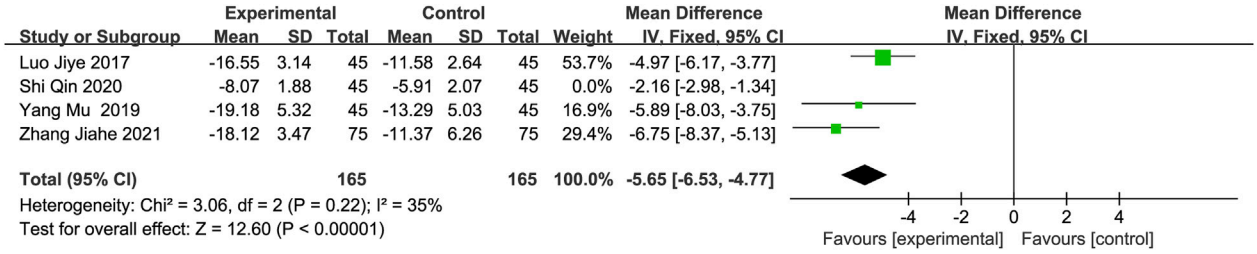

FIGURE 5
Forest plot of BI after excluding Wang's study.

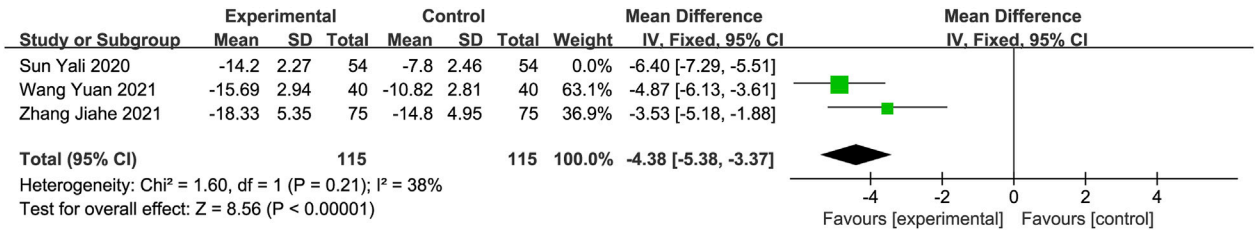

FIGURE 6
Forest plot of NSE after excluding Shi's study.

influenced the heterogeneity of this group. After excluding this study, the heterogeneity disappeared. The results were then analyzed using a fixed-effects model (MD: 15.86; 95% CI: 13.10, 18.63; $p < 0.00001$). Heterogeneity was assessed using Chi^2 and I^2 statistics, which showed no significant heterogeneity ($Chi^2 = 1.30$; $I^2 = 0\%$; $p = 0.52$, Figure 5).

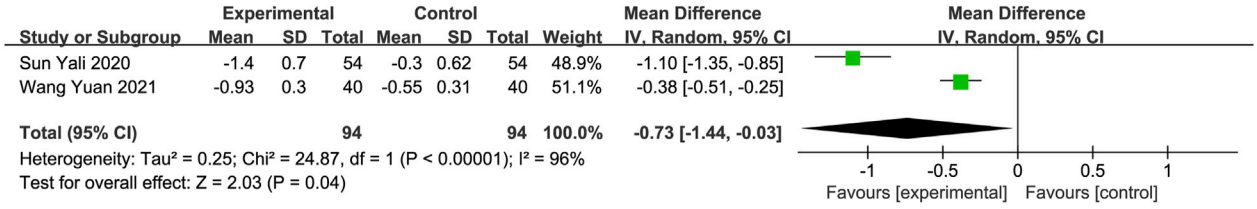

FIGURE 7
Forest plot of CRP after excluding Sun's study.

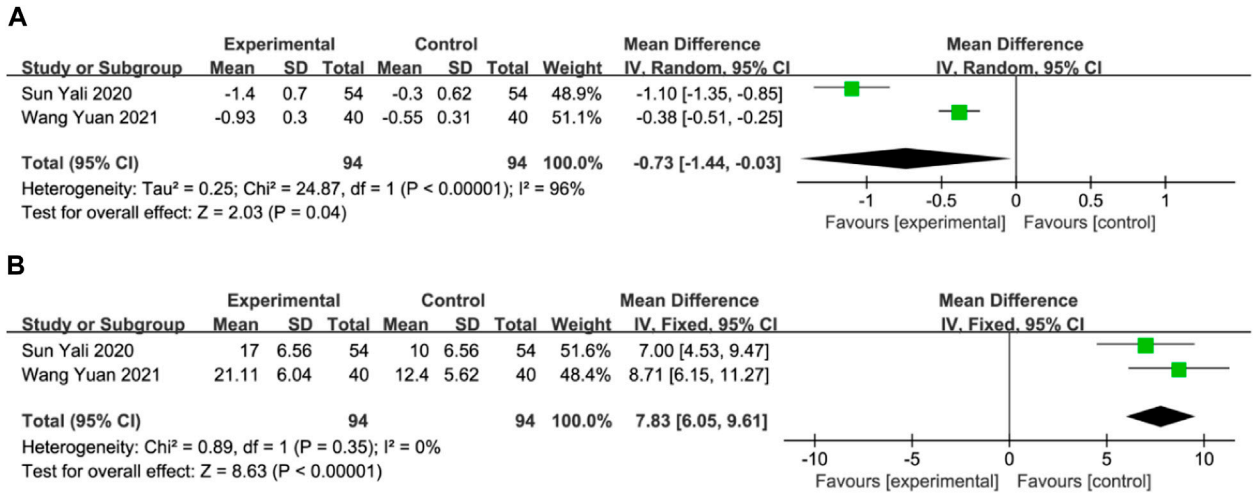

FIGURE 8
Forest plot of MDA **(A)** and SOD **(B)**.

Neuron-specific enolase (NSE)

Four studies (Luo and Chen, 2019; Yang, 2019; Shi and Fan, 2020; Zhang et al., 2021b) with 210 participants in each group reported NSE levels as an outcome measure. The random-effects model indicated that DGMI effectively reduced NSE levels. However, sensitivity analysis revealed that the study conducted by Shi et al. (Shi and Fan, 2020) had a significant effect on heterogeneity. After excluding this study, the heterogeneity decreased. A meta-analysis using a fixed-effects model confirmed this conclusion (MD: −5.65; 95% CI: −6.53, −4.77; $p < 0.00001$; heterogeneity: $Chi^2 = 3.06$; $I^2 = 35\%$; $p = 0.22$, Figure 6).

C-reactive protein (CRP)

CRP levels were reported in three studies (Sun, 2020; Zhang et al., 2021b; Wang and Fan, 2021) involving 338 participants. Meta-analysis using a random-effects model demonstrated a significant reduction in CRP levels in the experimental group compared to the control group. The sensitivity analysis identified the study conducted by Sun et al. (Sun, 2020) as a significant contributor to heterogeneity. After excluding this study, residual heterogeneity remained within an acceptable range. Therefore, a fixed-effects model was used for the analysis, resulting in the same conclusion (MD: −4.38; 95% CI: −5.38, −3.37; $p < 0.00001$; heterogeneity: $Chi^2 = 1.60$; $I^2 = 38\%$; $p = 0.21$, Figure 7).

Malondialdehyde (MDA) and superoxide dismutase (SOD)

Two studies with a total of 188 participants assessed MDA and SOD levels as outcome measures (Sun, 2020; Wang and Fan, 2021). The random-effects model revealed a significant reduction in MDA in the DGMI group compared to that in the control group (MD: −0.73; 95% CI: −1.44, −0.03; $p = 0.04$; heterogeneity: $Chi^2 = 24.87$; $I^2 = 96\%$; $p < 0.00001$, Figure 8A). No heterogeneity was observed in the two studies regarding SOD. A fixed-effects model was used for the meta-analysis, which demonstrated a significant improvement in SOD levels in the experimental group compared with the control group (MD: 7.83; 95% CI: 6.05, 9.61; $p < 0.00001$; heterogeneity: $Chi^2 = 0.89$; $I^2 = 0\%$; $p = 0.35$, Figure 8B).

Blood Rheology Indices

Three studies reported the hematocrit, plasma viscosity, platelet adhesion rate, and erythrocyte deformation index (Chen et al., 2020; Zhang et al., 2021b; Lu, 2021), whereas two studies reported the erythrocyte deformation index (Chen et al., 2020; Zhang et al., 2021b). Meta-analysis using a fixed-effects model revealed that the DGMI group was more effective than edaravone alone in reducing the hematocrit (MD: −0.66; 95% CI: −0.81, −0.51; $p < 0.00001$;

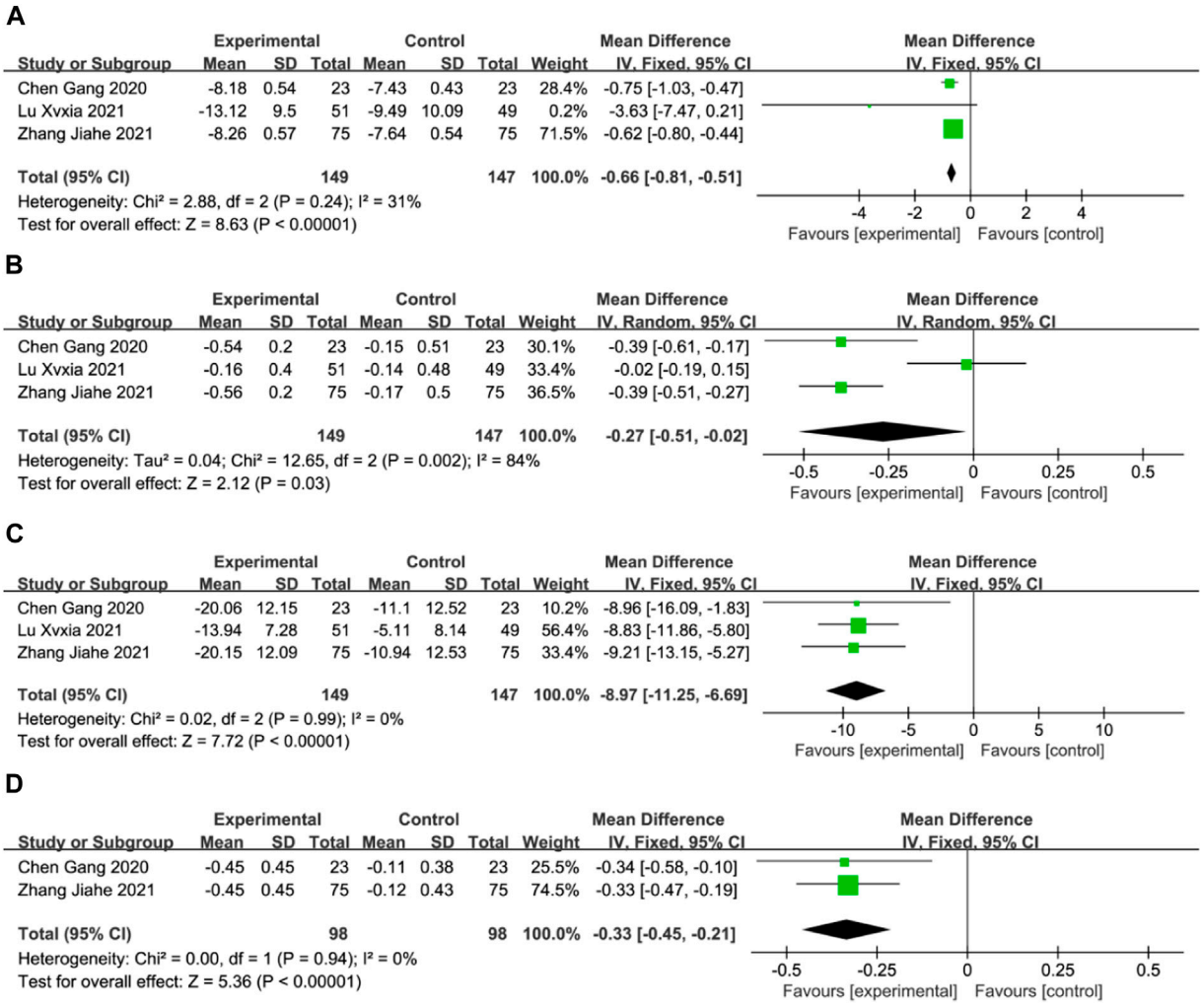

FIGURE 9
Forest plot of Blood Rheology Indices (A: forest plot of hematocrit, **(B)** forest plot of plasma viscosity, **(C)** forest plot of platelet adhesion rate, **(D)** forest plot of platelet erythrocyte deformation index).

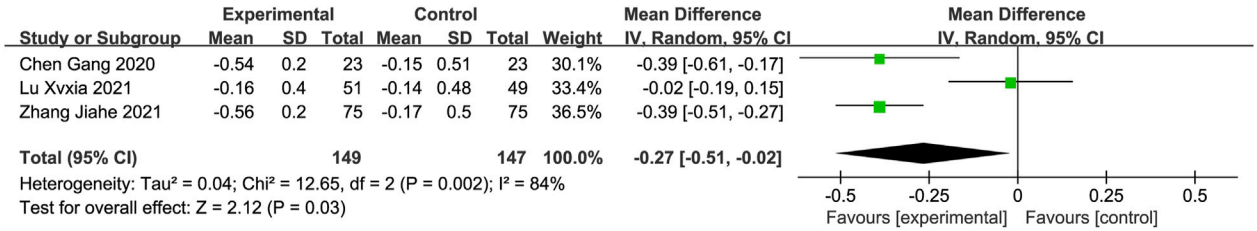

FIGURE 10
Forest plot of mRS.

heterogeneity: $Chi^2 = 2.88$; $I^2 = 31\%$; $p = 0.24$, Figure 9A), platelet adhesion rate (MD: −8.97; 95% CI: −11.25, −6.69; $p < 0.00001$; heterogeneity: $Chi^2 = 0.02$; $I^2 = 0\%$; $p = 0.99$, Figure 9 C), and erythrocyte deformation index (MD: −0.33; 95% CI: −0.45, −0.21; $p < 0.00001$; heterogeneity: $Chi^2 = 0.00$; $I^2 = 0\%$; $p = 0.94$, Figure 9 D).

Due to heterogeneity in plasma viscosity, the meta-analysis was performed using a random-effects model, and the results indicated that DGMI was effective in reducing plasma viscosity compared to the control group (MD: −0.27; 95% CI: −0.51, −0.02; $p = 0.003$; heterogeneity: $Chi^2 = 12.65$; $I^2 = 84\%$; $p = 0.002$, Figure 9B).

Modified Rankin Scale (mRS)

Only two studies reported mRS scores (Bao and Peng, 2019; Wang et al. 2024), with 105 participants in the DGMI group and 103 in the control group. Data analysis using a fixed-effects model revealed that DGMI was more effective in reducing mRS than the control group (MD: −0.39; 95% CI: −0.52, −0.25; $p < 0.00001$; heterogeneity: $Chi^2 = 0.77$; $I^2 = 0\%$; $p = 0.38$, Figure 10).

Adverse reactions

Only three of the 18 studies analyzed (Luo and Chen, 2019; Hu et al., 2021; Lu, 2021) provided information on adverse reactions, as presented in Table 2. Although the adverse reactions reported in the experimental group were milder and fewer than those in the control group, they did not interfere with the treatment or lead to worse outcomes. This finding suggests the safety of DGMI in combination with edaravone. However, the inclusion of a limited number of articles and the absence of adverse reactions in several studies could introduce bias when assessing treatment safety.

Discussion

Ischemic stroke, is the second leading cause of death worldwide and accounts for approximately 68% of all cerebrovascular diseases. The prevalence of ischemic stroke is a significant health concern owing to the characteristics of modern lifestyles, such as excessive consumption of oil, sugar, salt, and fat. Clinical research has focused on treating ischemic stroke and implementing primary prevention measures to address unhealthy lifestyles. Current treatment approaches primarily involve anticoagulation and thrombolysis with the aim of restoring blood flow in obstructed blood vessels. Thrombolytic drugs, when administered at specific doses, are considered the optimal treatment because of their ability to restore blood flow without inducing adverse effects, such as bleeding. However, certain medical conditions and patient factors limit the number of individuals who can receive thrombolytic therapy within the recommended timeframe. Consequently, clinicians are exploring alternative treatment options to improve their effectiveness.

In China, numerous clinical trials have demonstrated that combining TCM with Western medicine for the treatment of ischemic stroke can provide additional advantages. These include reducing the occurrence of complications, alleviating symptoms, lowering disability rates, and improving the long-term survival rates. The pathogenesis of acute ischemic stroke is complex and encompasses small hypertensive arteriosclerosis, cerebral atherosclerosis, reduced cerebral blood flow, hypercoagulability, hyper-adhesiveness of the blood, platelet aggregation, and thrombus formation. This intricate mechanism disrupts blood flow and causes neurological deficits in the brain. Infarct lesions in ischemic stroke can be categorized as ischemic foci and ischemic penumbra. During reperfusion in the ischemic penumbra, excess free radicals are generated, potentially resulting in nerve cell damage and apoptosis.

Edaravone is frequently prescribed for patients with acute ischemic stroke who are unable to receive intravenous thrombolytic therapy in time (Edaravone Acute Infarction Study Group, 2003). It functions as a potent hydroxyl radical scavenger and an antioxidant. It rapidly crosses the blood-brain barrier and has various beneficial effects, such as scavenging free radicals, inhibiting lipid peroxidation, and providing protection against apoptosis, necrosis, cytokine-induced damage, and neurovascular injury (Inokuchi et al., 2009; Kikuchi et al., 2009). Diterpene ginkgolide meglumine injection (DGMI) is composed of ginkgolides A, B, and K, which are the primary constituents derived from *Ginkgo biloba*. According to TCM, these components promote blood circulation, activate blood flow, and resolve blood stasis. From a modern medicine perspective, they can significantly dilate blood vessels in the area affected by cerebral ischemia, reduce vascular resistance, scavenge oxygen free radicals, and affect the concentration and ratio of central neurotransmitters, such as dopamine, dihydroxyphenylacetic acid, and 5-hydroxytryptamine. These neurotransmitters are closely associated with cerebral ischemia and reperfusion (Ma et al., 2012; Zhang et al., 2015; Zhang et al., 2016). However, the mechanism of action of DGMI in brain protection extends beyond its effect on neurotransmitters.

SOD activity decreases and MDA content increases following cerebral ischemia, resulting in alterations in mitochondrial permeability and release of apoptotic factors. Caspases are crucial for apoptosis, and animal experiments have demonstrated that DGMI can reduce caspase activity and prevent neuronal cell apoptosis following cerebral ischemia-reperfusion. This could be one of the mechanisms by which DGMI exerts neuroprotective effects (Yan et al., 2010; Chen et al., 2014). Blood rheological indicators are significant in the pathogenesis of cerebral infarction. The active ingredient in *G. biloba,* diterpene lactone dextran, exhibits platelet-activating factor receptor antagonism, which can prevent platelet activation and inhibit platelet aggregation by antagonizing the PI3K-Akt signaling pathway, reducing thrombus formation, and correcting hemodynamic abnormalities (Liu et al., 2015; Song et al., 2021). NSE is a protein that specifically indicates brain tissue injuries. The detection of NSE can be used to diagnose acute cerebral infarction and evaluate the extent of tissue damage. DGMI combined with edaravone has been shown to significantly reduce NSE concentration (Gelderblom et al., 2013).

In conclusion, the combination of DGMI and edaravone showed therapeutic benefits in patients with acute ischemic stroke. It has been observed to decrease NIHSS scores, improve the Barthel Index and other scales, decrease MDA levels, improve SOD activity, and positively affect blood rheological indices. Furthermore, the combination therapy demonstrated a favorable safety profile. However, it is important to note that the literature included in this study was of low quality, which inevitably introduced bias and affected the overall quality of the evidence. Therefore, more rigorous and high-quality clinical trials are necessary to validate the efficacy of DGMI combined with edaravone.

Comparison with previous studies

To date, only two meta-analyses on DGMI treatment for cerebral infarction have been published in China. One study

analyzed 26 studies involving 2,332 patients (Zhang et al., 2021c). The results of the study showed that the NIHSS scores, Barthel Index scores, and total effective rates were better than those of a single Western medicine. However, this conclusion was based on an analysis of randomized controlled trials that combined DGMI with multiple Western medications. This could potentially introduce bias and compromise the reliability of the conclusions. The other study analyzed data from 9 randomized controlled trials involving 1,129 patients (Jin et al., 2019).The study found that DGMI was effective in treating cerebral infarction and showed positive outcomes in terms of improving NIHSS and ADL scores, indicating its high clinical efficacy. However, the control group in this study was not limited to a specific treatment method and included conventional treatment and other *G. biloba* extracts. Moreover, this study examined both the acute and recovery stages of cerebral infarction. Owing to the presence of confounding variables, definitive conclusions cannot be drawn. Furthermore, neither of these studies analyzed laboratory indicators, and clinical efficacy was the primary outcome measure. The use of different definitions of clinical efficacy can affect the effectiveness of meta-analyses for identifying heterogeneity. Therefore, this study excluded clinical efficacy analysis, focused on objective indicators, such as laboratory parameters, and specifically limited the scope to acute ischemic stroke (AIS) and the drugs DGMI and edaravone. This approach provides more direct evidence for evaluating the efficacy of DGMI and enriches the scope of the study. Additionally, this study manually excluded studies with suspicious or incomplete data to minimize heterogeneity. The research design was clear and focused, and all included studies were randomized controlled trials, thus minimizing bias. Heterogeneity and subgroup analyses were performed after data analysis, making the logical flow more rigorous and the conclusions more reliable.

Strengths of this study

This study summarizes all relevant clinical studies on the topic and provides a comprehensive evaluation of the efficacy and safety of combining DGMI with edaravone for the treatment of acute ischemic stroke. This study has significant therapeutic implications owing to the limited benefits of Western medicine alone in treating AIS and the observed additional benefits in patients receiving adjuvant TCM treatment. Furthermore, the study's research objective, robust methodology involving randomized controlled trials, and comprehensive analysis encompassing heterogeneity and subgroup analysis contribute to the reliability of the conclusions.

Another strength of this study is its focus on a highly pure form of TCM extract, DGMI, which exhibits higher purity than other TCM injections. Moreover, the efficacy of each component of DGMI, namely, ginkgolides A, B, and K, is supported by robust evidence and established mechanisms of action (Nabavi et al., 2015; Chen et al., 2018). Recent studies have demonstrated that TCM offers numerous complementary advantages for the treatment of diseases (Wang et al., 2023). This study aligns with the ongoing endeavor to modernize TCM and enhance its integration with Western medicine, thereby offering potential clinical benefits.

Limitations

However, this study has certain limitations. First, there may be a language bias due to the inclusion of exclusively Chinese-language papers. Second, the quality of the included studies was low as they lacked sufficient descriptions of allocation concealment, blinding, dropped visits, or participant attrition. Third, inconsistencies were observed in the treatment courses, drug dosages, and underlying treatments across the trials. This could potentially result in biased outcomes and contribute to a lack of homogeneity in some outcome indicators. Additionally, the total sample size was relatively small, with only 1,636 cases, all of which were single-center trials, potentially affecting the reliability of the findings. Moreover, the limited generalizability of the conclusions is attributed to the potential influences of the underlying diseases of the patients and the use of single outcome indicators. The long-term outcomes of patients with AIS who receive a combination of the two drugs remain uncertain. Finally, only three studies reported adverse effects, limiting our ability to confirm their relationship with the combination of the two drugs. Further safety evaluations should be conducted using larger sample sizes in future clinical studies.

Conclusion

In conclusion, available evidence suggests that DGMI can enhance the effectiveness of edaravone in the treatment of patients with acute ischemic stroke. However, the low quality of the included literature introduces bias and necessitates more rigorous and high-quality clinical trials to validate these findings further.

Data availability statement

The original contributions presented in the study are included in the article/Supplementary Materials, further inquiries can be directed to the corresponding author.

Author contributions

MY and JW conceived and drafted the systematic review, registered the protocol, conducted literature screening, collected and analyzed the data, and wrote the first draft of the paper. LW, KW, and LL participated in the study design, data analysis, and content correction of the paper. TS, HZ, and MiZ contributed to data collection and analysis and provided support for statistical analysis. LZ and SY participated in the literature review and revised the contents of the article. JL provided overall guidance on research plan design and critically revised the content of the study.

Funding

This research is supported by the Fundamental Research Funds for the Central Universities (2020-JYB-ZDGG-131).

Conflict of interest

The authors declare that the research was conducted in the absence of any commercial or financial relationships that could be construed as a potential conflict of interest.

Publisher's note

All claims expressed in this article are solely those of the authors and do not necessarily represent those of their affiliated organizations, or those of the publisher, the editors and the reviewers. Any product that may be evaluated in this article, or claim that may be made by its manufacturer, is not guaranteed or endorsed by the publisher.

Supplementary material

The Supplementary Material for this article can be found online at: https://www.frontiersin.org/articles/10.3389/fphar.2023.1236684/full#supplementary-material

References

Bao, T. C., and Peng, M. (2019). Clinical effect analysis of ginkgo diterpene lactone glucosamine injection in the treatment of acute progressive cerebral infarction. *Heilongjiang J. Traditional Chin. Med.* 48 (03), 1–2.

Chen, C. M., Zhou, J., Chen, J., Chang, X. J., Zhang, L. L., Wang, Z. Z., et al. (2014). Effects of ginkgo biloba diterpene lactone glucosamine injection on acute cerebral ischemia-reperfusion injury in rats. *Chin. J. Exp. Traditional Med. Formulae* 20 (17), 133–136. doi:10.13422/j.cnki.syfjx.2014170133

Chen, G., Lu, W., and Fu, Y. (2020). Effect of ginkgo biloba diterpene lactone glucosamine injection combined with edaravone on NIHSS scores in patients with acute cerebral infarction. *Contemp. Med.* 26 (26), 26–28. doi:10.3969/j.issn.1009-4393.2020.26.012

Chen, M., Zou, W., Chen, M., Cao, L., Ding, J., Xiao, W., et al. (2018). Ginkgolide K promotes angiogenesis in a middle cerebral artery occlusion mouse model via activating JAK2/STAT3 pathway. *Eur. J. Pharmacol.* 833, 221–229. doi:10.1016/j.ejphar.2018.06.012

Edaravone Acute Infarction Study Group (2003). Effect of a novel free radical scavenger, edaravone (MCI-186), on acute brain infarction. Randomized, placebo-controlled, double-blind study at multicenters. *Cerebrovasc. Dis.* 15 (3), 222–229. doi:10.1159/000069318

Feigin, V. L., Forouzanfar, M. H., Krishnamurthi, R., Mensah, G. A., Connor, M., Bennett, D. A., et al. (2014). Global and regional burden of stroke during 1990-2010: findings from the global burden of disease study 2010. *Lancet* 383 (9913), 245–254. doi:10.1016/s0140-6736(13)61953-4

Gao, C. Y., Wu, C. H., Zhao, J. G., Cao, X. L., Xu, B. Y., Wu, B. S., et al. (2017). Chinese guidelines for the diagnosis and treatment of cerebral infarction with Chinese and Western medicine. *Chin. J. Integr. Traditional West. Med.* 38 (02), 136–144. doi:10.7661/j.cjim.20171221.483

GBD 2019 Stroke Collaborators (2021). Global, regional, and national burden of stroke and its risk factors, 1990-2019: a systematic analysis for the Global Burden of Disease Study 2019. *Lancet Neurol.* 20 (10), 795–820. doi:10.1016/S1474-4422(21)00252-0

Gelderblom, M., Daehn, T., Schattling, B., Ludewig, P., Bernreuther, C., Arunachalam, P., et al. (2013). Plasma levels of neuron specific enolase quantify the extent of neuronal injury in murine models of ischemic stroke and multiple sclerosis. *Neurobiol. Dis.* 59, 177–182. doi:10.1016/j.nbd.2013.07.017

Heinrich, M., Jalil, B., Abdel-Tawab, M., Echeverria, J., Kulić, Ž., McGaw, L. J., et al. (2022). Best Practice in the chemical characterisation of extracts used in pharmacological and toxicological research-The ConPhyMP-Guidelines. *Front. Pharmacol.* 13, 953205. doi:10.3389/fphar.2022.953205

Higgins, J. P., Altman, D. G., Gøtzsche, P. C., Jüni, P., Moher, D., Oxman, A. D., et al. (2011). The Cochrane Collaboration's tool for assessing risk of bias in randomised trials. *BMJ* 343, d5928. doi:10.1136/bmj.d5928

Hu, J. P., Guo, J., Zhang, T. H., Jin, J., Chen, Z. J., Wang, J. C., et al. (2021). Efficacy and safety analysis of ginkgo diterpene lactone glucosamine and butalbital combined with edaravone in the treatment of phlegm-stasis blocked cerebral infarction. *Hebei Med. J.* 43 (2), 219–222. doi:10.3969/j.issn.1002-7386.2021.02.012

Inokuchi, Y., Imai, S., Nakajima, Y., Shimazawa, M., Aihara, M., Araie, M., et al. (2009). Edaravone, a free radical scavenger, protects against retinal damage *in vitro* and *in vivo*. *J. Pharmacol. Exp. Ther.* 329 (2), 687–698. doi:10.1124/jpet.108.148676

Jin, F. H., Chen, J., and Yang, W. C. (2019). The efficacy and safety of diterpene ginkgolides meglumine injection in stroke: a Meta analysis. *J. Pharm. Pract. Serv.* 37 (01), 80–85. doi:10.3969/j.issn.1006-0111.2019.01.019

Kikuchi, K., Kawahara, K., Tancharoen, S., Matsuda, F., Morimoto, Y., Ito, T., et al. (2009). The free radical scavenger edaravone rescues rats from cerebral infarction by attenuating the release of high-mobility group box-1 in neuronal cells. *J. Pharmacol. Exp. Ther.* 329 (3), 865–874. doi:10.1124/jpet.108.149484

Li, J. F. (2019). Effect of ginkgo biloba diterpene lactone glucosamine injection combined with argatroban on NIHSS score and blood rheology in patients with acute ischemic stroke. *J. North Pharm.* 16 (05), 118–119. doi:10.3969/j.issn.1672-8351.2019.05.094

Li, S. L., Zhou, W., Zhu, X. H., Xu, S., Li, J., Wu, M., et al. (2017a). Efficacy of edaravone combined with ginkgo bilaterolactone glucosamine injection in the treatment of acute cerebral infarction. *Clin. Res. Pract.* 2 (18), 35–36. doi:10.19347/j.cnki.2096-1413.201718016

Li, Y., Wu, Y., Yao, X., Hao, F., Yu, C., Bao, Y., et al. (2017b). Ginkgolide A ameliorates LPS-induced inflammatory responses *in vitro* and *in vivo*. *Int. J. Mol. Sci.* 18 (4), 794. doi:10.3390/ijms18040794

Liu, C. (2020). Efficacy of ginkgo biloba diterpene lactone glucosamine in combination with edaravone in the treatment of progressive ischemic stroke. *Clin. Res.* 28 (6), 71–73.

Liu, J., Heng, W. W., Liu, H., Zhang, G. Q., Wang, J. B., Li, J., et al. (2019). Analysis of the efficacy of ginkgo diterpene lactone glucosamine injection combined with butylphthalide in the treatment of acute cerebral infarction. *Chin. J. Pract. Nerv. Dis.* 22 (17), 1900–1904. doi:10.12083/SYSJ.2019.17.318

Liu, Q., Xu, Z. L., Zhou, J., Li, N., Bi, Y. A., Wang, Z. Z., et al. (2015). Protective effects of ginkgo biloba diterpene lactone glucosamine injection on SH-SY5Y cells damaged by glucose and oxygen deprivation. *Chin. Pharmacol. Bull.* 31 (07), 994–999. doi:10.3969/j.issn.1001-1978.2015.07.021

Liu, Y., Shields, L. B. E., Gao, Z., Wang, Y., Zhang, Y. P., Chu, T., et al. (2017). Current understanding of platelet-activating factor signaling in central nervous system diseases. *Mol. Neurobiol.* 54 (7), 5563–5572. doi:10.1007/s12035-016-0062-5

Liu, Y. G., Li, F. J., Wang, J., and Wang, X. D. (2010). Effects of Ginkgolide B on inflammation induced by cerebral ischemia-reperfusion in rats. *J. Chin. Med. Mater.* 33 (04), 578–580. doi:10.13863/j.issn1001-4454.2010.04.036

Lu, X. X. (2021). Effectiveness and safety analysis of ginkgo biloba diterpene lactone glucosamine injection in the treatment of acute cerebral infarction combined with multiple intracranial artery stenosis. *China Pract. Med.* 16 (23), 149–151. doi:10.14163/j.cnki.11-5547/r.2021.23.051

Luo, B. H., and Chen, J. J. (2019). Study on the effectiveness of a new ginkgo biloba preparation ginkgo diterpene lactone glucosamine injection in the treatment of acute cerebral infarction. *Strait Pharm. J.* 31 (9), 159–161. doi:10.3969/j.issn.1006-3765.2019.09.060

Luo, J. Y., Xie, Y. P., Chen, X. B., Chen, X. F., and Wang, Y. L. (2017). Efficacy of ginkgo biloba diterpene lactone glucosamine injection in the treatment of acute cerebral infarction in the elderly. *World Latest Med. Inf.* 17 (58), 16–18. doi:10.19613/j.cnki.1671-3141.2017.58.007

Lv, C., Tang, K. D., Feng, Q., Wang, Y. Z., and Feng, Y. B. (2020). Efficacy of edaravone combined with ginkgo biloba diterpene lactone glucosamine injection in the treatment of acute cerebral infarction. *World Latest Med. Inf.* 20 (89), 213–214. doi:10.3969/j.issn.1671-3141.2020.89.098

Ma, S., Yin, H., Chen, L., Liu, H., Zhao, M., and Zhang, X. (2012). Neuroprotective effect of ginkgolide K against acute ischemic stroke on middle cerebral ischemia occlusion in rats. *J. Nat. Med.* 66 (1), 25–31. doi:10.1007/s11418-011-0545-7

Moher, D., Liberati, A., Tetzlaff, J., Altman, D. G., and PRISMA Group (2009). Preferred reporting items for systematic reviews and meta-analyses: the PRISMA statement. *J. Clin. Epidemiol.* 62 (10), 1006–1012. doi:10.1016/j.jclinepi.2009.06.005

Nabavi, S. M., Habtemariam, S., Daglia, M., Braidy, N., Loizzo, M. R., Tundis, R., et al. (2015). Neuroprotective effects of ginkgolide B against ischemic stroke: a review of current literature. *Curr. Top. Med. Chem.* 15 (21), 2222–2232. doi:10.2174/1568026615666150610142647

Peng, B., and Wu, B. (2018). Chinese guidelines for the diagnosis and treatment of acute ischemic stroke 2018. *Chin. J. Neurology* 51 (09), 666–682. doi:10.3760/cma.j.issn.1006-7876.2018.09.004

Shi, Q., and Fan, T. (2020). Observation on the effect of edaravone combined with ginkgo biloba diterpene lactone glucosamine injection in elderly patients with cerebral infarction. *Med. Forum* 24 (31), 4506–4507. doi:10.19435/j.1672-1721.2020.31.037

Song, S., Liang, L, Fonarow, G. C., Smith, E. E., Bhatt, D. L., Matsouaka, R. A., et al. (2019). Comparison of clinical care and in-hospital outcomes of asian american and white patients with acute ischemic stroke. *JAMA Neurol.* 76, 430–439. doi:10.1001/jamaneurol.2018.4410

Song, Y. Q., Ma, J., and Li, G. (2021). Effects of ginkgo biloba diterpene lactone glucosamine combined with butylphthalide on neurological function and blood rheology in patients with acute cardiogenic stroke. *Drug Eval.* 18 (14), 891–893. doi:10.19939/j.cnki.1672-2809.2021.14.19

Sun, T., Wang, P., Deng, T., Tao, X., and Xu, Y. (2021). Effect of panax notoginseng saponins on focal cerebral ischemia-reperfusion in rat models: a meta-analysis. *Front. Pharmacol.* 11, 572304. doi:10.3389/fphar.2020.572304

Sun, Y. L. (2020). Clinical effect study of ginkgo diterpene lactone glucosamine combined with edaravone in the treatment of ischemic stroke. *Chin. Remedies Clin.* 20 (21), 3599–3601. doi:10.11655/zgywylc2020.21.026

Wang, C. L. (2019). Analysis of the efficacy of ginkgo diterpene lactone glucosamine injection combined with injectable eurycomycin in the treatment of 53 cases of acute ischemic stroke. *J. North Pharm.* 16 (05), 28–29. doi:10.3969/j.issn.1672-8351.2019.05.021

Wang, W., Jiang, B., Sun, D., Sun, H., Wang, L., Wang, L., et al. (2017). Prevalence, incidence, and mortality of stroke in China: results from a nationwide population-based survey of 480 687 adults. *Circulation* 135 (8), 759–771. doi:10.1161/CIRCULATIONAHA.116.025250

Wang, X., Gu, Z. L., Qin, Z. H., and Zhang, H. L. (2007). Protective effect of ginkgolide A and B mixture on permanent focal cerebral ischemia in rats. *Chin. Traditional Herb. Drugs* (02), 241–244. doi:10.3321/j.issn:0253-2670.2007.02.032

Wang, X. Y., Luo, S. Z., and Cui, C. L. (2024). Clinical study on the treatment of acute cerebral infarction with ginkgo diterpene lactone glucosamine injection.[J]. *Hebei Journal of Traditional Chinese, 2017* 39 (9), 1328–1331. doi:10.3969/j.issn.1002-2619.2017.09.012

Wang, Y., and Fan, T. (2021). Clinical observation of ginkgo diterpene lactone glucosamine injection in the treatment of acute ischemic stroke. *China's Naturop.* 29 (20), 85–87. doi:10.19621/j.cnki.11-3555/r.2021.2031

Wang, Y., Liu, S., Zhang, Y., Zhu, G., Wang, H., Xu, B., et al. (2023). Effect of traditional Chinese medicine on postoperative depression of breast cancer: a systematic review and meta-analysis. *Front. Pharmacol.* 14, 1019049. doi:10.3389/fphar.2023.1019049

Xiao, B. (2020). Efficacy analysis of edaravone combined with ginkgo biloba diterpene lactone glucosamine in the treatment of acute cerebral infarction. *Chin. J. Mod. Drug Appl.* 14 (5), 107–109. doi:10.14164/j.cnki.cn11-5581/r.2020.05.048

Yan, F. X., Gao, W. J., Qian, T., Ye, D. Q., Zhang, Y. L., Hou, Z. P., et al. (2010). Effects of Astragalus injection on caspase-3 expression in hippocampal neurons of hypoxia-hypoglycemia/reoxygenation-reoxygenation rats. *Chin. Pharmacol. Bull.* 26 (07), 898–903. doi:10.3969/j.issn.1005-9202.2011.08.029

Yang, H., Li, G. P., Liu, Q., Zong, S. B., Li, L., Xu, Z. L., et al. (2021). Neuroprotective effects of Ginkgolide B in focal cerebral ischemia through selective activation of prostaglandin E2 receptor EP4 and the downstream transactivation of epidermal growth factor receptor. *Phytother. Res.* 35, 2727–2744. doi:10.1002/ptr.7018

Yang, M. (2019). Efficacy of Ginkgo biloba diterpene lactone glucosamine injection adjuvant to edaravone in the treatment of acute cerebral infarction and changes in serum Hcy and NSE. *J. Med. Forum* 40 (3), 148–149.

Zhang, C. F., Cao, L., Deng, Y., Li, N., Wang, Z. Z., Xiao, W., et al. (2015). Effects of ginkgo biloba diterpene lactone glucosamine injection on behavioral and cerebrospinal fluid composition in rats with cerebral ischemia-reperfusion. *Chin. J. Exp. Traditional Med. Formulae* 21 (20), 118–122. doi:10.13422/j.cnki.syfjx.2015200118

Zhang, J. H., Shi, J. S., and Zhang, Q. (2021b). Clinical effects of ginkgo biloba diterpene lactone glucosamine injection in the treatment of acute cerebral infarction. *Clin. Res. Pract.* 6 (29), 147–149. doi:10.19347/j.cnki.2096-1413.202129048

Zhang, L. L., Lian, X. F., Zhao, J., Chen, X., Bai, Y. J., Li, X. T., et al. (2021c). Meta-analysis on diterpene ginkgolides meglumine injection with Western Medicine in treating cerebral infarction. *Chin. J. Neuroimmunol. Neurology* 28 (02), 152–157. doi:10.3969/j.issn.1006-2963.2021.02.011

Zhang, Q., Zhang, L., Liu, Y., Tian, X., Li, X., Han, B., et al. (2021a). Research progress on the pharmacological effect and clinical application of Tongqiao Huoxue Decoction in the treatment of ischaemic stroke. *Biomed. Pharmacother.* 138, 111460. doi:10.1016/j.biopha.2021.111460

Zhang, W., Dong, L. G., Wang, X. P., and Zu, J. (2017). Clinical effects of ginkgo biloba diterpene lactone glucosamine combined with eurycomycin in the treatment of cerebral infarction with middle cerebral artery stenosis. *Contemp. Med. Symp.* 15 (11), 2–4. doi:10.3969/j.issn.2095-7629.2017.11.002

Zhang, W., Song, J. K., He, G. R., Zhang, X., Zhou, Q. M., Wang, Z. Z., et al. (2016). Effects of ginkgo diterpene lactones on neurotransmitters in brain tissue of ischemic/reperfused rats. *Chin. Pharmacol. Bull.* 32 (12), 1648–1656. doi:10.3969/j.issn.1001-1978.2016.12.005

Zhao, G. Q., Li, Y. S., Jiang, C. H., and Wen, S. Q. (2017). Clinical efficacy of ginkgo diterpene lactone glucosamine injection combined with edaravone injection in the treatment of acute cerebral infarction. *Guide China Med.* 15 (30), 210–211. doi:10.15912/j.cnki.gocm.2017.30.169

Zhong, X. N. (2020). Chinese expert consensus on platelet-activated factor receptor antagonists for the treatment of ischemic stroke. *Chin. J. Neuroimmunol. Neurology* 27 (01), 1–5+8. doi:10.3969/j.issn.1006-2963.2020.01.001

Zhu, Y. (2020). Effect of ginkgo biloba diterpene lactone glucosamine injection combined with edaravone in the treatment of acute cerebral infarction. *Chin. J. Misdiagnostics* 15 (05), 199–200.

frontiers | Frontiers in Pharmacology

TYPE Original Research
PUBLISHED 18 June 2024
DOI 10.3389/fphar.2024.1395167

OPEN ACCESS

EDITED BY
Syed Shadab Raza,
ERA's Lucknow Medical College, India

REVIEWED BY
Yuxiang Fei,
China Pharmaceutical University, China
Zhong-Yan Zhou,
Shanghai University of Traditional Chinese Medicine, China

*CORRESPONDENCE
Daiyin Peng,
pengdaiyin@163.com
Lan Han,
hanlan56@ahtcm.edu.cn

†These authors have contributed equally to this work and share first authorship

RECEIVED 03 March 2024
ACCEPTED 22 May 2024
PUBLISHED 18 June 2024

CITATION
Tang L, Liu Z, Ji Z, Zhang X, Zhao M, Peng D and Han L (2024), Promotion of mature angiogenesis in ischemic stroke by Taohong Siwu decoction through glycolysis activation. *Front. Pharmacol.* 15:1395167. doi: 10.3389/fphar.2024.1395167

Promotion of mature angiogenesis in ischemic stroke by Taohong Siwu decoction through glycolysis activation

Linfeng Tang[1,2†], Zhuqing Liu[1,2†], Zhaojie Ji[1,2], Xueting Zhang[1,2], Mengdie Zhao[1,2], Daiyin Peng[1,2,3*] and Lan Han[1,2,3*]

[1]Department of Pharmacy, Anhui University of Chinese Medicine, Hefei, China, [2]Anhui Province Key Laboratory of Chinese Medicinal Formula, Hefei, China, [3]MOE-Anhui Joint Collaborative Innovation Center for Quality Improvement of Anhui Genuine Chinese Medicinal Materials, Hefei, China

Backgrounds: Mature angiogenesis plays a critical role in improving cerebral ischemia-reperfusion injury (CIRI). Glycolysis serves as the primary energy source for brain microvascular endothelial cells (BMECs), whereas other vascular cells rely on aerobic respiration. Therefore, intercellular variations in energy metabolism could influence mature angiogenesis. Taohong Siwu Decoction (THSWD) has demonstrated efficacy in treating ischemic stroke (IS), yet its potential to promote mature angiogenesis through glycolysis activation remains unclear.

Methods: In this study, we established a middle cerebral artery occlusion/reperfusion (MCAO/R) model *in vivo* and an oxygen-glucose deprivation/reoxygenation (OGD/R) model *in vitro*. We assessed neuroprotective effects using neurobehavioral scoring, 2,3,5-triphenyltetrazolium chloride (TTC) staining, Hematoxylin-eosin (HE) staining, and Nissl staining in MCAO/R rats. Additionally, we evaluated mature angiogenesis and glycolysis levels through immunofluorescence, immunohistochemistry, and glycolysis assays. Finally, we investigated THSWD's mechanism in linking glycolysis to mature angiogenesis in OGD/R-induced BMECs.

Results: *In vivo* experiments demonstrated that THSWD effectively mitigated cerebral damage and restored neurological function in MCAO/R rats. THSWD significantly enhanced CD31, Ang1, PDGFB, and PDGFR-β expression levels, likely associated with improved glucose, pyruvate, and ATP levels, along with reduced lactate and lactate/pyruvate ratios. *In vitro* findings suggested that THSWD may boost the expression of mature angiogenesis factors (VEGFA, Ang1, and PDGFB) by activating glycolysis, increasing glucose uptake and augmenting lactate, pyruvate, and ATP content, thus accelerating mature angiogenesis.

Abbreviations: IS, Ischemic stroke; ECs, Endothelial cells; TCM, Traditional Chinese medicine; THSWD, Taohong Siwu Decoction; CIRI, Cerebral ischemia-reperfusion injury; MCAO/R, Middle cerebral artery occlusion/reperfusion; OGD/R, Oxygen-glucose deprivation/reoxygenation; TTC, 2,3,5-triphenyltetrazolium chloride; HE, Hematoxylin-eosin; 2DG, 2-Deoxy-D-glucose; NBP, Butylphthalide; UPLC MS/MS, Ultra-performance chromatography-mass spectrometry; SD, Sprague-Dawley; ELISA, Enzyme-linked immunosorbent assay; mNSS, Modified neurologic severity score; WB, Western Blotting; BMECs, Brain microvascular endothelial cells.

Conclusion: THSWD could alleviate CIRI by activating the glycolysis pathway to promote mature angiogenesis. Targeting the glycolysis-mediated mature angiogenesis alongside THSWD therapy holds promise for IS treatment.

KEYWORDS

ischemic stroke, cerebral ischemia-reperfusion injury, mature angiogenesis, glycolysis, Taohong Siwu decoction

Introduction

Ischemic stroke (IS) is a prominent cause of mortality and permanent disability worldwide, posing substantial economic and quality of life challenges (GBD, 2019 Stroke Collaborators, 2021; Behera et al., 2020). Current clinical interventions for IS patients are largely limited to interventional therapy or thrombolytic therapy with recombinant tissue plasminogen activator, constrained by a narrow therapeutic window (Behera et al., 2020). Following a stroke, blood flow can reach the ischemic area through collateral or neovascularization, which may compensate for cerebral tissue (Liu D. et al., 2016). The restoration of collateral circulation in the ischemic penumbra is a pivotal factor in stroke prognosis (Chng et al., 2008), underscoring the potential of promoting collateral formation and angiogenesis in IS treatment.

However, compensatory neovascularization in stroke patients is often limited, with the risk of vessel no-reflow or exacerbated cerebral edema (Li et al., 2007). Consequently, there is considerable interest in promoting angiogenesis in ischemic regions through exogenous gene, protein, or drug supplementation (Kumar et al., 2008). Notably, localized brain injections of VEGFA for therapeutic angiogenesis have shown limitations, including high permeability and low perfusion in neovascularization (Zhang et al., 2000; Zhang et al., 2017). Consequently, while focusing on the number of neovascularization, we should pay more attention to the maturity and functionality of the neovascularization. Thus, the focus has shifted towards enhancing the maturity and functionality of neovascularization.

Mature angiogenesis is a highly dynamic process involving endothelial cell (EC) differentiation, proliferation, migration,

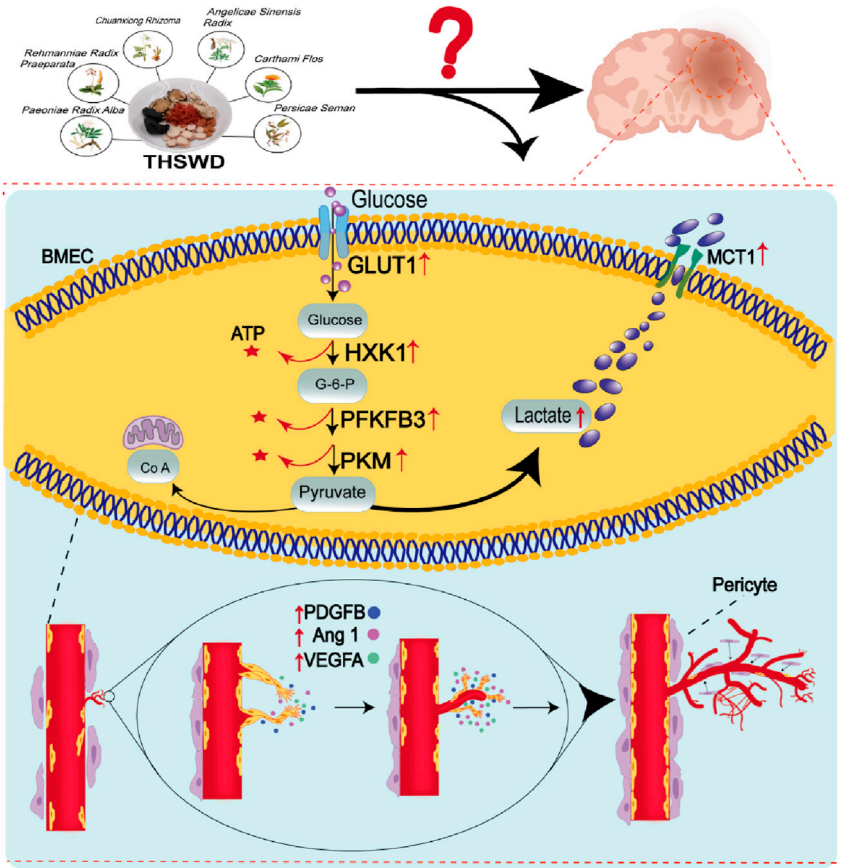

GRAPHICAL ABSTRACT

pericyte recruitment, and basement membrane remodeling, culminating in the formation of perfused vessels in ischemic areas (Chang et al., 2017; Gete et al., 2021). EC hyperglycolysis, akin to the Warburg effect in tumors, plays a critical role in this process (Cruys et al., 2016). Studies have shown that manipulating glycolysis can modulate angiogenesis; for instance, PFKFB3 gene knockdown inhibits EC glycolysis and angiogenesis (Schoors et al., 2014), while increased hexokinase expression boosts glycolysis and promotes angiogenesis (Yu et al., 2017).

Additionally, ECs recruit pericytes to stabilize vascular structures (Armulik et al., 2011), with other vascular cells primarily relying on aerobic respiration (Cunnane et al., 2020). Ischemia and hypoxia stimulate increased glycolysis, promoting EC proliferation and differentiation but potentially impairing other vascular cell functions. Thus, understanding the interplay and molecular mechanisms of ECs glycolysis levels in mature angiogenesis after IS warrants further investigation.

Traditional Chinese medicine (TCM) views IS as a manifestation of blood stasis syndrome, focusing on "stasis-removing and regeneration-promoting" in treatment (Liu et al., 2016; Li et al., 2017). Taohong Siwu Decoction (THSWD), a classic TCM formulation for this purpose, consists of *Prunus persica* (L.) Batsch, *Carthamus tinctorius* L, *Angelica sinensis* (Oliv.) Diels, *Rehmannia glutinosa* (Gaertn.) DC, *Ligusticum chuanxiong* Hort, *Paeonia lactiflora* Pall, as documented in the Golden Mirror of Medicine of the Qing Dynasty (Xia et al., 2021). Our previous research has shown that TSHWD effectively treats cerebral ischemia-reperfusion injury (CIRI) (Li et al., 2015; Chen et al., 2020; Wang et al., 2020), and it promotes angiogenesis by increasing VEGFA, CD34, and BrdU/vWF levels in the ischemic penumbra (Chen et al., 2020). Therefore, we aim to investigate whether THSWD alleviates CIRI by promoting mature angiogenesis and whether this involves the activation of the ECs glycolysis pathway.

To address these questions, we utilized middle cerebral artery occlusion/reperfusion (MCAO/R) *in vivo* and oxygen-glucose deprivation/reoxygenation (OGD/R) *in vitro* models. We examined the role of THSWD in mature angiogenesis after IS and explored the underlying molecular mechanisms involving glycolysis pathways.

Materials and methods

Herbs and reagents

The details of the six herbs comprising THSWD are presented in Table 1. These herbs were sourced from Anhui Bozhou Xiehecheng Pharmaceutical Co., Ltd. Butylphthalide (NBP, 1182110134) was acquired from Shiyao Group Enbip Pharmaceutical Co. The 2% 2,3,5-triphenyltetrazolium chloride (TTC, BL1215A) staining solution was obtained from Beijing G-CLONE Biotechnology Co, and the Hematoxylin-eosin (HE) stain (G1003) kit was purchased from Wuhan Servicebio Biotechnology Co. Additionally, the Nissl staining kit (10262109) was procured from Hefei eBioGo Biotechnology Co. For biochemical analyses, glucose (012522220429), lactate (20020421), pyruvate (20020525), and ATP (20220919) kits were acquired from Nanjing Jianjian Biotechnology Co.

Primary antibodies, including CD31 (25u3337), PDGFR-β (01052356), PDGFB (57n6785), and Ang1 (00081292), were purchased from Wuhan Sanying Biotechnology Co. The 2-Deoxy-D-glucose (2DG) (156249) was sourced from Shanghai MCE Biotechnology Ltd., and the Matrigel matrix (356234) was obtained from Corning Incorporated, United States. Enzyme-linked immunosorbent assay (ELISA) kits for Ang1, PDGFB, and VEGFA (202210) were obtained from Shanghai Jianglai Biotechnology Ltd. Furthermore, the primary antibodies, GLUT1 (B1157), HXKI (B1218), PKM (I3022), MCT1 (D0522), and PFKFB3 (D1022) were procured from Santa Cruz, United States.

THSWD preparation and quality control

The specified amounts of herbs were weighed according to the proportions outlined in Table 1. They were initially decocted in 10 volumes of water for 2 h, followed by filtration and storage. Subsequently, a second decoction was carried out using 8 volumes of water for 1.5 h, and the resulting filtrate was combined with the first batch and concentrated to a density of 1.8 g/mL (Pan et al., 2022).

Furthermore, quality control of THSWD was conducted using ultra-performance chromatography-mass spectrometry (UPLC MS/MS), adhering to established experimental protocols (Chen et al., 2020).

MCAO/R modeling

All Sprague-Dawley (SD) rats (SCXK 2019-0003) used in this study were procured from the Laboratory Animal Center of Anhui University of TCM (Ethics Committee No. AHUCM-rats-2021041) and weighed approximately 250 g ± 20 g. The MCAO/R model was induced using the thread-embolism technique (Wu et al., 2020). Briefly, rats were anesthetized with intraperitoneal pentobarbital injection (30 mg/kg), followed by isolation of the common carotid artery, external carotid artery, and internal carotid artery. A small incision was made in the common carotid artery, and a thread embolus (0.40 ± 0.02 mm) was inserted into the internal carotid artery approximately 18–22 mm. The sham group underwent the same procedure without artery ligation or thread embolus insertion. After 2 h of ischemia, the thread embolus was removed to restore perfusion for 24 h, and the efficacy of the model was evaluated using the Zea Longa score. The rats were then randomly divided into sham, model, and THSWD groups (4.5 g/kg, 9 g/kg, 18 g/kg), as well as a group receiving NBP (25 mg/kg). Subsequently, the corresponding indexes were assessed following 7 days of continuous drug or saline gavage for each group.

Neurological function score

After completing the treatment protocol, the rats underwent neurological assessments using the Zea Longa score

TABLE 1 The basic information of THSWD.

Herbal name	Plant scientific name	Lot number	Weight ratio	Representative components
Paeoniae Radix Alba	*Paeonia lactiflora* Pall	22073002	3	paeoniflorin
Rehmanniae Radix Praeparata	*Rehmannia glutinosa* (Gaertn.) DC.	23010311	4	verbascoside
Angelicae Sinensis Radix	*Angelica sinensis* (Oliv.) Diels	23070403	3	ferulic acid
Chuanxiong Rhizoma	*CLigusticum chuanxiong* Hort	22070701	2	ligustilide
Persicae Seman	*Prunus persica* (L.) Batsch	23060504	3	amygdalin
Carthami Flos	*Carthamus tinctorius* L	23060504	2	hydroxysafflor yellow A

(Li et al., 2023) and the modified neurologic severity score (mNSS) (Chen et al., 2001). The Zea Longa score was assigned as follows: 0 for normal walking, 1 for inability to extend the left forelimb, 2 for tilt walking, 3 for counterclockwise circling, and 4 for inability to walk or unconsciousness. The mNSS, as previously described, assigns a higher score (ranging from 0 for normal function to 18 for maximal deficit) to indicate more severe neurological impairment. All assessments of animal neurological function were conducted by trained researchers who were unaware of grouping information.

Cerebral infarction volume

The rat brain tissue was washed with pre-cooled PBS and sliced into 2 mm sections along the sagittal plane. These brain slices were then incubated in a 2% TTC staining solution for 30 min at 37°C, protected from light. Subsequently, the slices were immersed in 4% paraformaldehyde for 24 h. The cerebral infarct volume was quantified using ImageJ software.

HE staining and Nissl staining

Fresh brain tissues were fixed in 4% paraformaldehyde for 24 h and then embedded in paraffin to prepare 4 mm coronal sections. HE staining and Nissl staining were conducted according to standard protocols. Brain tissue damage was assessed using a light microscope. Additionally, Nissl bodies were quantitatively analyzed using ImageJ software.

Biochemical kits and ELISA

Glucose, pyruvate, and lactate levels were determined in rat serum and cell culture media using biochemical kits. Additionally, the VEGFA, Ang1, and PDGFB levels in cell culture media were measured using ELISA kits. Protein concentrations in cerebral cortical tissue from the ischemic area and cellular extracts were quantified separately using a BCA kit. Furthermore, the glucose, pyruvate, lactate, and ATP levels in the cerebral cortex and cellular ATP content were assessed using biochemical assay kits. All procedures were conducted in accordance with the manufacturers' instructions.

Immunofluorescence

The rat brains were swiftly extracted to prepare frozen sections. The sections were incubated with anti-CD31 (1:500) antibodies at 4°C overnight and restained with DAPI for 5 min following incubation with secondary antibodies (1:1000). All images were acquired using a fluorescence microscope (Nikon/Eclipse, Tokyo, Japan), and the fluorescence intensity was assessed using ImageJ.

Immunohistochemistry

The cerebral specimens underwent fixation, paraffin embedding, section preparation, programmed dewaxing, dehydration, antigen repair, and sealing procedures. Subsequently, the sections were incubated overnight at 4°C with primary antibodies against Ang1 (1:100), PDGFB (1:200), and PDGFR-β (1:200). The following day, the specimens were washed with PBS and then incubated with secondary antibodies (1:1000) for 30 min at room temperature. They were subsequently stained using DAB and hematoxylin before being sealed for photograph collection. In parallel, mature angiogenesis protein expression was analyzed using ImageJ software.

THSWD drug-containing serum preparation

SD rats were administered THSWD (1.8 g/mL) via oral gavage twice daily for three consecutive days. Rats in the normal group received saline supplementation instead. Following the final THSWD administration, rats were anesthetized, and blood samples were immediately collected from the abdominal aorta. The samples were allowed to stand for 2 hours, followed by centrifugation at 3000 rpm for 20 min at 4°C. The supernatant was then heated in a 56°C water bath for 30 min for inactivation, filtered through a 0.22 μm microporous filter membrane for sterilization, and stored at −80°C until analysis. The analysis of blood components was performed according to established protocols detailed in our previous research (Duan et al., 2020).

OGD/R

Brain microvascular endothelial cells (BMECs) were obtained from the BeNa Culture Collection (337717), while rat brain microvascular pericytes were purchased from iCell Bioscience

Inc. (2022092701). Both cell types were cultured in high glucose DMEM medium with 10% FBS in a standard cell culture incubator (5% CO_2, 95% O_2). To simulate CIRI, BMECs were exposed to glucose-free DMEM medium and placed in a hypoxic incubator (1% O_2, 5% CO_2 with 94% N_2) for 4 hours (Shi et al., 2023). Subsequently, the medium was replaced with glucose-containing DMEM, and the cells were transferred to a standard cell culture incubator for 24 h of reoxygenation.

Drug concentration screening and grouping

A total of 100 μL of BMECs (1×10^5 cells/mL) were seeded into each well of a 96-well plate and randomly assigned to either a normal group or an OGD/R group. Following 4 hours of OGD, each group received different concentrations of THSWD drug-containing serum and 2DG. After 24 h of reoxygenation, 10 μL CCK8 solution was added to each well and incubated for 1 h, with the optical density (OD) value measured at 450 nm.

To further assess the impact of THSWD on glycolysis levels and angiogenesis in OGD/R-induced BMECs, cells were categorized into the following groups: normal group (10% blank serum), OGD/R group (10% blank serum), THSWD group (OGD/R+10% THSWD drug-containing serum), 2DG group (OGD/R+10% blank serum+5 mM 2DG), and 2DG + THSWD group (OGD/R+10% THSWD drug-containing serum+5 mM 2DG).

Mature angiogenesis

CCK8

The proliferation of BMECs in the normal and drug-processed groups was assessed using the same procedure as the previous description of the CCK8 approach.

Scratch test

BMECs were seeded in 6-well plates and grown to the shape of a "paving stone road." After an OGD treatment of 4 h, scratches were made using a sterile toothpick. After cleaning with PBS, the 0-h scratch locations were marked and photographed for recording. After 24 h of reoxygenation treatment, pictures of recordings were retaken, and the cell migration rate of all groups was examined using ImageJ.

Sprouting test

The sphere sprouting assay of BMECs was performed with slight modifications (De Bock et al., 2013). We spread the cell culture dish using 0.5% sterile agarose solution. After the solution was cooled, 3 mL of BMECs (1×10^5 cells/mL) were seeded to form cell spheroids. We combined the rat tail tendon collagen type I and M199 medium in a 10:1 ratio to produce a light yellow solution. Next, we immediately transferred the cell spheroid suspension to the light yellow solution and allowed it to stand for 2 hours in the cell culture incubator. Finally, we conducted OGD/R modeling and observed the sphere sprouting after 24 h. Additionally, the length of the sphere sprouting and the number of sprouts were assessed using ImageJ.

Tube formation assay

We inoculated 50 μL of precooled Matrigel matrix into 96-well plates (Liu et al., 2023). After modeling and drug intervention, we digested the BMECs, along with 100 μL (1×10^5 cells/mL) of suspension per well, and transferred it to the Matrigel matrix. After culturing for 3 h, photographs were taken to record the tube formation in each group. ImageJ analysis was performed to assess the tube number and branching.

Transwell assay

The day preceding the assay, 1 mL of pericytes (1×10^5 cells/mL) and BMECs (1×10^5 cells/mL) were seeded in the upper and lower chambers of the Transwell, respectively, and allowed to incubate overnight. The following day, both upper and lower chamber cells were recycled with glucose-free medium and placed in a low-oxygen incubator for 4 hours. We changed the upper pericytes to a culture medium supplemented with 1% FBS, and the lower chamber BMECs were changed to a culture medium containing 10% FBS. They were incubated in a normal cell culture incubator for 24 h and fixed using 4% paraformaldehyde for 30 min before staining with 0.5% crystal violet staining solution. After photographs were taken, they were analyzed using ImageJ to assess the number of pericyte migrations.

Western Blotting (WB)

The BMECs were lysed in a pre-cooled RIPA solution containing PMSF for 20 min to obtain total proteins. We measured the protein concentration using a BCA kit and included a consistent protein content in each group. Using 10% or 12% SDS-PAGE electrophoresis for 2 hours, the proteins were transferred to an NC membrane for 1 hour. After incubating with 5% skimmed milk powder for 2 hours and primary antibody overnight at 4°C, the membranes were washed three times with TBST, and incubated with HRP-labeled secondary antibody for 2 hours for chemiluminescence reaction.

Statistical analysis

All experimental findings were presented using Mean ± SD. Comparisons between two groups were made using a two-tailed Student's t-test, while comparisons between three or more groups were performed using a one-way analysis of variance. SPSS 25.0 software was adopted for statistical analysis. $p < 0.05$ was considered statistically significant.

Results

UPLC MS/MS profile of THSWD

A total of six THSWD-indicative components were characterized using the UPLC MS/MS approach (Figures 1A–C). We calculated the contents of the THSWD (1 mg/mL) components according to the standard curve method: hydroxysafflor yellow A (2.572 μg/mL), amygdalin (6.793 μg/mL), paeoniflorin (25.374 μg/mL), verbascoside (0.165 μg/mL), ferulic acid (0.989 μg/mL), and ligustilide (8.023 μg/mL). The mass spectrometry data was shown in Supplementary Material 1.

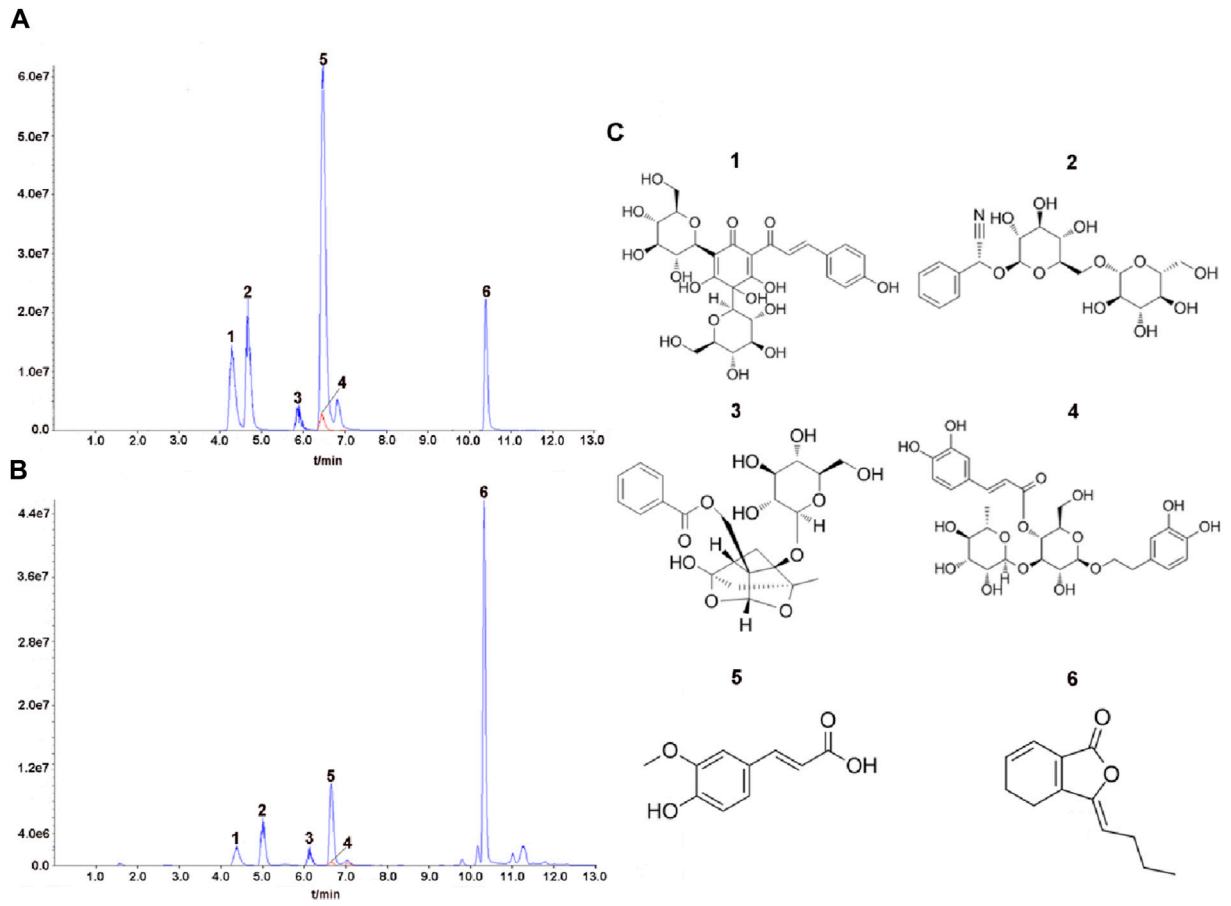

FIGURE 1
Analysis of representative components of THSWD using UPLC MS/MS. The chromatograms of six representative components of the mixed standard compounds **(A)** and THSWD **(B)**. **(C)** The chemical structures of six representative components. 1: hydroxysafflor yellow A; 2: amygdalin; 3: paeoniflorin; 4: verbascoside; 5:ferulic acid; 6:ligustilide.

THSWD ameliorated cerebral ischemia and neurological function in MCAO/R rats

After developing the MCAO/R model, we administered treatment by supplementing varying doses of THSWD and NBP (Figure 2A). Compared to the Sham group, MCAO/R modeling significantly increased Zea Longa and mNSS scores. After the intervention, the Zea Longa and mNSS scores in the THSWD group were significantly lower than those in the MCAO/R group (Figures 2B,C). HE results suggested that the brain tissue in the ischemic area of rats in the model group possessed severe vacuolation and necrosis. Conversely, THSWD could effectively alleviate pathologic damage (Figure 2D). The milky white area denotes the site of cerebral infarction. The TTC results indicated that the rats in the model group had prominent areas of cerebral infarction (Figure 2E). Differing doses of THSWD significantly reduced cerebral infarct volume (Figures 2E,F). We used Nissl staining to evaluate the neuronal damage, finding that THSWD significantly increased the number of Nissl bodies in the ischemic cortical region of MCAO/R rats and improved cerebral neurological impairment (Figures 2G,H). In conclusion, THSWD exhibited a favorable neuroprotective effect on MCAO/R rats.

THSWD accelerated mature angiogenesis in MCAO/R rats

As previously identified, promoting mature angiogenesis may be critical for improving CIRI. To confirm the microvessel density, the expression of CD31 in ischemic areas was detected using immunofluorescence staining (Hui et al., 2022). The immunofluorescence findings indicated that the expression of CD31 was slightly increased in the MCAO/R group, but it was significantly elevated after the administration of THSWD (Figures 3A,B).

Pericyte recruitment can increase vascular structural stability and accelerate neovascularization maturation (Armulik et al., 2011). Ang1 is primarily expressed in growing vascular ECs and pericytes, attracting pericyte recruitment upon binding to Tie2 receptors on ECs (Lee et al., 2009; Koh, 2013). While PDGFB is mainly secreted by ECs, interacting with PDGFR-β expressed by pericytes, which

10.3389/fphar.2024.1395167

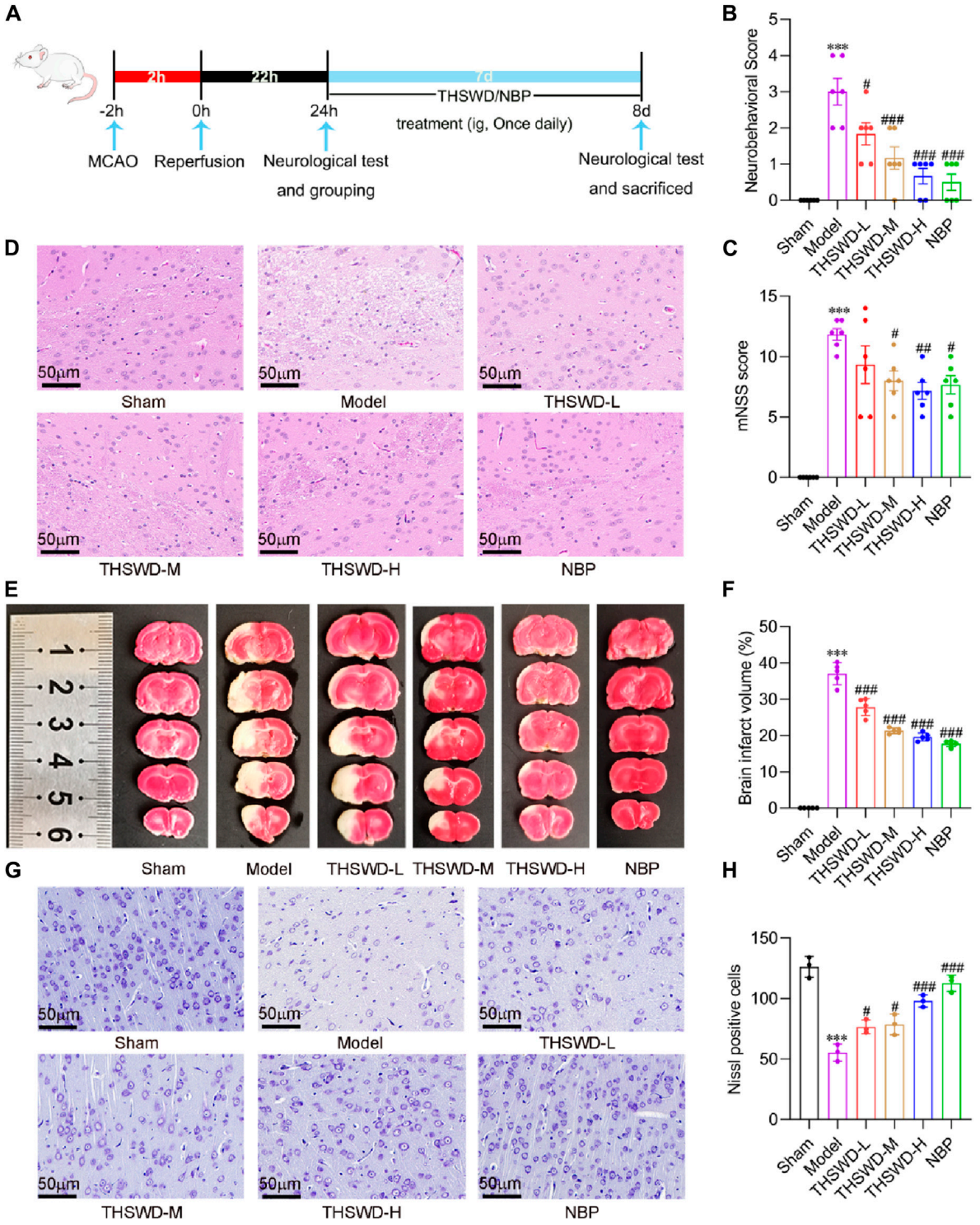

FIGURE 2
The effects of THSWD on neurological function, cerebral infarct volume, histopathology, and neuronal injury in MCAO/R rats. **(A)** The flow diagram of the experiment. **(B)** Neurobehavioral score (n = 6). **(C)** mNSS score (n = 6). **(D)** Representative images of HE staining of the cerebral cortex on the Ischemia side (n = 3). **(E)** Representative images of TTC staining. **(F)** Quantification of cerebral infarct volume (n = 5). **(G)** Representative images and quantitative analysis of Nissl bodies **(H)** in the cerebral cortex of the ischemic side. The scale bar represents 50 μm. Data were expressed as mean ± SD. ***$p < 0.001$ vs. the sham group; $^{\#}p < 0.05$, $^{\#\#}p < 0.01$, $^{\#\#\#}p < 0.001$ vs. the model group.

promotes pericyte aggregation, proliferation and migration (Hellström et al., 2001). Immunohistochemical results demonstrated that the expression levels of Ang1, PDGFB, and PDGFR-β were significantly reduced in the ischemic region of MCAO/R rats. Conversely, treatment with THSWD effectively elevated the expression of the indicators (Figures 4A–F),

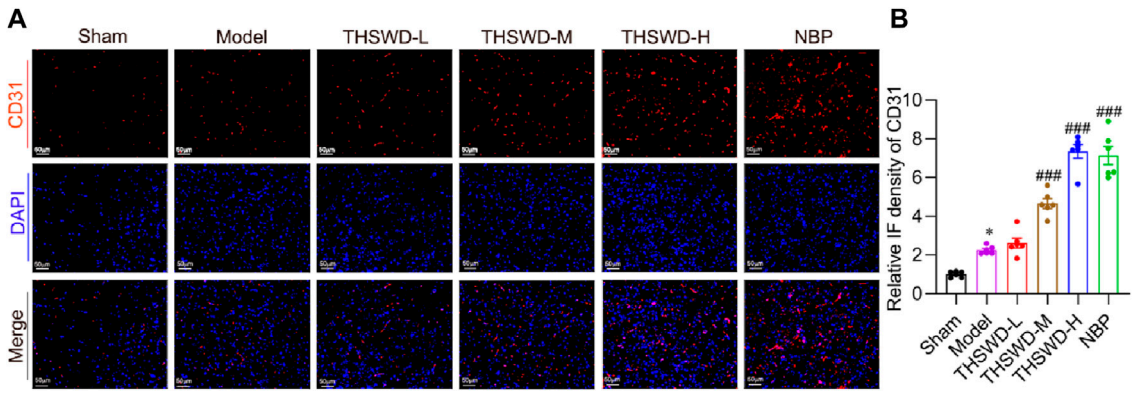

FIGURE 3
THSWD accelerated angiogenesis in MCAO/R rats. **(A)** Representative images of CD31 detected by Immunofluorescence staining and **(B)** quantitative analysis (n = 6). The scale bar represents 50 μm. Data were expressed as mean ± SD. $^{*}p < 0.05$ vs. the sham group; $^{###}p < 0.001$ vs. the model group.

suggesting that THSWD may improve CIRI by promoting mature angiogenesis.

THSWD activated the glycolysis pathway in MCAO/R rats

Diversity in energy metabolism across different cells may be a significant cause of defective vascular function. The products of aerobic and anaerobic glycolysis of glucose are pyruvate and lactate, respectively (Helms et al., 2007). The lactate/pyruvate levels reflect the degree of ischemia and hypoxia, with higher ratios indicating worsened ischemia and hypoxia (Raudam and Rivis, 1976; Chen et al., 2000). Compared to the sham group, the serum and ischemic cortex's glucose (Figure 5A) and pyruvate (Figure 5B) levels in model rats were significantly lower. Conversely, the lactate content (Figure 5C) and the lactate/pyruvate ratio (Figure 5D) were significantly higher. Supplementing THSWD reverses the alterations in the contents of the above indexes. The variation in ATP content further confirms our hypothesis (Figure 5E). THSWD may promote the vascular differentiation of BMECs into vessels via activation of glycolysis while restoring the recruitment function of pericytes, facilitating mature angiogenesis. However, the molecular mechanisms of glycolysis and mature angiogenesis and the interventional effects of THSWD remain unclear.

THSWD enhanced glycolysis level in OGD/R-induced BMECs

2DG, a glucose analog, inhibits glycolysis by competing for glucose binding to hexokinase (Chen et al., 2022). We integrated the survival rates of BMECs under normal and model groups following pharmacological interventions (Figures 6A–D), determining the concentration of drug administration as THSWD (10%) and 2DG (5 mM).

Glycolysis kit findings demonstrated that glucose uptake (Figure 6E), pyruvate (Figure 6F), lactate release (Figure 6G), and ATP (Figure 6H) content decreased significantly in the OGD/R group relative to the normal group. In addition, THSWD supplementation effectively reversed these indicators. Compared to the OGD/R group, supplementation with 2DG further reduced glycolysis levels, indicating that 2DG has a favorable influence on inhibiting glycolysis. Compared to the THSWD group, the glycolysis level decreased significantly in the 2DG + THSWD group, suggesting that THSWD activated glycolysis.

THSWD promoted mature angiogenesis in OGD/R-induced BMECs

As outlined previously, we employed CCK8, scratch assay, sprouting, tube formation, and transwell assay, to simulate the process of mature angiogenesis *in vivo*. CCK8 and morphological results (Figures 7A, F) demonstrated that the cells in the OGD/R group had a crumpled and floating state, and the number of cells decreased significantly relative to the normal group. Compared to the OGD/R group, the THSWD group significantly improved cell injury and promoted proliferation, while the 2DG group had an aggravated injury state. Compared to the THSWD group, the 2DG + THSWD group substantially attenuated the improvement effect of treatment with THSWD. The scratch assay effectively assesses the migration ability of cells (Sun and Liu, 2022). As illustrated in Figures 7B,G, THSWD may promote the migration of BMECs in the OGD/R model by elevating the glycolysis level. Spheroid sprouting is a central step in angiogenesis, allowing the examination of EC proliferation and division capacity (De Bock et al., 2013). As depicted in Figures 7C,H, THSWD may significantly increase the number of sphere sprouts and sprout length under the OGD/R model by elevating the glycolysis level. The tube formation assay offers an excellent simulation of vascular remodeling *in vivo* (Sun and Liu, 2022). As illustrated in Figures 7D, I, J, THSWD may significantly enhance the tube lengths alongside the number of tube branches in BMECs in the OGD/R model by enhancing glycolysis. Recruitment of pericytes by BMECs is necessary for evaluating vascular maturation (Armulik et al., 2011). As shown in Figures 7E,K, THSWD may elevate the number of pericytes recruited in the OGD/R model by increasing glycolysis levels. Interestingly, it is

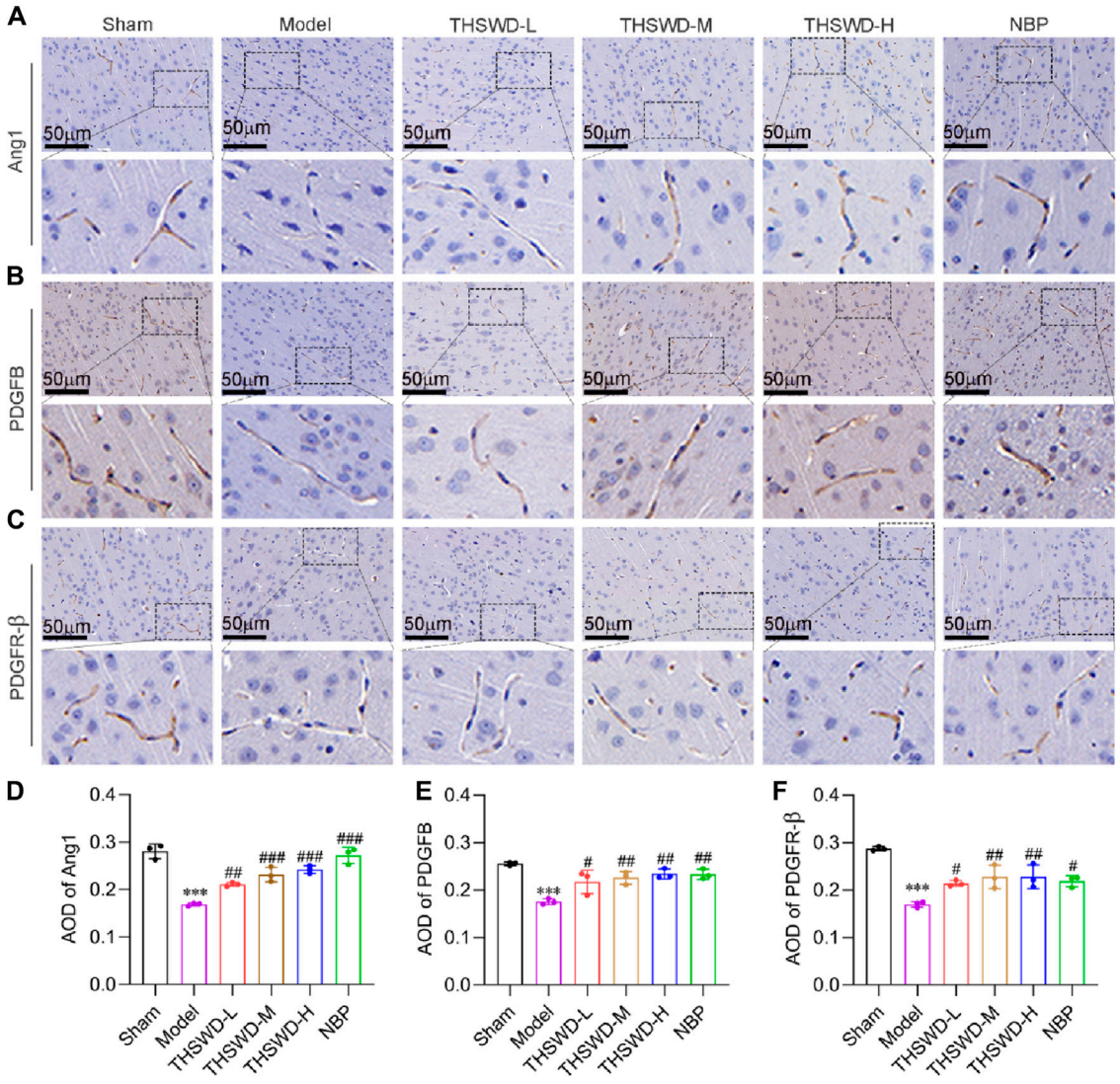

FIGURE 4
THSWD promotes the expression of mature angiogenesis factors in MCAO/R rats. Representative images of **(A)** Ang1, **(B)** PDGFB, and **(C)** PDGFR-β in the cortical vessels on the ischemic side of the cerebral in MCAO/R rats and **(D–F)** corresponding quantitative analysis. The scale bar represents 50 μm. Data were expressed as mean ± SD (n = 3). ***p < 0.01 vs. the sham group; $^{\#}p$ < 0.05, $^{\#\#}p$ < 0.01, $^{\#\#\#}p$ < 0.001vs. the model group.

consistent with the results of pericyte recruitment in animal level. In summary, THSWD promotes mature angiogenesis in BMECs in the OGD/R model by enhancing glycolysis.

THSWD improved the expression of mature angiogenesis proteins in OGD/R-induced BMECs

To further illustrate the molecular mechanism of glycolysis and mature angiogenesis, we assayed the expression of mature angiogenesis proteins. VEGFA, an essential regulator of angiogenesis, participates in the process of vascularization (Bikfalvi and Bicknell, 2002). As previously mentioned, the binding of Ang1 to Tie2 and PDGFB to PDGFR-β promotes EC recruitment of pericytes and accelerates vascular remodeling and maturation (Bjarnegård et al., 2004; Zhang et al., 2020). ELISA findings (Figures 8A–C) indicated that the protein content of VEGFA increased significantly in the OGD/R group, while the content of Ang1 and PDGFB decreased significantly relative to the normal group. Compared to the OGD/R group, the 2DG group reduced the expression of mature angiogenesis proteins. Additionally, 2DG also decreases the promotion of THSWD on protein content, indicating that THSWD may enhance the expression of VEGFA, Ang1, PDGFB in BMECs via activation of the glycolysis pathway, promoting mature angiogenesis.

THSWD regulated glycolysis pathway in BMECs after OGD/R injury

To further elucidate the molecular mechanism of glycolysis activation by THSWD, we examined the expression of glycolysis proteins. The WB results (Figures 8D–I) demonstrated that the

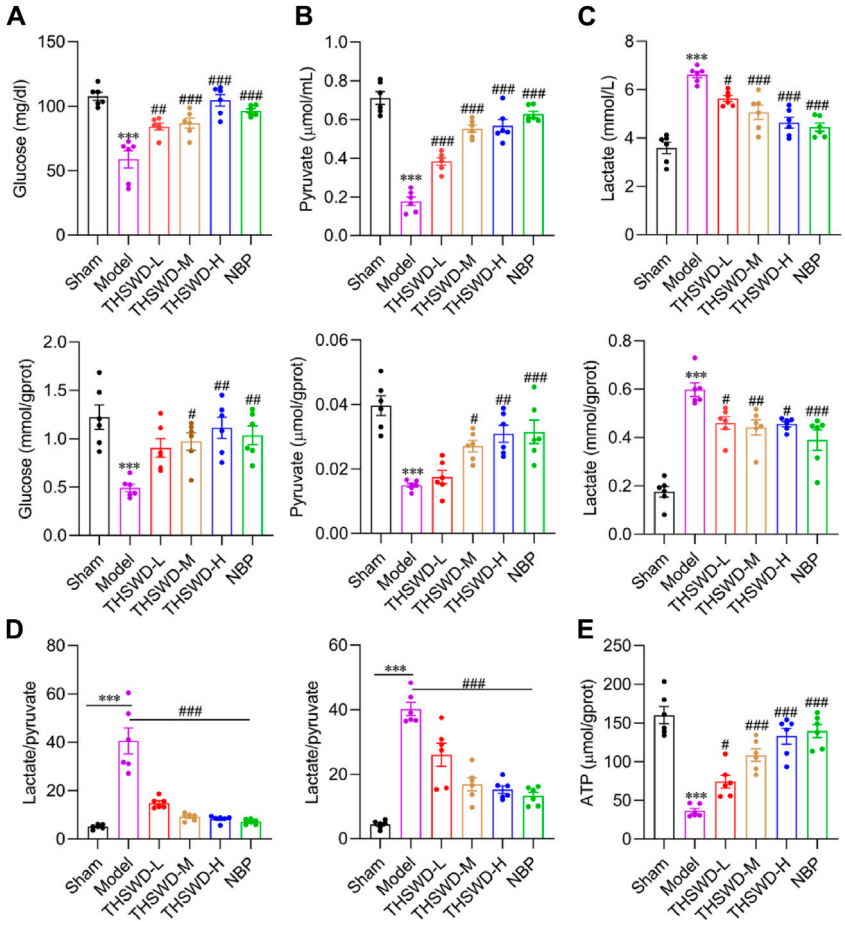

FIGURE 5
Effect of THSWD on glycolysis levels in MCAO/R rats. The glycolysis kit assays the expression of glucose **(A)**, pyruvate **(B)**, lactate **(C)**, and lactate/pyruvate **(D)** in the serum and the ischemic side cortex of MCAO/R rats. **(E)** Cortical ATP content in the ischemic side. Data were expressed as mean ± SD (n = 6). ***p < 0.01 vs. the sham group; $^{\#}p$ < 0.05, $^{\#\#}p$ < 0.01, $^{\#\#\#}p$ < 0.001 vs. the model group.

glycolysis protein content decreased significantly in the OGD/R group, while it was effectively reversed by THSWD supplementation. Compared to the OGD/R group, the 2DG group could further inhibit glycolysis protein expression, indicating that inhibition of hexokinase could significantly change the expression of upstream and downstream proteins. The above findings indicate that THSWD may hasten glucose uptake into ECs by enhancing GLUT1 expression. Additionally, it increased the activity of the three rate-limiting enzymes, facilitated lactate production, and released huge amounts of ATP. Ultimately, it elevated the expression of MCT1, facilitated lactate efflux to the extracellular compartment, and accelerated the EC glycolysis process.

Discussion

As angiogenesis can effectively elevate the supply of cerebral blood flow in IS, restore cerebral neurological function, and improve the prognosis of IS patients, some therapeutic strategies promoting angiogenesis have been applied clinically (Chng et al., 2008; Liu X. T. et al., 2016). However, emerging research suggests that neovascularization produced under IS ischemic-hypoxic stimuli, instead of restoring blood flow supply, may exacerbate the development of cerebral edema (Li et al., 2007). This indicates that the function of neovascularization may be more significant than the count of neovessels. Our previous study determined that THSWD could enhance angiogenesis and effectively improve CIRI in MCAO/R rats. Notably, MCAO/R rats promoted angiogenesis yet had little effect on CIRI treatment (Chen et al., 2020). We hypothesized that this might be related to improved neovascularization function by THSWD. BMECs have glycolysis-preferring properties resembling tumor cells (Cruys et al., 2016), while other cell types constituting the neurovascular unit are predominantly aerobically respiratory (Cunnane et al., 2020), attracting a great deal of attention. We hypothesized that the function of mature vessels may be associated with differences in cellular energy metabolism preferences. In this study, we developed the MCAO/R model *in vivo* and the OGD/R model *in vitro*, evaluated the effects of THSWD on mature angiogenesis, and explored its molecular mechanisms.

Mature angiogenesis takes place due to ischemia and hypoxia in the body, and its significant processes involve the initial, progressive,

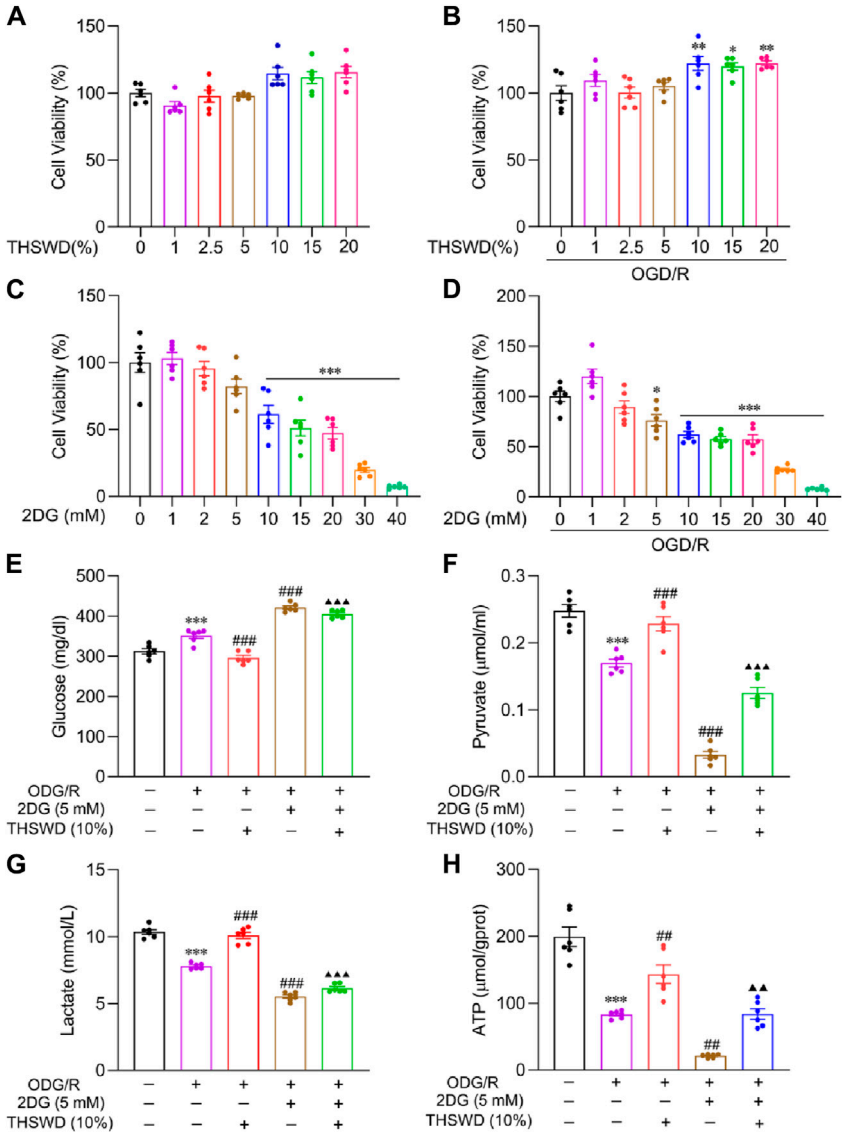

FIGURE 6
The effect of THSWD on glycolysis levels in OGD/R-induced BMECs. Effects of THSWD and 2DG on survival of BMECs under **(A, C)** normal and **(B, D)** OGD/R. The glycolysis Kit assays the **(E)** glucose, **(F)** pyruvate, **(G)** lactate, and **(H)** intracellular ATP content of the culture medium. Data were expressed as mean ± SD ($n = 6$). $^{*}p < 0.05$, $^{**}p < 0.01$, $^{***}p < 0.001$ vs. the normal group; $^{\#\#}p < 0.01$, $^{\#\#\#}p < 0.001$ vs. the OGD/R group; $^{\blacktriangle\blacktriangle}p < 0.01$, $^{\blacktriangle\blacktriangle\blacktriangle}p < 0.001$ vs. the THSWD group.

and mature-terminal stages. The process of angiogenesis is modulated by a series of angiogenic regulators (Oyama et al., 1996; Thurston et al., 2000), and under-expression or over-expression of these regulators in the organism may cause defects in vascular function. Following a stroke, the organism increases the content of neovascularization factors like VEGFA, Ang-2, and bFGF during the initial and progressive phases (Oyama et al., 1996; Zhang et al., 2017). However, mature-terminal vascular regulators require further study. Therefore, we hypothesized that the neovascularized no-reflow phenomenon in patients with IS may be associated with defective vascular function due to insufficient expression of mature angiogenic regulators. Our prior study identified that MCAO/R rats with significantly increased levels of angiogenic factors failed to lower the volume of cerebral infarcts, potentially related to the insufficient expression of mature angiogenic factors (Chen et al., 2020). In this study, we identified that the content of mature neovascular factors Ang1 and PDGFB, alongside the number of pericytes recruited (PDGFR-β), were significantly reduced in the model group in both the *in vivo* and *in vitro* assays. The mature angiogenesis factor levels and the number of recruited pericytes were substantially elevated following THSWD supplementation. Therefore, we hypothesized that THSWD may accelerate neovascularization into the mature-terminal phase, increase the number of mature neovessels, and restore cerebral blood flow supply.

Recent studies have demonstrated that the level of glycolysis in BMECs is critical for angiogenesis. Both in the resting state and the activated state, the energy source of BMECs comes primarily from glycolysis rather than oxidative phosphorylation (Perrotta et al., 2020). When the organism is in a hypoxic state, glycolysis

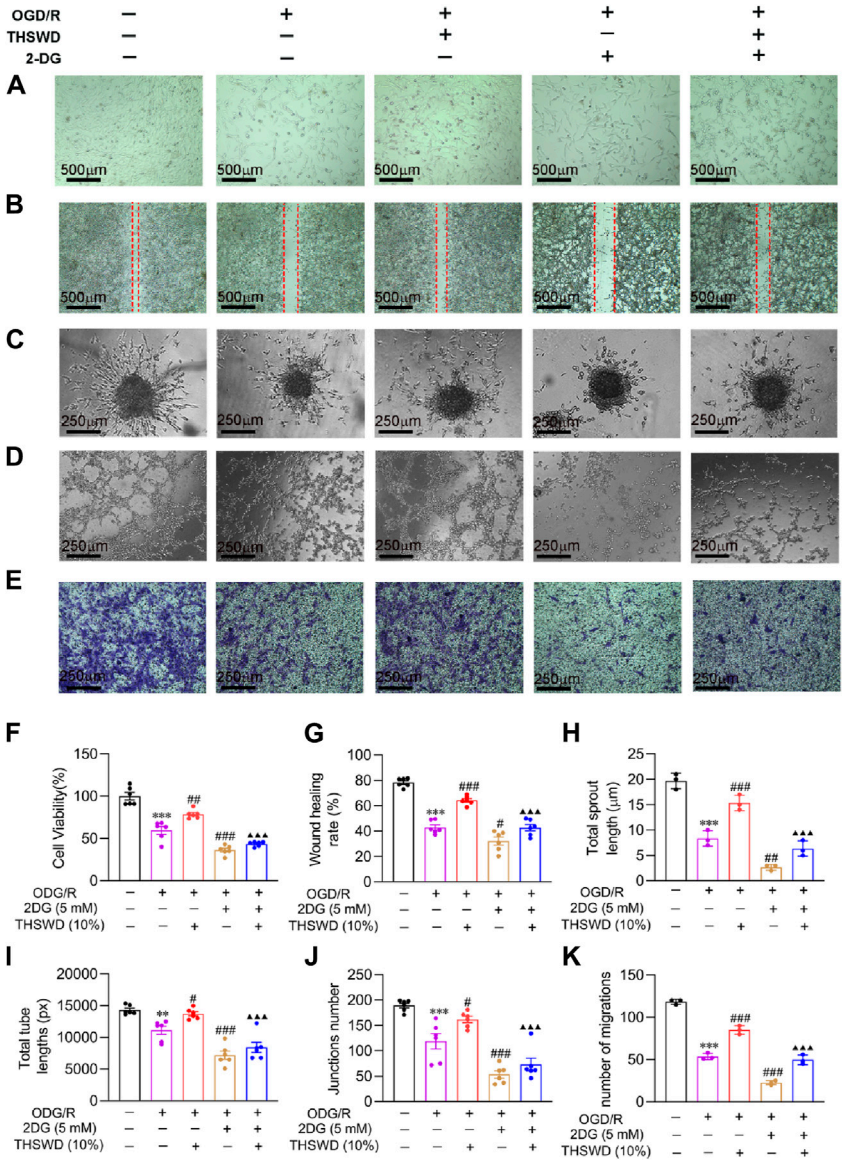

FIGURE 7
Effect of THSWD on mature angiogenesis of in OGD/R-induced BMECs. **(A)** Morphology (scale bar = 500 μm). **(B)** Wound healing (scale bar = 500 μm). **(C)** Sprouting assay (scale bar = 250 μm). **(D)** Tube formation assay (scale bar = 250 μm). **(E)** Pericyte recruitment (scale bar = 250 μm). **(F)** Quantification of proliferation rate (n = 6). **(G)** Wound healing rate (n = 6). **(H)** Sprouting length (n = 3). **(I,J)** Total tube length and number (n = 6). **(K)** Number of pericytes recruited (n = 3). Data were expressed as mean ± SD. $^{**}p < 0.01$, $^{***}p < 0.001$ vs. the normal group; $^{\#}p < 0.05$, $^{\#\#}p < 0.01$, $^{\#\#\#}p < 0.001$ vs. the OGD/R group; $^{\blacktriangle\blacktriangle\blacktriangle}p < 0.001$ vs. the THSWD group.

can rapidly supply ATP to the migrating and extending filamentous pseudopods (Wang et al., 2019). Conversely, other types of vascular cells, including pericytes, astrocytes, and smooth muscle cells, use oxidative phosphorylation as the primary energy source (Cunnane et al., 2020). Such variability in energy preferences of various types of vascular cells represents a critical factor affecting IS vascular function. The experimental findings of the animal studies indicated that the level of anaerobic glycolysis was remarkably increased in IS model rats, while the ATP content was significantly reduced. After supplementing with THSWD, aerobic glycolysis and the number of recruited pericytes increased, confirming our suspicions. However, the impact of THSWD on glycolysis in BMECs and its molecular mechanisms remain unclear.

EC glycolysis is a complex process encompassing the synergistic action of multiple enzymatic reactions. Studies have uncovered that GLUT1 assists in the passage of glucose through the blood-brain barrier into BMECs and other vascular cells, and its deficiency produces severely impaired energy metabolism (Jurcovicova, 2014). During EC glycolysis, hexokinase, 6-phosphofructokinase-2, and pyruvate kinase are the most prominent regulatory enzymes. Blocking or inhibiting these regulatory enzymes effectively inhibits the EC glycolysis processes (Schoors et al., 2014; Yu et al., 2017). In addition, glycolysis flux mirrors the expression of

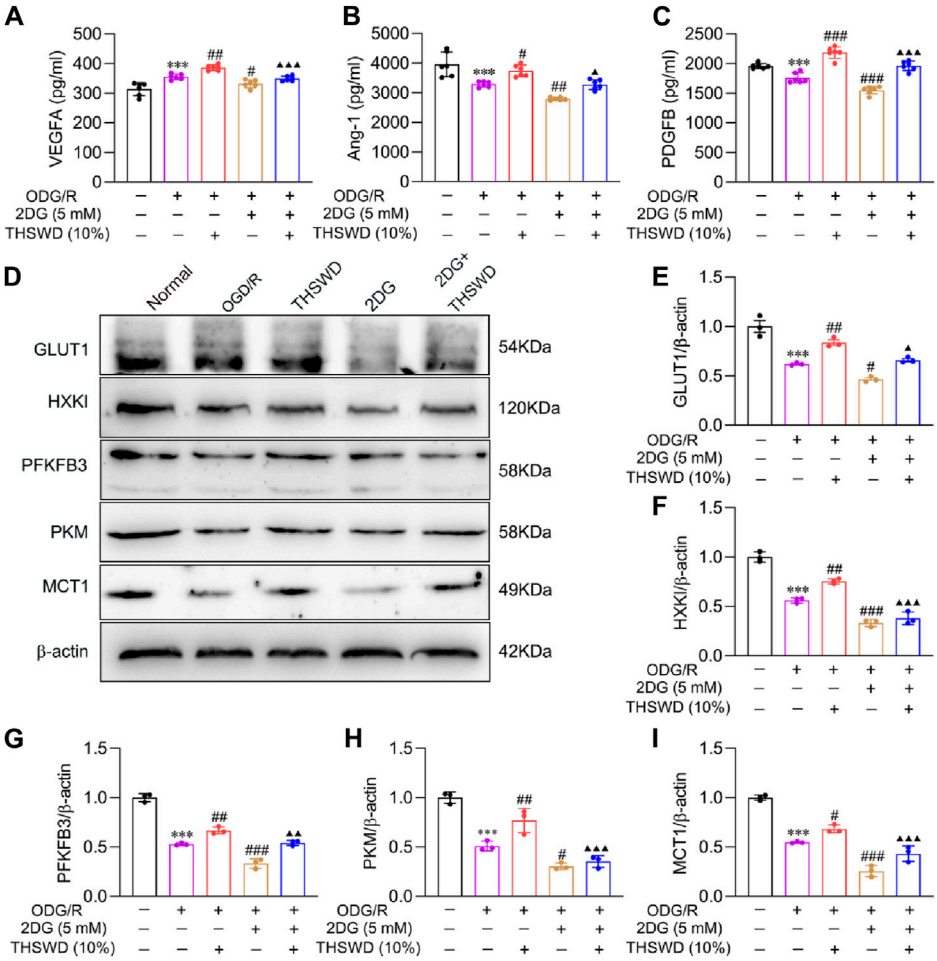

FIGURE 8
Effect of THSWD on mature angiogenesis factors and glycolysis pathway proteins in OGD/R-induced BMECs. The ELISA detected **(A)** VEGFA, **(B)** Ang1, and **(C)** PDGFB concentrations (n = 6). **(D)** The representative protein bands of GLUT1, HXKI, PFKFB3, PKM, and MCT1. **(E–I)** Quantitative statistical results of GLUT1, HXKI, PFKFB3, PKM, and MCT1 (n = 3). Data were expressed as mean ± SD. ***$p < 0.001$ vs. the normal group; $^{\#}p < 0.05$, $^{\#\#}p < 0.01$, $^{\#\#\#}p < 0.001$ vs. the OGD/R group; $^{\blacktriangle}p < 0.05$, $^{\blacktriangle\blacktriangle}p < 0.01$, $^{\blacktriangle\blacktriangle\blacktriangle}p < 0.001$ vs. the THSWD group.

MCT1 (Végran et al., 2011). The high glycolysis activity of ECs can generate large amounts of accumulated lactate. If not transported promptly, it can inhibit the activity of phosphofructokinase 1, reduce the rate of glycolysis, and even cause glycolysis inactivation in severe cases (Noble et al., 2017). MCT1 is a major transporter that regulates lactate efflux from ECs and maintains homeostasis in the intracellular environment (Végran et al., 2011). When impaired, its function aggravates lactate accumulation in ECs and reduces glycolysis flux. We found that THSWD could significantly enhance the glucose uptake and release of pyruvate and lactate in BMECs. Moreover, the ATP expression level was also significantly increased. Compared to the THSWD group, the 2DG + THSWD group suppressed glycolysis levels, suggesting that THSWD could effectively activate glycolysis in BMECs and increase its levels. As previously described, THSWD could effectively promote the mature angiogenesis process in BMECs, potentially related to its increased glycolysis flux. The results of WB assays unveiled that THSWD effectively increased the expression of GLUT1, glycolysis kinases (HXK1, PKM, PFKFB3), and MCT1. These findings suggest that THSWD may effectively increase glycolysis by up-regulating the content of critical proteins and enzymes in the glycolysis pathway and promoting the expression of mature angiogenic factors, accelerating the process of mature angiogenesis.

As described previously, THSWD for IS treatment is characterized by multiple pathways, multiple targets, and limited side effects. This can compensate for the issues of single targets and numerous side effects present in the Western medical treatment of IS. This study offers a new research strategy for treating IS in THSWD. However, it can be improved via the following aspects: 1) examining the mature angiogenesis at different time points (days 3, 14, and 21); 2) using EC glycolysis gene knockout mice for subsequent validation; 3) additional IS patient clinical data.

Conclusion

These findings suggest that THSWD may exert a critical protective influence in CIRI by promoting mature angiogenesis

via activation of the glycolysis pathway. Therefore, promoting mature angiogenesis is an effective therapeutic strategy for IS. In addition, this study offers a theoretical basis for preclinical studies of the TCM compound THSWD in treating IS.

Data availability statement

The original contributions presented in the study are included in the article/Supplementary Material, further inquiries can be directed to the corresponding authors.

Ethics statement

The animal study was reviewed and approved by Animal Ethics Committee of Anhui University of Traditional Chinese Medicine. The study was conducted in accordance with the local legislation and institutional requirements.

Author contributions

LT: Writing–original draft. ZL: Writing–original draft. ZJ: Data curation, Funding acquisition, Methodology, Resources, Writing–review and editing. XZ: Data curation, Software, Visualization, Formal Analysis, Writing–review and editing. MZ: Data curation, Formal Analysis, Software, Writing–review and editing. DP: Writing–review and editing. LH: Writing–review and editing.

Funding

The author(s) declare financial support was received for the research, authorship, and/or publication of this article. This work was supported by the National Natural Science Foundation of China (82074152, 82304912, and 81903953) and the Provincial Natural Science Project of Anhui Colleges (KJ 2020A0420 and 2023AH050744).

Conflict of interest

The authors declare that the research was conducted in the absence of any commercial or financial relationships that could be construed as a potential conflict of interest.

Publisher's note

Supplementary material

The Supplementary Material for this article can be found online at: https://www.frontiersin.org/articles/10.3389/fphar.2024.1395167/full#supplementary-material

References

Armulik, A., Genové, G., and Betsholtz, C. (2011). Pericytes: developmental, physiological, and pathological perspectives, problems, and promises. *Dev. Cell* 21 (2), 193–215. doi:10.1016/j.devcel.2011.07.001

Behera, A., Adjei Boakye, E., Trivedi, J., Armbrecht, E., Alshekhlee, A., and Edgell, R. (2020). Real-world impact of retrievable stents for acute ischemic stroke on disability utilizing the national inpatient sample. *Interv. Neurol.* 8 (1), 60–68. doi:10.1159/000495160

Bikfalvi, A., and Bicknell, R. (2002). Recent advances in angiogenesis, anti-angiogenesis and vascular targeting. *Trends Pharmacol. Sci.* 23 (12), 576–582. doi:10.1016/s0165-6147(02)02109-0

Bjarnegård, M., Enge, M., Norlin, J., Gustafsdottir, S., Fredriksson, S., Betsholtz, C., et al. (2004). Endothelium-specific ablation of PDGFB leads to pericyte loss and glomerular, cardiac and placental abnormalities. *Dev. Camb. Engl.* 131 (8), 1847–1857. doi:10.1242/dev.01080

Chang, J., Mancuso, M. R., Maier, C., Liang, X., Andreasson, K., Kuo, C. J., et al. (2017). Gpr124 is essential for blood-brain barrier integrity in central nervous system disease. *Nat. Med.* 23 (4), 450–460. doi:10.1038/nm.4309

Chen, C. J., Cheng, F. C., Liao, S. L., Chen, W. Y., Lin, N. N., and Kuo, J. S. (2000). Effects of naloxone on lactate, pyruvate metabolism and antioxidant enzyme activity in rat cerebral ischemia/reperfusion. *Neurosci. Lett.* 287 (2), 113–116. doi:10.1016/s0304-3940(00)01151-4

Chen, F. F., Wang, M. M., Xia, W. W., Peng, D. Y., and Han, L. (2020). Tao-Hong-Si-Wu Decoction promotes angiogenesis after cerebral ischaemia in rats via platelet microparticles. *Chin. J. Nat. Med.* 18 (8), 620–627. doi:10.1016/S1875-5364(20)30074-1

Chen, J., Sanberg, P. R., Li, Y., Wang, L., Lu, M., Willing, A. E., et al. (2001). Intravenous administration of human umbilical cord blood reduces behavioral deficits after stroke in rats. *Stroke* 32 (11), 2682–2688. doi:10.1161/hs1101.098367

Chen, S., Cui, W., Chi, Z., Xiao, Q., Hu, T., Wang, D., et al. (2022). Tumor-associated macrophages are shaped by intratumoral high potassium via Kir2.1. *Cell metab.* 34 (11), 1843–1859.e11. doi:10.1016/j.cmet.2022.08.016

Chng, S. M., Petersen, E. T., Zimine, I., Sitoh, Y. Y., Lim, C. C., and Golay, X. (2008). Territorial arterial spin labeling in the assessment of collateral circulation: comparison with digital subtraction angiography. *Stroke* 39 (12), 3248–3254. doi:10.1161/STROKEAHA.108.520593

Cruys, B., Wong, B. W., Gerhardt, H., Dewerchin, M., Bentley, K., Carmeliet, P., et al. (2016). Glycolytic regulation of cell rearrangement in angiogenesis. *Nat. Commun.* 7, 12240. doi:10.1038/ncomms12240

Cunnane, S. C., Trushina, E., Morland, C., Prigione, A., Swerdlow, R. H., Millan, M. J., et al. (2020). Brain energy rescue: an emerging therapeutic concept for neurodegenerative disorders of ageing. *Nat. Rev. Drug Discov.* 19 (9), 609–633. doi:10.1038/s41573-020-0072-x

De Bock, K., Georgiadou, M., Schoors, S., Chesney, J., Dewerchin, M., Carmeliet, P., et al. (2013). Role of PFKFB3-driven glycolysis in vessel sprouting. *Cell* 154 (3), 651–663. doi:10.1016/j.cell.2013.06.037

Duan, X., Pan, L., Peng, D., Wu, H., Peng, C., Chen, W., et al. (2020). Analysis of the active components and metabolites of Taohong Siwu decoction by using ultra high performance liquid chromatography quadrupole time-of-flight mass spectrometry. *J. Sep. Sci.* 43 (22), 4131–4147. doi:10.1002/jssc.202000498

GBD 2019 Stroke Collaborators (2021). Global, regional, and national burden of stroke and its risk factors, 1990-2019: a systematic analysis for the Global Burden of Disease Study 2019. *Lancet. Neurology* 20 (10), 795–820. doi:10.1016/S1474-4422(21)00252-0

Gete, Y. G., Koblan, L. W., Mao, X., Trappio, M., Mahadik, B., Liu, D. R., et al. (2021). Mechanisms of angiogenic incompetence in Hutchinson-Gilford progeria via downregulation of endothelial NOS. *Aging Cell* 20 (7), e13388. doi:10.1111/acel.13388

Hellström, M., Gerhardt, H., Kalén, M., Li, X., Eriksson, U., Wolburg, H., et al. (2001). Lack of pericytes leads to endothelial hyperplasia and abnormal vascular morphogenesis. *J. Cell Biol.* 153 (3), 543–553. doi:10.1083/jcb.153.3.543

Helms, A. K., Whelan, H. T., and Torbey, M. T. (2007). Hyperbaric oxygen therapy of acute ischemic stroke. *Stroke* 38 (4), 1137; author reply 1138–1139. doi:10.1161/01.STR.0000259832.57823.83

Hui, Z., Wang, S., Li, J., Wang, J., and Zhang, Z. (2022). Compound Tongluo Decoction inhibits endoplasmic reticulum stress-induced ferroptosis and promoted angiogenesis by activating the Sonic Hedgehog pathway in cerebral infarction. *J. Ethnopharmacol.* 283, 114634. doi:10.1016/j.jep.2021.114634

Jurcovicova, J. (2014). Glucose transport in brain - effect of inflammation. *Endocr. Regul.* 48 (1), 35–48. doi:10.4149/endo_2014_01_35

Koh, G. Y. (2013). Orchestral actions of angiopoietin-1 in vascular regeneration. *Trends Mol. Med.* 19 (1), 31–39. doi:10.1016/j.molmed.2012.10.010

Kumar, D., Branch, B. G., Pattillo, C. B., Lefer, D. J., Patel, R. P., Kevil, C. G., et al. (2008). Chronic sodium nitrite therapy augments ischemia-induced angiogenesis and arteriogenesis. *Proc. Natl. Acad. Sci. U. S. A.* 105 (21), 7540–7545. doi:10.1073/pnas.0711480105

Lee, S. W., Kim, W. J., Jun, H. O., Choi, Y. K., and Kim, K. W. (2009). Angiopoietin-1 reduces vascular endothelial growth factor-induced brain endothelial permeability via upregulation of ZO-2. *Int. J. Mol. Med.* 23 (2), 279–284.

Li, J. G., Wang, L. Q., Yang, X. Y., Xu, H., Liu, J. P., et al. (2017). Chinese herbal medicine Dengzhan Xixin injection for acute ischemic stroke: a systematic review and meta-analysis of randomised controlled trials. *Complementary Ther. Med.* 34, 74–85. doi:10.1016/j.ctim.2017.08.004

Li, L., Yang, N., Nin, L., Zeng, D., Qi, H., Xu, X., et al. (2015). Chinese herbal medicine formula tao hong si wu decoction protects against cerebral ischemia-reperfusion injury via PI3K/Akt and the Nrf2 signaling pathway. *J. Nat. Med.* 69 (1), 76–85. doi:10.1007/s11418-014-0865-5

Li, Y., Lu, Z., Keogh, C. L., Yu, S. P., and Wei, L. (2007). Erythropoietin-induced neurovascular protection, angiogenesis, and cerebral blood flow restoration after focal ischemia in mice. *J. Cereb. blood flow metabolism official J. Int. Soc. Cereb. Blood Flow Metabolism* 27 (5), 1043–1054. doi:10.1038/sj.jcbfm.9600417

Li, Y., Tan, L., Yang, C., He, L., Liu, L., Guo, J., et al. (2023). Distinctions between the Koizumi and Zea Longa methods for middle cerebral artery occlusion (MCAO) model: a systematic review and meta-analysis of rodent data. *Sci. Rep.* 13 (1), 10247. doi:10.1038/s41598-023-37187-w

Liu, D., Scalzo, F., Rao, N. M., Hinman, J. D., Liu, X., Liebeskind, D. S., et al. (2016a). Fluid-attenuated inversion recovery vascular hyperintensity topography, novel imaging marker for revascularization in middle cerebral artery occlusion. *Stroke* 47 (11), 2763–2769. doi:10.1161/STROKEAHA.116.013953

Liu, X. T., Ren, P. W., Peng, L., Hong, Q., Yang, W. J., Wen, S., et al. (2016b). Effectiveness and safety of ShenXiong glucose injection for acute ischemic stroke: a systematic review and GRADE approach. *BMC complementary Altern. Med.* 16, 68. doi:10.1186/s12906-016-1038-8

Liu, Z. L., Chen, H. H., Zheng, L. L., Sun, L. P., and Shi, L. (2023). Angiogenic signaling pathways and anti-angiogenic therapy for cancer. *Signal Transduct. Target. Ther.* 8 (1), 198. doi:10.1038/s41392-023-01460-1

Noble, R. A., Bell, N., Blair, H., Bomken, S., Critchlow, S. E., Wedge, S. R., et al. (2017). Inhibition of monocarboxyate transporter 1 by AZD3965 as a novel therapeutic approach for diffuse large B-cell lymphoma and Burkitt lymphoma. *Haematologica* 102 (7), 1247–1257. doi:10.3324/haematol.2016.163030

Oyama, K., Ohnuki, T., Ohnuki, N., and Nitta, S. (1996). The effect of basic fibroblast growth factor (bFGF) on early bronchial revascularization. *Nihon Kyobu Geka Gakkai* 44 (11), 2032–2039.

Pan, L., Peng, C., Wang, L., Wang, N., Chu, F., Peng, D., et al. (2022). Network pharmacology and experimental validation-based approach to understand the effect and mechanism of Taohong Siwu Decoction against ischemic stroke. *J. Ethnopharmacol.* 294, 115339. doi:10.1016/j.jep.2022.115339

Perrotta, P., Van der Veken, B., Van Der Veken, P., Pintelon, I., Roosens, L., Adriaenssens, E., et al. (2020). Partial inhibition of glycolysis reduces atherogenesis independent of intraplaque neovascularization in mice. *Arteriosclerosis, thrombosis, Vasc. Biol.* 40 (5), 1168–1181. doi:10.1161/ATVBAHA.119.313692

Raudam, E. I., and Rivis, E. K. (1976). The prognostic value of the lactate concentration and lactate/pyruvate ratio in cerebrospinal fluid following acute cerebral circulatory disorders. *Vopr. neirokhirurgii* (2), 32–37.

Schoors, S., De Bock, K., Cantelmo, A. R., Chesney, J., Dewerchin, M., Carmeliet, P., et al. (2014). Partial and transient reduction of glycolysis by PFKFB3 blockade reduces pathological angiogenesis. *Cell metab.* 19 (1), 37–48. doi:10.1016/j.cmet.2013.11.008

Shi, Y., Liu, Q., Chen, W., Wang, R., Wang, L., Liu, Z. Q., et al. (2023). Protection of Taohong Siwu Decoction on PC12 cells injured by oxygen glucose deprivation/reperfusion via mitophagy-NLRP3 inflammasome pathway *in vitro*. *J. Ethnopharmacol.* 301, 115784. doi:10.1016/j.jep.2022.115784

Sun, X., and Liu, B. (2022). Donepezil ameliorates oxygen-glucose deprivation/reoxygenation-induced brain microvascular endothelial cell dysfunction via the SIRT1/FOXO3a/NF-κB pathways. *Bioengineered* 13 (3), 7760–7770. doi:10.1080/21655979.2022.2045833

Thurston, G., Rudge, J. S., Ioffe, E., McDonald, D. M., Yancopoulos, G. D., Croll, S. D., et al. (2000). Angiopoietin-1 protects the adult vasculature against plasma leakage. *Nat. Med.* 6 (4), 460–463. doi:10.1038/74725

Végran, F., Boidot, R., Michiels, C., Sonveaux, P., and Feron, O. (2011). Lactate influx through the endothelial cell monocarboxylate transporter MCT1 supports an NF-κB/IL-8 pathway that drives tumor angiogenesis. *Cancer Res.* 71 (7), 2550–2560. doi:10.1158/0008-5472.CAN-10-2828

Wang, M., Liu, Z., Hu, S., Duan, X., Zhang, Y., Peng, C., et al. (2020). Taohong Siwu decoction ameliorates ischemic stroke injury via suppressing pyroptosis. *Front. Pharmacol.* 11, 590453. doi:10.3389/fphar.2020.590453

Wang, X., Hu, Z., Wang, Z., Cui, Y., and Cui, X. (2019). Angiopoietin-like protein 2 is an important facilitator of tumor proliferation, metastasis, angiogenesis and glycolysis in osteosarcoma. *Am. J. Transl. Res.* 11 (10), 6341–6355.

Wu, S. P., Wang, N., and Zhao, L. (2020). Network pharmacology reveals the mechanism of activity of tongqiao huoxue decoction extract against middle cerebral artery occlusion-induced cerebral ischemia-reperfusion injury. *Front. Pharmacol.* 11, 572624. doi:10.3389/fphar.2020.572624

Xia, W., Hu, S., Wang, M., Xu, F., Han, L., and Peng, D. (2021). Exploration of the potential mechanism of the Tao Hong Si Wu Decoction for the treatment of postpartum blood stasis based on network pharmacology and *in vivo* experimental verification. *J. Ethnopharmacol.* 268, 113641. doi:10.1016/j.jep.2020.113641

Yu, P., Wilhelm, K., Dubrac, A., Carmeliet, P., Chittenden, T. W., Eichmann, A., et al. (2017). FGF-dependent metabolic control of vascular development. *Nature* 545 (7653), 224–228. doi:10.1038/nature22322

Zhang, H. T., Zhang, P., Gao, Y., Li, Y. L., Jiang, C. L., Chen, L. C., et al. (2017). Early VEGF inhibition attenuates blood-brain barrier disruption in ischemic rat brains by regulating the expression of MMPs. *Mol. Med. Rep.* 15 (1), 57–64. doi:10.3892/mmr.2016.5974

Zhang, Y., Cedervall, J., Hamidi, A., Alitalo, K., Betsholtz, C., Dimberg, A., et al. (2020). Platelet-Specific PDGFB ablation impairs tumor vessel integrity and promotes metastasis. *Cancer Res.* 80 (16), 3345–3358. doi:10.1158/0008-5472.CAN-19-3533

Zhang, Z. G., Zhang, L., Jiang, Q., Zhang, R., Davies, K., Powers, C., et al. (2000). VEGF enhances angiogenesis and promotes blood-brain barrier leakage in the ischemic brain. *J. Clin. investigation* 106 (7), 829–838. doi:10.1172/JCI9369

frontiers | Frontiers in Pharmacology

TYPE Original Research
PUBLISHED 27 June 2024
DOI 10.3389/fphar.2024.1415445

OPEN ACCESS

EDITED BY
Viola B. Morris,
Emory University, United States

REVIEWED BY
Vidhya Prasad,
Emory University, United States
Josna Joseph,
Christian Medical College and Hospital, India

*CORRESPONDENCE
Hai-tong Wan,
whtong@126.com
Jiehong Yang,
yjhong@zcmu.edu.cn

†These authors contributed equally to this work and share the first authorship

RECEIVED 10 April 2024
ACCEPTED 03 June 2024
PUBLISHED 27 June 2024

CITATION
She Y, Shao C-y, Liu Y-f, Huang Y, Yang J and Wan H-t (2024), Catalpol reduced LPS induced BV2 immunoreactivity through NF-κB/NLRP3 pathways: an *in Vitro* and in silico study. *Front. Pharmacol.* 15:1415445.
doi: 10.3389/fphar.2024.1415445

Catalpol reduced LPS induced BV2 immunoreactivity through NF-κB/NLRP3 pathways: an *in Vitro* and in silico study

Yong She[1†], Chong-yu Shao[2†], Yuan-feng Liu[1], Ying Huang[1], Jiehong Yang[2*] and Hai-tong Wan[2*]

[1]School of Life Sciences, Zhejiang Chinese Medical University, Hangzhou, Zhejiang, China, [2]School of Basic Medical Sciences, Zhejiang Chinese Medical University, Hangzhou, Zhejiang, China

Background: Ischemic Stroke (IS) stands as one of the primary cerebrovascular diseases profoundly linked with inflammation. In the context of neuroinflammation, an excessive activation of microglia has been observed. Consequently, regulating microglial activation emerges as a vital target for neuroinflammation treatment. Catalpol (CAT), a natural compound known for its anti-inflammatory properties, holds promise in this regard. However, its potential to modulate neuroinflammatory responses in the brain, especially on microglial cells, requires comprehensive exploration.

Methods: In our study, we investigated into the potential anti-inflammatory effects of catalpol using lipopolysaccharide (LPS)-stimulated BV2 microglial cells as an experimental model. The production of nitric oxide (NO) by LPS-activated BV2 cells was quantified using the Griess reaction. Immunofluorescence was employed to measure glial cell activation markers. RT-qPCR was utilized to assess mRNA levels of various inflammatory markers. Western blot analysis examined protein expression in LPS-activated BV2 cells. NF-κB nuclear localization was detected by immunofluorescent staining. Additionally, molecular docking and molecular dynamics simulations (MDs) were conducted to explore the binding affinity of catalpol with key targets.

Results: Catalpol effectively suppressed the production of nitric oxide (NO) induced by LPS and reduced the expression of microglial cell activation markers, including Iba-1. Furthermore, we observed that catalpol downregulated the mRNA expression of proinflammatory cytokines such as IL-6, TNF-α, and IL-1β, as well as key molecules involved in the NLRP3 inflammasome and NF-κB pathway, including NLRP3, NF-κB, caspase-1, and ASC. Our mechanistic investigations shed light on how catalpol operates against neuroinflammation. It was evident that catalpol significantly inhibited the phosphorylation of NF-κB and NLRP3 inflammasome activation, both of which serve as upstream regulators of the inflammatory cascade. Molecular docking and MDs showed strong binding interactions between catalpol and key targets such as NF-κB, NLRP3, and IL-1β.

Conclusion: Our findings support the idea that catalpol holds the potential to alleviate neuroinflammation, and it is achieved by inhibiting the activation of

NLRP3 inflammasome and NF-κB, ultimately leading to the downregulation of pro-inflammatory cytokines. Catalpol emerges as a promising candidate for the treatment of neuroinflammatory conditions.

KEYWORDS

neuroinflammation, microglia, molecular docking analysis, molecular dynamics simulation, *in vitro*

1 Introduction

Stroke is a severe cardiovascular disease posing significant threats to human health, characterized by high incidence, disability, and mortality rates. Stroke is the second leading cause of disability and death globally, with low- and middle-income countries bearing the greatest burden. In 2016, there were 13.7 million new cases of stroke worldwide, with approximately 87% being ischemic strokes (Saini et al., 2021). Overall, stroke accounted for 11.6% of total deaths globally, reinforcing its status as a major public health concern (Feigin et al., 2021). An increasing body of evidence suggests that neuroinflammation is associated with the primary pathogenesis of ischemic stroke. (Maida et al., 2020). During the entire inflammatory process, various immune cells, including microglia and macrophages, become activated (Iadecola and Anrather, 2011). Among these innate immune cells, microglia take the central stage in the realm of neuroinflammation (DiSabato et al., 2016). After injury or infection, microglia shift towards a phenotype that promotes inflammation, such as exposure to bacterial-derived products like LPS. Thus, the cells release pro-inflammatory cytokines like TNF-α, interleukin (IL)-1β, and IL-6, along with inducible NO (iNOS) that contributes to nitric oxide creation (Orihuela et al., 2016). Therefore, controlling microglial activation and the inhibition of pro-inflammatory mediators and cytokines are viewed as promising treatment strategies in the onset and progression of ischemic stroke.

Rehmannia glutinosa, a commonly used herb in traditional Chinese medicine, has been widely employed to treat diabetes (Bian et al., 2023), neurological disorders (Pan et al., 2022), and inflammation (Zhang et al., 2023). Catalpol (CAT), an iridoid glycoside compound isolated from *Rehmannia glutinosa*, is a water-soluble component known for its anti-inflammatory and hepatoprotective properties. (Zhang J. et al., 2019). Recent studies have demonstrated the anti-inflammatory properties of catalpol in various conditions such as diabetes (Shu et al., 2021), nephropathy (Zaaba et al., 2023), and encephalopathy. In the context of ischemic stroke, *in vitro* experiments have utilized different cell types to study the effects of catalpol. These cell types include SY5Y cells, primary neurons, BMEC cells, and BV2 microglia, highlighting its potential therapeutic application across a range of neural and non-neural cell models. Nonetheless, the efficacy of catalpol in effectively mitigating the activation of the LPS-induced microglial remains to be established, and the underlying molecular mechanisms for anti-neuroinflammation remain unexplored.

In this investigation, we used BV2 cells treated with LPS, a mouse microglial cell line, as an experimental model to explore the anti-inflammatory characteristics of catalpol and to clarify the signaling pathways involved in its effects. To identify key catalpol targets, we used molecular docking to predict binding affinity with specific proteins. This was followed by validation through molecular dynamics (MD) simulation techniques and further *in vitro* experiments. Collectively, our findings strongly indicate that catalpol has a significant impact on neuroinflammatory responses induced by LPS in BV2 microglial cells.

2 Materials and methods

2.1 Cell lines and cell culture

Mouse microglial cells (BV2, Accession Number: CVCL_0182) were obtained from the Cell Bank of Type Culture Collection of the Chinese Academy of Sciences (Shanghai, China) and were cultured in a 37°C, 5% CO_2 environment using high-glucose DMEM (Gibco, ThermoFisher Scientific, US), supplemented with 10% fetal bovine serum (FBS, BI, Israel), and 1% penicillin/streptomycin. The subsequent experiments were conducted using BV2 cells at passages 3–5. Upon reaching 80% confluence, the cells were split using 0.25% trypsin and sub-cultured for subsequent experiments. Cells were pretreated with catalpol (250 and 500 μM) for 24 h, followed by treatment with or without LPS (500 ng/mL) for 6 h. The catalpol (product number: AB1238-100 mg; CAS number: 2415-24-9; HPLC ≥98%) was purchased from Chengdu Alfa Biotechnology Co., Ltd.

The BV2 cells were divided into four groups for subsequent experimental studies: the blank control group (C group), the model group (M group), the catalpol low-dose group (CAT-L group), and the catalpol high-dose group (CAT-H group).

2.2 CCK-8 cell viability assay

A CCK-8 assay followed the manufacturer's instructions with a commercial kit from Biosharp, Guangzhou, China. (Zhao et al., 2023). In summary, BV2 cells were plated in 96-well plates during the logarithmic growth phase (1×10^5 cells/well) and exposed to varying concentrations of catalpol (50–2000 μM) for 24 h. Subsequently, The cells were exposed to 10 μL/well of the CCK-8 solution and then placed in a 5% CO_2 incubator at 37°C for 1 hour, after which the absorbance was measured at 450 nm. For each concentration of catalpol, six technical replicates were used, and the entire experiment was repeated three times.

2.3 NO assay

50 μL/well of supernatants were collected, and the levels of total nitric oxide (NO) were determined using the Griess assay kit (Beyotime, Shanghai, China) by the manufacturer's instructions, as previously reported. The sodium nitrite standard was diluted in complete culture medium to concentrations of 0, 1, 2, 5, 10, 20, 40, 60, and 100 μM, and a standard curve was constructed. To calculate nitrite concentrations, sodium nitrite was used to create a standard

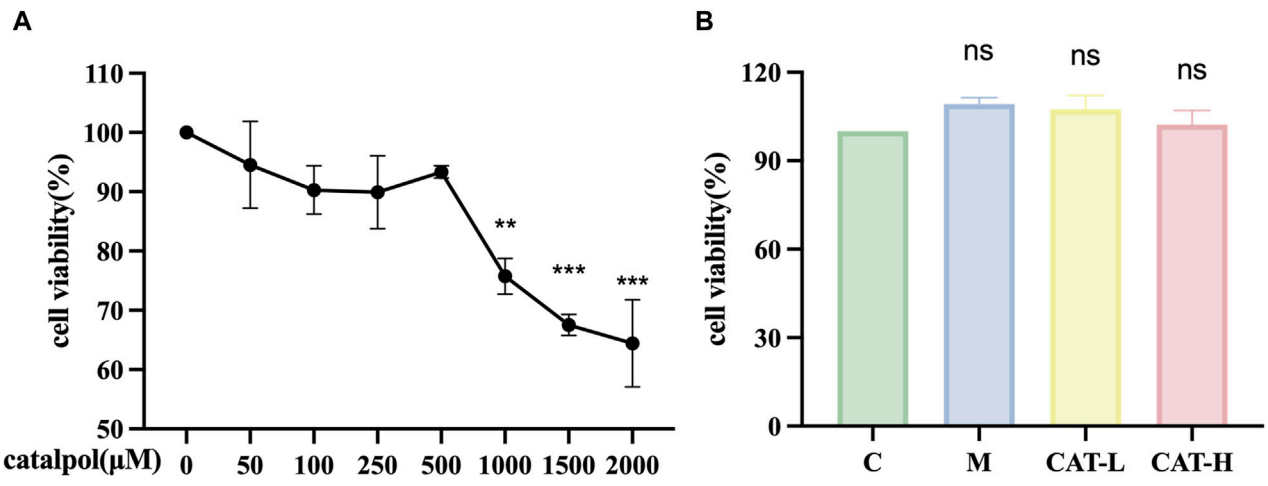

FIGURE 1
The effects of catalpol on proliferation in BV2 cells. CCK-8 assay was used to detect the viability of BV2 cells. **(A)** BV2 cells were treated with catalpol (0, 50, 100, 250, 500, 1,000, 1,500 or 2,000 μM) for 24 h **(B)**. BV2 cells were pretreated with 250 μM catalpol (CAT-L) or 500 μM catalpol (CAT-H) for 24 h, and then incubated with or without LPS (500 ng/mL) for 6 h.

curve of different dilutions. The reaction mixtures were measured for their absorbance at 540 nm using a microplate reader.

2.4 Real-time quantitative PCR (RT-qPCR)

Harvested BV2 cells were subjected to total RNA extraction using the FastPure Cell/Tissue Total RNA Isolation Kit V2 (Vazyme; Nanjing, China). The RNA was reverse transcribed (Biosharp, Guangzhou, China), and quantitative assessment (ABclonal, Wuhan, China) was performed as previously described (Yu et al., 2022). The amplification reactions were performed according to the ABclonal qPCR reagent kit instructions. The cycling conditions were 95°C for 3 min, followed by 40 cycles of 95°C for 5 s and 60°C for 30 s. GAPDH was used as the housekeeping gene, and the relative expression levels of the target genes were calculated using the $2^{-\Delta\Delta Ct}$ method with the control group as the reference. The primer sequences can be found in Supplementary Table S1.

2.5 Western blotting

Western blotting was performed as previously described (Zhao et al., 2023). Sixteen micrograms of protein were separated using sodium dodecyl sulfate-polyacrylamide gel electrophoresis (SDS-PAGE) and then transferred onto polyvinylidene fluoride (PVDF) membranes. After transfer, PVDF membranes were blocked with 5% BSA for 1.5 h and incubated overnight at 4°C with primary antibodies. The next day, the membranes were incubated with a secondary antibody for 1.5 h. The information about the antibodies is shown in Supplementary Table S2.

2.6 Immunofluorescence staining

The experimental procedure was performed as previously described (Zhao et al., 2023). The cells were fixed in 4% paraformaldehyde at room temperature for 30 min and then washed thrice with PBS. After permeabilization with 0.2% Triton X-100/PBS for 15 min, the cells were washed with PBS, blocked in PBS with 5% BSA at room temperature for 1 h, and then incubated overnight at 4°C with primary antibodies. The next day, after being washed with PBS, the cells were incubated with ABflo® 594 goat anti-rabbit (1:200) secondary antibody for 1 h in the dark. Then, the cells were washed with PBS and treated in the dark with an antifade mounting medium containing DAPI for 10 min at 37°C. Finally, the relative positive expression rates of the sections were determined using ImageJ, and information about the antibodies is shown in Supplementary Table S2.

2.7 Annexin V-FITC (apoptosis) assay

Apoptosis was assessed by flow cytometry using the Annexin V-FITC Apoptosis Detection kit (Beyotime, Shanghai, China) and performed according to the manufacturer's instructions. The cells were detached using trypsin and then pelleted by centrifugation at 1,000 rpm for 5 min. The obtained cells were washed with ice-cold PBS (1X) and resuspended in 400 μL binding solution. Next, the cells were stained with both Annexin V-FITC (5 μL) and propidium iodide (10 μL) in the dark for 20 min at room temperature, and their apoptosis rate was determined within 0.5 h using a flow cytometer (Beckman, US). Data were analyzed using FlowJo software.

2.8 Database websites and software

The databases and software used were as follows: PubChem database (https://pubchem.ncbi.nlm.nih.gov/), GeneCards (http://www.genecards.org), UniProt (https://www.uniprot.org), Acpype Server (https://www.bio2byte.be/acpype/), Autodock vina_1.2.3 software, Discovery Studio 2021 software, Gromacs 2019.6, and Gmx_MMPBSA software.

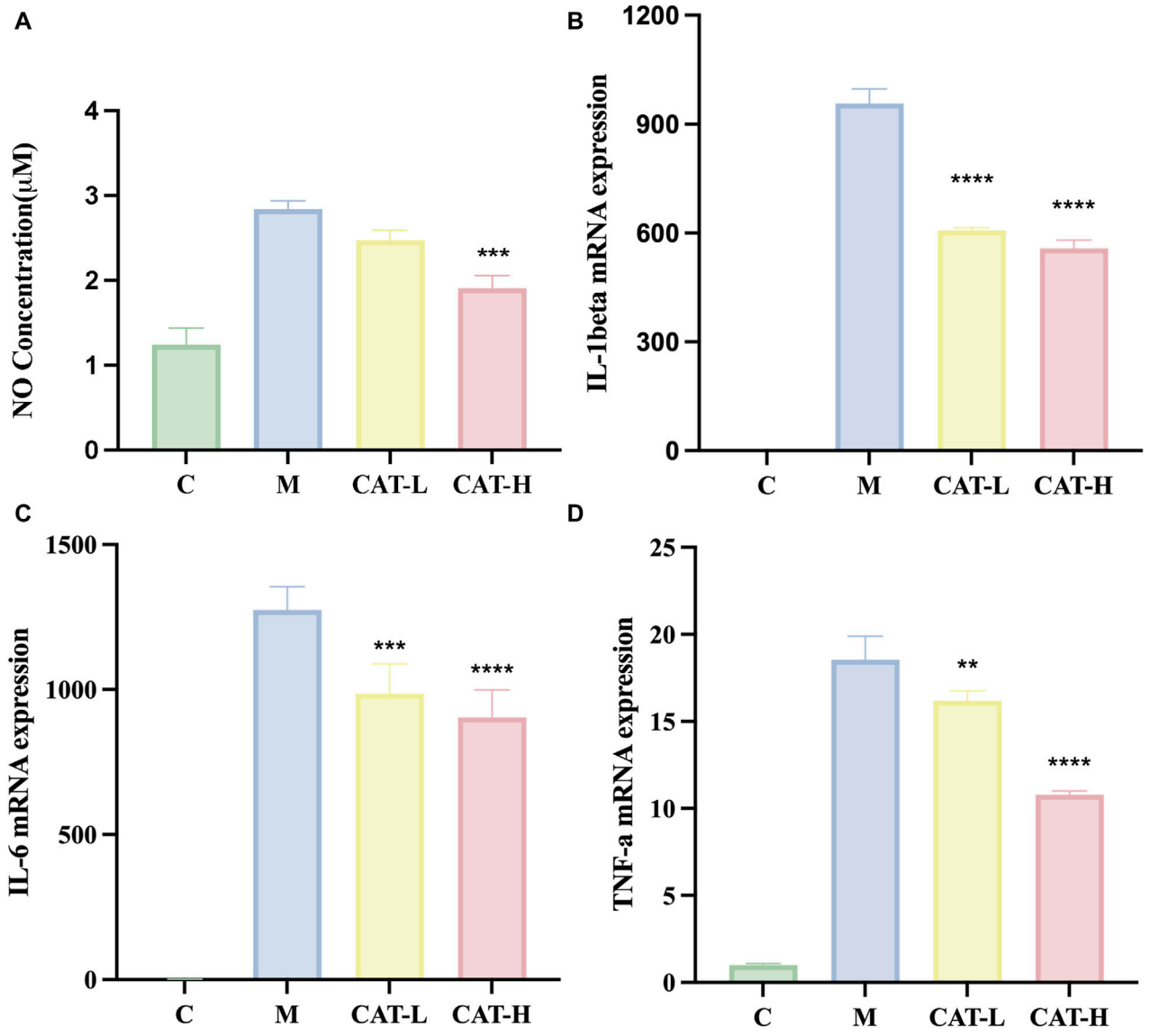

FIGURE 2
(A) NO concentration in the supernatant was measured using the Griess reaction. Gene expression levels of IL-1β, IL-6, and TNF-αwere assessed using RT-qPCR. **(B–D)**. All data are presented as the mean ± SD (n = 3). $^{**}p < 0.01$, $^{***}p < 0.001$ $^{****}p < 0.0001$.

2.9 Molecular docking

The protein structure files of IL-1β, NLRP3, and NF-κB were obtained from AlphaFold. The three-dimensional (3D) structure of Catalpol was retrieved from the PubChem database. Following the method of Liu et al. (2024), We used AutoDockTools to prepare the three-dimensional structures of key components and the crystal structures of core proteins. Subsequently, molecular docking of the ligands and receptors was performed using AutoDock Vina. Finally, visual analysis was conducted using PyMOL and Discovery Studio.

2.10 Molecular dynamics simulation

After docking, the MD simulation was performed using Gromacs 2022.2 software, the AMBERff14SB force field, and the TI3P model to check the stability of the combined pose with the lowest binding energy. The complexes were placed in a dodecahedral box with a minimum distance of 1.2 nm between the protein atoms and the box edges. Energy minimization was performed using the steepest descent method until the energy converged to 1,000 kJ mol^{-1} nm^{-1}. Finally, the simulation trajectories were analyzed using various scripts integrated within GROMACS.

2.11 Binding energy calculation through MM-PBSA

The binding free energy of protein-ligand complexes was calculated using the g_mmpbsa tool, which calculated the binding free energy of complex structures using the Molecular Mechanics Poisson–Boltzmann surface area (MM-PBSA) method.

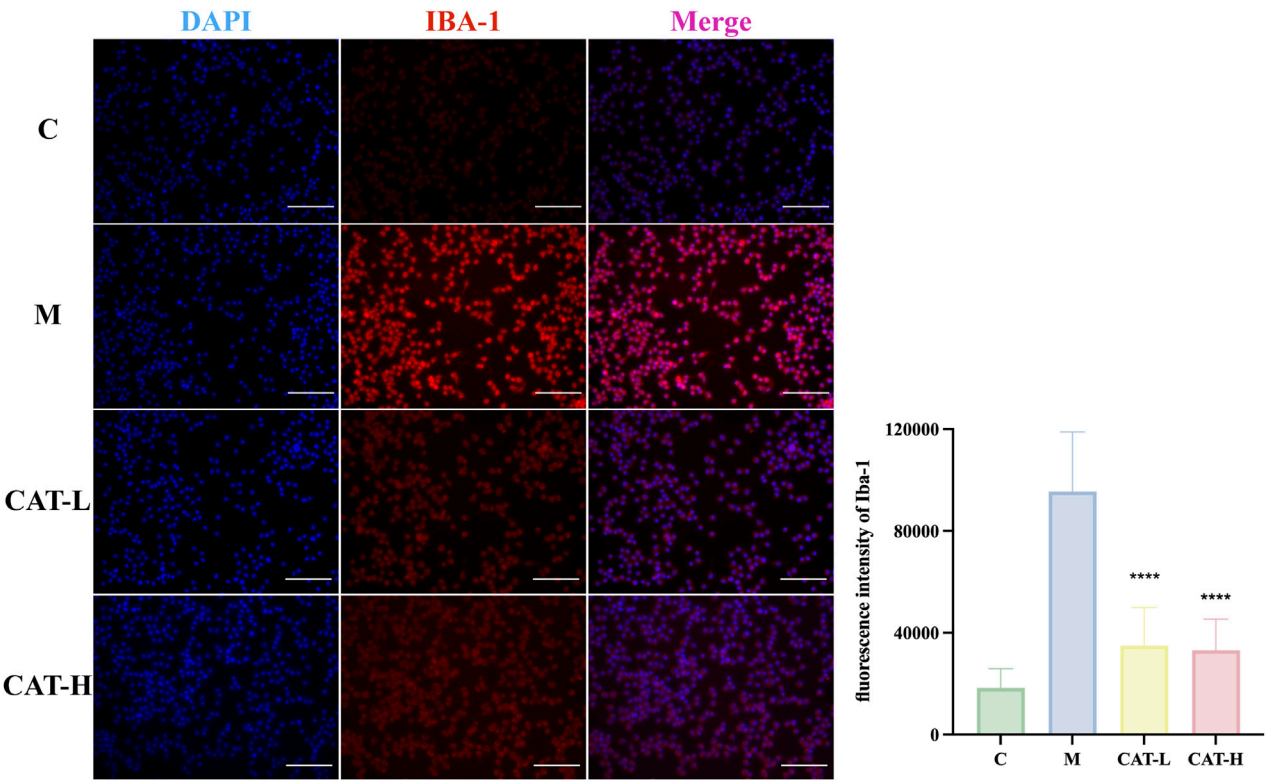

FIGURE 3
Cell morphology and IBA-1 protein expression were observed with immunofluorescence staining. Representative images of IF staining at × 20 magnification. Representative photomicrographs showed BV-2 cells labeled with an Iba-1 antibody (in red), with cell nuclei counterstained using DAPI (in blue). Scale bar: 500 μM. All data are presented as the mean ± SD (n = 3). ****$p < 0.0001$.

2.12 Statistical analysis

Results are expressed as mean ± SD. Statistical analysis of experimental data was performed using one-way analysis of variance (one-way ANOVA) on the results of at least three independent biological replicates. Multiple comparisons were subsequently performed using the Tukey test. All calculations were performed using GraphPad Prism 10 (GraphPad Software, San Diego, CA). $p < 0.05$ was considered statistically significant.

3 Results

3.1 Effects of catalpol on the viability of BV2 cells

To assess the impact of catalpol on BV2 cell viability, a CCK-8 assay was performed after treating with varying concentrations of catalpol (50–2000 μM) for 24 h. The results (Figure 1A) demonstrated that catalpol concentrations below 1 mM did not cause observable cytotoxic effects. Cytotoxic effects were observed above 1.5 mM. Consequently, concentrations of catalpol within the range of 250–500 μM were utilized in subsequent experiments. The BV2 cells underwent pretreatment with varying concentrations of catalpol for 24 h, followed by a 6-hour incubation period with LPS (500 ng/mL); the model group was not pretreated with catalpol, and the control group received no treatment. Catalpol showed no significant toxic effects on cell viability at different concentrations (250 and 500 μM) (Figure 1B).

3.2 Effects of catalpol on the production of NO inflammatory cytokines in LPS-induced BV2 cells

Nitric oxide (NO) serves as a crucial indicator of inflammation, playing a pivotal role in diverse manifestations of inflammation and carcinogenesis. (Choi et al., 2008). Hence, measuring NO production can offer insights into the impact of catalpol on the inflammatory process. The experimental procedure involved pretreating BV2 cells with different concentrations of catalpol for 24 h, followed by a 6-hour incubation period with LPS. The results, shown in Figure 2A, revealed a noteworthy increase in NO levels following LPS treatment in comparison to the control group. Nonetheless, the treatment of catalpol considerably reduced the production of NO induced by LPS.

3.3 Effects of catalpol on the level of proinflammatory cytokines in LPS-induced BV2 cells

We performed RT-qPCR experiments to explore the plausible regulatory impacts of catalpol on proinflammatory responses. Total RNA was isolated, and the levels of proinflammatory cytokines IL-

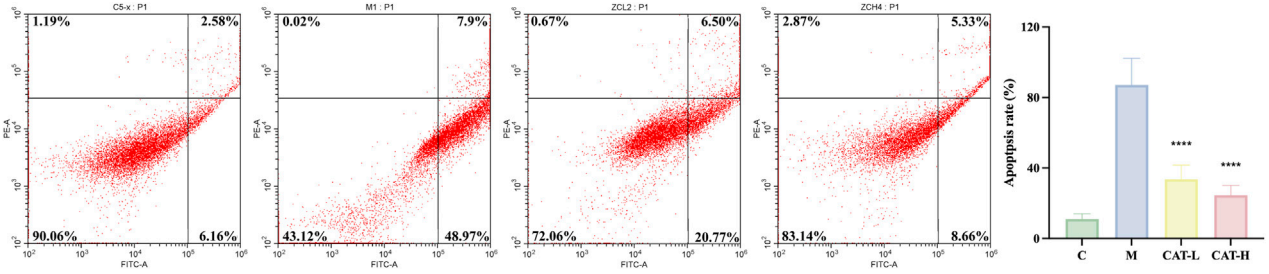

FIGURE 4
Catalpol abrogated the LPS-enhanced apoptosis in BV2 cells. The expression of apoptosis rate was determined using flow cytometry. Q1, cell debris or mechanically damaged cells; Q2, later apoptotic cells; Q3, early apoptotic cells; Q4, live cells. All data are presented as the mean ± SD ($n = 3$). ****$p < 0.0001$.

1β, IL-6, and TNF-α were quantified. The results (Figure 2) demonstrated a noteworthy elevation in the concentrations of pro-inflammatory cytokines following LPS stimulation, as evidenced by the increased production of IL-1β, IL-6, and TNF-α. Importantly, catalpol treatment mitigated the synthesis of pro-inflammatory cytokines triggered by LPS. These findings suggest that catalpol demonstrated anti-inflammatory properties in BV2 cells stimulated by LPS.

As activated microglia are recognized for releasing proinflammatory mediators within the brain parenchyma, we investigated the potential influence of catalpol on microglial activation. Specifically, we focused on Iba-1, a calcium-binding protein that exhibits specific expression in microglia and is upregulated upon their activation. Our findings revealed that the LPS-treated group exhibited pronounced microglial hypertrophy and a significant increase in microglial activation compared to the untreated control group. Following LPS treatment, microglia adopted a pro-inflammatory amoeboid morphology, featuring thick and short cell bodies. In contrast, after treatment with catalpol, the BV2 cells morphological changes induced by LPS were attenuated. The cells exhibited a morphology characterized by a spindle-shaped form, compact cell bodies, and elongated processes (Figure 3).

3.4 Effects of catalpol on LPS-induced apoptosis in BV2 cells

The apoptotic cell percentages were assessed through flow cytometry. As depicted in Figure 4, stimulation with LPS substantially elevated the apoptotic rate in BV2 cells, an effect that was notably alleviated by prior treatment with catalpol. Catalpol pre-treatment nearly entirely counteracted the LPS-induced increase in apoptosis among BV2 cells.

3.5 Effects of NF-κB/NLRP3 on Catalpol's impact on LPS-Induced BV2 cell activation

To investigate whether catalpol influences microglial activation via the NF-κB/NLRP3 signaling pathway, P65, Phospho-P65, NLRP3, and IL-1β (downstream genes of the NF-κB pathway) were selected as targets for further experiments. Phospho-P65 was considered to be an indicator of NF-κB activation. In BV2 microglia, the mRNA levels of NLRP3, NF-κB, Caspase1, and ASC exhibited a significant increase in response to LPS treatment. However, Catalpol administration markedly reduced the expression levels of these genes (Figure 5A). Additionally, the protein levels were evaluated using western blots. As illustrated in Figure 5B, the LPS group exhibited a substantial increase in the expression levels of phosphorylated P65, NLRP3, and IL-1β, whereas catalpol pretreatment remarkably suppressed these effects. In addition, an immunofluorescence assay revealed that catalpol significantly reduced the level of P65 in the nucleus of BV2 induced by LPS (Figure 5C).

3.6 Molecular docking

The more robust the interaction between the ligand and the receptor, the more negative the binding energy of the two. Three candidate target proteins, including NLRP3, IL-1β, and NF-κB, were conducted molecular docking with catalpol; the corresponding 2D-chemical structures were drawn using Discovery Studio software, whose results were visualized by Pymol. Our findings indicated that catalpol exhibited binding energies and the three core proteins were all ≤ −6 kcal/mol, the lowest binding free energy was NLRP3-catalpol (−7.309 kcal/mol), and the main forces involved were Alkyl, hydrophobic forces, and carbon-hydrogen bonds. Figure 6 shows the binding mode of catalpol to each target. In detail, for NLRP3 (Figure 6A), the compound was bound to the activity sites alkyl bonds with ILEA234. Moreover, catalpol could form hydrogen bonds with GLUA152, ASPA153, ARGA154, GLYA231, LYSA232, and THRA233. What's more, more H-bonds than the other three proteins may explain the reason that NLRP3 showed the best binding energy. In the binding mode (Figure 6B), IL-1β was bound to the active binding sites via three hydrogen bonds and one alkyl interaction. In detail, the compound formed alkyl interactions with LYSA210. Moreover, Catalpol was bound to HISA115, GLNA164, and TYRA113 by three hydrogen bonds. For NF-κB as shown in Figure 6C, catalpol could form hydrogen bonds with ALAA43, GLYA44, and ASNA115 respectively. Together, catalpol could bind well with three core targets, all of which might play key roles in the influence of microglial activation.

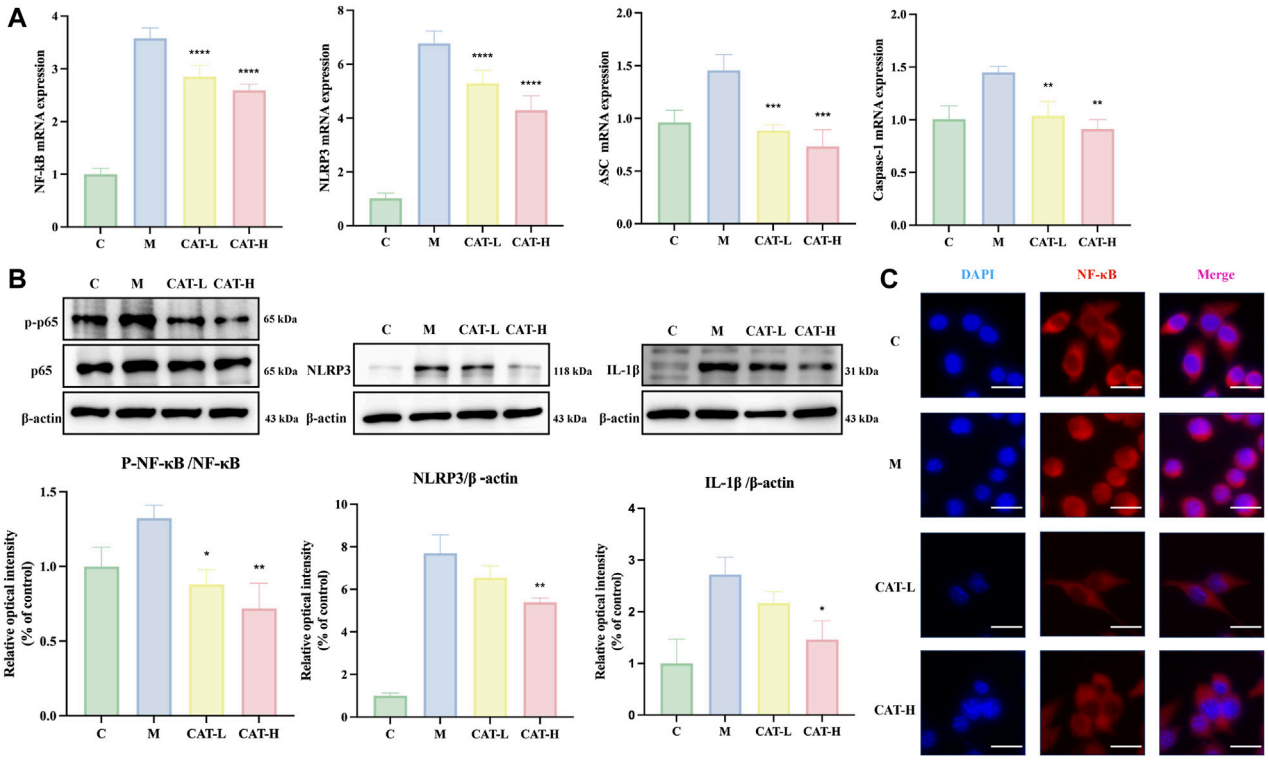

FIGURE 5
Catalpol effects on NF-κB/NLRP3 signaling in LPS-Induced BV2 cells. The whole cells were collected for assessing the gene expression of NLRP3, NF-κB, Caspase-1, and ASC using rt-qPCR **(A)**, and cells were collected to evaluate the protein expression of NF-κB p-65, p-NF-κB p-65, and NLRP3 via western blot analysis **(B)** Nuclear translocation of NF-κB p65 is significantly inhibited by catalpol in LPS-stimulated cells. Representative images of IF staining at ×20 magnification, Scale bar: 50 μM. **(C)** All data are presented as the mean ± SD ($n = 3$). *$p < 0.05$, **$p < 0.01$, ***$p < 0.001$ ****$p < 0.0001$.

3.7 Molecular dynamics simulations of catalpol

Given the inherent motion of proteins and small ligands, the conformation considered during molecular docking represents a relatively stable state for them. Molecular dynamics simulation is an extensively employed method for assessing the structural features of protein-ligand systems and examining the stability of binding between proteins and molecules. In this investigation, NF-κB, NLRP3, and IL-1β considered the most important targets in Catalpol against neuroinflammation, were selected for further assessment of the binding stability with Catalpol.

(1) RMSD analyses

The RMSD value of an individual protein and a protein-ligand complex can be compared to assess alterations in protein molecular dynamics and the conformational stability of the complex. The structural stabilization of the complex is indicated by a lower RMSD value of the protein-ligand complex compared to the solitary protein. In this study, the NLRP3-catalpol system had a sharp rise within 70 ns and tended to balance out the last 10 ns with the average RMSD value of 1.0748 ± 0.175. Meanwhile, the NLRP3 system was in an equilibrium state at 20–100 ns with a larger average RMSD value (1.2691 ± 0.1321), indicating that the stability of the catalpol-NLRP3 system was stronger (Figure 7A).

The IL-1β-catalpol complex was mostly stable throughout the simulation period. It attained a state of relative equilibrium at approximately 40 ns and remained stable until the end, with an average RMSD value of 2.0863 ± 0.286. The IL-1β system reached equilibrium after 50 ns, maintaining a smaller average RMSD value (1.7258 ± 0.2414), which reflects to a certain extent, the overall system stability. The equilibrium of both systems was achieved after a 50 ns simulation, indicating their satisfactory stability (Figure 7B).

The NF-κB-catalpol complexes experienced similar RMSD trends (Figure 7C). The NF-κB-catalpol complex rose to 2.3 nm at around 7 ns and remained stable till the end of NF-κB the simulation time with an average RMSD value of 2.132 ± 0.1665. The RMSD of NF-κB rose to 2.6 nm at 30 ns sustained stability until the conclusion of the simulation, with an average RMSD value of 2.5358 ± 0.3015 nm.

The absence of a break in the RMSD curve indicates that the compounds can firmly attach to proteins without dissociating from the protein pocket during the simulation. The RMSD outcomes for all complexes are noteworthy, indicating that small molecules can form stable bindings with proteins and sustain a relatively stable state.

(2) RMSF analyses

The RMSF plot serves as a typical representation of residues that underwent significant changes during the MD simulation process.

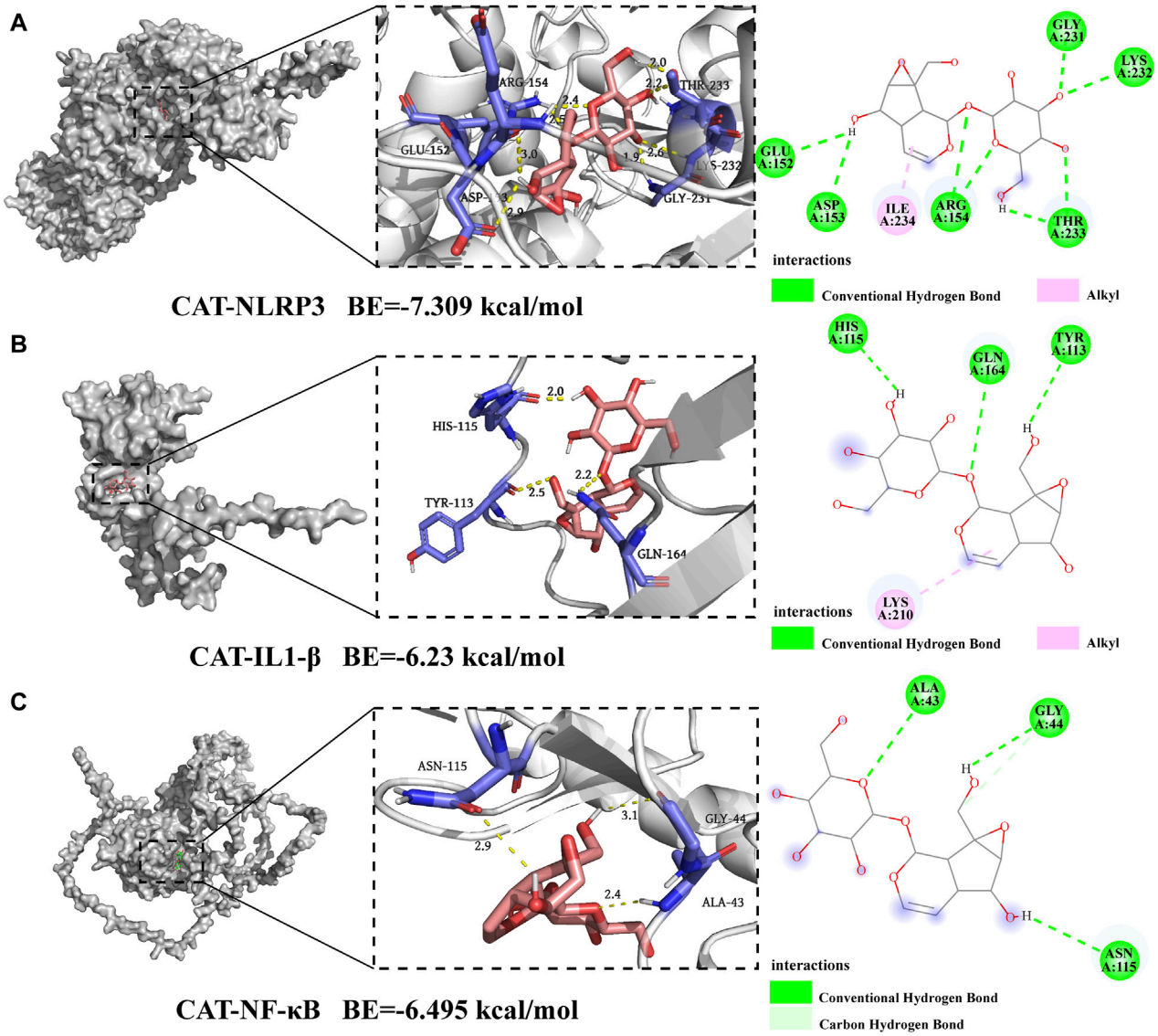

FIGURE 6
Molecular docking of catalpol with NLRP3, IL-1β, and NF-κB. **(A)** 2D and 3D binding models of NLRP3 and catalpol. **(B)** 2D and 3D binding models of IL-1β and catalpol. **(C)** 2D and 3D binding models of NF-κB and catalpol.

Peaks in the RMSF diagram signify residues experiencing pronounced oscillations throughout the simulation. Additionally, elevated RMSF values suggest greater flexibility in protein domains. The binding of the drug to the protein typically induces a reduction in protein flexibility, thereby achieving stabilization of the protein and facilitating enzymatic activity.

The RMSF of the NF-κB and NLRP3 proteins upon binding with catalpol are consistently low, indicating the overall rigidity of the protein as demonstrated in Figure 7D–F. However, for IL-1β, the effect of catalpol on protein RMSF was not different. The overall RMSF results reveal that these complexes are sufficiently stable.

(3) Radius of gyration (Rg) analysis

The radius of gyration, Rg, serves as a crucial parameter for quantifying the structural variability of a protein during molecular dynamics (MD) simulations. Lower Rg values indicate a more rigid structure during the simulation. The Rg values (Figure 7G) decrease gradually in all systems, except NLRP3-catalpol, showing that the other two protein structures are compressed when binding to catalpol. The Rg of IL-1β-catalpol decreases from 3.4091 nm to 1.9695 nm with an average Rg value of 2.2852 ± 0.3315 nm. Similarly, the Rg of NFκB-catalpol is in the range of 4.02804 to 3.08936 nm, the average is 3.2839 ± 0.15nm, reflecting a reduced level of fluctuation in the system. The NLRP3-catalpol complex ranges from 4.5612 to 4.1304 nm, with a mean of 4.2908 ± 0.0729 nm, and in the last 20 ns, the Rg of the protein is stable at around 4.200 nm. The results of Rg show that these systems are compact and converged well.

(4) Protein Solvent Accessible Surface Area (SASA)

Protein Solvent Accessible Surface Area (SASA) is considered a crucial element in investigations related to protein folding and

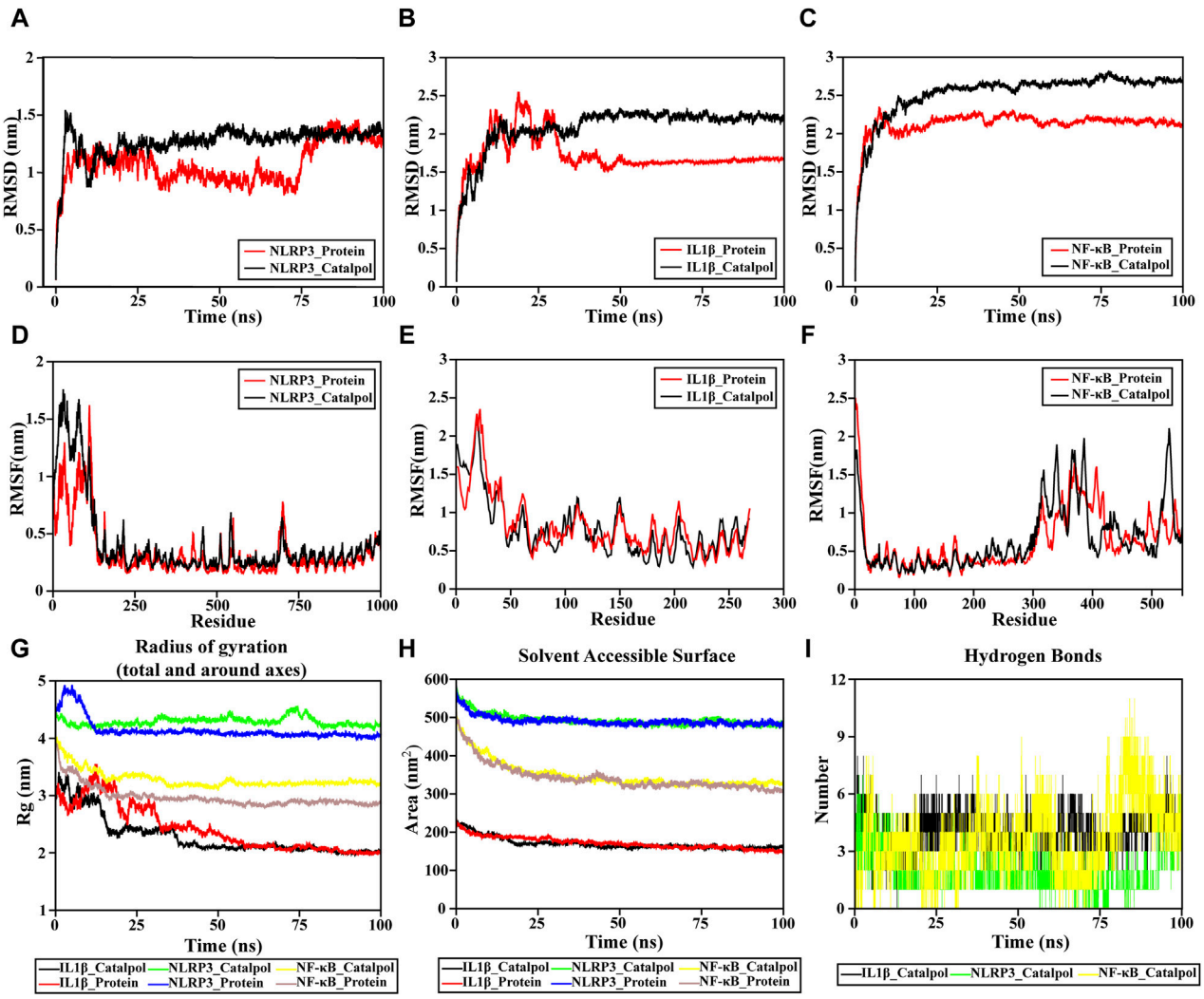

FIGURE 7
Molecular dynamic simulation. **(A–C)** RMSD of the complex MDS. **(D–F)** RMSF of the complex MDS is displayed in the high fluctuation range of the surface. **(G)** Rg variation diagram of the complex MDS. **(H)** SASA of the complex MDS. **(I)** HBNUM in the complex MDS.

stability. A decreased SASA value signifies enhanced compactness.

The solvent-accessible surface area of NLRP3-catalpol, IL-1β-catalpol, and NF-κB-catalpol complexes gradually decreased throughout the simulation, indicating that the bindings between them are gradually increased (Figure 7H).

(5) H-bond numbers analyses

Hydrogen bonds represent one of the most robust non-covalent binding interactions. The number of hydrogen bonds in the protein-compound complexes reflected their binding strengths. The larger the number, the better the binding.

The findings indicate a notably higher count of hydrogen bonds between catalpol and NF-κB compared to those formed with NLRP3. Among them, NF-κB-catalpol had the highest hydrogen bond density and strength, followed by IL-1β-catalpol, and NLRP3-catalpol (Figure 7I).

3.8 Binding free energy analysis

The Molecular Mechanics Poisson–Boltzmann Surface Area (MM/PBSA) method serves as a robust and dependable approach for computing the binding free energy of small molecule compounds to their respective protein targets. Typically, complexes exhibiting lower binding free energy are deemed more stable, suggesting that their ligands are likely to possess increased activity and potency.

The protein-ligand affinity in the NLRP3 system was recorded as −26.4 kcal/mol (Figure 8B), whereas in the IL-1β system, it amounted to −30.14 kcal/mol (Figure 8D), and in the NF-κB system, it was −25.51 kcal/mol (Figure 8F).

The free energy residue decomposition diagram provides insights into the amino acid residues that contribute to the binding during ligand simulation. The key residues contributing towards the binding interaction between NLRP3 and catalpol include ILE151 (−1.61 kcal/mol), GLU152

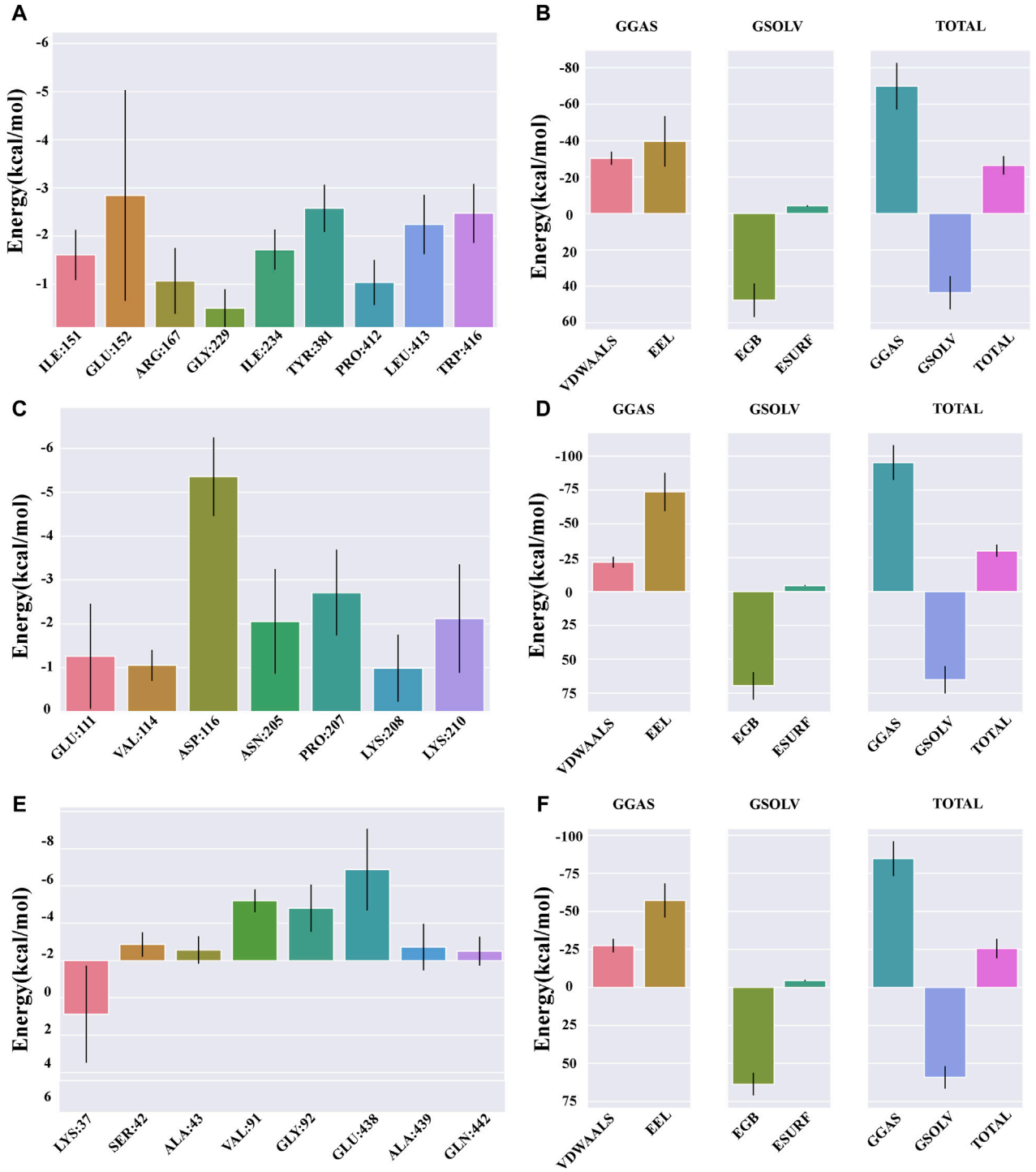

FIGURE 8
Binding free energy analysis. **(A)** Energy amino acid decomposition diagram for NLRP3–catalpol. **(B)** Energy attribute breakdown diagram for NLRP3–catalpol. **(C)** Energy amino acid decomposition diagram for IL-1β–catalpol. **(D)** Energy attribute breakdown diagram for IL-1β-catalpol. **(E)** Energy amino acid decomposition diagram for NF-κB–catalpol. **(F)** Energy attribute breakdown diagram for NF-κB–catalpol.

(−2.85 kcal/mol), ARG167 (−1.07 kcal/mol), ILE234 (−1.72 kcal/mol), TYR381 (−2.58 kcal/mol), PRO412 (−1.04 kcal/mol), LEU413 (−2.24 kcal/mol), and TRP416 (−2.47 kcal/mol) (Figure 8A). In case of IL-1β-Catalpol complex, residues such as GLU111 (−1.26 kcal/mol), VAL114 (−1.05 kcal/mol), ASP116 (−5.36 kcal/mol), ASN205 (−2.05 kcal/mol), PRO207 (−2.71 kcal/mol), LYS210 (−2.12 kcal/mol) contribute majorly to the total binding energy (Figure 8C). In case of NF-κB-Catalpol complex, residues such as LYS37 (−2.88 kcal/mol), VAL91 (−3.2 kcal/mol), GLY92 (−2.81 kcal/mol), and GLU438

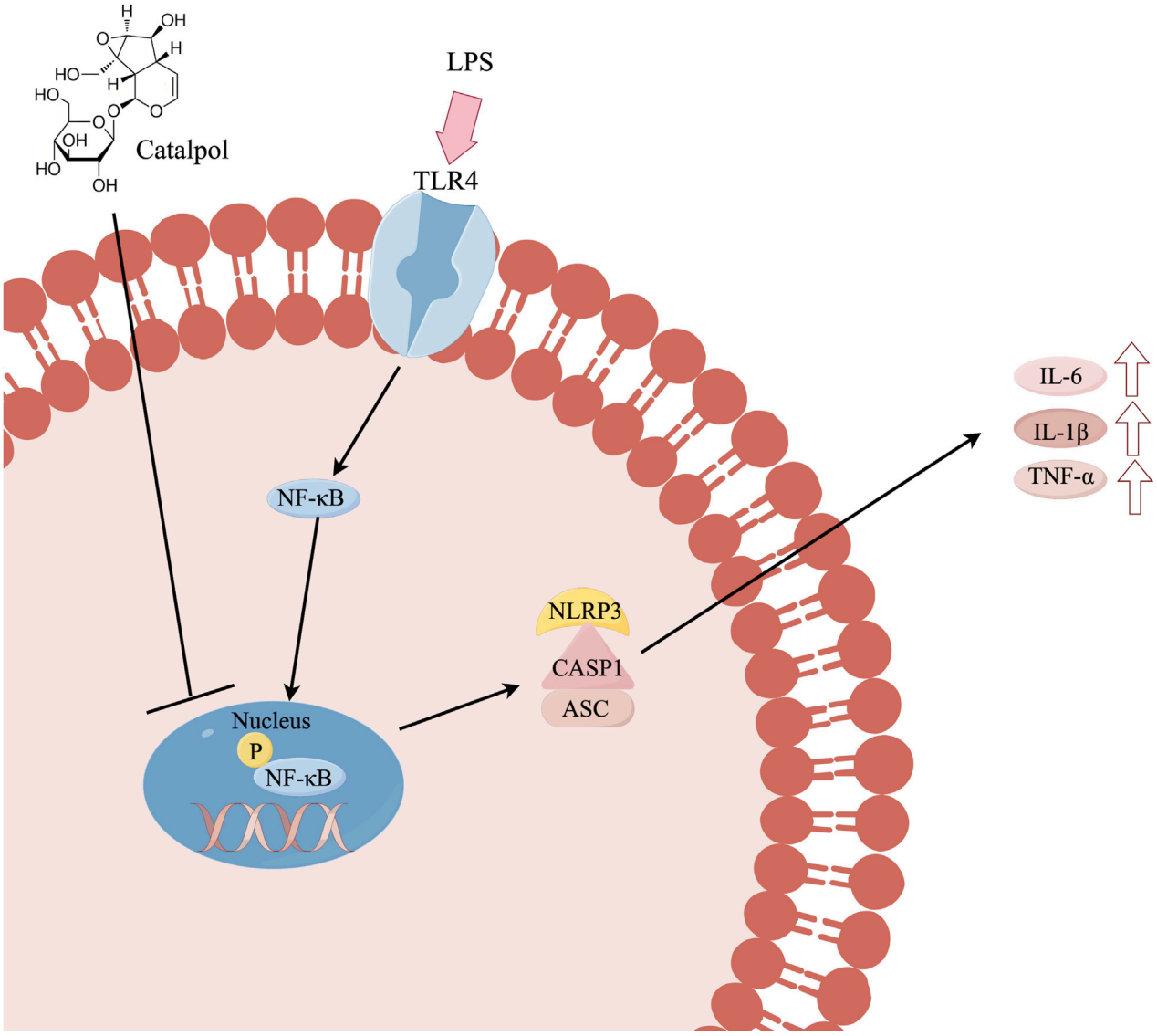

FIGURE 9
Schematic potential cellular mechanisms By Figdraw.

(−4.88 kcal/mol) have higher contribution toward the total binding energy (Figure 8E).

4 Discussion

Stroke stands as the second leading cause of mortality globally, accounting for approximately 12% of total deaths and imposing an escalating burden, especially in low-income countries (Feigin et al., 2021). Traditional Chinese Medicine (TCM) has a rich history of employing various medicinal herbs for stroke treatment, exhibiting robust therapeutic effects in both pharmacological experiments and clinical applications (Zhu et al., 2020). The responsive nature of microglia to injury suggests their potential as diagnostic markers for disease onset and progression, particularly given their involvement in neuroinflammation. Genetic studies have provided strong support for the pivotal role of microglia-mediated neuroinflammation in neurodegeneration (Perry et al., 2010; Crotti and Ransohoff, 2016; Rangaraju et al., 2018). Consequently, it is of paramount importance to identify bioactive ingredients in TCM that can regulate microglial function in the brain, thereby mitigating neurotoxic inflammatory mediators.

Prior research has underscored the anti-inflammatory characteristics of catalpol (Zhang H. et al., 2019; Yang et al., 2020; Wu et al., 2022; Ni et al., 2023). Additionally, researches have extensively explored catalpol for its potential effects in experimental models of various neurological disorders such as depression, Alzheimer's, and Parkinson's disease (Bhattamisra et al., 2019). In a specific study, patients experiencing depression exhibited heightened levels of pro-inflammatory cytokines, including interleukin-1β (IL-1β) and tumor necrosis factor-α (TNF-α). The inhibition of COX-2 led to a subsequent decrease

in these heightened cytokine levels, and catalpol exhibited a notable suppressive effect on the levels of COX-2 and prostaglandin E2 (PGE2) in the frontal cortex and hippocampus of mice (Kuwano et al., 2004; Wang et al., 2015).

In our study, we employed LPS as an inflammation stimulant to investigate the effects of catalpol on LPS-induced neuroinflammatory responses. Our findings illustrated that catalpol treatment led to a notable inhibition of NO production in LPS-activated cells. This suggests that catalpol has the potential to mitigate inflammation by reducing excessive NO levels. Additionally, the triggering of proinflammatory cytokines (TNF-α, IL-1β, and IL-6) and the upregulation of Iba-1 upon LPS treatment contributed to brain neuroinflammation. Intriguingly, catalpol treatment significantly mitigated these LPS-induced neuroinflammatory changes, highlighting its potential as an anti-inflammatory agent.

We obtained a significant result in our study. Primarily, catalpol significantly suppressed LPS-induced neuroinflammation by reducing the production of pro-inflammatory cytokines, phosphorylation of NF-κB, expression of Iba-1, and regulating NLRP3 to inhibit inflammasome activation. Catalpol indeed has broad medicinal value and application prospects due to its effects on multiple organs and tissues. However, most research on catalpol remains at the basic experimental stage, with clinical evaluations primarily focused on its anti-tumor activity (Fei et al., 2018). Other pharmacological effects have yet to be thoroughly evaluated in clinical settings. Therefore, more research is needed to establish a solid foundation for clinical trials and expedite its clinical application.

To clarify the underlying mechanisms involved in inhibiting the release of inflammatory factors and modulating microglial phenotypes, we investigated the activation of NF-κB/NLRP3 signaling pathways induced by LPS. LPS, a component found in the outer membrane of Gram-negative bacteria, functions as a ligand for TLR4, triggering several downstream signal pathways, including NF-κB (Nair et al., 2019). The NF-κB transcription factor is prominently expressed in various brain cells, encompassing neurons, microglia, and astrocytes. It's vital role lies in the regulation of inflammatory genes and its involvement in a multitude of brain functions (Sun et al., 2022). NF-κB activation entails the movement of the P50/P65 subunits of NF-κB from the cytoplasm to the nucleus in the majority of cell types (Tak and Firestein, 2001). Numerous research investigations have suggested that inhibiting NF-κB could serve as a pivotal factor in halting the progression of ischemic stroke (IS) pathology.

The NLRP3 inflammasome, consisting of multiple proteins, is recognized for its ability to activate procaspase-1. This activation subsequently triggers the cleavage and secretion of IL-1β and IL-18 (Lamkanfi and Dixit, 2014). Activation of NLRP3 involves two signals. The first is initiated by the binding of the TLR4 receptor to its ligand LPS, subsequently triggering NF-κB-mediated upregulation of NLRP3 along with proIL-1β (Bauernfeind et al., 2009). Upon activation, NLRP3 assembles into an inflammasome complex with the adaptor molecule ASC, regulating the activation of Caspase-1 (Dinarello, 2009). Extensive research has demonstrated the association between NLRP3 inflammasome activation and neuroinflammation in neurodegenerative disorders. Recent evidence has also proposed a potential connection between the increased activity of the inflammasome and neuronal/glial cell death in cerebral ischemia (Fann et al., 2013). Additionally, a recent study has proposed that NLRP3 deficiency distinctly alleviated microglial activation in mice (Tejera et al., 2019; Wu et al., 2021). Furthermore, there is another mechanism of inflammasome activation known as the non-canonical inflammasome pathway, triggered by the cytosolic sensing of LPS (Diamond et al., 2015). The non-canonical inflammasome also serves as a signal for activating the canonical inflammasome, playing a crucial role in inducing and promoting inflammatory responses (Chi et al., 2014; Down et al., 2020). A recent study has shown the activation of a novel NLRP1-ASC-caspase-8 non-canonical inflammasome in the mouse cortex during inflammation (Cyr et al., 2022). However, research on the non-canonical pathway in the context of ischemic stroke is relatively scarce, which is a limitation of our study. Future research should focus on understanding the mechanisms of the non-canonical inflammasome pathway in ischemic stroke, as this will be crucial for advancing our knowledge in this area.

The NF-κB/NLRP3 signaling pathways exert crucial functions in controlling the expression of proinflammatory cytokines in microglia following LPS stimulation (Lam et al., 2001). Consequently, we explored whether the suppressive impact of catalpol on the NF-κB/NLRP3 pathway could provide neuroprotective benefits against LPS-induced neuroinflammatory responses in BV2 cells. As anticipated, the outcomes showed a pronounced increase in the phosphorylation of NF-κB P65 in BV2 cells following LPS stimulation. However, catalpol administration successfully mitigated the hyperactivity of NF-κB induced by LPS in BV2 cells. Secondly, our data demonstrate a notable reduction in LPS-induced NF-κB P65 nuclear translocation upon catalpol administration in microglial cells. Therefore, catalpol may mitigate the LPS-induced neuroinflammatory response by restoring the balance of NF-κB activation and inhibiting NF-κB P65 nuclear translocation. The NF-kB signaling pathway plays a crucial role in triggering the activation of NLRP3 (Bauernfeind et al., 2011; Lamkanfi and Dixit, 2014). Furthermore, our results indicate that catalpol attenuated LPS-induced neuroinflammation by suppressing NLRP3 inflammasome signaling. More specifically, catalpol administration resulted in the inhibition of NLRP3 activation, caspase-1 cleavage, and ASC expression. Mechanistically, our results demonstrated that catalpol could alleviate the inflammatory response in microglia by downregulating the NF-κB and NLRP3 inflammasome pathways.

Progress in science and technology has facilitated the application of computational analyses and simulations in research, thereby surmounting experimental constraints and augmenting research efficiency This pivotal role has been instrumental in consolidating and propelling advancement in neuroinflammation research (Li et al., 2021).

This study involved molecular docking of catalpol with NLRP3, IL-1β, and NF-κB to investigate its pharmacological targets. Notably, catalpol, known for its efficacy against neuroinflammation, exhibited robust binding affinity to these three targets, highlighting its significant role in inflammation regulation. Additionally, we utilized MD simulation, a potent tool for assessing the stability of protein-ligand complexes and visualizing structural dynamics during the simulation period. This approach was instrumental in evaluating the stability of catalpol binding to NLRP3, IL-1β, and NF-κB in their respective binding pockets over a 100 ns duration.

Lower RMSD values indicate greater structural stability. In the case of the catalpol-NLRP3 system, a lower RMSD suggests robust stability. An illustrative representation of residue changes during MD simulation is the RMSF plot. Our RMSF results showed that NF-κB and NLRP3, when bound to small molecules, experienced generally low overall RMSF, indicating increased rigidity upon binding to small molecules and enhancing the overall protein structure stability. The radius of gyration (Rg) is another parameter used to measure structural fluctuations during MD simulations. For NF-κB-catalpol and IL-1β-catalpol, Rg suggested stable fluctuations in size, implying high binding potential. SASA is considered a crucial element in researching protein folding and stability. Hydrogen bond analysis, reflecting binding strengths, showed that IL-1β-catalpol and NF-κB-catalpol exhibited superior hydrogen bonding in terms of size and density. All three complexes demonstrated the ability to form stable hydrogen bonds, establishing a solid foundation for stable bonding.

Free energy analysis showed similar sign distribution for NLRP3, IL-1β, and NF-κB. However, the IL-1β affinity was stronger at −30.14 kcal/mol compared to NLRP3 and NF-κB. Stable binding was revealed through MDS, supporting the anti-neuroinflammatory role of catalpol via multiple targets. Furthermore, the breakdown diagram of free energy residues can be utilized to comprehend which amino acid residues contribute to the binding during ligand simulation. These findings, in turn, provide additional support to the earlier experiments.

Emerging evidence strongly implicates neuroinflammation as a pivotal mechanism in neurodegenerative diseases, including ischemic stroke (Stephenson et al., 2018; Endres et al., 2022; Amanollahi et al., 2023). The overactivation of microglia leads to the secretion of proinflammatory mediators, resulting in neuroinflammation. Moreover, augmented neuroinflammatory responses mediated by glial cells and elevated levels of pro-inflammatory mediators have been observed in both animal models of ischemic stroke and IS patients (Price et al., 2006; Ormstad et al., 2011; Ding et al., 2022; Cui et al., 2023). Therefore, targeting the regulation of microglial cell-mediated neuroinflammation represents a promising therapeutic approach for neurodegenerative diseases. In this study, we demonstrated that catalpol effectively modulates LPS-induced neuroinflammation in BV-2 cells. Collectively, our results highlight that catalpol can effectively regulate glia-induced neuroinflammatory responses, providing potential anti-inflammatory effects in the brain. Consequently, it may offer an effective treatment for neuroinflammation-related diseases, including neurodegenerative diseases such as ischemic stroke.

Although this study demonstrates the beneficial effect of catalpol on neuroinflammation and its regulatory role on NF-κB/NLRP3, given the intricate pathology and progression of IS injury, our study represents only a preliminary investigation. A thorough exploration of the potential mechanisms is needed in future research endeavors. Unfortunately, due to time constraints and other practical factors, we were unable to include a more extensive *in vivo* mechanism study in this paper. As a result, the *in vivo* experimental results cannot be presented in this manuscript. However, we are currently undertaking comprehensive *in vivo* studies to further investigate the neuroprotective effects of catalpol against ischemic stroke (IS).

To explore the anti-neuroinflammatory effects of catalpol in more detail, we are establishing a rat middle cerebral artery occlusion/reperfusion (MCAO/R) model. This will involve using TTC staining to calculate the volume of cerebral infarction, H&E staining and Nissl staining to observe histopathological changes, and immunofluorescence staining to assess the expression of IBA-1. Additionally, we will employ qRT-PCR and Western blots to measure the expression of inflammatory factors at both the gene and protein levels. These experiments aim to observe the protective effects of catalpol in the rat MCAO model and to further elucidate its underlying mechanisms. Future research endeavors will be crucial in providing deeper insights into the mechanisms by which catalpol exerts its neuroprotective effects in the context of IS.

5 Conclusion

Catalpol exhibited anti-inflammatory activity by attenuating inflammatory markers in BV-2 microglia. This inhibitory effect may be attributed to the suppression of the NF-κB/NLRP3 pathway. Schematic potential cellular mechanisms as shown in Figure 9.

Data availability statement

The original contributions presented in the study are included in the article/Supplementary Material, further inquiries can be directed to the corresponding author.

Ethics statement

Ethical approval was not required for the studies on animals in accordance with the local legislation and institutional requirements because only commercially available established cell lines were used.

Author contributions

YS: Conceptualization, Data curation, Formal Analysis, Investigation, Methodology, Software, Validation, Visualization, Writing–original draft, Writing–review and editing. C-yS: Conceptualization, Formal Analysis, Project administration, Supervision, Writing–review and editing. Y-fL: Data curation, Visualization, Writing–original draft. YH: Data curation, Validation, Writing–original draft. J-hY: Supervision, Validation, Writing–review and editing. H-tW: Conceptualization, Funding acquisition, Resources, Supervision, Writing–review and editing.

Funding

The author(s) declare that financial support was received for the research, authorship, and/or publication of this article. This work was supported by the National Natural Science Foundation of China

(grant number 82330120); and the Zhejiang Provincial Natural Science Foundation of China (grant number LZ23H270002).

Acknowledgments

We gratefully acknowledge the support and assistance provided by Provincial key Laboratory of TCM Cardio-Cerebrovascular Diseases of Zhejiang Province.

Conflict of interest

The authors declare that the research was conducted in the absence of any commercial or financial relationships that could be construed as a potential conflict of interest.

Publisher's note

Supplementary material

The Supplementary Material for this article can be found online at: https://www.frontiersin.org/articles/10.3389/fphar.2024.1415445/full#supplementary-material

References

Amanollahi, M., Jameie, M., Heidari, A., and Rezaei, N. (2023). The dialogue between neuroinflammation and adult neurogenesis: mechanisms involved and alterations in neurological diseases. *Mol. Neurobiol.* 60, 923–959. doi:10.1007/s12035-022-03102-z

Bauernfeind, F., Ablasser, A., Bartok, E., Kim, S., Schmid-Burgk, J., Cavlar, T., et al. (2011). Inflammasomes: current understanding and open questions. *Cell Mol. Life Sci.* 68, 765–783. doi:10.1007/s00018-010-0567-4

Bauernfeind, F., Horvath, G., Stutz, A., Alnemri, E. S., MacDonald, K., Speert, D., et al. (2009). Cutting edge: NF-kappaB activating pattern recognition and cytokine receptors license NLRP3 inflammasome activation by regulating NLRP3 expression. *J. Immunol.* 183, 787–791. doi:10.4049/jimmunol.0901363

Bhattamisra, S. K., Yap, K. H., Rao, V., and Choudhury, H. (2019). Multiple biological effects of an iridoid glucoside, catalpol and its underlying molecular mechanisms. *Biomolecules* 10, 32. doi:10.3390/biom10010032

Bian, Z., Zhang, R., Zhang, X., Zhang, J., Xu, L., Zhu, L., et al. (2023). Extraction, structure and bioactivities of polysaccharides from rehmannia glutinosa: a review. *J. Ethnopharmacol.* 305, 116132. doi:10.1016/j.jep.2022.116132

Chi, W., Li, F., Chen, H., Wang, Y., Zhu, Y., Yang, X., et al. (2014). Caspase-8 promotes NLRP1/NLRP3 inflammasome activation and IL-1β production in acute glaucoma. *Proc. Natl. Acad. Sci. U. S. A.* 111, 11181–11186. doi:10.1073/pnas.1402819111

Choi, S.-Y., Hwang, J.-H., Park, S.-Y., Jin, Y.-J., Ko, H.-C., Moon, S.-W., et al. (2008). Fermented guava leaf extract inhibits LPS-induced COX-2 and iNOS expression in mouse macrophage cells by inhibition of transcription factor NF-kappaB. *Phytother. Res.* 22, 1030–1034. doi:10.1002/ptr.2419

Crotti, A., and Ransohoff, R. M. (2016). Microglial physiology and pathophysiology: insights from genome-wide transcriptional profiling. *Immunity* 44, 505–515. doi:10.1016/j.immuni.2016.02.013

Cui, P., Lu, W., Wang, J., Wang, F., Zhang, X., Hou, X., et al. (2023). Microglia/macrophages require vitamin D signaling to restrain neuroinflammation and brain injury in a murine ischemic stroke model. *J. Neuroinflammation* 20, 63. doi:10.1186/s12974-023-02705-0

Cyr, B., Hadad, R., Keane, R. W., and de Rivero Vaccari, J. P. (2022). The role of non-canonical and canonical inflammasomes in inflammaging. *Front. Mol. Neurosci.* 15, 774014. doi:10.3389/fnmol.2022.774014

Diamond, C. E., Khameneh, H. J., Brough, D., and Mortellaro, A. (2015). Novel perspectives on non-canonical inflammasome activation. *Immunotargets Ther.* 4, 131–141. doi:10.2147/ITT.S57976

Dinarello, C. A. (2009). Immunological and inflammatory functions of the interleukin-1 family. *Annu. Rev. Immunol.* 27, 519–550. doi:10.1146/annurev.immunol.021908.132612

Ding, R., Li, H., Liu, Y., Ou, W., Zhang, X., Chai, H., et al. (2022). Activating cGAS-STING axis contributes to neuroinflammation in CVST mouse model and induces inflammasome activation and microglia pyroptosis. *J. Neuroinflammation* 19, 137. doi:10.1186/s12974-022-02511-0

DiSabato, D., Quan, N., and Godbout, J. P. (2016). Neuroinflammation: the devil is in the details. *J. Neurochem.* 139, 136–153. doi:10.1111/jnc.13607

Down, K. P., Nguyen, H., Dorfleutner, A., and Stehlik, C. (2020). An overview of the non-canonical inflammasome. *Mol. Asp. Med.* 76, 100924. doi:10.1016/j.mam.2020.100924

Endres, M., Moro, M. A., Nolte, C. H., Dames, C., Buckwalter, M. S., and Meisel, A. (2022). Immune pathways in etiology, acute phase, and chronic sequelae of ischemic stroke. *Circ. Res.* 130, 1167–1186. doi:10.1161/CIRCRESAHA.121.319994

Fann, D. Y.-W., Lee, S.-Y., Manzanero, S., Chunduri, P., Sobey, C. G., and Arumugam, T. V. (2013). Pathogenesis of acute stroke and the role of inflammasomes. *Ageing Res. Rev.* 12, 941–966. doi:10.1016/j.arr.2013.09.004

Fei, B., Dai, W., and Zhao, S. (2018). Efficacy, safety, and cost of therapy of the traditional Chinese medicine, catalpol, in patients following surgical resection for locally advanced colon cancer. *Med. Sci. Monit.* 24, 3184–3192. doi:10.12659/MSM.907569

Feigin, V. L., Stark, B. A., Johnson, C. O., Roth, G. A., Bisignano, C., Abady, G. G., et al. (2021). Global, regional, and national burden of stroke and its risk factors, 1990–2019: a systematic analysis for the global burden of disease study 2019. *Lancet Neurology* 20, 795–820. doi:10.1016/S1474-4422(21)00252-0

Iadecola, C., and Anrather, J. (2011). The immunology of stroke: from mechanisms to translation. *Nat. Med.* 17, 796–808. doi:10.1038/nm.2399

Kuwano, T., Nakao, S., Yamamoto, H., Tsuneyoshi, M., Yamamoto, T., Kuwano, M., et al. (2004). Cyclooxygenase 2 is a key enzyme for inflammatory cytokine-induced angiogenesis. *FASEB J.* 18, 300–310. doi:10.1096/fj.03-0473com

Lam, A. G., Koppal, T., Akama, K. T., Guo, L., Craft, J. M., Samy, B., et al. (2001). Mechanism of glial activation by S100B: involvement of the transcription factor NFkappaB. *Neurobiol. Aging* 22, 765–772. doi:10.1016/s0197-4580(01)00233-0

Lamkanfi, M., and Dixit, V. M. (2014). Mechanisms and functions of inflammasomes. *Cell* 157, 1013–1022. doi:10.1016/j.cell.2014.04.007

Li, H., Yang, W., Wang, Z., Wang, X., Hao, Y., Xi, J., et al. (2021). Computational research of mTORC1 inhibitor on cerebral ischemia-reperfusion injury. *Aging (Albany NY)* 13, 19598–19613. doi:10.18632/aging.203371

Liu, Y., Li, Q., Shao, C., She, Y., Zhou, H., Guo, Y., et al. (2024). Exploring the potential mechanisms of guanxinshutong capsules in treating pathological cardiac hypertrophy based on network pharmacology, computer-aided drug design, and animal experiments. *ACS Omega* 9, 18083–18098. doi:10.1021/acsomega.3c10009

Maida, C. D., Norrito, R. L., Daidone, M., Tuttolomondo, A., and Pinto, A. (2020). Neuroinflammatory mechanisms in ischemic stroke: focus on cardioembolic stroke, background, and therapeutic approaches. *Int. J. Mol. Sci.* 21, 6454. doi:10.3390/ijms21186454

Nair, S., Sobotka, K. S., Joshi, P., Gressens, P., Fleiss, B., Thornton, C., et al. (2019). Lipopolysaccharide-induced alteration of mitochondrial morphology induces a metabolic shift in microglia modulating the inflammatory response *in vitro* and *in vivo*. *Glia* 67, 1047–1061. doi:10.1002/glia.23587

Ni, H., Rui, Q., Kan, X., Gao, R., Zhang, L., and Zhang, B. (2023). Catalpol ameliorates oxidative stress and neuroinflammation after traumatic brain injury in rats. *Neurochem. Res.* 48, 681–695. doi:10.1007/s11064-022-03796-6

Orihuela, R., McPherson, C. A., and Harry, G. J. (2016). Microglial M1/M2 polarization and metabolic states. *Br. J. Pharmacol.* 173, 649–665. doi:10.1111/bph.13139

Ormstad, H., Aass, H. C. D., Lund-Sørensen, N., Amthor, K.-F., and Sandvik, L. (2011). Serum levels of cytokines and C-reactive protein in acute ischemic stroke patients, and their relationship to stroke lateralization, type, and infarct volume. *J. Neurol.* 258, 677–685. doi:10.1007/s00415-011-6006-0

Pan, L., Peng, C., Wang, L., Li, L., Huang, S., Fei, C., et al. (2022). Network pharmacology and experimental validation-based approach to understand the effect

and mechanism of thong siwu decoction against ischemic stroke. *J. Ethnopharmacol.* 294, 115339. doi:10.1016/j.jep.2022.115339

Perry, V. H., Nicoll, J. A. R., and Holmes, C. (2010). Microglia in neurodegenerative disease. *Nat. Rev. Neurol.* 6, 193–201. doi:10.1038/nrneurol.2010.17

Price, C. J. S., Wang, D., Menon, D. K., Guadagno, J. V., Cleij, M., Fryer, T., et al. (2006). Intrinsic activated microglia map to the peri-infarct zone in the subacute phase of ischemic stroke. *Stroke* 37, 1749–1753. doi:10.1161/01.STR.0000226980.95389.0b

Rangaraju, S., Dammer, E. B., Raza, S. A., Rathakrishnan, P., Xiao, H., Gao, T., et al. (2018). Identification and therapeutic modulation of a pro-inflammatory subset of disease-associated-microglia in Alzheimer's disease. *Mol. Neurodegener.* 13, 24. doi:10.1186/s13024-018-0254-8

Saini, V., Guada, L., and Yavagal, D. R. (2021). Global epidemiology of stroke and access to acute ischemic stroke interventions. *Neurology* 97, S6–S16. doi:10.1212/WNL.0000000000012781

Shu, A., Du, Q., Chen, J., Gao, Y., Zhu, Y., Lv, G., et al. (2021). Catalpol ameliorates endothelial dysfunction and inflammation in diabetic nephropathy via suppression of RAGE/RhoA/ROCK signaling pathway. *Chem. Biol. Interact.* 348, 109625. doi:10.1016/j.cbi.2021.109625

Stephenson, J., Nutma, E., van der Valk, P., and Amor, S. (2018). Inflammation in CNS neurodegenerative diseases. *Immunology* 154, 204–219. doi:10.1111/imm.12922

Sun, E., Motolani, A., Campos, L., and Lu, T. (2022). The pivotal role of NF-kB in the pathogenesis and therapeutics of alzheimer's disease. *Int. J. Mol. Sci.* 23, 8972. doi:10.3390/ijms23168972

Tak, P. P., and Firestein, G. S. (2001). NF-kappaB: a key role in inflammatory diseases. *J. Clin. Invest.* 107, 7–11. doi:10.1172/JCI11830

Tejera, D., Mercan, D., Sanchez-Caro, J. M., Hanan, M., Greenberg, D., Soreq, H., et al. (2019). Systemic inflammation impairs microglial Aβ clearance through NLRP3 inflammasome. *EMBO J.* 38, e101064. doi:10.15252/embj.2018101064

Wang, J.-M., Yang, L.-H., Zhang, Y.-Y., Niu, C.-L., Cui, Y., Feng, W.-S., et al. (2015). BDNF and COX-2 participate in anti-depressive mechanisms of catalpol in rats undergoing chronic unpredictable mild stress. *Physiol. Behav.* 151, 360–368. doi:10.1016/j.physbeh.2015.08.008

Wu, X., Gong, L., Xie, L., Gu, W., Wang, X., Liu, Z., et al. (2021). NLRP3 deficiency protects against intermittent hypoxia-induced neuroinflammation and mitochondrial ROS by promoting the PINK1-parkin pathway of mitophagy in a murine model of sleep apnea. *Front. Immunol.* 12, 628168. doi:10.3389/fimmu.2021.628168

Wu, X., Liu, C., Wang, J., Guan, Y., Song, L., Chen, R., et al. (2022). Catalpol exerts antidepressant-like effects by enhancing anti-oxidation and neurotrophy and inhibiting neuroinflammation via activation of HO-1. *Neurochem. Res.* 47, 2975–2991. doi:10.1007/s11064-022-03641-w

Yang, C., Shi, Z., You, L., Du, Y., Ni, J., and Yan, D. (2020). Neuroprotective effect of catalpol via anti-oxidative, anti-inflammatory, and anti-apoptotic mechanisms. *Front. Pharmacol.* 11, 690. doi:10.3389/fphar.2020.00690

Yu, L., Zhang, Y., Chen, Q., He, Y., Zhou, H., Wan, H., et al. (2022). Formononetin protects against inflammation associated with cerebral ischemia-reperfusion injury in rats by targeting the JAK2/STAT3 signaling pathway. *Biomed. Pharmacother.* 149, 112836. doi:10.1016/j.biopha.2022.112836

Zaaba, N. E., Al-Salam, S., Beegam, S., Elzaki, O., Yasin, J., and Nemmar, A. (2023). Catalpol attenuates oxidative stress and inflammation via mechanisms involving sirtuin-1 activation and NF-κB inhibition in experimentally-induced chronic kidney disease. *Nutrients* 15, 237. doi:10.3390/nu15010237

Zhang, H., Wu, Z.-M., Yang, Y.-P., Shaukat, A., Yang, J., Guo, Y.-F., et al. (2019a). Catalpol ameliorates LPS-induced endometritis by inhibiting inflammation and TLR4/NF-κB signaling. *J. Zhejiang Univ. Sci. B* 20, 816–827. doi:10.1631/jzus.B1900071

Zhang, H., Yue, Y., Zhang, Q., Liang, L., Li, C., Chen, Y., et al. (2023). Structural characterization and anti-inflammatory effects of an arabinan isolated from rehmannia glutinosa libosch. *Carbohydr. Polym.* 303, 120441. doi:10.1016/j.carbpol.2022.120441

Zhang, J., Bi, R., Meng, Q., Wang, C., Huo, X., Liu, Z., et al. (2019b). Catalpol alleviates adriamycin-induced nephropathy by activating the SIRT1 signalling pathway *in vivo* and *in vitro*. *Br. J. Pharmacol.* 176, 4558–4573. doi:10.1111/bph.14822

Zhao, Y., Shao, C., Zhou, H., Yu, L., Bao, Y., Mao, Q., et al. (2023). Salvianolic acid B inhibits atherosclerosis and TNF-α-induced inflammation by regulating NF-κB/NLRP3 signaling pathway. *Phytomedicine* 119, 155002. doi:10.1016/j.phymed.2023.155002

Zhu, T., Wang, L., Tian, F., Zhao, X., Pu, X.-P., Sun, G.-B., et al. (2020). Anti-ischemia/reperfusion injury effects of notoginsenoside R1 on small molecule metabolism in rat brain after ischemic stroke as visualized by MALDI-MS imaging. *Biomed. Pharmacother.* 129, 110470. doi:10.1016/j.biopha.2020.110470

frontiers | Frontiers in Pharmacology

TYPE Original Research
PUBLISHED 24 September 2024
DOI 10.3389/fphar.2024.1365642

OPEN ACCESS

EDITED BY
Viola B. Morris,
Emory University, United States

REVIEWED BY
Sergei V. Fedorovich,
Belarusian State University, Belarus
Manoj Veleeparambil,
University of Kentucky, United States
Naijil George,
St. Joseph's College, Irinjalakuda, India

*CORRESPONDENCE
Qihai Gong,
gqh@zmu.edu.cn

RECEIVED 04 January 2024
ACCEPTED 09 September 2024
PUBLISHED 24 September 2024

CITATION
Liu D, Wu W, Wang T, Zhan G, Zhang Y, Gao J and Gong Q (2024) *Lithocarpus polystachyus* Rehd. ameliorates cerebral ischemia/reperfusion injury through inhibiting PI3K/AKT/NF-κB pathway and regulating NLRP3-mediated pyroptosis.
Front. Pharmacol. 15:1365642.
doi: 10.3389/fphar.2024.1365642

Lithocarpus polystachyus Rehd. ameliorates cerebral ischemia/reperfusion injury through inhibiting PI3K/AKT/NF-κB pathway and regulating NLRP3-mediated pyroptosis

Daifang Liu[1,2,3], Wendan Wu[1,2], Tingting Wang[1,2], Guiyu Zhan[1,2], Yuandong Zhang[1,2], Jianmei Gao[1,2] and Qihai Gong[1,2]*

[1]Key Laboratory of Basic Pharmacology, Ministry of Education and Joint International Research Laboratory of Ethnomedicine, Zunyi Medical University, Zunyi, China, [2]Key Laboratory of Basic Pharmacology of Guizhou Province, Department of Pharmacology, School of Pharmacy, Zunyi Medical University, Zunyi, China, [3]Department of Neurology, Affiliated Hospital of Zunyi Medical University, Zunyi, China

Introduction: Ischemic stroke (IS) is a serious threat to human life and health, and cerebral ischemia/reperfusion injury (CIRI) exacerbates IS by enhancing neuroinflammation and oxidative stress. Sweet tea (ST) comprises several bioactive components, such as phlorizin, trilobatin, and phloretin, with diverse pharmacological activities. However, it remains uncertain whether ST can confer protection against CIRI. In this study, we aimed to investigate the impact and potential underlying mechanism of ST in the context of CIRI.

Methods: CIRI model were established in male sprague dawley (SD) rats. The neurobehavioral assessment, the volume of cerebral infarction and the morphology of neurons were measured to complete the preliminary pharmacodynamic study. The therapeutic targets and pathways of ST on IS were obtained by protein-protein interaction, molecular docking and Metascape database. The predicted results were further verified *in vivo*.

Results: Our results revealed that ST treatment significantly ameliorated brain damage in rats subjected to CIRI by mitigating mitochondrial oxidative stress and neuroinflammation. Additionally, we identified the PI3K/AKT/NF-κB pathway and the NLRP3-mediated pyroptosis axis as crucial processes, with molecular docking suggested direct interactions between the main compounds of ST and NLRP3.

Abbreviations: IS, Ischemic stroke; MCAO, Middle cerebral artery occlusion; CIRI, Cerebral ischemia/reperfusion injury; ST, sweet tea (*Lithocarpus polystachyus* Rehd.); PI3K, phosphatidylinositol-3-kinase; AKT, protein kinase B; NF-κB, nuclear factor-κB; NLRP3, NOD-like receptor family pyrin domain-containing 3; GO, Gene ontology; KEGG, Kyoto Encyclopedia of genes and genomes; PPI, protein-protein interaction.

Conclusion: ST safeguards against CIRI-induced neuronal loss, neuroinflammation and oxidative stress through the inhibition of the PI3K/AKT/NF-κB pathway and the regulation of NLRP3-mediated pyroptosis.

KEYWORDS

ischemic stroke, *Lithocarpus polystachyus* Rehd., pyroptosis, PI3K/Akt/NF-κB, oxidative stress, inflammation

1 Introduction

Ischemic stroke refers to a central nervous system disorder caused by impaired blood supply, leading to ischemic and hypoxic necrosis of brain tissue (Baillieul et al., 2022). It is characterized by a high occurrence rate of incidence, mortality and disability, imposing a dreadful incubus on patients and society (Khanna et al., 2021). Up to now, recombinant tissue-type plasminogen activator is the only drug approved by FDA to overcome ischemic stroke (Goncalves et al., 2022). However, its limitations, including a narrow treatment time window, contraindications, and the risk of hemorrhagic transformation, have restricted its benefits for patients (Yuan et al., 2021). Furthermore, restoring blood flow to ischemic brain tissue can exacerbate neuronal death and neurological dysfunction, a condition known as cerebral ischemia-reperfusion injury (CIRI) (Zeng et al., 2022).

CIRI is a critical link in ischemic stroke, involving highly complex pathological processes, amobg which oxidative stress and neuroinflammation playing pivotal roles (Liao et al., 2020; Tuo et al., 2022). Following ischemia and hypoxia, endogenous antioxidant substances in brain tissue were depleted, leading to an accumulation of excessive reactive oxygen species (ROS) (Sies and Jones, 2020; Li et al., 2021). This accumulation induces toll-like receptor 4 (TLR4) activation, which subsequently phosphorylates nuclear factor-κB (NF-κB) (Gao et al., 2020). NF-κB then translocates from the cytoplasm to the nucleus, initiating pro-inflammatory cytokines release involving tumor necrosis factor-alpha (TNF-α), interleukin-1 beta (IL-1β), and interleukin-6 (IL-6) (Yu et al., 2020; Capece et al., 2022). The vicious cycle between oxidative stress and inflammatory responses can trigger the NOD-like receptor pyrin domain containing 3 (NLRP3) inflammasome activation (Han X. et al., 2021; Ma, 2023). The activated NLRP3 inflammasome, in turn, activates cysteinyl aspartate specific proteinase-1 (Caspase-1), which, on one hand, cleaves and activates IL-1β and interleukin-18 (IL-18), thereby mediating and amplifying the inflammatory response (Ising et al., 2019; Ma, 2023). On the other hand, Caspase-1 cleaves Gasdermin D (GSDMD), causing cell membrane perforation and initiating cell pyroptosis, exacerbating CIRI (Frank et al., 2020; Evavold et al., 2021). Therefore, targeting oxidative stress and neuroinflammation regulated by cell pyroptosis holds promise as a therapeutic approach for CIRI.

Sweet Tea (ST), also known as *Lithocarpus Polystachyus* Rehd., is an ethnobotanical medicine primarily found in Guizhou Province, China, and various provinces south of the Yangtze River (Goncalves et al., 2022). It possesses several medicinal properties, including blood sugar reduction, lipid-lowering, anti-inflammatory, antioxidant, and anti-tumor effects (Liao et al., 2020). The main active constituents of ST are phlorizin, trilobatin, and phloretin, and previous literature has suggested that ST can exert neuroprotective effects by inhibiting oxidative stress and inflammatory responses (Shang et al., 2022; Gao et al., 2020). However, there have been no reports on the effects of ST on ischemic stroke. Network pharmacology, a new interdisciplinary field that combines systems biology and computer technology, which analyzes the molecular associations between drugs and diseases from a systems-level perspective (Qin et al., 2022). Meanwhile, natural plants typically have complex active ingredients, multi-target effects, and multiple pathways (Sies and Jones, 2020). Therefore, this study combines network pharmacology, molecular docking technology, and experimental validation to systematically explore and validate the potential mechanisms of ST in preventing ischemic stroke.

2 Materials and methods

2.1 Materials

The following reagents and antibodies were used in this study: Enzyme-linked immunosorbent assay (ELISA) Kits from Shanghai Renjie Biotechnology Co., Ltd.: IL-6 (RJ15478), IL-18 (RJ15463), IL-1β (RJ15465), TNF-α (RJ16622), Interferon-γ (IFN-γ, RJ15676), Lactate dehydrogenase (LDH, RJ16172), ROS (RJ15780), Superoxide dismutase (SOD, RJ16691), Malondialdehyde (MDA, RJ15503), Glutathione (GSH, RJ29397). Antibodies from Abcam: NLRP3 (ab263899), Apoptosis associated speck-like protein (ASC, ab175449), GSDMD (ab209845), IL-18 (ab191860), IL-1β (ab254360), Caspase-1 (ab286125), Phosphatidylinositol 3-kinase (PI3K, ab1916061), Phosphorylation PI3K (p-PI3K, ab182651), Protein kinase B (AKT, ab8805), Phosphorylation AKT (p-AKT, ab38449), NF-κB (ab16502), Phosphorylation NF-κB (p-NF-κB, Catalog No: ab76302), NF-κB inhibitory protein α (IκB-α, ab32518), Glial fibrillary acidic protein (GFAP, ab7260), Ionized calcium-binding adapter molecule 1 (IBA1, ab178847), Antibodies from Wuhan Sanying Biotechnology Co., Ltd.: Cleaved-Caspase-1 (AF4022), β-actin internal reference (20536-1-AP), GAPDH internal reference (60004-1-lg). Reagents and Standards from Other Sources: TTC staining solution (T8170) from Beijing Solaibao Technology Co., Ltd. Rutin standard (SP8240) from Beijing Solaibao Technology Co., Ltd. Quercetin standard (161009) from Nanjing Zelang Biotech Co., Ltd.

2.2 Preparation and analysis of ST

The fresh leaves of *Lithocarpus polystachyus* Rehd. were collected from Guizhou Province in summer, which were deposited in the herbarium and identified by Jianyong Zhang of

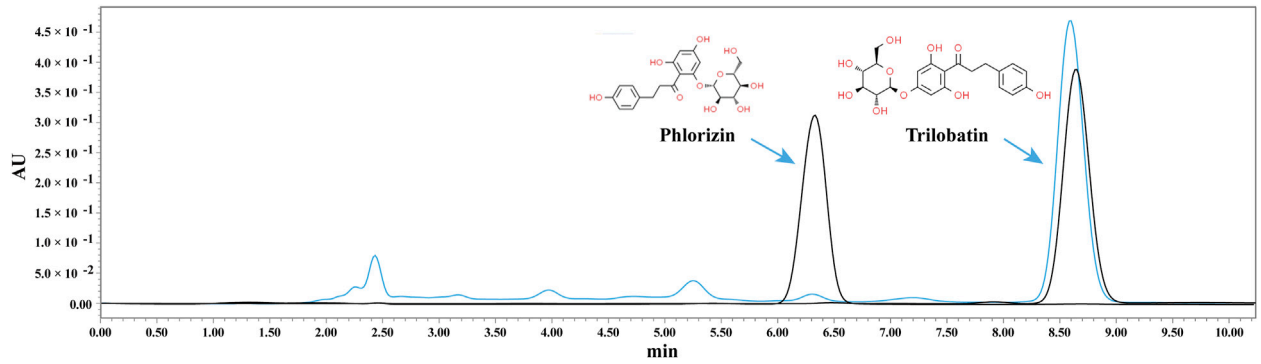

FIGURE 1
HPLC analysis of ST aqueous extract. The black line represents the standard, and the blue line represents the sample.

Zunyi Medical University. The dried ST leaves were ground in a mortar and then transferred to a round-bottom flask. Purified water was added in a 1:20 ratio (plant material to water). After heating and refluxing for 30 min, the mixture was filtered through sterile gauze. This filtration process was repeated twice, and the filtrates were combined. The filtrate was rotary evaporated to obtain an extract, which was then dried in a vacuum dryer. The collected product is the dried powder, which was stored in a −80°C freezer for future use (Gao et al., 2018).

For the analysis of the main representative compounds, trilobatin and phlorizin, in ST based on previous studies, HPLC (High-Performance Liquid Chromatography) was employed. The chromatographic conditions were as follows: Column: Exten-C18 (5 μm, 4.6 × 150 mm), Mobile phase: 1% acetic acid aqueous solution (A)-Methanol (B), Gradient elution (trilobatin: 0–40 min, 70%A-30%B; phlorizin: 0 min, 95%A-5%B; 40 min, 40%A-60%B; 50 min, 0%A-100%B), Maximum wavelength: 286 nm, Injection volume: 10 μL, Column temperature: 30°C, Flow rate: 1 mL/min.

2.3 Animal and drug treatment

Male Sprague Dawley (SD) rats weighing 260–280 g from a specific pathogen-free (SPF) environment were obtained from Hunan SJA Laboratory Animal Co., Ltd. (Certificate No: SCXK (Xiang) 2019–0004, Changsha, China). The rats were housed in separate cages (5-6 rats per cage) within an SPF-grade animal facility. During their one-week acclimation period, the animals were kept in rooms with good ventilation, maintained at a constant temperature of 23°C ± 1°C, and a constant humidity of 55% ± 5%. Throughout the acclimation period, the SD rats had free access to food and water. The animal experiments strictly adhered to the ethical guidelines and regulations of the Ethics Committee for Animal Experiments at Zunyi Medical University.

The rats were randomly divided into seven groups using a simple randomization method: the Sham group, middle cerebral artery occlusion (MCAO) group, MCAO + ST 200 mg/kg group, MCAO + ST 400 mg/kg group, and MCAO + ST 600 mg/kg group. ST was administered through intragastric gavage for 7 consecutive days, with one dose per day. Rats in the sham group and the model group were administered intragastrically volume-matched vehiclean equivalent volume of distilled water by intragastric gavage. Twenty-four hours after the last administration, the MCAO model was induced to simulate CIRI.

2.4 Animal model

In brief, rats were anesthetized with a 2% solution of pentobarbital sodium (30 mg/kg). Following, the rats were fixed on a board, and the neck area was disinfected with iodine. 2 cm incision was made in the neck area to expose the right common carotid artery, internal carotid artery, and external carotid artery. The external carotid artery was ligated near the common carotid artery. Then, a "V"-shaped incision was made in the common carotid artery, and a filament was inserted until the marked black point. The timer was started, and the incision was sutured. After 2 h of ischemia, the filament was pulled out until the black point was visible, and the excess filament was cut (Gao et al., 2023). The modeling procedure was completed. Throughout the surgery, a constant-temperature heating blanket was used to maintain the rat's body temperature at around 37°C.

2.5 Laser speckle contrast imaging (LSCI) monitoring

To assess the success of the model, cerebral blood flow (CBF) in the whole brain of rats was monitored using a laser speckle blood flow imaging system before modeling, during modeling, and during reperfusion (Gao et al., 2023). The MCAO model was considered successful when CBF decreased to approximately 20% of the preoperative level during modeling and then recovered to around 80% of the preoperative level during reperfusion.

2.6 Neurobehavioral assessment

To assess the recovery of rat neurological function, the Longa 5-point method was employed 24 h after reperfusion (Gao et al., 2020). The scoring criteria were as follows: 0 points: No neurological damage; 1 point: Mild neurological impairment, inability to fully extend the

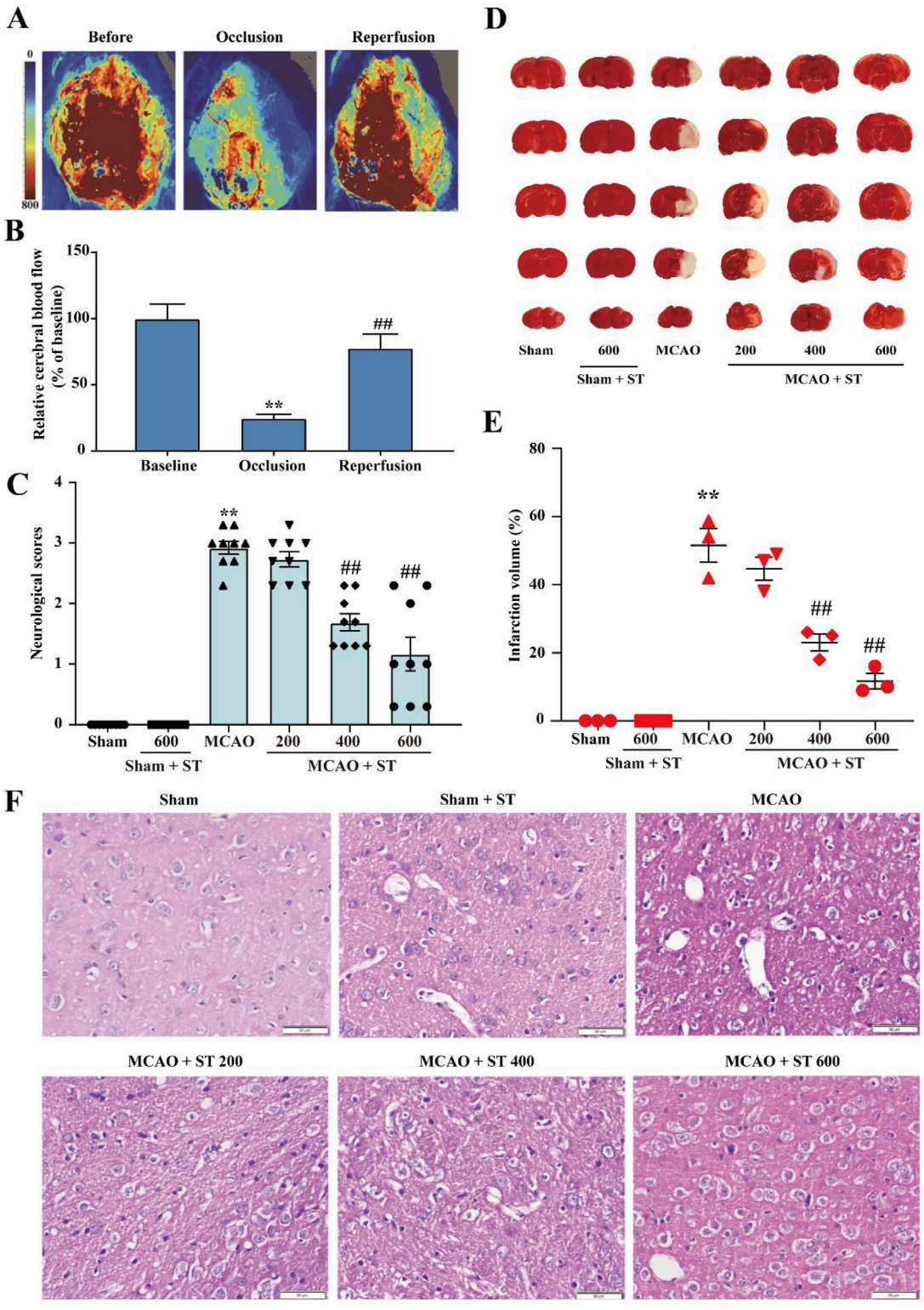

FIGURE 2
ST significantly improves CIRI in rats. **(A)** Laser speckle imaging representative images. **(B)** Representative images of TTC staining. **(C)** Quantitative analysis of CBF (n = 3). **(D)** Results of neurological function scoring (n = 9). **(E)** Quantitative analysis of brain infarct volume in each group (n = 3). **(F)** HE staining (n = 3, Scale bar: 50 μm). Data presented are mean ± SEM. $^{*}P < 0.05$, $^{**}P < 0.01$ vs. Sham group; $^{\#}P < 0.05$, $^{\#\#}P < 0.01$ vs. MCAO group.

paralyzed forelimb on the affected side, walking with a tilted posture; 2 points: Moderate neurological impairment, circling towards the paralyzed side while walking; 3 points: Severe neurological impairment, falling to the paralyzed side when walking, or nearly rotating around the head as the center; 4 points: Inability to walk spontaneously, with signs of loss of consciousness.

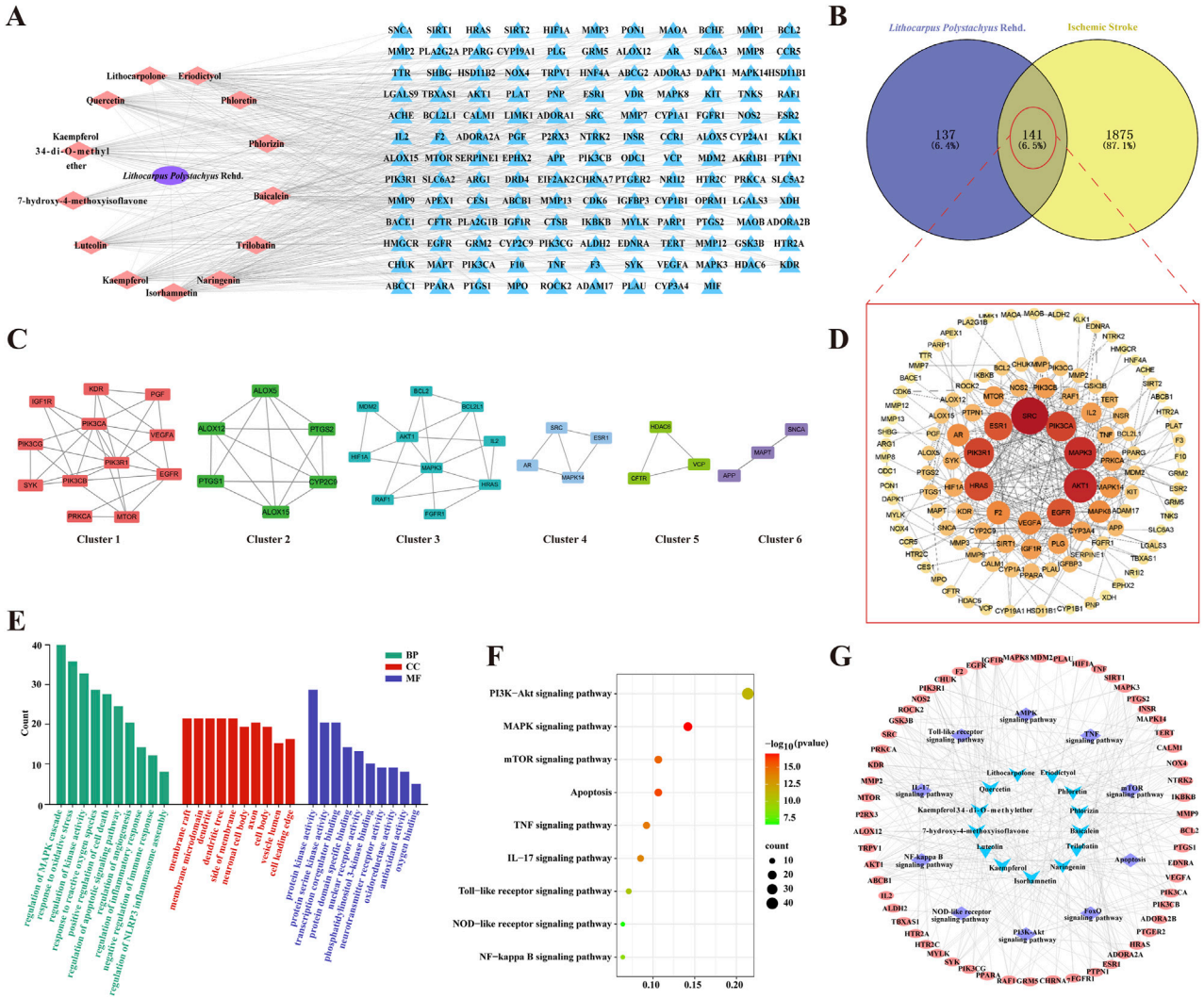

FIGURE 3
The potential mechanisms of ST in neuroprotection against IS. **(A)** Compound-target network of active ingredients in ST; pink nodes represent active compounds found in ST, and blue nodes represent their corresponding target proteins. **(B)** Venn diagram depicting the overlap between ST targets and IS targets. **(C)** Six clusters obtained from the PPI network. **(D)** PPI network of intersected targets, with the color gradient from yellow to red indicating the significance level of these overlapping targets, with red being the highest and yellow being the lowest. **(E)** Enrichment analysis of GO functions. **(F)** Bubble chart of KEGG pathways. **(G)** Network of drug ingredients, pathways, and targets. Blue nodes represent active compounds found in ST, purple nodes represent signaling pathways these compounds participate in, and pink nodes represent the target proteins of these compounds.

2.7 Measurement of cerebral infarct volume

After the completion of the modeling process, rats were euthanized, and their brains were carefully and rapidly removed. Subsquently, the brain tissue was sliced into uniform thickness of 5 sections using a blade. These sections were then incubated at 37 C in a constant temperature oven for 60 min with 2,3,5-triphenyltetrazolium chloride (TTC) dye. Following the TTC reaction, the solution was discarded, and a 4% paraformaldehyde solution was added for fixation at room temperature for 2 days, and then TTC-stained slices was quantified by ImageJ software.

2.8 Hematoxylin and eosin staining (HE)

The rats underwent cardiac perfusion with PBS (200 mL), followed by perfusion with 4% paraformaldehyde. Subsequently, the brains were carefully and rapidly removed and fixed in 4% paraformaldehyde for 48 h. After dehydration with ethanol, the brain tissues were embedded in paraffin. The paraffin-embedded brain tissues were then cut into 5 μm-thick sections, and the tissue sections were deparaffinized using xylene, and stained with hematoxylin solution for 5 min followed by soaking in eosin solution for 5 min. Finally, the sections were observed and photographed under an optical microscope (BX 43 Olympus, Tokyo, Japan).

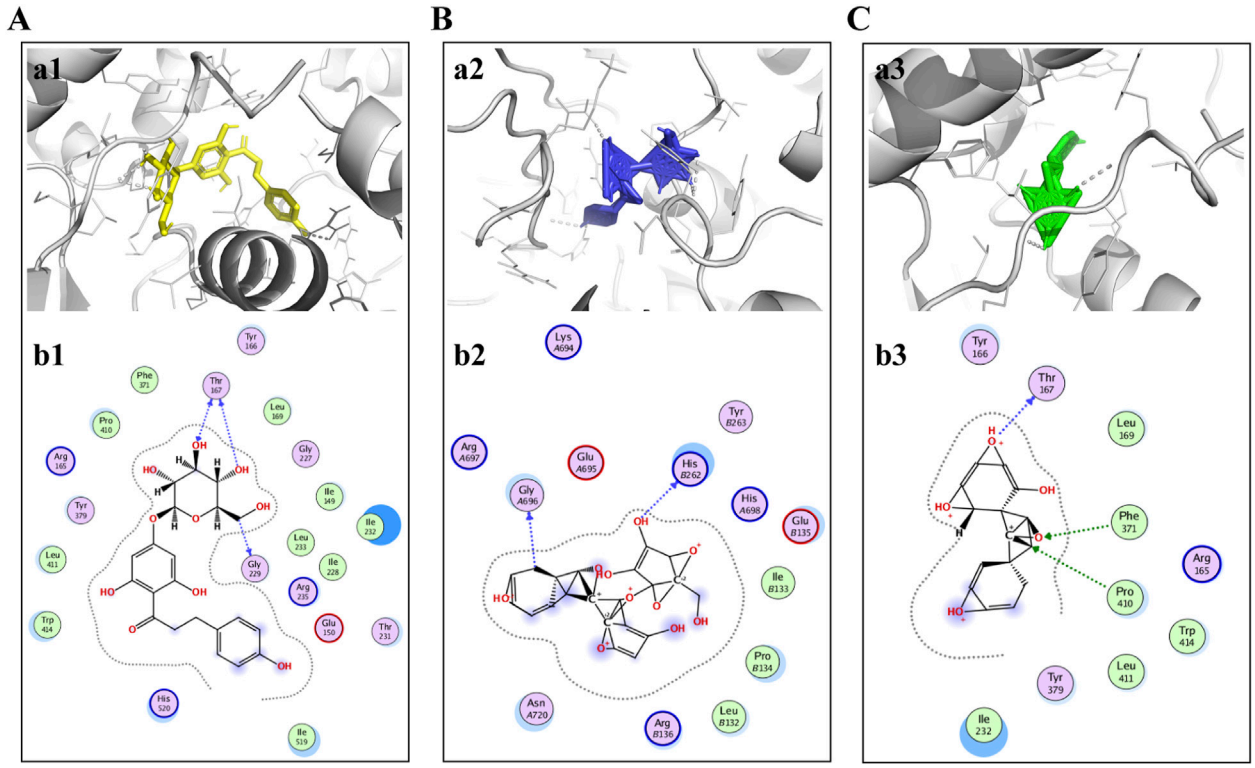

FIGURE 4
Trilobatin, phlorizin, and phloretin directly bind to NLRP3. **(A)** Trilobatin bound to NLRP3. (a1) Crystal structure of trilobatin (yellow) showing its binding to the docking pocket of NLRP3 (grey). (b1) Amino acid residues involved in the interaction between trilobatin and NLRP3. **(B)** Phlorizin bound to NLRP3. (a2) Crystal structure of phlorizin (blue) demonstrating its binding to the docking pocket of NLRP3 (grey). (b2) Amino acid residues involved in the interaction between phlorizin and NLRP3. **(C)** Phloretin bound to NLRP3. (a3) Crystal structure of phloretin (green) illustrating its binding to the docking pocket of NLRP3 (grey). (b3) Amino acid residues involved in the interaction between phloretin and NLRP3.

2.9 Collection and screening of active chemical composition in ST

ST, as a regional ethnic medicine, is not cataloged in various databases. Therefore, this study employed different keywords, including "sweet tea", "*Lithocarpus Polystachyus Rehd.*," and others, to search various databases. From the extensive literature related to ST, information on its active components was gathered. Duplicate and structurally unclear compounds were removed, and the data were compiled. These data were then input into the PubChem database (https://pubchem.ncbi.nlm.nih.gov/) to extract the Canonical SMILES names for each component. Subsequently, the SWISS ADME database (https://www.swissadme.ch/) was used to predict the pharmacokinetic properties and drug-likeness of these compound SMILES names. The criteria for selection included "High" gastrointestinal absorption and positive results for Lipinski, Ghose, Veber, Egan, and Muegge filters, with a requirement of "yes" for each and a score of ≥2.

2.10 Prediction of potential drug targets and construction of component-target network

SWISS Target Prediction database (http://swisstargetprediction.ch/SwissTargetPrediction) was used to identify the SMILES names of the selected active compounds of ST. The results, in "tsv" format, were downloaded. The duplicate targets and the genes whose credibility value was 0 were removed. Then Cytoscape 3.7.0 software was applied to construct the component-target network.

2.11 Acquisition of intersecting target genes

To discover target genes related to ischemic stroke, searches were conducted in the Disgenet database (http://www.disgenet.org/) and GeneCards database (http://www.disgenet.org/) using "Ischemic stroke" as the keyword. An online analysis tool, Venny 2.1 (http://bioinfogp.cnb.csic.es/tools/venny/), was used to create a Venn diagram to visualize the intersection of active components in ST and ischemic stroke-related target genes.

2.12 Protein-protein interaction (PPI) network construction

String database (https://string-db.org/) was utilized with a species constraint of "*Homo sapiens*" and a confidence score threshold set at greater than 0.9. This helped in constructing a protein-protein interaction (PPI) network. Nodes that were not connected in the network were hidden. The results, in "tsv" format,

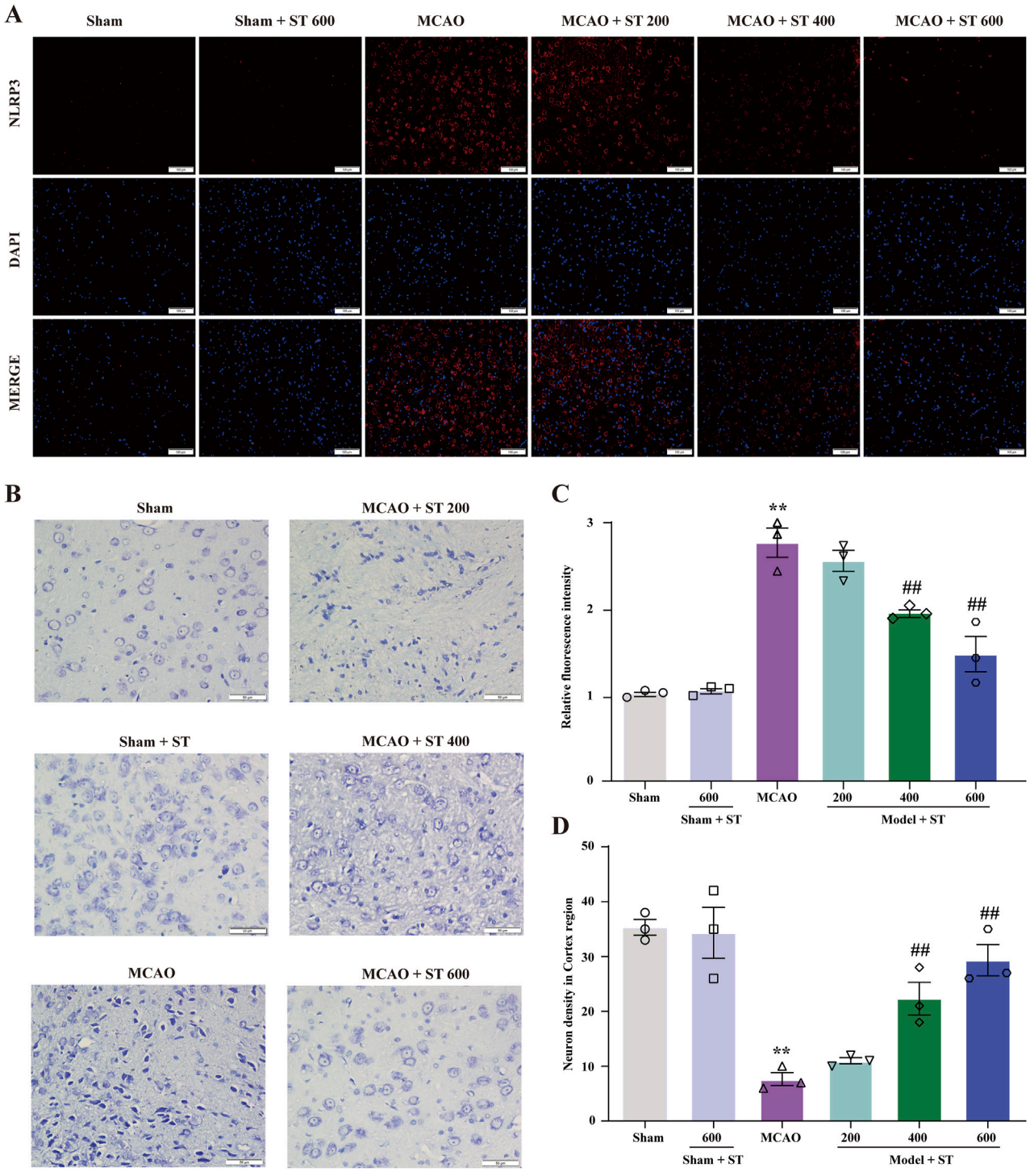

FIGURE 5
ST reduces CIRI-induced NLRP3 expression and neuronal damage. **(A)** Expression of NLRP3 in the cortical region. **(B)** Nissl staining in the cortical region (scale bar: 50 μm). **(C)** Statistical analysis of relative fluorescence intensity of NLRP3 in the cortical region (n = 3). **(D)** Quantification of surviving neurons in the cortical region (n = 3). Data presented are mean ± SEM. $^{**}P < 0.01$ vs. Sham group; $^{\#\#}P < 0.01$ vs. MCAO group.

were downloaded and imported into Cytoscape 3.7.0 software. A drug-active component-target network was constructed, and the molecular complex detection algorithm (MCODE) plugin was used to identify highly interconnected clusters with default parameters. This comprehensive methodology allowed for the prediction of potential targets for ST and the construction of a network illustrating the relationships among compounds, target proteins, and their interactions.

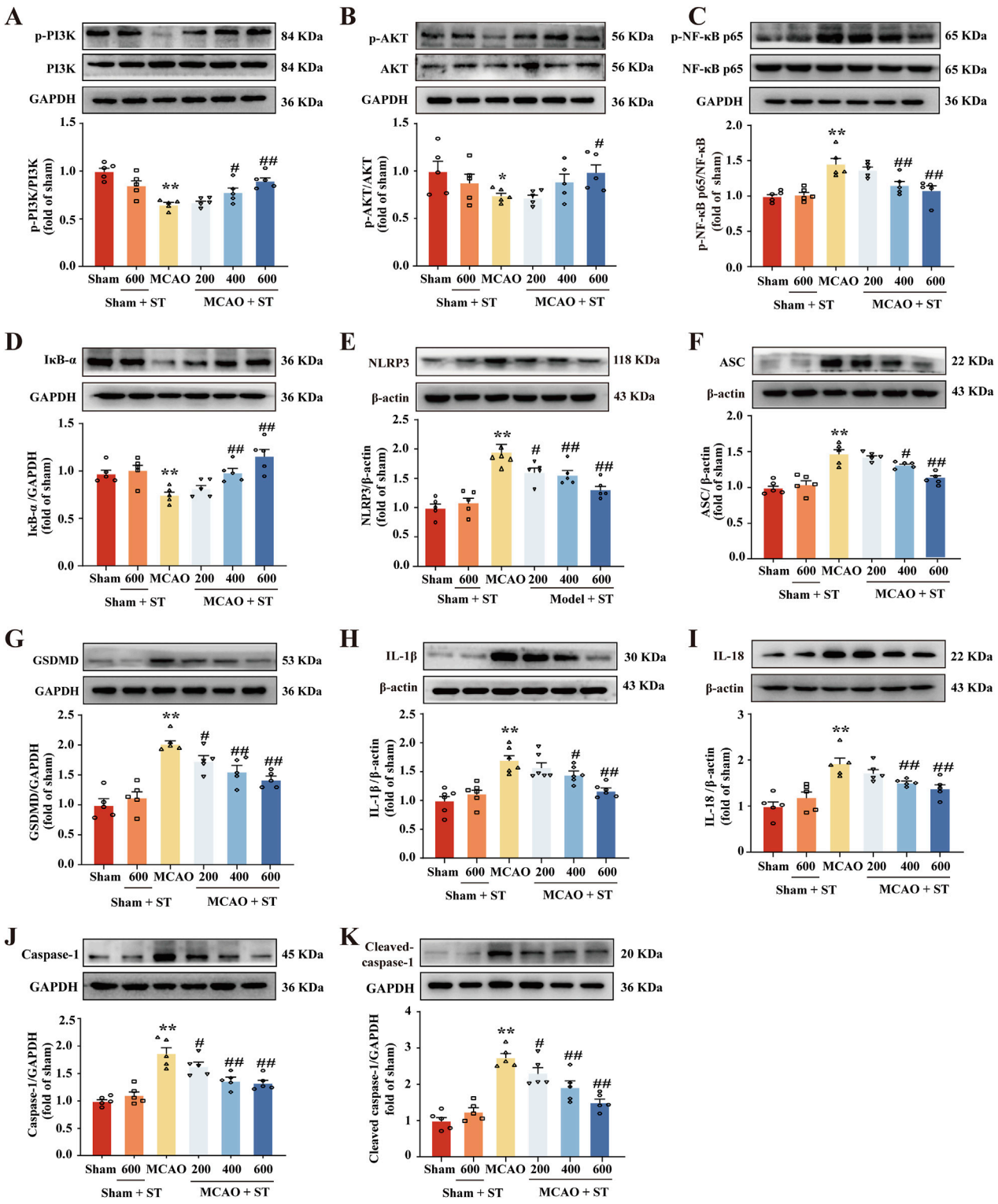

FIGURE 6
ST dampens pyroptosis induced by CIRI through suppressing the PI3K/AKT/NF-κB pathway. **(A)** Quantitation of p-PI3K (n = 5). **(B)** Quantitation of p-AKT (n = 5). **(C)** Quantitation of p-NF-κB (n = 5). **(D)** Quantitation of IκB-α (n = 5). **(E)** Quantitation of NLRP3 (n = 5). **(F)** Quantitation of ASC (n = 5). **(G)** Quantitation of GSDMD (n = 5). **(H)** Quantitation of IL-1β (n = 6). **(I)** Quantitation of IL-18 (n = 5). **(J)** Quantitation of Caspase-1 (n = 5). **(K)** Quantitation of Cleaved-caspase-1 (n = 5). $^{*}P < 0.05$, $^{**}P < 0.01$ vs. Sham group; $^{\#}P < 0.05$, $^{\#\#}P < 0.01$ vs. MCAO group.

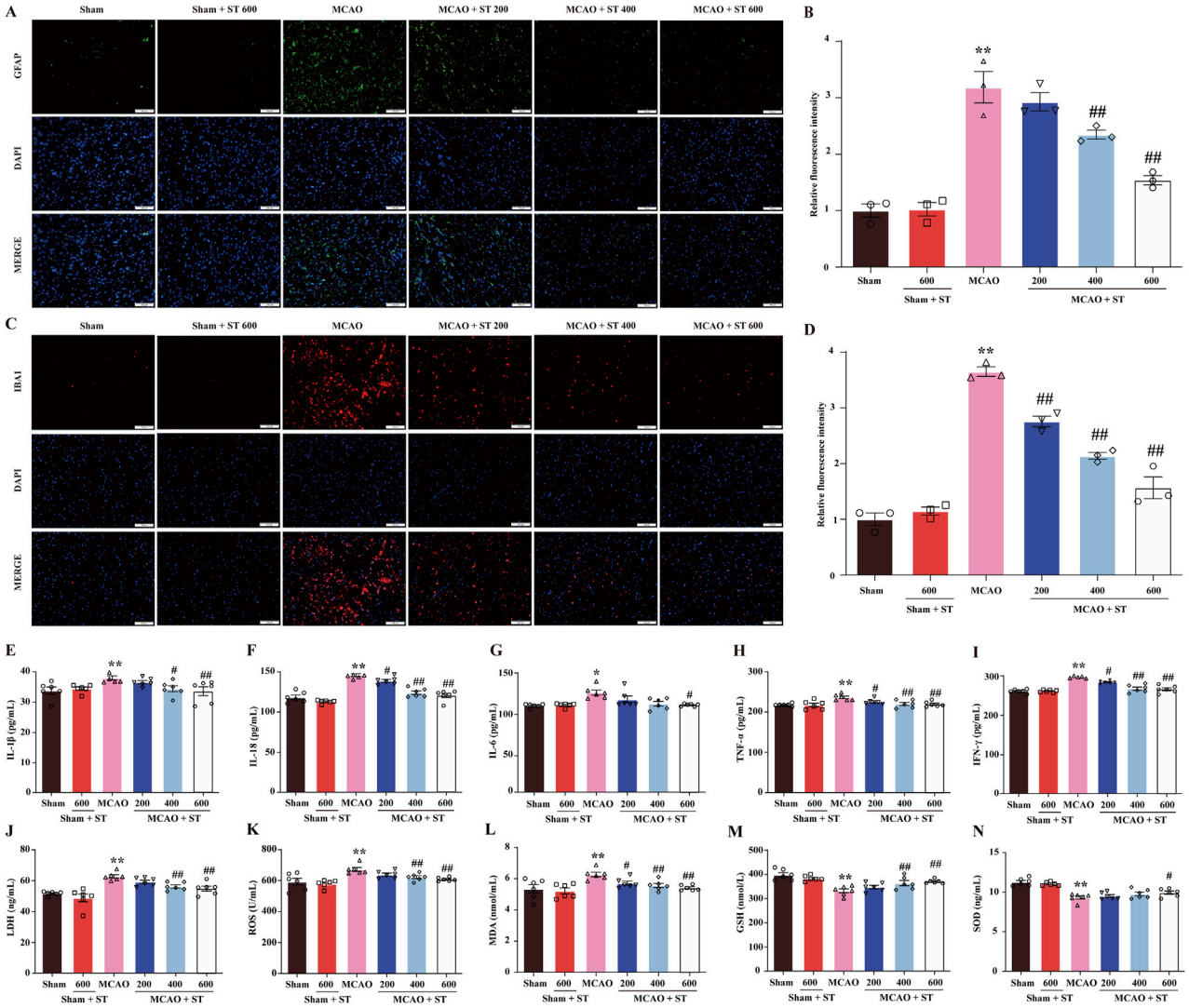

FIGURE 7
ST mitigates inflammatory responses and oxidative stress induced by CIRI through inhibiting the activation of gliocyte. **(A)** Representative images of GFAP expression (scale bar = 100 μm). **(B)** Representative images of IBA1 expression (scale bar = 100 μm). **(C)** Quantitation of astrocyte fluorescence intensity (n = 3). **(D)** Quantitation of microglia fluorescence intensity (n = 3). **(E)** IL-1β level (*n* = 6). **(F)** IL-18 level (n = 6). **(G)** IL-6 level (n = 6). **(H)** TNF-α level (n = 6). **(I)** IFN-γ level (n = 6). **(J)** LDH level (n = 6). **(K)** ROS (n = 6). **(L)** MDA (n = 6). **(M)** GSH (n = 6). **(N)** SOD (n = 6). Data presented are mean ± SEM. $^{**}P< 0.01$ vs. Sham group; $^{\#}P< 0.05$, $^{\#\#}P< 0.01$ vs. MCAO group.

2.13 GO analysis and KEGG pathway enrichment analysis

We conducted a gene ontology (GO) functional enrichment analysis and Kyoto Encyclopedia of Genes and Genomes (KEGG) pathway enrichment analysis on the overlapping targets using the Metascape database (http://metascape.org/gp/index.html). The analysis results were visualized by creating bar graphs and bubble charts using a bioinformatics platform (http://www.bioinformatics.com.cn/). This process aimed to provide a comprehensive understanding of the enriched functions and pathways associated with the intersection targets.

2.14 Construction the network of drug ingredients, main pathways, and targets

The active chemical composition in ST, main signal pathways enriched in KEGG analysis, and the corresponding targets of each pathway were imported into Ctyoscape3.7.0 to draw the drug ingredient-main pathway-target network diagram.

2.15 Molecular docking

Based on the drug-component-target network results, molecular docking was performed between the main active components of ST

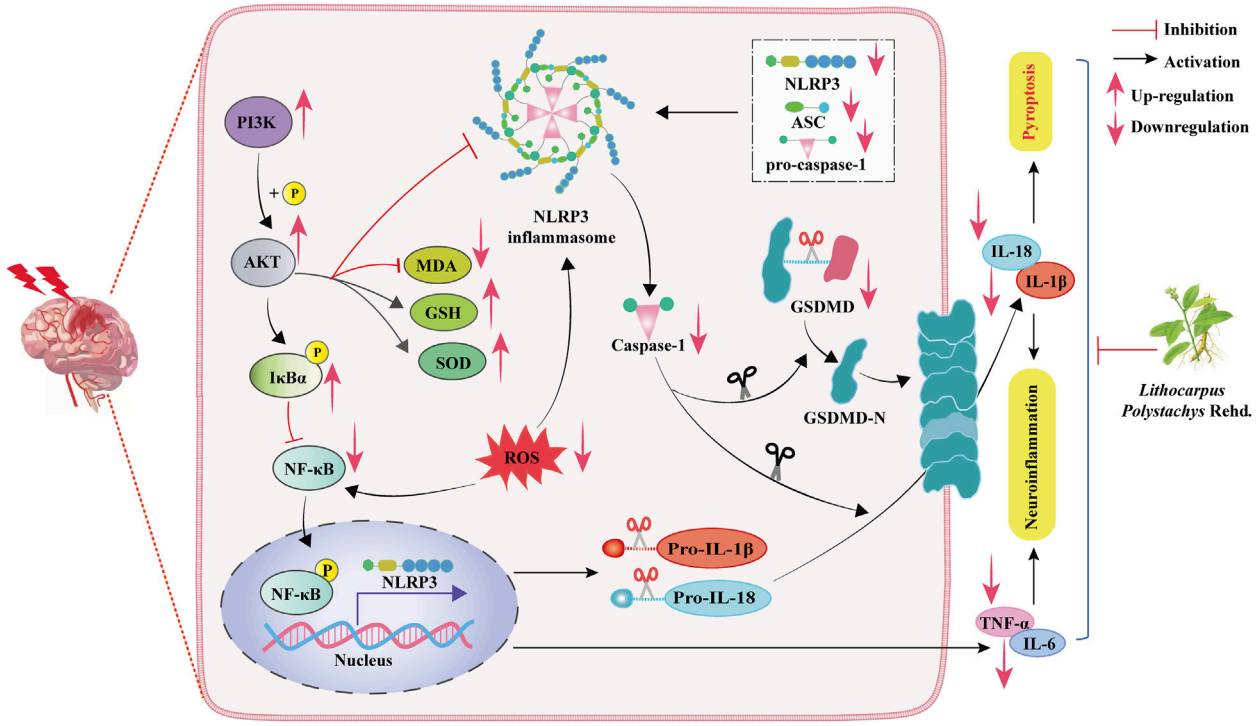

FIGURE 8
Schematic representation of the molecular mechanisms underlying the protective effects of ST against CIRI.

(trilobatin, phlorizin, phloretin) and NLRP3. In summary, the 3D crystal structure of the NLRP3 protein (PDB ID: 6NPY) was obtained from the Protein Data Bank (http://www.rcsb.org). The structures of trifolirhizin, root bark glycosides, and quercetin were obtained from the PubChem database and converted to the mol2 format for storage. The target protein and ligands underwent preprocessing, which included steps such as dehydration, hydrogen addition, and atom type assignment, using PyMOL and AutoDock Tools software. Subsequently, molecular docking were performed using AutoDock 4.2. The results were visualized using PyMOL software to gain insights into the interactions between the ligands and the target protein.

2.16 Nissl staining

The paraffin-embedded brain tissue sections underwent standard deparaffinization. They were immersed in xylene (55°C, 30 min), followed by double-distilled water to remove excess staining solution. After ensuring clear Nissl bodies under a microscope, the sections were air-dried in a fume hood. Subsequently, neutral resin containing xylene was used to mount the slides. Neuron quantification was performed using the ImageJ 1.80 software.

2.17 Immunofluorescence staining (IF)

Brain tissue paraffin sections were subjected to routine deparaffinization, followed by antigen retrieval with citrate buffer using microwave treatment. Non-specific antigen blocking was carried out using goat serum, and the primary antibodies were incubated overnight under 4°C. Subsequently, the corresponding secondary antibodies were added. DAPI staining was performed at room temperature for 5–7 min. Finally, fluorescence was observed using a fluorescence microscope (BX 53 Olympus, Tokyo, Japan), and fluorescence intensity was analyzed by ImageJ software.

2.18 Enzyme-linked immunosorbent assay (ELISA)

Blood was obtained from the abdominal aorta, and the serum was collected after centrifuged (3000 × g, 10 min) at 4°C. ELISA were performed following the instructions provided in the respective assay kits to measure the concentrations of IL-6, IL-18, IL-1β, TNF-α, IFN-γ, LDH, ROS, SOD, MDA, and GSH in the serum. Brifly, the standard group, control group and sample group were divided on the 96-well plate, and the standard product, sample diluent, and serum samples diluted 5 times were added in sequence. Then, enzyme-labeled antibodies were added (except control group) and incubated at 37°C for 1 h. After washing for 5 times, add chromogenic solution A and B respectively and incubate at 37°C for 15 min. Finally, add the termination solution. The absorbance value was detected at a wavelength of 450 nm on microplate reader and the sample concentration was calculated according to the standard curve.

2.19 Western blot (WB)

In brief, the ischemic penumbra was isolated, and the tissue was completely homogenized on ice. Protein quantification was

performed using a BCA assay kit, and the protein samples were denatured by heating. A 10% sodium dodecyl sulfate-polyacrylamide gel electrophoresis (SDS-PAGE) was prepared to separate the proteins, followed by blocking with 5% skim milk powder for 3 h. Subsequently, primary antibodies were used for overnight incubation under 4°C: NLRP3 (1:1,000), GSDMD (1:1,000), NF-κB p65 (1:1,000), p-NF-κB p65 (1:1,000), IL-1β (1:1,000), IL-18 (1:1,000), ASC (1:1,000), Caspase-1 (1:1,000), Cleaved-Caspase-1 (1:1,000), PI3K (1:1,000), p-PI3K (1:1,000), AKT (1:1,000), p-AKT (1:1,000), IκB-α (1:1,000), β-actin (1:10,000), and GAPDH (1:10,000). The following day, HRP-conjugated secondary antibodies were incubated at room temperature for 40 min (1:5,000). Images were exposed and saved, and the grayscale values were analyzed using ImageJ software.

2.20 Statistical analysis

All data from this experiment were analyzed using SPSS 18.0 statistical software and are presented as mean ± standard error of the mean (mean ± SEM). Multiple group comparisons were performed using the one-way ANOVA test. If homogeneity of variances was observed, the LSD test was applied. If variances were not homogeneous, the Dunnett's T3 test was used. A significance level of $P < 0.05$ was considered statistically significant.

3 Results

3.1 Preparation and analysis of ST

ST aqueous extract was prepared from dried ST leaves, and its composition was analyzed using HPLC. Chromatographic results from the HPLC analysis revealed that among the detected peaks, the iconic components of ST, trilobatin and phlorizin, were found (Figure 1).

3.2 ST exhibits neuroprotective effect on CIRI

To investigate the protective effects of ST on CIRI in rats, neurological function scoring, brain infarct volume measurement, and HE staining were performed at the 24-h time point after successful establishment of the MCAO model. Laser speckle imaging monitoring showed that CBF in rats decreased to approximately 20% of preoperative levels after modeling, and it increased to around 80% of preoperative levels after reperfusion (Figures 2A, B), confirming the successful establishment of the model in this study. Experimental results of neurological function scoring and brain infarct volume measurement demonstrated that the neurological function score and brain infarct volume in the model group were significantly increased compared to the sham surgery group. In comparison to the model group, the administration of ST at 200 mg/kg did not affect the neurological function score and brain infarct volume, whereas the 400 mg/kg and 600 mg/kg groups exhibited significant reductions (Figures 2C–E). Furthermore, HE staining results indicated that after MCAO, there was a significant loss of neurons in the cortical region, or phenomena such as blurred cell boundaries and dark-stained nuclei. However, ST clearly reversed these changes (Figure 2F). These results collectively suggest that ST exhibits neuroprotective effects, significantly attenuating CIRI in rats.

3.3 The potential mechanisms of ST in neuroprotection against IS

From published literature, a total of 13 potentially active compounds were gathered. These compounds included trilobatin, phlorizin, phloretin, and others (Supplementary Table S1). The SWISS Target Prediction tool was employed to predict target genes for these compounds, resulting in 278 unique target genes after removing duplicates. A compound-target network was constructed and visualized using Cytoscape 3.7.0, comprising 155 nodes and 514 edges (Figure 3A). A total of 2,016 target genes linked to CIRI were obtained from the GeneCards and DisGeNet databases. By comparing disease-related targets with drug-related targets using the Venny 2.1 platform, 141 overlapping targets were identified as core genes for further investigation (Figure 3B). A protein-protein interaction (PPI) network composed of these targets was constructed using the STRING database, resulting in visual graphics and data (Figure 3D). Next, targets in the PPI network was analyzed using MCODE revealed six clusters (Figure 3C; Supplementary Table S2). These results offer new insights into the pharmacological effects of ST to treat CIRI.

Importing core targets into Metascape database for GO analysis: following filtering with a significance level of $P< 0.05$, a total of 216 biological process (BP), 88 cellular component (CC), and 99 molecular function (MF) entries were enriched. In BP analysis, target proteins were primarily involved in processes such as regulation of oxidative stress, inflammatory response, apoptosis, and NLRP3 inflammasome assembly. MF analysis highlighted crucial molecular functions, including protein kinase activity, phosphatidylinositol 3-kinase binding, and antioxidant activity. CC analysis indicated that target proteins were predominantly distributed in membrane rafts, membrane microdomains, dendrites, dendritic spines, membrane periphery, neuronal cell bodies, axons, cell bodies, vesicle lumens, and cell leading edges (Figure 3E). Additionally, a total of 175KEGG signaling pathways were screened out with a significance level of $P< 0.05$. Key pathways such as the NOD-like receptor signaling pathway, PI3K-Akt signaling pathway, TNF signaling pathway, and NF-kappa B signaling pathway were identified as crucial for the anti-IS effects of ST (Figure 3F). Furthermore, our compound-target-pathway network analysis demonstrated that each compound could impact multiple targets and participate in various pathways. Among them, trilobatin, phlorizin and phloretin were identified as key active ingredients in the treatment of IS with ST (Figure 3G).

3.4 Molecular docking

As previously mentioned, NLRP3 may be a possible target for ST in the treatment of ischemic stroke. Therefore, molecular coupling

method was used to further explore the interaction of key active ingredients trilobatin, phlorizin and phloretin with the target protein NLRP3 (PDBID:6NPY). The results indicated that the binding energies of the three compounds with the target proteins were −5.67 kcal/mol, −5.82 kcal/mol, and −6.28 kcal/mol, respectively. This suggests that the compounds exhibited strong binding affinities with the target proteins. The molecular docking results are detailed below (Figure 4).

3.5 ST inhibits NLRP3 activation induced by CIRI and reduces neuronal loss in rats

To further validate the potential target NLRP3, we conducted immunofluorescence staining (IF). Following CIRI, the NLRP3 fluorescence intensity markedly increased. However, upon treatment with ST, the fluorescence intensity significantly decreased (Figures 5A, C). Furthermore, Nissl staining results showed that in the sham group, neuronal morphology in the cortical region of rats was intact, with full nuclei and clear nucleoli appearing light blue. In contrast, in the model group, Nissl bodies were disorganized, some cell membranes ruptured with vacuoles, nucleoli were deeply stained and shrunken, there was an increase in neuronal loss, and cell degeneration was observed. However, after ST intervention, the 400 and 600 mg/kg dosage groups significantly ameliorated these abnormal changes (Figures 5B, D).

3.6 ST dampens pyroptosis induced by CIRI through suppressing the PI3K/AKT/NF-κB pathway

We utilized WB to validate the findings from the network pharmacology analysis. In rats with CIRI, ASC, GSDMD, IL-18, IL-1β, Caspase-1, Cleaved-Caspase-1, p-NF-κB, and NLRP3 protein expressions were significantly upregulated compared to the sham group. Whereas, after treatment with ST, the expression of these proteins was obviously reduced (Figures 6C, E–K). Additionally, in the model group, p-PI3K, p-Akt, and IκB-α proteins levels were significantly decreased in comparison of the sham group, and this effect was reversed in the ST treatment groups (Figures 6A, B, D).

3.7 ST mitigates inflammatory responses and oxidative stress induced by CIRI through inhibiting the activation of gliocyte

The IF staining was employed to evaluate the fluorescence intensity of GFAP and IBA1 to assess the activation of astrocytes and microglia in the ischemic penumbra of rat brain tissue. The results revealed that in the sham surgery group, both astrocytes and microglia in the ischemic penumbra region were in a resting state. In contrast, in the model group, astrocytes and microglia were significantly activated, exhibiting enlarged cell bodies, increased branching, and a significantly enhanced relative fluorescence intensity. However, intervention with ST reversed these morphological changes (Figures 7A, B) and significantly reduced the relative fluorescence intensity of GFAP and IBA1 (Figures 7C, D). Moreover, the results showed that the levels of IL-6, IL-18, IL-1β, TNF-α, IFN-γ, and LDH in CIRI rats were significantly increased in comparison of sham group. However, following ST intervention, the levels of these pro-inflammatory cytokines were dose-dependently decreased than those of model group (Figures 7E–J). Additionally, it is worth noting that ST significantly improved the levels of oxidative stress-related indicators than those of model group (Figures 7K–N). These findings suggest that ST inhibits the activation of gliocyte, thereby reducing neuroinflammation and oxidative stress following CIRI challenge.

4 Discussion

This study demonstrates that: (1) ST aqueous extract has a significant anti-CIRI effect. (2) ST exerts CIRI protection by modulating the PI3K/AKT/NF-κB and NLRP3-triggered pyroptotic signaling pathways to inhibit oxidative stress and neuroinflammation (Figure 8).

Thus far, due to its complex pathogenesis, there is no ideal treatment for CIRI in clinical practice. Emerging evidence indicates that oxidative stress and neuroinflammation play a pivotal role in worsening neuronal dysfunction and loss following CIRI (Campbell et al., 2019; Qin et al., 2022). Hence, effective drugs for CIRI treatment should exhibit robust anti-neuroinflammatory and antioxidant properties. Prior studies have pinpointed the primary active compounds in ST, including trilobatin, phlorizin, and phloretin, which have demonstrated significant anti-neuroinflammatory and antioxidant effects against various diseases, including IS(Gao et al., 2020; Anan et al., 2022; Li et al., 2023). ST is a medicinal and edible Chinese medicine that integrates the functions of tea, sugar and medicine, and has been approved as a new food raw material with the characteristics of low toxicity and high edible safety (Shang et al., 2022; Liu et al., 2022). So in this study, and considering the pharmacological properties of ST, we embarked on an in-depth exploration of the therapeutic effects of ST on CIRI and its potential targets, with a view to prevent IS through drinking of ST.

Our research results indicate that, through behavioral and neurological assessments, as well as TTC staining, ST can effectively alleviate neurological deficits and cerebral infarction volume, suggesting a protective effect of ST on CIRI. However, the comprehensive and detailed mechanisms of ST are not yet fully understood. Therefore, we employed network pharmacology analysis and molecular docking simulations to predict the potential mechanisms of ST in CIRI. The results suggest that the beneficial effects of ST after CIRI involve the PI3K/AKT/NF-κB pathway and pyroptosis-related pathways, with NLRP3 identified as a key target for ST action. Interestingly, the main active compounds of ST, trilobatin, phlorizin, and phloretin, can directly bind with NLRP3. Earlier study suggests that activation of NLRP3 is elicited within hours of ischemic stroke onset, driving neuroinflammation, ultimately leading to neuronal death (Han B. et al., 2021; Torices et al., 2023). As expected, ST significantly reduced NLRP3 expression and neuronal loss in rats of ischemic penumbra, as confirmed by IF staining and Nissl staining. Moreover, ST reduced the protein expressions associated with the PI3K/AKT/NF-κB pathway and the regulation of pyroptosis following CIRI injury, in alignment with the findings from the

network pharmacology analysis. These results indicate that, which indicate that ST may defeat CIRI-induced pyroptosis through modulating the PI3K/AKT/NF-κB pathway. Following brain ischemia, endogenous microglia become activated, secreting inflammation-related cytokines such as IL-1β, IL-18, and TNF-α. Concurrently, activated perivascular astrocytes release numerous vascular permeability factors to exacerbate brain injury (Li et al., 2020; Cramer et al., 2022). In addition, ROS accumulation induced by cerebral ischemia participates in the inflammatory process, resulting in neuronal damage (Wu et al., 2021). Our results show that ST significantly reduced the activation of microglia and astrocytes. Simultaneously, ST significantly lowered serum levels of pro-inflammatory cytokines and oxidative biomarkers, while significantly increased the contents of SOD and GSH in CIRI rats. These findings infer that ST mitigates inflammatory responses and oxidative stress induced by CIRI through inhibiting the activation of gliocyte.

Of note, there are still limitations in current study. Firstly, the precise molecular mechanisms of ST against the acute phase of CIRI, as well as the potential side effects and sustained neuroprotective effects associated with long-term treatment of ST deserve further in-depth exploration. Secondly, more robust data would be needed to be provided to substantiate these findings using a larger sample size, independent replication of results in different settings or with different ischemic models, and data from different layers such as protein, RNA, imaging, etc. Thirdly, this study is limited to an animal model, so human cell-based or 3D models could be further utilized to evaluate the therapeutic potential of ST in humans in the future.

5 Conclusion

In summary, the current research results suggest that ST preconditioning evokes robust anti-CIRI effect. ST preconditioning can inhibit NLRP3 inflammasome- mediated pyroptosis by modulating the PI3K/AKT/NF-KB signaling pathway, to exert beneficial effect on CIRI-induced neuronal loss, neuroinflammation and oxidative stress.

Data availability statement

The original contributions presented in the study are included in the article/Supplementary Material, further inquiries can be directed to the corresponding author.

Ethics statement

The animal study was approved by Experimental Animal Ethics Committee of the Zunyi Medical University (No. ZMU21-2203-538). The study was conducted in accordance with the local legislation and institutional requirements.

Author contributions

DL: Data curation, Methodology, Software, Validation, Writing–original draft. WW: Data curation, Methodology, Validation, Writing–original draft. TW: Data curation, Methodology, Validation, Writing–original draft. GZ: Methodology, Validation, Writing–original draft. YZ: Supervision, Writing–original draft. JG: Conceptualization, Project administration, Supervision, Writing–review and editing. QG: Conceptualization, Project administration, Supervision, Writing–review and editing.

Funding

The author(s) declare financial support was received for the research, authorship, and/or publication of this article. This work was supported by the "hundred" level of high-level innovative talents in Guizhou Province [No. GCC(2023)042], 2011 Collaborative Innovation Center of Traditional Chinese Medicine in Guizhou Province [No. (2022)026], Guizhou Province Science and Technology Project [No. Qian Ke He (ZK2023)549].

Acknowledgments

The author would like to thank all those who suggested valuable comments to improve the quality of article.

Conflict of interest

The authors declare that the research was conducted in the absence of any commercial or financial relationships that could be construed as a potential conflict of interest.

Publisher's note

Supplementary material

The Supplementary Material for this article can be found online at: https://www.frontiersin.org/articles/10.3389/fphar.2024.1365642/full#supplementary-material

References

Anan, G., Hirose, T., Kikuchi, D., Takahashi, C., Endo, A., Ito, H., et al. (2022). Inhibition of sodium-glucose cotransporter 2 suppresses renal stone formation. *Pharmacol. Res.* 186, 106524. doi:10.1016/j.phrs.2022.106524

Baillieul, S., Dekkers, M., Brill, A. K., Schmidt, M. H., Detante, O., Pépin, J. L., et al. (2022). Sleep apnoea and ischaemic stroke: current knowledge and future directions. *Lancet Neurol.* 21 (1), 78–88. doi:10.1016/s1474-4422(21)00321-5

Campbell, B. C. V., De Silva, D. A., Macleod, M. R., Coutts, S. B., Schwamm, L. H., Davis, S. M., et al. (2019). Ischaemic stroke. *Nat. Rev. Dis. Prim.* 5 (1), 70. doi:10.1038/s41572-019-0118-8

Capece, D., Verzella, D., Flati, I., Arboretto, P., Cornice, J., and Franzoso, G. (2022). NF-κB: blending metabolism, immunity, and inflammation. *Trends Immunol.* 43 (9), 757–775. doi:10.1016/j.it.2022.07.004

Cramer, T., Gill, R., Thirouin, Z. S., Vaas, M., Sampath, S., Martineau, F., et al. (2022). Cross-talk between GABAergic postsynapse and microglia regulate synapse loss after brain ischemia. *Sci. Adv.* 8 (9), eabj0112. doi:10.1126/sciadv.abj0112

Evavold, C. L., Hafner-Bratkovič, I., Devant, P., D'Andrea, J. M., Ngwa, E. M., Boršić, E., et al. (2021). Control of gasdermin D oligomerization and pyroptosis by the Ragulator-Rag-mTORC1 pathway. *Cell* 184 (17), 4495–4511.e19. doi:10.1016/j.cell.2021.06.028

Frank, M. G., Baratta, M. V., Zhang, K., Fallon, I. P., Pearson, M. A., Liu, G., et al. (2020). Acute stress induces the rapid and transient induction of caspase-1, gasdermin D and release of constitutive IL-1β protein in dorsal hippocampus. *Brain Behav. Immun.* 90, 70–80. doi:10.1016/j.bbi.2020.07.042

Gao, J., Chen, N., Li, N., Xu, F., Wang, W., Lei, Y., et al. (2020). Neuroprotective effects of trilobatin, a novel naturally occurring Sirt3 agonist from Lithocarpus polystachyus rehd., mitigate cerebral ischemia/reperfusion injury: involvement of TLR4/NF-κB and nrf2/keap-1 signaling. *Antioxid. Redox Signal* 33 (2), 117–143. doi:10.1089/ars.2019.7825

Gao, J., Ma, C., Xia, D., Chen, N., Zhang, J., Xu, F., et al. (2023). Icariside II preconditioning evokes robust neuroprotection against ischaemic stroke, by targeting Nrf2 and the OXPHOS/NF-κB/ferroptosis pathway. *Br. J. Pharmacol.* 180 (3), 308–329. doi:10.1111/bph.15961

Gao, J., Xu, Y., Zhang, J., Shi, J., and Gong, Q. (2018). Lithocarpus polystachyus Rehd. leaves aqueous extract protects against hydrogen peroxide-induced SH-SY5Y cells injury through activation of Sirt3 signaling pathway. *Int. J. Mol. Med.* 42 (6), 3485–3494. doi:10.3892/ijmm.2018.3916

Goncalves, A., Su, E. J., Muthusamy, A., Zeitelhofer, M., Torrente, D., Nilsson, I., et al. (2022). Thrombolytic tPA-induced hemorrhagic transformation of ischemic stroke is mediated by PKCβ phosphorylation of occludin. *Blood* 140 (4), 388–400. doi:10.1182/blood.2021014958

Han, B., Jiang, W., Cui, P., Zheng, K., Dang, C., Wang, J., et al. (2021a). Microglial PGC-1α protects against ischemic brain injury by suppressing neuroinflammation. *Genome Med.* 13 (1), 47. doi:10.1186/s13073-021-00863-5

Han, X., Xu, T., Fang, Q., Zhang, H., Yue, L., Hu, G., et al. (2021b). Quercetin hinders microglial activation to alleviate neurotoxicity via the interplay between NLRP3 inflammasome and mitophagy. *Redox Biol.* 44, 102010. doi:10.1016/j.redox.2021.102010

Ising, C., Venegas, C., Zhang, S., Scheiblich, H., Schmidt, S. V., Vieira-Saecker, A., et al. (2019). NLRP3 inflammasome activation drives tau pathology. *Nature* 575 (7784), 669–673. doi:10.1038/s41586-019-1769-z

Khanna, P., Totten, D., Novik, L., Roberts, J., Morecraft, R. J., and Ganguly, K. (2021). Low-frequency stimulation enhances ensemble co-firing and dexterity after stroke. *Cell* 184 (4), 912–930.e20. doi:10.1016/j.cell.2021.01.023

Li, C., Liu, B., Xu, J., Jing, B., Guo, L., Wang, L., et al. (2023). Phloretin decreases microglia-mediated synaptic engulfment to prevent chronic mild stress-induced depression-like behaviors in the mPFC. *Theranostics* 13 (3), 955–972. doi:10.7150/thno.76553

Li, C., Zhao, Z., Luo, Y., Ning, T., Liu, P., Chen, Q., et al. (2021). Macrophage-disguised manganese dioxide nanoparticles for neuroprotection by reducing oxidative stress and modulating inflammatory microenvironment in acute ischemic stroke. *Adv. Sci. (Weinh)* 8 (20), e2101526. doi:10.1002/advs.202101526

Li, Q., Cao, Y., Dang, C., Han, B., Han, R., Ma, H., et al. (2020). Inhibition of double-strand DNA-sensing cGAS ameliorates brain injury after ischemic stroke. *EMBO Mol. Med.* 12 (4), e11002. doi:10.15252/emmm.201911002

Liao, B., Geng, L., Zhang, F., Shu, L., Wei, L., Yeung, P. K. K., et al. (2020). Adipocyte fatty acid-binding protein exacerbates cerebral ischaemia injury by disrupting the blood-brain barrier. *Eur. Heart J.* 41 (33), 3169–3180. doi:10.1093/eurheartj/ehaa207

Liu, M., Li, N., Lu, X., Shan, S., Gao, X., Cao, Y., et al. (2022). Sweet tea (Rubus Suavissmus S. Lee) polysaccharides promote the longevity of *Caenorhabditis elegans* through autophagy-dependent insulin and mitochondrial pathways. *Int. J. Biol. Macromol.* 15 (207), 883–892. doi:10.1016/j.ijbiomac.2022.03.138

Ma, Q. (2023). Pharmacological inhibition of the NLRP3 inflammasome: structure, molecular activation, and inhibitor-NLRP3 interaction. *Pharmacol. Rev.* 75 (3), 487–520. doi:10.1124/pharmrev.122.000629

Qin, C., Yang, S., Chu, Y. H., Zhang, H., Pang, X. W., Chen, L., et al. (2022). Signaling pathways involved in ischemic stroke: molecular mechanisms and therapeutic interventions. *Signal Transduct. Target Ther.* 7 (1), 215. doi:10.1038/s41392-022-01064-1

Shang, A., Liu, H. Y., Luo, M., Xia, Y., Yang, X., Li, H. Y., et al. (2022). Sweet tea (Lithocarpus polystachyus rehd.) as a new natural source of bioactive dihydrochalcones with multiple health benefits. *Crit. Rev. Food Sci. Nutr.* 62 (4), 917–934. doi:10.1080/10408398.2020.1830363

Sies, H., and Jones, D. P. (2020). Reactive oxygen species (ROS) as pleiotropic physiological signalling agents. *Nat. Rev. Mol. Cell Biol.* 21 (7), 363–383. doi:10.1038/s41580-020-0230-3

Torices, S., Daire, L., Simon, S., Mendoza, L., Daniels, D., Joseph, J. A., et al. (2023). The NLRP3 inflammasome and gut dysbiosis as a putative link between HIV-1 infection and ischemic stroke. *Trends Neurosci.* 46 (8), 682–693. doi:10.1016/j.tins.2023.05.009

Tuo, Q. Z., Liu, Y., Xiang, Z., Yan, H. F., Zou, T., Shu, Y., et al. (2022). Thrombin induces ACSL4-dependent ferroptosis during cerebral ischemia/reperfusion. *Signal Transduct. Target Ther.* 7 (1), 59. doi:10.1038/s41392-022-00917-z

Wu, A. G., Zhou, X. G., Qiao, G., Yu, L., Tang, Y., Yan, L., et al. (2021). Targeting microglial autophagic degradation in NLRP3 inflammasome-mediated neurodegenerative diseases. *Ageing Res. Rev.* 65, 101202. doi:10.1016/j.arr.2020.101202

Yu, H., Lin, L., Zhang, Z., Zhang, H., and Hu, H. (2020). Targeting NF-κB pathway for the therapy of diseases: mechanism and clinical study. *Signal Transduct. Target Ther.* 5 (1), 209. doi:10.1038/s41392-020-00312-6

Yuan, J., Li, L., Yang, Q., Ran, H., Wang, J., Hu, K., et al. (2021). Targeted treatment of ischemic stroke by bioactive nanoparticle-derived reactive oxygen species responsive and inflammation-resolving nanotherapies. *ACS Nano* 15 (10), 16076–16094. doi:10.1021/acsnano.1c04753

Zeng, X., Zhang, Y. D., Ma, R. Y., Chen, Y. J., Xiang, X. M., Hou, D. Y., et al. (2022). Activated Drp1 regulates p62-mediated autophagic flux and aggravates inflammation in cerebral ischemia-reperfusion via the ROS-RIP1/RIP3-exosome axis. *Mil. Med. Res.* 9 (1), 25. doi:10.1186/s40779-022-00383-2

frontiers | Frontiers in Pharmacology

TYPE Review
PUBLISHED 26 September 2024
DOI 10.3389/fphar.2024.1409317

OPEN ACCESS

EDITED BY
Viola B. Morris,
Emory University, United States

REVIEWED BY
François Canonne-Hergaux,
Institut National de la Santé et de la Recherche Médicale (INSERM), France
Zhong-Bao Yang,
The affiliated Changsha hospital of hunan normal university, China
Chong Song,
Changsha Social Work College, China
Anna Vasilaki,
University of Thessaly, Greece

*CORRESPONDENCE
Yongpan Huang,
yongpanhuangyxy@163.com
Jiayu Tang,
tangjiayu1978@163.com

RECEIVED 29 March 2024
ACCEPTED 16 September 2024
PUBLISHED 26 September 2024

CITATION
Peng G, Huang Y, Xie G and Tang J (2024) Exploring Copper's role in stroke: progress and treatment approaches.
Front. Pharmacol. 15:1409317.
doi: 10.3389/fphar.2024.1409317

Exploring Copper's role in stroke: progress and treatment approaches

Gang Peng[1,2], Yongpan Huang[3]*, Guangdi Xie[4] and Jiayu Tang[1,2]*

[1]The School of Clinical Medicine, Hunan University of Chinese Medicine, Changsha, Hunan, China, [2]Department of Neurology, Brain Hospital of Hunan Province, Changsha, Hunan, China, [3]School of Medicine, Changsha Social Work College, Changsha, Hunan, China, [4]Department of Neurology, Huitong People's Hospital, Huitong, Hunan, China

Copper is an important mineral, and moderate copper is required to maintain physiological processes in nervous system including cerebral ischemia/reperfusion (I/R) injury. Over the past few decades, copper induced cell death, named cuprotosis, has attracted increasing attention. Several lines of evidence have confirmed cuprotosis exerts pivotal role in diverse of pathological processes, such as cancer, neurodegenerative diseases, and I/R injury. Therefore, an in-depth understanding of the interaction mechanism between copper-mediated cell death and I/R injury may reveal the significant alterations about cellular copper-mediated homeostasis in physiological and pathophysiological conditions, as well as therapeutic strategies deciphering copper-induced cell death in cerebral I/R injury.

KEYWORDS

copper ions, cerebral ischemia/reperfusion injury, cuproptosis, apoptosis, oxidative stress

Introduction

Copper is an essential trace nutrient required for various cellular functions, meanwhile, copper accumulation beyond cellular needs is toxic (Khalfaoui-Hassani et al., 2021). Copper exists in two states, Cu^{+} and Cu^{2+}, in body. In bodily fluids, copper is predominantly in the form of Cu^{2+}, while inside cells, primarily exists as Cu^{+} (Kucková et al., 2015). Under the action of oxidoreductases, a conversion between Cu^{+} and Cu^{2+} existed, which electron transfer occurs through the Fenton reaction, leading to the generation of ROS, including superoxide anion (O^{2-}), nitric oxide (NO-), hydroxyl radical (OH), and hydrogen peroxide (H_2O_2) (Valko et al., 2005). ROS could oxidize and damage biological molecules, including proteins, nucleic acids, and lipids. Additionally, ROS could interfer with the synthesis of iron-sulfur clusters (Slezak et al., 2021). Copper, assimilated from the digestive tract, undergoes hepatic metabolism to form ceruloplasmin, the primary copper-containing protein in the bloodstream, extensively present in diverse bodily organs. Ceruloplasmin is responsible for transporting 95% of copper in the bloodstream, making it a reliable marker for assessing the body's copper levels (Piacenza et al., 2021). The diagnosis of specific copper metabolism disorders involves evaluating internal copper levels through the measurement of ceruloplasmin (CP) content (Bandmann et al., 2015). When ceruloplasmin (CP) amounts to the surface of target cells, which interacts with its corresponding receptors to release copper. The released copper is then absorbed and utilized by the targeted cells. The binding and release of copper ions by CP allow for distinct distribution of copper in multiple tissues and organs (Liu Z. et al., 2022). However, copper not bound to

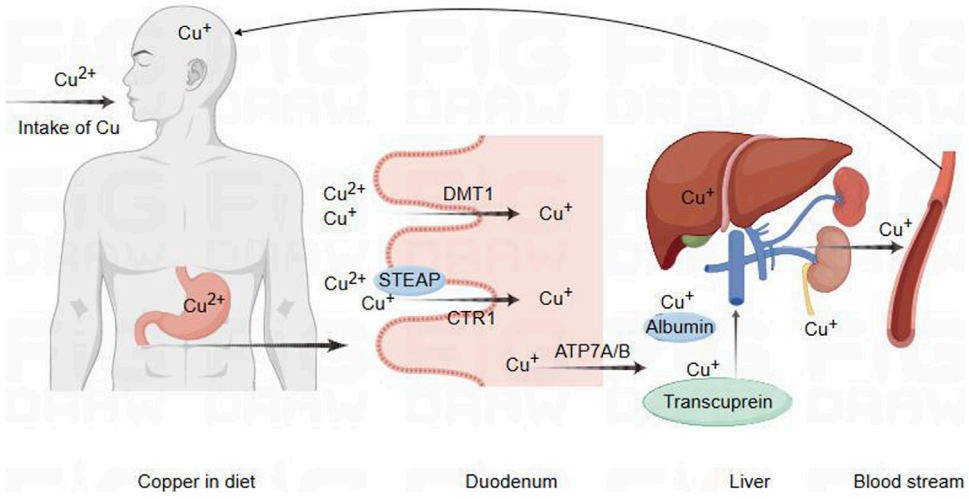

FIGURE 1
Schematic diagram of copper ion regulation in cells for cellular function. Copper metabolism and transport to the brain pathway. Copper in food is first reduced by STEAP, which promotes the absorption of copper by intestinal epithelial cells through the action of CTR1. In addition, DMT1 can also transport and absorb copper in certain situations. Subsequently, copper is transported to the portal vein through copper ATP7A, where it binds to plasma proteins such as albumin and copper transporter protein for transport to the liver. A small amount of copper is processed or transported from the liver and released into the bloodstream for circulation into the brain, while excess copper is excreted through bile.

ceruloplasmin could still be continuously absorbed by tissues in the blood. Ceruloplasmin could oxidize ferrous ions (Fe^{2+}) to ferric ions (Fe^{3+}), facilitating the transportation of iron in the plasma, which plays a crucial role in maintaining the iron homeostasis in living organisms (Raia et al., 2023). During the oxidation of ferrous iron to ferric iron, ceruloplasmin facilitates the transfer of ferric iron into transferrin, preventing oxidative stress damage caused by the Fenton reaction (Vasilyev, 2019). Therefore, ceruloplasmin possesses certain antioxidant capabilities, manifested through its oxidase activity towards low-valent metal ions and glutathione peroxidase. It also exhibits the ability to eliminate reactive oxygen species (ROS) (Liu Z. et al., 2022; Samygina et al., 2017).

Copper enters the cell through binding with a copper chaperone, enters the mitochondria. Within the mitochondria, COX17 forms a complex with Cu^{+}, and subsequently, Cu^{+} could be transferred to SCO1 or COX11, which is involved in the synthesis of cytochrome c oxidase (CcO), the terminal component of the mitochondrial respiratory chain. CcO catalyzes the transfer of electrons from reduced cytochrome c to oxygen, facilitating the oxidative phosphorylation process (McCann C. et al., 2022; Horng et al., 2004; Banci et al., 2008). CCS [Copper Chaperone for superoxide dismutase (SOD)] serves as the copper companion for Superoxide Dismutase 1 (SOD1) and involves transferring copper ions to SOD1, thereby activating the active site of SOD1, which exerts a crucial regulatory role in the cellular redox balance (Boyd et al., 2020; Boulis and Donsante, 2023). In cellular cytoplasm, Metallothionein 1/2 (MT1/2) forms complexes with numerous copper ions, acting as a repository for copper. This interaction is potentially involved in regulating the equilibrium of copper ions within the cell (Tapiero et al., 2003; Ruttkay-Nedecky et al., 2013; Yu et al., 2022). Glutathione (GSH), featuring thiol groups, functions as an antioxidant within cells by directly engaging in enzymatic antioxidant reactions. This involvement manifests anti-oxidative and anti-apoptotic effects. Additionally, GSH may play a role in directly or indirectly regulating the cellular copper pool (Ulrich and Jakob, 2019; Ferguson and Bridge, 2019). Copper transport protein (ATP7A) is expressed in most tissues and organs, while ATP7B is primarily expressed in the liver. ATP7A and ATP7B are located in the trans-Golgi network (TGN), which supply copper to copper-dependent enzymes synthesized in the secretory pathway. The copper efflux rate is determined by the transport or fusion of vesicles containing ATP7A with the plasma membrane (Chun et al., 2017; Janardhanan et al., 2022; Chen et al., 2020) (Figure 1).

Copper metabolism and internal balance

Copper metabolism

Copper is extensively distributed in the biological entities of the natural environment, and it is a crucial trace nutrient for human body. It plays a vital role in numerous redox reactions occurring within human cells, contributing to cellular processes (Chen et al., 2021; Chelyadina et al., 2023). As is well known, Cu is a static cofactor, serving as a catalytic or structural cofactor in the formation of enzymes and proteins, which might be buried and protected within its active sites of enzymes, participating in numerous vital biological activities. Cu is involved in various life processes by constituting enzymes such as cytochrome c oxidase (CCO), SOD, metallothionein (MT), cuproprotein (CP), and lysyl oxidase (LOX). Its participation extends to functions like energy metabolism, antioxidant stress response, vascular formation, and neurotransmitter synthesis (Chen et al., 2020; Tsang et al., 2021; Zhou et al., 2023). Internal copper metabolism is tightly regulated, and extreme deficiency or excess of copper disrupts the copper balance, leading to the onset of diseases and even posing a threat to life (Kirsipuu et al., 2020). Copper deficiency could influence the activity of SOD and the antioxidant capacity of

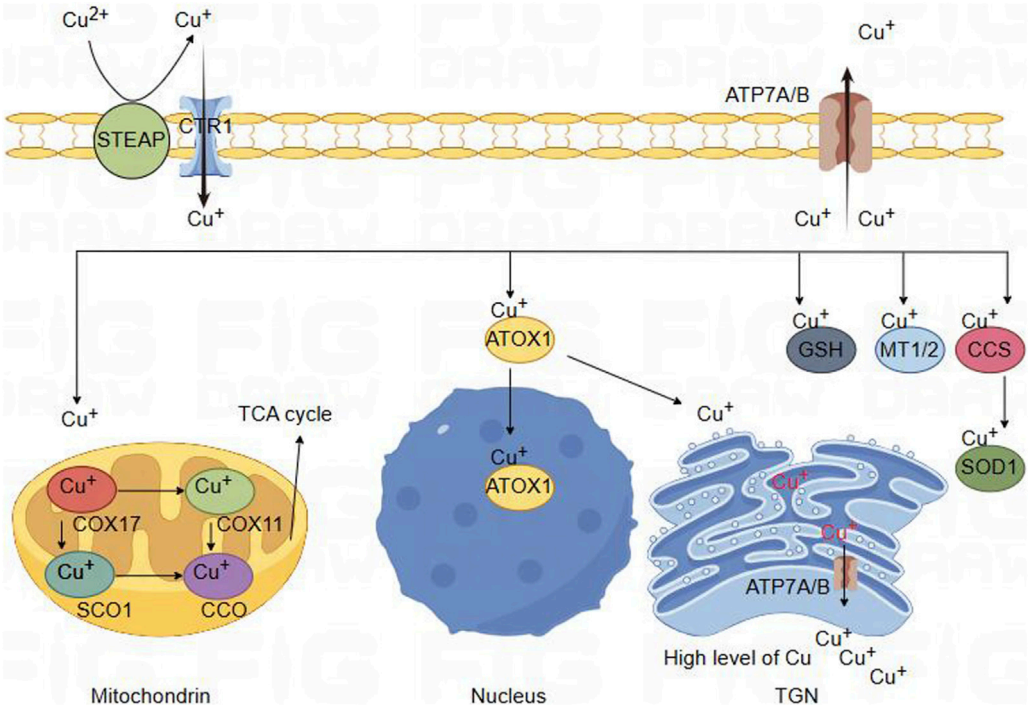

FIGURE 2
Schematic diagram of copper ion metabolism in body. Copper metabolism in brain cells. Divalent copper cannot be directly absorbed. It is first reduced by STEAP and enters cells through the high affinity of CTR1 for copper absorption on the plasma membrane. Copper binds to copper partners and enters mitochondria, where COX17 forms a complex with copper. Copper can then be transferred to SCO1 or COX11, which participate in the synthesis of CcO, the terminal component of the tricarboxylic acid cycle energy metabolism mitochondrial respiratory chain. Copper could bind with ATOXI into the nucleus and participate in gene expression regulation. It can also be transferred to the Golgi apparatus and released by binding with ATP7A/B, providing copper for copper dependent enzymes synthesized in the secretion pathway. In the cytoplasm, MT1/2 forms complexes with many copper ions, serving as a storage reservoir for copper. This interaction may be involved in regulating the balance of copper ions within cells. GSH can also directly or indirectly participate in regulating cellular copper pools. In addition, CCS acts as a copper partner of SOD1, involving the transfer of copper ions to SOD1. Finally, the efflux of copper is determined by the transport or fusion of ATP7A/B vesicles with the plasma membrane.

other cellular components, such as iron, selenium, and glutathione (Altarelli et al., 2019; Trist et al., 2021). Copper deficiency may be associated with early pregnancy miscarriage, inflammatory responses, severe anemia, cardiovascular system issues, optic nerve function, and neuro-degenerative changes (Gurnari and Rogers, 2021; Hu et al., 2023; Cendrowska-Pinkosz et al., 2022; Wu et al., 2023). Similarly, copper accumulation could lead to abnormal oxidative metabolism, attacking to the structures and functions of biomolecules such as proteins, which could lead to the occurrence of diseases such as diabetes, neurological disorders, and cardiovascular dysfunctions (Bjørklund et al., 2020; Shi et al., 2023; Gaetke and Chow, 2003). Thus, copper homeostasis is regarded as crucial mechanism for maintaining the balance in the body. The absorption of dietary copper depends on the chemical form of copper and the interaction with dietary components. Daily intake below 0.8 mg/day results in a net loss of copper, while intake above 2.4 mg/day leads to a net increase (Bost et al., 2016). Studies indicates that excessive dietary copper intakes are associated with atherosclerosis, cardiovascular diseases, abdominal aortic calcification, neuronal and mixed neuronal-glial tumors, diabetes, and various neurodegenerative diseases (Yang et al., 2024; Li X. et al., 2023; Liu and Liang, 2024; Eljazzar et al., 2023; Zhang W. et al., 2023; Zhang Y. et al., 2023). In the mammalian digestive tract, copper in food is reduced from its divalent state by the metal-reducing enzyme (STEAP) to a monovalent state. Subsequently, it is absorbed by intestinal cells through the high-affinity copper transporter 1 (CTR1) (Li, 2020). Divalent metal transporter 1 (DMT1) could also transport copper under certain circumstances. The intestinal DMT1 is crucial for the absorption of iron but not essential for the absorption of copper or manganese in mice. A high-iron diet inhibited the intestinal transport of copper through DMT1 (Lin et al., 2015; Sánchez-González et al., 2022; Shawki et al., 2015). As previously reported, copper absorbed in the intestine is transported to the portal vein through ATP7A. In the portal vein, copper binds to plasma proteins such as albumin and transcuprein, facilitating transport to liver, which serves as the central control system for copper homeostasis (Alessi et al., 2021; Horn and Wittung-Stafshede, 2021). Most excess copper is excreted through the bile into the feces, with only a small amount excreted through the kidneys. Impairment of biliary copper excretion could lead to hepatic copper retention (Lenartowicz et al., 2015; Schilsky et al., 2023) (Figure 2).

Cu protein in mammal metabolism

Ferredoxin (Fdx)

In mitochondrial matrix of eukaryotic cells, there is an unstable copper pool, which serves as the location for the assembly of mitochondrial iron-sulfur (Fe/S) clusters (Du et al., 2023).

Ferredoxin (FDX) is a vital protein mediator in biological electron transfer reactions, which characterized by the presence of [2Fe-2S] or [4Fe-4S] clusters, allowing it to efficiently accept and release electrons, contributing to its active involvement in oxidation-reduction reactions (Nzuza et al., 2021). Disruption of copper homeostasis may negatively impact the formation of mitochondrial Fe/S clusters, which could lead to impaired iron-sulfur cluster biogenesis, affecting mitochondrial function. The impact extends beyond the respiratory chain, influencing various mitochondrial functions like citric acid cycle, heme biosynthesis, and sulfur-containing amino acid synthesis may be compromised (Ruiz et al., 2021; Cobine et al., 2021). FDX, as an electron donor, engages in various metabolic processes due to its versatile nature, which include participation in the synthesis of steroids, hemoglobin, vitamin D, and the biogenesis of Fe-S clusters in different organisms. Although Fdx1 and Fdx2 share significant functional similarities, they exhibit specific and distinct roles in different physiological pathways (Dreishpoon et al., 2023a; Braymer et al., 2021). Lipoic acid synthase (LIAS) generates lipoic acid cofactors, crucial components for tricarboxylic acid cycle (TCA) cycle enzymes like pyruvate dehydrogenase (PDH). FDX1 acts as an upstream regulator of LIAS, participating in the regulation of the PDH complex. DLAT is a component of the mitochondrial PDH. Loss of FDX1 resulted in the accumulation of pyruvate and α-ketoglutarate, impacting the TCA cycle (Joshi et al., 2023; Dreishpoon et al., 2023b). FDX1 is a crucial regulator of copper ionophore-induced cell death and serves as an upstream regulator of cellular protein lipidation. FDX1 directly binds to LIAS, facilitating its functional interaction with the lipoic acid carrier protein (glycine cleavage system protein H, GCSH), which direct interaction allows FDX1 to regulate protein lipoylation, bypassing indirect modulation of cellular Fe-S cluster biogenesis.

FDX1 promotes the formation of LIAS-GCSH bonds and activation of lipoic acid, which is crucial for cellular processes (Wang Z. et al., 2023; Ke et al., 2023; Schulz et al., 2023). The reductase encoded by FDX1 undergoes protein thioylation regulation during the reduction of Cu^{2+} to Cu^{+}, promoting oligomerization of dihydrothioacyl S-acetyltransferase (DLAT). The regulatory mechanism subsequently induces protein toxicity stress, indicating the significant role of FDX1 in copper ion metabolism and cellular stress response (Joshi et al., 2023; Weiler et al., 2020; Li Y. et al., 2023). FDX1 knockdown results in a decrease in the lipoylation level of DLAT and DLST in thyroid cancer cells, which contributes to the alleviation of cell death induced by copper accumulation (Chen G. et al., 2023). FDX1 could regulate the activity of cytochrome c oxidase and mitochondrial respiration, and has multiple targets *in vivo*. FDX1 knockout led to a specific reduction in cytochrome c oxidase, influencing copper and heme A/a3 levels (Zulkifli et al., 2023).

Cytochrome c oxidase (COX)

Mitochondrial Cytochrome c Oxidase is located in the inner mitochondrial membrane and serves as a crucial enzyme in the respiratory chain. As the fourth central enzyme complex, also known as Complex IV, it receives electrons on cytochrome C molecules and transfers them to oxygen, generating water and releasing a substantial amount of energy (Blomberg, 2020; Ramzan et al., 2021; Brischigliaro and Zeviani, 2021). Copper serves as a necessary cofactor for COX, with three copper ions needed to construct the dual-core CuA and mononuclear CuB sites, ensuring the enzyme's stability and activity (Maghool et al., 2019). The assembly of the CuA center necessitates the presence of copper chaperones SCO1, SCO2, and COA6. COA6 knockout in HEK293T cells resulted in decreased activities of both complex I and IV, accompanied by a reduction in mitochondrial membrane potential (Pacheu-Grau et al., 2020). The cellular COX is a complex comprising 13 subunits, and its functionality involves a highly coordinated process. The regulation of COX expression and function is essential for sustaining cellular respiration and energy production (Watson and McStay, 2020). The involvement of Cytochrome c oxidase subunit 5a (COX5a) is essential for preserving regular mitochondrial function.

Metabolism of copper ions in brain

Copper has been confirmed abundantly present in the brain, playing a crucial role in brain function and development. The subventricular zone (SVZ) in the lateral ventricles, containing a high amount of copper, is the largest neurogenic region in the adult brain and plays a crucial role in neurogenesis (Liu L. L. et al., 2022). Clinical studies confirmed that the severity of brain atrophy is associated with the functional and neurological impairments in patients with Wilson's disease (WD). Brain volume serves as an indicator of neuro-degeneration induced by copper (Shang et al., 2023). Disruption of copper homeostasis may be a primary cause of various neurological disorders, particularly when elevated copper ion levels occur during brain I/R injury, leading to neuronal damage (Zhang et al., 2020; Chen X. et al., 2023). The potential mechanisms underlying the toxicity induced by the excessive accumulation of free copper within neural cells remain unclear, which are associated with oxidative stress attacks, cell apoptosis, copper death, and other factors (Chen X. et al., 2023; Goto et al., 2020; Gao et al., 2024). In 2022, Peter Tsvetkov, et al. first proposed a novel form of cell death induced by copper ions, which named "cuproptosis" (Kahlson and Dixon, 2022). Emerging evidence supports the facts that copper death is a novel form of cell death involved in regulating cerebral I/R injury. In a rat model of cerebral I/R injury, elevated copper ions and abnormal expression of copper death-related proteins were observed (Guo Q. et al., 2023). Thus, much progress has been made in understanding the pathophysiological mechanisms of copper death in cerebral I/R, it has attracted more and more attention worldwide. It is accepted that the mechanism of I/R is an important driving force for cerebral I/R injury. In this review, we intended to discuss the recent advances in the copper balance.

Endothelial cells within the blood-brain barrier acquire copper from the blood through CTR1 and transport it to the brain parenchyma via ATP7A. Copper homeostasis in the brain involves a complex interplay between uptake, distribution, utilization, and efflux mechanisms (Washington-Hughes et al., 2023; An et al., 2022). Copper ions traverse the blood-brain barrier to enter the brain parenchyma, initially encountering astrocytes. Astrocytes possess the capability to absorb, store, and release copper (Li B. et al., 2024). Copper is allocated to various brain cells according to the demands of different cell types. The copper concentration within astrocytes is the highest, influencing copper

homeostasis in the brain. When astrocytes die due to brain injury or aging, copper may be released from astrocytes, potentially exerting adverse effects on neighboring brain cells (Górska et al., 2023; Bhattacharjee et al., 2020). The copper transporter protein CTR1 on the cytoplasmic membrane of brain nerve cells could efficiently uptake copper with high affinity (Wen et al., 2021).

Biological functions of copper in brain/and neuronal cells

Cu protein in brain metabolism

Copper is crucial for the normal functioning of the brain, participating in the synthesis of neurotransmitters such as dopamine and adrenaline. Copper distribution in the brain is uneven, with the highest concentration in the locus coeruleus region of brainstem neurons (Rihel, 2018; Scheiber et al., 2014). This region serves as a primary source of norepinephrine (NA) in CNS. The neurotransmitter NA plays a role in regulating wakefulness, sensory processing, attention, aversion, adaptive stress responses, as well as higher-order cognitive functions and memory (Ma et al., 2023; Kawahara et al., 2021). The copper content is higher in the substantianigra, and the decreased levels of copper in the substantia nigra of Parkinson's disease (PD) brain further indicate the significant role of copper in this brain region (Bisaglia and Bubacco, 2020). Copper also plays a crucial role in synaptic transmission. In the synaptic cleft, copper could directly or indirectly modulate the activity of neurotransmitter receptors (NMDA, AMPA, GABAA, P2X receptors), influencing neural excitability. Neurotransmission could influence the transport and transmission of copper within neuronal cells (D'Ambrosi and Rossi, 2015; Wang et al., 2020). Copper in brain, besides participating in specific functions mentioned earlier, is also associated with general metabolism, which includes energy metabolism (cytochrome c oxidase, TCA cycle (FDX1)), antioxidant defense (superoxide dismutase containing zinc and copper, copper blue protein), iron metabolism (copper blue protein), neurotransmitter synthesis (dopamine-β-monooxygenase), and neuropeptide synthesis (peptide glycine-α-amidating enzyme) (Liu L. L. et al., 2022; Scheiber et al., 2014; Wang et al., 2020; Masaldan et al., 2018; Li et al., 2022). Neural cells require enzymes and proteins that depend on copper coordination to perform their normal functions. Additionally, some proteins rely on copper for metabolic regulation. Several important proteins expressed in brain and involved in these processes are described as following:

Ceruloplasmin (both soluble and GPI-anchored ceruloplasmin)

Genetic mutations in the CP gene result in aceruloplasminemia, a hereditary condition characterized by progressive degeneration of the retina and basal ganglia neurons (Bonaccorsi di Patti et al., 2021). Patients with WD undergo impaired copper excretion from the liver, leading to copper ion deposition in the brain and the manifestation of neurological symptoms, even after undergoing liver transplantation (Xu et al., 2022). Additionally, in a mouse model of permanent middle cerebral artery occlusion-induced cerebral ischemia, mice lacking CP exhibit an increased area of cerebral infarction, leading to more severe oxidative stress damage to lipids and proteins (Ryan et al., 2019).

COX

Overexpressing COX5a in the SAMP8 aging mouse model led to improvements in spatial recognition, memory, and hippocampal synaptic plasticity and also restored hippocampal CA1 dendrites, playing a crucial role in modulating age-related cognitive decline (Xiyang et al., 2020). In hypoxia-ischemia (HI) rat model, a manifestation of severe neurological dysfunction, cerebral infarction, cell apoptosis, and notable neuronal loss is concomitant with reduction in COX5a expression. Conversely, COX5a upregulation facilitated neuronal survival post-oxygen-glucose deprivation (OGD), decreasing apoptosis and notably increasing the length of neuronal dendrites (Jiang et al., 2020). In addition, COX6b1 overexpression alleviated I/R-induced hippocampal neuron damage in rat (Yang et al., 2019).

Fdx

In a rat MCAO model, a significant upregulation of FDX1 was observed, while interventions with DEX resulted in reduction in FDX1 expression, which alleviates cerebral infarction area and decreases copper-induced neuronal death. Furthermore, in PC12 cells, post-OGD/R treatment led to increased FDX1 expression, causing DLAT oligomerization and triggering copper-induced neuronal death (Wang D. et al., 2023).

SOD

The structure, function, and mutations of copper-zinc SOD are associated with neurodegenerative disorders, particularly amyotrophic lateral sclerosis (ALS) (Altobelli et al., 2020; Sanghai and Tranmer, 2021). The activation of immature SOD1 involves in the copper chaperone (Ccs1), which includes Ccs1 delivering copper and promoting the oxidation of the intramolecular disulfide bonds within SOD1, or activation through the entry of copper ions into the sulfur-containing intermediate at the binding site (Fetherolf et al., 2017). In rats subjected to cerebral I/R injury, overexpression of transgenic SOD1 alleviates oxidative stress injury, which exhibited protective effects on nerve cells (Chan et al., 1998). The key to combating cerebral I/R injury is enhancing the activity of endogenous antioxidant enzymes, with SOD1 capable of clearing excessive ROS production (Park et al., 2021). Therefore, external intervention to enhance SOD1 activity could be utilized in the development of protective agents against ischemic injury.

Dopamine β-hydroxylase (DBH)

DBH is a member of the copper-dependent monooxygenase family, located in the endoplasmic reticulum, which encoded by the DBH gene and catalyzed the conversion of dopamine to norepinephrine (Juárez-Cedillo et al., 2023). Functionally similar to DBM, and both may be different names for the same enzyme. Dietary copper deficiency in rats leads to a downregulation of dopamine beta-monooxygenase levels in brain tissues (Prohaska and Brokate, 2001). In patients with Menkes disease, the reduction of copper content led to an increased ratio of DBM deficiency in dopamine/norepinephrine, resulting in abnormal behavioral and psychological manifestations (Guthrie et al., 2020; Ohkubo et al., 2019). DBH is the enzyme responsible for producing norepinephrine (NE), while dopamine (DA) and NE are crucial neurotransmitters necessary for normal brain function, which are associated with various diseases such as hypertension, congestive

heart failure, Alzheimer's disease, PD, and Huntington's disease (Gonzalez-Lopez and Vrana, 2020; Vendelboe et al., 2016).

Peptidylglycine α-amidating monooxygenase (PAM)

Peptide hormones are synthesized, stored, and released in the anterior pituitary. The activation of inactive peptide hormone precursors requires the post-translational processing enzyme PAM (Bonnemaison et al., 2016), which converts peptides with extended glycine to amidated products, involved two single-electron transfer steps catalyzed by copper ions at two specific sites. This process is involved in the biosynthesis of peptide hormones (Bäck et al., 2022; Merkler et al., 2022). PAM, an ascorbate- and copper-dependent membrane enzyme that enters secretory granules along with its soluble substrates. Biological studies elucidated the highly conserved mechanism for amidated peptide production and raised many questions about PAM trafficking and the effects of PAM on cytoskeletal organization and gene expression. With the identification of PAM, it showed that PAM was composed of two soluble catalytic cores, including PHMcc (the catalytic core of PHM) and PALcc (the catalytic core of PAL) and a protease-sensitive cytoplasmic domain. Copper ions bound at two sites separated by an 11 Å aqueous cleft participate in the two single electron transfer steps needed to generate a peptidyl-α-hydroxyglycine product (Grechnikova et al., 2020). As previously reported, $PAM^{-/-}$ mice could only survive until mid-pregnancy (Kumar et al., 2016). PAM (+/−) heterozygous mice exhibited anxiety-like behavior, alterations in temperature regulation, and increased susceptibility to seizures, which could be reversed by dietary copper supplementation, suggesting that physiological functions sensitive to PAM genetic constraints could be reversed by copper supplementation (Bousquet-Moore et al., 2010). In primary pituitary cells subjected to 4 h of hypoxia, hypoxia-inducible factor 1α (HIF-1α) exhibited an upregulation, which restricts the ability of PAM to generate amidated peptides, further impacting the enzyme's activity (Rao et al., 2021).

The pathophysiological role of copper in cerebral I/R injury

Cerebral I/R injury and cuproptosis

Stroke is a severe neurological disease, which remains the second leading cause of death (GBD, 2019 Stroke Collaborators, 2021). Early identification, thrombolytic therapy, and emergency intervention for acute ischemic stroke could significantly reduce the incidence and mortality associated with strokes (Herpich and Rincon, 2020). The recovery reperfusion of acute ischemic stroke has a high degree of time dependence (Reziya et al., 2023). In clinical trials, it is challenging to grasp the time window for vascular reconstruction. When the recovery of cerebral blood flow exceeds the time window, it cannot improve the tissue state of reversible damage, and may even deteriorate irreversible sequelas, such as malignant edema and even bleeding (Magoufis et al., 2021). However, the molecular mechanisms remained not fully elucidated, which are associated with oxidative stress, apoptosis, ferroptosis, calcium overload, and copper death. Increasing evidence has showed that copper death participates in brain I/R injury. In cerebral I/R injury, ischemia or hypoxia causes decreases in mitochondrial ATP production, which restricts copper transportation, and results in the of copper accumulation (Cunnane et al., 2020). As previously reported, copper-targeted delivery alleviates neuronal damage in ischemic stroke (Huuskonen et al., 2017). During cerebral I/R, the intracellular copper ion uptake and excretion reached a homeostatic balance, which could be disrupted by mitochondrial respiratory attack and limitation in ATP production, potentially the accumulation of copper ions within the cell and cellular cuproptosis (Lin et al., 2021). Therefore, inhibiting neuronal cuproptosis could decrease the levels of copper ions inside nerve cells, mitigating neuronal injury during cerebral I/R.

Copper accumulation and cuproptosis

Reperfusion of blood supply in ischemic region of the brain after an ischemic stroke yields to irreversible cellular and biochemical consequences, including generation of ROS, expressions of inflammatory cytokines, and inflammation (Lim et al., 2021). Brain tissue is rich in polyunsaturated fatty acids, which is particularly susceptible to attack by ROS and undergoing lipid peroxidation. Intervention with polyunsaturated fatty acids also held potentials for improving neurological outcomes in neonatal hypoxic/ischemic encephalopathy (sHIE) (Martinat et al., 2021; Ng et al., 2022; Dyall et al., 2023). Cu^{2+} exposure reduced levels of glutathione (GSH) and antioxidant capacity while promoting lipid peroxidation in tissues. Some studies indicate that copper (Cu-HCF) nanocomposites catalyze the conversion of reduced glutathione (GSH) to oxidized glutathione within tumor cells, leading to the depletion of GSH (Li C. et al., 2024). The generation of mitochondrial ATP occurs through the process of oxidative phosphorylation (OXPHOS), where the OXPHOS system operates the following five enzyme complexes in the electron transport chain (ETC): Complex I (NADH: ubiquinone oxidoreductase), Complex II (succinate dehydrogenase, SDH), Dimeric Complex III2 (cytochrome bc1 oxidoreductase), and Complex IV (cytochrome c oxidase) (Vercellino and Sazanov, 2022). Due to the presence of two crucial copper sites essential for its functionality, respiratory Complex IV in mitochondria requires copper to sustain the functionality of cytochrome c oxidase (CcO). Therefore, its activity could be easily manipulated by either copper removal/chelation or copper overload, thus influencing the structural and functional aspects of the Electron Transport Chain (ETC) (Ruiz et al., 2021; Swaminathan and Gohil, 2022). Some studies indicate that prolonged exposure to copper in liver and muscles of the viviparous killifish leads to a reduction in energy production, which attribute to copper inhibiting anaerobic pathways and the mitochondrial respiratory chain (Abou Anni et al., 2019). Furthermore, in the liver of patients with Wilson's disease (WD), copper overload could lead to mitochondrial injury, impairing energy metabolism (Mazi et al., 2020). In cerebral I/R injury, the level of copper ions increases. Cu^{+} directly binds to the sulfur-containing components in the mitochondrial TCA, leading to copper-induced reduction of Fe-S (iron-sulfur) proteins, which triggers protein toxicity stress, inducing copper-dependent cell death. Recent study indicates that Disulfiram (DSF), a widely

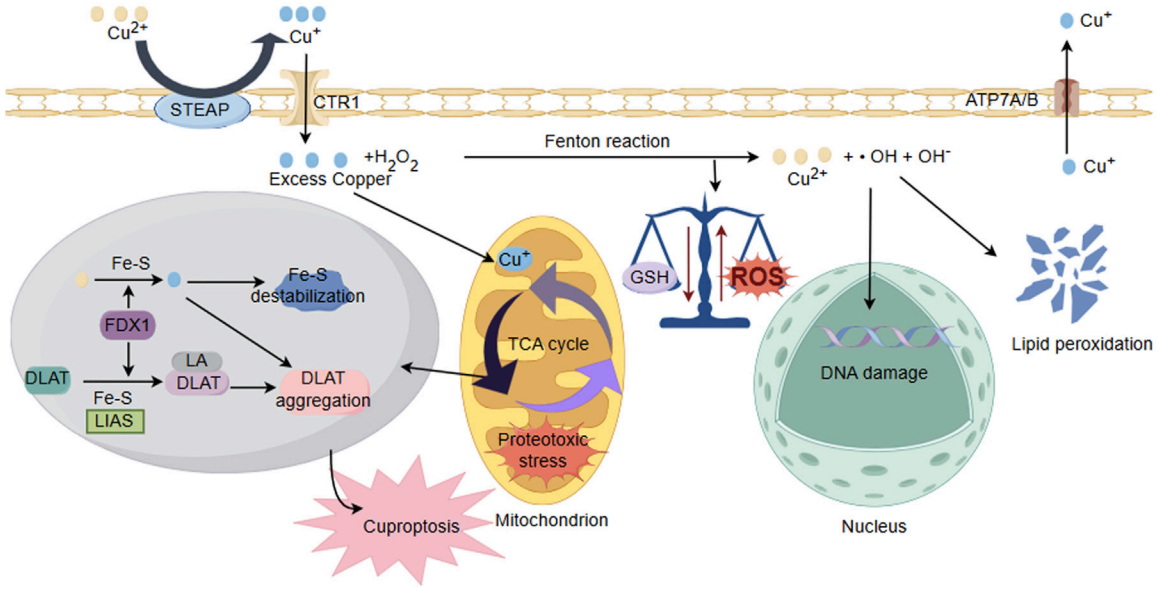

FIGURE 3
Schematic illustration of copper ion overload inducing neuronal cell injury. Under the action of cytoplasmic oxidoreductases, there is a conversion between Cu^{+} and Cu^{2+}, and electron transfer occurs through the Fenton reaction, producing ROS. The accumulation of Cu^{2+} reduces GSH levels and antioxidant capacity, disrupting the balance of cellular redox states and damaging biomolecules including proteins, nucleic acids, and lipids. In addition, ROS could interfere with the synthesis of iron sulfur clusters. Cu binds to thiolated mitochondrial enzymes in the TCA cycle (such as DLAT), inducing the aggregation of these proteins. FDX1/LIAS is an upstream regulator of protein sulfhydrylation. FDX1 reduces Cu^{2+} to more toxic Cu^{+}, leading to inhibition of Fe-S cluster protein synthesis, aggregation of mitochondrial proteins and loss of Fe-S clusters, blocking the TCA cycle of the tricarboxylic acid cycle. Collectively, these abnormal processes lead to protein toxicity stress and induce cell death.

used drug for controlling alcoholism, possesses anticancer activity by inducing apoptosis in a copper Cu-dependent manner (You et al., 2019). DSF/Cu could accelerate copper death in liver cancer cells (HCC), accompanied by GSH depletion and increased lipid peroxides (Zhang et al., 2024). Taken together, these findings suggest that sustained copper accumulation may induce oxidative stress damage, mitochondrial dysfunction, and the occurrence of cuproptosis in cerebral I/R injury (Figure 3).

Regulating the level of copper ion and inhibit cuproptosis in cerebral I/R

Clinical studies have found a significant increase in free copper ions in blood samples collected from patients with acute myocardial infarction and successful percutaneous coronary intervention (Hao et al., 2022). Similarly, there is an increase in copper ion levels in the kidney and small intestine models of mice with I/R injury (Akçil et al., 2000; Lee et al., 2019). In a rat cerebral I/R model, the copper ion content in the hippocampal CA1 region of the brain tissue significantly increased compared with the sham group (Shang et al., 2023). In another MCAO rat study, pretreatment with the copper chelator D-penicillamine significantly reduced cerebral infarct volume and copper ion levels which could be improved mitochondrial respiration and membrane potential, possibly exerting its effects by blocking the cuproptosis pathway mediated by FDX1 (Guo Qingduo et al., 2023). Therefore, reducing the increase in copper ion levels in tissues and organs can inhibit the occurrence of cuproptosis. By regulating the copper ion transport, storage, and output processes in neural cells, the copper ion levels in neuronal cells could be reduced, thereby inhibiting the occurrence of cuproptosis. Seeking targeted therapeutic strategies to alleviate I/R injury by specifically reducing cuproptosis is becoming urgent.

Regulating copper ion levels by blocking the entry of copper ions into CTR1

CTR, located at the plasma membrane and composed of two types of subunits including CTR1 and CTR2, especially which CTR1 belongs to the superfamily of membrane spanning transport proteins responsible for dietary copper homeostasis in mammalian cells (Schoeberl et al., 2022a). Under a normal physiological copper homeostasis, CTR1 is described to be mainly located at the plasma membrane. However, when the cells are medicated with a high amount of Cu, CTR1 is internalized to Early Endosomal Antigen (EEA1)- and Rab5-marked compartments by endocytosis. After removal of extracellular Cu, the transport protein recycles back to the plasma membrane via the slower recycling endosomes (Garmann et al., 2008; Mandal et al., 2020). The missense mutation of the CTR1 coding gene leads to copper deficiency in the central nervous system, thereby affecting the mitochondrial function of nerve cells (Batzios et al., 2022). The increase in copper content during the aging process of the human brain may be attributed to the dysfunction of the brain barrier CTR1, which may be a trigger for neurodegenerative diseases (Haywood and Vaillant, 2014). The increase of intracellular copper is parallel to the expression of CTR1 mRNA. Chakraborty

K, et al. found that the differentiation of PC-12 cells (neurons) involves an increase in intracellular copper (Chakraborty et al., 2022). Copper ions must be transported into cells through the transporter protein CTR1, so it is possible to reduce intracellular copper ions by regulating CTR1.

Interference in copper and platinum uptake mediated by CTR1

CTR1 is responsible for copper transport through the N-terminal domain of its amino acid residues. Interestingly, CTR1 also affects platinum uptake in tumor cells (Wang X. et al., 2023). Cisplatin, as a competitor to hCtr1 mediated copper transport, leads to a decrease in cellular copper levels (Akerfeldt et al., 2017). Liang et al.'s study reported that cisplatin reduced copper uptake by at least 50% in ovarian cancer cells (Liang et al., 2014). In addition, Pt (II) drugs can also specifically affect Cu (I) homeostasis by interfering with the rapid exchange of Cu (I) between Atox1 and Cu ATPases (Lasorsa et al., 2019). Which indicated that interference existed between copper and platinum that are substrates for cellular uptake mediated by CTR1. Several *in vitro* studies have disclosed that platinum drugs disrupt cellular copper uptake. In the ovarian cancer cell lines A2780 and the cisplatin-resistant A2780cis cells, utilizing cisplatin treatment exhibited a significant decrease in copper content compared with untreated cells (Schoeberl et al., 2022b). Therefore, platinum based drugs may become a backup drug for intervening in elevated copper ion levels in the future, by reducing intracellular copper ion concentration and inhibiting copper induced cell death.

Factors influencing CTR1 expression

In the study of improving the anti-tumor efficacy of platinum-based drugs, upregulation of CTR1 expression can be achieved. NSCLC cells, through glucose restriction, upregulate ROS and induce CTR1 expression in AMPK. Similarly, mice fed a low carbohydrate ketogenic diet (glucose restriction) showed an increase in CTR1 expression in tumor tissue, significantly enhancing the efficacy of cisplatin (Zhang et al., 2022). Changes in the expression of CTR1 within cells can directly affect the transport of copper ions. Downregulation of CTR1 expression reduces copper ion uptake. In the investigation of anti-pancreatic cancer, Song, et al. used targeted CTR1 mRNA therapy to effectively inhibit the expression of CTR1 in PANC-1 cells, reduce copper intake, and delay the progress of pancreatic cancer (Song et al., 2021). In a rat brain I/R injury model, the expression of intracellular CTR1 is downregulated, the concentration of copper ions decreases, and copper induced neuronal death is alleviated, effectively protecting neural function (Strenkert et al., 2024).

However, there are many factors that affect the expression of CTR1, such as the regulation of gene transcription encoded by CTR1. Treatment of M21 melanoma cell lines with the Sp1 selective inhibitor Plicamycin for 24 h or knockout of the Sp1 gene resulted in a decrease in the expression of Sp1 and CTR1, as well as a decrease in intracellular copper ion levels and an increase in cell survival rate (Lin et al., 2014). In U2OS cells, SP1 can directly bind to the CTR1 promoter. Overexpression SP1 stimulates CTR1 expression, increases copper ions and inhibits nuclear translocation of (SP1), knockout of p53 promotes CTR1 expression and cisplatin uptake, while p53 overexpression inhibits CTR1 expression and cisplatin uptake (Yong et al., 2023). In VPS35 knockout in HeLa cells, the results showed a significant decrease in the abundance of CTR1 on the cell surface and a significant decrease in copper ion levels in the absence of reverse transcriptase function, indicating that reverse transcriptase affects the transport of copper by CTR1 (Curnock and Cullen, 2020). Carine White's et al. found that RAW264.7 macrophages pre-exposed to hypoxic conditions showed a significant increase in copper ion uptake compared to normoxia (White et al., 2009). Experimental evidence points that the copper uptake of Caco-2 cells under hypoxia is five times higher than normoxia, and the increase in copper uptake in Caco-2 cells under hypoxic conditions is related to the increase in Ctr1mRNA expression (Pourvali et al., 2012). In addition, studies have found that the expression of CTR1 gene is regulated by hypoxia inducible factor (HIF) and Myc transcription (Feng et al., 2009; Porcu et al., 2018).

After the transcription of the CTR1 gene, the stability of its protein can be translated in order to perform its function. Jianping Guo, et al. found that Nedd4l can induce CTR1 ubiquitination and subsequently degrade CTR1 (Guo et al., 2021). Nedd4l can negatively regulate CTR1 copper signaling to regulate AKT kinase activity and reduce tumor occurrence. Based on CRISPR/Cas9, the upstream kinase of CTR1 was identified through transcriptome screening. It was found that AMPK can enhance the localization of CTR1 membrane, and phosphorylation and stabilization of CTR1 are present and play a role in the plasma membrane (Zhang X. et al., 2023). CTR1 is essential for the activation of the MAPK signaling pathway by ligands of three major receptor tyrosine kinases (RTKs): FGF, PDGF, and EGF (Tsai et al., 2012). In summary, during cerebral I/R, modulation of post-translational modifications of CTR1, such as ubiquitination and phosphorylation, could influence its function and inhibit neuronal uptake of copper ions.

Factors influencing CTR1 activity

X-ray diffraction shows that CTR1 adopts a homologous trimeric structure similar to Cu^{+} selective ion channels. Two layers of cysteine triad form a selective filter that coordinates two bound copper ions near the extracellular entrance (Ren et al., 2019). Changes in the activity of CTR1 in cells may interfere with intracellular copper ion levels. Initially, it was believed that, similar to other ion channels, its activity could be altered by affecting energy metabolism. However, studies have shown that both mammalian and yeast CTR families lack clear ATP binding domains, and CTR1 mediated copper uptake may not be energy dependent (Margaret et al., 2023). Moreover, Peter Tsvetkov et al.'s research show that mitochondrial respiration is involved in copper-induced cell death, on the contrary, disrupting ATP generation with mitochondrial uncoupling agents showed no effect on copper-induced cell death (Tsvetkov et al., 2022). However, changes in the extracellular environment may affect CTR1 activity. The N-terminal region of the human copper transporter protein Ctr1 exhibits pH and metal oxidation state-dependent multi-metal binding capabilities (Lee et al., 2002). Experimental findings on the impact of extracellular pH, Na, and K+ on copper absorption indicated a significant increase in copper accumulation in Hek5 cells at pH 5.5 and 5.7 compared to pH 7.5. Compared with low K buffer, incubation of Hek5 cells in high K buffer significantly increased copper accumulation (Ren et al., 2019). Collectively, these findings suggest that acidic or

high potassium could activate CTR1 activity, once neuronal cells undergo anaerobic glycolysis, acidosis, and high potassium levels, changes in the cellular microenvironment might cause stimulation on CTR1 activity, which led to increased copper ion uptake and subsequent copper-induced neuronal cell death. Furthermore, emerging studies indicate that the endogenous retrovirus envelope glycoprotein Refrex1 could interact with CTR1, reducing its transport activity to regulate copper uptake (Nardella et al., 2022). These results indicated that altering CTR1 activity through changes in the extracellular environment and protein interactions represents a potential target against copper-induced cell death due to elevated copper ion levels.

Regulating copper ion levels by modulating the copper efflux pathway ATP7A/B

ATP7A/B is a Cu + transporter ATPase, which maintains copper homeostasis within cells and involves the transmembrane transfer of Cu + ions from the cytoplasm to receptor proteins, and requires ATP hydrolysis (Tury et al., 2023). Mutations in ATP7A and ATP7B (more specific to liver where it plays an important role to deliver Cu to apoceruloplasmin) are the basis for MD and WD, respectively. ATP7A facilitates the extrusion of copper through the cell membrane to maintain cellular copper homeostasis. The copper accumulation in motor neurons is the pathogenic mechanism associated with ATP7A in the hereditary motor neuropathy dHMN (Tadini-Buoninsegni and Smeazzetto, 2017). However, some results indicated that genetic mutations in the genes encoding copper efflux proteins ATP7A/B could lead to functional impairment, which might impair Cu^{+} efflux within cells, copper overload, and induction of copper related cell death. A study in a Wilson Disease (WD) mouse model demonstrated that a decrease in Fe-S proteins, protein sulfhydration, and expression of copper death-related proteins showed shared occurrence of copper-induced cell death mechanisms in genetic models (Dong et al., 2021). Hepatolenticular degeneration is a mutation in the ATP7B gene, where copper ions continue to accumulate in brain, liver, and other tissues. The intervention strategy for WD primarily depended on the utilization of copper ion chelators such as D-penicillamine and tetrathiomolybdate (TTM) (Litwin et al., 2019). Studies have revealed that heterogeneous nuclear ribonucleoprotein hnRNPA2/B1 regulates Cu + homeostasis by modulating the Cu(I)-transporting protein ATP7A (McCann Courtney J. et al., 2022). In Hela cells, hnRNPA2/B1 downregulation increases ATP7A mRNA and protein levels, significantly decreasing cellular copper levels (Natera-de Benito et al., 2021). In HPrEC cells, certain anticancer drugs, like flavonoids, disrupt the expression of the copper transport gene ATP7A, leading to impaired copper ion transport and subsequent cell death (McCann C. J. et al., 2022). Furthermore, in human neuroblastoma SH-SY5Y cells, NaHS significantly reduces the levels of ATP7A, promotes intracellular Cu + accumulation, which induce cellular toxicity (Goto et al., 2020). COMMD1 performs intracellular ATP7A/B stability chaperone function, and copper levels increase in cells lacking functional COMMD1 protein (Singla et al., 2021). Therefore, by regulating the expression of ATP7A/B, it is possible to influence the intracellular copper ion levels. In the study of cerebral I/R in rats, it was found that the expression of ATP7B was significantly downregulated compared to the control group, and the intracellular copper ion level was increased. Dexmedetomidine pretreatment in cerebral I/R causes increase in ATP7B strongly expressed in brain, reduce intracellular copper ions, and inhibit neuronal copper death (Guo Qingduo et al., 2023). These results indicate that overexpression of ATP7A/B in neuronal cells, increased excretion of copper ions, and inhibition of copper induced neuronal cell death, which provided significant implications for the treatment of cerebral I/R injury.

Future prospectives

Taken together, the primary treatment approach for stroke is early perfusion to alleviate ischemic damage. However, early reperfusion could result in I/R injury, necessitating urgent exploration of therapeutic strategies to mitigate these assaults. During cerebral I/R, there is an elevation in copper ion levels, abnormal expression of copper death-related proteins, and the occurrence of copper-induced cell death in neurons. Understanding the physiological metabolism of copper ions in the brain, reducing cerebral copper ion levels during I/R injury aims to alleviate copper-induced cell death, offering a novel avenue for treating cerebral ischemic injury. While current research on cuproptosis primarily focuses on tumor treatment and drug resistance mechanisms, lessons from various strategies to decrease intracellular copper ions in cancer research could be applied to inhibit cuproptosis, contributing to studies aimed at alleviating cerebral I/R injury. Recently, although substantial progress has been made in unraveling the mechanisms of cuproptosis during cerebral I/R, there are still no effective remedies available for reliving cerebral I/R injury. This requires further studies and novel approaches to facilitate the molecular features and excavate more rational strategies.

Author contributions

GP: Writing–original draft, Software, Writing–review and editing. GX: Formal Analysis, Data curation, Writing–review and editing. YH: Supervision, Funding acquisition, Conceptualization, Writing–review and editing. JT: Writing–review and editing, Validation, Supervision.

Funding

The author(s) declare that financial support was received for the research, authorship, and/or publication of this article. This study was partly funded by Hunan Natural Science Foundation (2023JJ60262).

Conflict of interest

The authors declare that the research was conducted in the absence of any commercial or financial relationships that could be construed as a potential conflict of interest.

The reviewer CS declared a shared affiliation with the author YH to the handling editor at the time of review.

Publisher's note

References

Abou Anni, I. S., Zebral, Y. D., Afonso, S. B., Moreno Abril, S. I., Lauer, M. M., and Bianchini, A. (2019). Life-time exposure to waterborne copper III: effects on the energy metabolism of the killifish Poecilia vivipara. *Chemosphere* 227, 580–588. doi:10.1016/j.chemosphere.2019.04.080

Akçil, E., Tuğ, T., and Döşeyen, Z. (2000). Antioxidant enzyme activities and trace element concentrations in ischemia-reperfusion. *Biol. Trace Elem. Res.* 76 (1), 13–17. doi:10.1385/BTER:76:1:13

Akerfeldt, M. C., Tran, C. M., Shen, C., Hambley, T. W., and New, E. J. (2017). Interactions of cisplatin and the copper transporter CTR1 in human colon cancer cells. *J. Biol. Inorg. Chem.* 22 (5), 765–774. doi:10.1007/s00775-017-1467-y

Alessi, K., Delima, M., Pfautsch, M., Shriver, M. E., and Parmar, M. S. (2021). Neurological type Wilson's disease: a case report. *SN Compr. Clin. Med.* 3 (9), 1946–1950. doi:10.1007/s42399-021-00960-x

Altarelli, M., Ben-Hamouda, N., Schneider, A., and Berger, M. M. (2019). Copper deficiency: causes, manifestations, and treatment. *Nutr. Clin. Pract.* 34 (4), 504–513. doi:10.1002/ncp.10328

Altobelli, G. G., Van Noorden, S., Balato, A., and Cimini, V. (2020). Copper/zinc superoxide dismutase in human skin: current knowledge. *Front. Med. (Lausanne)* 7, 183. doi:10.3389/fmed.2020.00183

An, Y., Li, S., Huang, X., Chen, X., Shan, H., and Zhang, M. (2022). The role of copper homeostasis in brain disease. *Int. J. Mol. Sci.* 23 (22), 13850. doi:10.3390/ijms232213850

Bäck, N., Mains, R. E., and Eipper, B. A. (2022). PAM: diverse roles in neuroendocrine cells, cardiomyocytes, and green algae. *FEBS J.* 289 (15), 4470–4496. doi:10.1111/febs.16049

Banci, L., Bertini, I., Ciofi-Baffoni, S., Hadjiloi, T., Martinelli, M., and Palumaa, P. (2008). Mitochondrial copper(I) transfer from Cox17 to Sco1 is coupled to electron transfer. *Proc. Natl. Acad. Sci. U. S. A.* 105 (19), 6803–6808. doi:10.1073/pnas.0800019105

Bandmann, O., Weiss, K. H., and Kaler, S. G. (2015). Wilson's disease and other neurological copper disorders. *Lancet Neurol.* 14 (1), 103–113. doi:10.1016/S1474-4422(14)70190-5

Batzios, S., Tal, G., DiStasio, A. T., Peng, Y., Charalambous, C., Nicolaides, P., et al. (2022). Newly identified disorder of copper metabolism caused by variants in CTR1, a high-affinity copper transporter. *Hum. Mol. Genet.* 31 (24), 4121–4130. doi:10.1093/hmg/ddac156

Bhattacharjee, A., Ghosh, S., Chatterji, A., and Chakraborty, K. (2020). Neuron-glia: understanding cellular copper homeostasis, its cross-talk and their contribution towards neurodegenerative diseases. *Metallomics.* 12 (12), 1897–1911. doi:10.1039/d0mt00168f

Bisaglia, M., and Bubacco, L. (2020). Copper ions and Parkinson's disease: why is homeostasis so relevant? *Biomolecules* 10 (2), 195. doi:10.3390/biom10020195

Bjørklund, G., Dadar, M., Pivina, L., Doşa, M. D., Semenova, Y., and Aaseth, J. (2020). The role of zinc and copper in insulin resistance and diabetes mellitus. *Curr. Med. Chem.* 27 (39), 6643–6657. doi:10.2174/0929867326666190902122155

Blomberg, M. R. A. (2020). The structure of the oxidized state of cytochrome c oxidase - experiments and theory compared. *J. Inorg. Biochem.* 206, 111020. doi:10.1016/j.jinorgbio.2020.111020

Bonaccorsi di Patti, M. C., Cutone, A., Nemčovič, M., Pakanová, Z., Baráth, P., and Musci, G. (2021). Production of recombinant human ceruloplasmin: improvements and perspectives. *Int. J. Mol. Sci.* 22 (15), 8228. doi:10.3390/ijms22158228

Bonnemaison, M. L., Duffy, M. E., Mains, R. E., Vogt, S., Eipper, B. A., and Ralle, M. (2016). Copper, zinc and calcium: imaging and quantification in anterior pituitary secretory granules. *Metallomics* 8 (9), 1012–1022. doi:10.1039/c6mt00079g

Bost, M., Houdart, S., Oberli, M., Kalonji, E., Huneau, J. F., and Margaritis, I. (2016). Dietary copper and human health: current evidence and unresolved issues. *J. Trace Elem. Med. Biol.* 35, 107–115. doi:10.1016/j.jtemb.2016.02.006

Boulis, N. M., and Donsante, A. (2023). A novel antibody to treat SOD1-related amyotrophic lateral sclerosis. *Mol. Ther. Methods Clin. Dev.* 29, 236–237. doi:10.1016/j.omtm.2023.03.011

Bousquet-Moore, D., Prohaska, J. R., Nillni, E. A., Czyzyk, T., Wetsel, W. C., Mains, R. E., et al. (2010). Interactions of peptide amidation and copper: novel biomarkers and mechanisms of neural dysfunction. *Neurobiol. Dis.* 37 (1), 130–140. doi:10.1016/j.nbd.2009.09.016

Boyd, S. D., Ullrich, M. S., Skopp, A., and Winkler, D. D. (2020). Copper sources for Sod1 activation. *Antioxidants (Basel)* 9 (6), 500. doi:10.3390/antiox9060500

Braymer, J. J., Freibert, S. A., Rakwalska-Bange, M., and Lill, R. (2021). Mechanistic concepts of iron-sulfur protein biogenesis in Biology. *Biochim. Biophys. Acta Mol. Cell Res.* 1868 (1), 118863. doi:10.1016/j.bbamcr.2020.118863

Brischigliaro, M., and Zeviani, M. (2021). Cytochrome c oxidase deficiency. *Biochim. Biophys. Acta Bioenerg.* 1862 (1), 148335. doi:10.1016/j.bbabio.2020.148335

Cendrowska-Pinkosz, M., Ostrowska-Lesko, M., Ognik, K., Krauze, M., Juskiewicz, J., Dabrowska, A., et al. (2022). Dietary copper deficiency leads to changes in gene expression indicating an increased demand for NADH in the prefrontal cortex of the rat's brain. *Int. J. Mol. Sci.* 23 (12), 6706. doi:10.3390/ijms23126706

Chakraborty, K., Kar, S., Rai, B., Bhagat, R., Naskar, N., Seth, P., et al. (2022). Copper dependent ERK1/2 phosphorylation is essential for the viability of neurons and not glia. *Metallomics.* 14 (4), mfac005. doi:10.1093/mtomcs/mfac005

Chan, P. H., Kawase, M., Murakami, K., Chen, S. F., Li, Y., Calagui, B., et al. (1998). Overexpression of SOD1 in transgenic rats protects vulnerable neurons against ischemic damage after global cerebral ischemia and reperfusion. *J. Neurosci.* 18 (20), 8292–8299. doi:10.1523/JNEUROSCI.18-20-08292.1998

Chelyadina, N. S., Kapranov, S. V., Popov, M. A., Smirnova, L. L., and Bobko, N. I. (2023). The mussel *Mytilus galloprovincialis* (Crimea, Black Sea) as a source of essential trace elements in human nutrition. *Biol. Trace Elem. Res.* 201 (11), 5415–5430. doi:10.1007/s12011-023-03607-1

Chen, C. H., Chou, Y. T., Yang, Y. W., and Lo, K. Y. (2021). High-dose copper activates p53-independent apoptosis through the induction of nucleolar stress in human cell lines. *Apoptosis* 26 (11-12), 612–627. doi:10.1007/s10495-021-01692-y

Chen, G., Zhang, J., Teng, W., Luo, Y., and Ji, X. (2023a). FDX1 inhibits thyroid cancer malignant progression by inducing cuprotosis. *Heliyon* 9 (8), e18655. doi:10.1016/j.heliyon.2023.e18655

Chen, J., Jiang, Y., Shi, H., Peng, Y., Fan, X., and Li, C. (2020). The molecular mechanisms of copper metabolism and its roles in human diseases. *Pflugers Arch.* 472 (10), 1415–1429. doi:10.1007/s00424-020-02412-2

Chen, X., Cai, Q., Liang, R., Zhang, D., Liu, X., Zhang, M., et al. (2023b). Copper homeostasis and copper-induced cell death in the pathogenesis of cardiovascular disease and therapeutic strategies. *Cell Death Dis.* 14 (2), 105. doi:10.1038/s41419-023-05639-w

Chun, H., Catterton, T., Kim, H., Lee, J., and Kim, B. E. (2017). Organ-specific regulation of ATP7A abundance is coordinated with systemic copper homeostasis. *Sci. Rep.* 7 (1), 12001. doi:10.1038/s41598-017-11961-z

Cobine, P. A., Moore, S. A., and Leary, S. C. (2021). Getting out what you put in: copper in mitochondria and its impacts on human disease. *Biochim. Biophys. Acta Mol. Cell Res.* 1868 (1), 118867. doi:10.1016/j.bbamcr.2020.118867

Cunnane, S. C., Trushina, E., Morland, C., Prigione, A., Casadesus, G., Andrews, Z. B., et al. (2020). Brain energy rescue: an emerging therapeutic concept for neurodegenerative disorders of ageing. *Nat. Rev. Drug Discov.* 19 (9), 609–633. doi:10.1038/s41573-020-0072-x

Curnock, R., and Cullen, P. J. (2020). Mammalian copper homeostasis requires retromer-dependent recycling of the high-affinity copper transporter 1. *J. Cell Sci.* 133 (16), jcs249201. doi:10.1242/jcs.249201

D'Ambrosi, N., and Rossi, L. (2015). Copper at synapse: release, binding and modulation of neurotransmission. *Neurochem. Int.* 90, 36–45. doi:10.1016/j.neuint.2015.07.006

Dong, J., Wang, X., Xu, C., Gao, M., Wang, S., Zhang, J., et al. (2021). Inhibiting NLRP3 inflammasome activation prevents copper-induced neuropathology in a murine model of Wilson's disease. *Cell Death Dis.* 12 (1), 87. doi:10.1038/s41419-021-03397-1

Dreishpoon, M. B., Bick, N. R., Petrova, B., Warui, D. M., Cameron, A., Booker, S. J., et al. (2023b). FDX1 regulates cellular protein lipoylation through direct binding to LIAS. *J. Biol. Chem.* 299 (9), 105046. doi:10.1016/j.jbc.2023.105046

Dreishpoon, M. B., Bick, N. R., Petrova, B., Warui, D. M., Cameron, A., Booker, S. J., et al. (2023a). FDX1 regulates cellular protein lipoylation through direct binding to LIAS. *J. Biol. Chem.* 299 (9), 105046. doi:10.1016/j.jbc.2023.105046

Du, J., Huang, Z., Li, Y., Ren, X., Zhou, C., Liu, R., et al. (2023). Copper exerts cytotoxicity through inhibition of iron-sulfur cluster biogenesis on ISCA1/ISCA2/ISCU assembly proteins. *Free Radic. Biol. Med.* 204, 359–373. doi:10.1016/j.freeradbiomed.2023.05.017

Dyall, S. C., Nessel, I., Sharpe, J. A., Yip, P. K., Michael-Titus, A. T., and Shah, D. K. (2023). Long-chain omega-3 polyunsaturated fatty acids are reduced in neonates with substantial brain injury undergoing therapeutic hypothermia after hypoxic-ischemic encephalopathy. *Front. Neurol.* 14, 1231743. doi:10.3389/fneur.2023.1231743

Eljazzar, S., Abu-Hijleh, H., Alkhatib, D., Sokary, S., Ismail, S., Al-Jayyousi, G. F., et al. (2023). The role of copper intake in the development and management of type 2 diabetes: a systematic review. *Nutrients* 15 (7), 1655. doi:10.3390/nu15071655

Feng, W., Ye, F., Xue, W., Zhou, Z., and Kang, Y. J. (2009). Copper regulation of hypoxia-inducible factor-1 activity. *Mol. Pharmacol.* 75 (1), 174–182. doi:10.1124/mol.108.051516

Ferguson, G. D., and Bridge, W. J. (2019). The glutathione system and the related thiol network in *Caenorhabditis elegans*. *Redox Biol.* 24, 101171. doi:10.1016/j.redox.2019.101171

Fetherolf, M. M., Boyd, S. D., Taylor, A. B., Kim, H. J., Wohlschlegel, J. A., Blackburn, N. J., et al. (2017). Copper-zinc superoxide dismutase is activated through a sulfenic acid intermediate at a copper ion entry site. *J. Biol. Chem.* 292 (29), 12025–12040. doi:10.1074/jbc.M117.775981

Gaetke, L. M., and Chow, C. K. (2003). Copper toxicity, oxidative stress, and antioxidant nutrients. *Toxicology* 189 (1-2), 147–163. doi:10.1016/s0300-483x(03)00159-8

Gao, S., Zhou, M., and Tang, Z. (2024). The Tao of copper metabolism: from physiology to pathology. *Curr. Med. Chem.* 31 (35), 5805–5817. doi:10.2174/0929867331666230915162405

Garmann, D., Warnecke, A., Kalayda, G. V., Kratz, F., and Jaehde, U. (2008). Cellular accumulation and cytotoxicity of macromolecular platinum complexes in cisplatin-resistant tumor cells. *J. Control. Release.* 131 (2), 100–106. doi:10.1016/j.jconrel.2008.07.017

GBD 2019 Stroke Collaborators (2021). Global, regional, and national burden of stroke and its risk factors, 1990-2019: a systematic analysis for the Global Burden of Disease Study 2019. *Lancet Neurol.* 20 (10), 795–820. doi:10.1016/S1474-4422(21)00252-0

Gonzalez-Lopez, E., and Vrana, K. E. (2020). Dopamine beta-hydroxylase and its genetic variants in human health and disease. *J. Neurochem.* 152 (2), 157–181. doi:10.1111/jnc.14893

Górska, A., Markiewicz-Gospodarek, A., Markiewicz, R., Chilimoniuk, Z., Borowski, B., Trubalski, M., et al. (2023). Distribution of iron, copper, zinc and cadmium in glia, their influence on glial cells and relationship with neurodegenerative diseases. *Brain Sci.* 13 (6), 911. doi:10.3390/brainsci13060911

Goto, N., Hara, H., Kondo, M., Yasuda, N., Kamiya, T., Okuda, K., et al. (2020). Hydrogen sulfide increases copper-dependent neurotoxicity via intracellular copper accumulation. *Metallomics.* 12 (6), 868–875. doi:10.1039/d0mt00015a

Grechnikova, M., Ženíšková, K., Malych, R., Mach, J., and Sutak, R. (2020). Copper detoxification machinery of the brain-eating amoeba Naegleria fowleri involves copper-translocating ATPase and the antioxidant system. *Int. J. Parasitol. Drugs Drug Resist* 14, 126–135. doi:10.1016/j.ijpddr.2020.10.001

Guo, J., Cheng, J., Zheng, N., Zhang, X., Dai, X., Zhang, L., et al. (2021). Copper promotes tumorigenesis by activating the PDK1-AKT oncogenic pathway in a copper transporter 1 dependent manner. *Adv. Sci. (Weinh)* 8 (18), e2004303. doi:10.1002/advs.202004303

Guo, Q., Ma, M., Yu, H., Han, Y., and Zhang, D. (2023a). Dexmedetomidine enables copper homeostasis in cerebral ischemia/reperfusion via ferredoxin 1. *Ann. Med.* 55 (1), 2209735. doi:10.1080/07853890.2023.2209735

Guo, Q., Ma, M., Yu, H., Han, Y., and Zhang, D. (2023b). Dexmedetomidine enables copper homeostasis in cerebral ischemia/reperfusion via ferredoxin 1. *Ann. Med.* 55 (1), 2209735. doi:10.1080/07853890.2023.2209735

Gurnari, C., and Rogers, H. J. (2021). Copper deficiency. *N. Engl. J. Med.* 385 (7), 640. doi:10.1056/NEJMicm2103532

Guthrie, L. M., Soma, S., Yuan, S., Silva, A., Zulkifli, M., Snavely, T. C., et al. (2020). Elesclomol alleviates Menkes pathology and mortality by escorting Cu to cuproenzymes in mice. *Science* 368 (6491), 620–625. doi:10.1126/science.aaz8899

Hao, P., Li, H., Zhou, L., Sun, H., Han, J., and Zhang, Z. (2022). Serum metal ion-induced cross-linking of photoelectrochemical peptides and circulating proteins for evaluating cardiac ischemia/reperfusion. *ACS Sens.* 7 (3), 775–783. doi:10.1021/acssensors.1c02305

Haywood, S., and Vaillant, C. (2014). Overexpression of copper transporter CTR1 in the brain barrier of North Ronaldsay sheep: implications for the study of neurodegenerative disease. *J. Comp. Pathol.* 150 (2-3), 216–224. doi:10.1016/j.jcpa.2013.09.002

Herpich, F., and Rincon, F. (2020). Management of acute ischemic stroke. *Crit. Care Med.* 48 (11), 1654–1663. doi:10.1097/CCM.0000000000004597

Horn, N., and Wittung-Stafshede, P. (2021). ATP7A-Regulated enzyme metalation and trafficking in the Menkes disease puzzle. *Biomedicines* 9 (4), 391. doi:10.3390/biomedicines9040391

Horng, Y. C., Cobine, P. A., Maxfield, A. B., Carr, H. S., and Winge, D. R. (2004). Specific copper transfer from the Cox17 metallochaperone to both Sco1 and Cox11 in the assembly of yeast cytochrome C oxidase. *J. Biol. Chem.* 279 (34), 35334–35340. doi:10.1074/jbc.M404747200

Hu, Y., Zhang, D., Zhang, Q., Yin, T., Jiang, T., He, S., et al. (2023). Serum Cu, Zn and IL-1β levels may predict fetal miscarriage risk after IVF cycles: a nested case-control study. *Biol. Trace Elem. Res.* 201 (12), 5561–5574. doi:10.1007/s12011-023-03621-3

Huuskonen, M. T., Tuo, Q. Z., Loppi, S., Dhungana, H., Korhonen, P., McInnes, L. E., et al. (2017). The copper bis(thiosemicarbazone) complex CuII(atsm) Is protective against cerebral ischemia through modulation of the inflammatory milieu. *Neurotherapeutics* 14 (2), 519–532. doi:10.1007/s13311-016-0504-9

Janardhanan, P., Somasundaran, A. K., Balakrishnan, A. J., and Pilankatta, R. (2022). Sensitization of cancer cells towards Cisplatin and Carboplatin by protein kinase D inhibitors through modulation of ATP7A/B (copper transport ATPases). *Cancer Treat. Res. Commun.* 32, 100613. doi:10.1016/j.ctarc.2022.100613

Jiang, Y., Bai, X., Li, T. T., Al-Hawwas, M., Jin, Y., Zou, Y., et al. (2020). COX5A over-expression protects cortical neurons from hypoxic ischemic injury in neonatal rats associated with TPI up-regulation. *BMC Neurosci.* 21 (1), 18. doi:10.1186/s12868-020-00565-5

Joshi, P. R., Sadre, S., Guo, X. A., McCoy, J. G., and Mootha, V. K. (2023). Lipoylation is dependent on the ferredoxin FDX1 and dispensable under hypoxia in human cells. *J. Biol. Chem.* 299 (9), 105075. doi:10.1016/j.jbc.2023.105075

Juárez-Cedillo, T., Martínez-Rodríguez, N., Fragoso, J. M., Islas-Pérez, V., López-Martínez, A., and Valle-Medina, A. (2023). Multifactor dimensionality reduction analysis to evaluate the association of dopamine beta-hydroxylase (dβh) polymorphisms with susceptibility to dementia (SADEM study). *Mol. Neurobiol.* 60 (8), 4731–4737. doi:10.1007/s12035-023-03367-y

Kahlson, M. A., and Dixon, S. J. (2022). Copper-induced cell death. *Science* 375 (6586), 1231–1232. doi:10.1126/science.abo3959

Kawahara, M., Tanaka, K. I., and Kato-Negishi, M. (2021). Copper as a collaborative partner of zinc-induced neurotoxicity in the pathogenesis of vascular dementia. *Int. J. Mol. Sci.* 22 (14), 7242. doi:10.3390/ijms22147242

Ke, D., Zhang, Z., Liu, J., Chen, P., Li, J., Sun, X., et al. (2023). Ferroptosis, necroptosis and cuproptosis: novel forms of regulated cell death in diabetic cardiomyopathy. *Front. Cardiovasc Med.* 10, 1135723. doi:10.3389/fcvm.2023.1135723

Khalfaoui-Hassani, B., Trasnea, P. I., Steimle, S., Koch, H. G., and Daldal, F. (2021). Cysteine mutants of the major facilitator superfamily-type transporter CcoA provide insight into copper import. *mBio* 12 (4), e0156721. doi:10.1128/mBio.01567-21

Kirsipuu, T., Zadorožnaja, A., Smirnova, J., Friedemann, M., Plitz, T., Tõugu, V., et al. (2020). Copper (II)-binding equilibria in human blood. *Sci. Rep.* 10 (1), 5686. doi:10.1038/s41598-020-62560-4

Kucková, L., Jomová, K., Švorcová, A., Valko, M., Segľa, P., Moncoľ, J., et al. (2015). Synthesis, crystal structure, spectroscopic properties and potential biological activities of salicylate–neocuproine ternary copper(II) complexes. *Molecules* 20 (2), 2115–2137. doi:10.3390/molecules20022115

Kumar, D., Mains, R. E., and Eipper, B. A. (2016). 60 Years of POMC: from POMC and α-MSH to PAM, molecular oxygen, copper, and vitamin C. *J. Mol. Endocrinol.* 56 (4), T63–T76. doi:10.1530/JME-15-0266

Lasorsa, A., Nardella, M. I., Rosato, A., Mirabelli, V., Caliandro, R., Caliandro, R., et al. (2019). Mechanistic and structural basis for inhibition of copper trafficking by platinum anticancer drugs. *J. Am. Chem. Soc.* 141 (30), 12109–12120. doi:10.1021/jacs.9b05550

Lee, E. J., Kolb, J., Hwee, D. T., Malik, F. I., and Granzier, H. L. (2019). Functional characterization of the intact diaphragm in a nebulin-based nemaline myopathy (NM) model-effects of the fast skeletal muscle troponin activator tirasemtiv. *Int. J. Mol. Sci.* 20 (20), 5008. doi:10.3390/ijms20205008

Lee, J., Peña, M. M., Nose, Y., and Thiele, D. J. (2002). Biochemical characterization of the human copper transporter Ctr1. *J. Biol. Chem.* 277 (6), 4380–4387. doi:10.1074/jbc.M104728200

Lenartowicz, M., Krzeptowski, W., Lipiński, P., Grzmil, P., Starzyński, R., Pierzchała, O., et al. (2015). Mottled mice and non-mammalian models of Menkes disease. *Front. Mol. Neurosci.* 8, 72. doi:10.3389/fnmol.2015.00072

Li, B., Yu, W., and Verkhratsky, A. (2024a). Trace metals and astrocytes physiology and pathophysiology. *Cell Calcium* 118, 102843. doi:10.1016/j.ceca.2024.102843

Li, C., Jia, W., Guo, Z., Kang, Y., Zhou, C., Zhao, R., et al. (2024b). A copper-platinum nanoplatform for synergistic photothermal and chemodynamic tumor therapy via ROS outburst and GSH exhaustion. *J. Mater Chem. B* 12 (3), 800–813. doi:10.1039/d3tb02288a

Li, S. R., Bu, L. L., and Cai, L. (2022). Cuproptosis: lipoylated TCA cycle proteins-mediated novel cell death pathway. *Signal Transduct. Target Ther.* 7 (1), 158. doi:10.1038/s41392-022-01014-x

Li, X., Dehghan, M., Tse, L. A., Lang, X., Rangarajan, S., Liu, W., et al. (2023a). Associations of dietary copper intake with cardiovascular disease and mortality: findings from the Chinese Perspective Urban and Rural Epidemiology (PURE-China) Study. *BMC Public Health* 23 (1), 2525. doi:10.1186/s12889-023-17441-6

Li, Y. (2020). Copper homeostasis: emerging target for cancer treatment. *IUBMB Life* 72, 1900–1908. doi:10.1002/iub.2341

Li, Y., Du, Y., Zhou, Y., Chen, Q., Luo, Z., Ren, Y., et al. (2023b). Iron and copper: critical executioners of ferroptosis, cuproptosis and other forms of cell death. *Cell Commun. Signal* 21 (1), 327. doi:10.1186/s12964-023-01267-1

Liang, Z. D., Long, Y., Chen, H. H., Savaraj, N., and Kuo, M. T. (2014). Regulation of the high-affinity copper transporter (hCtr1) expression by cisplatin and heavy metals. *J. Biol. Inorg. Chem.* 19 (1), 17–27. doi:10.1007/s00775-013-1051-z

Lim, S., Kim, T. J., Kim, Y. J., Kim, C., Ko, S. B., and Kim, B. S. (2021). Senolytic therapy for cerebral ischemia-reperfusion injury. *Int. J. Mol. Sci.* 22 (21), 11967. doi:10.3390/ijms222111967

Lin, C., Zhang, Z., Wang, T., Chen, C., and James Kang, Y. (2015). Copper uptake by DMT1: a compensatory mechanism for CTR1 deficiency in human umbilical vein endothelial cells. *Metallomics* 7 (8), 1285–1289. doi:10.1039/c5mt00097a

Lin, M. C., Liu, C. C., Liao, C. S., and Ro, J. H. (2021). Neuroprotective effect of Quercetin during cerebral ischemic injury involves regulation of essential elements, transition metals, Cu/Zn ratio, and antioxidant activity. *Molecules* 26 (20), 6128. doi:10.3390/molecules26206128

Lin, X., Shang, X., Manorek, G., Fofana, M., and Stephen, B. H. (2014). Integrin αV modulates the cellular pharmacology of copper and cisplatin by regulating expression of the influx transporter CTR1. *Oncoscience* 1 (3), 185–195. doi:10.18632/oncoscience.22

Litwin, T., Dzieżyc, K., and Członkowska, A. (2019). Wilson disease-treatment perspectives. *Ann. Transl. Med.* 7 (Suppl. 2), S68. doi:10.21037/atm.2018.12.09

Liu, C., and Liang, D. (2024). High copper intake is associated with decreased likelihood of abdominal aortic calcification in middle-aged and older US adults. *Biol. Trace Elem. Res.* 202 (4), 1390–1400. doi:10.1007/s12011-023-03765-2

Liu, L. L., van Rijn, R. M., and Zheng, W. (2022b). Copper modulates adult neurogenesis in brain subventricular zone. *Int. J. Mol. Sci.* 23 (17), 9888. doi:10.3390/ijms23179888

Liu, Z., Wang, M., Zhang, C., Zhou, S., and Ji, G. (2022a). Molecular functions of ceruloplasmin in metabolic disease pathology. *Diabetes Metab. Syndr. Obes.* 15, 695–711. doi:10.2147/DMSO.S346648

Ma, H. T., Zhang, H. C., Zuo, Z. F., and Liu, Y. X. (2023). Heterogeneous organization of Locus coeruleus: an intrinsic mechanism for functional complexity. *Physiol. Behav.* 268, 114231. doi:10.1016/j.physbeh.2023.114231

Maghool, S., Cooray, N. D. G., Stroud, D. A., Aragão, D., Ryan, M. T., and Maher, M. J. (2019). Structural and functional characterization of the mitochondrial complex IV assembly factor Coa6. *Life Sci. Alliance* 2 (5), e201900458. doi:10.26508/lsa.201900458

Magoufis, G., Safouris, A., Raphaeli, G., Kargiotis, O., Psychogios, K., Krogias, C., et al. (2021). Acute reperfusion therapies for acute ischemic stroke patients with unknown time of symptom onset or in extended time windows: an individualized approach. *Ther. Adv. Neurol. Disord.* 14, 17562864211021182. doi:10.1177/17562864211021182

Mandal, T., Kar, S., Maji, S., Sen, S., and Gupta, A. (2020). Structural and functional diversity among the members of CTR, the membrane copper transporter family. *J. Membr. Biol.* 253 (5), 459–468. doi:10.1007/s00232-020-00139-w

Margaret, B. D., Bick, N. R., Petrova, B., Douglas, M. W., Cameron, A., Booker, S. J., et al. (2023). FDX1 regulates cellular protein lipoylation through direct binding to LIAS. *J. Biol. Chem.* 299 (9), 105046. doi:10.1016/j.jbc.2023.105046

Martinat, M., Rossitto, M., Di Miceli, M., and Layé, S. (2021). Perinatal dietary polyunsaturated fatty acids in brain development, role in neurodevelopmental disorders. *Nutrients* 13 (4), 1185. doi:10.3390/nu13041185

Masaldan, S., Clatworthy, S. A. S., Gamell, C., Smith, Z. M., Francis, P. S., Denoyer, D., et al. (2018). Copper accumulation in senescent cells: interplay between copper transporters and impaired autophagy. *Redox Biol.* 16, 322–331. doi:10.1016/j.redox.2018.03.007

Mazi, T. A., Shibata, N. M., and Medici, V. (2020). Lipid and energy metabolism in Wilson disease. *Liver Res.* 4 (1), 5–14. doi:10.1016/j.livres.2020.02.002

McCann, C., Quinteros, M., Adelugba, I., Morgada, M. N., Castelblanco, A. R., Davis, E. J., et al. (2022a). The mitochondrial Cu+ transporter PiC2 (SLC25A3) is a target of MTF1 and contributes to the development of skeletal muscle *in vitro*. *Front. Mol. Biosci.* 9, 1037941. doi:10.3389/fmolb.2022.1037941

McCann, C. J., Hasan, N. M., Padilla-Benavides, T., Roy, S., and Lutsenko, S. (2022b). Heterogeneous nuclear ribonucleoprotein hnRNPA2/B1 regulates the abundance of the copper-transporter ATP7A in an isoform-dependent manner. *Front. Mol. Biosci.* 9, 1067490. doi:10.3389/fmolb.2022.1067490

McCann, C. J., Hasan, N. M., Padilla-Benavides, T., Roy, S., and Lutsenko, S. (2022c). Heterogeneous nuclear ribonucleoprotein hnRNPA2/B1 regulates the abundance of the copper-transporter ATP7A in an isoform-dependent manner. *Front. Mol. Biosci.* 9, 1067490. doi:10.3389/fmolb.2022.1067490

Merkler, D. J., Hawley, A. J., Eipper, B. A., and Mains, R. E. (2022). Peptidylglycine α-amidating monooxygenase as a therapeutic target or biomarker for human diseases. *Br. J. Pharmacol.* 179 (13), 3306–3324. doi:10.1111/bph.15815

Nardella, M. I., Fortino, M., Barbanente, A., Natile, G., Pietropaolo, A., and Arnesano, F. (2022). Multinuclear metal-binding ability of the N-terminal region of human copper transporter Ctr1: dependence upon pH and metal oxidation state. *Front. Mol. Biosci.* 9, 897621. doi:10.3389/fmolb.2022.897621

Natera-de Benito, D., Sola, A., Sousa, P. R., Boronat, S., Expósito-Escudero, J., Carrera-García, L., et al. (2021). Copper toxicity associated with an ATP7A-related complex phenotype. *Pediatr. Neurol.* 119, 40–44. doi:10.1016/j.pediatrneurol.2021.03.005

Ng, S. C. W., Furman, R., Axelsen, P. H., and Shchepinov, M. S. (2022). Free radical chain reactions and polyunsaturated fatty acids in brain lipids. *ACS Omega* 7 (29), 25337–25345. doi:10.1021/acsomega.2c02285

Nzuza, N., Padayachee, T., Chen, W., Gront, D., Nelson, D. R., and Syed, K. (2021). Diversification of ferredoxins across living organisms. *Curr. Issues Mol. Biol.* 43 (3), 1374–1390. doi:10.3390/cimb43030098

Ohkubo, N., Aoto, M., Kon, K., and Mitsuda, N. (2019). Lack of zinc finger protein 521 upregulates dopamine β-hydroxylase expression in the mouse brain, leading to abnormal behavior. *Life Sci.* 231, 116559. doi:10.1016/j.lfs.2019.116559

Pacheu-Grau, D., Wasilewski, M., Oeljeklaus, S., Gibhardt, C. S., Aich, A., Chudenkova, M., et al. (2020). COA6 facilitates cytochrome c oxidase biogenesis as thiol-reductase for copper metallochaperones in mitochondria. *J. Mol. Biol.* 432 (7), 2067–2079. doi:10.1016/j.jmb.2020.01.036

Park, Y. E., Noh, Y., Kim, D. W., Lee, T.-K., Ahn, J. H., Kim, B., et al. (2021). Experimental pretreatment with YES-10®, a plant extract rich in scutellarin and chlorogenic acid, protects hippocampal neurons from ischemia/reperfusion injury via antioxidant role. *Exp. Ther. Med.* 21 (3), 183. doi:10.3892/etm.2021.9614

Piacenza, F., Giacconi, R., Costarelli, L., Basso, A., Bürkle, A., Moreno-Villanueva, M., et al. (2021). Age, sex, and BMI influence on copper, zinc, and their major serum carrier proteins in a large European population including nonagenarian offspring from MARK-AGE study. *J. Gerontol. A Biol. Sci. Med. Sci.* 76 (12), 2097–2106. doi:10.1093/gerona/glab134

Porcu, C., Antonucci, L., Barbaro, B., Illi, B., Nasi, S., Martini, M., et al. (2018). Copper/MYC/CTR1 interplay: a dangerous relationship in hepatocellular carcinoma. *Oncotarget* 9 (10), 9325–9343. doi:10.18632/oncotarget.24282

Pourvali, K., Matak, P., Latunde-Dada, G. O., Solomou, S., Mastrogiannaki, M., Peyssonnaux, C., et al. (2012). Basal expression of copper transporter 1 in intestinal epithelial cells is regulated by hypoxia-inducible factor 2α. *FEBS Lett.* 586 (16), 2423–2427. doi:10.1016/j.febslet.2012.05.058

Prohaska, J. R., and Brokate, B. (2001). Dietary copper deficiency alters protein levels of rat dopamine beta-monooxygenase and tyrosine monooxygenase. *Exp. Biol. Med. (Maywood)* 226 (3), 199–207. doi:10.1177/153537020122600307

Raia, S., Conti, A., Zanardi, A., Ferrini, B., Scotti, G. M., Gilberti, E., et al. (2023). Ceruloplasmin-deficient mice show dysregulation of lipid metabolism in liver and adipose tissue reduced by a protein replacement. *Int. J. Mol. Sci.* 24 (2), 1150. doi:10.3390/ijms24021150

Ramzan, R., Napiwotzki, J., Weber, P., Kadenbach, B., and Vogt, S. (2021). Cholate disrupts regulatory functions of cytochrome c oxidase. *Cells* 10 (7), 1579. doi:10.3390/cells10071579

Rao, V. K. S., Eipper, B. A., and Mains, R. E. (2021). Multiple roles for peptidylglycine α-amidating monooxygenase in the response to hypoxia. *J. Cell Physiol.* 236 (11), 7745–7758. doi:10.1002/jcp.30457

Ren, F., Logeman, B. L., Zhang, X., Liu, Y., Thiele, D. J., and Yuan, P. (2019). X-ray structures of the high-affinity copper transporter Ctr1. *Nat. Commun.* 10 (1), 1386. doi:10.1038/s41467-019-09376-7

Reziya, H., Sayifujiamali, K., Han, H. J., Wang, X. M., Nuerbiya, T., Nuerdong, D., et al. (2023). Real-time feedback on mobile application use for emergency management affects the door-to-needle time and functional outcomes in acute ischemic stroke. *J. Stroke Cerebrovasc. Dis.* 32 (4), 107055. doi:10.1016/j.jstrokecerebrovasdis.2023.107055

Rihel, J. (2018). Copper on the brain. *Nat. Chem. Biol.* 14 (7), 638–639. doi:10.1038/s41589-018-0089-1

Ruiz, L. M., Libedinsky, A., and Elorza, A. A. (2021). Role of copper on mitochondrial function and metabolism. *Front. Mol. Biosci.* 8, 711227. doi:10.3389/fmolb.2021.711227

Ruttkay-Nedecky, B., Nejdl, L., Gumulec, J., Zitka, O., Masarik, M., Eckschlager, T., et al. (2013). The role of metallothionein in oxidative stress. *Int. J. Mol. Sci.* 14 (3), 6044–6066. doi:10.3390/ijms14036044

Ryan, F., Zarruk, J. G., Lößlein, L., and David, S. (2019). Ceruloplasmin plays a neuroprotective role in cerebral ischemia. *Front. Neurosci.* 12, 988. doi:10.3389/fnins.2018.00988

Samygina, V. R., Sokolov, A. V., Bourenkov, G., Schneider, T. R., Anashkin, V. A., Kozlov, S. O., et al. (2017). Rat ceruloplasmin: a new labile copper binding site and zinc/copper mosaic. *Metallomics* 9 (12), 1828–1838. doi:10.1039/c7mt00157f

Sánchez-González, C., Moreno, L., Aranda, P., Montes-Bayón, M., Llopis, J., and Rivas-García, L. (2022). Effect of bis (maltolato) oxovanadium (IV) on zinc, copper, and manganese homeostasis and DMT1 mRNA expression in streptozotocin-induced hyperglycemic rats. *Biol. (Basel).* 11 (6), 814. doi:10.3390/biology11060814

Sanghai, N., and Tranmer, G. K. (2021). Hydrogen peroxide and amyotrophic lateral sclerosis: from biochemistry to pathophysiology. *Antioxidants (Basel)* 11 (1), 52. doi:10.3390/antiox11010052

Scheiber, I. F., Mercer, J. F., and Dringen, R. (2014). Metabolism and functions of copper in brain. *Prog. Neurobiol.* 116, 33–57. doi:10.1016/j.pneurobio.2014.01.002

Schilsky, M. L., Roberts, E. A., Bronstein, J. M., Dhawan, A., Hamilton, J. P., Rivard, A. M., et al. (2023). A multidisciplinary approach to the diagnosis and management of Wilson disease: executive summary of the 2022 practice guidance on Wilson disease from the American association for the study of liver diseases. *Hepatology* 77 (4), 1428–1455. doi:10.1002/hep.32805

Schoeberl, A., Gutmann, M., Theiner, S., Corte-Rodríguez, M., Braun, G., Vician, P., et al. (2022a). The copper transporter CTR1 and cisplatin accumulation at the single-cell level by LA-ICP-TOFMS. *Front. Mol. Biosci.* 9, 1055356. doi:10.3389/fmolb.2022.1055356

Schoeberl, A., Gutmann, M., Theiner, S., Corte-Rodríguez, M., Braun, G., Vician, P., et al. (2022b). The copper transporter CTR1 and cisplatin accumulation at the single-cell level by LA-ICP-TOFMS. *Front. Mol. Biosci.* 9, 1055356. doi:10.3389/fmolb.2022.1055356

Schulz, V., Basu, S., Freibert, S. A., Webert, H., Boss, L., Mühlenhoff, U., et al. (2023). Functional spectrum and specificity of mitochondrial ferredoxins FDX1 and FDX2. *Nat. Chem. Biol.* 19 (2), 206–217. doi:10.1038/s41589-022-01159-4

Shang, J., Jiao, J., Yan, M., Wang, J., Li, Q., Shabuerjiang, L., et al. (2023). Chrysin protects against cerebral ischemia-reperfusion injury in hippocampus via restraining oxidative stress and transition elements. *Biomed. Pharmacother.* 161, 114534. doi:10.1016/j.biopha.2023.114534

Shawki, A., Anthony, S. R., Nose, Y., Engevik, M. A., Niespodzany, E. J., Barrientos, T., et al. (2015). Intestinal DMT1 is critical for iron absorption in the mouse but is not required for the absorption of copper or manganese. *Am. J. Physiol. Gastrointest. Liver Physiol.* 309 (8), G635–G647. doi:10.1152/ajpgi.00160.2015

Shi, W., Zhang, H., Zhang, Y., Lu, L., Zhou, Q., Wang, Y., et al. (2023). Co-exposure to Fe, Zn, and Cu induced neuronal ferroptosis with associated lipid metabolism disorder via the ERK/cPLA2/AA pathway. *Environ. Pollut.* 336, 122438. doi:10.1016/j.envpol.2023.122438

Singla, A., Chen, Q., Suzuki, K., Song, J., Fedoseienko, A., Wijers, M., et al. (2021). Regulation of murine copper homeostasis by members of the COMMD protein family. *Dis. Model Mech.* 14 (1), dmm045963. doi:10.1242/dmm.045963

Slezak, J., Kura, B., LeBaron, T. W., Singal, P. K., Buday, J., and Barancik, M. (2021). Oxidative stress and pathways of molecular hydrogen effects in medicine. *Curr. Pharm. Des.* 27 (5), 610–625. doi:10.2174/1381612826666200821114016

Song, G., Dong, H., Ma, D., Wang, H., Ren, X., Qu, Y., et al. (2021). Tetrahedral framework nucleic acid delivered RNA therapeutics significantly attenuate pancreatic cancer progression via inhibition of CTR1-dependent copper absorption. *ACS Appl. Mater Interfaces* 13 (39), 46334–46342. doi:10.1021/acsami.1c13091

Strenkert, D., Schmollinger, S., Paruthiyil, S., Brown, B. C., Green, S., Shafer, C. M., et al. (2024). Distinct function of Chlamydomonas CTRA-CTR transporters in Cu assimilation and intracellular mobilization. *Metallomics* 16 (3), mfae013. doi:10.1093/mtomcs/mfae013

Swaminathan, A. B., and Gohil, V. M. (2022). The role of COA6 in the mitochondrial copper delivery pathway to cytochrome c oxidase. *Biomolecules* 12 (1), 125. doi:10.3390/biom12010125

Tadini-Buoninsegni, F., and Smeazzetto, S. (2017). Mechanisms of charge transfer in human copper ATPases ATP7A and ATP7B. *IUBMB Life* 69 (4), 218–225. doi:10.1002/iub.1603

Tapiero, H., Townsend, D. M., and Tew, K. D. (2003). Trace elements in human physiology and pathology. Copper. *Copp. Biomed. Pharmacother.* 57 (9), 386–398. doi:10.1016/s0753-3322(03)00012-x

Trist, B. G., Hilton, J. B., Hare, D. J., Crouch, P. J., and Double, K. L. (2021). Superoxide dismutase 1 in health and disease: how a frontline antioxidant becomes neurotoxic. *Angew. Chem. Int. Ed. Engl.* 60 (17), 9215–9246. doi:10.1002/anie.202000451

Tsai, C. Y., Finley, J. C., Ali, S. S., Patel, H. H., and Howell, S. B. (2012). Copper influx transporter 1 is required for FGF, PDGF and EGF-induced MAPK signaling. *Biochem. Pharmacol.* 84 (8), 1007–1013. doi:10.1016/j.bcp.2012.07.014

Tsang, T., Davis, C. I., and Brady, D. C. (2021). Copper biology. *Curr. Biol.* 31 (9), R421–R427. doi:10.1016/j.cub.2021.03.054

Tsvetkov, P., Coy, S., Petrova, B., Dreishpoon, M., Verma, A., Abdusamad, M., et al. (2022). Copper induces cell death by targeting lipoylated TCA cycle proteins. *Science* 375 (6586), 1254–1261. doi:10.1126/science.abf0529

Tury, S., Chauveau, L., Lecante, A., Courgnaud, V., and Battini, J. L. (2023). A co-opted endogenous retroviral envelope promotes cell survival by controlling CTR1-mediated copper transport and homeostasis. *Cell Rep.* 42 (9), 113065. doi:10.1016/j.celrep.2023.113065

Ulrich, K., and Jakob, U. (2019). The role of thiols in antioxidant systems. *Free Radic. Biol. Med.* 140, 14–27. doi:10.1016/j.freeradbiomed.2019.05.035

Valko, M., Morris, H., and Cronin, M. T. (2005). Metals, toxicity and oxidative stress. *Curr. Med. Chem.* 12 (10), 1161–1208. doi:10.2174/0929867053764635

Vasilyev, V. B. (2019). Looking for a partner: ceruloplasmin in protein-protein interactions. *Biometals* 32 (2), 195–210. doi:10.1007/s10534-019-00189-1

Vendelboe, T. V., Harris, P., Zhao, Y., Walter, T. S., Harlos, K., El Omari, K., et al. (2016). The crystal structure of human dopamine β-hydroxylase at 2.9 Å resolution. *Sci. Adv.* 2 (4), e1500980. doi:10.1126/sciadv.1500980

Vercellino, I., and Sazanov, L. A. (2022). The assembly, regulation and function of the mitochondrial respiratory chain. *Nat. Rev. Mol. Cell Biol.* 23 (2), 141–161. doi:10.1038/s41580-021-00415-0

Wang, D., Tian, Z., Zhang, P., Zhen, L., Meng, Q., Sun, B., et al. (2023b). The molecular mechanisms of cuproptosis and its relevance to cardiovascular disease. *Biomed. Pharmacother.* 163, 114830. doi:10.1016/j.biopha.2023.114830

Wang, L., Yin, Y. L., Liu, X. Z., Shen, P., Zheng, Y. G., Lan, X. R., et al. (2020). Current understanding of metal ions in the pathogenesis of Alzheimer's disease. *Transl. Neurodegener.* 9, 10. doi:10.1186/s40035-020-00189-z

Wang, X., Lou, Q., Fan, T., Zhang, Q., Yang, X., Liu, H., et al. (2023c). Copper transporter Ctr1 contributes to enhancement of the sensitivity of cisplatin in esophageal squamous cell carcinoma. *Transl. Oncol.* 29, 101626. doi:10.1016/j.tranon.2023.101626

Wang, Z., Jin, D., Zhou, S., Dong, N., Ji, Y., An, P., et al. (2023a). Regulatory roles of copper metabolism and cuproptosis in human cancers. *Front. Oncol.* 13, 1123420. doi:10.3389/fonc.2023.1123420

Washington-Hughes, C. L., Roy, S., Seneviratne, H. K., Karuppagounder, S. S., Morel, Y., Jones, J. W., et al. (2023). Atp7b-dependent choroid plexus dysfunction causes transient copper deficit and metabolic changes in the developing mouse brain. *PLoS Genet.* 19 (1), e1010558. doi:10.1371/journal.pgen.1010558

Watson, S. A., and McStay, G. P. (2020). Functions of cytochrome c oxidase assembly factors. *Int. J. Mol. Sci.* 21 (19), 7254. doi:10.3390/ijms21197254

Weiler, B. D., Brück, M. C., Kothe, I., Bill, E., Lill, R., and Mühlenhoff, U. (2020). Mitochondrial [4Fe-4S] protein assembly involves reductive [2Fe-2S] cluster fusion on ISCA1-ISCA2 by electron flow from ferredoxin FDX2. *Proc. Natl. Acad. Sci. U. S. A.* 117 (34), 20555–20565. doi:10.1073/pnas.2003982117

Wen, M. H., Xie, X., Huang, P. S., Yang, K., and Chen, T. Y. (2021). Crossroads between membrane trafficking machinery and copper homeostasis in the nerve system. *Open Biol.* 11 (12), 210128. doi:10.1098/rsob.210128

White, C., Kambe, T., Fulcher, Y. G., Sachdev, S. W., Bush, A. I., Fritsche, K., et al. (2009). Copper transport into the secretory pathway is regulated by oxygen in macrophages. *J. Cell Sci.* 122 (Pt 9), 1315–1321. doi:10.1242/jcs.043216

Wu, Y., Liu, C., and Dong, W. (2023). Adjunctive therapeutic effects of micronutrient supplementation in inflammatory bowel disease. *Front. Immunol.* 14, 1143123. doi:10.3389/fimmu.2023.1143123

Xiyang, Y. B., Liu, R., Wang, X. Y., Li, S., Zhao, Y., Lu, B. T., et al. (2020). COX5A plays a vital role in memory impairment associated with brain aging via the BDNF/ERK1/2 signaling pathway. *Front. Aging Neurosci.* 12, 215. doi:10.3389/fnagi.2020.00215

Xu, W. Q., Wang, R. M., Dong, Y., and Wu, Z. Y. (2022). Emerging neurological symptoms after liver transplantation: a 6-year follow-up of an adolescent patient with Wilson's disease. *CNS Neurosci. Ther.* 28 (5), 788–791. doi:10.1111/cns.13798

Yang, S., Li, Y., Zhou, L., Wang, X., Liu, L., and Wu, M. (2024). Copper homeostasis and cuproptosis in atherosclerosis: metabolism, mechanisms and potential therapeutic strategies. *Cell Death Discov.* 10 (1), 25. doi:10.1038/s41420-023-01796-1

Yang, S., Wu, P., Xiao, J., and Jiang, L. (2019). Overexpression of COX6B1 protects against I/R-induced neuronal injury in rat hippocampal neurons. *Mol. Med. Rep.* 19 (6), 4852–4862. doi:10.3892/mmr.2019.10144

Yong, L., Shi, Y., Wu, H. L., Dong, Q. Y., Guo, J., Hu, L. S., et al. (2023). p53 inhibits CTR1-mediated cisplatin absorption by suppressing SP1 nuclear translocation in osteosarcoma. *Front. Oncol.* 12, 1047194. doi:10.3389/fonc.2022.1047194

You, S. Y., Rui, W., Chen, S. T., Chen, H. C., Liu, X. W., Huang, J., et al. (2019). Process of immunogenic cell death caused by disulfiram as the anti-colorectal cancer candidate. *Biochem. Biophys. Res. Commun.* 513 (4), 891–897. doi:10.1016/j.bbrc.2019.03.192

Yu, Y., Wu, Q., Niu, M., Gou, L., Tan, L., Fu, C., et al. (2022). A core-shell liquid metal-Cu nanoparticle with glutathione consumption via an *in-situ* replacement strategy for tumor combination treatment of chemodynamic, microwave dynamic and microwave thermal therapy. *Biomater. Sci.* 10 (13), 3503–3513. doi:10.1039/d2bm00435f

Zhang, M., Li, W., Wang, Y., Wang, T., Ma, M., and Tian, C. (2020). Association between the change of serum copper and ischemic stroke: a systematic review and meta-analysis. *J. Mol. Neurosci.* 70 (3), 475–480. doi:10.1007/s12031-019-01441-6

Zhang, P., Li, B., Chen, Q., Wang, H., and Feng, Q. (2022). Glucose restriction induces ROS-AMPK-mediated CTR1 expression and increases cisplatin efficiency in NSCLC. *Cancer Lett.* 543, 215793. doi:10.1016/j.canlet.2022.215793

Zhang, P., Zhou, C., Ren, X., Jing, Q., Gao, Y., Yang, C., et al. (2024). Inhibiting the compensatory elevation of xCT collaborates with disulfiram/copper-induced GSH consumption for cascade ferroptosis and cuproptosis. *Redox Biol.* 69, 103007. doi:10.1016/j.redox.2023.103007

Zhang, W., He, Y., Kang, X., Wang, C., Chen, F., Kang, Z., et al. (2023a). Association between dietary minerals and glioma: a case-control study based on Chinese population. *Front. Nutr.* 10, 1118997. doi:10.3389/fnut.2023.1118997

Zhang, X., Jiang, Q., Su, Y., Bu, L., Sun, Z., Wu, X., et al. (2023c). AMPK phosphorylates and stabilises copper transporter 1 to synergise metformin and copper chelator for breast cancer therapy. *Br. J. Cancer* 128 (8), 1452–1465. doi:10.1038/s41416-022-02127-4

Zhang, Y., Zhou, Q., Lu, L., Su, Y., Shi, W., Zhang, H., et al. (2023b). Copper induces cognitive impairment in mice via modulation of cuproptosis and CREB signaling. *Nutrients* 15 (4), 972. doi:10.3390/nu15040972

Zhou, C., Yang, J., Liu, T., Jia, R., Yang, L., Sun, P., et al. (2023). Copper metabolism and hepatocellular carcinoma: current insights. *Front. Oncol.* 13, 1186659. doi:10.3389/fonc.2023.1186659

Zulkifli, M., Okonkwo, A. U., and Gohil, V. M. (2023). FDX1 is required for the biogenesis of mitochondrial cytochrome c oxidase in mammalian cells. *J. Mol. Biol.* 435 (23), 168317. doi:10.1016/j.jmb.2023.168317

frontiers | Frontiers in Pharmacology

TYPE Systematic Review
PUBLISHED 22 October 2024
DOI 10.3389/fphar.2024.1407669

OPEN ACCESS

EDITED BY
Viola B. Morris,
Emory University, United States

REVIEWED BY
Mina Bagheri Varzaneh,
University of Illinois Chicago, United States
Yongsheng Chen,
Jinan University, China

*CORRESPONDENCE
Lechang Zhan,
zlc6612@163.com

RECEIVED 15 April 2024
ACCEPTED 07 October 2024
PUBLISHED 22 October 2024

CITATION
Zhan J, Xu X, Zhu Y, Liu L, Chen H and Zhan L (2024) Shuxuening injection for treating acute ischemic stroke: a PRISMA-compliant systematic review and meta-analysis of randomized controlled trials.
Front. Pharmacol. 15:1407669.
doi: 10.3389/fphar.2024.1407669

Shuxuening injection for treating acute ischemic stroke: a PRISMA-compliant systematic review and meta-analysis of randomized controlled trials

Jie Zhan[1,2], Xiaowen Xu[3], Yanzhen Zhu[2], Lin Liu[3], Hongxia Chen[1,3,2] and Lechang Zhan[1,2]*

[1]Department of Rehabilitation, Guangdong Provincial Hospital of Chinese Medicine, The Second Affiliated Hospital of Guangzhou University of Chinese Medicine, Guangzhou, China, [2]The Second Clinical College of Guangzhou University of Chinese Medicine, Guangzhou, China, [3]Medical College of Acu-Moxi and Rehabilitation, Guangzhou University of Chinese Medicine, Guangzhou, China

Background: Using Shuxuening injection (SXNI) for acute ischemic stroke (AIS) is popular in China, but its efficacy and safety remain controversial.

Purpose: This study aims to assess the efficacy and safety of SXNI as an add-on therapy for AIS.

Study design: Systematic review and meta-analysis.

Methods: We searched for randomized controlled trials (RCTs) on SXNI for AIS in seven databases and two clinical trial registration platforms from their inception to January 2023. We used the Cochrane risk of bias tool to assess the methodological quality of the included studies and performed the meta-analysis with R software. The primary outcome was clinical efficacy, assessed by the clinical effective rate (CER). The secondary outcomes were neurological function, activities of daily living (ADL), and adverse events (AEs).

Results: In total, 116 studies with 12,401 participants were included in this review. Fifteen (12.9%) studies were judged to be of moderate to high quality. SXNI plus conventional treatments (CTs) improved the CER compared with CTs alone (risk ratio [RR]: 1.21, 95% confidence interval [CI]: 1.17–1.25, $p < 0.0001$) or CTs plus other injections (RR: 1.18, 95% CI: 1.15–1.21, $p < 0.0001$). SXNI plus CTs reduced the National Institute of Health Stroke Scale score compared with CTs alone (mean difference [MD]: −4.00, 95% CI: −5.22 to −2.78, $p < 0.0001$) or CTs plus other injections (MD: −2.28, 95% CI: −3.41 to −1.16, $p < 0.0001$). SXNI plus CTs also decreased the Chinese Stroke Scale score compared with CTs alone (MD:

Abbreviations: ADL, activities of daily living; AEs, adverse events; AIS, acute ischemic stroke; BI, Barthel index; CBM, Chinese biological medicine database; CI, confidence interval; CER, clinical effective rate; CNKI, China national knowledge infrastructure; CONSORT, consolidated standards of reporting trials; CSS, Chinese Stroke Scale; CT, computed tomography; CTs, conventional treatments; EVT, endovascular thrombectomy; GBE, Ginkgo biloba extract; GRADE, Grading of Recommendation, Assessment, Development, and Evaluation; IVT, intravenous thrombolysis; MRI, magnetic resonance imaging; CND, clinical neurological deficit; NIHSS, National Institutes of Health Stroke Scale; RCTs, randomized controlled trials; ROB, risk of bias; RR, risk ratio; SMD, standardized mean difference; SXNI, shuxuening injection; PAF, platelet-activating factor; PRISMA, preferred reporting items for systematic reviews and meta-analysis; VIP, Chinese scientific journal database; WMD, weighted mean difference.

−5.01, 95% CI: −7.38 to −2.65, $p < 0.0001$) or CTs plus other injections (MD: −4.31, 95% CI: −5.75 to −2.88, $p < 0.0001$). SXNI plus CTs was superior for increasing the Barthel index score compared with CTs alone (MD: 11.58, 95% CI: 8.27–14.90, $p < 0.0001$) or CTs plus other injections (MD: 5.43, 95% CI: 0.48–10.39, $p = 0.0317$). The level of evidence for each outcome was assessed as low to very low. The most common AEs of SXNI were cardiovascular system events, and all these AEs were mild.

Conclusion: SXNI combined with CTs maybe better than CTs alone or CTs plus other injections for improving the clinical efficacy, neurological function, and ADL of AIS patients, with relatively reliable safety. However, due to the low quality of the included studies, more rigorously designed RCTs with large sample sizes should be conducted in the future.

Systematic Review Registration: www.crd.york.ac.uk, identifier (CRD42023418565).

KEYWORDS

shuxuening injection, acute ischemic stroke, traditional Chinese medicine, systematic review, meta-analysis

1 Introduction

Stroke is the third leading cause of death and disability globally, especially in low- and middle-income countries (GBD, 2019 Stroke Collaborators, 2021). From 1990 to 2019, the absolute number of global stroke events increased by 70.0%, and stroke mortality increased by 43.0% worldwide (GBD, 2019 Stroke Collaborators, 2021). Stroke patients often have motor dysfunction, loss of activities of daily living (ADL) (Jørgensen et al., 1999), and a significant decline in quality of life, which prevents them from returning to work, thereby resulting in economic losses for the country's productivity (Rochmah et al., 2021). According to the American Heart Association, the total cost of stroke, including direct and indirect expenditures, is projected to increase from $105.2 billion in $2012 to $240.7 billion in 2030 (Ovbiagele et al., 2013).

Acute ischemic stroke (AIS) accounts for most of all strokes. The appropriate treatment for AIS is significantly associated with prognosis (Hasan et al., 2021; Rosa et al., 2022). The primary therapeutic goal of AIS is to restore perfusion of ischemic brain tissue, and the main treatments include intravenous thrombolysis (IVT) and/or endovascular thrombectomy (EVT) (Hasan et al., 2021). However, 3%–8% of patients receiving IVT experience symptomatic cerebral hemorrhage (Gumbinger et al., 2012). Due to the narrow time window, contraindications, and the relatively low recanalization rate of large artery occlusions, the number of AIS patients who benefit from IVT is not as large as expected (Bhatia et al., 2010). EVT can significantly improve the prognosis of stroke; however, most interventional neuroradiologists work in urban areas, while half of the world's population lives in rural areas, resulting in limited access to EVT (Wassélius et al., 2022). Therefore, it is necessary to find an effective and safe therapy with a longer time window to improve the prognosis of stroke and address its burden.

Shuxuening injection (SXNI) extracted from *Ginkgo biloba* is a commercial Chinese polyherbal preparation that is widely used for stroke in China (Cui et al., 2020; Li et al., 2023). SXNI can dilate blood vessels and improve blood circulation, and it is mainly used for ischemia cardio-cerebrovascular diseases, such as cerebral infarction, vasospasm and coronary heart disease. The pharmacologically active metabolites of SXNI are flavonol glycosides and ginkgolide (Smith et al., 1996; Shi et al., 2009). Numerous *in vitro* and *in vivo* studies have confirmed the neuroprotective effect of *G. biloba* extract (GBE) (Oyama et al., 1996; Guidetti et al., 2001; Ahlemeyer and Krieglstein, 2003). GBE can improve blood circulation, strengthen capillary walls, prevent thrombosis, and protect nerve cells from damage during hypoxia (Singh et al., 2019). Two studies (Oskouei et al., 2013; Li et al., 2017) showed that GBE was better than placebo or aspirin in improving stroke patients' neurological function, as assessed by the National Institutes of Health Stroke Scale (NIHSS). More interestingly, GBE can work within 1–3 h (Diamond et al., 2000). Compared with IVT or EVT, SXNI not only has a longer treatment time window and cheaper costs with fewer side effects (Li et al., 2023) but can also be implemented in urban and rural medical places without specially higher professional requirements for doctors. However, due to the complexity of the metabolites of SXNI, it requires more careful monitoring for patients to prevent adverse events (AEs) while administering the drug.

Previous systematic reviews published in 2011, 2012, and 2016 confirmed the efficacy of SXNI for treating AIS in terms of the clinical efficacy assessed by the clinical effective rate (CER), with a very low level of evidence. However, some outcomes that are conducive to assessing the overall status of stroke patients, such as neurological function assessed by internationally recognized tools (e.g., the NIHSS), activities of daily living (ADL), and AEs, were not reported in these reviews. In addition, numerous RCTs on SXNI for AIS have been published since 2016, and it is necessary to update the evidence. We aimed to comprehensively assess the efficacy and safety of SXNI as an add-on therapy for AIS in terms of clinical efficacy, neurological function, ADL, and AEs.

2 Methods

This study was conducted strictly following the Preferred Reporting Items for Systematic Reviews and Meta-Analysis (PRISMA) guidelines (Page et al., 2021). The protocol was registered at PROSPERO (www.crd.york.ac.uk), and the registration number was CRD42023418565.

2.1 Types of studies

All RCTs about SXNI for AIS were eligible for inclusion. The language of publication was not limited. We excluded case-control studies, retrospective studies, case reports, animal experiments, cell experiments, reviews, meta-analyses, clinical experiences, commentaries, and conference abstracts.

2.2 Participants

Patients who were older than 18 years and diagnosed with AIS according to the recognized guidelines or criteria and confirmed by computed tomography (CT) or magnetic resonance imaging (MRI) were included without limitations on sex, culture, nationality, or race. The duration of the stroke should have been less than 14 days. We excluded patients with hypoxic-ischemic encephalopathy and *postpartum* apoplexy.

2.3 Types of interventions

The SXNI group received SXNI combined with conventional treatments (CTs), and the non-SXNI group received CTs alone or CTs combined with other injections. According to the Chinese guidelines for the diagnosis and treatment of AIS 2018; Chinese Society of Neurology Chinese Stroke Society, 2018), CTs include IVT, EVT, antiplatelet drugs, neuroprotective agents, and symptomatic supportive treatment, such as the management of blood pressure and blood lipid and sugar levels. Other injections were defined as any monodrug of non-Ginkgo biloba extract, such as compound Danshen injection, Shuxuetong injection, and so on. The duration of treatment had to be between 14 and 30 days. There were no restrictions on daily dose or frequency.

2.4 Outcome measures

The primary outcome was clinical efficacy assessed by the CER. According to the scoring criteria for clinical neurological deficit (CND) in stroke patients (Fourth Session of Chinese National Cerebrovascular Conference, 1996), improvements in CND were classified into five categories: a) recovery: 90%–100% reduction in CND with a disability level of 0; b) significant improvement: 46%–89% reduction in CND with a disability level of 1–3; c) progress: 18%–45% reduction in CND; d) inefficacy: less than 17% reduction in CND; e) deterioration: greater increase in CND. CER = (a + b + c) cases/total cases × 100% (National Administration of Traditional Chinese Medicine, 1994; Zheng, 2002).

The secondary outcomes included a) neurological function assessed by the Chinese Stroke Scale (CSS) and the NIHSS; b) ADL assessed by the Barthel Index (BI); c) AEs. The CSS consists of eight dimensions with a total score of 45. A higher CSS score indicates that a patient's stroke is more severe (Fourth Session of Chinese National Cerebrovascular Conference, 1996). The NHISS consists of 15 items with a total score of 42 and is a validated tool for assessing the severity of acute stroke. The greater the NIHSS score is, the more severe the neurological deficit (Brott et al., 1989; Kwah and Diong, 2014). The highest BI score is 100, and the higher the BI score is, the better the individual's ability to perform ADLs (Mahoney and Barthel, 1965). The common AEs related to SXNI are headache, flushing, and so on.

2.5 Data sources and searches

Seven databases were searched from their inception to January 2023, including PubMed, the Cochrane Library, Embase, the China National Knowledge Infrastructure (CNKI), the WanFang Database, the Chinese Scientific Journal Database (VIP), and the Chinese Biological Medicine Database (CBM). We also searched the Chinese Clinical Trial Registry (http://www.chictr.org.cn/) and the U.S. Clinical Trial Registry (https://clinicaltrials.gov/). We screened the reference lists of all included studies to identify more eligible studies. The search terms included ("stroke" OR "palsy" OR "apoplexy" OR "apoplexia" OR "cerebrovascular disorders" OR "cerebral infarction" OR "infarct of brain" OR "cerebral hemorrhage" OR "intracerebral hemorrhage" OR "brain hemorrhage") AND ("shuxuening" OR "shuxuening injection" OR "Ginkgo Leaf" OR "Folium Ginkgo" OR "Chinese patent medicine"). The detailed search strategy is described in Supplementary Appendix 1.

2.6 Selection of studies

We not only removed reduplicated articles using NoteExpress 3.6 but also performed manual de-duplication. Then, two reviewers independently screened the literature based on predefined eligibility criteria. We first excluded irrelevant literature by reading the titles and abstracts and then reading the full texts to select eligible studies. When two or more studies reported the same RCT, we selected the study with the largest sample size, appropriate outcomes, and the earliest publication. We consulted a third reviewer to resolve any disagreements.

2.7 Data extraction and management

We developed standardized data extraction forms that included study information (e.g., author, publication year, city, and country), characteristics of participants (e.g., age, sex, and course of stroke), study design (e.g., sample size, interventions, administration methods, duration of intervention, and SXNI manufacturing company), and outcomes (e.g., CER, NIHSS, CSS, BI, and AEs). Two reviewers extracted the data independently and cross-checked the extracted data. We contacted the authors via email when the information in the article was unclear or insufficient. If there were disagreements on data extraction, a third reviewer was consulted.

2.8 Quality assessment

The quality of the included studies was evaluated by two reviewers using the Cochrane risk of bias (ROB) assessment tool (Higgins and Green, 2011). The ROB tool includes seven items:

random sequence generation, allocation concealment, blinding of participants and personnel, blinding of outcome assessment, incomplete outcome data, selective reporting, and other biases. Each item can be judged as "low risk", "high risk" or "unclear risk". If a study had a "low risk" of more than four domains, its overall quality was judged as high. Any disagreements between the two reviewers were resolved by a third reviewer.

2.9 Data synthesis

We used R software (version 4.1.2, https://cran.r-project.org/) and Review Manager software (version 5.4, Cochrane Collaboration, Copenhagen, Denmark) to analyze the data. Dichotomous data are expressed as risk ratios (RRs) and 95% confidence intervals (CIs). Continuous data assessed using the same scale are expressed as weighted mean differences (WMDs) and 95% CIs, whereas standardized mean differences (SMDs) and 95% CIs were used for the different scales. Statistical heterogeneity was assessed by I^2 and p values from the Cochrane Q test. $I^2 < 50\%$ and $p \geq 0.05$ indicated no heterogeneity among studies. A random effects model was used if heterogeneity existed; otherwise, the fixed effects model was used. $p < 0.05$ was considered to indicate a statistically significant difference.

2.10 Sensitivity analysis

We tested the stability of the meta-analysis results by alternating the random and fixed effects models. Moreover, we excluded each study in turn to test the robustness of the results.

2.11 Subgroup analysis

We performed a subgroup analysis based on the duration of intervention, daily dose, and different injections used in the control group. We also conducted mixed-effects meta-regression analysis using sample size (n ≤ 107 vs. n > 107), quality of studies (high vs. low), publication year, mean age (≤60 years old vs. > 60 years old vs. mixed), and total dose of SXNI (≤280 mL vs. > 280 mL) as covariates to search for sources of heterogeneity.

2.12 Publication bias

Publication bias was assessed with "funnel" and Egger's tests when the number of included studies was more than 10.

2.13 Quality of evidence

We evaluated the quality of evidence for each outcome using the Grading of Recommendation, Assessment, Development, and Evaluation (GRADE) tool (https://www.gradepro.org/). The GRADE included five domains: a) risk of bias, b) inconsistency, c) indirectness, d) imprecision, and e) other considerations, such as publication bias and number of included studies. The overall level of evidence for every outcome was judged as high, moderate, low, or very low. Any disagreement regarding the level of evidence was resolved through discussion and consultation.

3 Results

3.1 Study selection

A total of 4,061 records were retrieved, 2075 of which were duplicate publications. After removing 1,775 records that did not meet the criteria by screening the titles and abstracts, we read the full texts of 211 articles. Finally, 116 eligible studies were included in the meta-analysis. The details of the study selection process are displayed in Figure 1. The full citation details of the included and excluded studies are described in Supplementary Appendix 2.

3.2 Characteristics of the included studies

All included studies were conducted in China and published in Chinese, with publication years distributed between 2002 and 2023. The most frequent provinces of author affiliation were Henan, Shandong, Guangdong, and Hebei. The sample sizes were between 40 and 438, and the duration of AIS ranged from less than 12 h to 14 days. The intervention duration ranged from 14 to 30 days. The daily dose of SXNI varied from 2 to 30 mL. The total dose of SXNI was between 28 and 900 mL. Thirty-six studies with 3,568 participants compared the efficacy of SXNI plus CTs vs. CTs alone, and eight studies with 8,833 participants compared the efficacy of SXNI plus CTs vs. CTs plus other injections. Of the 116 studies, 102 reported the CER, 14 reported the BI, 44 reported the CSS, and 16 reported the NIHSS. The characteristics of the included studies are described in Table 1.

3.3 The quality of the included studies

Fifteen (12.9%) studies were judged to be of moderate to high quality (Table 2; Figure 2). Of 116 studies, 110 (94.8%) mentioned the word "randomization", 15 (12.9%) used random number table methods, and the remaining studies used incorrect or undetailed randomization methods. Five (4.3%) studies mentioned the word "blinding" without a detailed description of the specific methods. None of the studies reported allocation concealment. Three (2.6%) studies were judged as high risk because they did not conduct intention-to-treat analysis and did not specify the reason for case dropout. Nine (7.8%) studies were assessed as high risk for selective reporting based on the description of the methods in the article. All included studies were free of other sources of ROB.

3.4 Primary outcome

3.4.1 Clinical efficacy

3.4.1.1 SXNI plus CTs vs. CTs alone

Thirty-two studies with 3,056 participants reported the CER. We used a fixed effects model due to the low heterogeneity ($I^2 = 0\%$, $p =$

TABLE 1 Characteristics of the included RCTs. (Note. AEs, adverse events; BI, Barthel index; C, control group; CER, clinical effective rate; CSS, Chinese Stroke Scale; CTs, conventional treatments; d, day; F, female; h, hour; IVGTT, intravenous injection; M, male; NIHSS, National Institutes of Health Stroke Scale; NR, not reported; SXNI, shuxuening injection; T, treatment group; w, week.)

Study	Study sites	Sample size	Time since stroke		Age		Sex (M/F)		Interventions		Daily dose of SXNI	Intervention duration	SXNI manufacturing company	Outcomes
		T/C	T	C	T	C	T	C	T	C				
Cao M 2004	Hebei, China	35/40	11h-6d	12h-7d	41-78	43-76	22/13	26/14	SXNI + CTs	CTs + Compound Danshen injection	15 ml, qd, ivgtt	14 d	China Resources Double-crane Pharmaceutical Co., Ltd	CER, AEs
Cao XM 2015	Hebei, China	56/56	10–28h	10-28h	60 ± 1.2	60 ± 1.2	NR	NR	SXNI + CTs	CTs + Danshen injection	20 ml, qd, ivgtt	14 d	NR	CER, CSS
Chang CF 2015	Henan, China	150/128	6–72h	6-72h	64.9	63.7	98/52	84/44	SXNI + CTs	CTs + Compound Danshen injection	20 ml, qd, ivgtt	14 d	NR	CER, CSS, BI, AEs
Che YQ 2005	Liaoning, China	46/44	6–72h	6-72h	50-76	48-78	29/17	34/10	SXNI + CTs	CTs + Danshen injection	20 ml, qd, ivgtt	14 d	Xiamen Pengdao Pharmaceutical Co., Ltd	CER, CSS, AEs
Chen JJ 2014	Jiangsu, China	30/30	48h–1w	48h-1w	61 ± 5.26	62 ± 5.77	20/10	18/12	SXNI + CTs	CTs + Compound Danshen injection	20 ml, qd, ivgtt	14 d	NR	CER, AEs
Chen LY 2021	Hunan, China	35/35	<3d	<3d	57.84 ± 1.55	56.68 ± 1.39	20/15	18/17	SXNI + CTs	CTs + Edaravone injection	2 ml, qd, ivgtt	14 d	China Shineway Pharmaceutical Group Limited	NIHSS, BI
Chen R 2015	Jiangsu, China	39/39	32.47 ± 6.52h	32.47 ± 6.52h	65.38 ± 7.49	65.38 ± 7.49	NR	NR	SXNI + CTs	CTs + Compound Danshen injection	20 ml, qd, ivgtt	28 d	NR	CSS
Chen YF 2009	Shanghai, China	40/40	1-5d	1-5d	74.60 ± 7.53	72.95 ± 7.37	16/24	13/27	SXNI + CTs	CTs + Danshen injection	20 ml, qd, ivgtt	14 d	China Shineway Pharmaceutical Group Limited	CER
Chen ZC 2014	Guangdong, China	34/34	12-72 h	12-72 h	61.6 ± 4.3	58.6±5.3	22/12	18/16	SXNI + CTs	CTs + Chuanxiongqin injection	20 ml, qd, ivgtt	14 d	SHIYAO YINHU PHARMACENRTICAL CO., LTD	CER, AEs
Cheng ZL 2016	Hebei, China	40/40	15.4 ± 4.8h	16.1 ± 5.2h	58.7 ± 7.2	60.1 ± 6.8	25/15	23/17	SXNI + CTs	CTs	10 ml, qd, ivgtt	14 d	China Shineway Pharmaceutical Group Limited	CER
Cui YM 2014	Henan, China	62/62	≤48 h	≤48 h	62.8 ± 12.6	62.8 ± 12.6	NR	NR	SXNI + CTs	CTs + Venoruton injection	20 ml, qd, ivgtt	14 d	China Shineway Pharmaceutical Group Limited	CER
Dai YP 2008	Henan, China	80/80	l-7d	l-7d	38-82	40-81	44/36	47/33	SXNI + CTs	CTs + Venoruton injection	20 ml, qd, ivgtt	14 d	China Shineway Pharmaceutical Group Limited	CER, AEs
Du PK 2016	Henan, China	49/49	6.1 ± 1.9d	6.5 ± 1.4d	61.2 ± 3.7	63.1 ± 4.0	31/18	29/20	SXNI + CTs	CTs	20 ml, qd, ivgtt	14 d	Heilongjiang Zbd Pharmaceutical Co., Ltd	CER, CSS

(Continued on following page)

10.3389/fphar.2024.1407669

TABLE 1 (*Continued*) Characteristics of the included RCTs. (Note. AEs, adverse events; BI, Barthel index; C, control group; CER, clinical effective rate; CSS, Chinese Stroke Scale; CTs, conventional treatments; d, day; F, female; h, hour; IVGTT, intravenous injection; M, male; NIHSS, National Institutes of Health Stroke Scale; NR, not reported; SXNI, shuxuening injection; T, treatment group; w, week.)

Study	Study sites	Sample size	Time since stroke		Age		Sex (M/F)		Interventions		Daily dose of SXNI	Intervention duration	SXNI manufacturing company	Outcomes
		T/C	T	C	T	C	T	C	T	C				
Du XL 2010	Beijing, China	99/99	1.7 ± 0.5d	1.9 ± 0.3d	69.1 ± 4.4	67.3 ± 3.7	54/50	51/51	SXNI + CTs	CTs	20 ml, qd, ivgtt	14 d	China Shineway Pharmaceutical Group Limited	NIHSS, AEs
Feng JW 2017	Shandong, China	47/47	6.15 ± 1.29h	6.02 ± 1.26h	56.89 ± 12.67	58.05 ± 10.38	26/21	27/20	SXNI + CTs	CTs + Danshen injection	30 ml, qd, ivgtt	14 d	China Shineway Pharmaceutical Group Limited	CER
Gao YD 2011	Zhejiang, China	60/60	<72h	<72h	45-85	46-87	39/21	40/20	SXNI + CTs	CTs	20 ml, qd, ivgtt	14 d	NR	CER, CSS, AEs
Ge J 2013	Henan, China	70/67	6-24h	6-24h	61.23 ± 12.98	60.88 ± 11.75	39/31	38/29	SXNI + CTs	CTs + Compound Danshen injection	10 ml, qd, ivgtt	14 d	Langzhi Group Wanrong Pharmaceutical Co., Ltd.	CER, AEs
Guo WJ 2013	Hebei, China	35/35	l-3d	l-3d	58.38 ± 4.27	61.32 ± 5.88	20/15	19/16	SXNI + CTs	CTs	20 ml, qd, ivgtt	14 d	China Resources Double-crane Pharmaceutical Co., Ltd	CER, AEs
He J 2010	Anhui, China	40/40	1-3d	1-3d	58-72	59-74	32/8	28/12	SXNI + CTs	CTs + Compound Danshen injection	20 ml, qd, ivgtt	30 d	NR	CER, AEs
He JQ 2013	Guangdong, China	39/39	<12h	<12h	71.2 ± 2.3	72.1±2.1	30/9	31/8	SXNI + CTs	CTs	10 ml, qd, ivgtt	20 d	NR	CER
He XY 2006	Sichuan, China	30/30	<12h	<12h	78.69 ± 6.21	78.69 ± 6.21	NR	NR	SXNI + CTs	CTs	25 ml, qd, ivgtt	15 d	NR	CER, AEs
Hua GC 2002	Shanghai, China	60/32	36 ± 0.4h	35 ± 0.6h	69 ± 3.2	68 ± 4.1	36/24	17/15	SXNI + CTs	CTs + Ginaton injection	25 ml, qd, ivgtt	15 d	Beijing Wanhui Pharmaceutical Group	AEs
Huang DL 2009	Guangdong, China	40/40	12-96h	12-96h	38-72	39-71	27/13	28/12	SXNI + CTs	CTs + Compound Danshen injection	20 ml, qd, ivgtt	14 d	NR	CER, AEs
Huang JL 2010	Shaanxi, China	60/60	30 min-42 h	1-39 h	55.2 ± 8.5	56.6 ± 7.9	35/25	37/23	SXNI + CTs	CTs	20 ml, qd, ivgtt	28 d	Boan Brothers Pharmaceutical Co., Ltd	ESS, CER, BI
Huang M 2004	Guangdong, China	30/30	6 h-3 d	6 h-3 d	65.3 ± 7.5	64.2 ± 8.1	18/12	20/10	SXNI + CTs	CTs + Compound Danshen injection	10 ml, qd, ivgtt	14 d	Langzhi Group Wanrong Pharmaceutical Co., Ltd	CSS
Huang XZ 2014	Fujian, China	64/60	<14d	<14d	86.7 ± 3.6	87.7 ± 2.8	44/20	38/22	SXNI + CTs	CTs + Rhadiola extract injection	20 ml, qd, ivgtt	14 d	Beijing China Rescources High-Tech Natural Pharmaceutical Co., Ltd	CER, AEs
Jia HB 2008	Liaoning, China	62/61	12-72h	12-72h	43-85	42-86	39/23	37/24	SXNI + CTs	CTs + Chuanxiongqin injection	20 ml, qd, ivgtt	14 d	Beijing China Rescources High-Tech Natural Pharmaceutical Co., Ltd	CER, CSS, AEs

(Continued on following page)

10.3389/fphar.2024.1407669

TABLE 1 (*Continued*) Characteristics of the included RCTs. (Note. AEs, adverse events; BI, Barthel index; C, control group; CER, clinical effective rate; CSS, Chinese Stroke Scale; CTs, conventional treatments; d, day; F, female; h, hour; IVGTT, intravenous injection; M, male; NIHSS, National Institutes of Health Stroke Scale; NR, not reported; SXNI, shuxuening injection; T, treatment group; w, week.)

Study	Study sites	Sample size	Time since stroke		Age		Sex (M/F)		Interventions		Daily dose of SXNI	Intervention duration	SXNI manufacturing company	Outcomes
		T/C	T	C	T	C	T	C	T	C				
Jia HY 2021	Henan, China	41/41	11.52 ± 1.47h	11.74 ± 1.51h	57.38 ± 4.67	57.95 ± 4.16	22/19	23/18	SXNI + CTs	CTs	20 ml, qd, ivgtt	14 d	NR	NIHSS, CER
Jiang BN 2009	Shandong, China	55/55	<72h	<72h	67 ± 8.31	70 ± 9.14	35/20	33/22	SXNI + CTs	CTs + Xuesaitong injection	10 ml, qd, ivgtt	21 d	Tonghua Guhong Pharmaceutical Co., Ltd	CER, CSS
Jiao XL 2008	Zhejiang, China	30/22	3h-7d	3h-7d	46-89	46-89	NR	NR	SXNI + CTs	CTs + Compound Danshen injection	20 ml, qd, ivgtt	28 d	NR	CER
Ji DY 2014	Shaanxi, China	62/60	8-28h	7-29h	41-77	40-78	38/24	36/24	SXNI + CTs	CTs + Danshen injection	20 ml, qd, ivgtt	14 d	NR	CER, AEs
Kou XF 2012	Henan, China	50/50	<72h	<72h	66.7 ± 9.3	66.7±9.3	NR	NR	SXNI + CTs	CTs	20 ml, qd, ivgtt	14 d	China Shineway Pharmaceutical Group Limited	NIHSS, CER, AEs
Lei GR 2014	Jiangxi, China	45/45	18.3 ± 5.1h	18.3 ± 5.1h	59.21 ± 7.4	59.21 ± 7.4	NR	NR	SXNI + CTs	CTs + Danshen injection	20 ml, qd, ivgtt	14 d	NR	CER
Li JH 2008	Beijing, China	44/44	<48h	<48h	61-82	61-80	32/12	34/10	SXNI + CTs	CTs + Compound Danshen injection	20 ml, qd, ivgtt	14 d	NR	CER, CSS, AEs
Li SJ 2014	Shaanxi, China	60/60	≤72h	≤72h	63.8 ± 1.5	63.8 ± 1.5	NR	NR	SXNI + CTs	CTs + Danshen injection	20 ml, qd, ivgtt	14 d	NR	CER, CSS, BI, AEs
Li XF 2014	Shandong, China	48/42	2.1 ± 1.0h	2.2 ± 1.2h	63.7 ± 5.9	64.1 ± 6.3	26/22	22/20	SXNI + CTs	CTs	20 ml, qd, ivgtt	28 d	NR	CSS
Li XH 2011	Jilin, China	120/120	≤7d	≤7d	42-78	40-77	NR	NR	SXNI + CTs	CTs	20 ml, qd, ivgtt	14 d	SHIYAO YINHU PHARMACENRTICAL CO., LTD	CER, CSS
Li XJ 2010	Sichuan, China	28/30	3.78 ± 1.96d	4.08 ± 2.11d	63.5 ± 4.3	62.8 ± 4.6	18/10	19/11	SXNI + CTs	CTs + Xuesaitong injection	20 ml, qd, ivgtt	14 d	China Resources Double-crane Pharmaceutical Co., Ltd	CER, CSS
Li XL 2023	Jiangsu, China	35/35	<14d	<14d	63.79 ± 4.83	63.02 ± 4.57	23/12	25/10	SXNI + CTs	CTs	20 ml, qd, ivgtt	14 d	China Shineway Pharmaceutical Group Limited	NIHSS, CER, BI
Li XR 2011	Guizhou, China	90/60	<72h	<72h	50.8 ± 8.7	60.7 ± 9.5	39/51	26/34	SXNI + CTs	CTs	10 ml, qd, ivgtt	14 d	China Shineway Pharmaceutical Group Limited	CSS
Li YJ 2018	Hebei, China	62/62	6-72h	6-72h	58.6 ± 3.4	59.2 ± 3.5	32/30	34/28	SXNI + CTs	CTs	20 ml, qd, ivgtt	14 d	Beijing China Rescources High-Tech Natural Pharmaceutical Co., Ltd	NIHSS, CER, BI

(Continued on following page)

10.3389/fphar.2024.1407669

TABLE 1 (*Continued*) Characteristics of the included RCTs. (Note. AEs, adverse events; BI, Barthel index; C, control group; CER, clinical effective rate; CSS, Chinese Stroke Scale; CTs, conventional treatments; d, day; F, female; h, hour; IVGTT, intravenous injection; M, male; NIHSS, National Institutes of Health Stroke Scale; NR, not reported; SXNI, shuxuening injection; T, treatment group; w, week.)

Study	Study sites	Sample size	Time since stroke		Age		Sex (M/F)		Interventions		Daily dose of SXNI	Intervention duration	SXNI manufacturing company	Outcomes
		T/C	T	C	T	C	T	C	T	C				
Li ZY 2013	Neimenggu, China	80/80	9-72h	9-72h	41-76	41-76	NR	NR	SXNI + CTs	CTs + Troxerutin injection	20 ml, qd, ivgtt	15 d	NR	NIHSS, CER, AEs
Lin YQ 2006	Guangdong, China	50/50	48h-1w	48h-1w	35-79	40-82	27/23	30/20	SXNI + CTs	CTs + Venoruton injection	6 ml, qd, ivgtt	15 d	NR	CER, AEs
Ling YX 2006	Guangdong, China	220/218	8.2 ± 4.5h	8.3 ± 4.8h	56.5 ± 21.5	57.2 ± 22.4	124/96	120/98	SXNI + CTs	CTs + Compound Danshen injection	12 ml, qd, ivgtt	15 d	NR	CER, AEs
Liu JX 2004	Shaanxi, China	60/46	1-5d	1-6d	41-83	42-84	32/28	24/22	SXNI + CTs	CTs	30 ml, qd, ivgtt	30 d	Beijing China Rescources High-Tech Natural Pharmaceutical Co., Ltd.	CER
Liu JX 2010	Tianjin, China	50/50	<72h	<72h	45-75	45-75	NR	NR	SXNI + CTs	CTs + Xuesaitong injection	20 ml, qd, ivgtt	14 d	Beijing China Rescources High-Tech Natural Pharmaceutical Co., Ltd	CER, AEs
Liu MF 2009	Henan, China	60/60	≤3d	≤3d	63.9 ± 8.7	63.9 ± 8.7	NR	NR	SXNI + CTs	CTs + Compound Danshen injection	16 ml, qd, ivgtt	14 d	NR	CER, AEs
Liu S 2004	Shandong,China	60/60	1-3d	1-3d	45-78	45-78	34/26	38/22	SXNI + CTs	CTs + Venoruton injection	12 ml, qd, ivgtt	14 d	Sanjiu Enterprise Group(Shenzhen Nanfang Pharmaceutical Plant)	AEs
Liu XH 2013	Hunan, China	82/82	≤12h	≤12h	77.8±9.2	76.5±8.7	75/7	76/6	SXNI + CTs	CTs + Compound Danshen injection	25 ml, qd, ivgtt	30 d	NR	CER
Liu XJ 2008	Liaoning, China	68/30	≤7d	≤7d	36-80	36-80	41/27	17/13	SXNI + CTs	CTs + Danshen injection	20 ml, qd, ivgtt	14 d	NR	CER, AEs
Liu XY 2016	Neimenggu, China	47/47	4.92 ± 1.21h	4.86 ± 1.12h	64.39 ± 9.26	64.28 ± 9.17	27/20	25/22	SXNI + CTs	CTs + Shuxuetong injection	20 ml, qd, ivgtt	14 d	China Shineway Pharmaceutical Group Limited	CER, CSS
Liu Y 2003	Jiangsu, China	56/48	≤48h	≤48h	<75	<75	NR	NR	SXNI + CTs	CTs + Danshen injection	20 ml, qd, ivgtt	14 d	China Resources Double-crane Pharmaceutical Co., Ltd	CER
Ma YX 2016	Jilin, China	43/43	2.18 ± 0.41d	2.34 ± 0.42d	60.34 ± 5.28	60.23 ± 5.32	24/19	23/20	SXNI + CTs	CTs + Danshen injection	20 ml, qd, ivgtt	14 d	NR	CER, CSS, BI
Mai Y 2005	Yunnan, China	34/30	1-5d	1-5d	61-84	63-86	28/6	25/5	SXNI + CTs	CTs	20 ml, qd, ivgtt	30 d	Langzhi Group Wanrong Pharmaceutical Co., Ltd	CER, CSS, AEs
Nie XP 2020	Jiangxi, China	44/44	4.62 ± 1.79h	4.57 ± 1.62h	66.8 ± 2.5	66.4 ± 2.6	22/22	20/24	SXNI + CTs	CTs	20 ml, qd, ivgtt	20 d	Beijing China Rescources High-Tech Natural Pharmaceutical Co., Ltd	CER, AEs

(Continued on following page)

10.3389/fphar.2024.1407669

TABLE 1 (*Continued*) Characteristics of the included RCTs. (Note. AEs, adverse events; BI, Barthel index; C, control group; CER, clinical effective rate; CSS, Chinese Stroke Scale; CTs, conventional treatments; d, day; F, female; h, hour; IVGTT, intravenous injection; M, male; NIHSS, National Institutes of Health Stroke Scale; NR, not reported; SXNI, shuxuening injection; T, treatment group; w, week.)

Study	Study sites	Sample size	Time since stroke		Age		Sex (M/F)		Interventions		Daily dose of SXNI	Intervention duration	SXNI manufacturing company	Outcomes
		T/C	T	C	T	C	T	C	T	C				
Peng J 2021	Hunan, China	37/37	4.21 ± 0.57h	4.39 ± 0.66h	64.25 ± 0.37	64.53 ± 0.84	20/17	21/16	SXNI + CTs	CTs	20 ml, qd, ivgtt	14 d	Shanxi Taiyuan Pharmaceutical Co., Ltd	NIHSS, BI
Qin DY 2014	Guangxi, China	30/30	6-24h	6-24h	42-78	45-76	20/10	18/12	SXNI + CTs	CTs	20 ml, qd, ivgtt	14 d	China Shineway Pharmaceutical Group Limited	CER, CSS
Qin QA 2013	Henan, China	120/116	9-28h	10-29h	41-75	40-76	76/44	70/46	SXNI + CTs	CTs + Danshen injection	20 ml, qd, ivgtt	14 d	NR	CER, CSS, AEs
Ren JM 2006	Jiangsu, China	38/34	≤48h	≤48h	64±8	62±7	20/18	18/16	SXNI + CTs	CTs + Danshen injection	20 ml, qd, ivgtt	14 d	NR	CER, AEs
Shang S 2014	Henan, China	44/44	<72h	<72h	37-81	36-79	27/17	26/18	SXNI + CTs	CTs + Compound Danshen injection	20 ml, qd, ivgtt	15 d	NR	CER, AEs
Shen DD 2017	Zhejiang, China	57/57	16.1 ± 4.12h	15.67 ± 3.78h	62.34 ± 4.01	61.46 ± 3.69	33/24	37/20	SXNI + CTs	CTs	20 ml, qd, ivgtt	14 d	NR	NIHSS, CER, AEs
Shi JP 2008	Henan, China	41/41	48-72h	48-72h	40-79	37-78	26/15	24/17	SXNI + CTs	CTs + Compound Danshen injection	20 ml, qd, ivgtt	15 d	Guizhou Yibai Pharmaceutical Co., Ltd	CER, CSS, AEs
Su HM 2007	Shanghai, China	36/32	8h-6d	9h-5d	53.5	55	22/14	21/11	SXNI + CTs	CTs + Danshen injection	20 ml, qd, ivgtt	15 d	NR	CER
Sun BJ 2014	Hebei, China	100/100	36.5 ± 13.5h	39.5 ± 16.3h	60.5 ± 14.6	63.5 ± 14.6	55/45	54/46	SXNI + CTs	CTs + Shuxuetong injection	20 ml, qd, ivgtt	14 d	NR	CER, CSS
Sun HY 2005	Zhejiang, China	52/51	9h-3d	9h-3d	39-78	41-77	34/18	32/19	SXNI + CTs	CTs + Danshen injection	12 ml, qd, ivgtt	15 d	Langzhi Group Wanrong Pharmaceutical Co., Ltd.	CER, CSS, AEs
Sun T 2019	XinJiang, China	20/20	≤24h	≤24h	59.4 ± 6.7	59.4 ± 6.7	NR	NR	SXNI + CTs	CTs + Compound Xueshuantong injection	20 ml, qd, ivgtt	14 d	Heilongjiang Zbd Pharmaceutical Co., Ltd	NIHSS, CER, AEs
Tai SEGL 2011	Xinjiang, China	60/60	≤3d	≤3d	58-86	56-86	48/12	47/13	SXNI + CTs	CTs + Compound Danshen injection	20 ml, qd, ivgtt	30 d	NR	CER, CSS
Tian ZC 2008	Shandong, China	56/24	1-10d	1-10d	62 ± 3.72	64.1 ± 3.86	NR	NR	SXNI + CTs	CTs + Danshen injection	20 ml, qd, ivgtt	21 d	NR	CSS, AEs
Wang DH 2023	Beijing, China	60/60	26.14 ± 5.32h	25.32 ± 4.94h	57.32 ± 8.56	58.59 ± 7.88	35/25	33/27	SXNI + CTs	CTs	20 ml, qd, ivgtt	14 d	SHIYAO YINHU PHARMACENRTICAL CO., LTD	NIHSS, CER, BI, AEs

(Continued on following page)

10.3389/fphar.2024.1407669

TABLE 1 (*Continued*) Characteristics of the included RCTs. (Note. AEs, adverse events; BI, Barthel index; C, control group; CER, clinical effective rate; CSS, Chinese Stroke Scale; CTs, conventional treatments; d, day; F, female; h, hour; IVGTT, intravenous injection; M, male; NIHSS, National Institutes of Health Stroke Scale; NR, not reported; SXNI, shuxuening injection; T, treatment group; w, week.)

Study	Study sites	Sample size	Time since stroke		Age		Sex (M/F)		Interventions		Daily dose of SXNI	Intervention duration	SXNI manufacturing company	Outcomes
		T/C	T	C	T	C	T	C	T	C				
Wang HL 2013	Beijing, China	40/40	19.1 ± 10.6h	18.6 ± 9.9h	66.7 ± 8.5	67.4 ± 9.1	22/18	23/17	SXNI + CTs	CTs + Edaravone injection	20 ml, qd, ivgtt	14 d	Heilongjiang Zbd Pharmaceutical Co., Ltd.	NIHSS, CER
Wang HR 2010	Chongqing, China	53/53	1-65h	0.5-61h	43-77	41-78	24/29	21/32	SXNI + CTs	CTs	20 ml, qd, ivgtt	28 d	Boan Brothers Pharmaceutical Co., Ltd	CER, CSS
Wang JF 2018	Shandong, China	32/32	15.27±4.24h	15.34±4.11h	70.41±1.33	70.34 ± 1.41	21/11	20/12	SXNI + CTs	CTs	20 ml, qd, ivgtt	14 d	SHIYAO YINHU PHARMACENRTICAL CO., LTD	CER
Wang MS 2012	Henan, China	106/106	<48h	<48h	67.4 ± 8.7	69.0 ± 9.8	70/36	68/38	SXNI + CTs	CTs	20 ml, qd, ivgtt	14 d	NR	CER, AEs
Wang QY 2012	Shanxi, China	40/40	<72h	<72h	48-67	44-70	27/13	25/15	SXNI + CTs	CTs + Compound Danshen injection	20 ml, qd, ivgtt	14 d	NR	CER, CSS, AEs
Wang SW 2014	Guangxi, China	31/30	0.5-7d	1-7d	49-78	50-77	20/11	21/9	SXNI + CTs	CTs + Compound Danshen injection	20 ml, qd, ivgtt	15 d	NR	CER, CSS, AEs
Wang WH 2006	Sichuan, China	30/30	<12h	<12h	78.69 ± 6.21	78.69 ± 6.21	NR	NR	SXNI + CTs	CTs	25 ml, qd, ivgtt	15 d	NR	CER, AEs
Wang XH 2015	Henan, China	51/51	4.01 ± 0.22d	4.01 ± 0.22d	62.1 ± 2.3	62.1 ± 2.3	NR	NR	SXNI + CTs	CTs + Xuesaitong injection	20 ml, qd, ivgtt	14 d	China Resources Double-crane Pharmaceutical Co., Ltd	CER, CSS
Wu J 2011	Henan, China	33/31	6h-3d	6h-3d	55.42 ± 11.72	56.03 ± 12.49	17/16	15/16	SXNI + CTs	CTs + Edaravone injection	16 ml, qd, ivgtt	14 d	Langzhi Group Wanrong Pharmaceutical Co., Ltd	CER, CSS
Wu XJ 2006	Hunan, China	30/30	1-3d	1-3d	65.80 ± 8.62	65.40 ± 8.40	16/14	17/13	SXNI + CTs	CTs + Compound Danshen injection	20 ml, qd, ivgtt	14 d	Shanxi Zhendong Taisheng Pharmaceutical Co., Ltd	CER, AEs
Wu Y 2011	Guangdong, China	30/30	6-72h	6-72h	60.21 ± 8.72	60.21 ± 8.72	NR	NR	SXNI + CTs	CTs	10 ml, qd, ivgtt	14 d	Langzhi Group Wanrong Pharmaceutical Co., Ltd	CER, AEs
Wu ZX 2004	Zhejiang, China	50/34	1-2d	1-2d	36-70	40-72	27/23	15/19	SXNI + CTs	CTs + Danshen injection	20 ml, qd, ivgtt	14 d	Langzhi Group Wanrong Pharmaceutical Co., Ltd	CER, AEs
Xiao DF 2022	Liaoning, China	40/40	18.02 ± 2.57h	17.96 ± 2.64h	66.84 ± 4.93	67.03 ± 5.22	21/19	22/18	SXNI + CTs	CTs	20 ml, qd, ivgtt	14 d	Heilongjiang Zbd Pharmaceutical Co., Ltd	NIHSS, CER, BI, AEs
Xie RP 2010	Shanxi, China	40/40	12-72h	12-72h	42-80	42-80	NR	NR	SXNI + CTs	CTs + Compound Danshen injection	20 ml, qd, ivgtt	15 d	China Shineway Pharmaceutical Group Limited	CER, AEs

(Continued on following page)

10.3389/fphar.2024.1407669

TABLE 1 (*Continued*) Characteristics of the included RCTs. (Note. AEs, adverse events; BI, Barthel index; C, control group; CER, clinical effective rate; CSS, Chinese Stroke Scale; CTs, conventional treatments; d, day; F, female; h, hour; IVGTT, intravenous injection; M, male; NIHSS, National Institutes of Health Stroke Scale; NR, not reported; SXNI, shuxuening injection; T, treatment group; w, week.)

Study	Study sites	Sample size	Time since stroke		Age		Sex (M/F)		Interventions		Daily dose of SXNI	Intervention duration	SXNI manufacturing company	Outcomes
		T/C	T	C	T	C	T	C	T	C				
Xie YQ 2004	Hunan, China	30/30	<7d	<7d	59.4	57.7	17/13	18/12	SXNI + CTs	CTs	25 ml, qd, ivgtt	15 d	China Resources Double-crane Pharmaceutical Co., Ltd	CER, CSS, BI, AEs
Xin FB 2005	Hubei, China	121/121	<24h	<24h	58 ± 8	60 ± 7	76/45	71/50	SXNI + CTs	CTs + Danshen injection	20 ml, qd, ivgtt	14 d	Langzhi Group Wanrong Pharmaceutical Co., Ltd	CER, CSS, AEs
Xiong SC 2011	Sichuan, China	40/40	5-22h	4-24h	51-75	50-72	22/28	23/17	SXNI + CTs	CTs + Danshen injection	20 ml, qd, ivgtt	20 d	NR	CER, CSS
Xu CY 2012	Shandong, China	60/60	<7d	<7d	41-82	40-81	32/28	38/22	SXNI + CTs	CTs + Compound Danshen injection	20 ml, qd, ivgtt	14 d	SHANGHAI ASIA PIONEER PHARMACENRTICAL CO., LTD	AEs
Xu L 2008	Henan, China	30/30	8h-1w	8h-1w	55.42 ± 11.72	56.03 ± 12.49	18/12	19/11	SXNI + CTs	CTs + Sodium Ozagrel injection	16 ml, qd, ivgtt	14 d	Langzhi Group Wanrong Pharmaceutical Co., Ltd	CER, CSS, AEs
Xu PF 2011	Guangdong, China	35/35	1-5d	1.05-5d	65 ± 9.2	66.8 ± 10.3	19/16	20/15	SXNI + CTs	CTs + Compound Danshen injection	20 ml, qd, ivgtt	14 d	Heilongjiang Zbd Pharmaceutical Co., Ltd	CER, AEs
Xue JY 2013	Henan, China	24/24	4.5 ± 1.8h	4.5 ± 1.8h	65.8 ± 5.2	65.8 ± 5.2	NR	NR	SXNI + CTs	CTs + Danshen injection	20 ml, qd, ivgtt	14 d	NR	CER
Yan TQ 2016	Shandong, China	45/45	12.4 ± 1.6h	14.1 ± 1.8h	54.2 ± 2.4	53.5 ± 2.5	25/20	23/22	SXNI + CTs	CTs	20 ml, qd, ivgtt	14 d	NR	CER
Yan XY 2010	Anhui, China	30/30	6-72h	6-72h	52.13 ± 9.71	58.32 ± 8.79	18/12	16/14	SXNI + CTs	CTs	20 ml, qd, ivgtt	14 d	China Shineway Pharmaceutical Group Limited	CER, AEs
Yang JH 2010	Hunan, China	48/48	<7d	<7d	46-75	47-75	26/22	25/23	SXNI + CTs	CTs	20 ml, qd, ivgtt	14 d	NR	CER, AEs
Yang M 2009	Anhui,China	30/30	<7d	<7d	66.3 ± 9.3	67.4 ± 8.6	NR	NR	SXNI + CTs	CTs + Sodium Ozagrel injection	20 ml, qd, ivgtt	14 d	NR	CER, AEs
Yang XW 2006	Guangdong, China	46/35	<48h	<48h	46-74	45-75	28/18	21/14	SXNI + CTs	CTs + Compound Xueshuantong injection	10 ml, qd, ivgtt	14 d	Langzhi Group Wanrong Pharmaceutical Co., Ltd	CER, AEs
Yin HX 2004	Guangdong, China	95/90	<48h	<48h	35-78	38-76	68/27	65/25	SXNI + CTs	CTs + Compound Danshen injection	10 ml, qd, ivgtt	14 d	Langzhi Group Wanrong Pharmaceutical Co., Ltd	CER, CSS, AEs
Yin ZL 2020	Jilin, China	34/34	12.46 ± 1.61h	12.48 ± 1.62h	56.17 ± 3.24	56.14 ± 3.26	20/14	19/15	SXNI + CTs	CTs	20 ml, qd, ivgtt	14 d	Tonghua Guhong Pharmaceutical Co., Ltd	NIHSS, CER

(Continued on following page)

10.3389/fphar.2024.1407669

TABLE 1 (*Continued*) Characteristics of the included RCTs. (Note. AEs, adverse events; BI, Barthel index; C, control group; CER, clinical effective rate; CSS, Chinese Stroke Scale; CTs, conventional treatments; d, day; F, female; h, hour; IVGTT, intravenous injection; M, male; NIHSS, National Institutes of Health Stroke Scale; NR, not reported; SXNI, shuxuening injection; T, treatment group; w, week.)

Study	Study sites	Sample size	Time since stroke		Age		Sex (M/F)		Interventions		Daily dose of SXNI	Intervention duration	SXNI manufacturing company	Outcomes
		T/C	T	C	T	C	T	C	T	C				
Yu BQ 2003	Jiangsu, China	66/75	11h-6d	11h-7d	67 ± 11.5	64 ± 12.4	42/36	49/41	SXNI + CTs	CTs + Compound Danshen injection	20 ml, qd, ivgtt	14 d	NR	CER, CSS, BI, AEs
Zang ZX 2010	Heilongjiang, China	65/62	9-72h	8-72h	62.5 ± 10.3	63.4 ± 9.89	41/24	38/24	SXNI + CTs	CTs + Danshen injection	20 ml, qd, ivgtt	14 d	China Shineway Pharmaceutical Group Limited	CER, CSS
Zhang GJ 2010	Heilongjiang, China	124/122	12-72h	12-72h	41-83	41-83	78/46	74/48	SXNI + CTs	CTs + Chuanxiongqin injection	20 ml, qd, ivgtt	14 d	NR	AEs
Zhang H 2009	Hubei, China	60/58	9-28h	10-29h	42-76	41-77	38/22	35/23	SXNI + CTs	CTs + Danshen injection	20 ml, qd, ivgtt	14 d	Beijing China Rescources High-Tech Natural Pharmaceutical Co., Ltd	CER, CSS, BI, AEs
Zhang HM 2004	Shandong, China	74/70	<7d	<7d	54-80	56-79	NR	NR	SXNI + CTs	CTs + Compound Danshen injection	20 ml, qd, ivgtt	14 d	NR	CER, CSS, AEs
Zhang HX 2006	Hebei, China	110/100	16.1 ± 8.4h	16 ± 8.5h	62.56 ± 12.37	62.52 ± 12.4	56/54	51/49	SXNI + CTs	CTs + Venoruton injection	20 ml, qd, ivgtt	15 d	China Resources Double-crane Pharmaceutical Co., Ltd	ESS, AEs
Zhang L 2007	Jilin, China	40/40	<72h	<72h	44-78	44-78	NR	NR	SXNI + CTs	CTs + Xuesaitong injection	10 ml, qd, ivgtt	14 d	NR	CER, AEs
Zhang L 2010	Henan, China	40/40	48h-1w	48h-1w	35-74	42-78	23/17	24/16	SXNI + CTs	CTs + Venoruton injection	6 ml, qd, ivgtt	15 d	NR	CER, AEs
Zhang MX 2018	Shanghai, China	40/40	<48h	<48h	43-81	43-81	26/14	26/14	SXNI + CTs	CTs + Compound Danshen injection	20 ml, qd, ivgtt	14 d	NR	CER, CSS
Zhang RL 2008	Shaanxi, China	67/62	1-6d	NR	36-75	36-75	46/21	44/18	SXNI + CTs	CTs	20 ml, qd, ivgtt	30 d	NR	CER, CSS, AEs
Zhang XK 2017	Shandong, China	62/62	<3d	<3d	58.66 ± 7.25	57.59 ± 9.31	32/30	33/29	SXNI + CTs	CTs + Danshen injection	20 ml, qd, ivgtt	14 d	NR	CER, CSS, AEs
Zhang XZ 2018	Henan, China	48/48	18.26 ± 2.32h	18.29 ± 2.30h	65.16 ± 4.62	65.19 ± 4.60	23/25	24/24	SXNI + CTs	CTs	20 ml, qd, ivgtt	14 d	China Shineway Pharmaceutical Group Limited	NIHSS, CER
Zhang YP 2004	Shanxi, China	66/58	6h-5d	6h-5d	45-78	42-80	38/28	35/23	SXNI + CTs	CTs + Compound Danshen injection	15 ml, qd, ivgtt	14 d	NR	CER, CSS
Zhao YX 2015	Henan, China	42/42	32.5 ± 9.4h	32.5 ± 9.4h	64.5 ± 8.1	64.5±8.1	NR	NR	SXNI + CTs	CTs + Edaravone injection	20 ml, qd, ivgtt	28 d	China Shineway Pharmaceutical Group Limited	NIHSS, BI, AEs

(Continued on following page)

10.3389/fphar.2024.1407669

10.3389/fphar.2024.1407669

TABLE 1 (*Continued*) Characteristics of the included RCTs. (Note. AEs, adverse events; BI, Barthel index; C, control group; CER, clinical effective rate; CSS, Chinese Stroke Scale; CTs, conventional treatments; d, day; F, female; h, hour; IVGTT, intravenous injection; M, male; NIHSS, National Institutes of Health Stroke Scale; NR, not reported; SXNI, shuxuening injection; T, treatment group; w, week.)

Study	Study sites	Sample size	Time since stroke		Age		Sex (M/F)		Interventions		Daily dose of SXNI	Intervention duration	SXNI manufacturing company	Outcomes
		T/C	T	C	T	C	T	C	T	C				
Zheng YZ 2014	Henan, China	36/36	<72h	<72h	47-76	47-76	NR	NR	SXNI + CTs	CTs + Xueshuantong injection	10 ml, bid, ivgtt	21 d	Datong Huida Pharmaceutical Co., Ltd	CER, AEs
Zhu L 2014	Shaanxi, China	73/73	5-24h	6-24h	62.5 ± 13.1	61.8 ± 12.5	40/33	38/35	SXNI + CTs	CTs + Compound Danshen injection	20 ml, qd, ivgtt	14 d	NR	CER, CSS, AEs
Zhu XJ 2013	Liaoning, China	51/30	18.02 ± 4.28h	18.02 ± 4.28h	62.41 ± 4.24	60.38 ± 6.02	21/30	18/12	SXNI + CTs	CTs	25 ml, qd, ivgtt	14 d	China Resources Double-crane Pharmaceutical Co., Ltd	CER
Zhuang JS 2004	Hebei, China	77/71	15-72h	15-72h	64.2 ± 9.7	65.4 ± 8.1	NR	NR	SXNI + CTs	CTs + Venoruton injection	20 ml, qd, ivgtt	15 d	NR	CER, AEs
Zi XH 2004	Hunan, China	28/26	<7d	<7d	69.2 ± 5.3	70 ± 6.6	NR	NR	SXNI + CTs	CTs + Sodium Ozagrel injection	25 ml, qd, ivgtt	15 d	NR	CER, AEs

Note: AEs, adverse events; BI, Barthel index; C, control group; CER, clinical effective rate; CSS, Chinese Stroke Scale; CTs, conventional treatments; d, day; F, female; h, hour; ivgtt, intravenous injection; M, male; NIHSS, National Institutes of Health Stroke Scale; NR, not report; SXNI, shuxuening injection; T, treatment group; w, week.

0.68). The meta-analysis results showed that SXNI plus CTs was superior to CTs alone in terms of the CER (*RR*: 1.21, *95% CI*: 1.17–1.25, $Z = 11.22$, $p < 0.05$) (Figure 3A). Sensitivity analysis was conducted by adjusting the random and fixed effects models (Supplementary Table S1) or excluding each study in turn (Supplementary Figure S1), which demonstrated that the results were robust. Subgroup analysis revealed that the effects of different daily doses and different intervention durations of SXNI on CER were not significantly different between SXNI plus CTs and CTs alone (Supplementary Figures S2, S3). Mixed-effect meta-regression analysis further revealed that the sample size, mean age, total dose of SXNI, publication year, and quality of studies were not the main sources of heterogeneity (Supplementary Table S2). Egger's test ($t = 4.80$, $p < 0.05$) and funnel plots revealed significant publication bias (Figure 4A).

3.4.1.2 SXNI plus CTs vs. CTs plus other injections

Seventy studies with 7,673 participants reported CER. A random effects model was used because of statistical heterogeneity ($I^2 = 25\%$, $p < 0.05$). The results of the meta-analysis showed that SXNI plus CTs was superior to CTs plus other injections in improving the CER (*RR*: 1.18, *95% CI*: 1.15–1.21, Z = 13.26, $p < 0.05$) (Figure 3B). By adjusting the analysis models (Supplementary Table S1) or removing each study in turn (Supplementary Figure S4), sensitivity analysis indicated that the results were robust. Subgroup analysis revealed that the effects of different daily doses, different intervention durations, and different injections on CER were not significantly different between SXNI plus CTs and CTs plus other injections (Supplementary Figures S5–7). Mixed-effect meta-regression models did not reveal sample size, mean age, total dose of SXNI, publication year, or quality of studies as sources of heterogeneity (Supplementary Table S2). The results of Egger's test ($t = 5.25$, $p < 0.05$) and funnel plots showed publication bias (Figure 4B).

3.5 Secondary outcomes

3.5.1 Neurological function

3.5.1.1 SXNI plus CTs vs. CTs alone

Eleven studies, including 1,126 participants, assessed neurological function using the NIHSS. We used a random effects model due to the significant heterogeneity ($I^2 = 98\%$, $p < 0.05$). SXNI plus CTs was superior for decreasing the NIHSS score compared with CTs alone (MD: −4.00, 95% CI: −5.22 to −2.78, Z = −6.42, $p < 0.05$) (Figure 5A). Sensitivity analysis was conducted by adjusting the random and fixed effects models (Supplementary Table S1) or deleting each study in turn (Supplementary Figure S8), which demonstrated that the meta-analysis results were robust. Mixed-effect meta-regression analysis revealed that the sample size, mean age, total dose of SXNI, publication year, and quality of studies did not contribute to the heterogeneity (Supplementary Table S2). Egger's test (t = −2.99, $p < 0.05$) and funnel plots revealed publication bias (Figure 4E).

Ten studies, including 1,117 participants, evaluated neurological function using CSS. Because of the significant heterogeneity ($I^2 = 99\%$, $p < 0.05$), we used a random effects model to pool the data. SXNI plus CTs was superior to CTs alone for decreasing the CSS

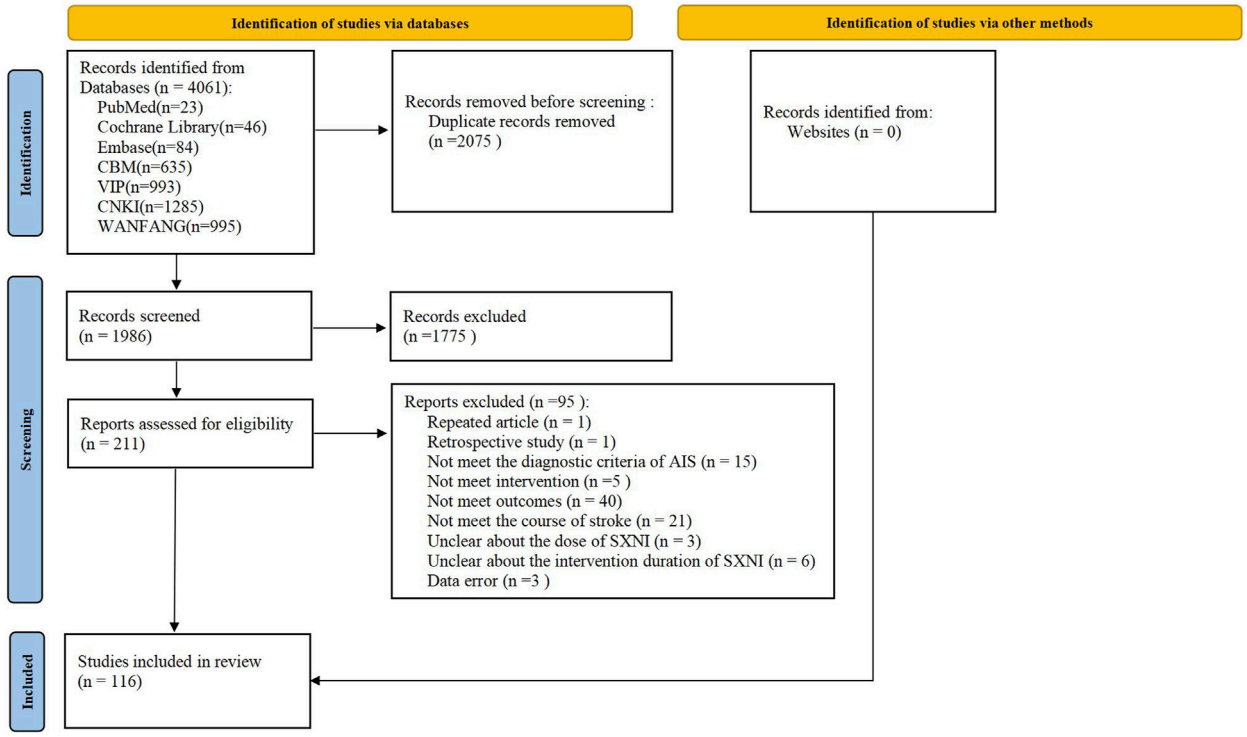

FIGURE 1
PRISMA flowchart of study selection.

(*MD*: −5.01, *95% CI*: −7.38 to −2.65, $Z = -4.15$; $p < 0.05$) (Figure 5B). By adjusting the analysis models (Supplementary Table S1) or removing each study in turn (Supplementary Figure S9), sensitivity analysis indicated that the results were robust. Mixed-effect meta-regression analysis based on sample size, mean age, total dose of SXNI, publication year, and quality of studies did not reveal sources of heterogeneity (Supplementary Table S2). Egger's test ($t = -0.36$, $p > 0.05$) and funnel plots revealed no publication bias (Figure 4C).

3.5.1.2 SXNI plus CTs vs. CTs plus other injections

Five studies with 434 participants assessed neurological function via the NIHSS. Because of significant heterogeneity ($I^2 = 84\%$, $p < 0.05$), we used a random effects model. The meta-analysis indicated that SXNI plus CTs improved the NIHSS score better than CTs plus other injections did (*MD*: −2.28, *95% CI*: −3.41 to −1.16, $Z = -3.97$, $p < 0.05$) (Figure 5C). Sensitivity analysis was conducted by adjusting the random and fixed effects models (Supplementary Table S1) or deleting each study in turn (Supplementary Figure S10), which demonstrated that the meta-analysis results were robust. No source of heterogeneity was found in mixed-effect meta-regression models based on sample size, mean age, total dose of SXNI, publication year, or quality of studies (Supplementary Table S2).

Thirty-four studies involving 3,996 participants assessed neurological function using the CSS. A random effects model was used to pool the data due to the significant heterogeneity ($I^2 = 99\%$, $p < 0.05$). The results of the meta-analysis showed that SXNI plus CTs decreased the CSS score in AIS patients more than CTs plus other injections did (*MD*: −4.31, *95% CI*: −5.75 to −2.88, $Z = -5.89$, $p < 0.05$) (Figure 5D). By adjusting the analysis models (Supplementary Table S1) or removing each study in turn (Supplementary Figure S11), sensitivity analysis indicated that the results were robust. Subgroup analysis indicated that the effects of different daily doses, different intervention durations, and different injections on decreasing the CSS score were not significantly different between SXNI plus CTs and CTs plus other injections (Supplementary Figures S12–14). Mixed-effect meta-regression models revealed that sample size, mean age, total dose of SXNI, publication year, and quality of studies were not the main sources of heterogeneity (Supplementary Table S2). Egger's test ($t = -1.20$, $p > 0.05$) and funnel plots revealed no publication bias (Figure 4D).

3.5.2 Activities of daily living

3.5.2.1 SXNI plus CTs vs. CTs alone

Seven studies with 648 participants assessed ADLs using the BI. We used a random effects model to pool the data because of the substantial heterogeneity ($I^2 = 96\%$, $p < 0.05$). The meta-analysis showed that SXNI plus CTs was better at improving the BI score than CTs alone (*MD*: 11.58, *95% CI*: 8.27–14.90, $Z = 6.84$, $p < 0.05$) (Figure 6A). By adjusting the analysis models (Supplementary Table S1) or removing each study in turn (Supplementary Figure S15), sensitivity analysis demonstrated the reliability of the results. Mixed-effect meta-regression analysis revealed that sample size, mean age, total dose of SXNI, publication year, and quality of studies were not the sources of heterogeneity (Supplementary Table S2).

10.3389/fphar.2024.1407669

TABLE 2 Quality assessment of the included studies using the Cochrane risk of bias (ROB) assessment tool[a].

Author, year	Random sequence generation	Allocation concealment	Blinding of participants and personnel	Blinding of outcome assessment	Incomplete outcome data	Selective reporting	Other bias	Overall quality
Cao M 2004	unclear	unclear	unclear	unclear	low	low	low	low
Cao XM 2015	unclear	unclear	unclear	unclear	low	low	low	low
Chang CF 2015	unclear	unclear	unclear	unclear	low	low	low	low
Che YQ 2005	unclear	unclear	unclear	unclear	low	low	low	low
Chen JJ 2014	unclear	unclear	unclear	unclear	low	low	low	low
Chen LY 2021	low	unclear	unclear	unclear	low	low	low	high
Chen R 2015	high	unclear	unclear	unclear	low	low	low	low
Chen YF 2009	unclear	unclear	unclear	unclear	low	low	low	low
Chen ZC 2014	low	unclear	unclear	unclear	low	low	low	high
Cheng ZL 2016	unclear	unclear	unclear	unclear	low	low	low	low
Cui YM 2014	unclear	unclear	unclear	unclear	low	low	low	low
Dai YP 2008	unclear	unclear	unclear	unclear	low	low	low	low
Du PK 2016	unclear	unclear	unclear	unclear	low	low	low	low
Du XL 2010	high	unclear	unclear	unclear	low	low	low	low
Feng JW 2017	low	unclear	unclear	unclear	low	low	low	high
Gao YD 2011	unclear	unclear	unclear	unclear	low	low	low	low
Ge J 2013	unclear	unclear	unclear	unclear	low	low	low	low
Guo WJ 2013	unclear	unclear	unclear	unclear	low	low	low	low
He J 2010	unclear	unclear	unclear	unclear	low	low	low	low
He JQ 2013	unclear	unclear	unclear	unclear	low	low	low	low
He XY 2006	unclear	unclear	unclear	unclear	low	low	low	low
Hua GC 2002	unclear	unclear	unclear	unclear	low	low	low	low
Huang DL 2009	high	unclear	unclear	unclear	low	low	low	low
Huang JL 2010	low	unclear	unclear	unclear	low	low	low	high
Huang M 2004	unclear	unclear	unclear	unclear	low	low	low	low
Huang XZ 2014	high	unclear	unclear	unclear	low	low	low	low
Ji DY 2014	unclear	unclear	unclear	unclear	low	low	low	low
Jia HB 2008	unclear	unclear	unclear	unclear	low	low	low	low
Jia HY 2021	unclear	unclear	unclear	unclear	low	low	low	low
Jiang BN 2009	unclear	unclear	unclear	unclear	low	low	low	low
Jiao XL 2008	unclear	unclear	unclear	unclear	low	low	low	low
Kou XF 2012	high	unclear	unclear	unclear	low	low	low	low
Lei GR 2014	unclear	unclear	unclear	unclear	low	low	low	low

(Continued on following page)

10.3389/fphar.2024.1407669

TABLE 2 (*Continued*) Quality assessment of the included studies using the Cochrane risk of bias (ROB) assessment tool[a].

Author, year	Random sequence generation	Allocation concealment	Blinding of participants and personnel	Blinding of outcome assessment	Incomplete outcome data	Selective reporting	Other bias	Overall quality
Li JH 2008	unclear	unclear	unclear	unclear	low	low	low	low
Li SJ 2014	high	unclear	unclear	unclear	low	low	low	low
Li XF 2014	high	unclear	unclear	unclear	low	low	low	low
Li XH 2011	unclear	unclear	unclear	unclear	low	low	low	low
Li XJ 2010	unclear	unclear	unclear	unclear	low	low	low	low
Li XL 2023	low	unclear	unclear	unclear	low	low	low	high
Li XR 2011	unclear	unclear	unclear	unclear	low	low	low	low
Li YJ 2018	low	unclear	unclear	unclear	low	low	low	high
Li ZY 2013	high	unclear	unclear	unclear	low	low	low	low
Lin YQ 2006	unclear	unclear	unclear	unclear	low	low	low	low
Ling YX 2006	unclear	unclear	unclear	unclear	low	low	low	low
Liu JX 2004	unclear	unclear	unclear	unclear	low	low	low	low
Liu JX 2010	unclear	unclear	unclear	unclear	low	low	low	low
Liu MF 2009	unclear	unclear	unclear	unclear	low	high	low	low
Liu S 2004	high	unclear	unclear	unclear	low	low	low	low
Liu XH 2013	unclear	unclear	unclear	unclear	low	low	low	low
Liu XJ 2008	unclear	unclear	unclear	unclear	low	low	low	low
Liu XY 2016	low	unclear	unclear	unclear	low	low	low	high
Liu Y 2003	unclear	unclear	unclear	unclear	low	high	low	low
Ma YX 2016	unclear	unclear	unclear	unclear	low	low	low	low
Mai Y 2005	unclear	unclear	unclear	unclear	low	high	low	low
Nie XP 2020	unclear	unclear	unclear	unclear	low	low	low	low
Peng J 2021	low	unclear	unclear	unclear	low	low	low	high
Qin DY 2014	unclear	unclear	unclear	unclear	low	low	low	low
Qin QA 2013	unclear	unclear	unclear	unclear	low	low	low	low
Ren JM 2006	unclear	unclear	unclear	unclear	low	low	low	low
Shang S 2014	unclear	unclear	unclear	unclear	low	low	low	low
Shen DD 2017	low	unclear	unclear	unclear	low	low	low	high
Shi JP 2008	unclear	unclear	unclear	unclear	low	low	low	low
Su HM 2007	unclear	unclear	unclear	unclear	low	low	low	low
Sun BJ 2014	unclear	unclear	unclear	unclear	low	low	low	low
Sun HY 2005	high	unclear	unclear	unclear	low	low	low	low
Sun T 2019	unclear	unclear	unclear	unclear	low	low	low	low
Tai SEGL 2011	unclear	unclear	unclear	unclear	low	high	low	low
Tian ZC 2008	unclear	unclear	unclear	unclear	low	low	low	low

(Continued on following page)

10.3389/fphar.2024.1407669

TABLE 2 (*Continued*) Quality assessment of the included studies using the Cochrane risk of bias (ROB) assessment tool[a].

Author, year	Random sequence generation	Allocation concealment	Blinding of participants and personnel	Blinding of outcome assessment	Incomplete outcome data	Selective reporting	Other bias	Overall quality
Wang DH 2023	low	unclear	unclear	unclear	low	low	low	high
Wang HL 2013	unclear	unclear	unclear	unclear	low	low	low	low
Wang HR 2010	low	unclear	unclear	unclear	low	low	low	high
Wang JF 2018	unclear	unclear	unclear	unclear	low	low	low	low
Wang MS 2012	unclear	unclear	unclear	unclear	low	low	low	low
Wang QY 2012	high	unclear	unclear	unclear	low	high	low	low
Wang SW 2014	unclear	unclear	unclear	unclear	low	low	low	low
Wang WH 2006	unclear	unclear	unclear	unclear	low	low	low	low
Wang XH 2015	high	unclear	unclear	unclear	low	low	low	low
Wu J 2011	low	unclear	unclear	unclear	low	low	low	high
Wu XJ 2006	unclear	unclear	unclear	unclear	low	low	low	low
Wu Y 2011	unclear	unclear	unclear	unclear	low	high	low	low
Wu ZX 2004	unclear	unclear	unclear	unclear	low	low	low	low
Xiao DF 2022	low	unclear	unclear	unclear	low	low	low	high
Xie RP 2010	unclear	unclear	unclear	unclear	low	low	low	low
Xie YQ 2004	unclear	unclear	unclear	unclear	low	low	low	low
Xin FB 2005	unclear	unclear	unclear	unclear	low	low	low	low
Xiong SC 2011	unclear	unclear	unclear	unclear	low	low	low	low
Xu CY 2012	unclear	unclear	unclear	unclear	low	low	low	low
Xu L 2008	unclear	unclear	unclear	unclear	low	low	low	low
Xu PF 2011	unclear	unclear	unclear	unclear	low	low	low	low
Xue JY 2013	unclear	unclear	unclear	unclear	low	low	low	low
Yan TQ 2016	unclear	unclear	unclear	unclear	low	low	low	low
Yan XY 2010	high	unclear	unclear	unclear	low	low	low	low
Yang JH 2010	low	unclear	unclear	unclear	low	low	low	high
Yang M 2009	unclear	unclear	unclear	unclear	low	low	low	low
Yang XW 2006	unclear	unclear	unclear	unclear	low	low	low	low
Yin HX 2004	unclear	unclear	unclear	unclear	low	low	low	low
Yin ZL 2020	low	unclear	unclear	unclear	low	low	low	high
Yu BQ 2003	high	unclear	unclear	unclear	low	low	low	low
Zang ZX 2010	unclear	unclear	unclear	unclear	high	high	low	low

(Continued on following page)

TABLE 2 (*Continued*) Quality assessment of the included studies using the Cochrane risk of bias (ROB) assessment tool[a].

Author, year	Random sequence generation	Allocation concealment	Blinding of participants and personnel	Blinding of outcome assessment	Incomplete outcome data	Selective reporting	Other bias	Overall quality
Zhang GJ 2010	unclear	unclear	unclear	unclear	low	low	low	low
Zhang H 2009	high	unclear	unclear	unclear	high	low	low	low
Zhang HM 2004	high	unclear	unclear	unclear	high	low	low	low
Zhang HX 2006	unclear	unclear	unclear	unclear	low	low	low	low
Zhang L 2007	unclear	unclear	unclear	unclear	low	low	low	low
Zhang L 2010	unclear	unclear	unclear	unclear	low	high	low	low
Zhang MX 2018	unclear	unclear	unclear	unclear	low	low	low	low
Zhang RL 2008	unclear	unclear	unclear	unclear	low	high	low	low
Zhang XK 2017	unclear	unclear	unclear	unclear	low	low	low	low
Zhang XZ 2018	unclear	unclear	unclear	unclear	low	low	low	low
Zhang YP 2004	high	unclear	unclear	unclear	low	low	low	low
Zhao YX 2015	unclear	unclear	unclear	unclear	low	low	low	low
Zheng YZ 2014	unclear	unclear	unclear	unclear	low	low	low	low
Zhu L 2014	unclear	unclear	unclear	unclear	low	low	low	low
Zhu XJ 2013	unclear	unclear	unclear	unclear	low	low	low	low
Zhuang JS 2004	unclear	unclear	unclear	unclear	low	low	low	low
Zi XH 2004	high	unclear	unclear	unclear	low	low	low	low

[a]Higgins, J.P.T., Green, S., 2011. Cochrane Handbook for Systematic Reviews of Interventions. London, The Cochrane Collaboration.

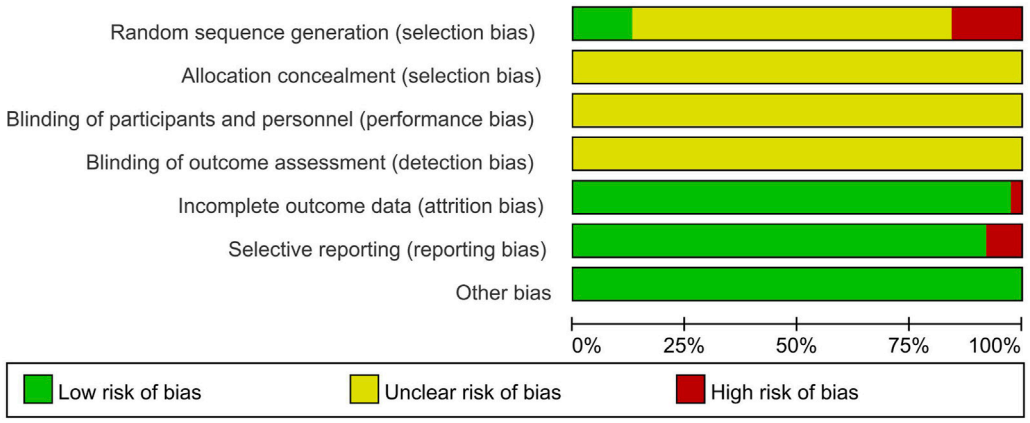

FIGURE 2
Risk of bias graph.

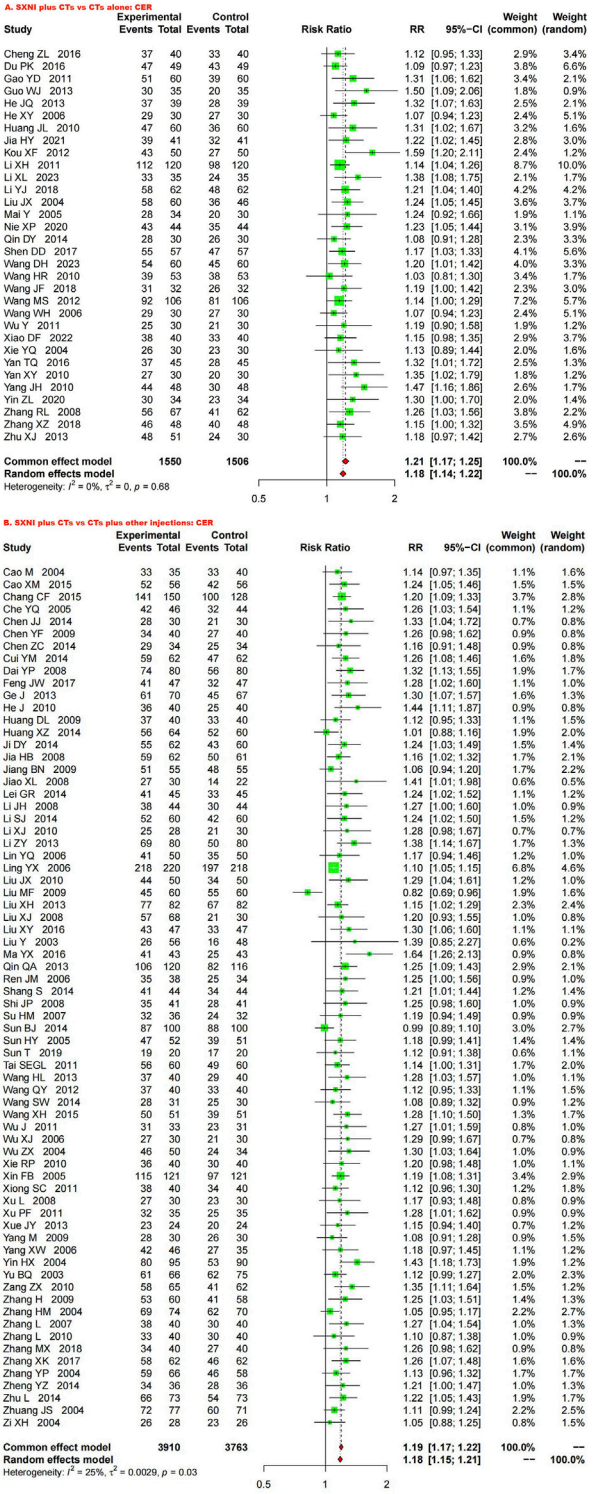

FIGURE 3
Forest plot and meta-analysis of clinical efficacy. (Note: CER, clinical effective rate; CTs, conventional treatments; SXNI, shuxuening injection).

3.5.2.2 SXNI plus CTs vs. CTs plus other injections

Seven studies involving 897 participants evaluated ADL by the BI. Due to significant heterogeneity (I^2 = 89%, p < 0.05), a random effects model was used. The results showed that SXNI plus CTs was superior to CTs plus other injections for increasing BI scores (*MD*: 5.43, *95% CI*: 0.48–10.39, Z = 2.15, p < 0.05) (Figure 6B). Sensitivity analysis by adjusting the statistical models showed that the meta-analysis results were robust (Supplementary Table S1). However, the difference in the BI scores between SXNI plus CTs and CTs plus other injections was not significant when five studies were removed one at a time (Chen, 2021; Li, 2014; Ma, 2016; Zhang et al., 2009; Zhao, 2015) (Supplementary Figure S16). Mixed-effect meta-regression did not reveal sample size, mean age, total dose of SXNI, publication year, or quality of studies as sources of heterogeneity (Supplementary Table S1).

3.6 AEs

Seventy-one studies reported AEs, and 49 reported no AEs. Twenty-two studies reported AEs related to the SXNI group or non-SXNI group, five of which did not report the number of AEs in the SXNI group, and two did not report the number of AEs in the non-SXNI group. SXNI plus CTs (1.53%, 61/3,994) was similarly safe to CTs alone or CTs plus other injections (1.32%, 50/3,797). The most common AEs related to SXNI were cardiovascular system events, and the five most common symptoms were dizziness, flushing, palpitations, nausea, and headache. The most common AEs related to the non-SXNI group were digestive system events, and the five most common symptoms were palpitations, nausea, dizziness, flushing, and vomiting. Moreover, all these symptoms in both the SXNI group and the non-SXNI group were mild and disappeared after discontinuation of the drug and symptomatic treatment. The symptoms of AEs are detailed in Supplementary Table S3.

3.7 Quality of evidence

We used the GRADE tool to systematically evaluate the quality of each outcome. The levels of evidence for CER and BI scores were low in SXNI plus CTs compared with CTs alone for AIS, while the levels of evidence for the NIHSS score and CSS score were very low (Table 3). Additionally, the level of evidence for the CER, NIHSS, CSS, and BI scores were all very low for SXNI plus CTs compared with CTs plus other injections for AIS (Table 3). The grade was decreased mainly because of the low methodological quality of the included studies, high heterogeneity among the included studies, and potential publication bias.

4 Discussion

4.1 Summary of the evidence

A total of 116 studies involving 12,401 participants were included in this review to assess the efficacy and safety of SXNI as an add-on therapy for patients with AIS. The meta-analysis results showed that SXNI plus CTs was superior to CTs alone or CTs plus other injections in improving patients' CER, NIHSS, CSS, and BI scores, suggesting that SXNI combined with CTs can significantly improve clinical efficacy, reduce neurological deficits,

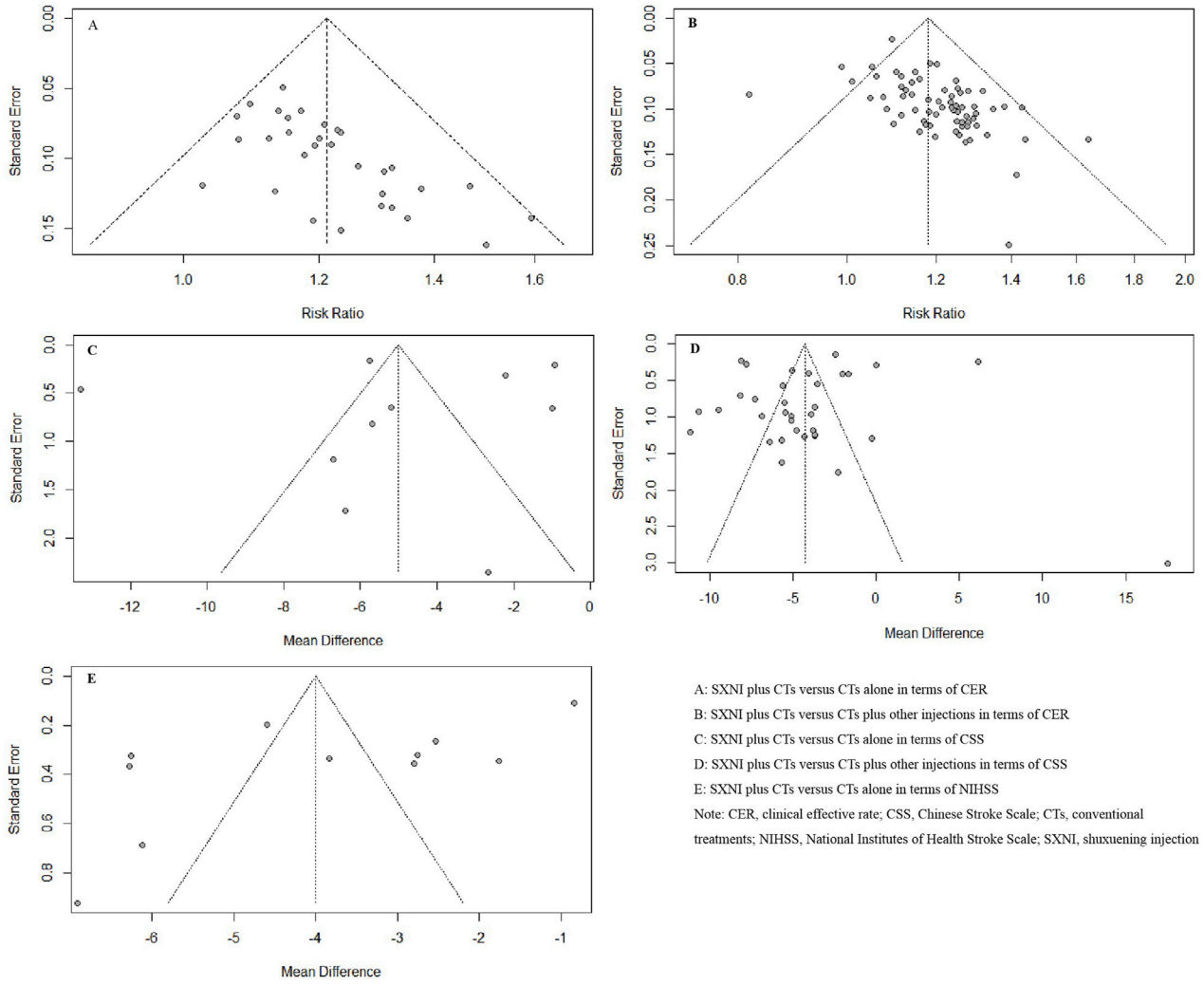

FIGURE 4
Funnel plots based on the CER, NIHSS, and CSS scores. (Note. CER, clinical effective rate; CSS, Chinese Stroke Scale; CTs, conventional treatments; NIHSS, National Institutes of Health Stroke Scale; SXNI, shuxuening injection).

and promote the recovery of ADL in patients with AIS. Subgroup analysis and mixed-effect meta-regression analysis indicated that duration of intervention, daily dose of SXNI, total dose of SXNI, sample size, mean age, different injections used in the control group, quality of studies, and publication year were not sources of heterogeneity. Except for the BI score between SXNI plus CTs and CTs plus other injections, the sensitivity analysis of the remaining indicators demonstrated that the meta-analysis results were robust. Sensitivity analysis revealed that the difference in BI scores between SXNI plus CTs and CTs plus other injections was not significant when five studies were removed one at a time (Chen, 2021; Li, 2014; Ma, 2016; Zhang et al., 2009; Zhao, 2015). In terms of safety, based on the results of this study, we cautiously believe that SXNI is relatively safe and reliable. Publication bias was found in the CER and NIHSS scores. Only 15 (12.9%) studies were judged to be of moderate to high quality. The levels of evidence for the CER, NIHSS, CSS, and BI scores were very low to low quality. Therefore, the results of this study should be considered with caution.

According to traditional Chinese medicine theory, the main pathological changes in AIS are qi deficiency and blood stasis. Qi is regarded as the main material basement that constitutes the human body and maintains life activities and an energy which manifests simultaneously on the physical and emotional-mental-spiritual level, and it has functions of promoting, warming, defense, transformative action and containment) (Jiang et al., 2023; Tian et al., 2024). Therefore, clinical treatment of this disease is mainly carried out by supplementing qi, promoting blood circulation, and dredging meridians and collaterals. SXNI is an extract of *G. biloba* leaves that promotes blood circulation, eliminates blood stasis, unblocks meridians, tonifies qi, and strengthens the brain (Ding, 2018; Zhang, 2019). From the perspective of Western medicine, SXNI can improve blood rheology, inhibit platelet aggregation, and reduce blood viscosity (Zhang et al., 2005). Ginkgolides can inhibit glutamate receptor-gated calcium channels, significantly reduce Ca^{2+} content in brain cells, prevent intracellular Ca^{2+} overload, and reduce cascade reaction-induced brain cell necrosis (Chandrasekaran et al., 2001). SXNI can improve the energy

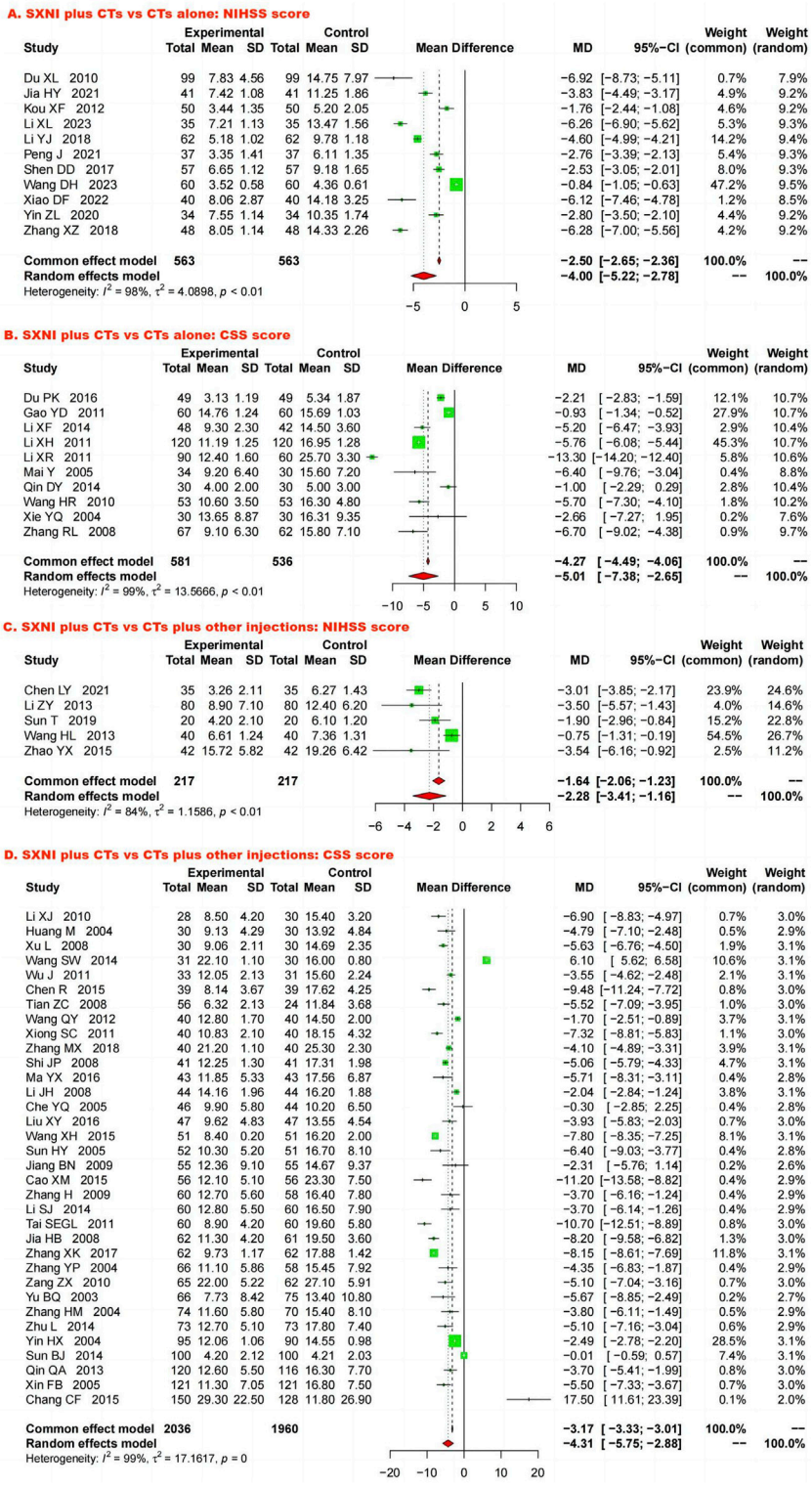

FIGURE 5
Forest plot and meta-analysis of neurological function. (Note. CSS, Chinese Stroke Scale; CTs, conventional treatments; NIHSS, National Institutes of Health Stroke Scale; SXNI, shuxuening injection).

metabolism and nutrition of hypoxic brain cells via its antioxidant properties (Smith et al., 2002; Nash and Shah, 2015) and reduce the apoptosis of neuronal cells in brain tissue through the inhibition of multiple inflammatory responses and the modulation of oxidative stress levels (Dong et al., 2023). Moreover, SXNI can increase superoxide dismutase activity against oxidative damage caused by

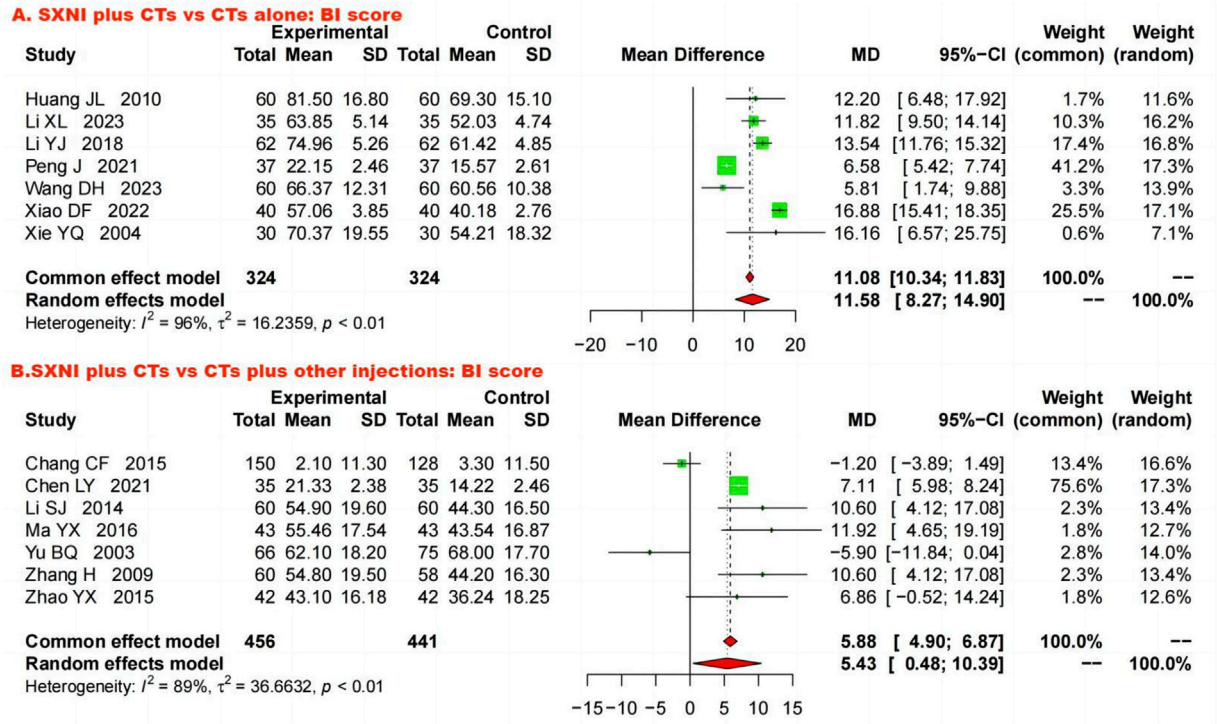

FIGURE 6
Forest plot and meta-analysis of activities of daily living. (Note. BI, Barthel index; CTs, conventional treatments; SXNI, shuxuening injection).

ischemia to protect muscle cells (Gao et al., 2007; Koyama et al., 2013; Powers and Lennon, 1999), and Ginkgolide B also can promote muscle regeneration by reviving osteocalcin–GPRC6A signalling (Wang et al., 2023). This may be the potential mechanism by which SXNI can reduce neurological deficits and improve limb function in AIS patients.

A centralized hospital monitoring study of the safety of SXNI injection in 9,735 patients showed that SXNI had a low incidence of AEs and good safety (Qu et al., 2023), which is consistent with our results. However, with the expanding application scope and increasing use frequency of SXNI in clinical practice, it is often abused. Reports of AEs related to SXNI were not uncommon. More than 80% of patients experienced AEs within 2 hours after administration (Chen, 2018; Gong and Shang, 2023), which prompted us to focus on monitoring the patient's condition during this time period. The occurrence of AEs to SXNI may be related to many factors, such as patient age, type of solvent, dosage, over-the-counter use, and coadministration (Wu, 2019). Therefore, we should pay attention to selecting the appropriate drug solvent, strictly follow the instructions for use, and try to avoid using other injections in combination.

In this review, 12.9% of the included studies were defined as moderate to high quality. Correct randomization and allocation concealment are important conditions for ensuring the minimization of selection bias; however, only 15 (12.9%) studies reported correct randomization methods, and none of the studies reported detailed allocation concealment, blinding, or implementation. Of all studies, 2.6% did not conduct intention-to-treat analysis and did not specify the reason for case dropout, 7.8% may not have completely reported outcomes, and none was registered in advance. Although all outcomes except CER showed significant heterogeneity, our subgroup analysis and mixed-effect regression analysis did not reveal the source of heterogeneity. Sensitivity analysis revealed differences in BI scores between SXNI plus CTs and CTs plus other injections when five studies (Chen, 2021; Li, 2014; Ma, 2016; Zhang et al., 2009; Zhao, 2015) were excluded one by one. The different manufacturers of SXNI, large sample size spans, different age-inclusion criteria, and populations in the different regions of these five studies may be potential sources of heterogeneity. The overall level of evidence for each outcome ranged from very low to low quality. The reasons for this were mainly the low methodological quality of the included studies, high heterogeneity among the included studies, and potential publication bias. Consequently, future RCTs with large sample sizes from multiple centers should be rigorously conducted in accordance with the consolidated standards of reporting trials (CONSORT) and should be registered in advance on the registration platform (Schulz et al., 2010).

4.2 Compared with previous studies

Our results suggested that SXNI in the treatment of AIS could not only increase CER and improve neurological function and ADL but also had good safety, which was consistent with the results of five systematic reviews previously published in 2011, 2012, and 2016 (Yan, et al., 2011; Xi et al., 2012; Zheng et al., 2012; Cai and Jiang, 2012; Tan, et al., 2016). We included patients who had AIS within

TABLE 3 Summary of findings according to the Grading Recommendations Assessment, Development, and Evaluations (GRADE) tool. (Note. CI, confidence interval; CTs, conventional treatments; MD, mean difference; RR, risk ratio; SXNI, shuxuening injection).

Certainty assessment							No of patients		Effect		Certainty	Importance
No of studies	Study design	Risk of bias	Inconsistency	Indirectness	Imprecision	Other considerations	SXNI plus CTs	CTs alone	Relative (95% CI)	Absolute (95% CI)		
A. SXNI plus CTs versus CTs alone												
Clinical Effective Rate												
32	randomised trials	seriousa	not serious	not serious	not serious	publication bias strongly suspectedd	1397/1550 (90.1%)	1119/1506 (74.3%)	RR 1.21 (1.17 to 1.25)	156 more per 1,000(from 126 more to 186 more)	⊕⊕◯◯◯ Low	CRITICAL
Chinese Stroke Scale												
10	randomised trials	very seriousb	very seriousc	not serious	not serious	none	581	536	-	MD 5.01 lower (7.38 lower to 2.65 lower)	⊕◯◯◯ Very low	IMPORTANT
National Institute of Health Stroke Scale												
11	randomised trials	not serious	very seriousc	not serious	not serious	publication bias strongly suspectedd	563	563	-	MD 4 lower (5.22 lower to 2.78 lower)	⊕◯◯◯ Very low	IMPORTANT
Barthel Index												
7	randomised trials	not serious	very seriousc	not serious	not serious	none	324	324	-	MD 11.58 higher (8.27 higher to 14.9 higher)	⊕⊕◯◯ Low	IMPORTANT
B. SXNI plus CTs versus CTs plus other injections												
Clinical Efficiency Rate												
70	randomised trials	very seriousb	not serious	not serious	not serious	publication bias strongly suspectedd	3528/3910 (90.2%)	2849/3763 (75.7%)	RR 1.18 (1.15 to 1.21)	136 more per 1,000 (from 114 more to 159 more)	⊕◯◯◯ Very low	CRITICAL
Chinese Stroke Scale												
34	randomised trials	very seriousb	very seriousc	not serious	not serious	none	2036	1960	-	MD 4.31 lower (5.75 lower to 2.88 lower)	⊕◯◯◯ Very low	IMPORTANT
National Institutes of Health Stroke Scale												
5	randomised trials	very seriousb	very seriousc	not serious	not serious	none	217	217	-	MD 2.28 lower (3.41 lower to 1.16 lower)	⊕◯◯◯ Very low	IMPORTANT

(Continued on following page)

10.3389/fphar.2024.1407669

TABLE 3 (*Continued*) Summary of findings according to the Grading Recommendations Assessment, Development, and Evaluations (GRADE) tool. (Note. CI, confidence interval; CTs, conventional treatments; MD, mean difference; RR, risk ratio; SXNI, shuxuening injection).

Certainty assessment							No of patients		Effect		Certainty	Importance
No of studies	Study design	Risk of bias	Inconsistency	Indirectness	Imprecision	Other considerations	SXNI plus CTs	CTs alone	Relative (95% CI)	Absolute (95% CI)		
Barthel Index												
7	randomised trials	very seriousb	very seriousc	not serious	not serious	publication bias strongly suspectedd	456	441	-	MD 5.43 higher (0.48 higher to 10.39 higher)	⊕OOO Very low	IMPORTANT

Note: CI, confidence interval; CTs, conventional treatments; MD, mean difference; RR, risk ratio; SXNI, shuxuening injection.

Explanations:

[a]: 50% - 75% of the studies were those with a higher risk of overall bias.

[b]: More than 75% of the studies were those with a higher risk of overall bias.

[c]: Heterogeneity among the studies was substantial.

[d]: There was a risk of publication bias.

14 days; however, Xi et al. and Zheng et al. included patients whose stroke occurred within 72 h and 7 days, respectively. According to the use requirements of SXNI, we included only adult stroke patients, but previous studies did not limit the age of AIS patients, which may have affected the scope of its application. Compared with previous meta-analyses (Yan, et al., 2011; Xi et al., 2012; Zheng et al., 2012; Cai and Jiang, 2012; Tan, et al., 2016), our study used more comprehensive outcomes (including CER, neurological function, ADL, and AEs) to evaluate the efficacy and safety of SXNI as an add-on therapy for AIS. However, Yan et al. included only 14 RCTs and did not report neurological deficit scores for outcome measures. Cai et al. only observed the CER of SXNI in AIS patients based on 22 RCTs. Tan et al. did not evaluate the effect of SXNI on the ability of patients with AIS to perform ADL. Moreover, the studies included in the previous meta-analyses (Yan, et al., 2011; Xi et al., 2012; Zheng et al., 2012; Cai and Jiang, 2012; Tan, et al., 2016) were all published before 2016, and many RCTs focusing on SXNI for AIS have been reported since 2016; therefore, our literature search deadline was 2023 to update the evidence.

4.3 Implications for practice and research

Our findings supported the clinical use of SXNI as an add-on treatment for AIS patients with a low level of evidence. Moreover, because no long-term follow-up studies have been performed to assess the effect of SXNI on the long-term prognosis of AIS patients, our study can only confirm that an intervention duration of 14–30 days with SXNI can effectively improve the neurological function and ADL of AIS patients. The usual daily dose of SXNI was 20 mL, and the most frequent treatment duration was 14 days. The five most common symptoms related to AEs were dizziness, flushing, palpitations, nausea, and headache, which is consistent with previous studies (Qu et al., 2023; Gong and Shang, 2023). Cardiovascular system events were the most common AEs of SXNI for AIS patients. Therefore, in clinical practice, SXNI should be used in strict accordance with the instructions, and patients should be monitored within 2 h after SXNI administration.

In this review, most (87.1%) included studies were judged as low quality. The lack of a detailed description of allocation concealment and blinding methods is a common problem in most studies. In all, 7.8% of the studies may have had a selective reporting bias. The included studies were all single-center RCTs conducted in China, which may mask the efficacy of SXNI in stroke patients of different ethnicities. Most of the studies were conducted in cities, and there is a lack of studies on SXNI for AIS in rural or primary medical institutions, while AIS patients in rural and primary medical institutions are in urgent need of effective and convenient drugs or technologies. SXNI has the advantages of being easy to use and safe. If SXNI is indeed effective in improving the prognosis of AIS patients, it will compensate for the deficiency caused by limited access to IVT and/or EVT. Large-sample, multicenter, placebo-controlled RCTs, especially in rural or primary medical institutions, should be conducted in the future. Moreover, all RCTs should be registered in an internationally recognized clinical trial registration platform and reported in accordance with the CONSORT guidelines.

4.4 Limitations and advantages

Some limitations of this study should be noted. First, all included trials were conducted in China and published in Chinese, which may have led to selection bias and publication bias and reduced the generalizability of the results to the applicable population. Second, most of the included studies were of low quality and had significant heterogeneity, which led to a low level of evidence.

There are also some advantages in our study. First, we carried out an extensive literature search, including seven databases and two clinical trial registration platforms, to obtain as many relevant studies as possible. Second, two reviewers independently performed literature screening, data extraction, and quality evaluation and cross-checked to ensure the accuracy of the data. Third, we conducted a sensitivity analysis, subgroup analysis, and mixed-effects meta-regression analysis to test the robustness of the meta-analysis results. We also assessed the level of evidence for each outcome based on the GRADE tool.

5 Conclusion

SXNI, as an add-on therapy, maybe safe and significantly improved the clinical efficacy, neurological function, and ADL of patients with AIS. However, due to the low quality of the included studies and the very low to low level of evidence in the meta-analysis results, more standardized, large sample, multicenter, and long follow-up RCTs are needed to confirm the efficacy and safety of SXNI for AIS.

Data availability statement

The original contributions presented in the study are included in the article/Supplementary Material, further inquiries can be directed to the corresponding authors.

Author contributions

JZ: Writing–review and editing, Writing–original draft, Methodology, Funding acquisition, Data curation, Conceptualization. XX: Writing–original draft, Project administration. YZ: Writing–original draft, Project administration. LL: Writing–original draft, Data curation, Project administration. HC: Writing–review and editing, Funding acquisition. LZ: Writing–review and editing, Conceptualization.

Funding

The author(s) declare that financial support was received for the research, authorship, and/or publication of this article. This study was funded by Medical Scientific Research Foundation of Guangdong Province (No. A2022239), special project of Science and Technology of Traditional Chinese Medicine of Guangdong Provincial Hospital of Chinese Medicine (No. YN2020QN23), Guangdong Basic and Applied Basic Research Foundation (No. 2022A1515220025), and special project of Lingnan modernization of traditional Chinese medicine in 2019 Guangdong Provincial R & D Program (No. 2020B1111100008). This study was also funded by the project of Traditional Chinese medicine rehabilitation talent training program of the Traditional Chinese Medicine Bureau of Guangdong Province (No. 01020184). The funders had no influence on the study design, data collection and analysis, decision to publish, or manuscript preparation.

Acknowledgments

We would like to thank all graduate students in the Department of Rehabilitation from Guangdong Provincial Hospital of Chinese Medicine for their assistance in finishing this paper. We also thank Home for Researchers editorial team (www.home-for-researchers.com) for English language editing.

Conflict of interest

The authors declare that the research was conducted in the absence of any commercial or financial relationships that could be construed as a potential conflict of interest.

Publisher's note

Supplementary material

The Supplementary Material for this article can be found online at: https://www.frontiersin.org/articles/10.3389/fphar.2024.1407669/full#supplementary-material

References

Ahlemeyer, B., and Krieglstein, J. (2003). Neuroprotective effects of Ginkgo biloba extract. *Cell Mol. Life Sci.* 60 (9), 1779–1792. doi:10.1007/s00018-003-3080-1

Bhatia, R., Hill, M. D., Shobha, N., Menon, B., Bal, S., Kochar, P., et al. (2010). Low rates of acute recanalization with intravenous recombinant tissue plasminogen activator in ischemic stroke: real-world experience and a call for action. *Stroke* 41 (10), 2254–2258. doi:10.1161/STROKEAHA.110.592535

Brott, T., Adams, H. P., Jr, Olinger, C. P., Marler, J. R., Barsan, W. G., Biller, J., et al. (1989). Measurements of acute cerebral infarction: a clinical examination scale. *Stroke* 20 (7), 864–870. doi:10.1161/01.str.20.7.864

Cai, L. M., and Jiang, J. Z. (2012). Summary analysis of the efficacy of Shuxuening injection for acute cerebral infarction. *Hebei Med. J.* 34 (8), 1217–1219. doi:10.3969/j.issn.1002-7386.2012.08.058

Chandrasekaran, K., Mehrabian, Z., Spinnewyn, B., Drieu, K., and Fiskum, G. (2001). Neuroprotective effects of bilobalide, a component of the Ginkgo biloba extract (EGb 761), in gerbil global brain ischemia. *Brain Res.* 922 (2), 282–292. doi:10.1016/s0006-8993(01)03188-2

Chen, J. (2018). Clinical analysis of adverse reactions of Shuxuening injection. *J. Med. Theory Pract.* 31 (3), 425–426. doi:10.19381/j.issn.1001-7585.2018.03.065

Chen, L. Y. (2021). Clinical effect of Shuxuening injection in the adjuvant treatment of acute cerebral infarction. *Chin. J. Clin. Ration. Drug Use* 14 (22), 47–49. doi:10.15887/j.cnki.13-1389/r.2021.22.017

Chinese Society of Neurology, Chinese Stroke Society (2018). Chinese guidelines for diagnosis and treatment of acute ischemic stroke. *Chin. J. Neurol.* 51, 666–682. doi:10.3760/cma.j.issn.1006-7876.2018.09.004

Cui, Q., Zhang, Y. L., Ma, Y. H., Yu, H. Y., Zhao, X. Z., Zhang, L. H., et al. (2020). A network pharmacology approach to investigate the mechanism of Shuxuening injection in the treatment of ischemic stroke. *J. Ethnopharmacol.* 257, 112891. doi:10.1016/j.jep.2020.112891

Diamond, B. J., Shiflett, S. C., Feiwel, N., Matheis, R. J., Noskin, O., Richards, J. A., et al. (2000). Ginkgo biloba extract: mechanisms and clinical indications. *Archives Phys. Med. rehabilitation* 81 (5), 668–678. doi:10.1016/s0003-9993(00)90052-2

Ding, Y. B. (2018). Effect of Shuxuening injection combined with Xingnao Kaiqiao acupuncture on blood lipid and neurological function in patients with cerebral infarction. *Clin. Res. Pract.* 3 (18), 119–120. doi:10.19347/j.cnki.2096-1413.201818055

Dong, W., Gong, T., Zhao, S., Wen, S., Chen, Q., Jiang, M., et al. (2023). A novel extract from Ginkgo biloba inhibits neuroinflammation and maintains white matter integrity in experimental stroke. *Neuroscience* 523, 7–19. doi:10.1016/j.neuroscience.2023.05.015

Fourth Session of Chinese National Cerebrovascular Conference (1996). Scoring criteria for clinical neurological deficit in stroke patients (1995). *Chin. J. Neurol.* 29 (6), 381–383.

Gao, J., Zhou, N., Hu, J. J., and Zhang, H. X. (2007). Protection of shuxuening injection on focal cerebral ischemic in rat. *Chin. J. Rehabilitation Theory Pract.* (08), 712–713. doi:10.3969/j.issn.1006-9771.2007.08.005

GBD 2019 Stroke Collaborators (2021). Global, regional, and national burden of stroke and its risk factors, 1990-2019: a systematic analysis for the Global Burden of Disease Study 2019. *Lancet Neurol.* 20 (10), 795–820. doi:10.1016/S1474-4422(21)00252-0

Gong, T., and Shang, B. (2023). Rationality and safety evaluation of the use of Shuxuening injection. *J. Navy Med.* 44 (5), 524–526. doi:10.3969/j.issn.1009-0754.2023.05.023

Guidetti, C., Paracchini, S., Lucchini, S., Cambieri, M., and Marzatico, F. (2001). Prevention of neuronal cell damage induced by oxidative stress *in-vitro*: effect of different Ginkgo biloba extracts. *J. Pharm. Pharmacol.* 53 (3), 387–392. doi:10.1211/0022357011775442

Gumbinger, C., Gruschka, P., Böttinger, M., Heerlein, K., Barrows, R., Hacke, W., et al. (2012). Improved prediction of poor outcome after thrombolysis using conservative definitions of symptomatic hemorrhage. *Stroke* 43 (1), 240–242. doi:10.1161/STROKEAHA.111.623033

Hasan, T. F., Hasan, H., and Kelley, R. E. (2021). Overview of acute ischemic stroke evaluation and management. *Biomedicines* 9 (10), 1486. doi:10.3390/biomedicines9101486

Higgins, J. P. T., and Green, S. (2011). *Cochrane handbook for systematic reviews of interventions*. London: The Cochrane Collaboration.

Jiang, J. C., Jiang, Y. L., and Wen, J. (2023). Cognitive load theory perspectives on Ma wanli's fundamentals of traditional Chinese medicine the inspiration of English translation and interpretation of the core concept of qi. *J. Guangxi Univ. Chin. Med.* 26 (02), 86–91. doi:10.3969/j.issn.2095-4441.2023.02.022

Jørgensen, H. S., Nakayama, H., Raaschou, H. O., and Olsen, T. S. (1999). Stroke. Neurologic and functional recovery the Copenhagen stroke study. *Phys. Med. rehabilitation Clin. N. Am.* 10 (4), 887–906. doi:10.1016/s1047-9651(18)30169-4

Koyama, H., Nojiri, H., Kawakami, S., Sunagawa, T., Shirasawa, T., and Shimizu, T. (2013). Antioxidants improve the phenotypes of dilated cardiomyopathy and muscle fatigue in mitochondrial superoxide dismutase-deficient mice. *Molecules* 18 (2), 1383–1393. doi:10.3390/molecules18021383

Kwah, L. K., and Diong, J. (2014). National Institutes of Health stroke scale (NIHSS). *J. Physiother.* 60 (1), 61. doi:10.1016/j.jphys.2013.12.012

Li, L. D., Zhou, Y., and Shi, S. F. (2023). Edaravone combined with Shuxuening versus edaravone alone in the treatment of acute cerebral infarction: a systematic review and meta-analysis. *Medicine* 102 (9), e32929. doi:10.1097/MD.0000000000032929

Li, S., Zhang, X., Fang, Q., Zhou, J., Zhang, M., Wang, H., et al. (2017). Ginkgo biloba extract improved cognitive and neurological functions of acute ischaemic stroke: a randomised controlled trial. *Stroke Vasc. neurology* 2 (4), 189–197. doi:10.1136/svn-2017-000104

Li, S. J. (2014). Clinical effect of Shuxuening injection in the treatment of acute cerebral infarction. *Jilin Med. J.* 35 (12), 2560. doi:10.3969/j.issn.1004-0412.2014.12.050

Ma, Y. X. (2016). Clinical effect and safety analysis of Shuxuening in the treatment of cerebral infarction. *China Health Care & Nutr.* 26 (29), 49. doi:10.3969/j.issn.1004-7484.2016.29.057

Mahoney, F. I., and Barthel, D. W. (1965). Functional evaluation: the barthel index. *Md. state Med. J.* 14, 61–65.

Nash, K. M., and Shah, Z. A. (2015). Current perspectives on the beneficial role of Ginkgo biloba in neurological and cerebrovascular disorders. *Integr. Med. insights* 10, 1–9. doi:10.4137/IMI.S25054

National Administration of Traditional Chinese Medicine (1994). *Standard for diagnosis and efficacy of Chinese medicine syndrome*. Nanjing: Nanjing University Press.

Oskouei, D. S., Rikhtegar, R., Hashemilar, M., Sadeghi-Bazargani, H., Sharifi-Bonab, M., Sadeghi-Hokmabadi, E., et al. (2013). The effect of Ginkgo biloba on functional outcome of patients with acute ischemic stroke: a double-blind, placebo-controlled, randomized clinical trial. *J. Stroke Cerebrovasc. Dis.* 22 (8), e557–e563. doi:10.1016/j.jstrokecerebrovasdis.2013.06.010

Ovbiagele, B., Goldstein, L. B., Higashida, R. T., Howard, V. J., Johnston, S. C., Khavjou, O. A., et al., and American Heart Association Advocacy Coordinating Committee and Stroke Council (2013). Forecasting the future of stroke in the United States: a policy statement from the American heart association and American stroke association. *Stroke* 44 (8), 2361–2375. doi:10.1161/STR.0b013e31829734f2

Oyama, Y., Chikahisa, L., Ueha, T., Kanemaru, K., and Noda, K. (1996). Ginkgo biloba extract protects brain neurons against oxidative stress induced by hydrogen peroxide. *Brain Res.* 712 (2), 349–352. doi:10.1016/0006-8993(95)01440-3

Page, M. J., McKenzie, J. E., Bossuyt, P. M., Boutron, I., Hoffmann, T. C., Mulrow, C. D., et al. (2021). The PRISMA 2020 statement: an updated guideline for reporting systematic reviews. *BMJ* 372, n71. doi:10.1136/bmj.n71

Powers, S. K., and Lennon, S. L. (1999). Analysis of cellular responses to free radicals: focus on exercise and skeletal muscle. *Proc. Nutr. Soc.* 58 (4), 1025–1033. doi:10.1017/s0029665199001342

Qu, Y., Ma, X. J., Li, Q. H., Li, H. L., Zhao, X. C., Sun, X. H., et al. (2023). Intensive hospital monitoring study on safety of 9735 cases of Shuxuening Injection. *Chin. Traditional Herb. Drugs* 54 (10), 3253–3260. doi:10.7501/j.issn.0253-2670.2023.10.022

Rochmah, T. N., Rahmawati, I. T., Dahlui, M., Budiarto, W., and Bilqis, N. (2021). Economic burden of stroke disease: a systematic review. *Int. J. Environ. Res. Public Health* 18 (14), 7552. doi:10.3390/ijerph18147552

Rosa, J. L., Alves, M., Ferreira, P., Papoila, A. L., and Nunes, A. P. (2022). Previous disability and benefit of acute phase therapy in functional prognosis of selected patients with ischemic stroke. *J. Stroke Cerebrovasc. Dis.* 31 (1), 106183. doi:10.1016/j.jstrokecerebrovasdis.2021.106183

Schulz, K. F., Altman, D. G., Moher, D., and CONSORT Group (2010). CONSORT 2010 statement: updated guidelines for reporting parallel group randomized trials. *Ann. Intern Med.* 152 (11), 726–732. doi:10.7326/0003-4819-152-11-201006010-00232

Shi, C., Zhao, L., Zhu, B., Li, Q., Yew, D. T., Yao, Z., et al. (2009). Protective effects of Ginkgo biloba extract (EGb761) and its constituents quercetin and ginkgolide B against beta-amyloid peptide-induced toxicity in SH-SY5Y cells. *Chem. Biol. Interact.* 181 (1), 115–123. doi:10.1016/j.cbi.2009.05.010

Singh, S. K., Srivastav, S., Castellani, R. J., Plascencia-Villa, G., and Perry, G. (2019). Neuroprotective and antioxidant effect of Ginkgo biloba extract against AD and other neurological disorders. *Neurotherapeutics* 16 (3), 666–674. doi:10.1007/s13311-019-00767-8

Smith, J. V., Burdick, A. J., Golik, P., Khan, I., Wallace, D., and Luo, Y. (2002). Anti-apoptotic properties of Ginkgo biloba extract EGb 761 in differentiated PC12 cells. *Cell Mol. Biol(Noisy-le-grand)* 48 (6), 699–707.

Smith, P. F., Maclennan, K., and Darlington, C. L. (1996). The neuroprotective properties of the Ginkgo biloba leaf: a review of the possible relationship to platelet-activating factor (PAF). *J. Ethnopharmacol.* 50 (3), 131–139. doi:10.1016/0378-8741(96)01379-7

Tan, D., Wu, J. R., Liu, S., and Zhang, B. (2016). Meta-analysis of efficacy of shuxuening injection in the treatment of cerebral infarction. *Chin. J. Pharmacoepidemiol.* 25 (8), 492–498.

Tian, J., Chen, L., Huang, X. L., Ding, Y. R., Wang, W., Huang, X. Y., et al. (2024). Understanding and relationship of qi and xue in traditional Chinese and western medicine. *Chin. J. Med. Guide* 26 (02), 171–175. doi:10.3969/j.issn.1009-0959.2024.02.020

Wang, B. Y., Chen, Y. F., Hsiao, A. W., Chen, W. J., Lee, C. W., and Lee, O. K. (2023). Ginkgolide B facilitates muscle regeneration via rejuvenating osteocalcin-mediated bone-to-muscle modulation in aged mice. *J. Cachexia Sarcopenia Muscle* 14 (3), 1349–1364. doi:10.1002/jcsm.13228

Wassélius, J., Arnberg, F., von Euler, M., Wester, P., and Ullberg, T. (2022). Endovascular thrombectomy for acute ischemic stroke. *J. Intern. Med.* 291 (3), 303–316. doi:10.1111/joim.13425

Wu, T. T. (2019). Retrospective analysis of adverse drug reaction of shuxuening injection in xi'an from 2013 to 2017. *Her. Med.* 38 (1), 49–53. doi:10.3870/j.issn.1004-0781.2019.01.011

Xi, B. C., Zhang, C., and Sun, L. L. (2012). Meta analysis of Shuxuening injection in treatment of patients with acute cerebral infarction. *Pharm. Care Res.* 12 (5), 354–357. doi:10.5428/pcar20120512

Yan, J., Wang, X. W., Zhou, J., Jing, J., Wang, C. X., and Li, J. J. (2011). Meta-analysis of shuxuening injection in the treatment for cerebral infarction. *Chin. J. Rehabil. Theory Pract.* 17 (9), 884–886. doi:10.3969/j.issn.1006-9771.2011.09.025

Zhang, A. L., Zhang, J. W., Sun, J. N., and Xu, Q. P. (2005). Progress on the mechanism of anti-ischemic action of Ginkgo biloba extracts. *China Pharm.* 16 (08), 626–629. doi:10.3969/j.issn.1001-0408.2005.08.031

Zhang, H., Zhou, M., and Zhang, J. J. (2009). The therapeutic effect of Shuxuening injection on acute cerebral infarction and its mechanism. *China J. Traditional Chin. Med. Pharm.* 24 (01), 81–84. doi:10.3969/j.issn.1004-7484(s).2013.09.542

Zhang, Z. W. (2019). Clinical observation of Pingganditantongluotang combined with Shuxuening injection in the treatment of cerebral infarction in the convalescent phase. *Guangming J. Chin. Med.* 34 (21), 3336–3338. doi:10.3969/j.issn.1003-8914.2019.21.047

Zhao, Y. X. (2015). Clinical observation of Shuxuening in the treatment of cerebral infarction. *J. Front. Med.* 5 (36), 87–88. doi:10.3969/j.issn.2095-1752.2015.36.086

Zheng, W. K., Zhang, L., and Shang, H. C. (2012). Systematic review on shuxuening injection in treating acute cerebral infarction. *China Licens. Pharm.* 9 (12), 33–41. doi:10.3969/j.issn.1672-5433.2012.12.007

Zheng, X. Y. (2002). *Guiding principles for clinical study of new Chinese medicines*. Beijing: China Medical Science Press.

Frontiers in Pharmacology

Explores the interactions between chemicals and living beings

The most cited journal in its field, which advances access to pharmacological discoveries to prevent and treat human disease.

Discover the latest Research Topics

See more →

Frontiers

Avenue du Tribunal-Fédéral 34
1005 Lausanne, Switzerland
frontiersin.org

Contact us

+41 (0)21 510 17 00
frontiersin.org/about/contact